SEISMIC PERFORMANCE OF REINFORCED CONCRETE TALL BUILDINGS WITH ADVANCED MATERIALS

A Dissertation

by

HUSAIN SALEEM ABBAS ALDAHLKI

Submitted to the Office of Graduate and Professional Studies of
Texas A&M University
in partial fulfillment of the requirements for the degree of

DOCTOR OF PHILOSOPHY

Chair of Committee,	Mary Beth Hueste
Committee Members,	John Niedzwecki
	Joeseph Bracci
	Theofanis Strouboulis
Head of Department,	Robin Autenrieth

December 2019

Major Subject: Civil Engineering

ABSTRACT

Utilizing new and advanced materials for reinforcing concrete structures in lieu of conventional steel bars could promote the response and behavior of concrete structures and provide reliable solutions for construction-related challenges in concrete structures.

The ACI 318-14 code does not allow the use of reinforcement with a yield strength higher than 60 ksi in special seismic force resisting systems in high seismic regions. ACI 318-19 limits the yield strength of reinforcement to 80 ksi in special frames and 100 ksi in special walls for seismic applications. In the first part of this study, high strength reinforcement was used instead of conventional bars in order to investigate the impact on the seismic performance of a concrete tall building that has been adopted as a case study.

In the second part of this study, an analytical study was performed utilizing shape memory alloy (SMA) bars as an alternative reinforcement for conventional steel bars in order to potentially improve the seismic performance of reinforced concrete tall buildings and reduce the residual strain upon subjecting the structure to severe earthquake shaking.

The study building was evaluated for four cases of reinforcement: conventional steel Grade 60, high strength ASTM A706 Grade 80, and high strength ASTM A1035 Grade 100 and 120. The response parameters were evaluated with the acceptance criteria of the Tall Building Initiative, TBI guidelines. Depending on the results, all cases with different grades satisfied the requirement of the TBI guidelines. In addition, an equivalent performance was noticed clearly between cases reinforced with a reduced area of high strength reinforcement and the reference case reinforced with conventional reinforcement.

The last case included both conventional steel bars and SMA bars which were used in specific regions where the plastic hinge is expected to occur. The performance of the case study building satisfied the TBI guidelines requirements. In addition, utilizing SMA bars improved the response of the building by eliminating the residual strain in reinforcing bars.

Finally, choosing the proper reinforcement material for concrete structures could be the key factor for meeting performance criteria while providing solutions for some construction problems.

DEDICATION

To my family

ACKNOWLEDGEMENTS

First thing that I want to emphasize that without the help and the guidance of the God, I could not do anything. Thanks for God for everything and every time.

I could not claim that this work is a result of an individual effort, however, this work represents a team work from my family to my advisor and committee members. To my advisor Dr. Mary Beth Hueste, thank you for your help, support, time, patience, and always encourage me. Thank you for give me this great opportunity for being one of your students. For my whole life, I will not forget the time that I was working with you. Thanks for Dr. John M. Niedzwecki for his support, help, time and advisements. One of the most unforgettable times in my life are the time I spent working with him. Thanks for Dr. Joseph M. Bracci, for his support, understanding and help. Thanks for Dr. Theofanis Strouboulis, for his help, time, and support.

For my Family thanks for unlimited support and help. For my wife Fanen, thanks for all you did for me and our children to complete my study successfully. For my kids, Fatema Alzahraa, Mohammed, Seraj, I will do my best for the rest of my life for you to be what you want to be.

CONTRIBUTORS AND FUNDING SOURCES

Contributors

This work was supervised by a dissertation committee consisting of Professor Mary Beth Hueste [advisor] and Professor John M. Niedzwecki and Professor Joseph M. Bracci of the Zachry Department of Civil and Environmental Engineering and Professor Theofanis Strouboulis of the Department of Aerospace Engineering.

All work conducted for the dissertation was completed by the student independently.

Funding Sources

Graduate study and research were supported mainly by a fellowship from the Higher Committee for Education Development in Iraq (HCED) and partially by Texas A&M University.

TABLE OF CONTENTS

Page

LIST OF FIGURES

Page

LIST OF TABLES

Page

CHAPTER I

INTRODUCTION

1.1 BACKGROUND

Reinforced concrete structural systems have many functions, however, the central one is to carry the gravity loads and withstand the effects of the surrounding environment. One of the most demanding environmental loads is the lateral load due to the shaking of structures during earthquakes. The main concern of structural engineers is that structures sustain their ability to carry gravity loads while experiencing large demands due to an earthquake event (FEMA 2015). All structural components respond to the applied loads in an integral form, however, some components that have the required design strength and details are designated as the seismic force resisting system (SFRS). The SFRS consists of horizontal and vertical members, and the foundation. To understand the role of each part of the SFRS, it is useful to consider the structural response during shaking of a building during an earthquake.

Earthquakes shake the ground below the foundation, such that foundation shaking occurs and the motion is transferred to the structure. The motion of the structure will create inertial forces (structure mass × acceleration of motion) according to Newton's second law. The inertial forces are distributed throughout the structure as a function of its mass distribution and the acceleration. The main role of the SFRS is to provide a path for inertial forces to be transferred to the foundation (Moehle 2014). Diaphragms represent the horizontal members of the SFRS and their function is to transfer the inertial forces at the floor level to the vertical members of the SFRS. The vertical members then transfer the inertial forces to the foundation. There are typically two types of vertical members: structural walls and moment-resisting frames.

The structural demand for buildings subject to earthquake shaking depends on the structure location, the characteristics of the earthquake such as intensity, and the strength and stiffness of the structure. For instance, when a linear elastic structure located in a high seismic region is subjected to the maximum expected earthquake, the lateral deformation may be several inches, and the lateral forces may be equal or greater than the weight of the structure. Designing structural systems to respond linearly during a severe earthquake is not typically an economic solution. Specifically, for a structural system to respond linearly to such high demands (forces and deformation), its components such as beams, and columns would need to be very large elements as compared to typical elements sizes. In addition, this type of structure will be very expensive and may reduce the functionality of the structure. Therefore, yielding or inelastic responses should be expected (Blume et al. 1961).

The structural building code for designing reinforced concrete structures in the United States, ACI 318-14, *Building Code Requirements for Structural Concrete and Commentary* (ACI 2014) (in time of writing this study the new edition of ACI 318 was issued (ACI 2019)), references the standard ASCE 7, *Minimum Design Loads and Associated Criteria for Buildings and other Structures* (ASCE 2016). In ASCE 7-16, the Risk-Targeted Maximum Considered Earthquake (MCER) corresponds to pseudo acceleration values that have an exceedance probability of 2% in 50 years (2475 year of return period). This value is the definition used by ASCE 7-16 for a ground motion for a particular region in the United States. However, ASCE 7-16 does not use MCER for design purposes, instead it uses the Design Earthquake (DE) value which is 2/3 of MCER (ASCE 2016). Based on the preceding brief discussion, the ACI 318-14 design philosophy accepts inelastic response of structures in areas of high seismic hazard. In all cases, engineers must anticipate inelastic responses and detail elements accordingly, therefore a good understanding of

the nature of nonlinear responses and where they would occur is crucial for structural engineers.

According to the preceding discussion, one could conclude that the main concern of the provisions of ACI 318-14 is life safety and prevention of structural collapse by allowing inelastic deformation in some specific regions in the SFRS of the structure. In some cases, the damage is very difficult to repair leading to a high cost of repair and a long time required to reoccupy the structure.

1.2 SIGNIFICANCE

Utilizing new and advanced materials for reinforcing concrete structures in lieu of conventional steel bars could promote the response and behavior of concrete structures subjected to earthquake shaking and provide reliable solutions for construction-related challenges in concrete structures. For instance, one issue in concrete construction is the congestion of steel reinforcing bars leading to difficulties such as concrete casting and reinforcement placement. In addition, tall concrete structures in high seismic regions usually have very congested steel bars reinforcement layouts. Utilizing high strength reinforcing bars could solve the congestion problem by reducing the required area of steel. It is crucial to mention that ACI 318-14 does not allow the use of high strength reinforcement for the primary reinforcement in SFRS. During the time of writing this work, ACI 318-19 was issued and this new version of the concrete code allows the use of Grade 80 reinforcement in special moment frames and special walls. In addition, ACI 318-19 allows the use of Grade 100 reinforcement for only special walls, but not for special moment frames. ACI 318-19 does not permit using Grade 120 reinforcement in special frames and special walls for seismic applications. More studies are needed to explore the performance of concrete structures reinforced with high strength reinforcement as compared to conventional steel bars. The goal of the first part of this study is to examine the seismic response of tall concrete buildings reinforced

with high strength reinforcement in lieu of conventional steel bars.

Another challenge is that the permanent deformation in some regions of concrete frames could lead to detrimental consequences such as high repair cost, longer time for repair, and eventual demolition of structures. The main goal of the second part of this study is to utilize a new and advanced material, shape memory alloys (SMA) in the form of reinforcing bars, for reinforced concrete structures in order to reduce the permanent deformation and to enhance the seismic performance.

These new and advanced reinforcing materials have unique characteristics that could be utilized to enhance the response and behavior of tall concrete buildings as well as facilitate the construction process.

1.3 OBJECTIVE AND SCOPE

1.3.1 Applications of High Strength Reinforcement

In the first part of this study, an investigation will be conducted to evaluate the use of high strength reinforcement in reinforced concrete tall buildings. The performance of a tall building reinforced with high strength reinforcement will be compared to that of the same building reinforced with conventional steel bars. High strength reinforcement can be defined as a reinforcement that has a yield strength of more than 72 ksi (NEHRP 2014). Production of reinforcement bars with a yield strength higher than 60 ksi is currently in progress in the United States and within a few years will be more common in the market. Tall buildings in high seismic regions have substantial gravity loads and seismic demands that can lead to very heavily congested reinforced concrete sections. Therefore, using high strength reinforcement with a reduced amount of steel area could introduce a valuable solution.

In general, the tensile characteristics of high strength reinforcement differ from

conventional steel (Tavallali et al. 2014). In addition, the provisions of ACI 318-19 limit the yield strength of reinforcement to 80 ksi in special frames and 100 ksi in special walls for seismic applications. Therefore, more studies are needed to explore deeply the behavior of structural members reinforced with high strength reinforcement under different loading conditions. Also, the effect of high strength reinforcement on the global behavior of frames should be investigated. In the first part of this study, high strength reinforcement is used instead of conventional bars in order to investigate the performance of a tall building that has been adopted as a case study. Three available types of high strength reinforcement will be used including Grades 80, 100, and 120. All three types are produced under the ASTM standards as described in Chapter 2.

The global and local response of the selected tall concrete case study building reinforced with high strength reinforcement, will be examined and evaluated according to the Tall Building Initiative (TBI) procedure of *Guidelines for Performance-Based Seismic Design of Tall Buildings* (TBI 2017). The seismic performance of the building is assessed and compared to the same building reinforced with conventional reinforcing bars, to determine if it has an equivalent performance. Nonlinear analyses will be performed to extract the response parameters that will be checked with the TBI guidelines acceptance criteria.

1.3.2 Applications of Shape Memory Alloy Reinforcement

The second part of this study focuses on utilizing shape memory alloy (Ozbulut et al.) bars as reinforcement in tall concrete buildings. SMAs are a type of new smart materials that show unique engineering properties (Lagoudas 2008). SMAs have unique characteristics, however, the most distinct one is their ability to experience large deformations and return to their original shape upon loading removal. SMAs have different properties than conventional steel bars, therefore using SMAs as reinforcement in concrete members will result in new structural sections with

different behavior and responses.

As part of this work, an analytical study was performed utilizing SMA bars as an alternative reinforcement for conventional steel bars in order to potentially improve the seismic performance of reinforced concrete tall buildings and reduce the residual strain or the damage upon subjecting the structure to severe earthquake shaking. Conventional steel reinforcement can yield and dissipate energy, however steel bars are not able to recover the inelastic deformation leading to permanent damage. On the other hand, SMAs have the ability to recover the inelastic strain upon loading removal leading to a negligible amount of residual strain.

Different scenarios for reinforcing with SMAs in the selected case study tall concrete building will be adopted. The performance of the case study building reinforced with SMAs will be studied and checked with the procedure of the TBI guidelines. The global and local responses of the case study building are examined through nonlinear analyses to two different shaking levels, service level and maximum considered earthquake level. The response parameters for global and local behavior are checked with the acceptance criteria of the TBI guidelines.

1.4 ORGANIZATION

This dissertation is comprised of 13 chapters. Chapter 1 provides background, objective, and scope. chapter 2 has three main parts. The first part gives the definition of tall buildings, while the second part provides a background about the types and tensile characteristics of high strength reinforcement. In addition, a review is provided of some recent works that focus on utilizing high strength reinforcement for structural members that are part of the lateral load resisting system. The third part provides background on the shape memory alloy effect, SMA types, and some recent studies that investigated utilizing SMA bars as an alternative reinforcing material for concrete structures. Chapter 3 provides a brief description of the case study building. The seismic design

spectrum of the location of the case study building is also provided.

The procedure of the TBI guidelines for assessing the seismic performance of tall buildings is described in chapter 4. In addition, a brief introduction about the reason behind the adoption of the TBI guidelines is presented.

The modeling procedure for simulation of different types of structural elements is explained in chapter 5. The validation of the selected models and materials with the experimental results is also provided.

The selection of the appropriate ground motions to match the target spectrum for the location of the case study building for SLE and MCER levels is provided in chapter 6 . In addition, the scaling procedure of the selected ground motions is explained.

chapter 7 shows the results of the case study building reinforced with conventional steel bars for both SLE and MCER levels. chapter 8 shows the results where the case study building is reinforced with ASTM A 706 Grade 80 reinforcement in all the structural members. The results for the use of ASTM 1305 A Grade 100 reinforcement are provided in chapter 9. The results of the case using ASTM 1035 A Grade 120 reinforcement are provided in chapter 10. The results of the case reinforced with SMA bars in some specific regions are depicted in chapter 11.

A comparison between the results of the reference case reinforced with conventional reinforcement and the cases of high strength reinforcement is depicted in Chapter 12. Another comparison between the reference case and the case reinforced with SMA bars in some specific regions is also depicted. chapter 13 provides a brief summary about the work. The main conclusions are presented in the same chapter.

CHAPTER II

LITERATURE REVIEW

2.1 TALL BUILDINGS DEFINITION

Three different terms may be used to describe buildings of a certain height: “tall buildings,” “high rise buildings,” and “skyscraper.” It is difficult to distinguish them based only on the dimensional perspective due to the fact that height is simply relative and would be changeable according to the place and time. During the late nineteenth century, the term “high rise buildings” was recognized, on the other hand, the term “tall buildings” has an older history than the term “high rise buildings” (Günel and Ilgin 2014). The reflection of people’s amazement and exaggeration may be the reason behind using the term “skyscraper” for some buildings. The 12-story Home Insurance Building in Chicago, built at the end of the nineteenth century, was the first appearance of the term “skyscraper” (Günel and Ilgin 2014).

Many researchers and engineering organizations stated different definitions for tall buildings and the criteria for this classification. There is no absolute definition for tall buildings. The Council on Tall Buildings and Urban Habitat (CTBUH) classified tall buildings into three categories according to the building height. The first category is “tall building” with 156 ft (50 m) or more in height, while a “supertall building” has a height of more than 984 ft (300 m). The third category is “megatall building” with a height more than 1968 ft (600 m). According to the way the height of a building is measured, the CTBUH established three categories of building heights. In all categories, the height is measured from the level of the lowest, significant, open-air, and pedestrian entrance. The measurement that is most often employed and used is the height to the “architectural top” which is defined as the architectural top of the building, including spires, but

not including antennae, signage, flag poles or other functional-technical equipment.

Moehle defined the threshold of the height for tall buildings as 240 ft (73 m) or taller (Moehle 2008). Some researchers have tried to give a definition for tall buildings without depending on the number of floors or the height. For instance, the need to use any additional techniques to construct a building is a threshold to distinguish tall buildings (Günel and Ilgin 2014). In Japan, a tall building has been defined as a building with a height of at least 197 ft (60 m) (Sugano 2008).

Other researchers tried to conceptualize the way by which one could distinguish tall, supertall, and skyscraper buildings by introducing two concepts: local and global. According to their definition, a tall building is a local concept, while on the other hand, a supertall or skyscraper building is a global concept. It is necessary for a tall building that is considered tall in its local region, to be recognized and classified globally to be defined as a supertall building or skyscraper (Günel and Ilgin 2014).

2.2 HIGH STRENGTH REINFORCEMENT

In this section, the types of available high strength reinforcement and their important properties will be introduced. Studies that examined the response of structural elements reinforced with high strength steel will also be presented.

2.2.1 Types of High Strength Reinforcement

High strength reinforcement could be defined as a reinforcement that has a yield strength of more than 72 ksi (NEHRP 2014). Japan has erected reinforced concrete buildings with high strength reinforcement bars with a yield strength as high as 100 ksi to resist seismic loads (Aoyama 2001). Reinforcing bars with a yield strength higher than 60 ksi are currently produced in the United States and within a few years they will be more common in the market. Three types of high

strength reinforcement that are available in the United States are introduced in this study. All three types are produced under the ASTM specifications as noted in the sections below. The first type is covered by ASTM A706, *Standard Specification for Low –Alloy Steel Deformed and Plain Bars for Concrete Reinforcement* (ASTM 2016a), and includes Grades 60 and 80. The other two types are covered by ASTM A1035, *Standard Specification for Deformed and Plain Low Carbon Chromium Steel Bars for Concrete Reinforcement* (ASTM 2016b), and includes Grades 100 and 120.

In this study, three types of high strength reinforcement that are available and produced in the United States, and cover a range of strength (80, 100, and 120 ksi) are considered.

2.2.1.1 ASTM A706 (Grade 80)

ASTM A706 (ASTM 2016a) has two reinforcement grades: Grade 60 and Grade 80. ACI 318-14 allows A706 Grade 60 to be used for seismic applications for reinforcing special moment frames and special walls. According to ASTM A706, Grade 80 has almost the same properties as Grade 60, therefore Grade 80 is accepted in the ACI 318-19 for special frames and walls for seismic applications. Table 2.1 summarizes critical requirements for ASTM A706 Grade 60 and Grade 80 reinforcement.

The tensile strength of reinforcement should be at least 1.25 times the actual yield strength according to ASTM A706. From Table 2.1, the similarity between both grades is obvious except for the yield strength and small differences in the elongation requirements. However, for bars with a size larger than no. 6, Grade 80 is required to match the same elongation requirements of Grade 60. From a practical point of view when designing primary structural elements, bar sizes larger than no. 6 would be more useful than smaller bars, therefore one could consider that there are no differences in the elongation requirements for both grades. Figures 2.1 and 2.2 show some

examples of the stress-strain relationship of ASTM A706 Grade 60 and 80 reinforcement.

2.2.1.2 ASTM A1035

ASTM A1035 (ASTM 2016b) reinforcement includes two reinforcement grades: Grade 100 and Grade 120. Grade 100 is allowed by ACI 318-14 to be used for confinement reinforcement. On the other hand, Grade 120 is not allowed to be used in any application according to ACI 318-14. ACI 318-19 allows the use of Grade 100 reinforcement in special walls, but not in special frames. ACI 318-19 does not allow the use of Grade 120 reinforcement for seismic applications. However, some studies have investigated the response of different structural members reinforced with both grades as described in Section 2.2.5. Table 2.2 shows the important tensile properties of A1035 reinforcement. The yield strength is measured by the 0.2% offset method because there is not a well-defined yield plateau. It is clear that the elongation requirements are less for A1035 than for A706. Figure 2.3 shows example stress-strain curves for A1035 reinforcement.

Table 2.1 ASTM A706 Grades 60 and 80 (adopted from (ASTM 2016a)).

Property	**Grade 60**	**Grade 80**
Yield strength (f_y), min. (ksi)	60	80
Yield strength (f_y), max. (ksi)	78	98
Tensile strength (f_u), min. (ksi)	80	100
Elongation in 8 in., min:		
Bar size 3, 4, 5, 6	14%	12%
Bar size: 7, 8, 9, 10, 11	12%	12%
Bar size: 14, 18	10%	10%

Table 2.2 ASTM A1035 Grades 100 and 120 (adopted from (ASTM 2016b)).

Property	**Grade 100**	**Grade 120**
Yield strength (f_y), min.	100	120
Tensile strength, min.	150	150
Stress corresponding to an extension under load 0.0035 in./in., min.	80	90
Elongation in 8 in., min.		
Bar size: 3 to 11	7%	7%
Bar size: 14, 18	6%	N.A.

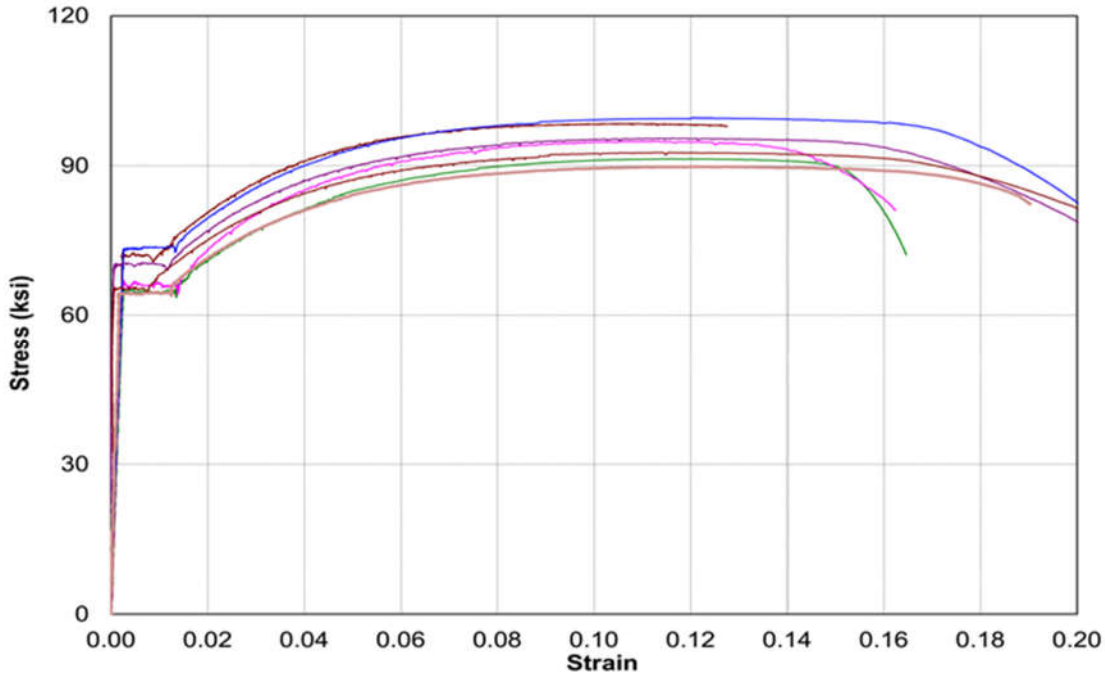

Figure 2.1 Example Stress-Strain Curves for ASTM A706 Grade 60 Reinforcement (NEHRP 2014).

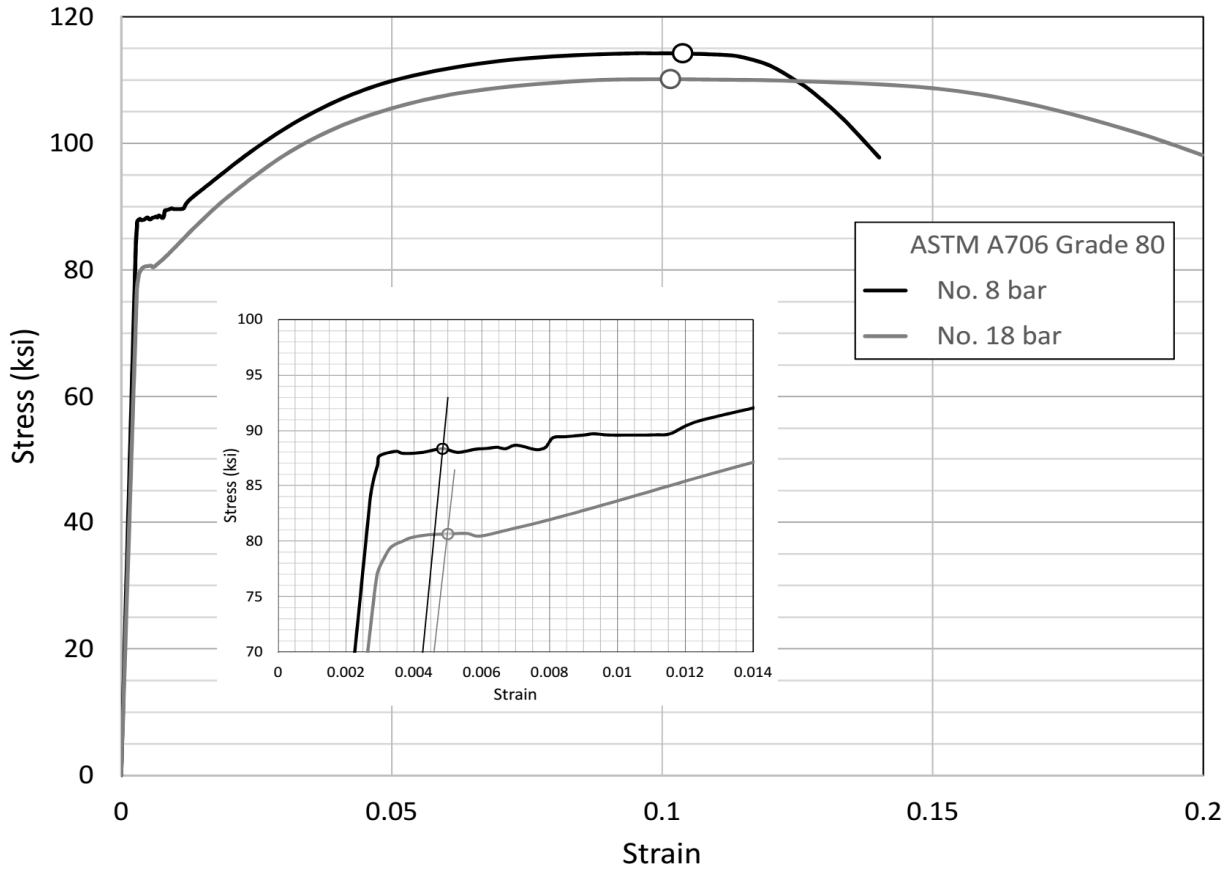

Figure 2.2 Example Stress-Strain Curves for ASTM A706 Grade 80; dots on the curves represent the tensile strength and uniform strain. The inset image shows a larger scale view of where the 2% offset lines cross the stress-strain curves (NEHRP 2014).

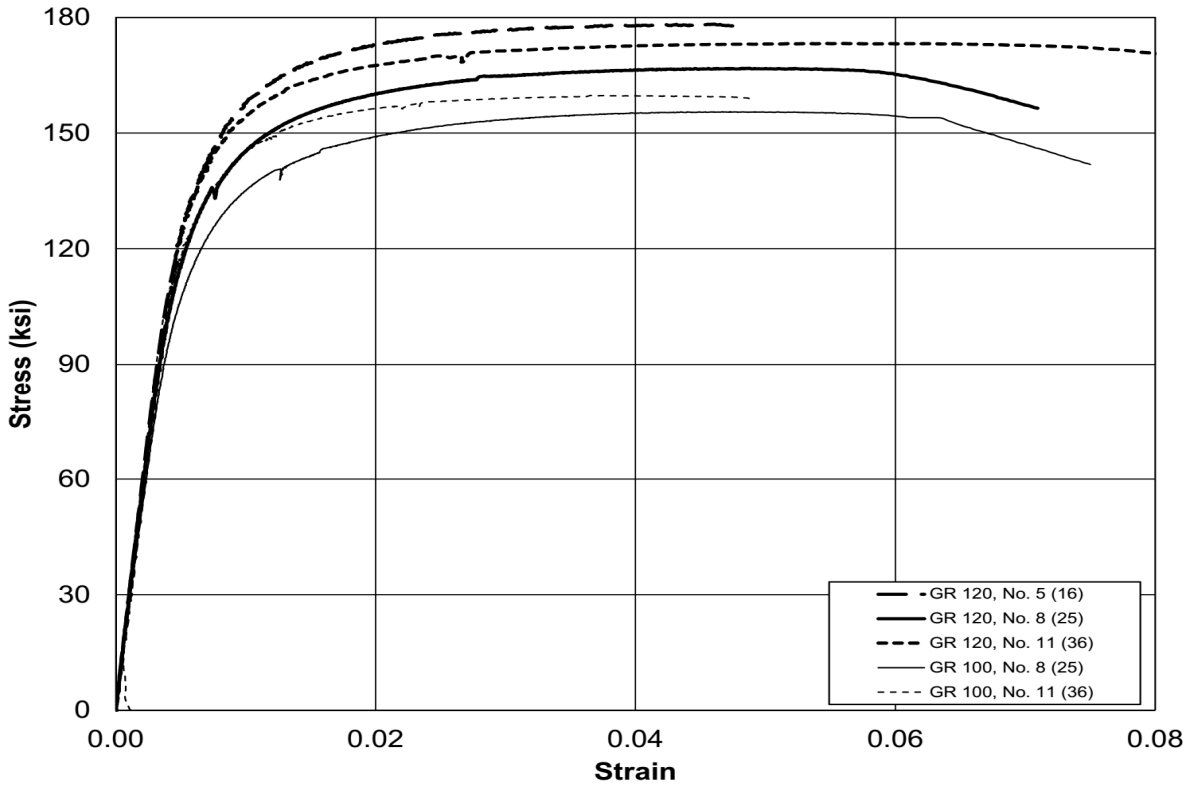

Figure 2.3 . Example stress-strain curves for ASTM A1035 Grade 100 and Grade 120 reinforcement (NEHRP 2014).

2.2.2 High Strength Reinforcement Properties

In this section, a brief explanation for defining the tensile properties of high strength reinforcing bars is introduced. Tensile properties are specific properties that are extracted from tensile tests of reinforcing bars specimens and are used to define the strength and ductility of reinforcing bars. Based on the tensile properties of a reinforcing bar, the bar could be evaluated for high strength reinforcement requirements according to the ASTM specifications. The essential tensile properties are the yield strength, tensile strength, elongation, ratio of tensile to yield strength, and ductility. It is worth mentioning that tensile properties are not only an indication of type or grade of reinforcing bars, they also play a crucial role in affecting the structural behavior

of members reinforced with steel bars as well as the global structural behavior, as will be explained in the sections below. In this section, a simple definition for each tensile property is provided and in a subsequent section, their effect on structural behavior is introduced.

2.2.2.1 Yield Strength

The definition of yield strength or yield point depends on the behavior of the reinforcing bar in the tensile test. The yield point is defined according to ASTM A370, *Standard Test Methods and Definitions for Mechanical Testing of Steel Products* (ASTM 2017), as "the first stress in a material less than the maximum obtainable stress, at which an increase in strain occurs without an increase in stress." It is clear from the ASTM A370 definition that the yield point represents a definitive point on the stress-strain curve, at which the steel bar strain increases with a negligible stress increase. In general, reinforcement with low strength (defined as having a strength less than 75 ksi), exhibits this type of behavior and consequently, has a yield point. On the other hand, a definitive yield point does not appear for high strength reinforcement. Therefore, a different definition is needed for describing the yield strength of high strength reinforcement. Yield strength is defined according to ASTM A370 as "the stress at which a material exhibits a specified limiting deviation from the proportionality of stress to strain." Two ways to determine yield strength according to ASTM A307 are the 0.2% offset method and the Extension under Load (EUL) method. High strength reinforcement of types A706, A615, and A1035 adopt the 0.2% offset method to determine the yield strength, with a requirement to use the EUL method for a strain of 0.0035 to determine the minimum yield strength.

2.2.2.2 Tensile Strength

In contrast with the yield strength, the tensile strength definition is consistent for all types of reinforcing steel. Tensile strength simply corresponds to the peak point in the stress-strain curve

and its value is determined by dividing the maximum applied load during the test by the nominal area of the specimen according to ASTM A370.

2.2.2.3 Elongation

Elongation is the most important property to determine the suitability of reinforcing steel to use in a member that is considered as part of the SFRS because it provides a measure of ductility. There are two terms related to the elongation: total elongation and uniform elongation. Uniform elongation is the strain of the peak point on the stress-strain curve, in other words, the strain at the peak stress. The most important feature of this elongation is the uniform distribution of strain throughout the whole length of the specimen. Therefore, uniform elongation represents the stage of the test just before the necking phenomenon occurs in the specimen. On the other hand, the total elongation represents the whole elongation that occurs from the beginning of the test until the fracture of the specimen. Therefore, the strain during the necking stage will be included in the total elongation. It should be noted that only the total elongation is required to be measured according to ASTM A307. However, the uniform elongation plays an important role in seismic design applications because the useable elongation should be taken as 75% or less of the uniform elongation. In seismic design, the useable elongation will be considered in the location of the plastic hinge at which the yielding of reinforcing bars is expected. It is very crucial to mention that the damage state for reinforcing bars at strains smaller than uniform elongation strain under cyclic loading may be equivalent to the damage state at the uniform elongation strain under monotonic loading. Consequently, the useable elongation should be taken to be less than the uniform elongation as mentioned above (Aoyama 2001; Rautenberg 2011).

2.2.3 Effect of Tensile Characteristics of High Strength Reinforcement on Structural Member Response

The tensile characteristics and the shape of the stress-strain curve of high strength reinforcement are changeable according to the manufacturing procedures (NEHRP 2014). In this brief discussion, the focus will be only on the most important characteristics such as the ratio of tensile to yield strength, the elongation, and the yield plateau. The structural response of a member is directly affected by the tensile characteristics and the stress-strain curves of the reinforcement, which play a crucial role in spreading or concentrating the plasticity within the plastic hinge zone. Spreading the plasticity leads to lengthen the plastic hinge zone length and decrease the imposed strain due to the same amount of drift. The high ratio of tensile to yield strength and a large elongation with the existence of a yield plateau will promote the spread of plasticity. The second effect of tensile characteristics is to maintain or degrade the strength of the member during rotation under the effect of earthquake events.

Similar to the concept of spreading the plasticity, reinforcement with a high ratio of tensile to yield strength and elongation, as well as a long yield plateau, will enhance the ability of a member to maintain its strength after experiencing large plastic cycles of deformation. It is noted that the ACI 318-14 code provisions allow ASTM A706 (Grade 60) reinforcement to be used in high seismicity regions for reinforcing special moment frames and walls due to its tensile characteristics, which would increase the spreading of plasticity and maintain the member strength. The tensile characteristics required by ASTM A706 are a ratio of tensile to yield strength of at least 1.25 and a total elongation of at least 12%. It should be mentioned that the ASTM standards for high strength reinforcement do not require a yield plateau. In general, the stress-strain curves of high strength steel do not have a distinctive yield plateau, and therefore their curves are rounded

as shown in Figure 2.3 for ASTM A1035.

2.2.4 Problem Description with High Strength Reinforcement

One of the primary parameters for designing steel reinforced concrete members is the yield strength of the steel bars. The 1956 ACI 318 code specified a limit of 60 ksi for the yield strength of steel bars (ACI 1956). Depending on full-scale concrete beams tests, the 1963 ACI 318 code increased the limit to 75 ksi (ACI 1963). A limit of 80 ksi was accepted and included in the 1971 ACI 318 code (ACI 1971). However, the manufacturers of reinforcing steel continued to develop methods for producing steel bars with a higher grade. In 2004, ASTM included a new standard, ASTM A1035, which deals with reinforcing steel with Grade 100. Responding to this growing area, the 2005 ACI 318 code (ACI 2005) allowed the use of 100 ksi steel for confinement purposes only. In 2010, ACI formed an Innovation Task Group 6, who developed design guidelines for using Grade 100 reinforcement for general applications but not for regions with high seismic design categories (D, E, and F) (ACI 2010). ACI 318-14 did not change the limit of 60 ksi for special seismic systems which are defined as seismic force resisting systems with ductile detailing intended for in highest seismicity areas. The current code provisions of ACI 318-14 do not allow the use of steel with a yield strength more than 60 ksi for the seismic force resisting systems in high seismicity regions. During the time of writing this work, ACI 318-19 is issued and this new version of the concrete code allows using Grade 80 in the special moment frame and the special walls. In addition, ACI 318-19 allows using Grade 100 for only the special walls not for special moment frames. ACI 318-19 does not permit using the Grade 120 in special frame and walls for seismic applications.

Currently, reinforcement with a yield strength of 80, 100, and 120 ksi are produced in the United States and are commercially available. Using reinforcement with high strength is associated

with using less volume of reinforcement for a given structural element for a typical structural element. Using a reduced amount of high strength reinforcements has some advantages such as reducing the congestion of steel bars, reducing the cost, placing concrete more easily, and reducing the environmental impact. Introducing high strength reinforcement with reduced amounts for seismic applications could be done by considering the following three important issues.

1. Cracks width and pattern under service loads conditions

Cracks could lead to more detrimental issues in concrete members such as reinforcing steel corrosion and increasing the permeability of concrete leading to more aggressive fluids to enter and deteriorate the concrete. Hognestad performed large-scale tests and confirmed that there is a proportionality between the crack width and the reinforcing steel stress (Hognestad 1962). Depending on Hognestad results, the 1963 ACI 318 code limited the yield strength of steel to 60 ksi (ACI 1963). Reducing the required area of reinforcing bars increases their stresses. The question here is what the effect of the reduced area of high strength reinforcement on crack width in SFRS under service-level loads? Longitudinal reinforcement in columns under service loads may or may not experience tensile stresses, therefore cracks in columns would not be a major concern under service loads. On the other hand, tensile stresses in the longitudinal reinforcement in columns under severe earthquakes would be considerably high due to lateral loads transfer, during an earthquake, cracks do not present the primary concern. Beams in a SFRS need a relatively large amount of reinforcement for resisting the effect of seismic loading compared to the required reinforcement for service loads effects, therefore the cracks width would not be a major issue. From the previous discussion, one could conclude that cracks could not be a critical concern if a reduced area of high strength reinforcement is utilized in seismic force resisting system (SFRS).

2. Post cracking stiffness

The member stiffness depends on the gross section properties before cracks occur. After the section cracks, the amount and layout of reinforcement play important role in calculating the effective stiffness of the member (Hognestad 1962). High strength reinforcement with reduced area relative to conventional reinforcement reduces member stiffness after cracking. Experimental and analytical studies are needed to investigate the effect of the reduced stiffness of structural members reinforced with high strength steel bars on the global response of the building SFRS. If the columns and beams of a frame have reduced post cracking stiffness, does the frame show similar reduction in its stiffness? It is noteworthy that the analysis or assessment by using nonlinear analyses could overcome the difficulties of evaluating the appropriate effective stiffness for members reinforced with high strength reinforcement.

3. Drift capacity

Studies mentioned that one of the factors that affects the drift capacity of a reinforced concrete member is the length of the plastic hinge (Kheyr and Naderpour 2007; Priestley and Park 1987). As mentioned above, the reinforcement tensile characteristics directly affect the spread of plasticity as well as the length of plastic hinge zone. High strength reinforcement with a low ratio of tensile to yield strength (less than 1.25) and a small amount of total elongation leads to a shorter length of the plastic hinge zone. As a consequence, the shortness of the plastic hinge length in a member requires more curvature to obtain the same drift. The increased curvature means more tensile strain and stress in the steel reinforcing bars. In addition, the concrete deformability should be increased. The equation for calculating the drift capacity that is proposed in some studies requires the length of the plastic hinge zone (Kheyr and Naderpour 2007; Priestley and Park 1987). The same studies suggested an equation for estimating the

length of a plastic hinge zone, but this equation does not consider using steel bars with yield strength greater than 60 ksi. Depending on the preceding discussion, more experimental studies are needed to establish an equation for calculating the drift capacity of concrete members reinforced with high strength reinforcement. In addition, analytical studies could provide information about the sensitivity of the response of the SFRS when using high strength steel reinforcement under cyclic loading conditions.

Reinforced concrete tall buildings are widely spread around the world. For instance, in 1930, steel tall buildings represented 96% of the world's 100 tallest buildings and the remaining were erected with concrete or composite systems. On the other hand, in 2010 the steel tall buildings percentage descended to 21% while a noticeable increase in the percentage of concrete and composite systems was observed with 79%. Tall buildings in high seismic regions have a substantial gravity loads and seismic demands, which usually lead to very heavily congested reinforced sections (TBI 2017). Therefore, using high strength reinforcement with a reduced area of steel reinforcing bars could introduce a valuable solution. Studies are needed to investigate the response of tall buildings reinforced with high strength reinforcement in their structural members under cyclic loading conditions. The results of the needed studies could increase the acceptance of using high strength reinforcement and make it a more reliable choice.

2.2.5 Previous Research on High Strength Reinforcement

In this section, studies that were performed to test experimentally or analytically the behavior of different structural members reinforced with high strength steel bars are introduced with emphasis on the behavior under cyclic loadings conditions.

2.2.5.1 Beams Reinforced with High Strength Reinforcement

According to the authors (Tavallali et al. 2014), a lot of researchers focused on utilizing

high strength reinforcement in normal applications (non-seismic applications), therefore the study intended to investigate experimentally using of high strength reinforcement in beams under reversed cyclic loading conditions.

In all seven specimens, transverse reinforcement was provided for resisting shear forces, preventing buckling of bars, and preventing any brittle failure modes prior to reaching the design flexure strength. After applying 5% drift cyclically, a monotonic push was applied till reaching the fracture of the specimen or the capacity of the testing apparatus. A good conclusion could be drawn through following the experimental results of two specimens CC4-X, and UC4-X that were typical except that the yield strength and the amount of the longitudinal reinforcement were different. CC4-X and UC4-X were reinforced with conventional reinforcing bars (ASTM A706 Grade 60) and high strength reinforcing bars (Grade 97 met the requirements of (ICC-ES 2009)) respectively. UC4-X had reduced amounts of longitudinal bars compared with CC4-X. The two beams specimens completed the testing protocol successfully and showed a stable hysteric behavior as in Figure 2.4. During the monotonic push, both beams reached more than 10% drift ratios. From the measured shear and drift ratios curves, a stable and similar hysteric response was observed for both specimens (Tavallali et al. 2014).

The measured strains at longitudinal steel bars for both specimens during the test showed that the length of the plastic hinge zone developed over a distance equal to d (the effective depth of a beam) from the face of the joint (critical section). From the measured shear-drift ratio relationship of the two specimens, the authors investigated the possible differences in the initial stiffness and unloading stiffness which they play important role in the nonlinear response of reinforced concrete members during seismic events. Due to the reduced amounts of steel bars in UC4-X specimen, the initial stiffness of high strength reinforcing steel specimen was

approximately (3/4) of the initial stiffness of conventional steel specimen. The effective stiffness of a reinforced concrete member after experiences large cycles of loadings and plastic deformation is referred to as the unloading stiffness. The specimen with high strength steel bars showed lower unloading stiffness (approximately 4/5 of conventional one) as compared to the conventional steel bars specimen. Using a reduced area of high strength reinforcing bars in concrete produces higher tensile stresses in steel reinforcing bars leading to wider cracks in concrete under service loading conditions.

Finally, the authors concluded that high strength reinforcement could be considered as a viable choice for reinforcing concrete members that would be a part of SFRS. In the Figure 2.4 below, the beam CC4-X is reinforced with conventional steel bars, while UC4-X is reinforced with Grade 97.

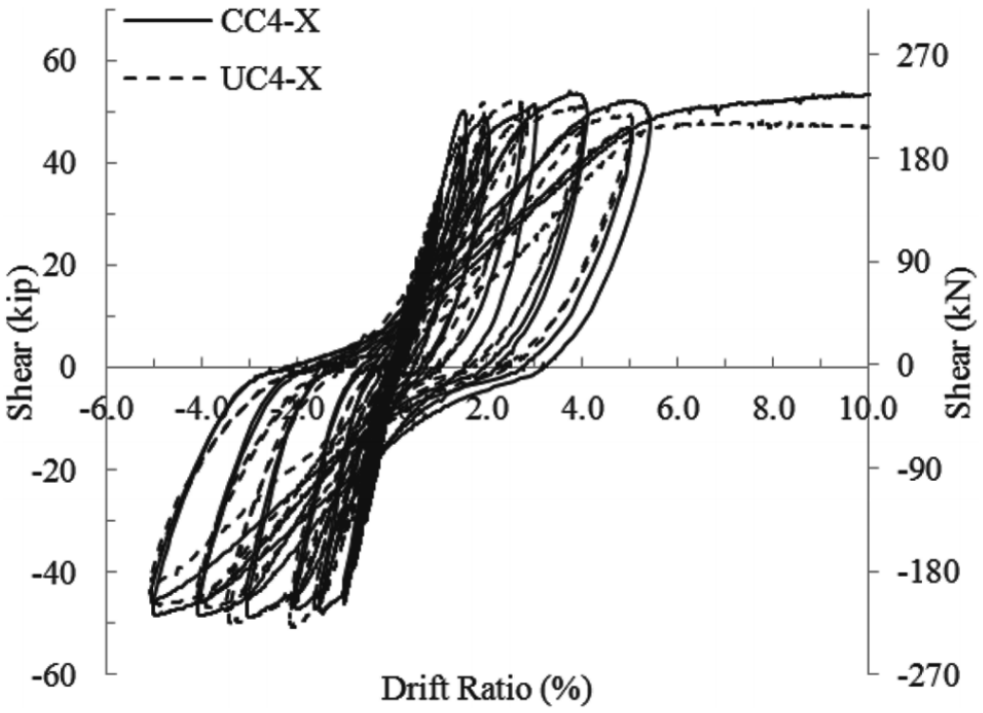

Figure 2.4 Comparison of Measured Cyclic Response for Grade 60 and Grade 97 Reinforced Beams (Tavallali et al. 2014).

2.2.5.2 Columns Reinforced with High Strength Reinforcement

In order to study the effect of using high strength steel bars in columns under cyclic loading conditions, the study (Rautenberg 2011) included two parts. In the first part, an experimental work was performed to investigate the response of columns reinforced with high strength steel bars under cyclic loads. Experimental data about the response of rectangular columns reinforced with high strength steel bars are not available. Eight columns were tested cyclically. The yield strength of longitudinal reinforcement were conventional bars with 60 ksi, 80 ksi ASTM A706, 120 ksi ASTM A1035. In the second part, the results of the eight columns was used to validate the numerical models which would be used to investigate the effect of using high strength steel bars in columns of multi-story buildings in their SFRS.

From the results of the experimental part, one can conclude that the axial loads capacities of all specimens were persevered as well as a valuable fraction of lateral loads capacities after applying drift ratios of at least 4%, as shown in Figure 2.5. The test results showed two types of failure mechanisms: fracture of longitudinal bars in a tension zone, and longitudinal bars buckling at a compression zone. In addition, using reduced amounts of high strength steel bars would increase the risk of bars buckling without decreasing the transverse reinforcement spacing. The drift capacities of high strength steel reinforced columns were 80% of conventional steel reinforced columns. The question is what are the effect of reduced stiffness of the high strength steel reinforced columns on the behavior of multi-stories frames using the same columns?

The second part of the study (Rautenberg 2011) tried to answer the previous question analytically by studying the response of four hypothetical buildings with different stories 3, 6, 12, and 20 stories. Each building had the same plan with only different stories. Two types of models for each building were made one reinforced with conventional steel bars in all its columns and the second was with high strength steel bars (Grade 120) in all its columns. All beams reinforcement was conventional steel bars (Grade 60). From the base shear-roof drift curves, one could conclude that the effect of high strength reinforcement decreased while the number of stories increased because taller buildings would experience more plastic hinges in its beams than low rise buildings. The results of nonlinear dynamics analysis for each building for 24 strong unscaled earthquakes showed that frames with columns reinforced with high strength steel bars experienced approximately same drift ratios as frames with conventional steel bars in their columns. In other words, the reduced stiffness that observed from experimental tests for individual columns reinforced with high strength steel bars would have negligible effects on the global response of whole frames.

In the study by (Sokoli and Ghannoum 2016), three full-scale columns reinforced with Grades 60, 80, 100 were tested cyclically under relatively high axial loads. High strength reinforcing bars (Grades 80 and 100) had a uniform elongation 20% less compared with Grade 60 reinforcement. The results showed that both Grades 60 and 80 reinforced columns showed comparable lateral response and exhibited similar and stable hysteric loops up to 5.5% drift ratio. In general, for all three columns, no bar buckling, or bar fracture was observed. The measured strain in the Grade 80 bars was 56% higher compared with Grade 60 bars for the same drift ratio, while Grade 100 bars showed 200% strain compared with Grade 60 for a 1.5% drift ratio. Bond degradation began in The Grade 100 reinforced column at a 1.5% drift ratio and continued to propagate along the column length. At a 3% drift ratio, bond splitting cracks extended along the column length and a significant drop of the lateral load strength and stiffness was taken place. The reduced area of steel bars by utilizing high strength steel increases the bond demand and makes the bar development length a major concern. According to the author more studies are needed to investigate the increased bond demand and the appropriate strategies to mitigate the bond failure while utilizing high strength reinforcement with a yield strength more than 80 ksi (Sokoli and Ghannoum 2016).

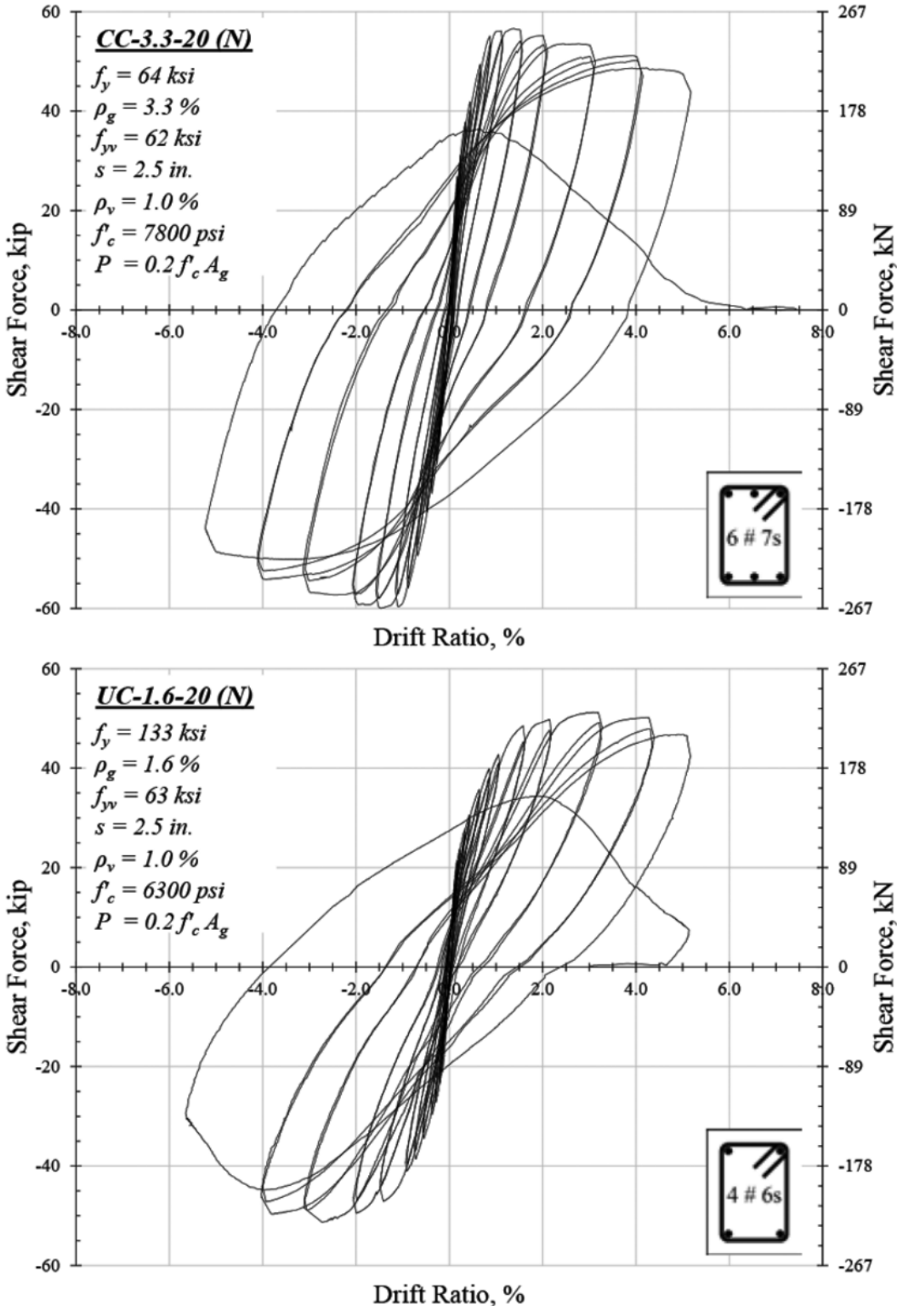

Figure 2.5 . Measured Shear Drift Curves for Columns (Rautenberg 2011).

2.2.5.3 Beam-Column Joint with High Strength Reinforcement

Using of high strength reinforcement arises a challenge about the bond demand and the bar development length especially where the available length is limited as in exterior beam-column joints. One of the valuable solutions is the use of headed reinforcing bars. However, ACI 318-14 code has limits on using the headed bars such as the yield strength of steel bars 60 ksi, maximum compressive strength of concrete 6 ksi, and the minimum space between bars not less than 3 times the bar diameter. These limitations reduce the use of the option of headed bars. A study by (Lee and Chang 2017) tried to investigate the use of high strength headed bars in beam column joints with a relaxation of the above ACI 318 limitations. Five beam column joints were reinforced with grade 100 and tested cyclically. The results showed the use of high strength concrete more than 6 ksi associated with using high strength reinforcement improve the compatibility in the structural response. The authors recommended increasing the maximum value of concrete strength from 6 ksi to 15 ksi in the future edition of ACI 318. In addition, the results showed that Grade 100 steel bars with a space of two times the bar diameter make the required development length by ACI 318-14 provides the intended yielding mechanism without bond failure (Lee and Chang 2017).

2.2.6 Knowledge Gaps with High Strength Reinforcement

Reinforced concrete tall buildings are widely spread around the world. Tall buildings in high seismic regions have substantial capacity requirements due to both gravity loads and seismic demands that often lead to very heavily congested sections. Therefore, using high strength reinforcement with a reduced area of steel bars introduces a valuable solution. However, the provisions of ACI 318-14 limit the yield strength of reinforcement to 60 ksi in SFRS in high seismic regions. In addition, the tensile characteristics of high strength reinforcement differ from conventional reinforcement leading to a different structural response behavior of structural

members. Consequently, the global response of building SFRS could be expected to vary from the response of conventional steel reinforced SFRS. This study aims to investigate the global and local response of tall concrete buildings reinforced with high strength reinforcement in their structural members when subject to earthquake shaking effects. To accomplish the goal of this study, a three-dimensional model for a case building, which is a tall building with 46 stories, will be prepared. By using the capabilities of nonlinear analyses in OpenSees (Mazzoni et al. 2006), the building model will be analyzed. The results of the analysis could help increase the acceptance of the use of high strength reinforcement and make it a more reliable choice by improving the understanding of its impact on the structural response. The performance of the tall building reinforced with high strength reinforcement will be investigated to check whether the tall building performs equivalently to the same building reinforced with conventional reinforcement according to the TBI guidelines.

2.3 SHAPE MEMORY ALLOYS

2.3.1 General

Shape memory alloys (SMAs) are a type of new smart materials that show unique engineering properties. The two main phases of SMAs are martensite and austenite. Martensite shows a stable state under low temperatures and high stress levels while austenite is stable under low stress levels and high temperatures. Figure 2.6 shows the phases of SMA and their crystal forms. From Figure 2.6, martensite also has two forms that are different in the orientation of the crystal direction. They are twinned martensite and detwinned martensite. It is worth to mention that the unique key property of SMAs or their ability to recover the strain, is a result of phase transformation between martensite and austenite. The phase transformation is induced by changing temperature (shape memory effect) or changing stresses (superelastic effect) (Saiidi and Wang

2006).

SMAs have four important temperatures that control the phase transformation in the case where no applied stresses exist, as explained in Figure 2.7:

1. A_s: Phase transformation begins from twinned martensite to austensite.
2. A_f: SMA finishes its transformation process from martensite to austensite. SMA is a pure austensite.
3. M_s: Phase transformation begins from austenite to twinned martensite.
4. M_f: Phase transformation to martensite has finished. SMA is a pure martensite.

It is worth noting that the effect of applied stresses on SMA will increase all of the above temperatures' values.

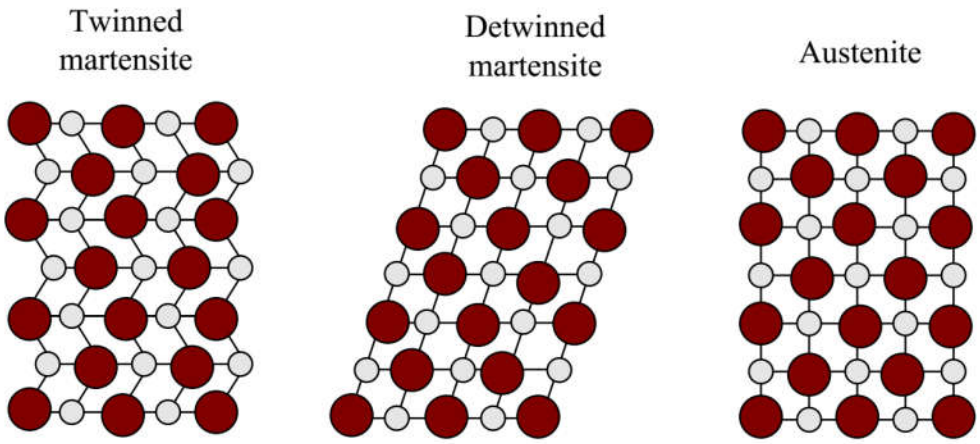

Figure 2.6 Different Phases of Shape Memory Alloy (Ozbulut et al. 2011).

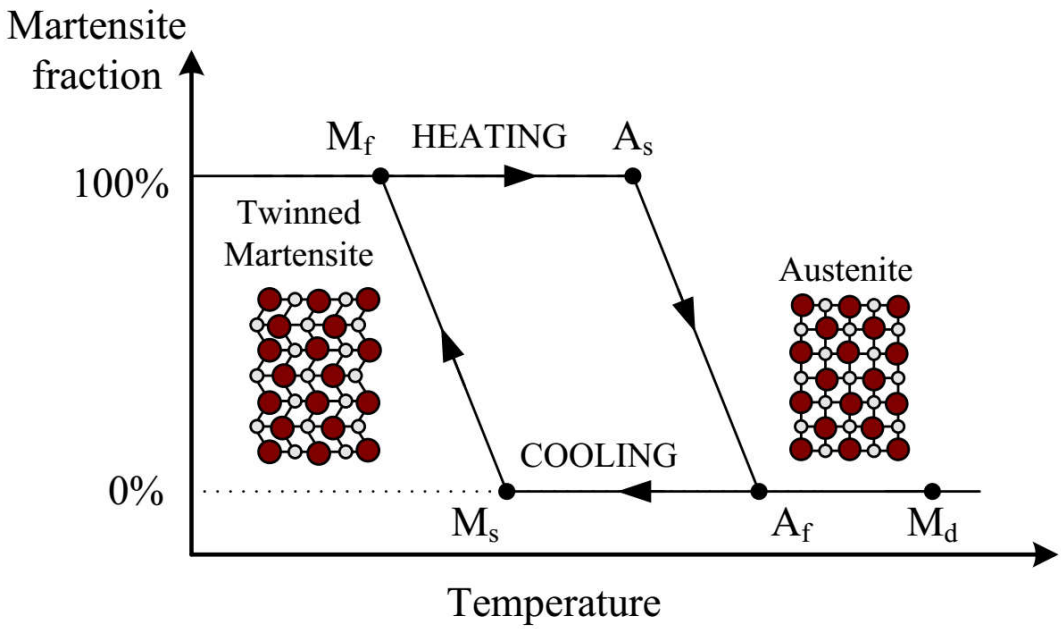

Figure 2.7 Martensite Fraction-Temperature of SMA (Ozbulut et al. 2011).

2.3.2 Shape Memory Effect

The shape memory effect is a thermal stress-induced transformation. This effect reflects the ability of SMAs to regain their original shape upon experiencing some deformation by a cycle of heating and cooling. For a temperature below M_s, the phase of SMA is the twinned martensite which in case of subjecting to a stress higher than critical levels will deform and transform to detwinned martensite. After loads removal, SMA will keep the detwinned martensite phase. SMA could return to their original shape (twinned martensite) by a cycle of heating and cooling. Heating the SMA to a temperature higher than A_f, austenite phase will be formed. After cooling below M_s, SMA will transform from austenite to twinned martensite with no residual deformation. One could easily see that the shape memory effect is a function of how the temperature plays a central role in phase transformation of SMA and eventually the original shape will be recovered (Lagoudas

2008). Figure 2.8 explains the phenomenon of shape memory effect and the temperature role and displays the qualitative stress-strain curve for SMA, while experiencing the shape memory effect.

2.3.3 Superelastic Effect

The superelastic effect exhibited by SMAs is the one that is very appealing and interesting in civil engineering applications. Superelastic SMAs can return to their original shape after undergoing large deformation upon stress removal. Recovery of the original shape will take place immediately upon removal of loading with no residual strain. To explain this phenomenon, at a temperature higher than A_f, SMA is in its austenite phase. This phase upon subjecting to loading will deform and with increasing stress level, a high level of strain will be gained. After a critical level of stress, SMA will transform to detwinned martensite. After removal of loads, SMA will experience a phase transformation to its original austenite and regain its original shape with no residual deformation. It is worth to mention that the superelastic effect of SMA can occur only if the temperature is above A_f to obtain the full recovery of the original shape. However, if the temperature is between A_f and A_s, partial recovery will occur with some residual strains. It is also important to note that the temperature value of A_f is approximately (-15,-10 C) degree. It is clear that A_f value is a very low temperature leading to increasing and broadening the applications of SMAs in civil engineering applications (Gaudenzi 2009). Figure 2.9 explains the phenomenon of superelastic effect (Ozbulut et al. 2011).

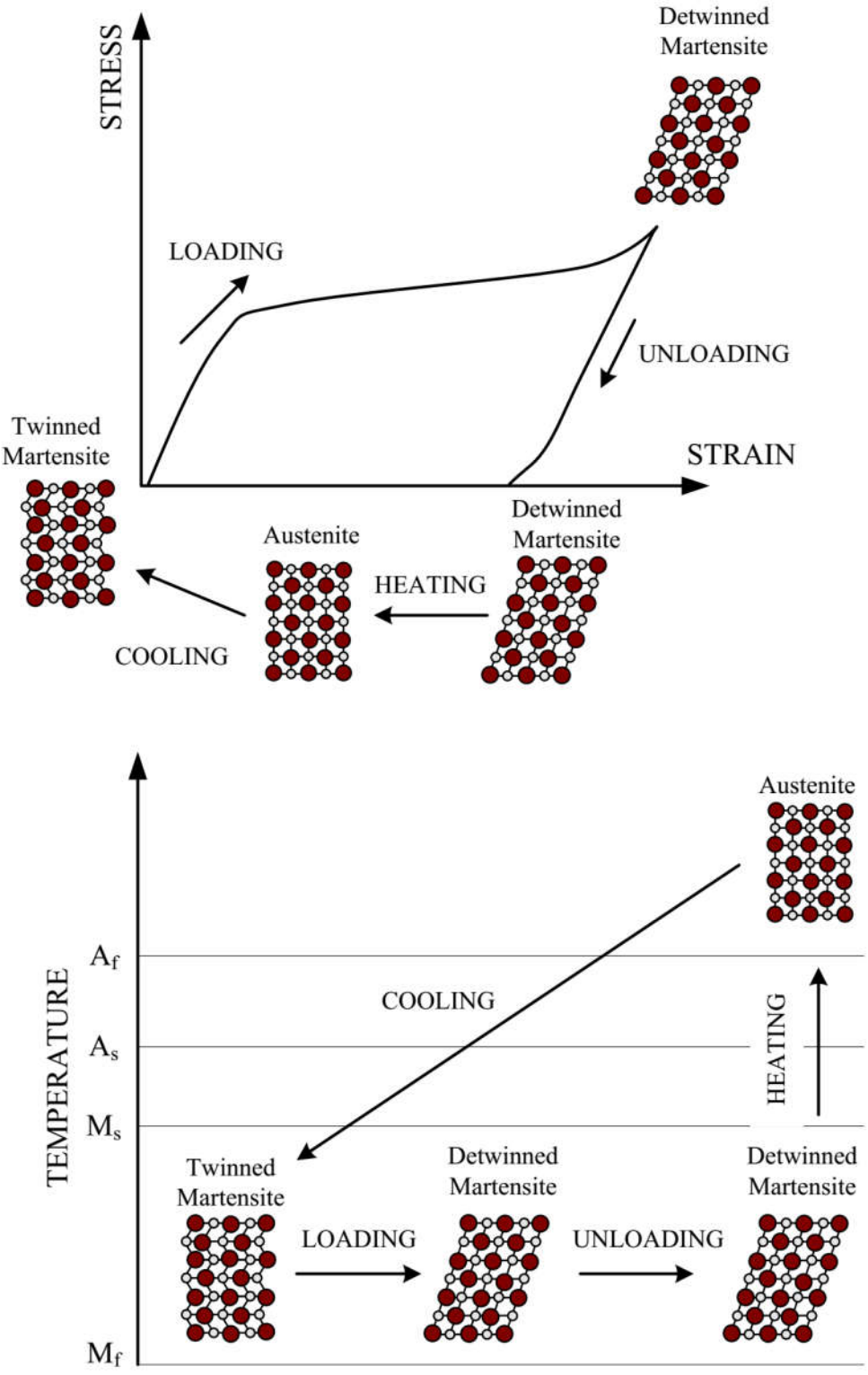

Figure 2.8 Shape Memory Effect (Ozbulut et al. 2011).

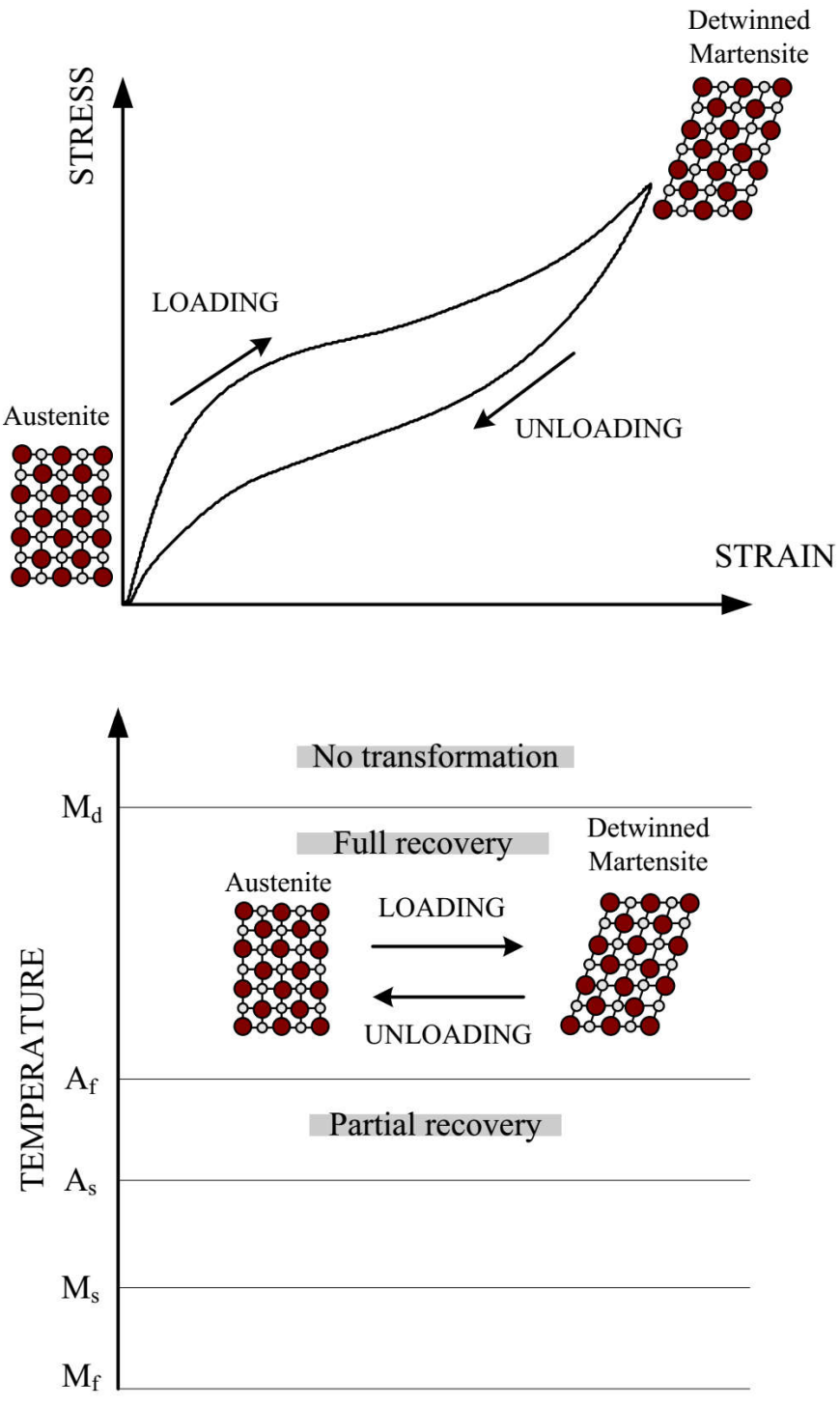

Figure 2.9 Superelastic Effect (Ozbulut et al. 2011).

2.3.4 Types of SMAs

In 1963, SMAs were discovered, and since that time, they had been investigated by many researchers (Gaudenzi 2009). However, two types of these alloys were the most common types that have been utilized in many applications. Ni-Ti based alloys and Cu-based alloys. A brief description of each type will be introduced, and then, this discussion will focus on Ni-Ti alloys due to their more appropriate characteristics for civil engineering applications.

2.3.4.1 Ni-Ti Based Alloys

The focus of studies on Ni-Ti based alloys led to increasing its importance for commercial usage. The most common alloy of this type is the one in which the participation percentage of the two elements is equal. In addition, the composition of these alloys has a direct effect on the temperature of the phase transformation. For example, a composition with Ni percentage above 50% will show a decrease in the required temperature for phase transformation.

One of the important properties of Ni-Ti alloys beside their superplastic behavior is their high resistance to corrosion. Without a doubt, this feature certainly has a great impact on increasing Ni-Ti alloys applications in civil engineering fields. Ni-Ti forms are wires, bars, tubes, and plates; however, the most appropriate forms for civil application are the wires and bars. In general, the limit of full strain recovery of Ni-Ti alloys is approximately 8% (Abdulridha et al. 2013).

2.3.4.2 Copper-Based SMA

The main advantage of Copper-based alloys over Ni-Ti alloys is their relatively low cost. However, the Cu-based alloy has low corrosion resistance and its recovery ability limit is about 2-4% (Lagoudas 2008). In this study, the focus is on using SMA as an alternative reinforcing bars to conventional steel bars. Therefore, this type of SMA will not be considered.

Depending on the properties of the two types of SMAs, one could conclude that Ni-Ti

alloys have more appropriate properties than Cu-based alloys when considering the required properties for a material to serve as reinforcing bars embedded in concrete structural members. In this study, the term shape memory alloys, SMAs, refers to superelastic Ni-Ti based shape memory alloys unless mentioning explicitly another type of SMAs.

2.3.5 Cyclic Response of SMAs

Cyclic loading is a simulation of the lateral demand under seismic loadings, and the behavior of a material subjected to cyclic loading could simulate the behavior of that material during an actual earthquake event. For superelastic SMAs, two distinct types of behavior in their cyclic response are observed as in Figure 2.10. SMAs experience a noticeable reduction in the stress of phase transformation associated with increasing numbers of loading cycles. As a consequence, the area under the stress-strain curve that represents the amount of dissipated energy will be reduced significantly. This reduction in stress of transformation is due to local slip which helps in the transformation process and occurs with small levels of stresses.

The second behavior that observed is that the ability of SMAs to fully recover will be decreased when subject to an increased number of loading cycles. In other words, some residual strain will occur upon loading removal (Alam et al. 2012).

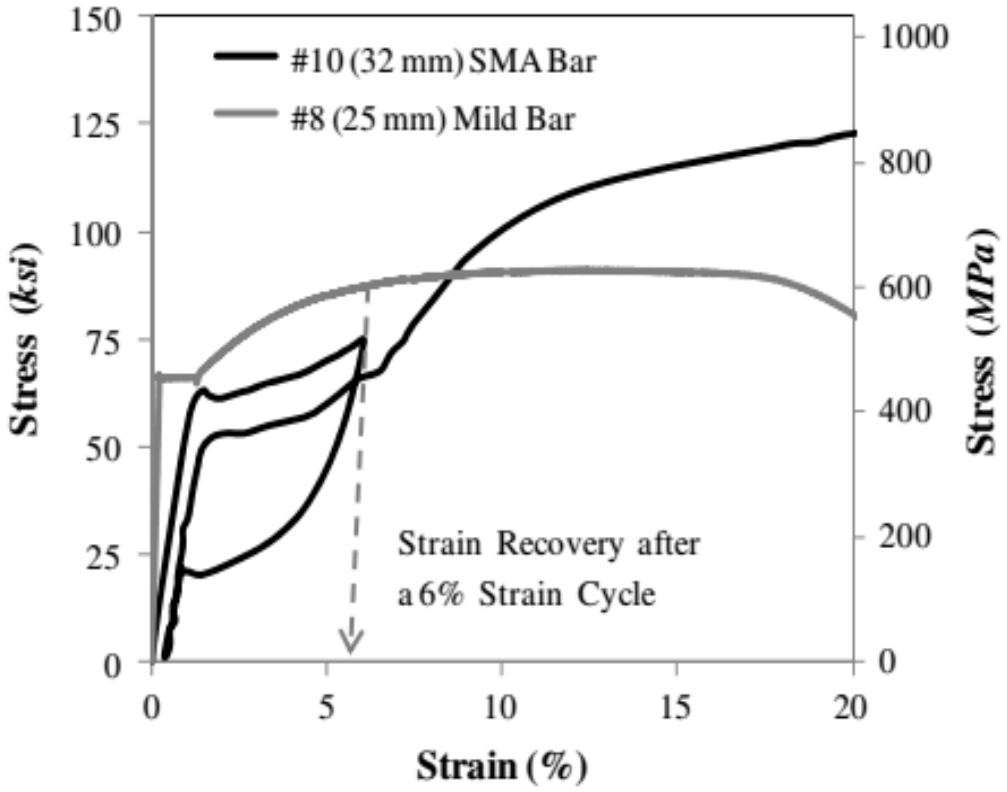

Figure 2.10 Stress-Strain Relationship for Conventional Steel and SMA (Tazarv and Saiidi 2014).

2.3.6 Problem Description for Shape Memory Alloys

The main function of civil Engineering structures is to carry the gravity loads and withstand environmental loads during its intended design life. Concrete structures are vulnerable to large demand forces and deformation while experiencing earthquake shaking. A massive structural frame would be needed to maintain a linear response of the structure leading to uneconomic designs. In addition, the current design procedure depends on design earthquake spectral values that represent a 2/3 of the MCER values. This means that inelastic response should be expected especially during strong earthquakes events. Therefore, the philosophy of the design code depends on the idea that dissipation of the input energy of the earthquake would be through allowing special

detailed regions in the structure to yield and undergo inelastic deformation without critical strength degradation (FEMA 2009a; Moehle 2014; FEMA 2105). The preceding design procedure aims to provide life safety and prevent structural collapse. However, structures could sustain permanent damage, which can have crucial impacts. The impacts could be on the cost of repair, the time required to close the buildings for retrofit purposes, the reduction of rescue operations following an earthquake by closing some important infrastructures.

In general, according to the current design codes and the observation of many structures responses upon an earthquake around the world, one could conclude that there are two main problems with the seismic response of concrete structures that are designed according to current codes: the problem of permanent deformation and the spalling of concrete cover (Saiidi and Wang 2006)). A lot of research has been conducted to find a solution to these problems in order to improve the response of structures, especially to severe earthquakes. Some research utilized smart structures techniques. One of the smart structures solutions is the using of smart materials that have certain and unique characteristics making it an excellent material for some specific applications. These unique characteristics would promote the performance of the structures and eliminate undesirable outputs.

Ni-Ti based SMAs are attractive and interesting smart materials with powerful features. Their unique characteristics have increased substantially the interest of researchers in using them in civil engineering applications. The most appealing feature of SMA is its ability to return to its original shape after undergoing a large deformation or strain (6-8%) upon the stress removal. In addition, it has a high strength, good corrosion and fatigue resistance, good energy dissipation (Ozbulut et al. 2011). Due to its unique mechanical properties and damping ability, a wide range of civil engineering applications in which SMA could be employed is growing increasingly. One

of the appealing applications that takes increasing interest by researchers is the using of SMA as alternative reinforcing bars in concrete structures. According to the preceding discussion about the way that concrete structures respond to an earthquake shaking, it is obvious that some regions in concrete frames will yield to dissipate the input energy of earthquakes. These regions are the plastic hinges zones usually they occur at the end of the beams. Yielding of reinforcing steel bars will cause the permanent deformations. Conventional steel bars are not able to recover the inelastic strains like the SMA. Some studies confirmed that utilizing SMA as an alternative for conventional steel bars in concrete structures could lead to better performance for concrete structures subjecting to cyclic loading with negligible residual strains (Abdulridha et al. 2013; Alam et al. 2012; Ghassemieh et al. 2016; Saiidi and Wang 2006).

SMA has different mechanical properties comparing to the conventional steel reinforcement. Depending on this fact, the response and behavior of SMA reinforced structural members should be expected to be also different than the behavior of steel reinforced structural members (Abdulridha et al. 2013). As consequence, frames with members reinforced with SMA should be expected to respond in a different manner compared with frames with conventional steel bars. More studies would be needed to investigate the response of SMA reinforced structural members and all related issues in order to increase the application of SMA bars in concrete structures. Some of these issues are bond strength between SMA bars and concrete, crack pattern (width and spacing), moment capacity, serviceability limitations for deformation under services loads, replacement scenarios between SMA bars and steel, the amount of the residual strains, etc. In addition, the tall building is one of the widely spread structural types around the world. Tall buildings are constructed in low and high seismicity regions. The seismic loads resisting systems in concrete tall buildings are usually the special moment frames and special walls. Therefore, it is

important to study the effect of using SMA as an alternative to conventional steel on the seismic behavior of tall buildings.

2.3.7 Previous Research on Shape Memory Alloys

2.3.7.1 Design Objective

The main concern of the provisions of the current code is life safety and prevention of structural collapse by allowing the inelastic deformation in some specific regions of the frame of the structure. There are four important principles through which one could ensure that the structure will respond safely to an earthquake while undergoing inelastic deformation. The four principles are (Blume et al. 1961; Mo 2013; Moehle 2014):

- "Strong column / weak beam" frames.
- Special reinforcement details for both columns and beams for ductile behavior in flexure mode.
- Design should avoid failure modes with more brittle responses such as shear and axial modes.
- Design should avoid interaction of nonstructural elements with structural elements.
  A brief discussion of each principle will be introduced.

- *"Strong column / weak beam" frame*

It is clear that the consequences of beams failure are less dangerous than failure in columns. Columns carry the loads that come from all stories above them while beams role is to support the floor slab only. According to the columns and beams strength, there are three scenarios that could occur for building subjected to an earthquake. A story mechanism occurs if the frame has weak columns. In this case, the lateral deformation tries to concentrate in one story or in few stories. In addition, the concentrated lateral drift demand may exceed the columns deformation capacity. For a frame with strong columns, the mode of deformation will be totally different from the case of weak columns. For the strong columns case (beam mechanism), the

deformation has a uniform distribution through the height of the frame with reduced of the local deformation. The intermediate mechanism occurs for frames which its columns strength exceeds beams strength by small differences. In this case, the deformation may be distributed through few stories, not just one story. It is important to mention that for beam mechanism, a frame needs its columns strength to be large by several times than its beams strength. This may appear uneconomic solution, therefore columns yielding could be expected. The "strong columns/weak beams" phenomenon is a fundamental property for frames that withstand safely against strong shaking.

- *Special reinforcement details for both columns and beams for ductile behavior in flexure mode.*

The design philosophy allows the inelastic deformation but there is a restriction on the location of this deformation. The ideal location of yield is the beams end through the overall structures and base of columns in the ground story. Practically, some other columns may undergo inelastic deformation also along the frame height. Therefore special reinforcement details for the regions of beams and columns ends ((regions at the face of beam-column joints)), are required in order for these regions to respond and experience the inelastic deformation without undergoing a critical strength degradation. Small spaced ties should be used in the plastic hinge zones (end of columns and beams members) in order to provide a confinement action for concrete core and prevent buckling of longitudinal bars. Confinement of concrete core is one of the fundamental reinforcing details for earthquakes design. Confined concrete will exhibit more ductile properties than unconfined concrete. Using continues longitudinal reinforcing bars through the plastic hinge zones is an important detail for earthquakes design.

- *Design should avoid failure modes with more brittle responses such as shear and axial modes.*

All design requirements such as material properties and member sizes should be characterized to develop the flexure yielding at the intended locations and prevent others types of failures which are commonly more brittle modes. One of the most serious brittle failure modes is the shear failure of columns. Shear failure mode in columns is recorded as the most common cause of severe damage and collapse during earthquakes. One of the code provisions is to neglect the concrete contribution to shear resistance equations of columns for seismic design.

The components that is most vulnerable to failure in the special moment frame is the beam-column joint, which is responsible for transfer of forces between beams and columns and anchoring the longitudinal steel bars of beams and columns. Beam-column joints can experience a high level of stress during earthquake events. Failure is more common in the exterior beam-column joints that located at the perimeter of the frame. This is due to that exterior joints have an exterior face that is not confined by any frame members. The code provision requires confining the concrete core of the joint with transverse reinforcement which similar to the same confinement requirement of plastic hinge zones of beams and columns.

- *Design should avoid interaction of nonstructural elements with structural elements*.

Examples of nonstructural components are stairways, masonry infills etc. Frames in seismic areas have to be free to vibrate, so any interaction from nonstructural elements will restrain the motion of some structural members and then steering to serious damages or collapse.

It is clear from the preceding discussion that the current design approach aims to save lives and prevent overall structural collapse through allowing the steel bars to yield and dissipate energy and form plastic hinges. In addition, damaging of unconfined concrete, concrete cover, occurs due to its low tensile strain capacity. These two reasons are behind the two consequences of earthquakes which are the permanent deformation or strain even upon loading removal and the spalling of the concrete cover (Saiidi and Wang 2006).

2.3.7.2 Study about modeling SMAs material

Studies have investigated the ways through which a promotion to the seismic responses of concrete structures could be obtained through utilizing SMA bars as an alternative reinforcement to conventional steel bars (Abdulridha et al. 2013; Alam et al. 2008; Alam et al. 2012; Billah and Alam 2016; Ghassemieh et al. 2016; Saiidi and Wang 2006). For the analytical investigation, an important factor is the accuracy of the models that used in the analysis. Therefore, some studies have offered different models for SMA.

A study by (Tazarv and Saiidi 2014) investigated the most important factors that affect the model of SMA. Although the stress-strain relationship of SMA is affected by several factors such as temperatures, and a large number of loading cycles, the authors selected a simple constitutive model of SMA to represent the actual response with sufficient accuracy for civil engineering applications. The authors mentioned some important considerations that support the idea of that taking the simple model of SMA would estimate the actual behavior of SMA reinforced structural components with a sufficient accuracy. First, SMA reinforcement bars embedded in concrete would not undergo detrimental temperature variation due to the insulating effect of concrete cover. Second, materials in structures may undergo degradation in its strength and stiffness during numerous cycles of loading. However, in reality, structures may only experience few cycles with large amplitudes. Therefore, one could neglect the stiffness and strength degradation that occurs upon large numbers of deformation cycles. All the above considerations support the adoption of the simple model for the stress-strain relationship of SMA. It is good to mention that in most civil engineering applications, SMA configurations are the wire or the bar, therefore, a one-dimensional stress-strain relationship is appropriate.

The authors (Tazarv and Saiidi 2014) provided a definition of the key mechanical

properties of SMA model and a method for extracting them from a standard tensile test in ASTM F2516-07 (ASTM 2007). The author proposed the model that takes into account the phase transformation and asymmetric response of SMA. This model has been used with finite element analysis. The model consists of three stages according to the level of strain in the SMA. Depending on the results from the literature review, tests by the authors, and tests by the SMA manufactures, the author could establish a range of values for each parameter of the model (k_1, k_2, f_y, ε_u, β, α), as in Figure 2.11. In order to study the effect of each of the model parameters on the structural response, an analytical column model was analyzed through moment-curvature relationship and the pushover analysis. For moment-curvature analysis, the results showed that the moment capacity of the column reinforced with SMA bars is the same as the one with conventional steel bars. In addition, the individual change of one of the model parameters had a minor effect on the moment-curvature curve. For pushover analysis, a drift ratio-force curves were utilized to show the effect of changing parameters values. From the curves, one could show that the stiffness of SMA-column was less than conventional steel columns. The SMA reinforced columns could exceed the displacement capacity of the conventional bars' columns.

The authors (Tazarv and Saiidi 2014) adopted the average values of the model parameters to be utilized in structural analysis and design for using SMA as a reinforcement in concrete structures. In addition, the authors proposed minimum values of the parameters in order to use it as a reference for SMA production. For the proposed (average values of the model parameters of SMA), an analytical procedure was made to validate the proposed values. Comparing the actual response of a SMA reinforced column (made by other researchers) with the calculated response using the proposed SMA model showed that the response was very close.

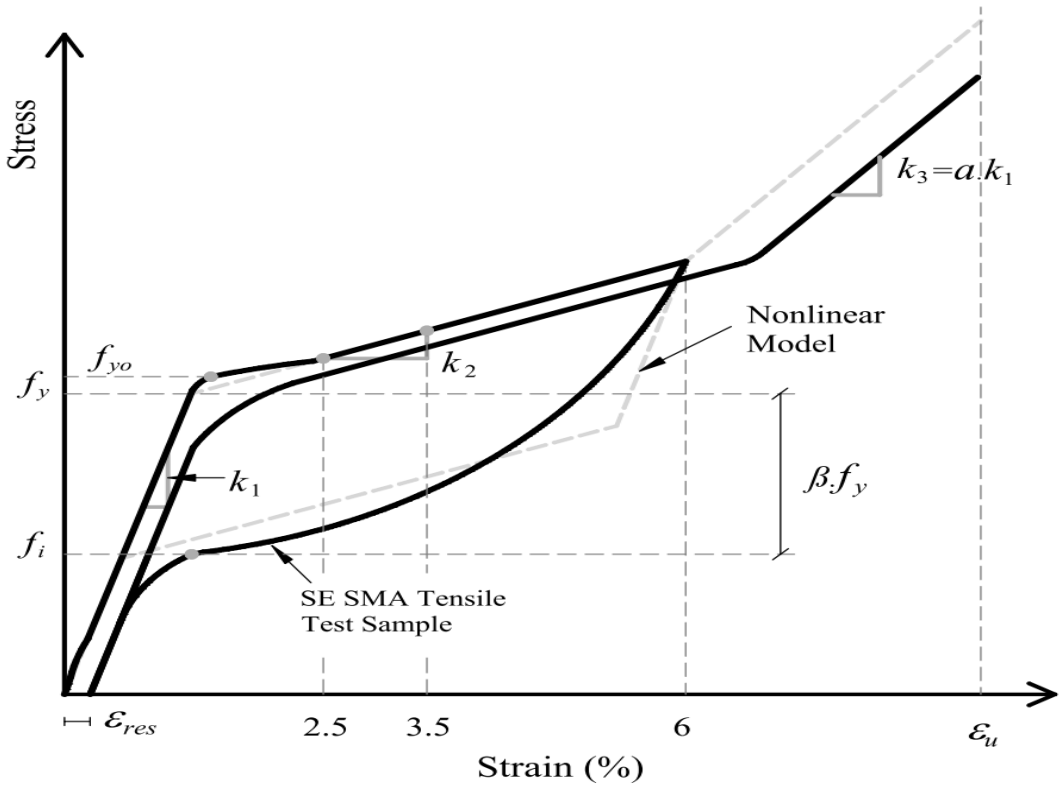

Figure 2.11 ASTM F2516-07 Ni-Ti SMA Tensile Test Sample and Nonlinear Model (Tazarv and Saiidi 2014).

2.3.7.3 Experimental study on large scale SMA reinforced beams

According to the authors (Abdulridha et al. 2013), limited experimental studies had made for small-scale concrete members reinforced with SMA to study the member's response and behavior under different types of loadings. In the paper of (Abdulridha et al. 2013), an experimental study was made to investigate the behavior of large-scale concrete beams reinforced with SMA bars as an alternative to conventional steel bars. In this study, three types of loadings (monotonic, cyclic, reverse cyclic) were conducted. In addition, examination of energy dissipation, deformation recovery, and cracks width was discussed. All specimens were tested to failure. The experimental program contained casting of seven simply supported concrete beams. The beams

long were 2.8 meter, as in Figure 2.12. Two types of reinforcement were utilized in this study, first the conventional steel bars, second SMA bars embedded only in the midspan section of the beam (critical section). The midspan section or the critical section refers to as the maximum moment section and could represent any maximum moment section in other structural members. For all beams, the reinforcing details were designed to make the flexure failure and response dominates. Three beams reinforced with steel bars were tested by three different types of loadings (one monotonic, one cyclic, one reverse cyclic). Other three beams reinforced with SMA bars in a critical section (midspan) were also tested by the same three loadings patterns.

The cracks width and residual crack width were observed for all beams during the test. For SMA reinforced beams, the crack width was higher than steel reinforced beams due to the smooth surface of the SMA. At a level of displacement at midspan of seven times the displacement at yielding, the crack width was 11 mm and 52 mm for steel reinforced beams and SMA reinforced beams respectively. However, the recoverability of displacement was more obvious in SMA reinforced beams than others. After reversing cyclic loadings, a SMA beam was able to recover approximately 89% while steel beam was able to recover 21% only, as in Figure 2.13. For both cyclic and reverse cyclic loadings, the energy dissipation of SMA beams was less than that for steel beams since SMA has flag-shaped hysterics loops. Depending on the experimental data, the authors proposed SMA model that could be implemented with finite element analysis. The model depended on a trilinear envelop response. The authors enhanced the model by including some important features such as consideration of permanent displacement and modeling the unloading stage by the trilinear response.

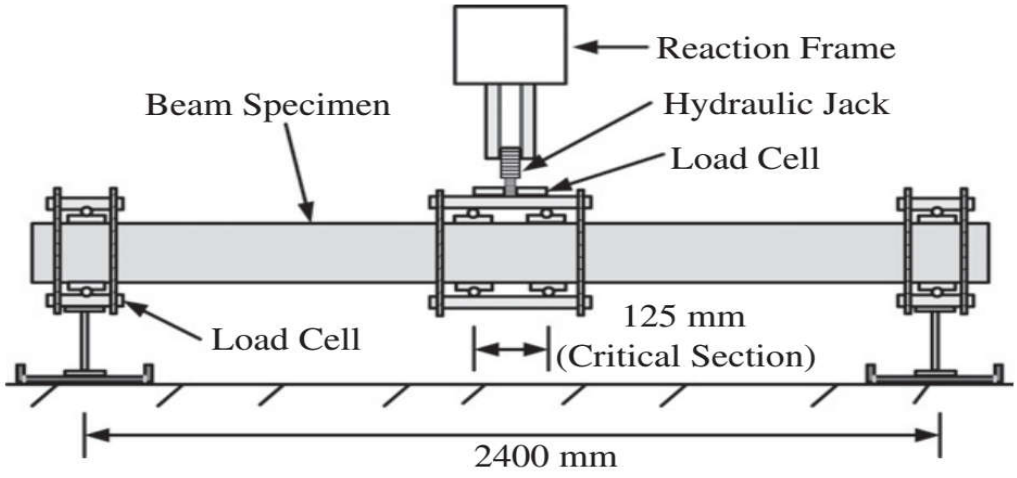

Figure 2.12 Test Setup (Abdulridha et al. 2013).

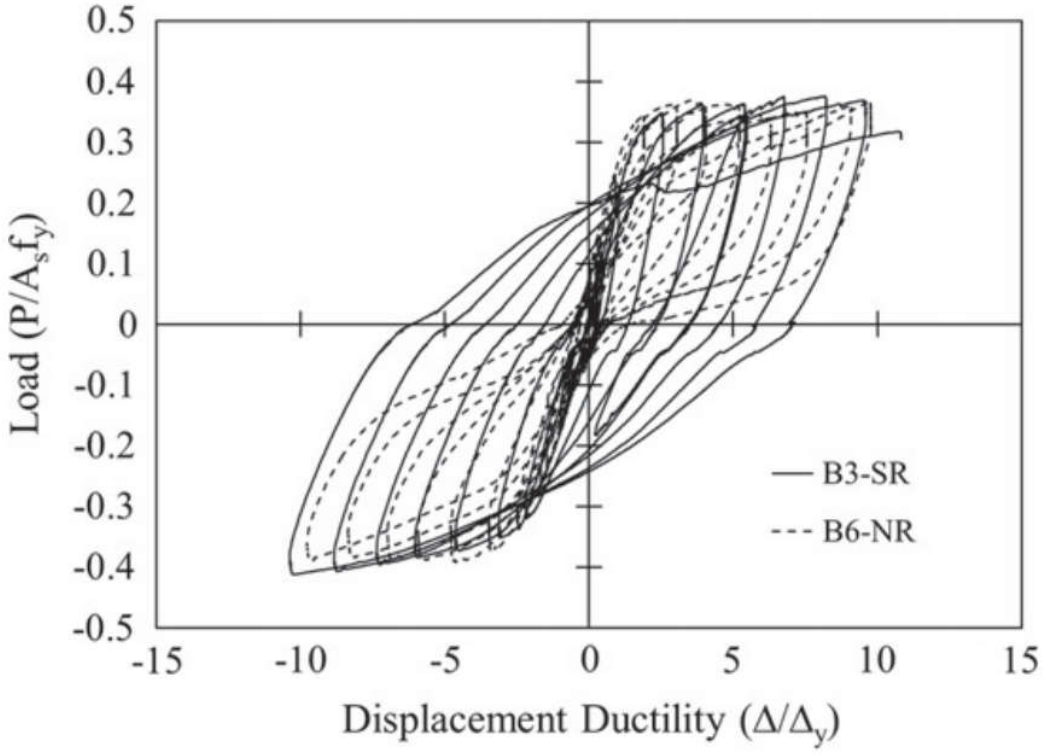

Figure 2.13 Test Results for Beams (Abdulridha et al. 2013).

2.3.7.4 Study about Bond Strength between SMAs and Concrete

Reinforced concrete is a composite material and its behavior is affected significantly by the bond between concrete and reinforcement bars. The bond strength is a crucial factor in controlling the deformation of reinforced concrete and the phenomenon of cracking. However, according to the authors of (Billah and Alam 2016), no study had been conducted to investigate the bond between concrete and SMA bars. The importance of the study of (Billah and Alam 2016) is obvious from the fact that most of SMA types ((especially Ni-Ti)) have a smooth surface without any lugs. For most commercial SMA, the machine process for making lugs with conventional devices is extremely difficult due to the hardness of the alloy. In addition, threading process on SMA bars will decrease its strength substantially. SMA smooth bars reinforced concrete members experience large cracks width in the critical sections. These wide cracks due to bond weakness will lead to shear failure in the critical sections of members due to losing the aggregate interlock that helps promote the shear strength of concrete. In the study of (Billah and Alam 2016), the authors conducted experimental tests to investigate the bond behavior between SMA bars and the concrete. For the surface condition, the authors performed a sand coating to increase the interlocking between SMA bars and concrete.

The experimental program includes 56 specimens test. The specimen was a concrete compressive test cylinder and the SMA bar embedded in its center. The test was a pushout due to its simplicity and no associated drawbacks such as the pullout test. The study parameters were the compressive strength of concrete, concrete cover, SMA bar diameter, the embedded length of the bar, and the surface condition of the SMA bars (smooth, sand coated). The approach for sand coating was using a layer of epoxy on the surface of the SMA bar and then rolling the bar on the sand. When a slippage of 30 mm occurs, the test would be terminated. From the experimental

results, many results and conclusions could be drawn. For failure mode, all smooth SMA bars specimens failed at the interface zone between bars and concrete without splitting cracks occur. Due to the smooth failure surface of concrete, one could conclude that no significant development of the bond between smooth SMA and concrete. For cases of sand-coated SAM bars, development of splitting cracks on the concrete surface was obvious. From the curve of load-slip, the maximum bond strength was defined as the peak load divided by the surface area of the embedded length of the bar. However, the residual bond strength was defined as the residual load on the load-slip curve divided by the surface area of embedded bar length. The results of the paper showed that concrete strength, bar diameter, and bars embedded length, have a significant effect on the bond between SMA bars and concrete. On the other hand, bond strength did not show a dependence on the concrete cover. Utilizing of sand coating technique had a noticeable enhancement of the bond strength. Sand coating provided friction forces between SMA bars and concrete. More enhancement of bond could be gained by using more coarse sand.

2.3.7.5 Studies about SMAs Reinforced Frames

The multistory building is one of the widely spread structural types around the world. Therefore, it is important to study the effect of using SMA as an alternative for conventional steel on the seismic behavior of multistory buildings. In the paper of (Alam et al. 2012), the authors studied analytically the effect of using SMA rebar on the seismic behavior of three different concrete buildings. Three, six, and eight stories concrete buildings were selected with three types of reinforcement for each one. Conventional steel, SMA reinforcement in plastic hinge only, and SMA in all beams longitudinal reinforcement were the three types of reinforcement for each type of previously mentioned buildings. Nonlinear pushover and dynamic time history analyses were conducted to show the effect of SMA rebar on the global response of buildings.

The roof drift at the strength capacity was higher for frames with SMA than frames with only steel bars. This is due to lower modulus of elasticity of SMA comparing with steel bars. It is worth to mention that for all frames (3, 6, 8 stories), the initial stiffness was very close, however, a reduction in stiffness of frames with SMA was noticed. The reason is that after concrete had cracked the SMA bars began to resist forces and due to SMA lower modulus of elasticity, a stiffness reduction would occur. The over strength factor showed close values for the three types of reinforcing for each number of stories.

For nonlinear dynamic analysis, ten different earthquakes were utilized to do the analysis for all frames. For the inter-story drift, 6 and 8 stories frames with SMA bars showed higher values of drift than the code limit ((2.5%)) due to the lower stiffness of SMA comparing with steel bars. Therefore, the stiffness of these frames needs to be increased. Increasing the stories number will lead to increase the inter-story drift for the frames with SMA bars replacing all longitudinal reinforcement of beams.

Utilizing SMAs as reinforcing bars in concrete structures is associated with using large quantities in actual applications. In addition, SMAs have a considerably higher cost compared with conventional steel bars. In order to reduce the required quantities of SMA, a study by (Shiravand et al. 2017) tried to investigate the optimal stories throughout the frame to implement SMA bars. Frames with 3, 5, 7, and 9 stories were investigated with three different reinforcing scenarios for each frame. The first scenario was the reference one using conventional steel only. The second one was to use SMA bars in all plastic hinge zones through all stories. The remaining scenarios were to implement SMA in the bottom stories and the middle stories, respectively. The results of the nonlinear time history analysis showed that frames reinforced with SMAs in the bottom stories only had equivalent performance compared with frames reinforced with SMAs within all stories

without a significant decreasing the ability of self-centering. Similarly, the results of incremental dynamics analyses showed that frames with SMAs in the bottom stories performed better than frames with SMAs in all their stories because the former still had a relatively high stiffness with a considerable recentering capacity. Finally, the cost of using SMA bars could be reduced significantly (Shiravand et al. 2017).

2.3.8 Knowledge Gaps with Shape Memory Alloy

From the previous discussion, one could conclude that limited studies have been performed to investigate experimentally the behavior of structural members reinforced with SMAs. In addition, limited studies have investigated the response of building frames reinforced with SMA analytically by considering two-dimensional buildings models with limited numbers of stories. No studies have been conducted to examine the response of tall buildings reinforced with SMAs as longitudinal reinforcement in the structural members under seismic loading conditions. In this study, a three-dimensional model will be prepared utilizing the advanced capabilities of nonlinear analysis that are available in OpenSees to investigate the response and behavior of a 46-story tall building. The seismic force resisting system of the adopted building is a dual system that is a combination of special moment frames with special structural walls. In this study, an investigation will be performed to identify whether the performance of tall buildings reinforced with SMAs is enhanced compared with the same buildings reinforced with conventional steel bars.

CHAPTER III

CASE STUDY TALL BUILDING

3.1 DESCRIPTION OF THE CASE STUDY

In order to study the potential effect of the new reinforcing materials, high strength reinforcing steel and SMAs, on the structural response of tall concrete buildings subjected to seismic loads and to assess the seismic performance of tall buildings reinforced with new materials, a tall building is selected from the PEER report as a case study (Moehle et al. 2011). The PEER report explored the potential differences in the response of the same building that was designed by three different procedures: ASCE-7-05, the Los Angeles Tall Buildings Seismic Design Guidelines (LATBSDC 2008), and the Tall Buildings Initiative (TBI 2010). The chosen building in this study was designed according to the ASCE7-05 and its seismic force resisting system consists of a dual system, that includes a core shear wall and special moment frames. In this section, a description of the case study building will be introduced.

The building has four stories below ground and 42 stories above ground. The story height is 10.5 ft except the ground story height is 13.67 ft. The penthouse is 20.0 ft tall. The SFRS consists of a dual system. The dual system contains a core shear wall and four special moment frames at the perimeter of the building. The special moment frames and the core wall continue from the base to the roof and the penthouse, respectively. The thickness of the shear wall is 24.0 in. for stories below the 20^{th} story, while the thickness for the remaining stories is 18.0 in. The concrete strength for the core wall varies from 5.0 to 6.0 ksi. The columns of the special moment frames have dimensions that vary from 46.0 in. × 46.0 in. to 36.0 in. × 36.0 in. All the beams are 36.0 in. deep × 30.0 in. wide. The concrete strength for columns varies from 5.0 to 10.0 ksi, while for beams the

strength is a constant 5.0 ksi. All reinforcement for the dual system is ASTM .A706 Grade 60.

Table 3.1 summarizes some of the features of the case study building. The slab thickness is 10.0 in, 12.0 in., and 8.0 in. for below grade levels, ground level, and above ground levels, respectively. The concrete strength for all slabs is 5.0 ksi. The building has basement walls at the below grade levels with a thickness of 16.0 in.

Table 3.1 Case Study Tall Building Properties (adopted from (Moehle et al. 2011)).

Parameter	Description
Story height	10.5 ft at levels below ground 13.67 ft from ground to 2nd floor 10.5 ft from 2nd to 42nd floors 11.5 ft 42nd floor to roof 20.0 ft roof to penthouse
Overall building height	484 ft
Number of stories	42 stories above ground 4 stories below ground
Slabs thickness and construction	10.0" at basement level (reinforced concrete) 12.0" at ground level (reinforced concrete) 8.0" above ground (post-tensioned concrete) 10.0" at roof (reinforced concrete)
Core walls	24.0" thick from foundation to 20th floor, f'_c 6.0 ksi 18.0" thick above 20th floor, f'_c 5.0 ksi
Coupling beams	30.0" deep.
Special moment frame beams	30.0"x36.0" cross section, f'_c 5.0 ksi
Special moment frame columns	46.0"x46.0" or 42.0"x42.0" or 36.0"x36.0"
	f'_c from 10.0 to 5.0 ksi
	For details see Figures 3.4 to 3.7
Basement shear walls	16.0" thick, f'_c 5.0 ksi.
Grade of all reinforcement	Grade 60 (ASTM A706).

Figures 3.1 to 3.7 provide details of the building, including an elevation view and typical plan views. Note that Frames A and F are special moment frames in the y-direction and Frames 2 and 5 are special moment frames in x-direction.

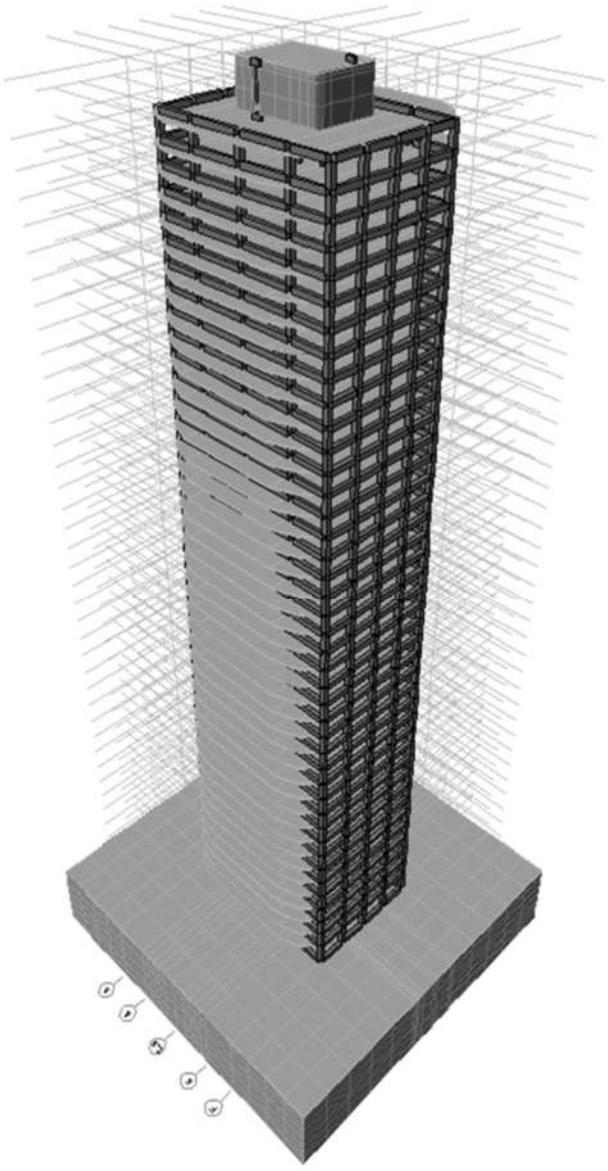

Figure 3.1 Three-Dimensional View of the Case Study Building (Moehle et al. 2011).

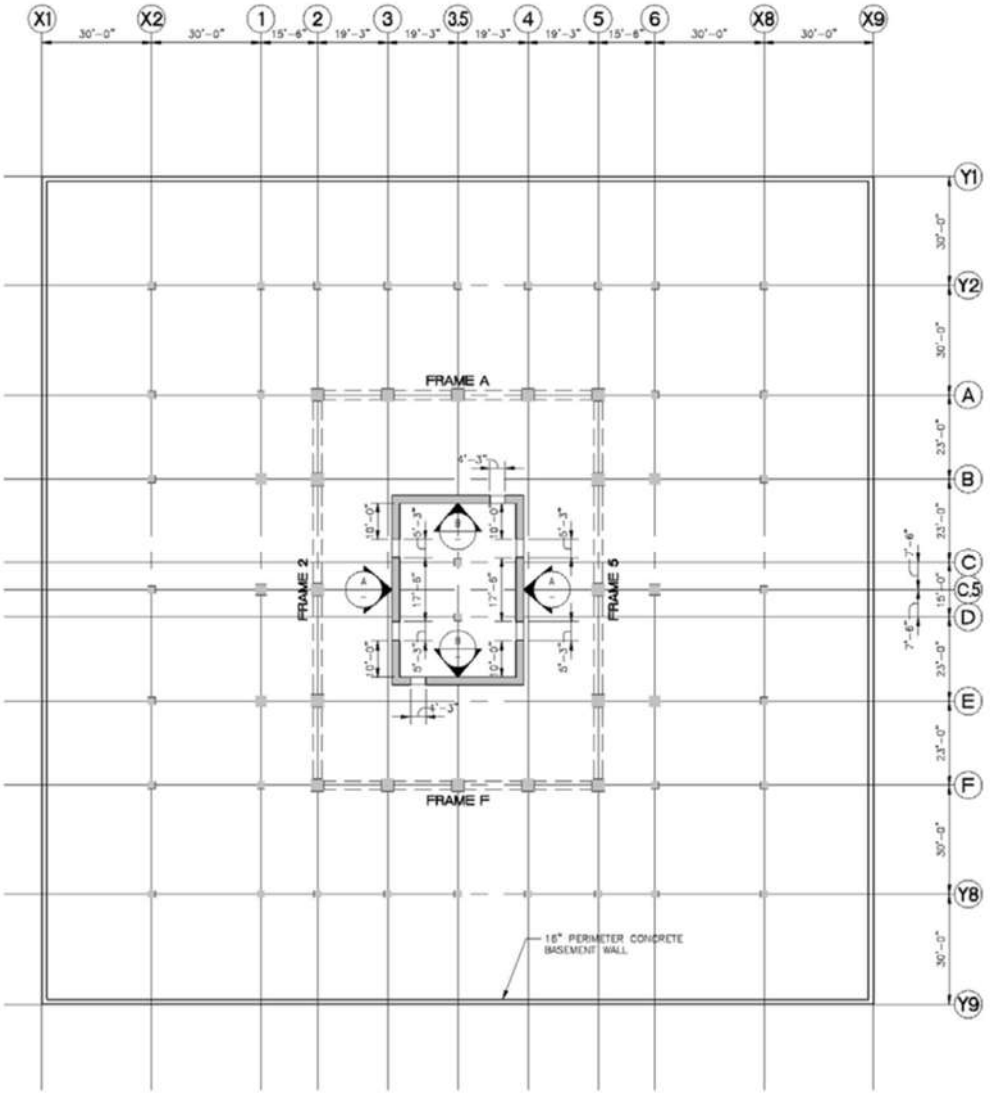

Figure 3.2 Plan View at the Tower (Moehle et al. 2011).

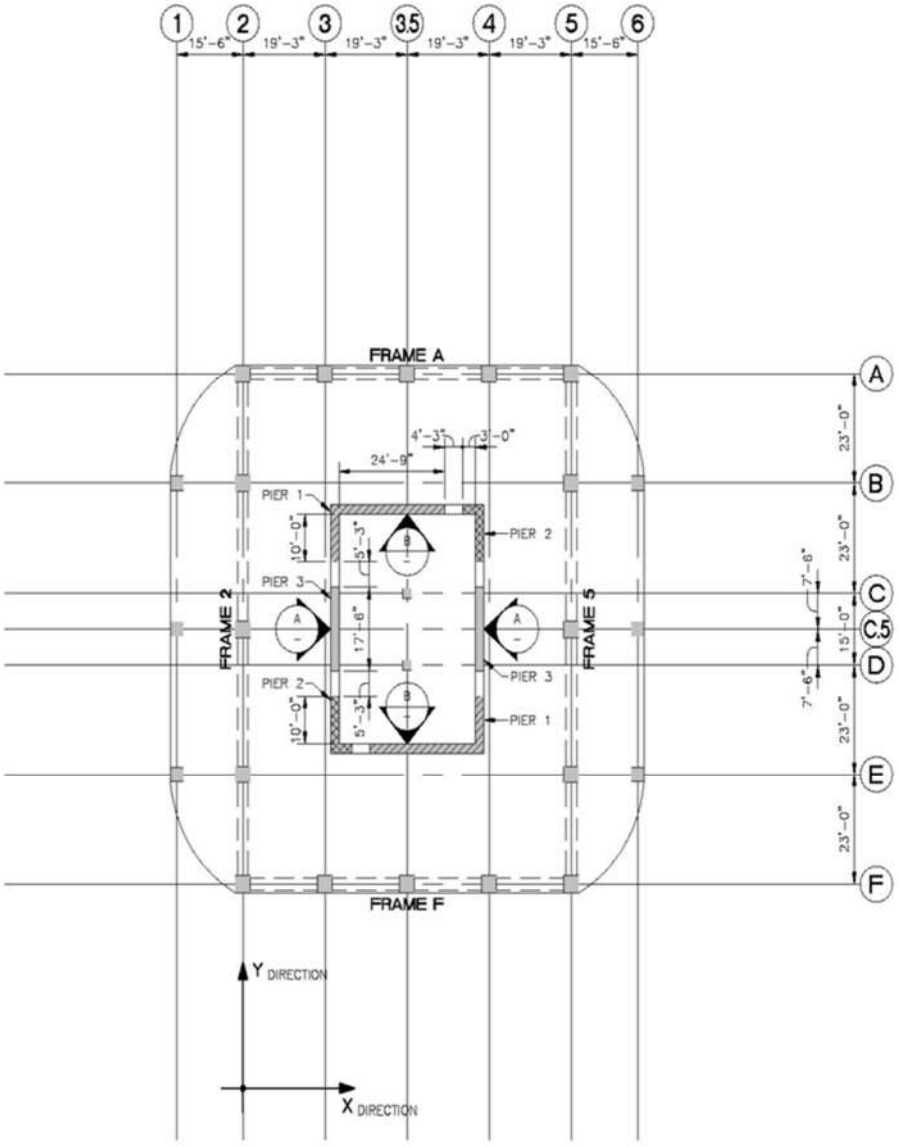

Figure 3.3 Plan View at the Tower (Moehle et al. 2011).

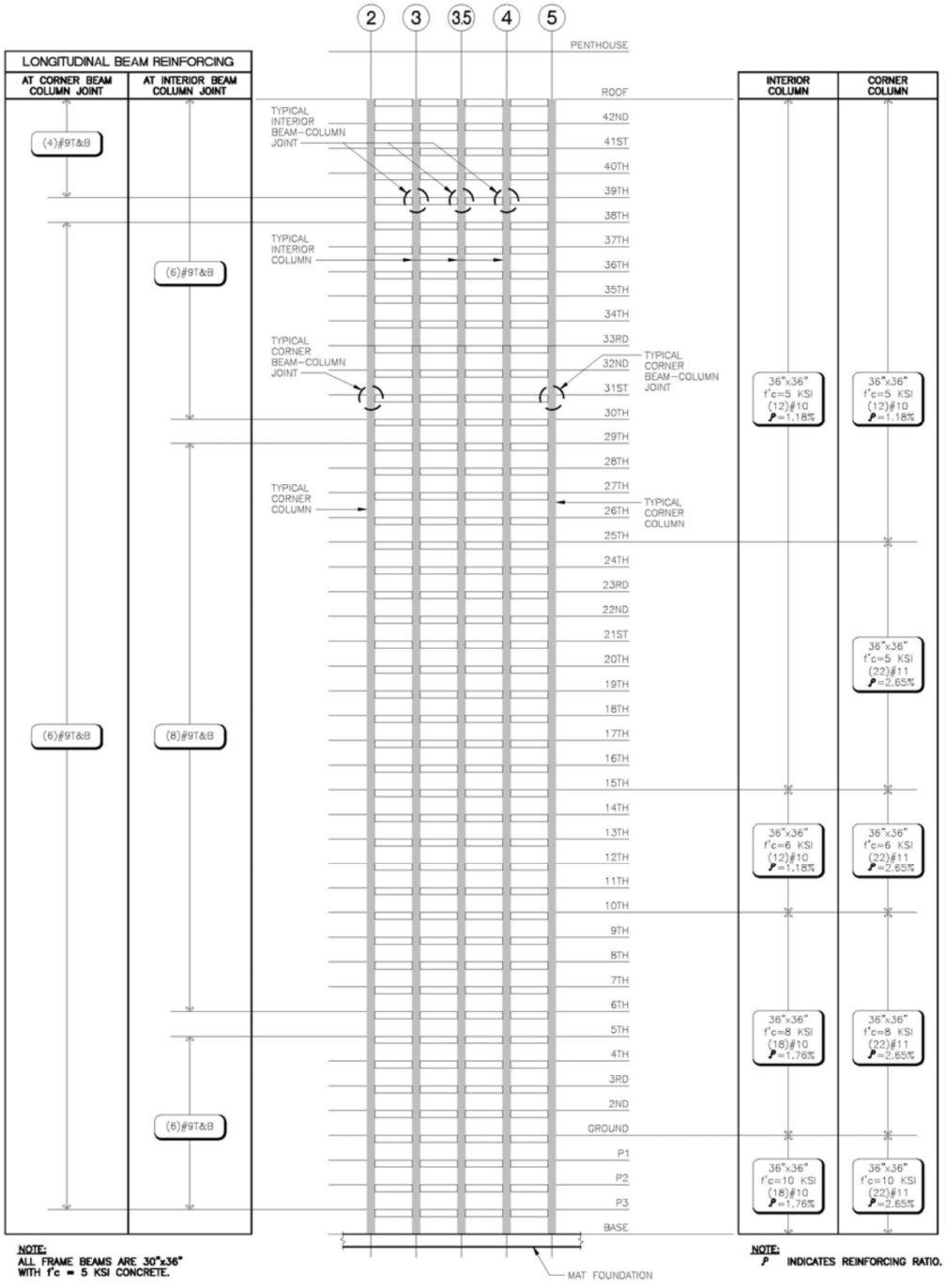

Figure 3.4 Elevation and Properties of Frames A and F for the Case Study Building (Moehle et al. 2011).

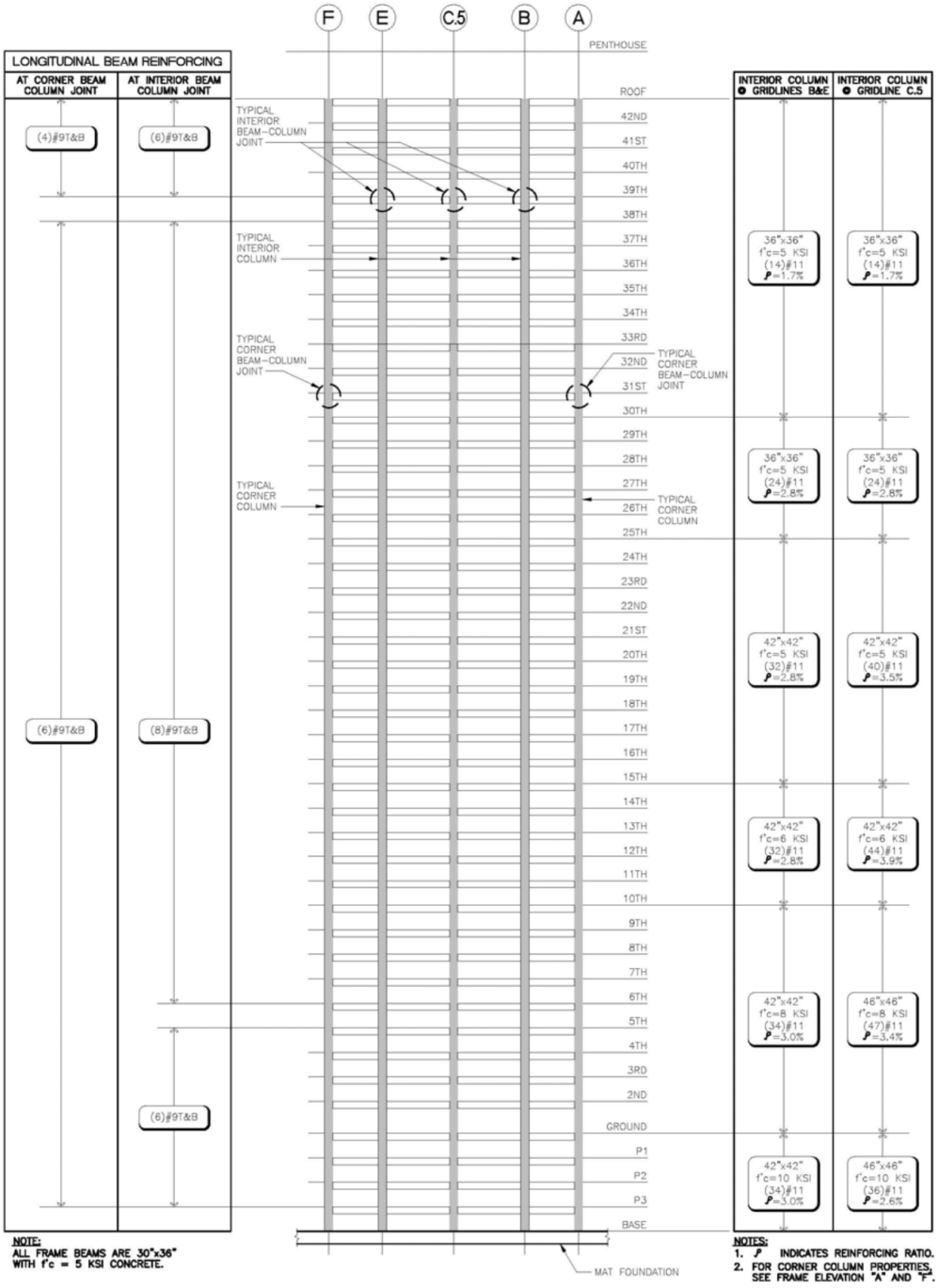

Figure 3.5 Elevation and Properties of Frames 2 and 5 for the Case Study Building (PEER, 2011).

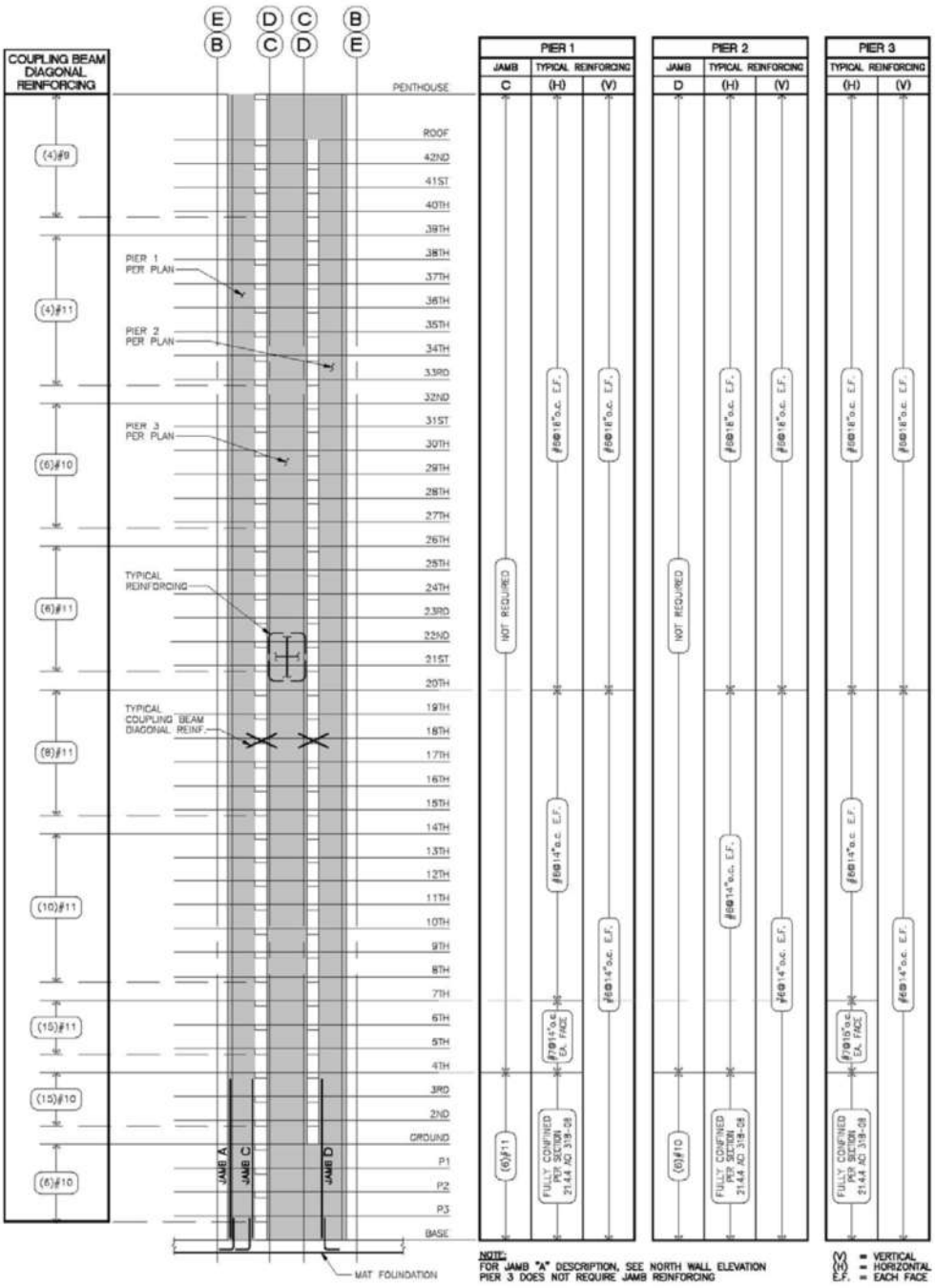

Figure 3.6 Elevation A and Shear Reinforcing for the Case Study Building (PEER 2011).

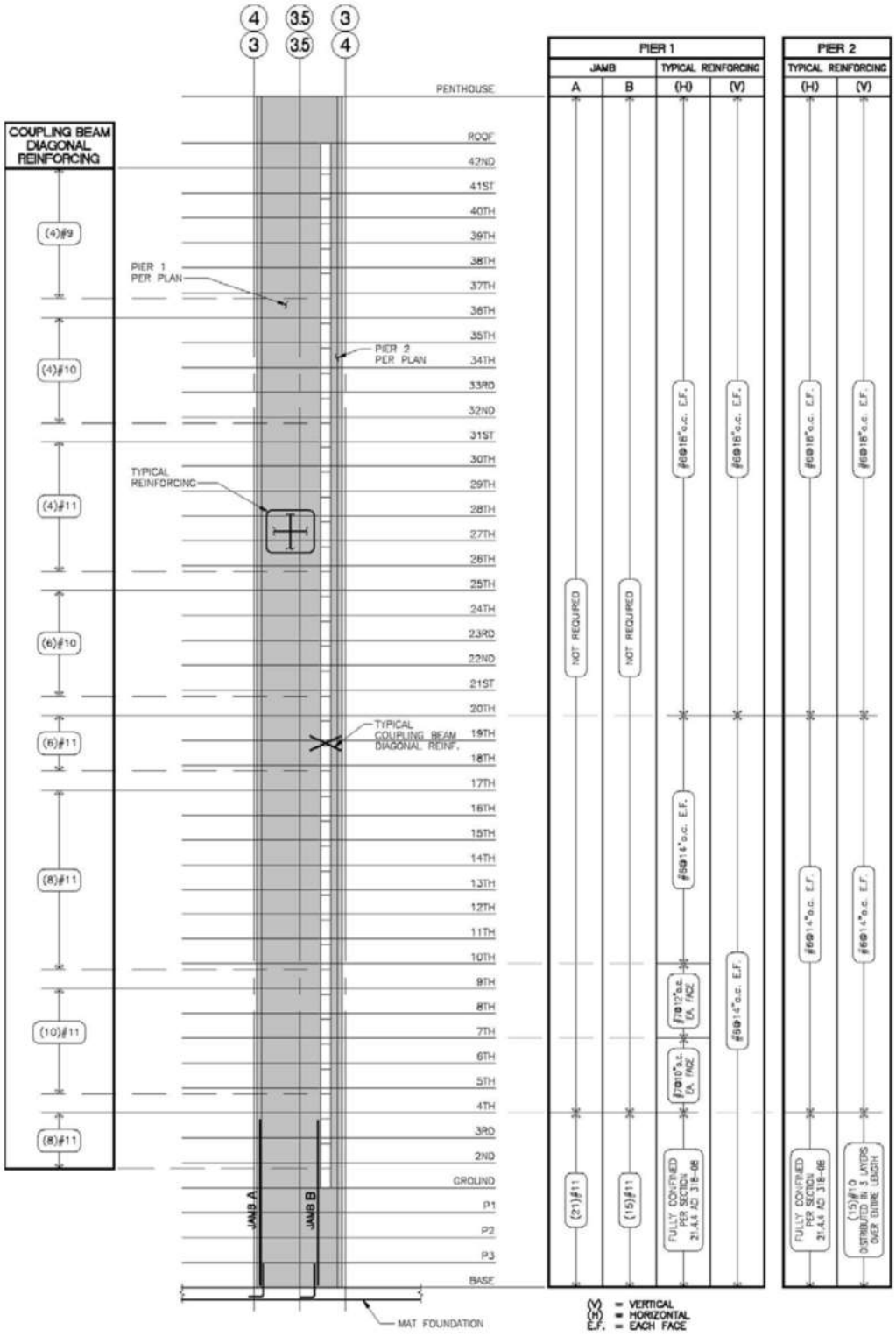

Figure 3.7 Elevation B and Shear Reinforcing for the Case Study Building (PEER 2011).

3.2 DESIGN SPECTRUM PARAMETERS FOR THE CASE STUDY BUILDING

The case study building is located at longitude=-118.25, latitude=34.05, on Site Class C soil in Los Angeles, California. Following ASCE 7-16 Chapter 11, the design spectrum parameters are summarized in Table 3.2. Figure 3.8 depicts the design spectrum for the case study building. The periods of the first three modes of the case study building are 5.15 sec, 4.7 sec, and 2.74 sec respectively.

Table 3.2 Design Spectrum Parameters for the Case Study Building.

Parameter	**Value**
S_s	1.970 g
S_1	0.701 g
Site class	C
F_a	1.2
F_v	1.4
S_{Ms}	2.364 g
S_{M1}	0.982 g
S_{Ds}	1.576 g
S_{D1}	0.654
Risk category	II
Seismic Design Category	D

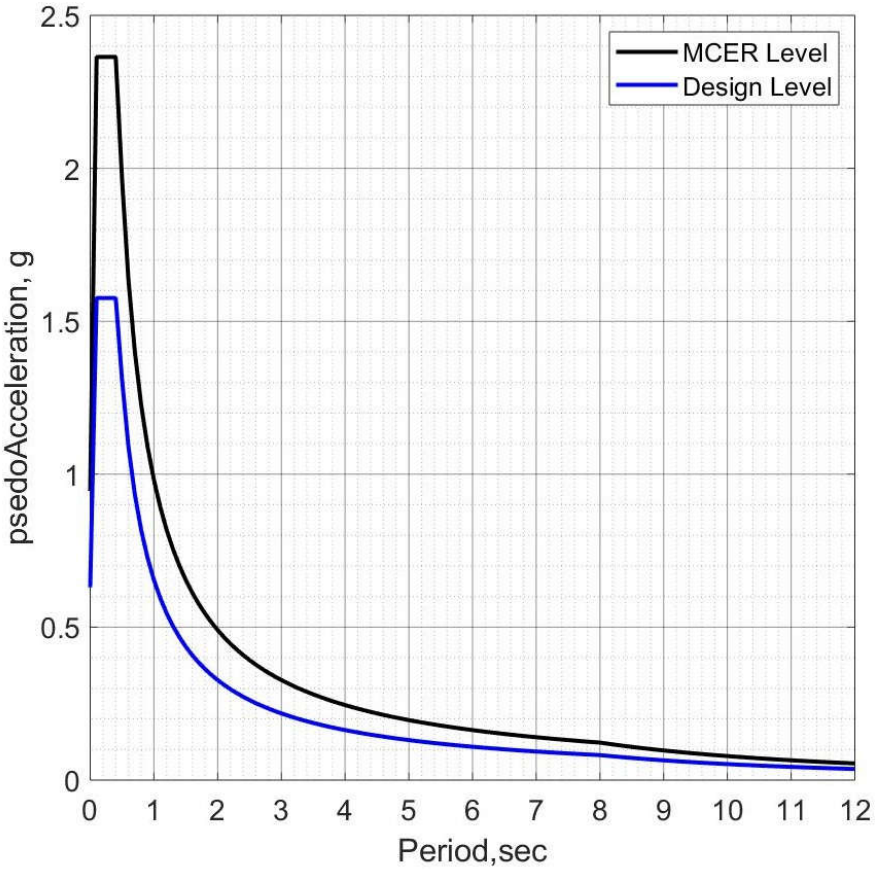

Figure 3.8 Design Spectrum for the Case Study Building.

3.3 PROPOSED CASES FOR EVALUATION

3.3.1 Cases for High Strength Reinforcement

As pointed out previously, the current code provisions of ACI 318-14 prevent the use of steel reinforcement with a yield strength more than 60 ksi in SFRS in high seismic regions. Currently, reinforcement with yield strength of 80, 100, and 120 ksi are produced in the United States and are commercially available. Using reinforcement with high strength is associated with a lower amount of reinforcement in the structural sections. This has some advantages such as reducing the congestion of steel bars, reducing the cost of placement, placing concrete more easily,

and reducing the environmental impact.

Tall buildings in high seismic regions have a substantial amount of both gravity loads and seismic demands that typically lead to very heavily congested reinforced sections. Therefore, using high strength reinforcement with a reduced amount of steel bars could introduce a valuable solution. Studies are needed to investigate the response of tall buildings reinforced with high strength reinforcement in its structural members under cyclic loading conditions. The results of the needed studies can improve the understanding of the response of tall buildings with high strength reinforcement and further its implementation into practice.

This part of the research is focused on providing analytical results for the response of a tall building reinforced with high strength reinforcement. The proposed cases for evaluation will be as follows.

- Case 1: ASTM A706 Grade 60 reinforcement will be used in the longitudinal reinforcement of all beams, columns, walls.
- Case 2: ASTM A706 Grade 80 reinforcement will be used in the longitudinal reinforcement of all beams, columns, and walls.
- Case 3: ASTM A1035 Grade 100 reinforcement will be used in the longitudinal reinforcement of all beams, columns, and walls.
- Case 4: ASTM A1035 Grade 120 reinforcement will be used in the longitudinal reinforcement of all beams, columns, and walls.

3.3.2 Cases for Shape Memory Alloys

As pointed in the previous sections, the design procedure depends on the design earthquake spectral values, which represent 2/3 of the MCER values. This means that inelastic responses should be expected especially during strong earthquakes events. Therefore, the philosophy of the

design code depends on the idea that dissipation of the input energy of the earthquake would be through allowing special detailed regions in the structure to yield and undergo inelastic deformation without critical strength degradation (FEMA 2015). This design procedure is intended to prevent overall structural collapse and loss of life. However, structures would undergo permanent damage, which has crucial impacts on the economy and future use of damaged structures.

The determination of the location of the special detailed regions that would experience inelastic deformation, plastic hinges, depends on the strength characteristics of the beams and columns in the frame. As mentioned in Section 2.3, according to the column and beam strength, there are three different scenarios for how the frame will respond and how the inelastic deformation will be distributed during seismic events. For the strong column and weak beam case (beam mechanism), the deformation has a uniform distribution through the height of the frame with reduced local deformation and the plastic hinges will develop at the ends of the beams. It is important to mention that for a beam mechanism, a frame needs its columns strength to be large by several times than its beams strength (Moehle 2014). This may be an uneconomical solution, therefore columns yielding should be expected. The "strong column/weak beam" phenomenon is a fundamental property for frames to safely withstand strong shaking (Moehle 2014).

It is obvious that some regions in concrete frames will yield to dissipate the input energy of earthquakes, these regions are the plastic hinges zones and yielding of reinforcing steel bars will cause permanent deformations. Conventional steel bars are not able to recover the inelastic strains like the SMAs. Studies confirm that utilizing SMA as an alternative for conventional steel bars in concrete structures leads to improved performance for concrete structures subjected to cyclic loading with negligible residual strains (Abdulridha et al. 2013; Alam et al. 2008; Ghassemieh et

al. 2016; Saiidi and Wang 2006). However, these studies have not considered tall buildings under strong earthquake shaking.

Depending on the above discussion, the proposed cases for evaluation will be as follows.

- Case 1: Shape memory alloy bars will be used in the plastic hinge zones where the tensile strain of the reinforcing bars expected to be high such as the beams of special moment frames and the boundary elements of the core wall. The final decision will be after exploring the response parameters of the case study building as in the Chapter 7.

CHAPTER IV

METHODS FOR ASSESSMENT

4.1 OVERVIEW

In this work, new reinforcing materials are utilized as alternatives to conventional reinforcing steel bars. The new materials, high strength reinforcing steel and shape memory alloys, have different characteristics that produce structural elements with a different response and behavior under different loads conditions. In addition, the current code provisions and standards, including ACI 318-14 and ASCE 7-16, provide a prescriptive procedure in which a complete procedure for analyzing and designing structures under different types of loads including seismic loads is introduced. Within the provisions of these prescriptive procedures, only conventional steel bars can be used as the primary reinforcement in concrete building structures. It should be noted that the code provisions do not intend to prevent any alternative new materials or methods of design to be used, but first the proposed materials and methods of design and construction must be approved to produce a structure that has performance at least equal to the performance objective intended by the codes.

4.2 IBC AND ASCE 7

The 2016 International Buildings Code (ICC 2016) states in Section 104.11 (Alternate materials, design and methods of construction and equipment) states, “The provisions of this code are not intended to prevent the installation of any material or to prohibit any design or method of construction not specifically prescribed in this code, provided that any such alternative has been approved. An alternative material, design or method of construction shall be approved where the building official finds that the proposed design is satisfactory and complies with the intent of the

provisions of this code, and that the material, method or work offered is, for the purpose intended, not less than the equivalent of that prescribed in this code in quality, strength, effectiveness, fire resistance, durability, and safety." ASCE 7-16 accepts alternative procedures that may adopt one or more requirements that differ from the requirements of the ASCE 7-16 prescriptive procedure. ASCE 7-16 Section 1.3.1.3 (Performance-based Procedures) states: "Structural and nonstructural components and their connections designed with performance-based procedures shall be demonstrated by analysis in accordance with Section 2.3.6 or by analysis procedures supplemented by testing to provide a reliability that is generally consistent with the target reliabilities stipulated in this section. Structural systems subjected to earthquake shall be based on the target reliabilities in Tables 1.3.2 and 1.3.3. The analysis procedures used shall account for uncertainties in loading and resistance."

From the previous code sections, one could conclude that it is permissible to use alternative procedures in which one or more of the requirements of the code prescriptive procedure might not be satisfied, as long as the performance of the alternative procedures has been shown to provide at least an equal or higher performance as compared to the prescriptive procedure of the code. ASCE 7-16 defines the performance objective for structures subjected to seismic loads as the target maximum probabilities of structural collapse measured upon subjecting the structure to MCER shaking level. According to Table 1.3.2 in ASCE 7-16, 10% maximum structural collapse is for risk category 1 and 2, 5% and 2.5% are for risk categories 3 and 4 respectively. ASCE 7-16 develops the structural collapse probabilities depending on the work of FEMA P695 (FEMA 2009b). In addition, procedures for estimating the collapse probabilities are also developed in FEMA P695. Using the procedures of FEMA P695, the collapse probability of a structure that designed by an alternative procedure could be estimated. Once the estimated probability of

collapse is within the acceptable values of in ASCE-7-16, Table 1.3.2, then the performance of the alternative procedure is equivalent or high than the performance objective of the prescriptive procedure of ASCE-7-16. Another available option for approving the equivalence between the performance of the alternative procedure and the prescriptive procedure is introduced by the Tall Buildings Initiative, TBI (TBI 2017), in the document, Guidelines for the performance-based seismic design of tall buildings. The following section focuses on these guidelines and how to implement them in this study.

4.3 TALL BUILDING INITIATIVE (TBI) GUIDELINES

4.3.1 Introduction

The Tall Building Initiative (TBI) developed guidelines for Performance-Based Seismic Design of Tall Buildings (TBI 2017). The TBI guidelines provide a complete procedure for selecting and scaling appropriate earthquakes records for time history analysis, modeling of different components for nonlinear analysis, and providing the acceptance criteria for evaluating the acceptability of the response and the behavior of the tall buildings designed according to the requirements of the TBI guidelines. The TBI guidelines adopt the ASCE 7-16 methods for selecting and scaling the earthquake records. For modeling of different structural components, the TBI guidelines modeling approach will be discussed in Chapter 5. The most important part of the TBI guidelines is the acceptance criteria that are provided to evaluate the performance of tall buildings. The TBI acceptance criteria are written to ensure that the seismic performance of a tall building designed in conformance with the TBI guidelines would be at least equal to or exceed the performance of a similar building designed completely with the prescriptive procedure of ASCE 7. While the TBI guidelines provide an alternative procedure in which one or more of ASCE 7-16 requirements would not be satisfied, it is important to mention that a building designed and

evaluated successfully with the TBI guidelines would perform at least equal to that required by ASCE 7 for seismic loading.

The TBI guidelines requires that the tall building response will be checked under two ground motion levels: the service level earthquake (SLE) and the MCER level. In the sections below, a brief introduction to the requirements for each shaking level is provided.

4.3.2 Evaluation of a Building for MCER

4.3.2.1 General

As discussed previously, the ASCE 7-16 standard allows the use of an alternative design procedure, performance-based design, upon showing that the probability of structural collapse under MCER shaking level is within the values in ASCE 7-16 Table 1.3.2. To estimate the structural collapse of buildings, the procedures of FEMA P695 could be applied (FEMA 2009b). However, the TBI guidelines provide another option. The TBI guidelines state the following "These Guidelines do not actually require implementation of the FEMA P695 procedures. Instead, these Guidelines establish acceptance criteria for evaluation of the acceptability of the structural response under MCER shaking. The acceptance criteria have been derived using the same concepts as the FEMA P695 procedures. These Guidelines should be deemed to conform to the requirements of ASCE 7-16 with regard to performance-based approaches." In other words, one could satisfy the requirements for probabilities of structural collapse of ASCE 7-16 (Table 1.3.2) by satisfying the acceptance criteria of TBI guidelines for MCER shaking levels.

The TBI guidelines require selecting a suite of ground motions records that represent MCER shaking level, Section 5.3 of this proposal discusses the selection and scaling of suitable ground motions. The second step is to prepare the model of the building that will be analyzed. Section 5.2 of this proposal introduces available techniques for modeling the structural

components such as beams-columns, walls, and joints. After completing the selection of ground motion records and modeling the structure, the TBI guidelines require performing the nonlinear response history analysis. The analysis results have to be checked with the acceptance criteria for selected structural response parameters provided in the TBI guidelines. Once the analysis results are shown to be within these limits, the performance objectives are achieved. Whenever the TBI guidelines performance objectives are satisfied, the required performance by the ASCE 7-16 (Table 1.3.2) for alternatives procedures, performance-based design, are also considered to be satisfied.

4.3.2.2 Global Acceptance Criteria

TBI guidelines satisfy the global performance by satisfying three requirements:

4.3.2.2.1 Unacceptable Response

The response of the building subjected to each ground motion from the selected suite would be considered as unacceptable if one or more of the following occurs.

- Convergence of the analysis is not achieved.
- For deformation-controlled elements, the demand exceeds the valid range of deformation in the modeling.
- For force-controlled elements, the demand exceeds the capacity.
- For any story, the peak drift ratio exceeds 0.045. It is important to mention that according to the authors of the TBI guidelines, the results of nonlinear response history analysis obtained by using current tools and software are unreliable once the drift ratio exceeds the recommended limit of 0.045.
- For any story, its residual drift ratio exceeds 0.015.

4.3.2.2.2 Peak Story Drift Ratio

The peak story drift ratio is evaluated for each story. The TBI guidelines require that the mean peak story drift calculated for all ground motion records in the suite should not exceed the limit of 0.03. According to the general consensus mentioned by the TBI guidelines, buildings designed and detailed properly will respond suitably up to the limit of 0.03 without critical degradation in its strength capacity. In addition, nonstructural components designed by considering the limit of 0.03 drift will not cause a considerable risk for life safety.

4.3.2.2.3 Residual Drift Ratio

Limiting residual drift ratio of 0.01 is used for each story. The residual drift is calculated as the mean value for all ground motions within the selected suite. The TBI guidelines add this criterion in order to improve the performance of the tall buildings. Excessive residual drifts could lead to detrimental consequences such as extra time for repair, high repair cost, and demolition of the building.

4.3.2.3 Element Level Acceptance Criteria

The TBI guidelines satisfy the performance at the local or element level by satisfying two requirements: deformation-based actions and force-based actions, as described below.

4.3.2.3.1 Deformation-Controlled Actions

The TBI guidelines require that for all components, the deformation capacity should not be exceeded by the deformation demand for any mode of deformation in any analysis for any ground motion within the suite of motions. The deformation demands are determined by using the nonlinear response history analysis. The TBI guidelines introduce two ways to determine the deformation capacities. For the first approach, the TBI guidelines suggest using the valid range of modeling parameters that has been validated by test data. Alternatively, the TBI guidelines adopt

the deformation capacities that are given by ASCE 41, *Seismic Evaluation and Retrofit of Existing Buildings* (ASCE 2013) . As pointed out previously, for any analysis to an individual ground motion, once the deformation demand exceeds the deformation capacity for any deformation-controlled components in any element, the response will be considered as an unacceptable one.

4.3.2.3.2 Force-Controlled Actions

For MCER shaking level, TBI guidelines introduce equations for checking the demands of the force-controlled actions with the available capacities. TBI guidelines recommend using the ACI-318 equations for determining the capacities of different force-controlled actions.

4.3.3 Evaluation of a Building for SLE

4.3.3.1 General

The TBI guidelines introduce acceptance criteria for tall buildings subjected to the service-level earthquake, SLE, which is defined as having 43-year return period or 50% probability of exceedance in 30 years. For SLE shaking level, the TBI guidelines allow the use of either linear analysis or nonlinear response history analysis to obtain the demands to compare to the acceptance criteria. For linear analysis, the TBI guidelines permit using either the response spectrum or the linear response history analysis. In this study, the nonlinear response history analysis will be performed. After selecting and scaling the suite of ground motions that represents SLE according to the procedure of ASCE 7-16 for selecting and scaling, a nonlinear building model is prepared. The demands are obtained by performing nonlinear response history analysis and then checked with the acceptance criteria for SLE.

4.3.3.2 Global Acceptance Criteria

The TBI guidelines satisfy the global performance by satisfying one requirement that still same whether performing linear or nonlinear analyses for SLE level: story drift ratio. In any story,

the calculated story drift ratio in any direction of the building should be equal or less than (0.005). TBI guidelines authors emphasize that a story drift ratio of limit 0.005 is chosen to ensure that buildings subjected to SLE shaking will experience very limited permanent deformation and nonstructural component damage.

4.3.3.3 Element Level Acceptance Criteria

The element-level requirements for SLE evaluation differ according to the adopted analysis procedure. In the sections below, requirements for linear and nonlinear analyses for the SLE level will be introduced. The TBI guidelines satisfy the performance at the local or element level by satisfying two requirements: deformation-based actions and force-based action, as described below.

4.3.3.3.1 Deformation-Controlled Actions

For linear analysis and for deformation-controlled actions, the ratio of calculated demands from the analysis to the capacities should be equal or less than 1.5. It is important to mention that the capacity of deformation-controlled actions for SLE shaking is defined as the nominal strength that is determined according to ACI 318-14 without multiplying by strength reduction factors.

For nonlinear analysis, the deformation capacity should not be exceeded by the deformation demand for any mode of deformation. The TBI guidelines permit using the acceptance criteria of ASEC 41-13 for the Immediate Occupancy performance level.

4.3.3.3.2 Force-Controlled Actions

For linear analysis and for force-controlled actions, the ratio of calculated demands from analysis to the corresponding capacities should be equal to or less than 1.0. The capacity of force–controlled actions for SLE shaking is defined as the nominal strength determined according to ACI 318-14 upon multiplying by the strength reduction factors in ACI 318-14.

For nonlinear analysis, the ratio of calculated demands from analysis to the capacities should be equal to or less than 1.0. The capacity of force–controlled actions for SLE shaking is defined as the expected strength that is determined by utilizing the expected materials properties according to ACI 318-14 upon multiplying by the strength reduction factors in ACI318-14.

CHAPTER V

DEVELOPMENT OF MODELING APPROACH

5.1 GENERAL ASSUMPTIONS

This chapter describes the basic modeling approach to be used for the modeling of the case study building. These assumptions are applicable for both the linear and nonlinear analyses.

5.1.1 Structure Idealization

A three-dimensional model is required to reliably predict the actual response and behavior of the case study tall building structure. Due to the powerful capabilities that are available in the current structural analysis software, the TBI guidelines require the use of three-dimensional models. The TBI guidelines note that accuracy of the response that is obtained by using three-dimensional models is more valuable than the simplicity in computational efforts that is obtained by using two-dimensional models. However, ASCE 7-16 only requires a three-dimensional model for any structure that has horizontal irregularities.

The TBI guidelines intend to estimate the seismic response with the maximum reliability to the extent possible, therefore these guidelines require including the gravity load carrying structural components in the model. The reason is that the frames not designated as part of the seismic force resisting system (gravity frames) contribute significantly to the lateral stiffness and strength. On the other hand, the ASCE 7-16 procedure does not include the gravity frames in the model.

The TBI guidelines recommend that the modeling parameters represent the expected values by utilizing their mean values. The modeling parameters include, but are not limited to, material and component properties, masses, and gravity loads.

5.1.2 Diaphragm Modeling

The classification of the diaphragm flexibility as rigid, semi-rigid, or flexible according to ASCE 7-16 is adopted by the TBI guidelines. For a semi-rigid diaphragm, the diaphragm stiffness should be included in the model.

For concrete slabs to be defined as rigid diaphragms, two conditions must be satisfied: span-to-width ratio of the slab must be equal to or less than three, and the structure must not have any horizontal irregularities described in Table 12.3.1 of ASCE 7-16. The concrete floor and roof diaphragms in the adopted case study building do satisfy the previous two conditions, therefore the diaphragms will be modeled as rigid diaphragms.

5.1.3 Seismic Mass and Expected Gravity Loads

Seismic mass is calculated from the effective seismic weight. The TBI guidelines follow the definition of the seismic weight provided by ASCE 7-16 in Section 12.7. The TBI guidelines require in general including the mass of the entire structure, superstructure and the substructure. The mass in the vertical degree of freedom should be included if the vertical ground motion input is included in the analysis and when the structure has vertical irregularities.

When performing the response history analyses, the expected gravity loads should be incorporated in the analyses. The TBI guidelines define the expected gravity loads as $D + 0.5L$, where D is the dead load and L is 40 percent of unreduced live loads that are below 100 psf, and 80 percent of other unreduced live loads.

5.1.4 Modeling of Damping Effect

The equivalent viscous damping represents the energy dissipation that is not considered through the hysteretic models in the analysis. This type of energy dissipation occurs through different mechanisms such as the small amount of yielding of elements that are assumed to remain

elastic, non-structural components, and the soil foundation interface. The TBI guidelines and other research show some test data that damping in tall buildings is less than in low-rise buildings. The main reason is the smaller contribution of damping from soil-foundation interfaces in tall buildings. The TBI guidelines give Equation (5-1) for estimating the value of the viscous damping critical ratio for SLE shaking

$$\zeta_{critical} = \frac{0.36}{\sqrt{H}} \leq 0.05 \quad \textbf{(5-1)}$$

where H is the total height of the building, in feet.

For the MCER shaking level, the critical damping ratio is also calculated from the above equation with the limit taken as not less than 0.025.

OpenSees uses the Rayleigh damping form to model the viscous damping. In the Rayleigh formulation, the damping matrix is defined as ($[C] = \alpha_m [M] + \alpha_k [K]$), where the α_m and α_k are defined at two periods to ensure that the modes that contribute significantly to the response will not be overdamped. The TBI guidelines suggest for tall buildings to use the periods of $0.2T$ and $1.5T$, where T is the fundamental period.

For nonlinear analysis, the stiffness matrix is changed, therefore OpenSees provides more than one approach to model the damping matrix. One approach is to use the initial stiffness matrix with or without the mass matrix. Another option is to use the tangent stiffness matrix with or without the mass matrix. Finally, one could choose to make the damping matrix proportional to the mass matrix only. In this study, the adopted approach is to make the damping matrix proportional to both the mass matrix and the tangent stiffness matrix.

5.1.5 Vertical Ground Motion Effect

The TBI guidelines require explicit modeling of the vertical ground motion in the analysis for structures that have a discontinuity in the vertical load carrying system. As pointed out earlier, the mass in the vertical degrees of freedom should be included when the vertical ground motion is included in the analysis. Examples of discontinuities in the vertical load carrying system include, but are not limited to, columns support some stories that are terminated, or major walls terminated on columns. According to the configuration of the adopted case study building, no vertical discontinuities occur in the building. Therefore, the model will not include the mass in the vertical degrees of freedom.

5.1.6 Expected Material Strength

The strength of concrete and reinforcing steel or any other construction materials should represent the expected strength values. Expected strength could be extracted from test data. In the case where test data is lacking, the TBI guidelines provide values for estimating the strength of concrete and reinforcing steel as in Table 5.1.

Table 5.1 Expected Material Strength (adopted from (TBI 2017)).

Materials	**Expected yield strength, f_{ye} (ksi)**	**Expected ultimate strength, f_{ue} (ksi)**
A615 Grade 80 Reinf.	82.0	114.0
A706 Grade 60 Reinf.	69.0	95.0
A706 Grade 80 Reinf.	85.0	112.0
Concrete	$1.3f_c'$, f_c' is the specified concrete strength	

5.2 COMPONENT MODELING

5.2.1 General

The modeling procedure for beams, columns, and joints should reflect, in general, all response modes such as the different modes of deformation or failure. The significant response modes include, but are not limited to, flexural hinging in beams and columns, shear deformation and forces in beams and columns, shear forces and deformation in beam-column joints, reinforcing bar splice failures, and buckling of reinforcing bars. However, if a building is designed and detailed according to the current code provisions, the modeling procedure could rely on the following response assumptions.

- *Beam and column shear design*: The ACI 318-14 design provisions for shear in beams and columns lead to a ratio of shear capacity to shear demand higher than one, but demand can be higher in the actual seismic event. Providing shear strength that resists the maximum probable moment M_{pr} reduces the likelihood of shear failure. This design will circumvent the premature failure due to shear deformation before the formation of flexural hinging. In other words, the behavior of the member will be dominated by only the flexure modes that already take into account the interaction effect of both the axial and moment forces. The maximum shear capacity-to-demand ratio from the analysis should be checked in order to confirm the mentioned assumption.
- *Beam-column joint design*: If the joint is designed in accordance with the ACI 318-14 code provisions, it is assumed that the joint resists forces induced by shear and bar anchorage without experiencing shear failure, bond slip, and reinforcing bar pullout. The joint shear-to-capacity ratio should be checked, based on the maximum demands from the analysis to confirm this assumption.

- *Longitudinal reinforcement splices*: The longitudinal bar splices are assumed to be designed and detailed in such a way to preclude splice failure due to its detrimental consequences such as sudden strength deterioration.
- *Sufficient confinement by transverse reinforcing bars*: The design is assumed to provide sufficient transverse reinforcement to confine the concrete core and supporting the longitudinal bars from buckling.

5.2.2 Modeling of Beam-Column Elements

The nonlinear models for beam-column elements are a line element with lumped plasticity, a line element with distributed plasticity, and a three-dimensional continuum finite element. The lumped plasticity model is less complex than the distributed plasticity model, while the continuum model is the most complex and needs more computational effort especially for the analyses of seismic loads. It is crucial to mention that using line or one-dimensional elements instead of a three-dimensional element leads to significant reduction in the analysis cost, while still maintaining the potential for excellent accuracy in predicting the response of columns and beams (Neuenhofer and Filippou 1997). The line element model with distributed plasticity does not limit the formation of the plastic hinge to the ends of the element like the model with lumped plasticity. In addition, the distributed plasticity model does not need to pre-define the length of the plastic hinge zone prior to the analysis. In the distributed plasticity model, the element is defined by sections, or integration points, that are distributed along the length of the element according to the numerical integration scheme.

To define the sections, there are two approaches. One approach is to define the force-deformation relationship of the section according to its dimensions and reinforcement details. The second approach is to use fiber discretization of the section. The section is divided into numbers

of fibers and each fiber is assigned a uniaxial stress-strain relationship, as in Figure 5.1. The section force and stiffness is determined by the integration of the forces and stiffness of all fibers that form the section.

The formulation of line element model in the finite element method uses either a displacement-based or a force-based method. In the displacement-based method, the displacement field along the element length is interpolated by shape functions with nodal displacements. In the force-based method, the internal forces along the element length are interpolated by shape functions with the forces at the nodes at the end of the element, nodal forces. The interpolation functions in the force-based element represent the exact distribution of the internal forces along the element regardless of the geometry and the type of materials for the sections of the element. Consequently, there is no discretization error which is common for modeling with the displacement-based element. Researchers (Neuenhofer and Filippou 1997) have shown the superior performance of the force-based element in predicting the nonlinear response of beams and columns when using one element for the modeling the structural member. In this work, the force-based element that is available in OpenSees will be used for modeling the nonlinear behavior of the beams and columns.

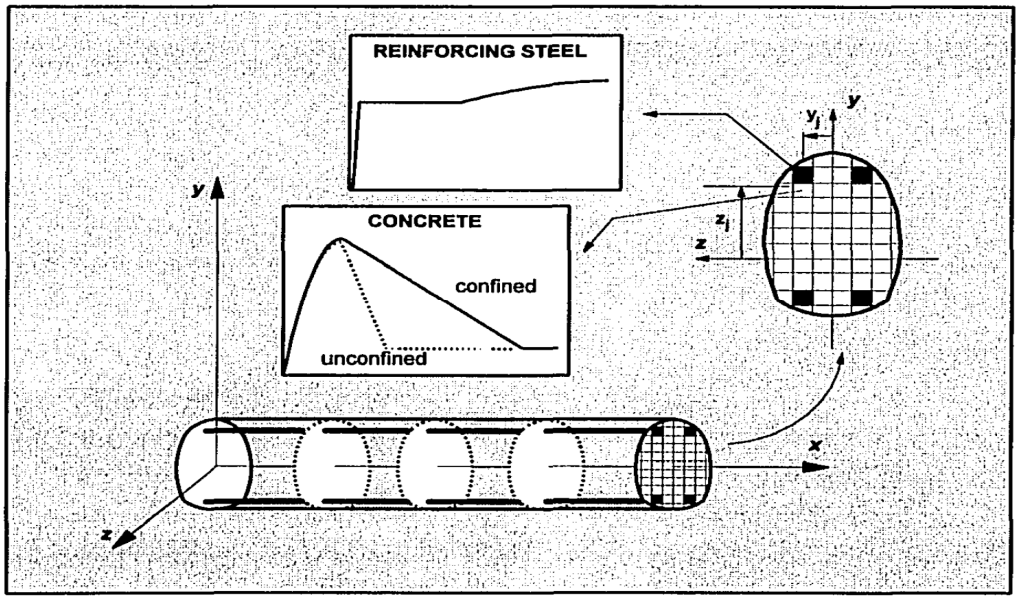

Figure 5.1 Fiber Section Discretization (Taucer et al. 1991).

5.2.3 Modeling of the Beam-Column Joints

The TBI guidelines accept the use of the ASCE 41-13 model for beam-column joints *(ASCE 2013)*. ASCE 41-13 provides a reasonably accurate model for joints by introducing rigid end offset as shown in Figure 5.2. The ratio of the strength of all columns to beams that are framing into the same joint determines the appropriate rigid end offset for modeling the joint as shown in Figure 5.2. According to (Moehle et al. 2010), for special moment frames designed with code provisions that require a column-to-beam strength ratio of at least 1.2, the joint model in Figure 5.2 (a) can be used.

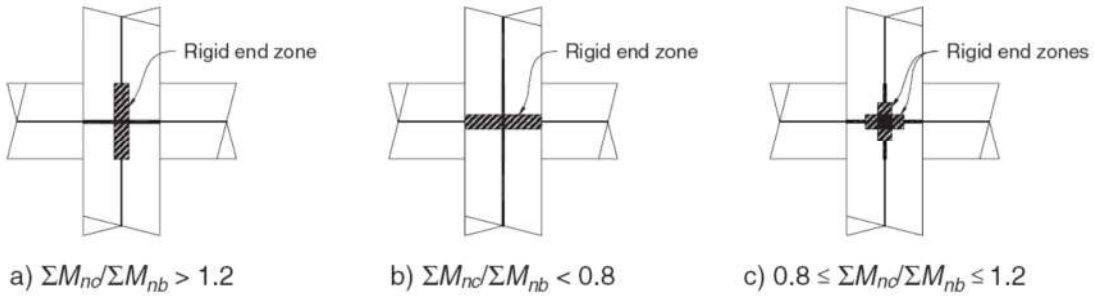

Figure 5.2 Rigid End Offset for Concrete Beam-Column Joint according to the Relative Strength of Beams and Columns Framing into the Joint (ASCE 2013).

5.2.4 Modeling of Shear Walls

Concrete walls are common structural elements that are used for supporting structures laterally. Walls have various configurations such as an isolated planar wall, a flanged wall, a three-dimensional form like a core wall. Modeling the shear wall mainly relies on the nature of the seismic response of the wall and the developed modes of failure in the wall during shaking. Two types of walls are recognized: slender walls and squat walls. The governed mode of failure in the slender walls is flexural yielding, while squat walls exhibit a shear mode of failure. Slender walls are defined as walls with height-to-length aspect ratio of at least 3 (Moehle 2014). A detailed discussion about the types of modeling approaches to simulate the behavior of slender walls are given in (Deierlein et al. 2010),(Moehle et al. 2010). The first common approach is the beam-column element with the fiber section. The main advantage of this approach is its reasonable computational time. On the other hand, this approach relies on the assumption of "plane section remains plane" which could be an important limit for simulating the behavior of non-planar walls especially the core walls. In addition, the beam-column model for walls is not an efficient model for a wall that has a three-dimensional assembly such as a building core. Many tests (Deierlein

et al. 2010) confirmed that wall sections do not remain plane especially when strong shaking levels are applied. Therefore, the shell element approach could be considered a useful model for simulating the response of concrete walls. The shell element model considers that sections do not remain plane. However, the shell element approach requires more computational time compared with the beam-column approach.

The lateral load resisting system of the case study building is a dual system in which the core wall is expected to carry a significant part of the total demands, therefore a suitable and accurate model should be utilized to capture the response appropriately. The shell element with the layered section is available in Opensees and is suitable for simulating the core wall in the case study building. A full description for the shell elements and the layered section is available in the Opensees website and in (Lu et al. 2015). The shell element needs four nodes to be defined. The layered section is used to define the cross section of the shell elements by defining the concrete and the reinforcement bars as layers that form the wall section. For each layer, a material model should be defined. Figure 5.3 shows a typical shell element with its four nodes and the layered section. Figure 5.4 depicts the way by which the layers of concrete and reinforcing bars are defined in the layered section.

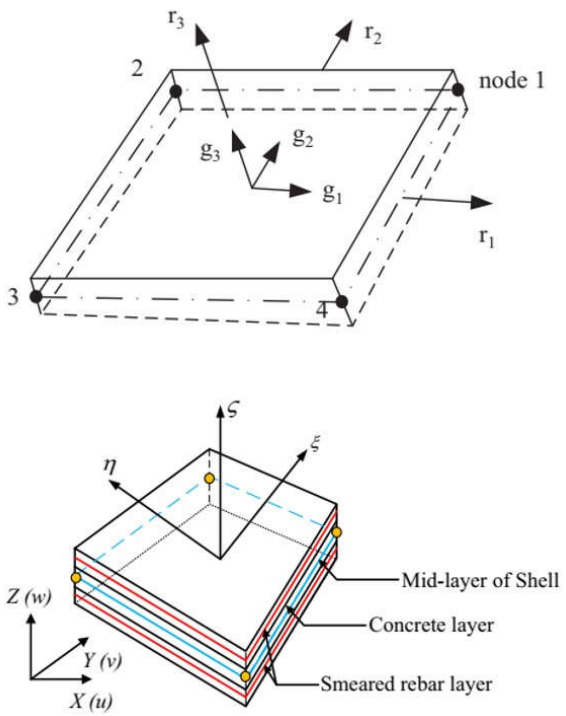

Figure 5.3 Multi-layer Shell Element (Lu et al. 2015).

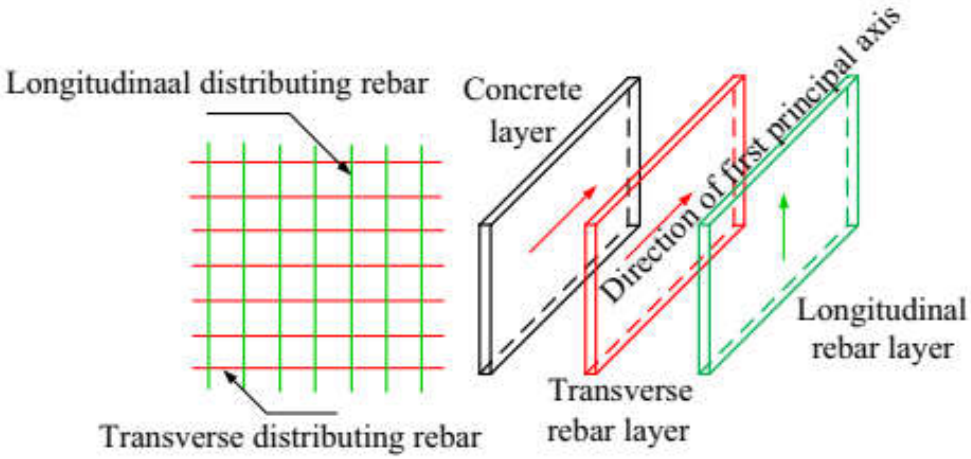

Figure 5.4 Layers of Concrete and Reinforcement Bars for Layered Section for Shell Element (Lu et al. 2015).

5.2.5 Modeling of Coupling Beams

All coupling beams in the case study building are diagonally reinforced and they are relatively deep (ratio of span to depth less than or equal to 2). A discussion about the potential modeling approaches for coupling beams are available in (Deierlein et al. 2010) and (Moehle et al. 2010). There are two common approaches for modeling the coupling beams as shown in Figure 5.5. The first one is to use the beam-column element and the other is to use the shell (wall) element. In general, deep beams behavior is governed by shear, therefore, the wall element could be used. The coupling beams in the case study building are controlled by shear yielding according to (Moehle et al. 2011). So, the model of shell element with the layered section will be used for modeling all coupling beams in the model of the case study building in this work. It is important to notice, when the shell element is used for modeling a coupling beam, the shear strain will be the demand that should be monitored and compared with the acceptance criteria of rotation of the coupling beams.

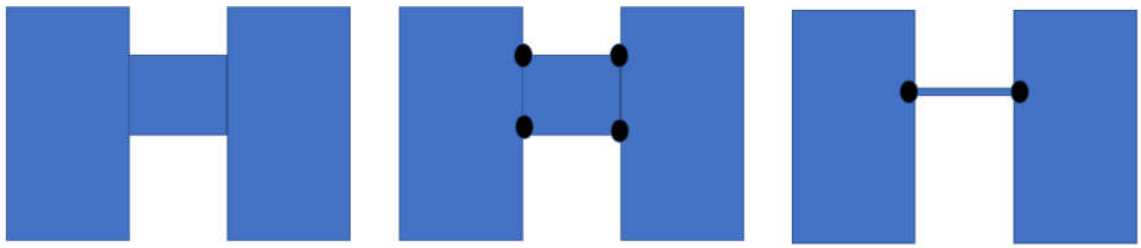

(a) Wall with coupling beam (b) Shell element model (c) Beam element model

Figure 5.5 The Two Approaches for Modeling A Coupling Beam.

5.3 MODELING REQUIREMENTS FOR SLE

The TBI guidelines allow linear or nonlinear analyses for SLE shaking. In addition to the general assumptions that are mentioned previously, here linear analysis requirements for SLE shaking will be introduced. Linear analyses could be performed either by response spectrum analysis or by linear response history analysis. The linear response history analysis recently is more popular than the response spectrum analysis due to the enhanced capabilities of available structural analysis software.

5.3.1 Effective Stiffness

For linear analysis, the effective stiffness for all members is used. The TBI guidelines provide the values for effective stiffness for structural elements for use in the linear analysis for SLE shaking, as in Table 5.2.

Table 5.2 Reinforced Concrete Elements Stiffness for SLE (adopted from (TBI 2017)).

Components	Axial Stiffness	Flexure Stiffness
Columns	1.0 E_cA_g	0.7 E_cI_g
Beams	1.0 E_cA_g	0.5 E_cI_g
Coupling beams	1.0 E_cA_g	$0.07\left(\frac{l_e}{h}\right)E_cI_g \leq 0.3E_cI_g$
Structural walls	1.0 E_cA_g	0.75 E_cI_g
Basement walls	1.0 E_cA_g	1.0 E_cI_g
Diaphragm	0.5 E_cA_g	0.5 E_cI_g

Ec is the modulus of elasticity of concrete. *Ag* is the gross area of the cross section. *Ig* is the moment of inertia calculated on gross properties of the cross section. *Ie* is the clear span of coupling beam *h* is coupling beam depth. Some values for effective stiffness in the above table may exceed the values of the prescriptive procedure that are intended for design level shaking. The reason is that structural members subjected to SLE shaking will experience limited cracks compared to crack widths and patterns for design level shaking.

5.3.2 Accidental Torsion Effect

For SLE shaking, the TBI guidelines do not require consideration of the effect of accidental torsion in the model.

5.4 MODELING REQUIREMENTS FOR NONLINEAR ANALYSIS

As noted above, nonlinear analysis can be used for both SLE and MCER levels.

5.4.1 Effective Stiffness for MCER

For SLE nonlinear analysis, effective stiffness in Table 5.2 will be used for any components that are assumed to be elastic during the SLE shaking level. In the nonlinear analysis for MCER, a component that remains elastic during the MCER shaking level needs to be modeled with its effective stiffness. The TBI guidelines provide the values for effective stiffness for structural elements that respond elastically for MCER shaking. Table 5.3 shows values of effective stiffness for reinforced concrete elements for MCER shaking level.

Table 5.3 Reinforcing Concrete Elements Stiffness for MCER (adopted from (TBI 2017)).

Component	Axial Stiffness	Flexure Stiffness
Column	1.0 E_cA_g	0.7 E_cI_g
Beam	1.0 E_cA_g	0.3 E_cI_g
Coupling Beam	1.0 E_cA_g	$0.07\left(\frac{l_e}{h}\right)E_cI_g \leq 0.3E_cI_g$
Structural Wall	1.0 E_cA_g	0.35 E_cI_g
Basement Wall	1.0 E_cA_g	0.8 E_cI_g
Diaphragm	0.25 E_cA_g	0.25 E_cI_g

5.5 OPENSEES

The Open System for Earthquake Engineering Simulation, OpenSees, is a software framework for simulating the characteristics of the seismic behavior of structural or geotechnical systems. OpenSees is developed at the Pacific Earthquake Engineering Research Center (PEER) for research in performance-based approaches for earthquake engineering. OpenSees has powerful capabilities for conducting nonlinear static and dynamic analyses. The modeling capabilities contain a wide range of materials models, various elements models, and various solution algorithms. Various uniaxial materials are provided and could be utilized for modeling concrete, steel bars, etc. In addition, discretization of structural sections into fibers is also provided. For elements modeling, OpenSees provide one-dimension elements and continuum elements. Various algorithms are provided for conducting the nonlinear analysis. A full description for all components of OpenSees are provided in its manual (Mazzoni et al. 2006).

5.6 SELECTED MODELING APPROACHES

The modeling approach that used for preparation the case study model was discussed in the previous sections. A brief summary about the final modeling approaches will be presented.

- Three-dimension model
- Core walls: the shell element with the layered section were used for simulating the behavior of the core wall from the base up to the roof. Fourteen layers were used for simulating the cross section of the core wall.
- Beam or column of special moment frame: the force-based beam-column element with fiber section were used for simulating the behavior of the columns and beams of the special moment frame. Four hundred fibers were used for simulating the core concrete of the columns and the beams. Forty fibers were used for simulating the cover concrete in the beams and columns. Each reinforcing steel bar was simulated by one fiber.
- Diaphragm: rigid diaphragm
- Basement walls: shell elements with elastic section
- Podiums: shell element with elastic section
- Concrete materials: concrete02
- Reinforcing steel materials: Steel02

Figure 5.6 depicts the nonlinear model that created by the available elements in Opensees. 7046 Nodes and 7200 elements were used for creating the model of the case study building. This model was used in all analyses for all cases for both SLE and MCER shaking levels.

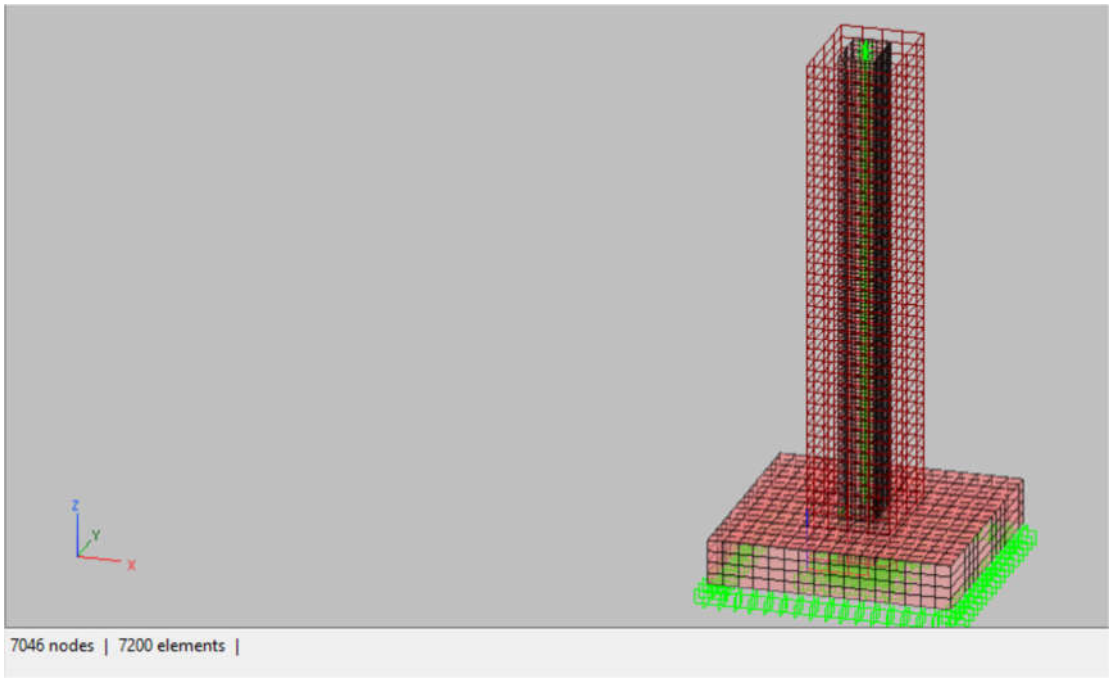

Figure 5.6 Nonlinear Model for the Case Study Building in Opensees.

5.7 VALIDATION OF SELECTED ELEMENT AND MATERIALS MODELS

To validate the model of the force-based beam-column element that will be used in modeling beams, columns, and walls of the case study building, experimental results from other works will be used. In addition, the material models for concrete, conventional reinforcement, high strength reinforcement, and shape memory alloys will be validated with experimental test results.

By using the capabilities in OpenSees, the model of experimental specimens was prepared by using the force-based beam column with five integration points. The fiber section was used for modeling the concrete and steel in the cross-sections. For the concrete material model, the concrete02 model in OpenSees was used. For steel reinforcing bars, the steel02 material in OpenSees was used. These material models are described in the OpenSees manual (Mazzoni et al. 2006). A brief presentation of the material models is provided in Section 5.8. The Mander model

for confined concrete was used for the concrete core (Mander et al. 1988).

5.7.1 Experimental Results from Haber et al. (2014)

The column specimen from the work of (Haber et al. 2014) will be chosen to validate the beam-column model. Table 5.4 shows dimensions and materials properties for the column specimen. The column was tested cyclically with a constant axial load of 200 kips. For each drift amplitude, two cycles were applied. The drift amplitudes were 0.25, 0.5, 0.75, 1, 2, 3, 4, 5, 6, 8, and 10 percent. The test setup ids depicted in Figure 5.7. Figure 5.8 depicts the comparison between the experimental results and numerical model.

Table 5.4 Column Specimen Characteristics Tested by Haber et al. (2014).

Column parameters	**Value**
Height	108 in.
Diameter	24.0 in.
Concrete cover	1.5 in.
Concrete compressive strength	4.33 ksi
Longitudinal steel	11 No. 8, Grade 60
Transverse steel	No. 3 spiral @ 2 in.

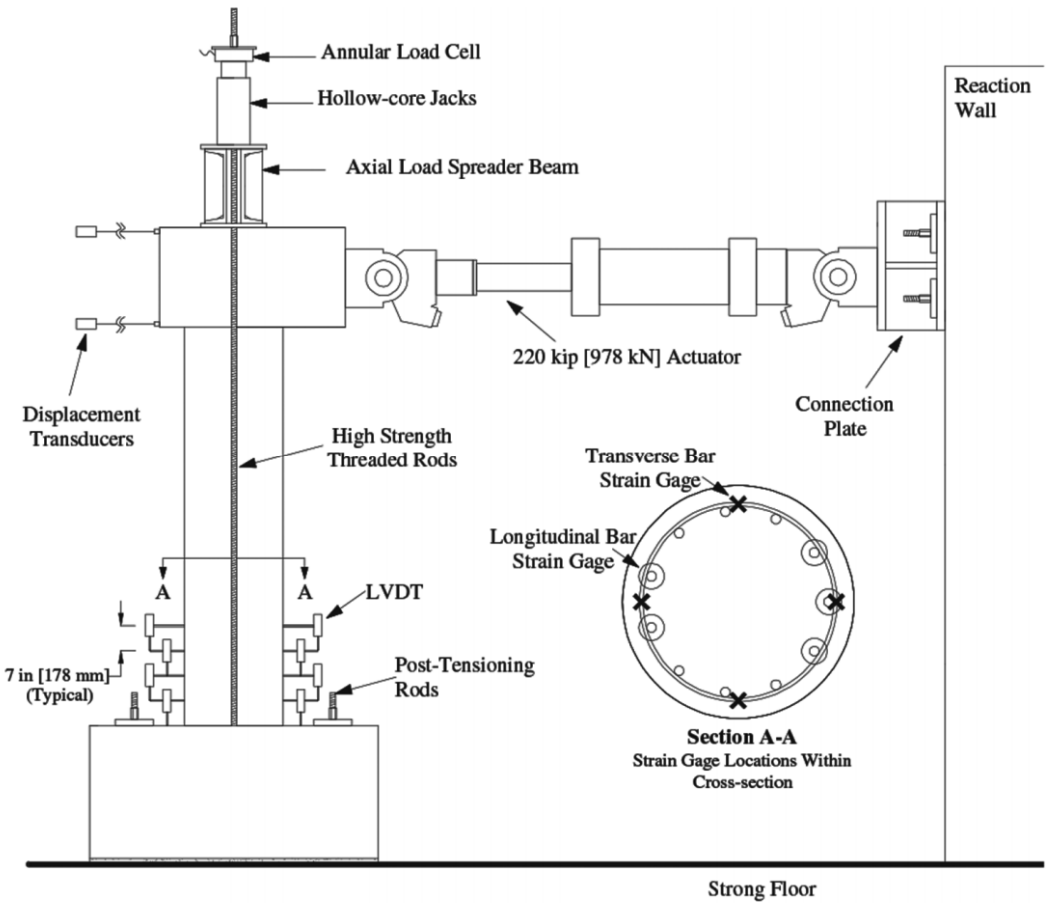

Figure 5.7 Test Setup (Haber et al. 2014).

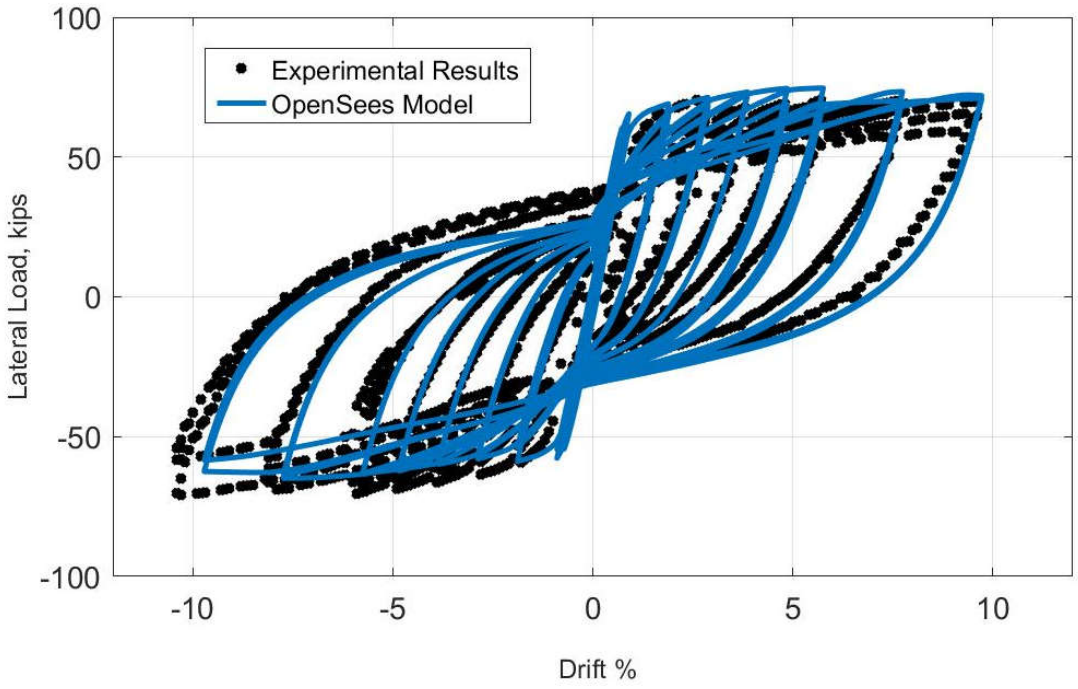

Figure 5.8 Experimental and Numerical Responses of a Column Tested by Haber et al. (2014).

5.7.2 Experimental Results from Dazio et al. (2009)

A large-scale wall specimen was tested under cyclic loading by (Dazio et al. 2009). The tested wall (WSH4) parameters are in Table 5.5. Figure 5.9 shows the dimensions of the tested wall and the cross-section with the reinforcement layout. The shell element with layered section in Opensees was used for simulating the tested wall. Figure 5.10 depicts the comparison between the experimental results and the numerical model for the wall specimen.

Table 5.5 Wall Specimen Characteristics Tested by Dazio et al. (2009).

Wall parameters	**Value**
Height	4950 mm
Width	2000 mm
Thickness	150 mm
Concrete compressive strength	41 MPa
Steel reinforcement Grade	60 A 706
Longitudinal steel, ρ_{bound} (%)	1.54
Longitudinal steel, ρ_{web} (%)	0.54
Horizontal steel, ρ_h (%)	0.25

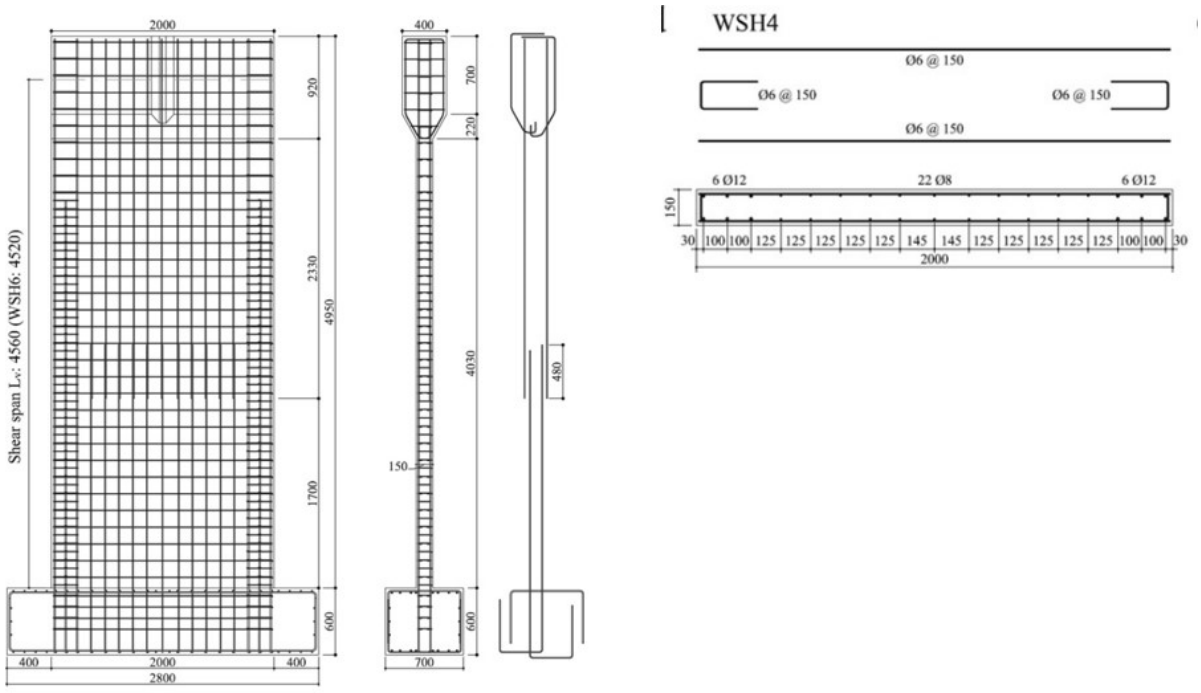

Figure 5.9 The Test Unit (WSH4) Dimensions and Cross Section (Dazio et al. 2009).

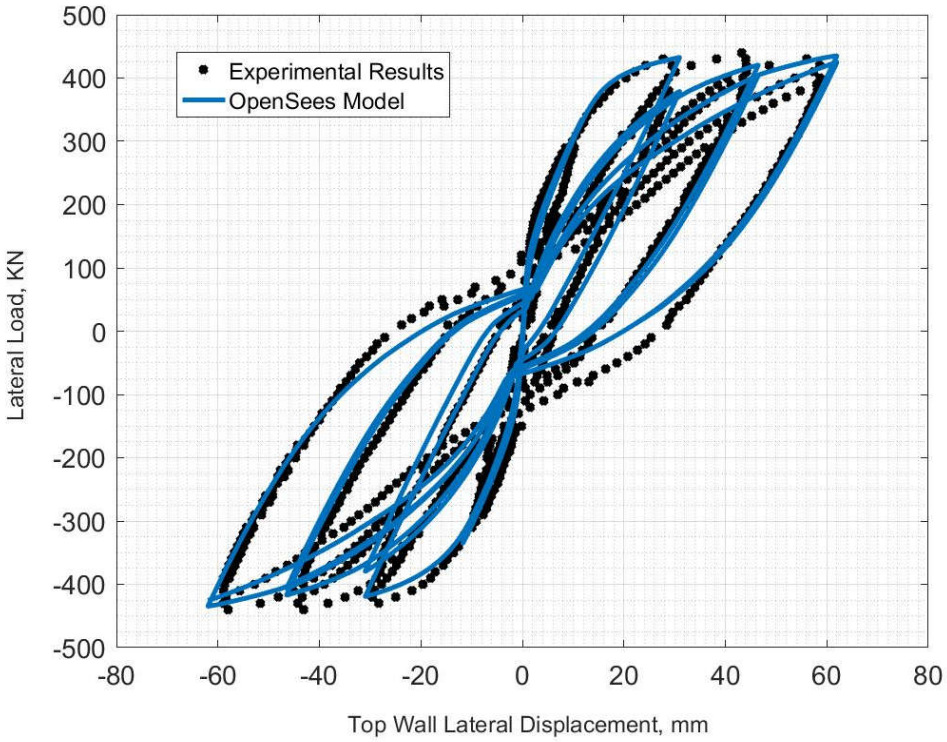

Figure 5.10 Experimental and Numerical Responses for Wall Tested by Dazio et al.(2009).

5.7.3 Experimental Results from Sokoli and Ghannoum (2016)

High strength Grade 80 reinforcement was used for longitudinal reinforcement in the column specimen in the work by (Sokoli and Ghannoum 2016). The dimension of the column and its cross-section are depicted in Figure 5.11. The column was tested cyclically. The model of (steel02) in Opensees was used for modeling the high strength steel bars for the tested column. The column parameters are shown in Table 5.6. Figure 5.12 depicts the comparison between the experimental results and the numerical model for the column specimen reinforced with Grade 80 reinforcement.

Table 5.6 Column Specimen Characteristics Tested by Sokoli and Ghannoum (2016).

Column parameters	**Value**
Height	84 in.
Cross-section	18 in. x 18 in.
Concrete compressive strength	4.5 ksi
Long. Steel reinforcement Grade	80 A 706
Longitudinal steel, ρ (%)	12#9 = 3.7
Transverse steel, ρ (%)	#4@5.5

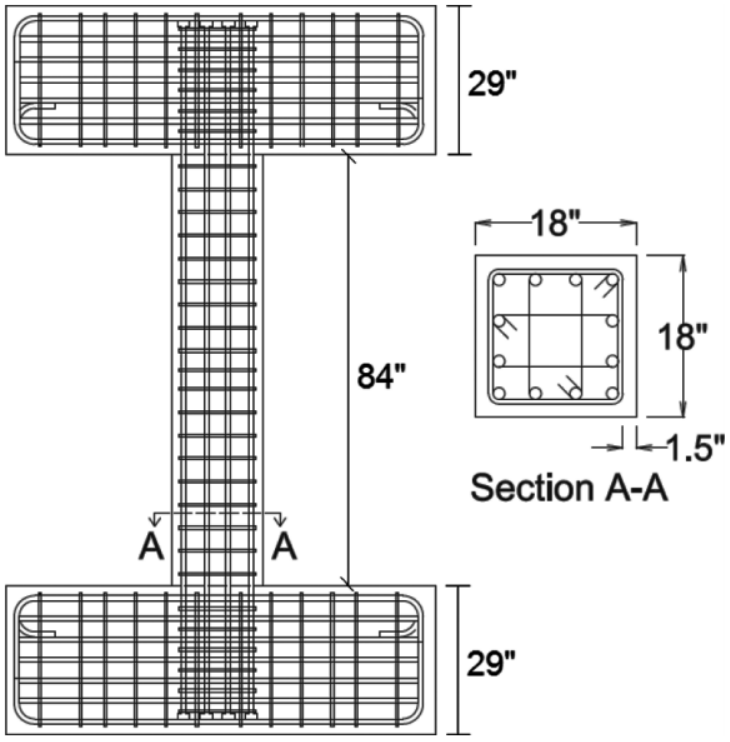

Figure 5.11 The Test Unit Dimensions and Cross Section (Sokoli and Ghannoum 2016).

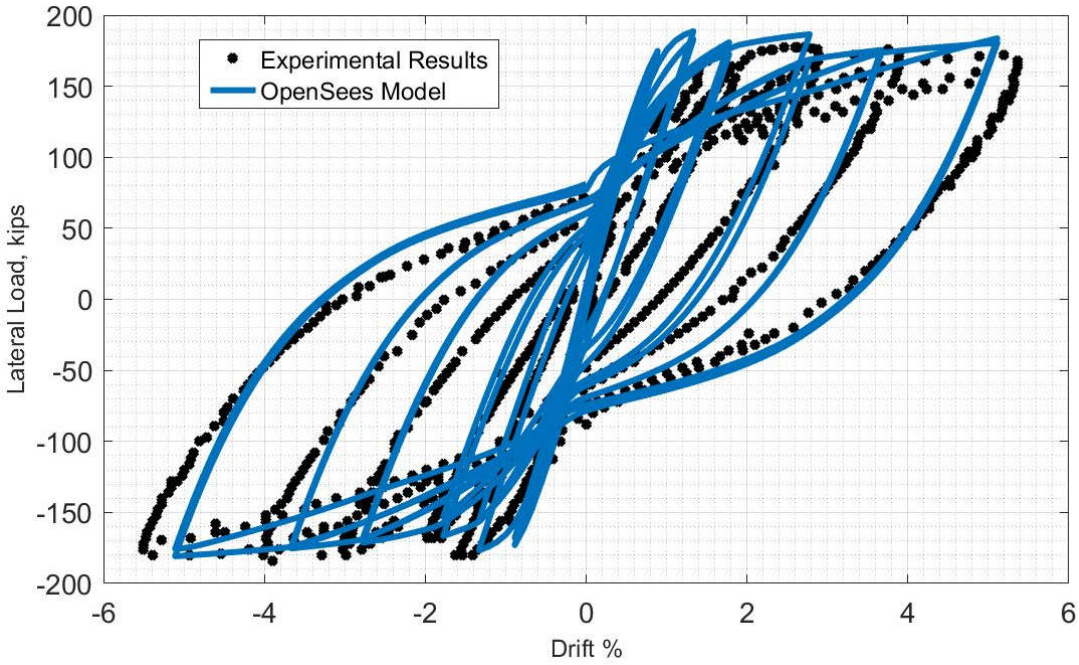

Figure 5.12 Experimental and Numerical Responses of a Column Tested by Sokoli and Ghannoum (2016).

5.7.4 Experimental Results from Sokoli et al. (2017)

High strength Grade 100 ASTM 1035 reinforcement was used for longitudinal reinforcement in the column specimen in the work by (Sokoli et al. 2017). The column was tested cyclically. The specimen dimension and reinforcement details are depicted in Figure 5.13. The model of (steel02) in Opensees was used for modeling the high strength steel bars (Grade 100 ASTM 1035) for the tested column. The column parameters are shown in Table 5.7. Figure 5.14 depicts the comparison between the experimental results and the numerical model for the column specimen reinforced with Grade 100 reinforcement.

Table 5.7 Column Specimen Characteristics Tested by Sokoli et al. (2017).

Column parameters	**Value**
Height	108 in.
Cross-section	18 in. x 18 in.
Concrete compressive strength	5.5 ksi
Long. Steel reinforcement Grade	100 A STM 1035
Longitudinal steel, ρ (%)	8#6=1.1
Transverse steel, ρ (%)	#4@3.5

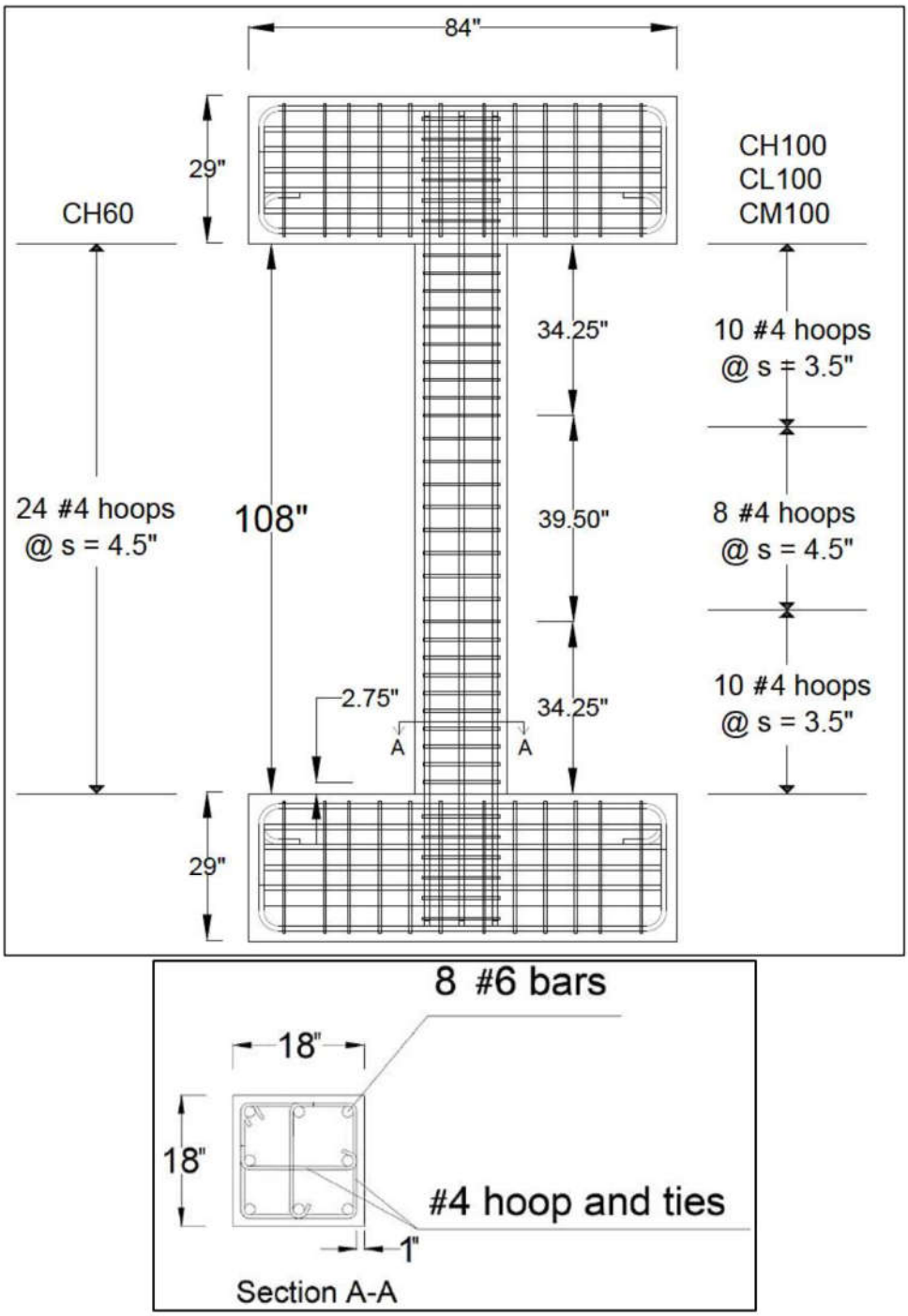

Figure 5.13 Dimensions and Reinforcement Details for Column tested by Sokoli et al. (2017).

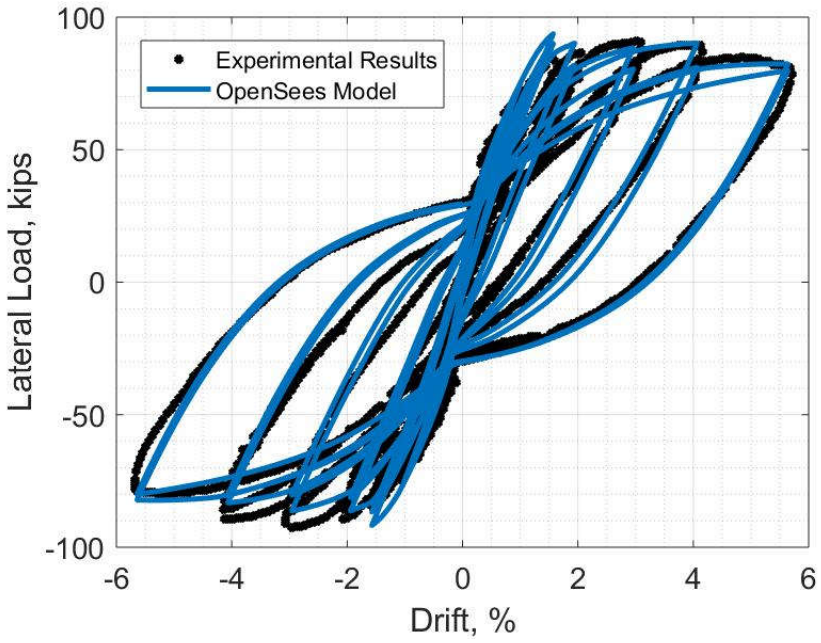

Figure 5.14 Experimental and Numerical Responses of a Column Tested by Sokoli et al. (2017).

5.7.5 Experimental Results from Pfund. (2012)

High strength Grade 120 ASTM 1035 reinforcement was used for longitudinal reinforcement in the beam specimen in the work by (Pfund 2012). The beam shown in Figure 5.15 was tested cyclically. The model of (steel02) in Opensees was used for modeling the high strength steel bars (Grade 120 ASTM 1035) for the tested beam. The beam parameters are shown in Table 5.8. Figure 5.16 depicts the comparison between the experimental results and the numerical model for the beam specimen reinforced with Grade 120 reinforcement.

Table 5.8 Beam Specimen Characteristics Tested by Pfund (2012).

Beam parameters	Value
Length	72in.
Cross-section	10 in. x 16 in.
Concrete compressive strength	5.8 ksi
Long. Steel reinforcement Grade	120 ASTM 1035
Longitudinal steel, ρ (%)	3#6 top & bot.

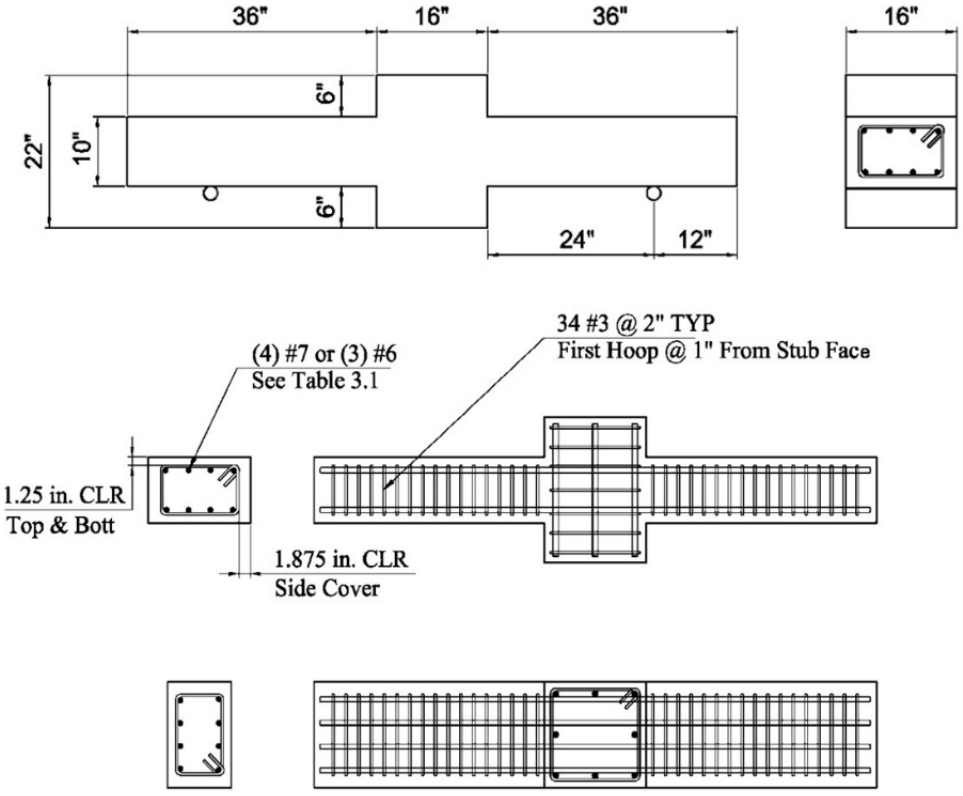

Figure 5.15 Specimen MC4-X Reinforced with Grade 120, Tested by (Pfund, 2012).

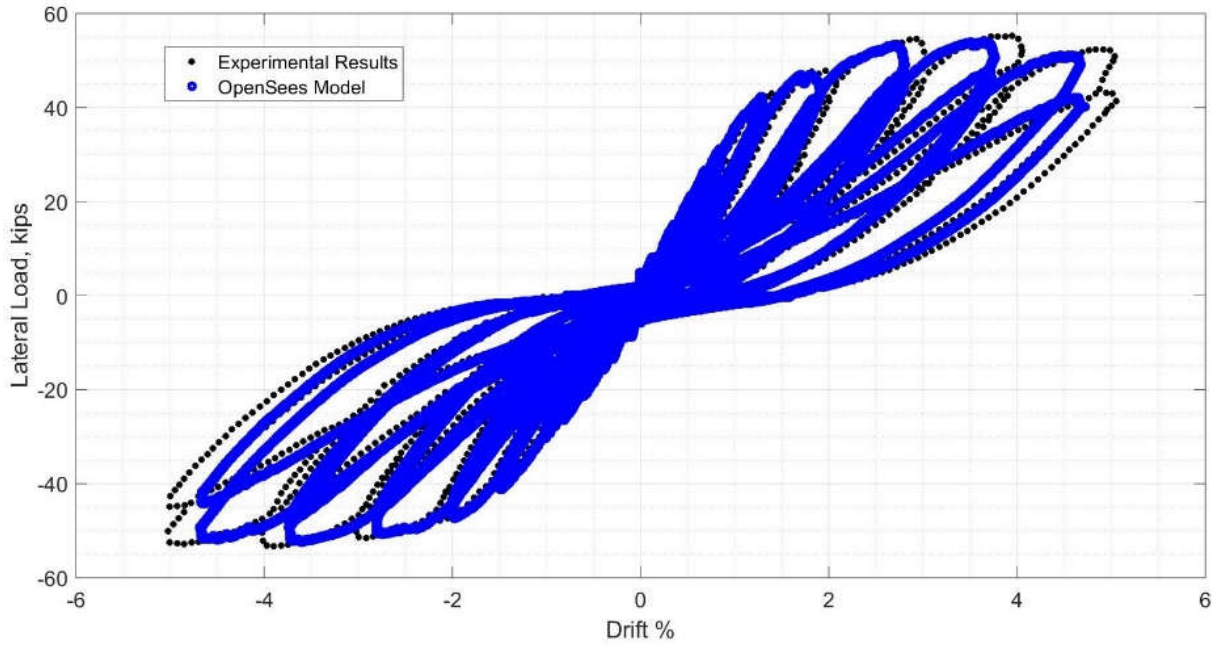

Figure 5.16 Experimental and Numerical Responses of a Beam Tested by Pfund (2012).

5.7.6 Experimental Results from Abdulridha et al. (2013)

In the study (Abdulridha et al. 2013), shape memory alloy reinforcement was used as alternative reinforcing bars for concrete beams. The beam specimen shown in Figure 5.17 was tested cyclically to show the effect of shape memory alloy bars in reducing the permanent deformation. The Self-Centering model in OpenSees was used for modeling the shape memory alloy bars. The specimen beam parameters are in Table 5.9. Figure 5.18 depicts the comparison between the experimental and the numerical model for the beam specimen reinforced with longitudinal SMA bars.

Table 5.9 Beam Specimen Characteristics Tested by Abdulridha et al. (2013).

Beam parameters	Value
Length	2400 mm
Cross section	125 mm * 250 mm
Concrete compressive strength	32.7 MPa
SMA bars diameter	9.5 mm

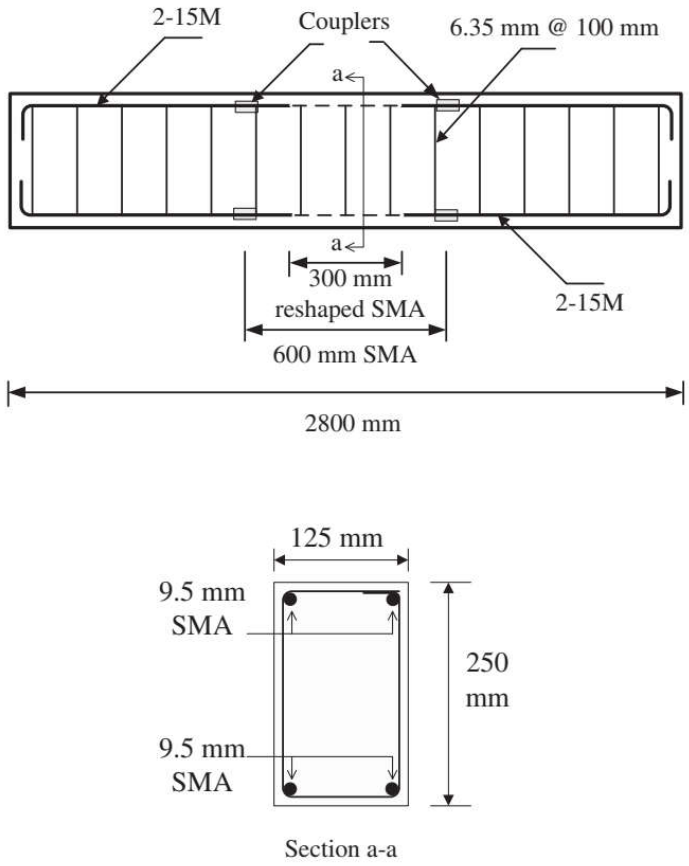

Figure 5.17 Reinforcement Details of the beam tested by Abdulridha et al.(2013).

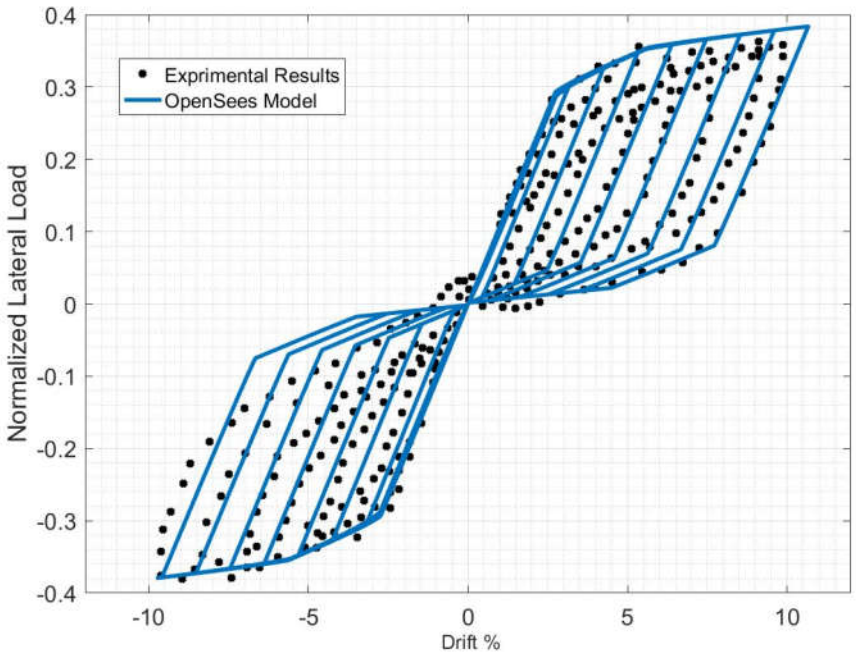

Figure 5.18 Experimental and Numerical Responses of a SMA reinforced Beam from Abdulridha et al. (2013).

5.8 MATERIAL MODELS

As shown in Section 5.7, the use of concrete02 and steel02 in OpenSees shows a good agreement between OpenSees models and the experimental data. In this section, a brief introduction about these two types of materials models is provided. In addition, These materials model are descripted in OpenSees manual (Mazzoni et al. 2006).

5.8.1 Concrete02 Model

A full description for the model and its hysteretic loops rules is provided in (Yassin 1994) . Here, a brief description about the envelope of the stress strain curve will be presented. Figure 5.19 depicts the stress strain curve for the concrete02. The monotonic envelope for compression stress strain relationship could be represented by three lines, as shown in Figure 5.19:

$$\text{Line OA} \qquad \varepsilon_c \le \varepsilon_0 \quad \sigma c = K\, f'_c \left[2\left(\frac{\varepsilon_c}{\varepsilon_0}\right) - \left(\frac{\varepsilon_c}{\varepsilon_0}\right)^2\right] \tag{5-2}$$

$$\text{Line AB} \qquad \varepsilon_0 \le \varepsilon_c \le \varepsilon_{20} \quad \sigma c = K\, f'_c \left[(1 - Z)(\varepsilon_c - \varepsilon_0)\right] \tag{5-3}$$

$$\text{Line BC} \qquad \varepsilon_c \ge \varepsilon_{20} \quad \sigma c = 0.2\, K\, f'_c \tag{5-4}$$

where ε_0 is the strain at the f'_c (the maximum compressive strength), ε_{20} is the strain at a stress of 20 percent of the maximum strength, K is the factor for confinement effects and is calculated from Mander model (Mander et al. 1988), and Z is the strain softening slope.

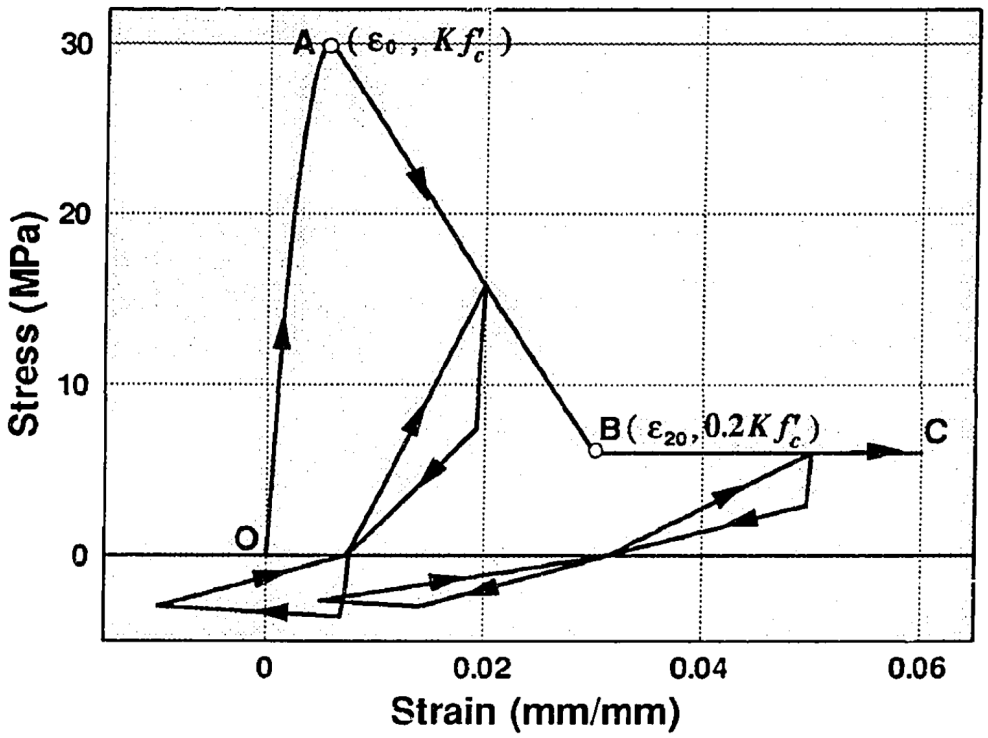

Figure 5.19 Stress Strain Relationship for Concrete Model (Concrete02) (Yassin 1994).

To define the model in OpenSees, the user needs to define the stress and strain at the maximum point and the point of crushing. The model also includes the tension effect by assuming a linear relationship up to the maximum tensile strength of concrete, which will be defined by the user.

5.8.2 Steel02 Model

A full description of the Steel02 model was introduced by (Filippou et al. 1983). A simple description is presented here. Figure 5.20 depicts the stress-strain curve of the model. The model is represented by Equation (5-5).

$$\sigma^* = b\,\varepsilon^* + \frac{(1-b)\varepsilon^*}{[1+\varepsilon^{*R}]^{\frac{1}{R}}} \tag{5-5}$$

$$\sigma^* = \frac{\sigma - \sigma_r}{\sigma_0 - \sigma_r} \tag{5-6}$$

$$\varepsilon^* = \frac{\varepsilon - \varepsilon_r}{\varepsilon_0 - \varepsilon_r} \tag{5-7}$$

$$R = R_0 - \frac{a_1 \xi}{a_2 + \xi} \tag{5-8}$$

The above equations give the curve transition from line with E_0 to line with slope E_1, as in Figure 5.20. Parameters σ_0 and ε_0 represent the point where the current two lines (with different slopes) intersect, as in Figure 5.21. Parameters σ_r and ε_r represent the point of the last strain reversal with the same sign stress with σ_0. The term b is the strain hardening ratio. The parameter R affects the shape of the curve and determined by Equation (5-5). Parameters (R_0, a_1, a_2) are calculated from experimental data. At the first cycle only, R is equal to R_0. Figure 5.21 shows the definition of (ξ). The user needs to define the yield strength, modulus of elasticity, hardening ratio,

and the parameters (R_0, a_1, a_2) in OpenSees.

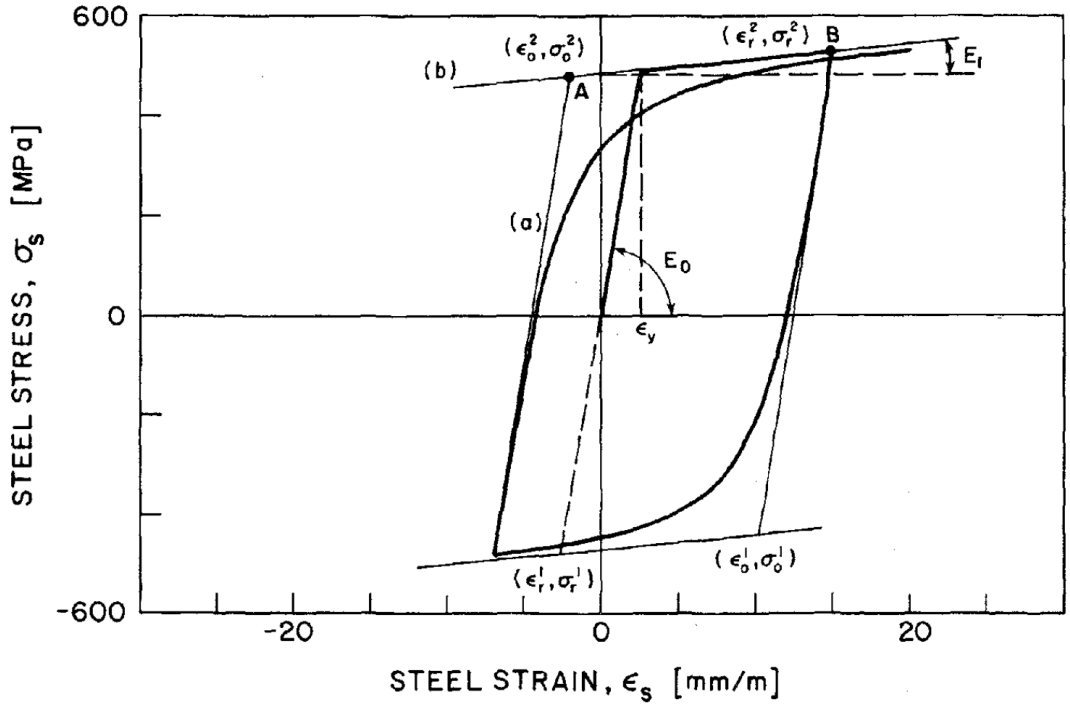

Figure 5.20 Stress Strain Relationship for Steel02 Model (Filippou et al. 1983).

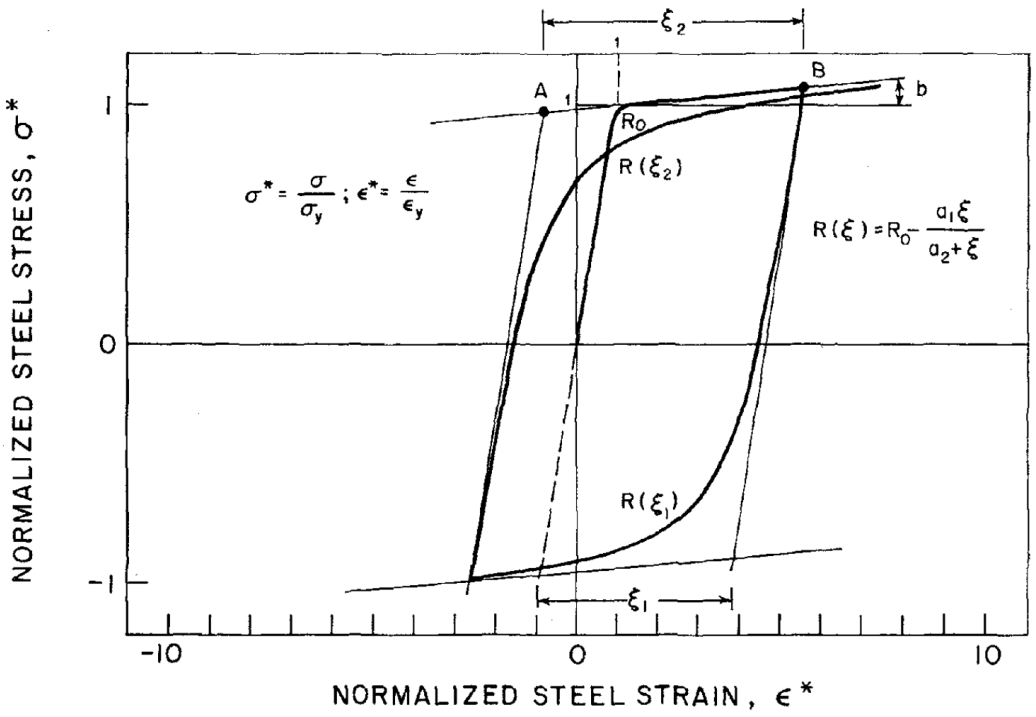

Figure 5.21 Definition of Curvature Parameter in Steel02 Model (Filippou et al. 1983).

5.8.3 Self-Centering Material

The available material for simulating the behavior of the shape memory alloy in Opensees is the (SelfCentering Material). A full description about this material model is available in (Tazarv and Saiidi 2014). A brief description about this model is presented in Section 2.3.7.2. The most important finding from the study is that depending on the results from the literature review, tests by the authors, and tests by the SMA manufactures, the author could establish a range of values for each parameter of the model *(k1, k2, fy, εu, β*), as in Figure 5.22. The recommended values for the parameters represent the expected values of the strength and strain of shape memory alloy and could be used for the seismic design and analysis. The values of (*k1, k2, fy, εu, β*) are (5500 ksi, 250 ksi, 55 ksi, 0.1, 0.65). The study recommended that the maximum recoverable strain is 0.06.

The recommended values were used in this work for defining the parameters of the model of (SelfCentering Material) in Opensees for simulating the behavior of the shape memory alloys bars.

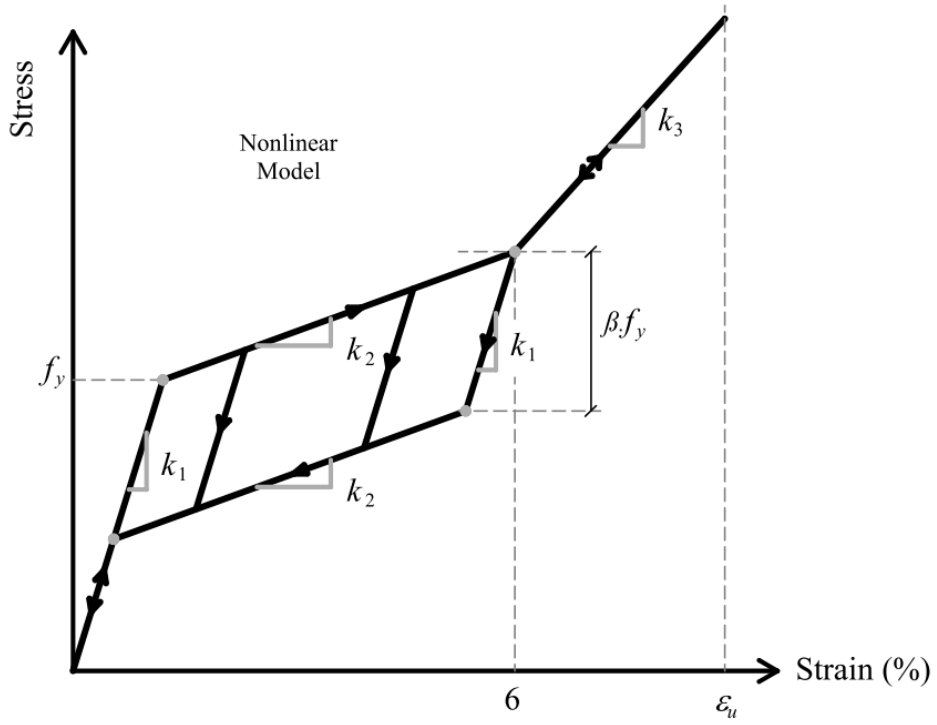

Figure 5.22 Nonlinear Model for Shape Memory alloy (Tazarv and Saiidi 2014).

CHAPTER VI

SELECTION AND MODIFICATION OF GROUND MOTION RECORDS

6.1 SELECTION OF SUITE OF GROUND MOTION RECORDS

The TBI guidelines recommend following the ASCE 7-16 procedure for selection and modification of ground motion records. The TBI guidelines, as well as ASCE 7-16, require a minimum number of 11 ground motion records in the suite for nonlinear response history analysis for MCER shaking. For SLE shaking, the TBI guidelines require a minimum number of seven records for nonlinear analysis. As pointed out in ASCE 7-16 and in its commentary for Chapter 16, the selection process can be performed through two stages. In the first stage, a suite of records from a ground motion database, such as the PEER Ground Motion Database, is preselected. The ground motion records should have a compatible source mechanism, magnitude, site to source distance, and site soil conditions with the target spectrum for the specific shaking level for the specific site. In the second stage, different criteria such as spectral shape, scale factor, and the number of records from the same event are applied to the records in order to choose the final records for the suite. The ground motion spectrum should have a similar shape as the target spectrum. In addition, the required scale factor for the ground motion must be limited and the allowable range is taken as 0.25 to 4.0. The last criterion is the number of records from the same seismic event. In general, only three to four records from a single event may be incorporated into the suite.

For the case study building, the analysis of site seismic hazard was done in the PEER report (Moehle et al. 2011). In the PEER report, it is recommended that any ground motion record with a maximum source distance of 100 km, and maximum shear velocity of 30 m/sec could be a

candidate record for the suite. According to the PEER report, these limitations are applied to make sure that all selected ground motions are compatible with the seismic characterization of the location of the case study building. After the initial selection which is done by considering the source distance and shear wave velocity, the other requirements such as the spectral shape, scale factor, and the number of records from the same event are applied to make the final selection. The same procedure was applied for both the SLE and MCER levels for ground motions selection.

6.2 SCALING AND MODIFYING GROUND MOTION RECORDS

The TBI guidelines follow the modification procedure of ASCE 7-16. The purpose of the scaling or modification of the ground motion records is to provide compatibility between the ground motions in the suite and the target spectrum for a specific shaking level.

After completing the selection of the required number of ground motion records for a specific shaking level, the scaling process is as follow:

- For each ground motion, find the maximum-direction spectrum. After finding the spectrum of each horizontal component of the ground motion, the maximum-direction spectrum for the ground motion can be determined by finding the geometric mean of the spectra of the horizontal components and then multiplying the geometric mean by the values from Table 6.1 for each period. In Table 6.1, linear interpolation can be used for the other periods.
- Specify the range of periods. According to ASCE 71-6, the period range is *2.0T* to *0.2T*, where *T* is the fundamental period of the structure.
- Find the initial scale factor for each ground motion. Scale the maximum-direction spectrum so that the value of the maximum-direction spectrum at the fundamental period value is the same as the value of the target spectrum of the shaking level. Repeating the same process for all ground motions, then each ground motion should have its own initial scale factor. It

is important to note that it is not necessary to choose the fundamental period value to make the equality between the maximum-direction spectrum and shaking level spectrum, however the period should be inside the selected range of periods as above.

- Find the mean value of the scaled maximum-direction spectrum. For each ground motion, multiply its initial scale factor by its maximum-direction spectrum and then find the mean value of the scaled maximum-direction spectra of all ground motions in the suite.
- Find the suite scale factor. The suite factor can be defined as one value that makes the mean value of the scaled maximum-direction spectrum of all ground motions equal or larger than 90% of the target spectrum for each period inside the period range.
- Finally, find the scale factor for each ground motion. The scale factor for a specific ground motion can be determined by multiplying its initial scale factor by the suite scale factor. This scale factor should be used for both horizontal components of the ground motion during the analysis.

Table 6.1 Values of the Maximum-direction Spectrum to the Geometric Spectrum (adopted from (FEMA 2015)).

Period (sec)	Value
0.0	1.1
0.1	1.1
0.2	1.1
0.3	1.1
0.5	1.2
1.0	1.3
2.0	1.3
4.0 and larger	1.4

6.3 GROUND MOTION FOR SLE LEVEL

According to the TBI guidelines, the minimum required number of ground motions for the SLE level is seven for nonlinear analysis. Figure 6.1 depicts the target spectrum for the SLE shaking level. Table 6.2 shows the seven ground motions that are selected and scaled to match the SLE spectrum. The unscaled maximum-direction spectrum for each ground motion with their mean spectrum are shown in Figure 6.2. The scaled spectrums with their mean are depicted in Figure 6.3. Only the mean values of the scaled and unscaled spectrum are shown in Figure 6.4, beside the SLE spectrum. Figure 6.4 depicts that the scaled mean spectrum of the suite of motions is equal to or larger than the value of 0.9 times the SLE spectrum for the range of 1 second to 10 seconds. Consequently, the scale factors applied to the selected ground motions satisfy the requirements of ASCE 7-16.

Table 6.2 Ground Motion Records for SLE Level.

No.	Record Sequence Number PEER	Earthquake Name	Year	Station Name	Magnitude	Distance (km)	V_{s30} (m/sec)	Points	*dt* (sec)	Scale Factor
1	1787	Hector Mine	1999	Hector	7.13	11.66	726	4531	0.01	1.13
2	1111	Kobe_ Japan	1995	Nishi-Akashi	6.9	7.08	609	4096	0.01	1.05
3	292	Irpinia_ Italy-01	1980	Sturno (STN)	6.9	10.84	382	16392	0.0024	0.55
4	832	Landers	1992	Amboy	7.28	69.21	382.93	2500	0.02	1.02
5	495	Nahanni, Canada	1985	Site 1	6.76	9.6	605.04	4113	0.0025	0.94
6	767	Loma Prieta	1989	Gilroy Array #3	6.93	12.82	349.85	7997	0.005	0.91
7	68	San Fernando	1971	LA,Hollywood Stor FF	6.61	22.77	316.46	7945	0.01	0.88

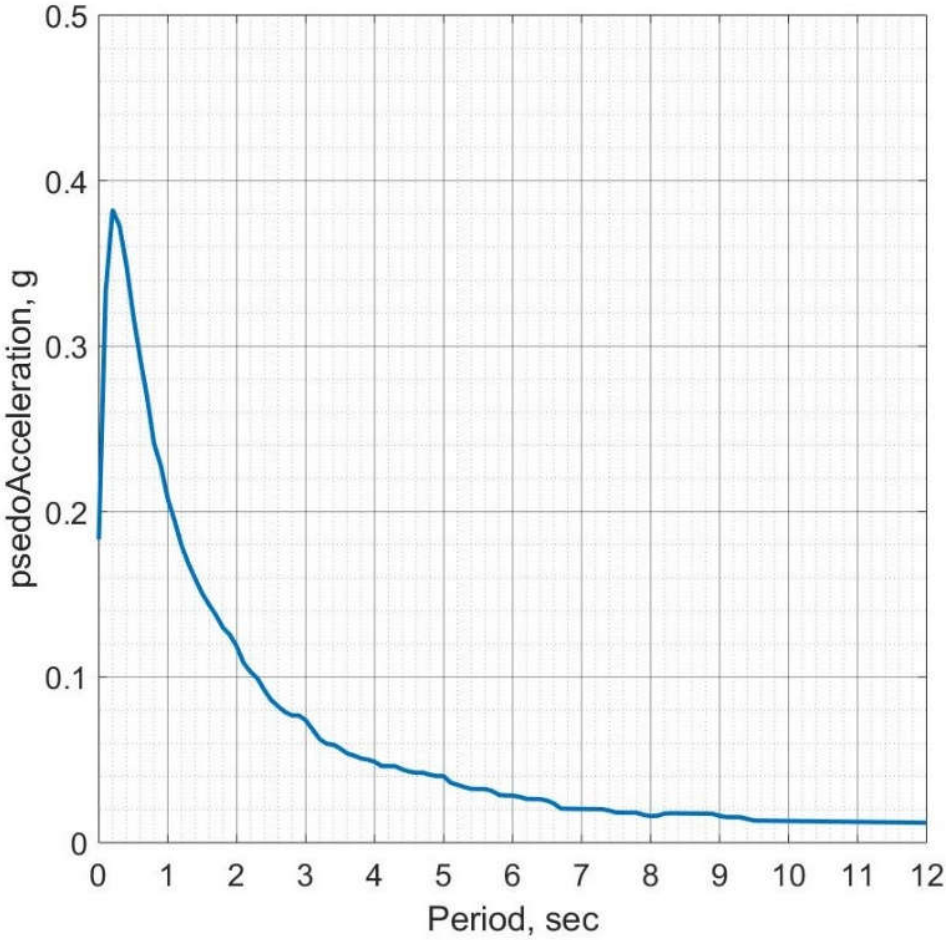

Figure 6.1 Service Level Earthquake Spectrum (adopted from (Moehle et al. 2011)).

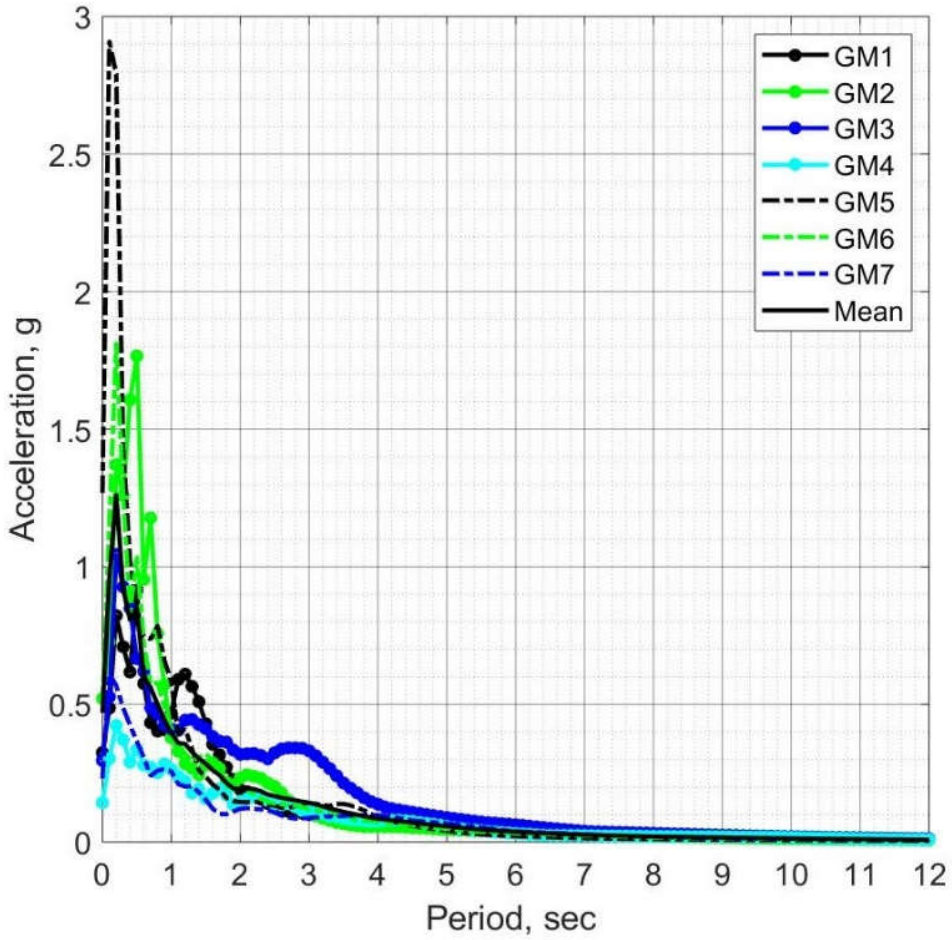

Figure 6.2 Unscaled Spectra for SLE Ground Motion Suite.

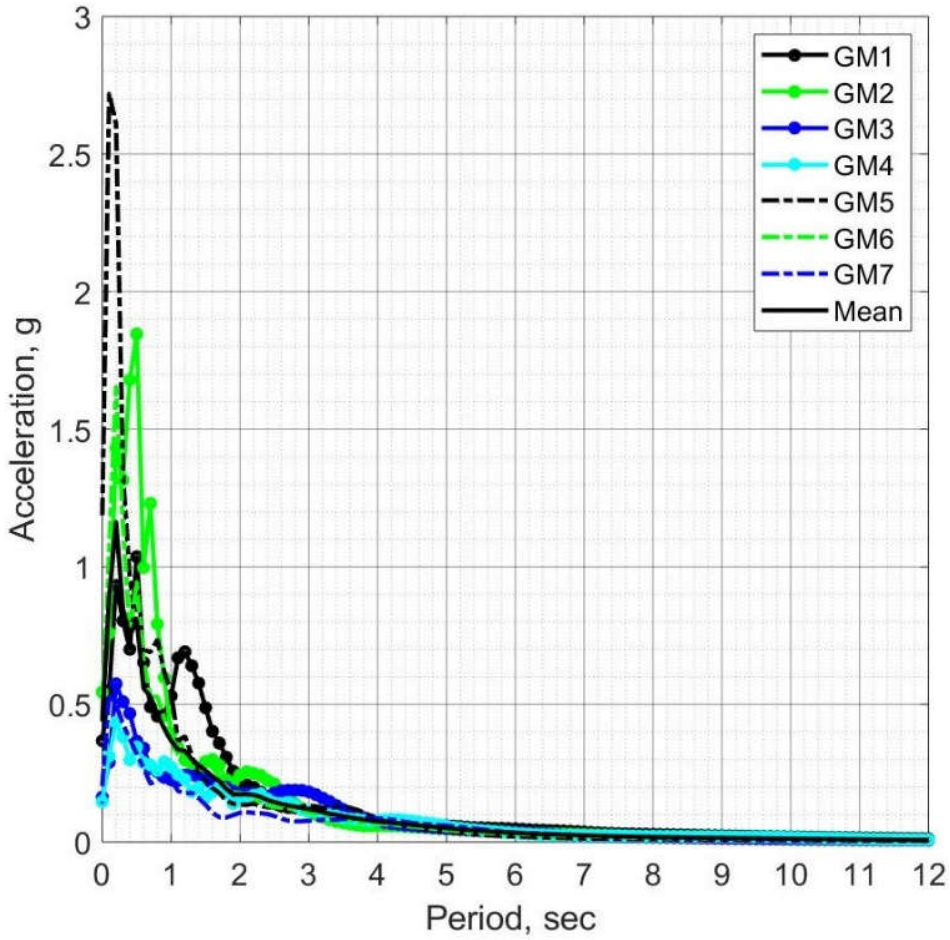

Figure 6.3 Scaled Spectra for SLE Ground Motion Suite.

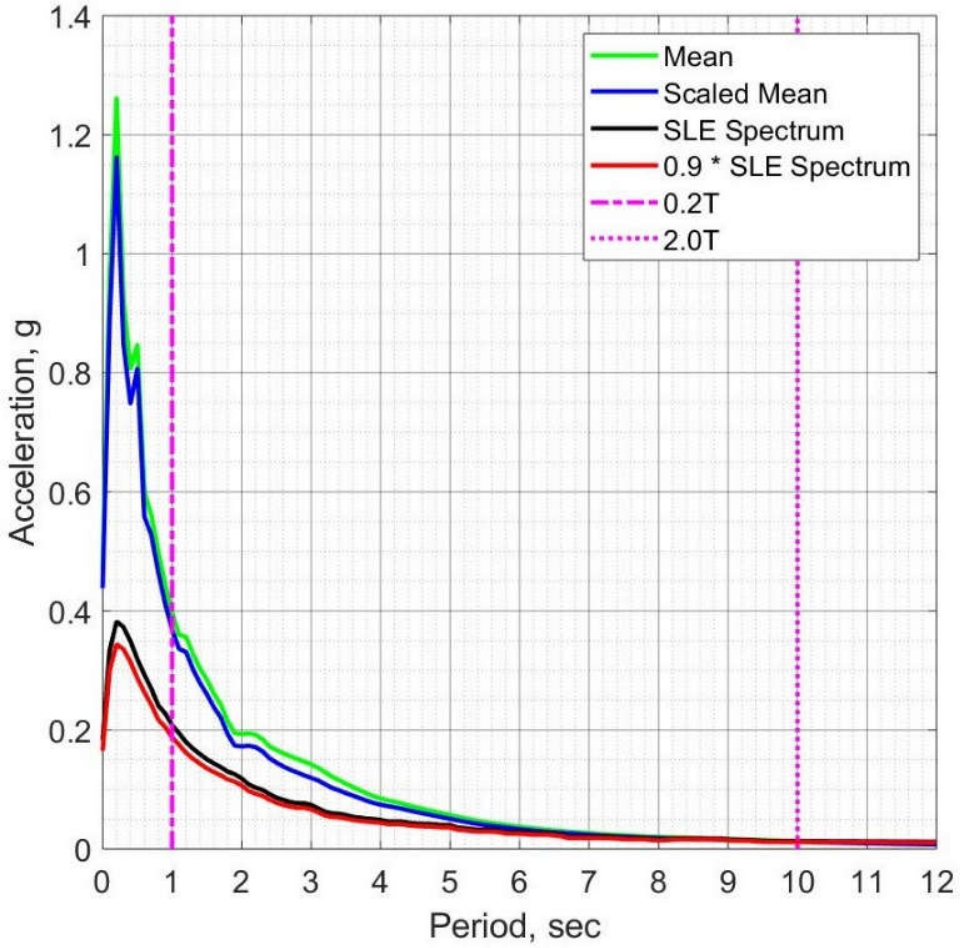

Figure 6.4 Scaled and Unscaled Mean for SLE Ground Motion Suite Spectra.

6.4 GROUND MOTION FOR MCER LEVEL

For the MCER level, the TBI guidelines require a minimum of 11 ground motions. Figure 3.8 depicts the target spectrum for the MCER shaking level. Table 6.3 shows the 11 ground motions that are selected and scaled to match the MCER spectrum. The unscaled maximum-direction spectrum for each ground motion with their mean spectrum are shown in Figure 6.5. The scaled spectrums with their mean are depicted in Figure 6.6. Only the mean values of the scaled and unscaled spectrum are shown in Figure 6.7, along with the MCER spectrum. Figure 6.7 depicts

that the scaled mean spectrum of the suite motions is equal or larger than the value of 90% of the MCER spectrum for the range of 1 second to 10 seconds. Consequently, the scale factors make the selected ground motions satisfy the requirements of ASCE 7-16.

Table 6.3 Ground Motion Records for MCER Level.

No.	Record Sequence Number	Earthquake Name	Year	Station Name	Magnitude	Distance (km)	V_{s30} (m/sec)	Points	*dt* (sec)	Scale Factor
1	1529	Chi-Chi, Taiwan	1999	TCU102	7.62	1.49	714.27	18000	0.005	1.2
2	2114	Denali, Alaska	2002	TAPS Pump Station #10	7.9	2.74	329.4	18419	0.005	1.4
3	1158	Kocaeli, Turkey	1999	Duzce	7.51	15.37	281.86	5437	0.005	2.2
4	721	Superstition Hills-02	1987	El Centro	6.54	18.2	192.05	11999	0.005	2.6
5	900	Landers	1992	Yermo, Fire Station	7.28	23.62	353.63	2200	0.02	2.6
6	1086	Northridge-01	1994	Sylmar - Olive View Med FF	6.69	5.3	440.54	2000	0.02	1.1
7	126	Gazli_ USSR	1976	Karakyr	6.8	5.46	259.59	2048	0.0066	2.1
8	181	Imperial Valley-06	1979	El Centro Array #6	6.53	1.35	203.22	7817	0.005	1.3
9	143	Tabas, Iran	1978	Tabas	7.35	2.05	766.77	1650	0.02	0.8
10	1244	Chi-Chi, Taiwan	1999	CHY101	7.62	9.94	258.89	1800	0.005	1.2
11	1605	Duzce, Turkey	1999	Duzce	7.14	6.58	281.86	5177	0.005	1.0

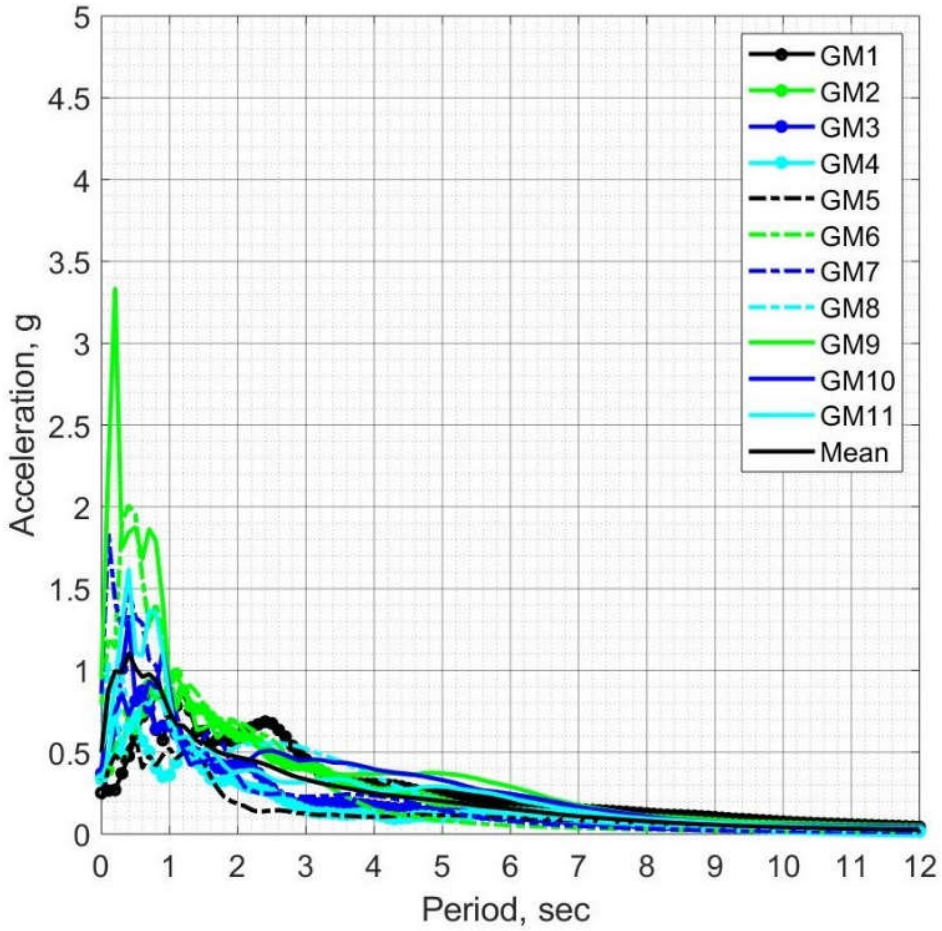

Figure 6.5 Unscaled Spectra for MCER Suite Motions.

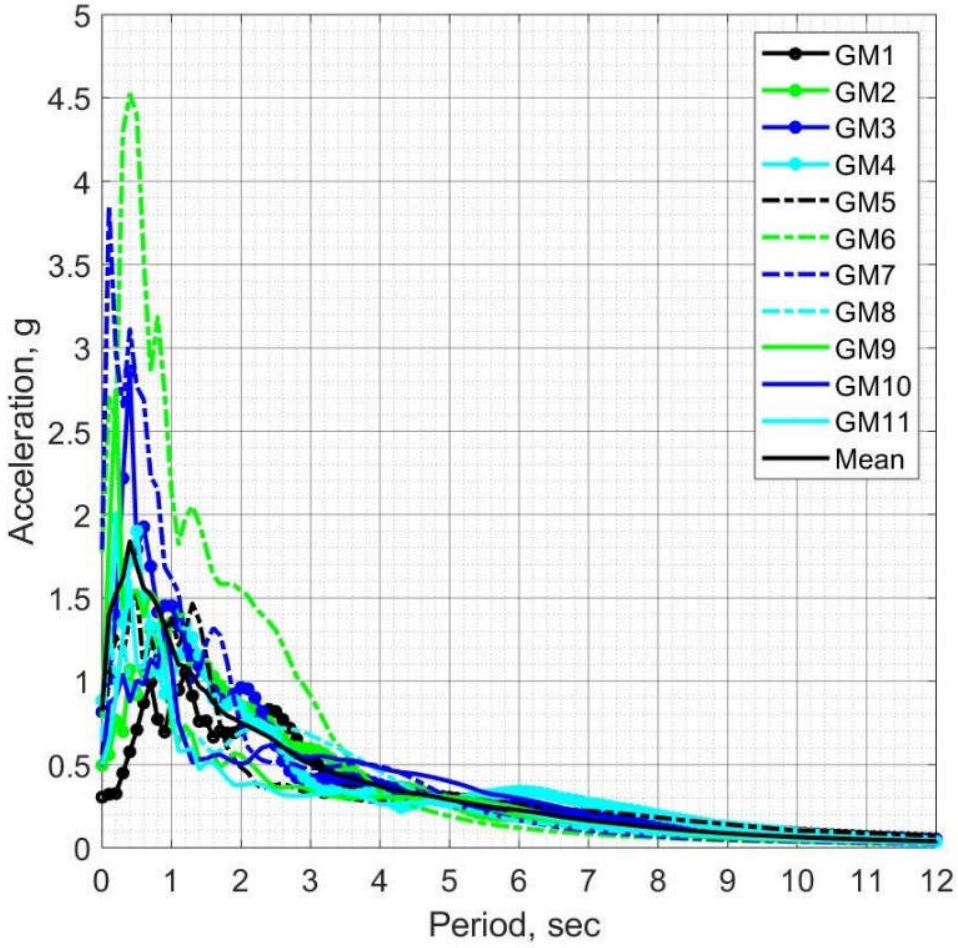

Figure 6.6 Scaled Spectrums for MCER Suite Motions.

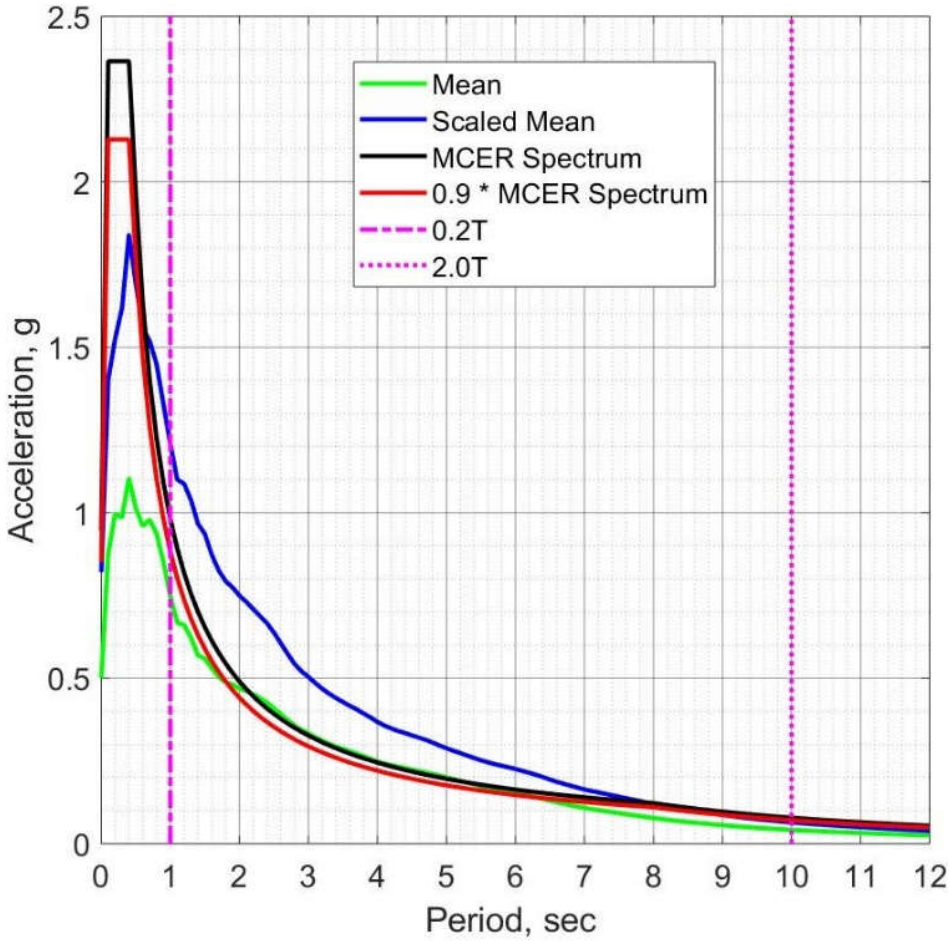

Figure 6.7 Scaled and Unscaled Mean for Spectrums for MCER Suite Motions.

CHAPTER VII

CASE 1 – GRADE 60 REINFORCEMENT RESULTS

7.1 INTRODUCTION

Case 1 consists of the case study building reinforced with conventional steel bars in all structural members. ASTM A706 Grade 60 reinforcement was used in the seismic force resisting system (SFRS) in both the core wall and the special moment frames. In the following sections, the response of the case study building will be examined and checked with the TBI guidelines acceptance criteria for both SLE and MCER levels.

7.2 SLE LEVEL

The results of seven analyses are presented and compared with the acceptance criteria of the TBI guidelines. According to the TBI guidelines, first, the mean value of the peak values of the response parameters from all ground motions in the suite should be checked with the acceptance criteria. Second, the TBI guidelines do not require checking the maximum response parameters from all ground motions in this level. However, the maximum response parameters will also be presented to examine the performance of the case study building in more depth.

7.2.1 Global Response

7.2.1.1 Drift Ratio

The drift ratio was calculated by dividing the difference in the lateral displacement in two points above and below the considered story by the height of that story.

Figure 7.1 show the mean and the maximum values of the drift ratios from all analyses over the building height. The mean peak interstory drift from the seven analyses was very close to 0.0045 in the x-direction and approximately 0.0030 in the y-direction, where both values were

within the acceptable limit of the TBI guidelines of 0.0050. Figures 7.2 and 7.3 show the peak drift ratios from all ground motions over the building height.

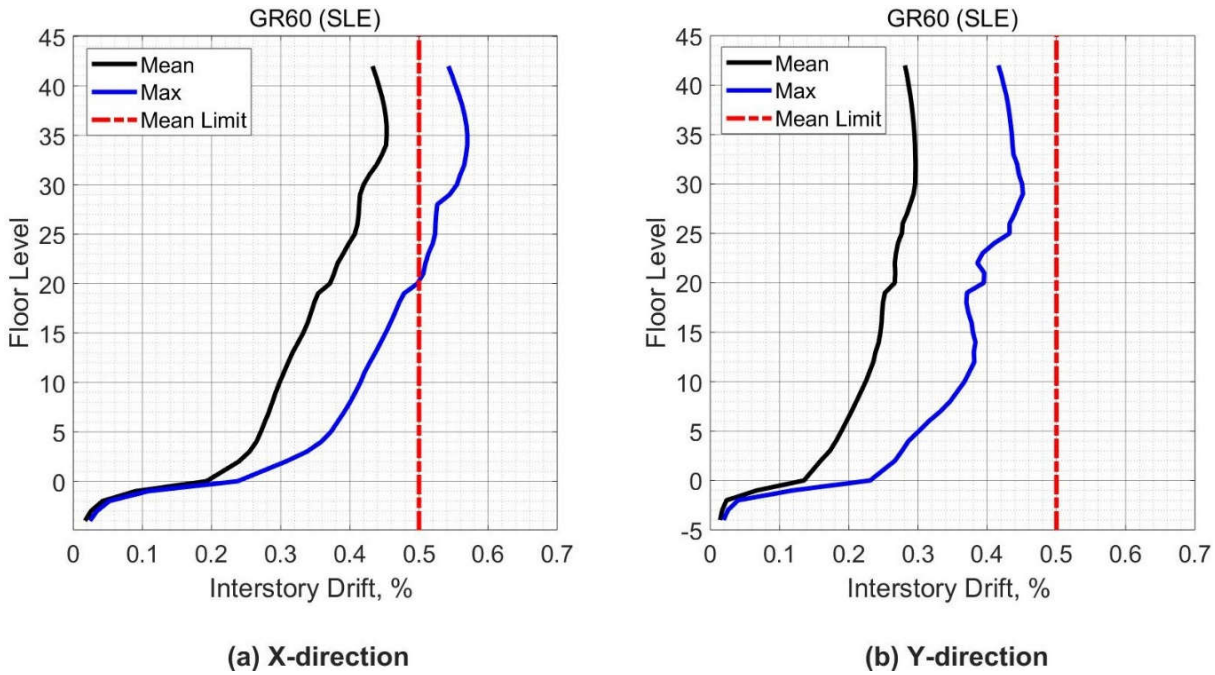

Figure 7.1 Peak Interstory Drift (Case 1 – SLE).

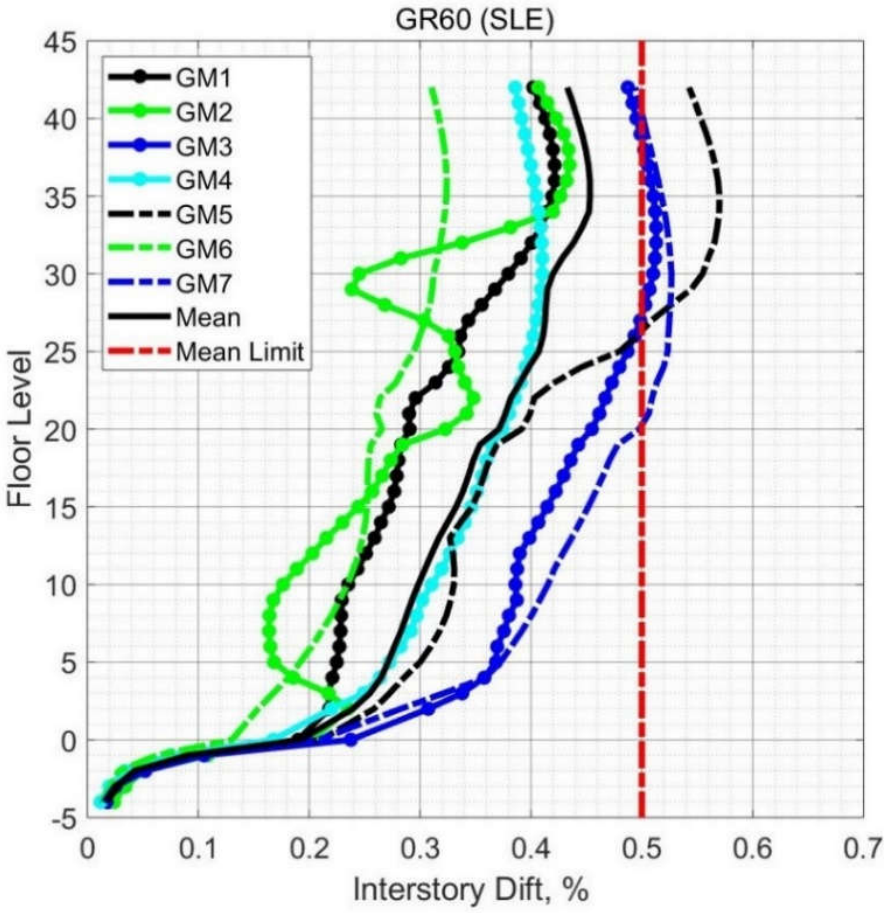

Figure 7.2 Peak Interstory Drift from All Ground Motions for X-direction (Case 1-SLE).

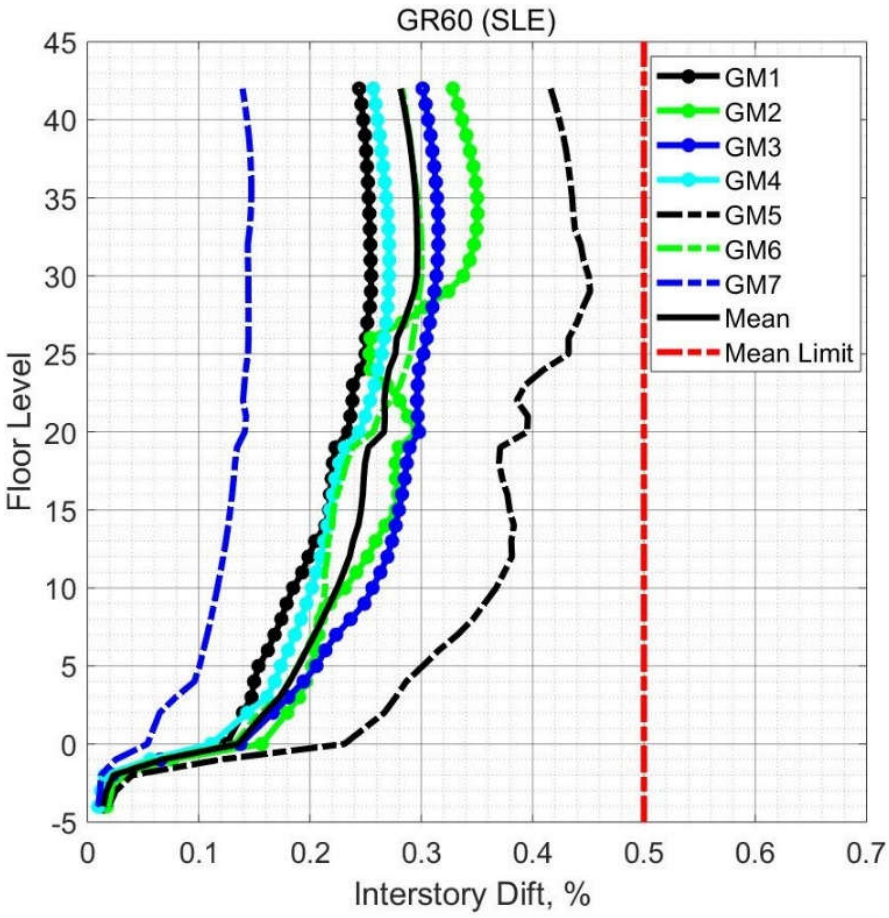

Figure 7.3 Peak Interstory Drift from All Ground Motions for Y-direction (Case 1-SLE).

7.2.1.2 Displacement

The TBI guidelines do not have requirements about the displacement of building stories. Figure 7.4 depicts the mean value of the displacement of each story at the same time step that the roof experiences a maximum displacement value. For each analysis, the displacement of each story was monitored during each time step, and whenever the roof experiences the maximum displacement, the displacements of other stories were recorded at the same time step.

Figures 7.5 and 7.6 show the time history of the roof displacement in the x-direction and y-direction, respectively from a ground motion at which the displacement demand of the roof was

the highest one among other ground motions. During the seventh ground motion, the roof experienced a maximum displacement in the x-direction while during the fifth ground motion the maximum roof displacement in the y-direction was observed.

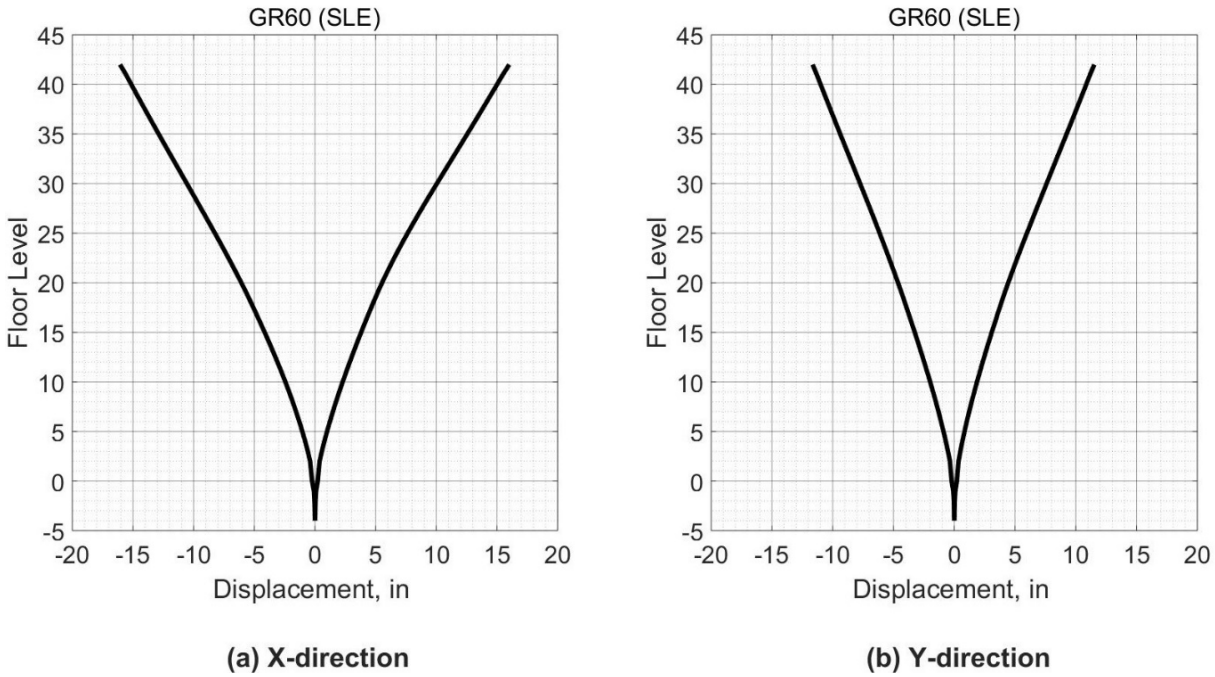

Figure 7.4 Floors Displacement Synchronous with Peak Roof Displacement (Case 1 - SLE).

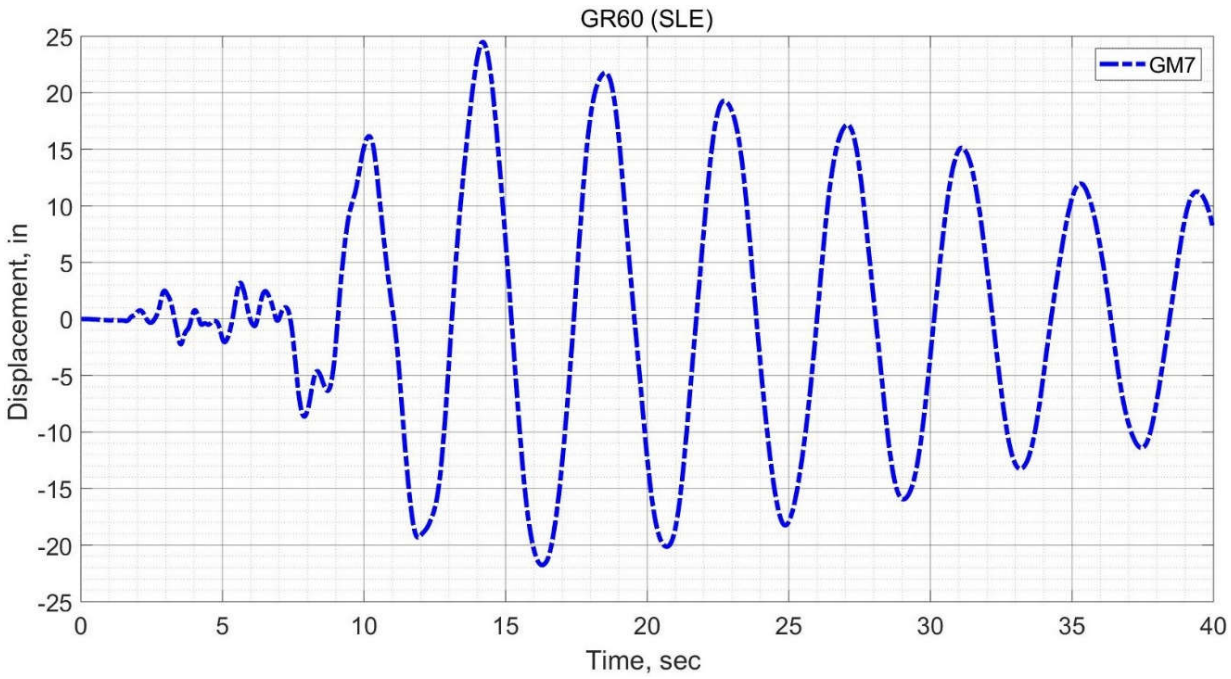

Figure 7.5 Time History for Peak Roof Displacement for X-direction (Case 1 – SLE).

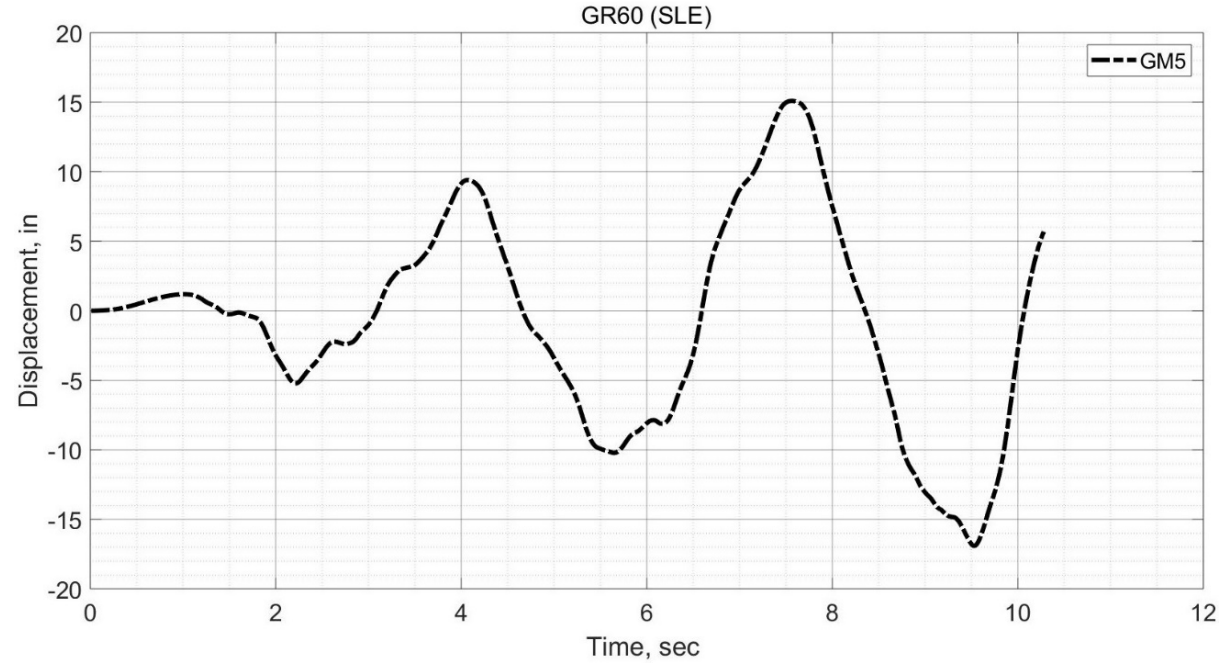

Figure 7.6 Time History for Peak Roof Displacement for Y-direction (Case 1 – SLE).

7.2.2 Element Level

The TBI guidelines require categorizing the actions in all structural members as force-based actions or deformation-based actions for the evaluation process. According to the TBI guidelines definition, actions that are not expected to experience inelastic behavior should be defined as force-based actions. On the other hand, actions that experience inelastic response should be defined as deformation-based actions.

The TBI guidelines require using only the mean value from all analyses for evaluation with the acceptance criteria for both actions in the SLE level. The maximum response parameters for both actions will also be presented to examine the response of the case study building in more depth. In the subsections below, the elements of the seismic force resisting system with their actions are presented and evaluated using the acceptance criteria of the TBI guidelines.

For force-based actions, the TBI guidelines require that the mean response action from all ground motions should be equal or less than the nominal strength capacity times the strength reduction factors according to ACI 318-14.

For deformation-based actions, the TBI guidelines require that the calculated mean deformation demands should not cause damage. The damage defined by the TBI guidelines as (a) deformation more than the yielding of reinforcement or concrete cracking, (b) deformation that lead to weaken the performance of the structure to withstand against a MCER earthquake, (c) an excessive level of permanent deformation. According to the TBI guidelines, the laboratory testing data could be considered to demonstrate that the deformation demands do not result in damage, or the acceptance criteria of ASCE-41 for Immediate Occupancy performance level could be used.

7.2.2.1 Core Wall Response

7.2.2.1.1 Core Wall Force-Based Action

The TBI guidelines specify that shear force in the core walls of tall buildings is a force-based action. To evaluate the shear demands of core walls, the TBI guidelines required that the shear force demands satisfy the following equations:

$$V_{mean} \leq \phi V_{exp} \quad \textbf{(7-1)}$$

$$V_{exp} = 1.5A_{cv}\left(2\sqrt{f'_{cexp}} + \rho_t f_{yexp}\right) \leq 15A_{cv}\sqrt{f'_{cexp}} \quad \textbf{(7-2)}$$

Where:

V_{mean}	The mean value of the maximum shear forces from all ground motions, lbs
V_{exp}	The expected shear strength, for core wall see Equation (7-2), lbs
ϕ	Strength reduction factor, 0.75 (ACI 318-14)
A_{cv}	The area of concrete bounded by the web thickness and the wall length, in^2
f'_{cexp}	The expected concrete compressive strength. TBI guidelines recommend 1.3 times the specified compressive strength, psi
ρ_t	The horizontal reinforcement ratio in the wall.
f_{yexp}	The expected yield strength of reinforcement. The TBI guidelines specify 69,000 psi for ASTM A 706 Grade 60.

Figure 7.7 shows the core wall shear forces over the building height and the values of $\phi V_{exp.}$ The shear demands in the core wall satisfy Equation (7-1) as required by the TBI guidelines. In addition, the shear force demands varied approximately in a linear manner with the height of the building. For the mean response, the demand was approximately the same in both the x- and y-directions. The maximum response was also less than the limit of the mean response. The peak shear force of the mean values is 6590 kips, and 6890 kips for x and y-direction, respectively.

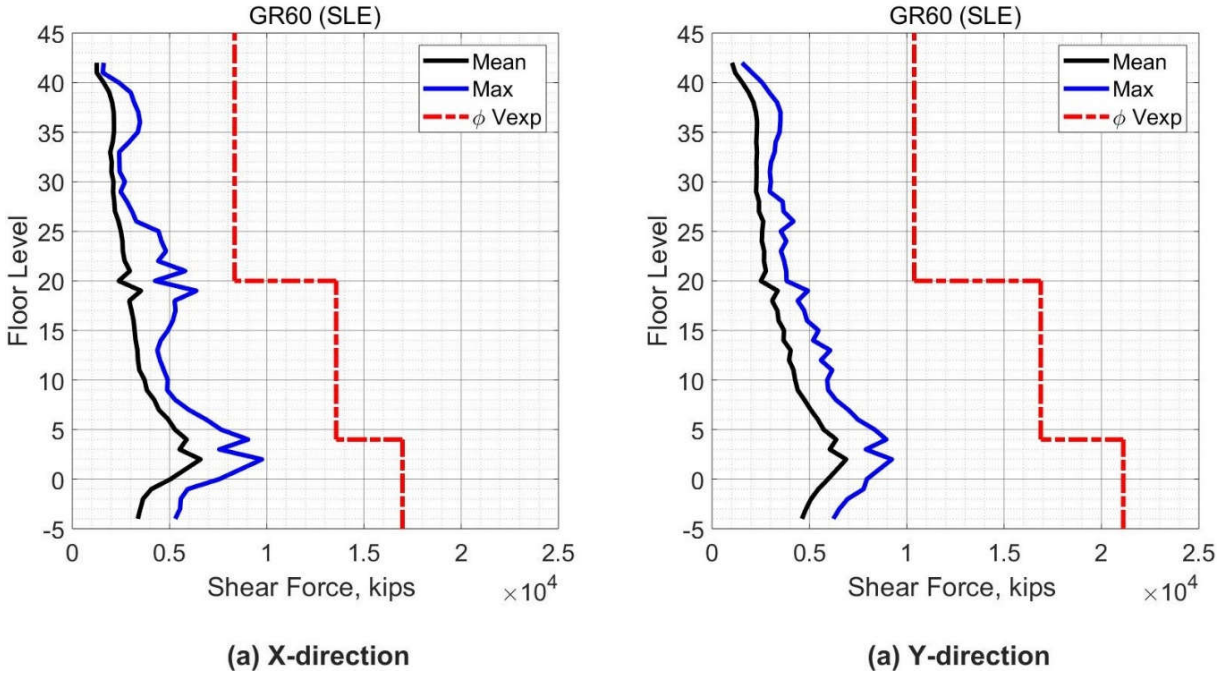

Figure 7.7 Shear Forces in Core Wall (Case 1 – SLE).

7.2.2.1.2 Core Wall Deformation-Based Actions

TBI guidelines specify the tensile strain in the reinforcing steel and the concrete compression strain as deformation-based actions for shear walls. The TBI guidelines require that the mean of the maximum strain demands in the steel bars and concrete should be less than the

acceptable limits. Therefore, the strain demands in the reinforcing steel and concrete were monitored during the analyses on all edges of the core wall. The strain was determined by using the vertical displacement (Δ_z) of the nodes of the core wall edges. Figure 7.8 shows the method that was used for calculating the strain by using Equations (7-3) and (7-4).

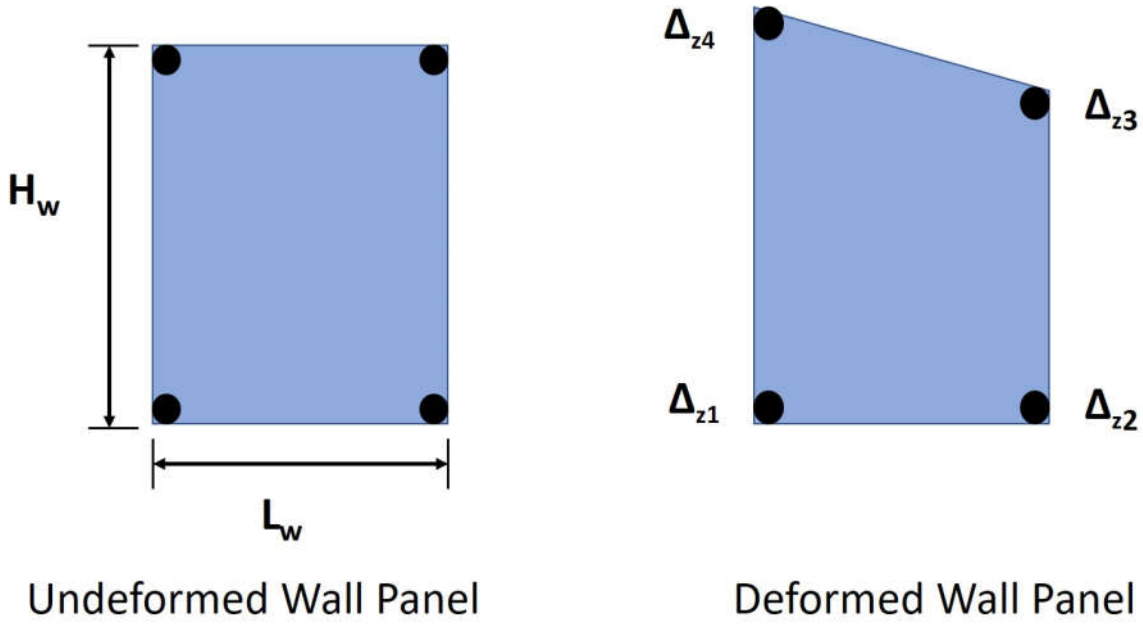

Figure 7.8 Core Wall Panel with Vertical Displacement of the Nodes.

$$\varepsilon_{(1-4)} = \frac{\Delta_{z4} - \Delta_{z1}}{H_w} \quad \textbf{(7-3)}$$

$$\varepsilon_{(2-3)} = \frac{\Delta_{z3} - \Delta_{z2}}{H_w} \quad \textbf{(7-4)}$$

ε is the tensile or compression strain in a wall edge. Δ_z is the vertical displacement of the node on a wall edge. H_w is the wall height. Figure 7.9 shows the position of the edge nodes of the core wall where the strains were calculated.

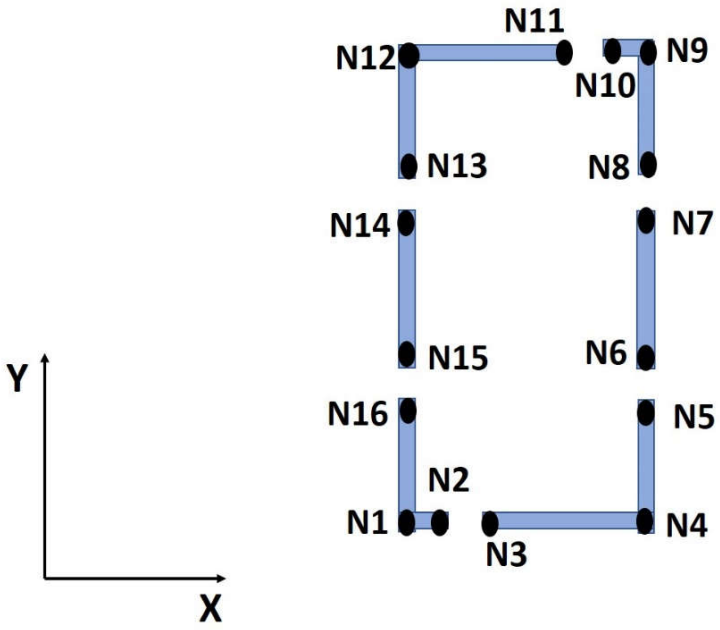

Figure 7.9 Edge Nodes for Core wall

Figures 7.10 to 7.13 show the mean values of the maximum tensile strain in the core wall reinforcement steel at locations shown in Figure 7.9 over the building height. The TBI guidelines consider the yielding of steel bars as damage that should be avoided in the SLE shaking level. The steel reinforcement in the core wall experienced maximum yielding strain of (0.002) which is below the expected yield strain of Grade 60 (0.0024), therefore the requirements of the TBI guidelines are satisfied. The maximum tensile strain was in the first story above the main podium A noticeable change in the response occurred at the twentieth story due to the wall thickness

changing from 24 in. to 18 in.

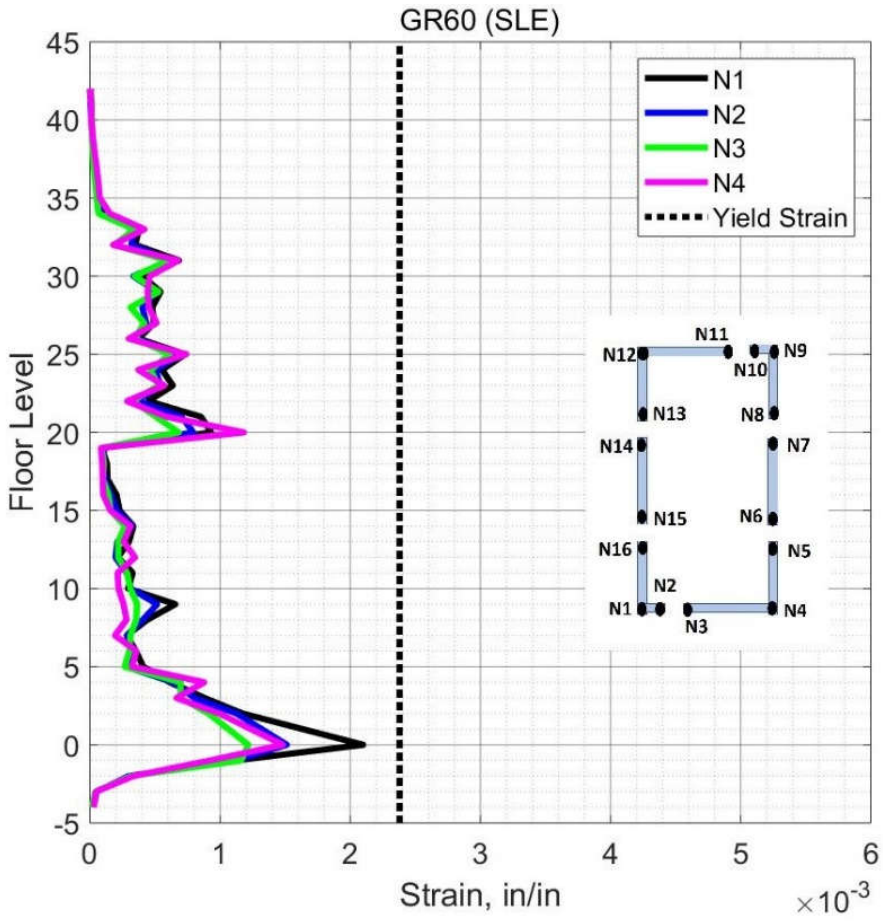

Figure 7.10 Mean Tensile Strain in Steel Bars in Core Wall Edges N1-N4 (Case 1 – SLE).

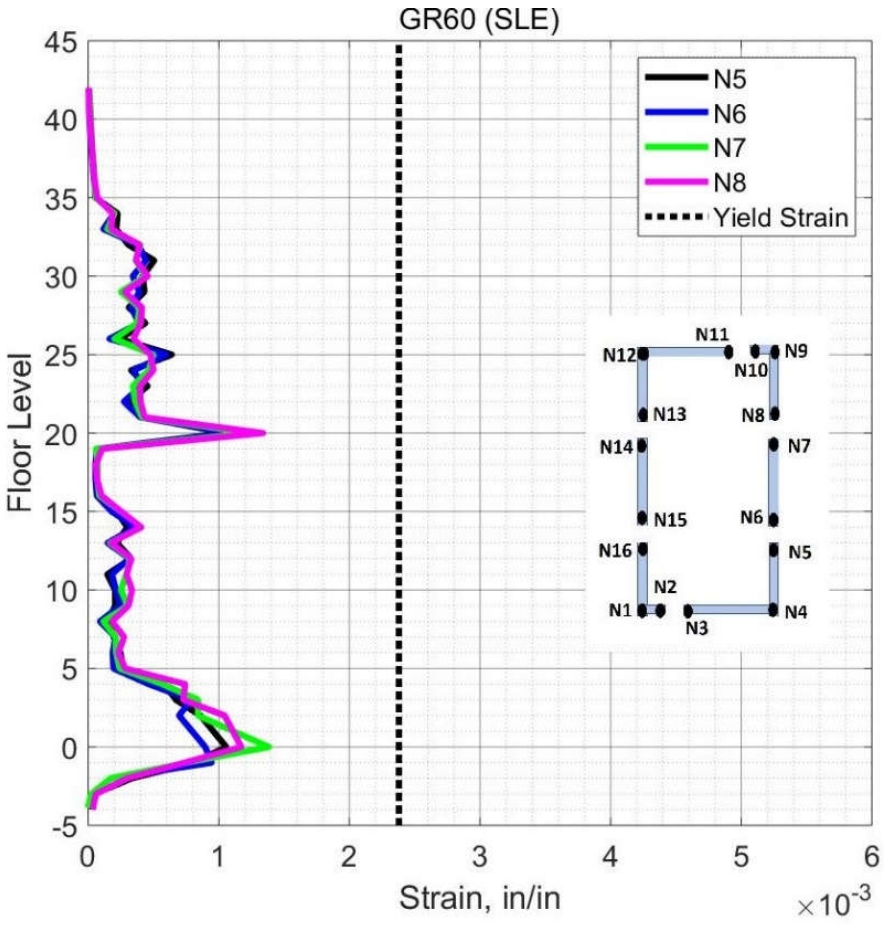

Figure 7.11 Mean Tensile Strain in Steel Bars in Core Wall Edges N5-N8 (Case 1 – SLE).

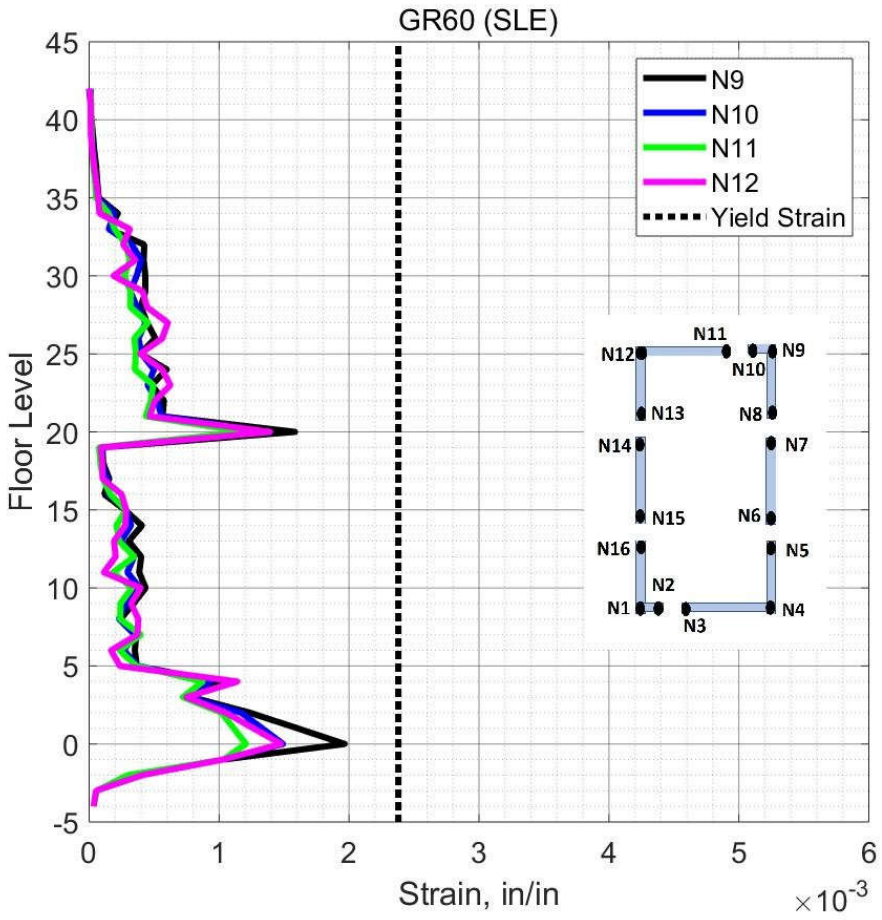

Figure 7.12 Mean Tensile Strain in Steel Bars in Core Wall Edges N9-N12 (Case 1 – SLE).

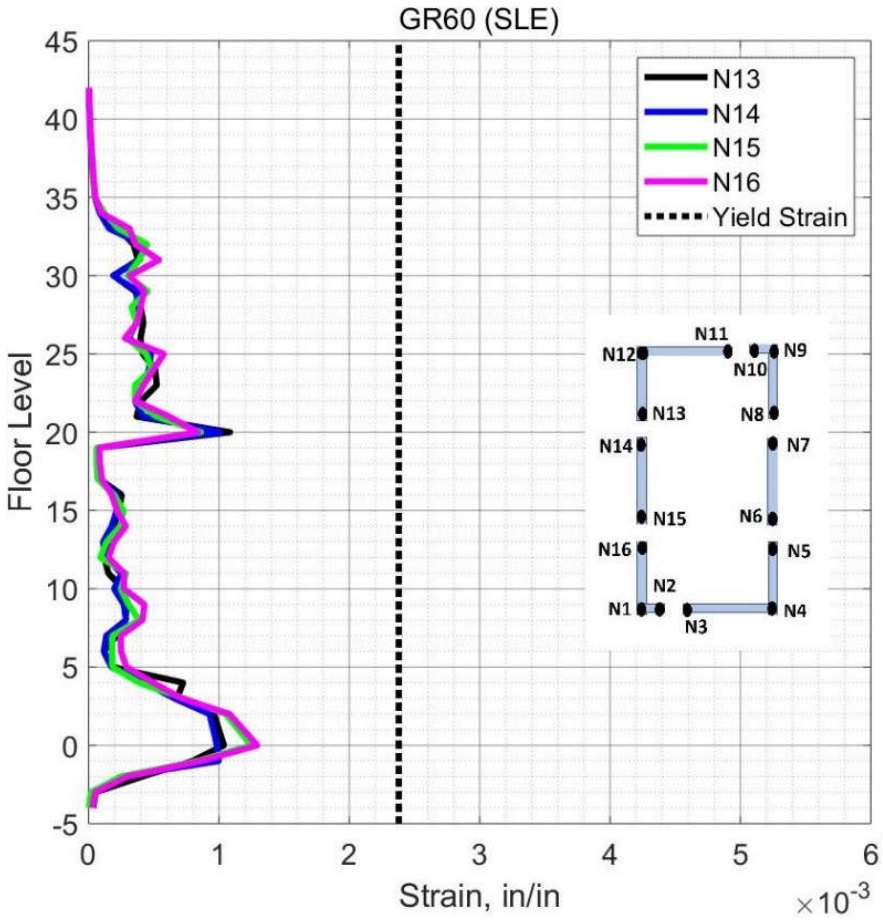

Figure 7.13 Mean Tensile Strain in Steel Bars in Core Wall Edges N13-N16 (Case 1 – SLE).

Figures 7.14 to 7.17 show the mean values of the maximum compression strain in the core wall concrete at locations shown in Figure 7.9 over the building height. The TBI guidelines consider the cracking of concrete as damage that should be avoided in the SLE shaking level. The concrete compression strain in the core wall was very low (< 0.0008), therefore the requirements of the TBI guidelines are satisfied. The maximum concrete compression strain was in the first story above the main podium. A noticeable change in the response of concrete strain occurred at the twentieth story due to the wall thickness changing from 24 in. to 18 in.

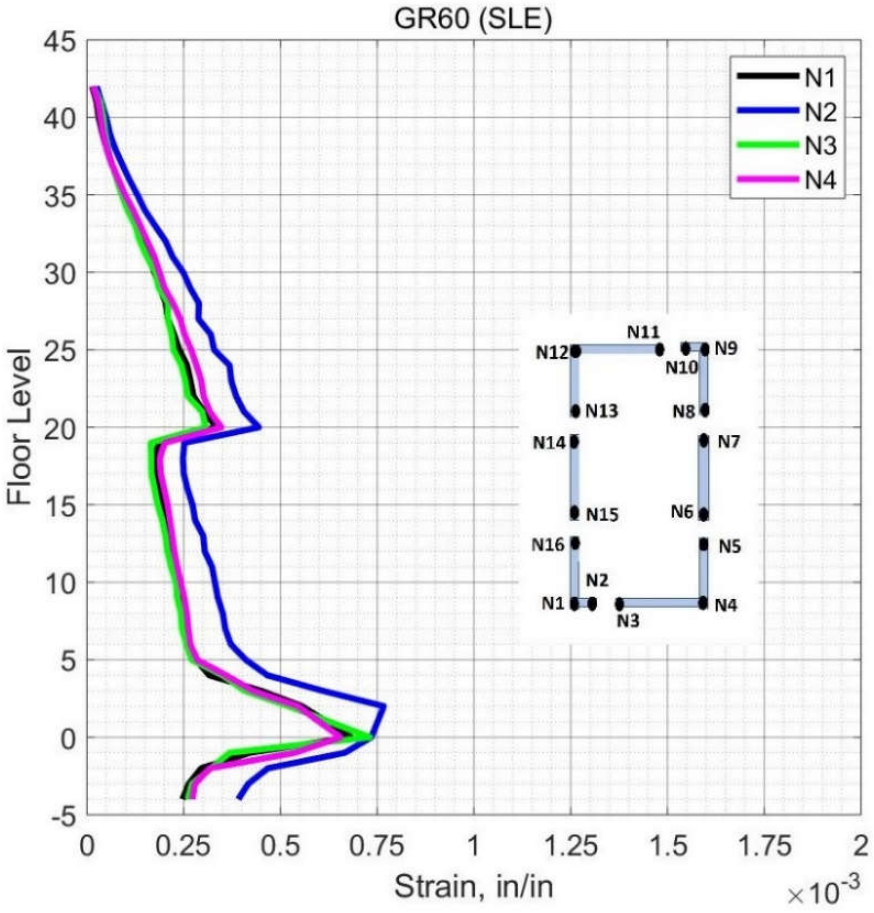

Figure 7.14 Mean Concrete Compression Strain in Core Wall Edges N1-N4 (Case 1 – SLE).

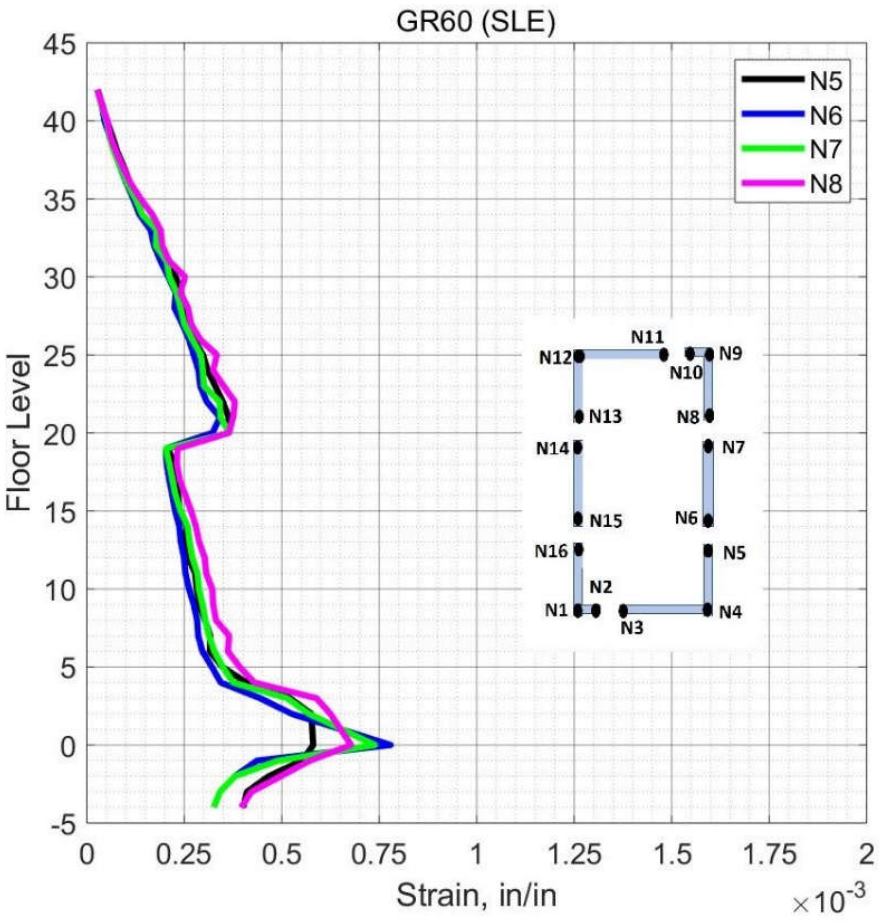

Figure 7.15 Mean Concrete Compression Strain in Core Wall Edges N5-N8 (Case 1 – SLE).

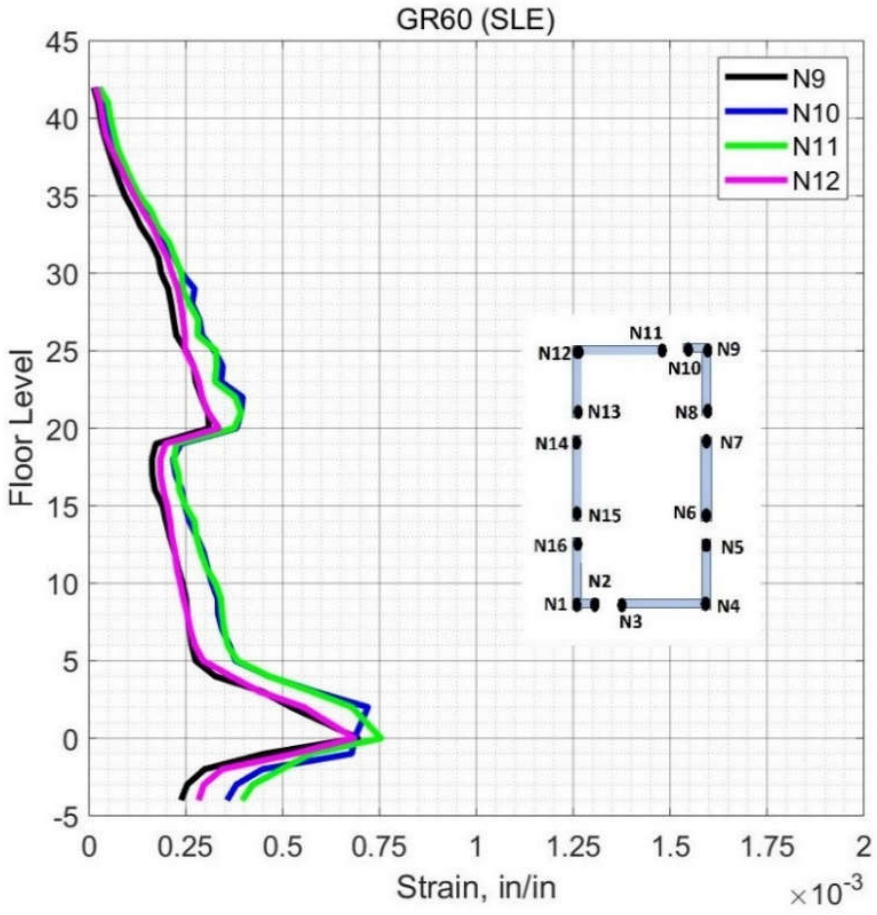

Figure 7.16 Mean Concrete Compression Strain in Core Wall Edges N9-N12 (Case 1 – SLE).

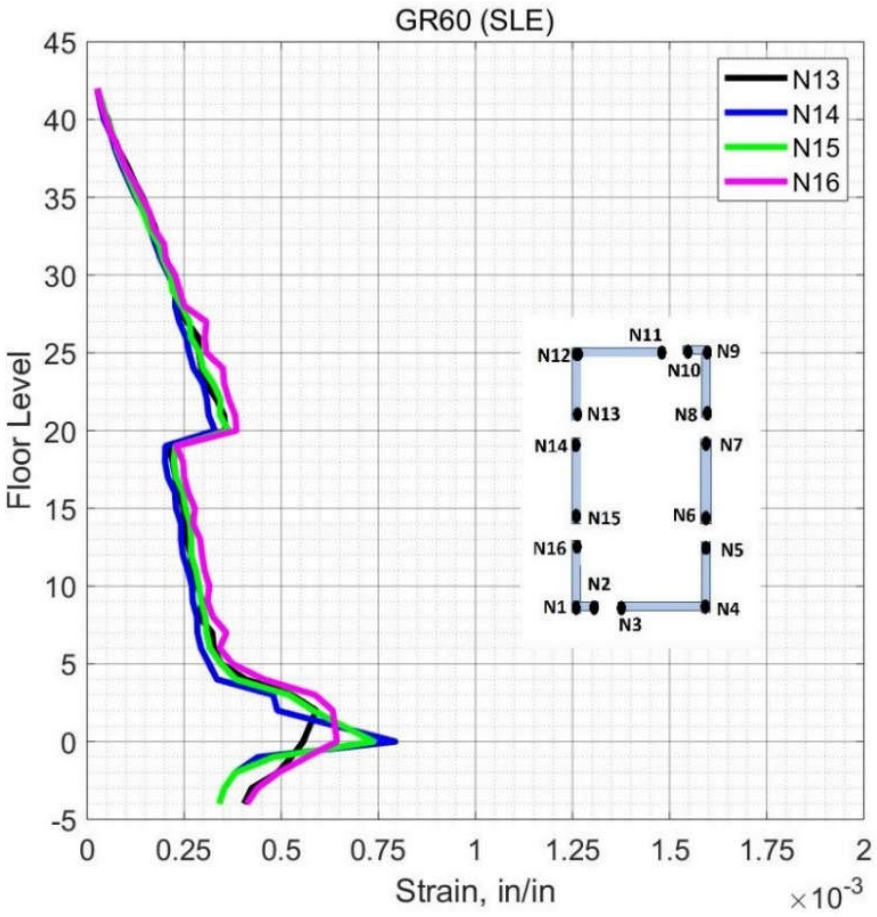

Figure 7.17 Mean Concrete Compression Strain in Core Wall Edges N13-N16 (Case 1 – SLE).

7.2.2.1.3 Coupling Beams

All coupling beams in the case study building are diagonally reinforced. The coupling beams in the x-direction have a 1.7 aspect ratio, while the coupling beams in the y-direction have a 2.1 aspect ratio. The rotation is the deformation based-action for coupling beams with diagonal reinforcing (TBI 2017). The rotation demand of all the coupling beams was monitored during all the analyses. To determine the acceptable capacity of coupling beams rotation, the TBI guidelines recommend using the acceptance criteria of ASCE 41 for Immediate Occupancy or the test data if

available. A study by (Naish 2010) provides fragility curves for coupling beams with diagonal reinforcing from collecting data as shown in Figure 7.18 for coupling beams with aspect ratios ($1 < l_n/h < 2$) and Figure 7.19 for coupling beams with aspect ratios ($2 < l_n/h < 4$).

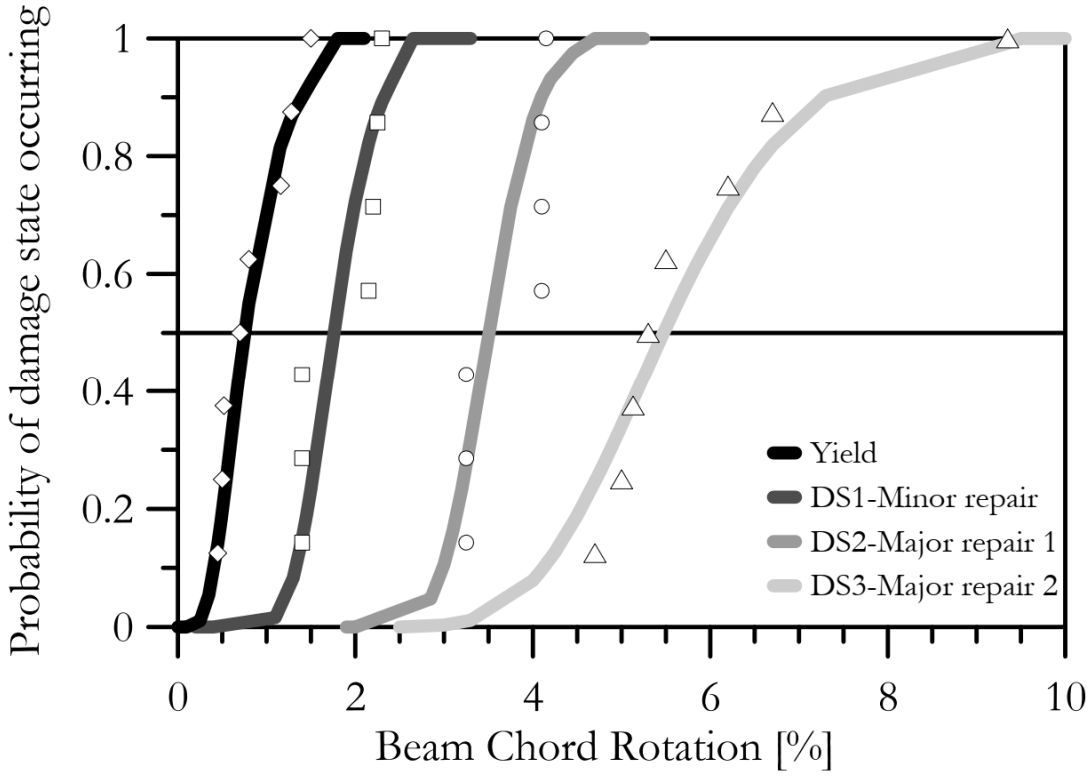

Figure 7.18 Fragility Curves for Diagonally-Reinforced Concrete Coupling Beams with Aspect Ratios $1.0 < l_n/h < 2.0$ (Naish 2010).

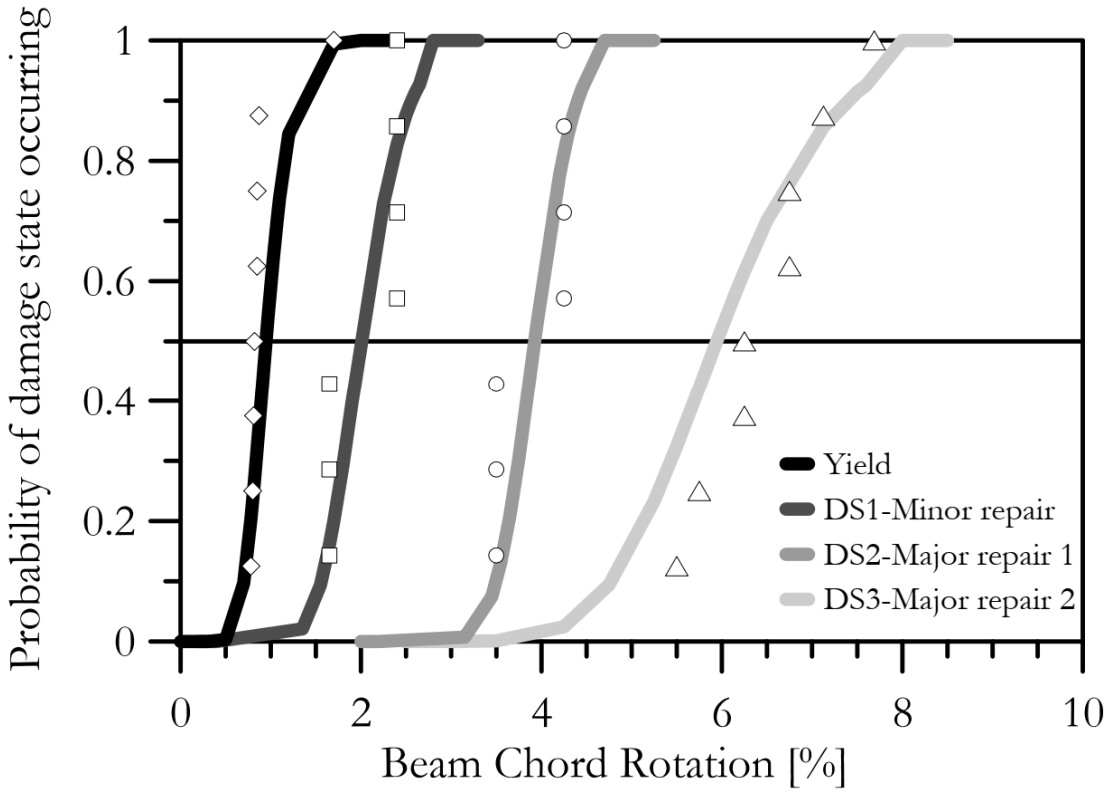

Figure 7.19 Fragility Curves for Diagonally-Reinforced Concrete Coupling Beams with Aspect Ratios 2.0 < l_n/h < 4.0 (Naish 2010).

Figures 7.18 and 7.19 can be read as: for a given rotation demand in the x axis, draw a vertical line and figure out the point of intersection with any curve in the graph and then read the probability of the damage state that the curve represents. According to the study (Naish 2010), yielding and three different damage states are presented. The yielding state occurs when a substantial reduction in the stiffness of the load deformation relationship initiates for the coupling beam. The first damage state (DS1) represents minor damage state and the member could be repaired by common and easy methods such as epoxy injection. The second damage state (DS2) is the major damage (I) in which a member needs to more work to repair such as replacement of spalling concrete or large epoxy injection. The third damage state (DS3) is the major damage (II)

in which a member experiences significant strength degradation, such as reinforcement buckling or fracture and concrete crushing.

Figure 7.20 (a) shows the mean and maximum values of the rotation of coupling beams with a 1.7 aspect ratio (coupling beams in the x-direction), over the building height. The peak value of the mean rotation is 0.0015 which indicate that coupling beams did not experience yielding of steel reinforcement according to the data in Figure 7.18. In addition, the peak values do not exceed the limit of (0.0060) of ASEC 41. Therefore, the rotation demands of coupling beams satisfy the requirement of the TBI guidelines.

Figure 7.20 (b) shows the mean and maximum values of the rotation of coupling beams with a 2.1 aspect ratio (coupling beams in the y-direction), over the building height. The peak value of the mean rotation is 0.0012 which indicate that coupling beams did not experience yielding of steel reinforcement according to the data in Figure 7.19. In addition, the peak values do not exceed the limit of (0.0060). Therefore, the rotation demands of coupling beams satisfy the requirement of the TBI guidelines.

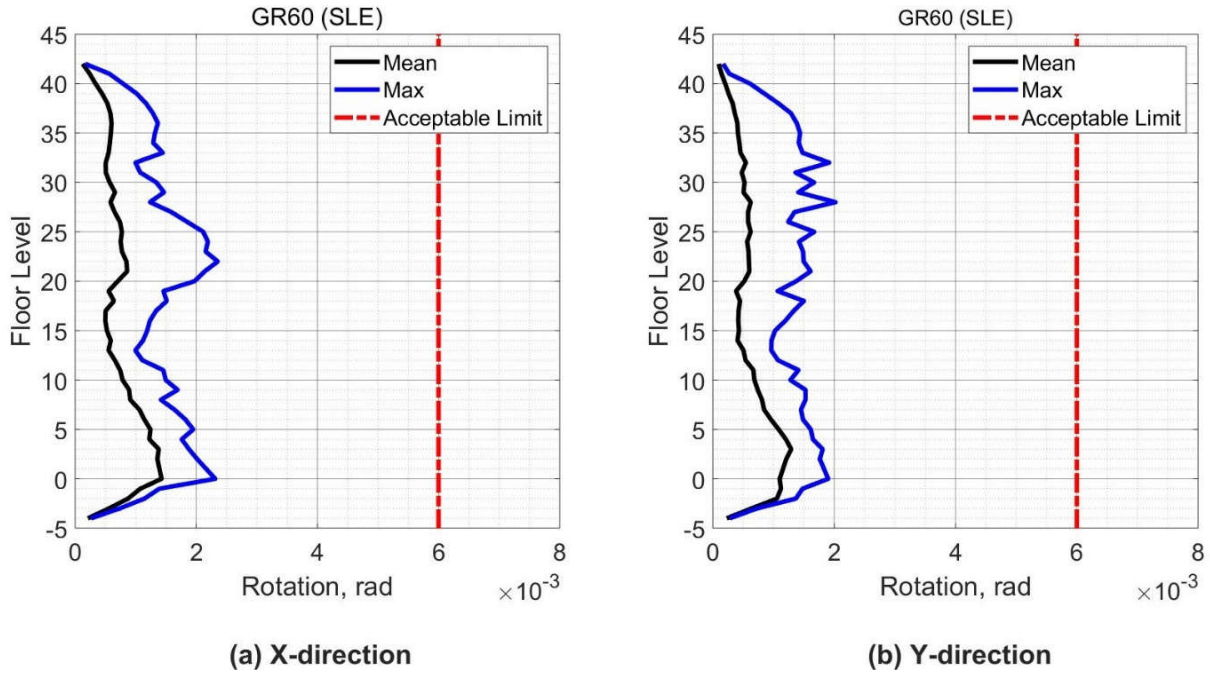

Figure 7.20 Rotation Demand in Coupling Beams (Case 1 – SLE).

7.2.2.2 Special Moment Frame Response

7.2.2.2.1 Beam Force-Based Action

The TBI guidelines specify the shear force in the beams of special moment frames as a force-based action. The shear demands should satisfy Equation (7-1). The expected shear strength (V_{exp}) of beams or columns is calculated by using Equation (7-5) from ACI 318-14.

$$V_{exp} = \frac{A_v f_{ytexp} d}{s} \quad \leq \quad 8 b_w d \sqrt{f'_{cexp}} \tag{7-5}$$

Where:

V_{exp}	The expected shear strength, for beams or columns, psi
A_v	Area of shear reinforcement, in^2
f_{ytexp}	The expected yield strength of shear reinforcement. The TBI guidelines specify 69,000 psi for ASTM A 706 Grade 60.
d	Distance from extreme compression fiber to the centroid of longitudinal tensile reinforcement, in
s	Center-to-center spacing of transverse reinforcement, in
b_w	Web width, in
f'_{cexp}	The expected concrete compressive strength. TBI guidelines recommend 1.3 times the specified compressive strength, psi

As stated previously, the TBI guidelines require that only the mean of the maximum from all analyses should be checked with the acceptance criteria for SLE shaking level. Figure 7.21 shows the mean and the maximum values of beams shear forces from all ground motions over the building height and the limiting values of (ϕV_{exp}). In addition, the mean shear forces demands in the beams of the special moment frame satisfy the requirements of the TBI guidelines by satisfying Equation (7-1). A slight increase in shear forces demands for the beams in the x-direction is noticed compared with beams in the y-direction. The maximum shear demand was approximately 200 kips while the reduced strength capacity 500 kips of the beams.

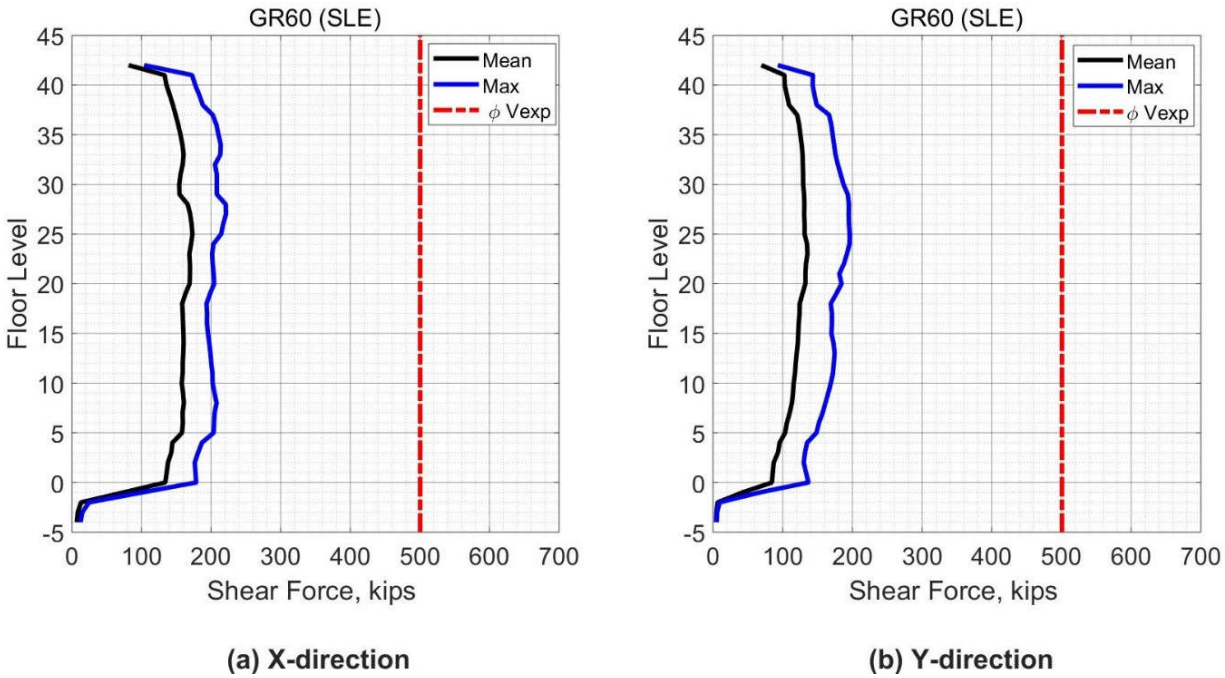

Figure 7.21 Peak Shear Force in Beams (Case 1 – SLE).

7.2.2.2.2 Beam Deformation-Based Action

The deformation-based action for beams is the plastic rotation of the beam chord. Due to the use of the fiber section for modeling the beam cross-sections, the tensile strains in the longitudinal reinforcing bars in beams were also monitored as another indicator for flexural demands on the beams. To calculate the plastic rotation demands in the beams and columns of special moment frame in both SLE and MCER shaking levels, the section curvature was monitored during the analysis and the following equation was used.

$$\theta_p = (\phi_u - \phi_y) l_p \quad \textbf{(7-6)}$$

$$l_p = 0.08l + 0.00015 d_b f_y \quad \textbf{(7-7)}$$

Where:

θ_p	The plastic rotation, rad.
ϕ_u	Ultimate curvature, rad/in.
ϕ_y	Curvature at yield, rad/in.
l_p	Plastic hinge length, in., see Equation (7-7).
l	Element length, in.
d_b	Reinforcing bar diameter, in.
f_y	Yield strength of reinforcing bar, psi

Both the tensile strain in the reinforcing bars and the section curvature were monitored with each time step during the analysis. Whenever the tensile strain of a reinforcing bar reached the yielding strain for the first time, the curvature at that time step was recorded as the yielding curvature. The ultimate curvature is the maximum curvature that the section experiences. After obtaining both yielding and ultimate curvatures, Equation (7-6) was applied to determine the plastic rotation demands. To calculate the acceptable limit of rotation capacity of the beams and columns for the SLE shaking level, the TBI guidelines permit using the acceptance criteria of ASCE 41-17 for the Immediate Occupancy level.

Figure 7.22 shows the mean and maximum tensile strain demands in the longitudinal reinforcement in the beams sections that are in the beam ends over the building height. The expected yield strain of Grade 60 A 706 is 0.0024. The TBI guidelines consider the yielding of steel bars as damage that should be avoided in the SLE shaking level. The mean tensile strain of the steel reinforcement in all beams did not exceed the expected yield strain, therefore, the requirements of the TBI guidelines are satisfied. A small increase in the tensile strain of the

reinforcing bars in the beams oriented in the x-direction was noticed compared with the beams oriented in the y-direction. No yielding of the steel bars in the beams means that the beams do not experience plastic rotation.

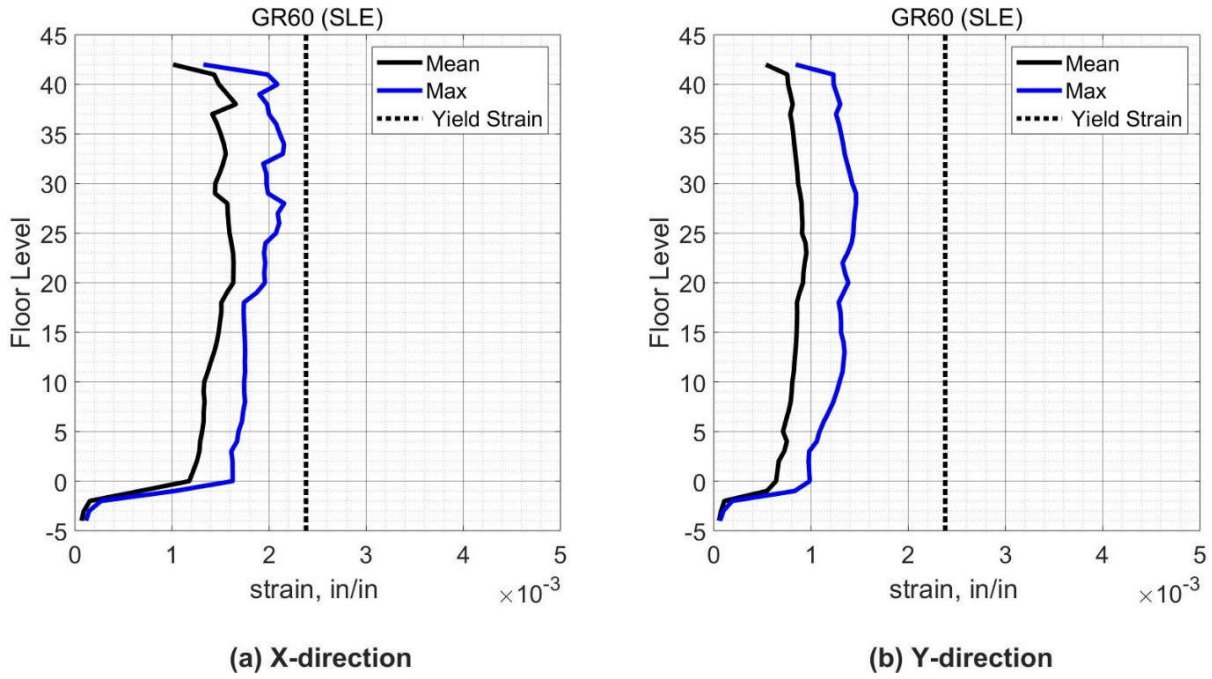

Figure 7.22 Peak Tensile Strain in Reinforcing bars in Beams (Case 1 – SLE).

7.2.2.2.3 Columns Force-Based Action

The same equations and procedure used in evaluating the shear forces demands in beams in Section 7.2.2.2.1 were applied to evaluate the shear force demands in the columns of the special moment frames. As mentioned previously, only the mean value of the response should be checked with the TBI guidelines acceptance criteria, however, presenting the maximum values is provided to examine the performance of the building in-depth.

Figures 7.23 to 7.26 show the mean and maximum values of the shear forces from all analyses in the building columns and the limiting values of (ϕV_{exp}) over the building height. The shear forces in the columns satisfies the requirements of the TBI guidelines by satisfying Equation (7-1) .

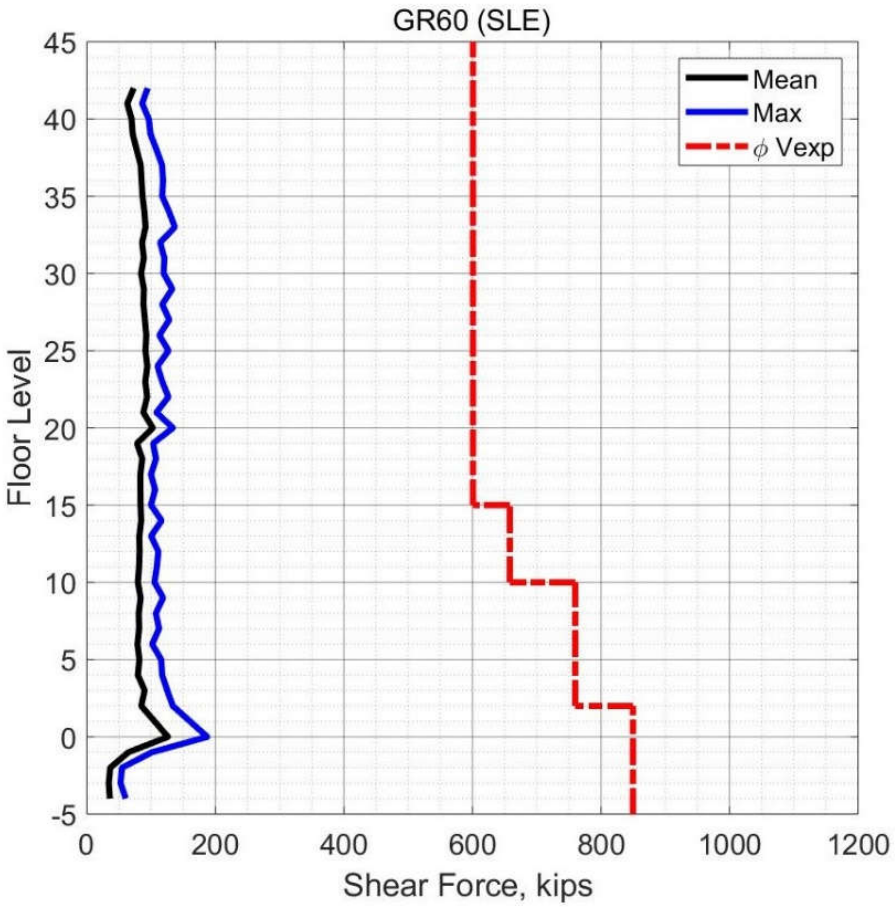

Figure 7.23 Peak Shear Force in Corner Columns (Case 1 – SLE).

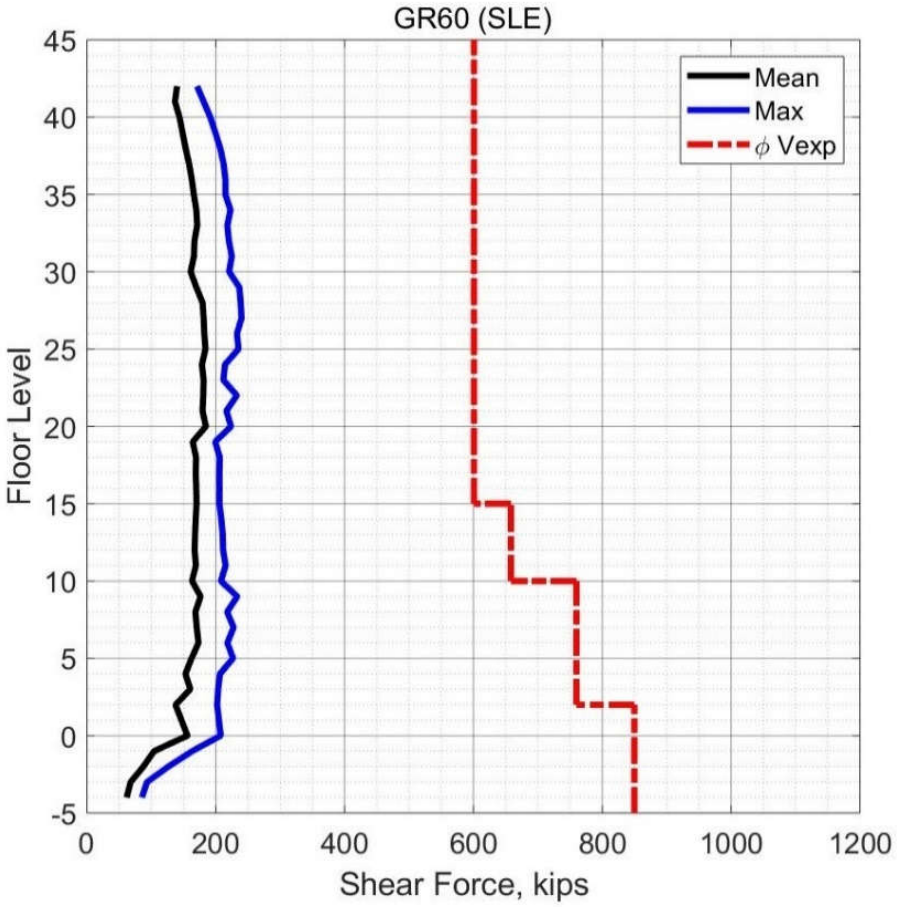

Figure 7.24 Peak Shear Force in Interior Columns X-direction (Case 1 – SLE).

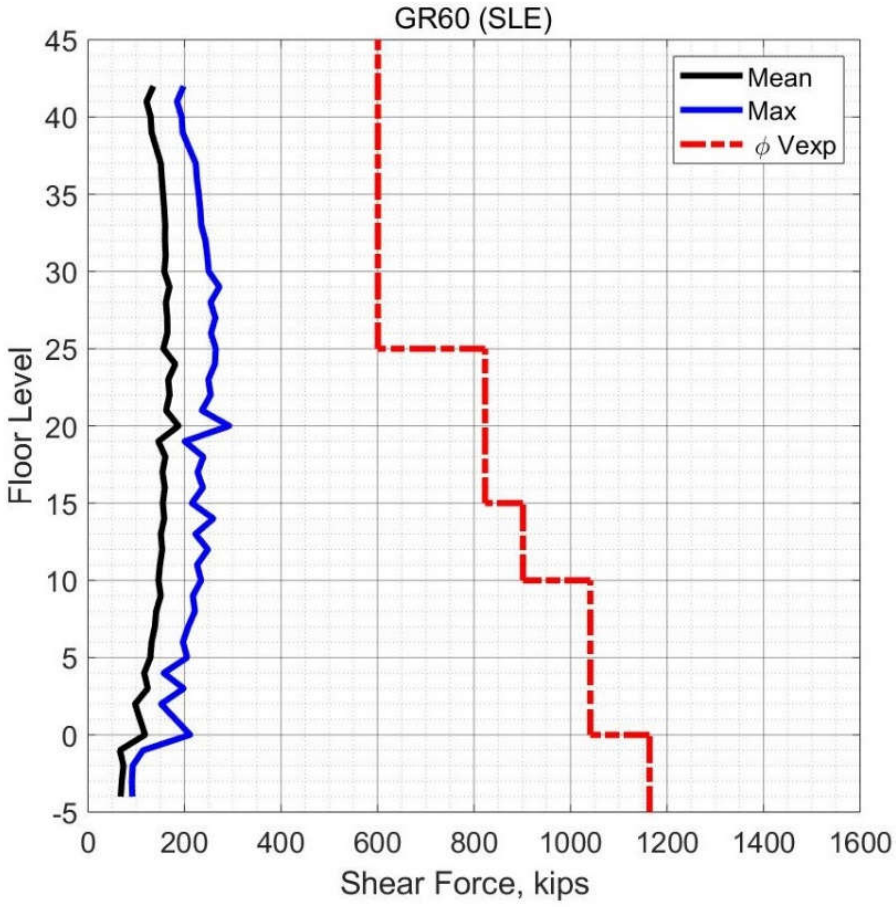

Figure 7.25 Peak Shear Force in Columns on Grid B and E (Case 1 – SLE).

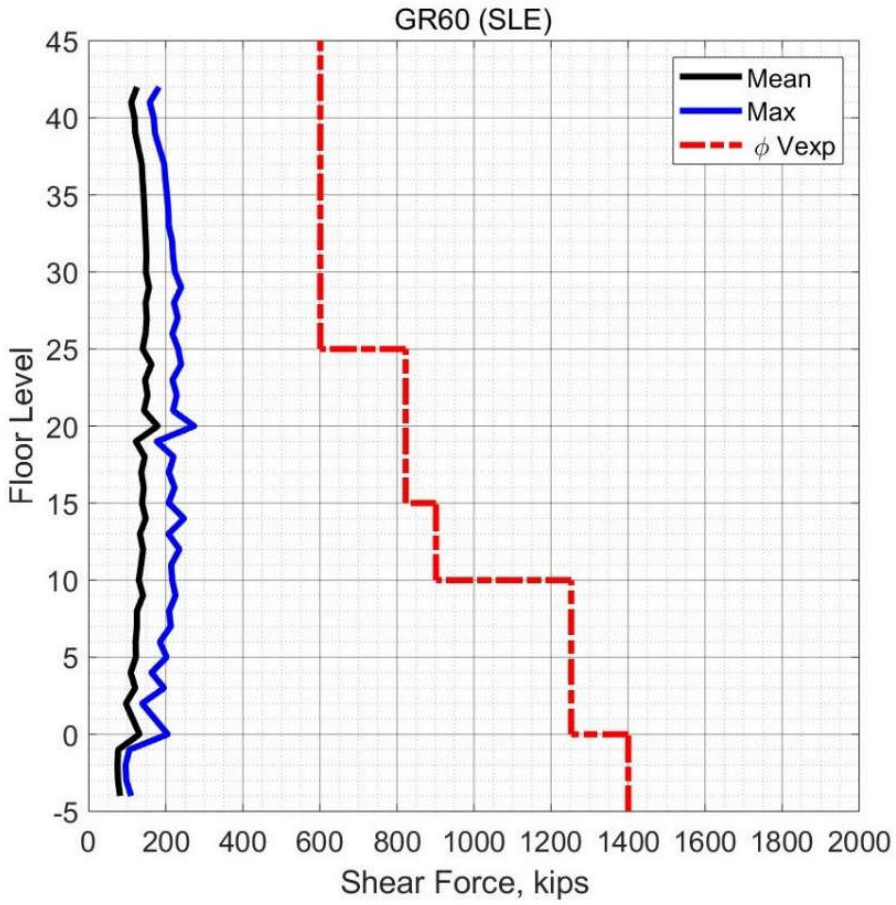

Figure 7.26 Peak Shear Force in Columns on Grid C.5 (Case 1 – SLE).

7.2.2.2.4 Column Deformation-Based Action

The deformation-based action for columns is the plastic rotation of the column chord. To satisfy the requirement of TBI guidelines, the mean value of the maximum values of the plastic rotation demands in the columns from all ground motions in the suite should be less than the rotation capacity of the columns. To calculate the plastic rotation demands on the columns, the same procedure and equations used in evaluating the beams plastic rotation demands in Section 7.2.2.2.2 were applied to evaluate the plastic rotation demands for the columns. To calculate the acceptable limit of the rotation capacity of the columns for SLE shaking level, the TBI guidelines

permit using the acceptance criteria of ASCE 41-17 for Immediate Occupancy level. In addition, modeling the columns cross sections with the fiber section provides a means to monitor the tensile strains in the longitudinal reinforcing bars in columns. The tensile strain in reinforcing bars of columns reflect the combined effect of axial and moment demands on columns.

Figure 7.27 show the maximum value of the tensile strain in the longitudinal bars in columns and the mean value from all ground motion in the suite over the building height. The TBI guidelines consider the yielding of steel bars as damage that should be avoided in the SLE shaking level. The maximum tensile strain demand (0.0012) did not exceed the expected yield strain (0.0024), which means no damage could be expected in the columns. Consequently, there is no plastic rotation in all the columns for this shaking level. Depending on the results of the tensile strain of the reinforcing bars, the columns satisfy the requirements of the TBI guidelines.

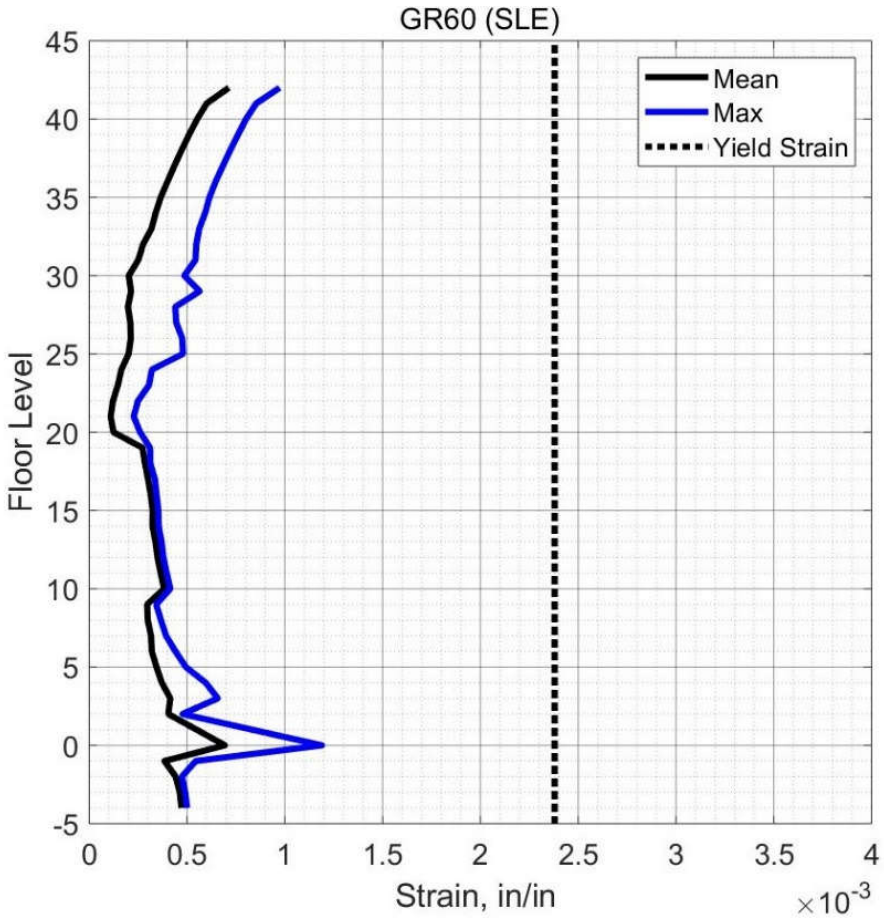

Figure 7.27 Peak Tensile Strain in Reinforcing Bars in Columns (Case 1 – SLE).

7.2.2.3 Contribution of Core Wall and Frame in Dual System

As mentioned previously, the seismic force resisting system (SFRS) of the case study building is a dual system that consists of the core wall and the special moment frame. To better understand the behavior of the dual system, the contribution of its components in resisting the story shear force is depicted in Figure 7.28 for the x and y-directions, respectively. Figure 7.29 shows the contribution percentage of the shear forces for the core wall and the frame over the building height. The frame contribution is approximately constant over the building height, while the core

wall contribution varies linearly. In general, the core wall contributes more than 80% of the total story shear for the lower stories and 50% for the upper stories.

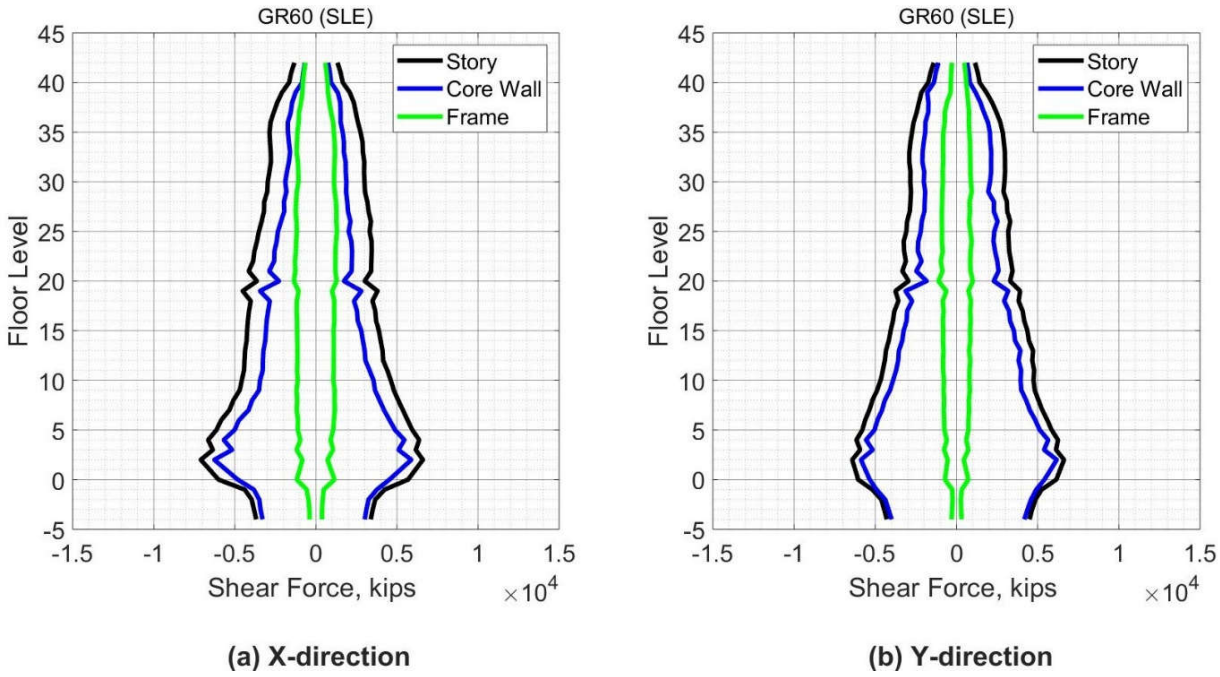

Figure 7.28 Shear Force Contribution of Core Wall & Frame (Case 1 – SLE).

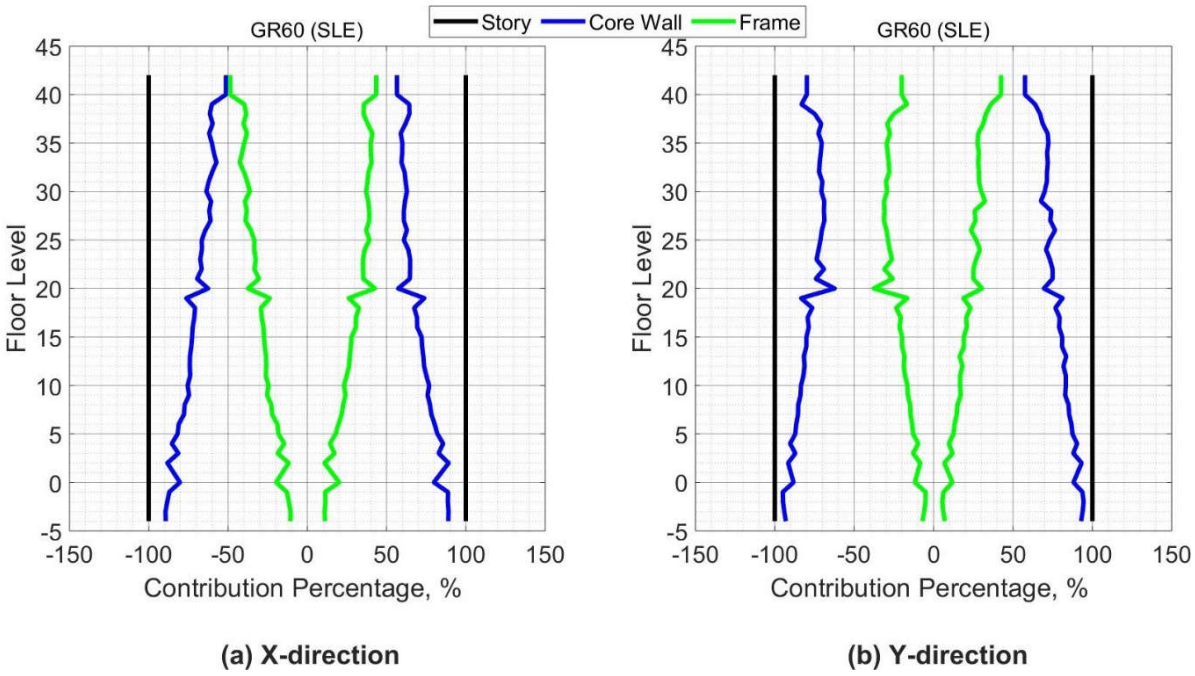

Figure 7.29 Contribution Percentage of Core wall & Frame Shear Force (Case 1 – SLE).

7.3 MCER LEVEL

The results of eleven analyses are presented and compared with the acceptance criteria of the TBI guidelines. According to the TBI guidelines, first, the mean value of the response parameters from all ground motions in the suite should be checked with the acceptance criteria. Second, the maximum response parameters from all ground motions should be checked to ensure that no unacceptable response was produced by any ground motion from the suite. All the response parameters were calculated by the same procedures that were described in Section 7.2 of the SLE level shaking.

7.3.1 Global Response

7.3.1.1 Drift Ratio

Figure 7.30 show the mean and the maximum values of the interstory drift ratios from all the ground motions analyses over the building height. The mean interstory drift from the eleven analyses was very close to 0.02 in the x-direction and approximately 0.012 in the y-direction, where both values were within the acceptable limit of TBI guidelines of 0.03. In addition, the maximum interstory drift was 0.03 and 0.018 for the x and y-directions, respectively. The maximum values of drift ratios were also within the acceptable limit of TBI guidelines (0.045), which indicates that no unacceptable response was produced when considering the drift ratios. Figures 7.31 and 7.32 depict the maximum drift ratios form each considered ground motion over the building height.

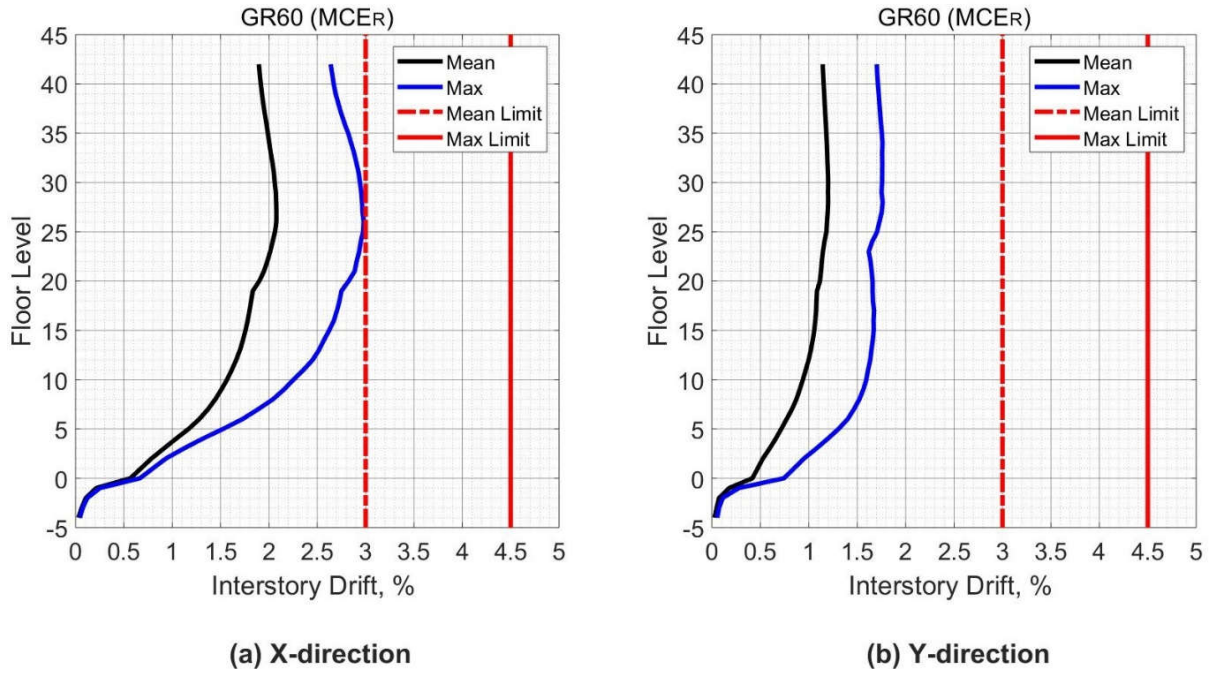

Figure 7.30 Peak Interstory Drift (Case 1 – MCER).

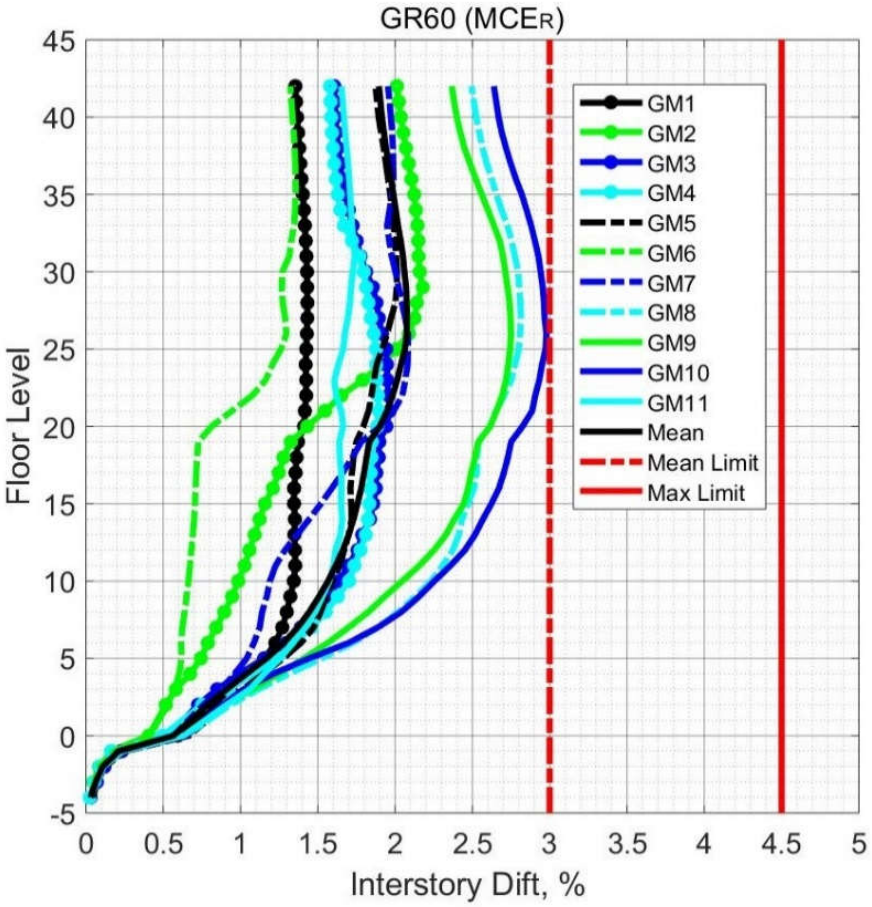

Figure 7.31 Peak Interstory Drift from All Ground Motions for X-direction (Case 1 - MCER).

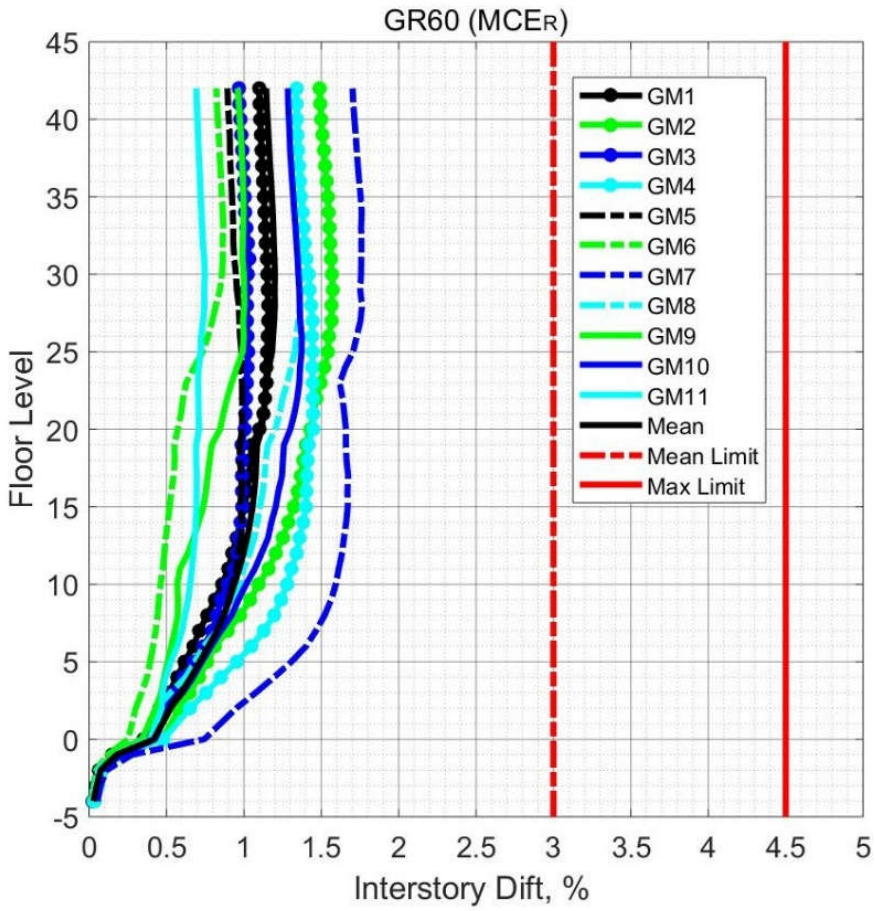

Figure 7.32 Peak Interstory Drift from All Ground Motions for Y-direction (Case 1 - MCER).

7.3.1.2 Residual Drift Ratio

The residual drift ratio was calculated by using the procedure of FEMA 58 (FEMA 58-2018). Figure 7.33 shows that the maximum of the mean values of the residual drift was 0.0075 in the x-direction and 0.0035 in the y-direction where both values are below the TBI limit (0.01). In addition, the maximum residual drift ratio obtained from all analyses was 0.0115, which is below the limit of the TBI guidelines for residual drift ratios (0.0150). Consequently, no unacceptable

response was produced from any ground motion when considering the values of the residual drift ratio.

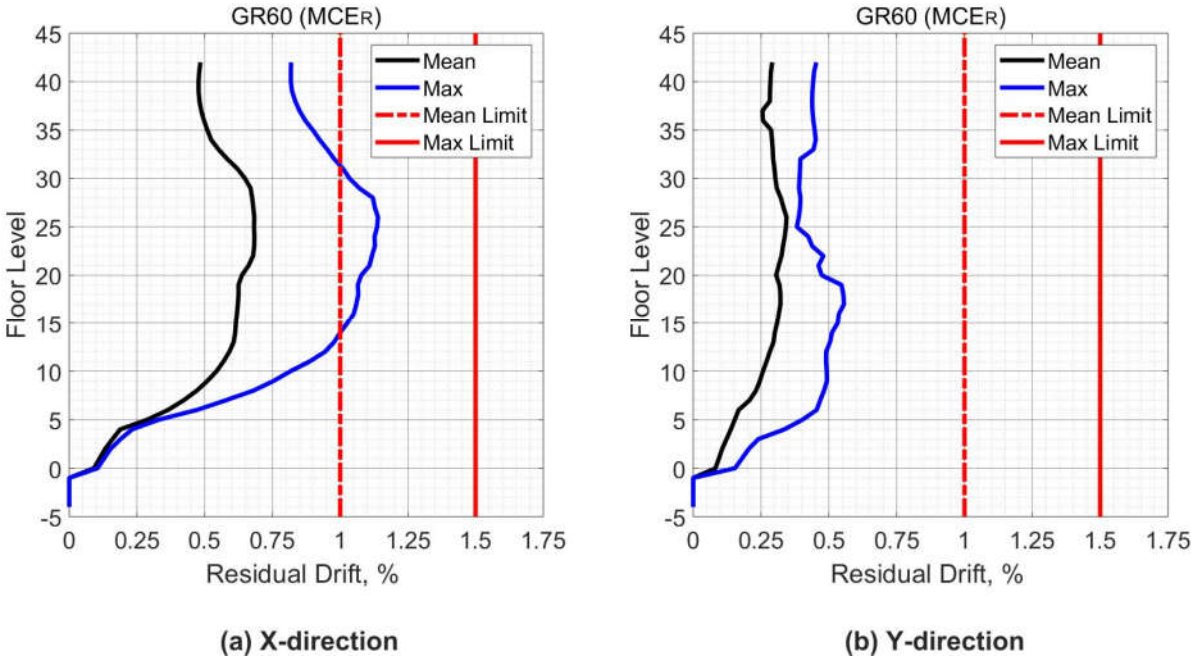

Figure 7.33 Peak Residual Drift (Case 1 – MCER).

7.3.1.3 Displacement

In the MCER level, the TBI guidelines do not require checking the displacement demands. As in section 7.2.1.2, Figure 7.34 depicts the mean value of the displacement of each story at the same time step that the roof experiences a maximum displacement value. The mean displacement of the roof was 80 in and 50 in for x and y-direction, respectively.

Figures 7.35 and 7.36 show the time history of the roof displacement in the x-direction and y-direction, respectively from a ground motion at which the displacement demand of the roof was the highest one among other ground motions. During the tenth ground motion, the roof experienced a maximum displacement in the x-direction while during the seventh ground motion the maximum

roof displacement in the y-direction was observed.

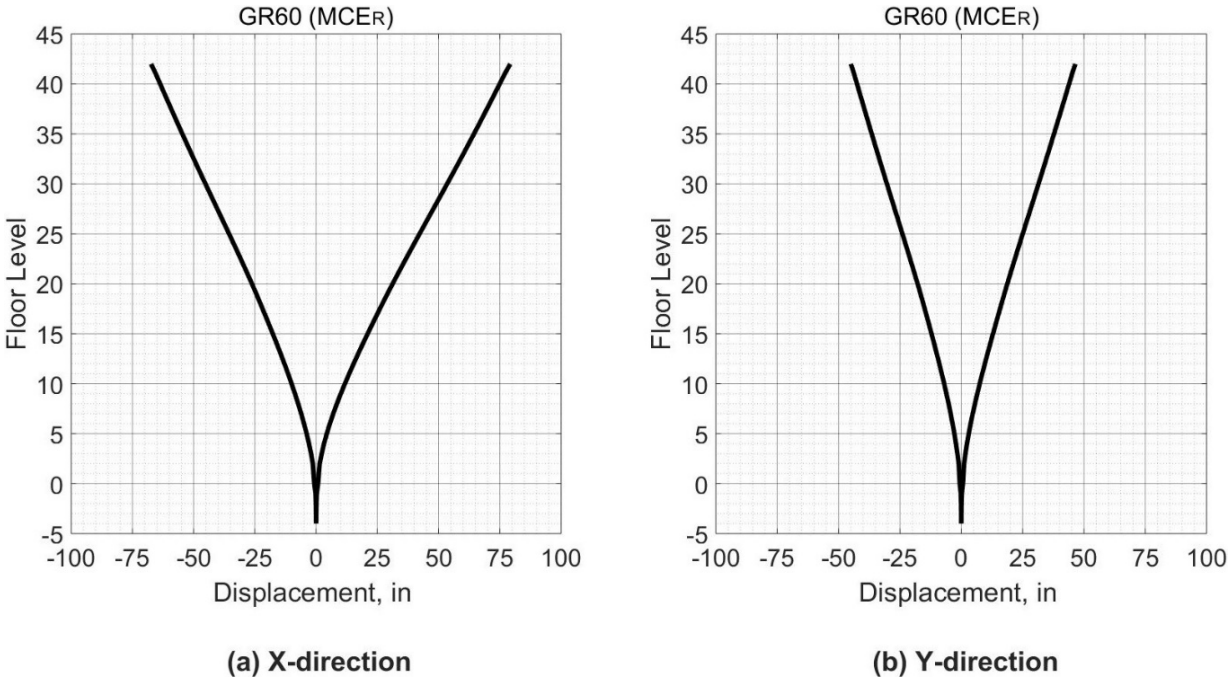

Figure 7.34 Floors Displacement Synchronous with Peak Roof Displacement (Case 1 - MCER).

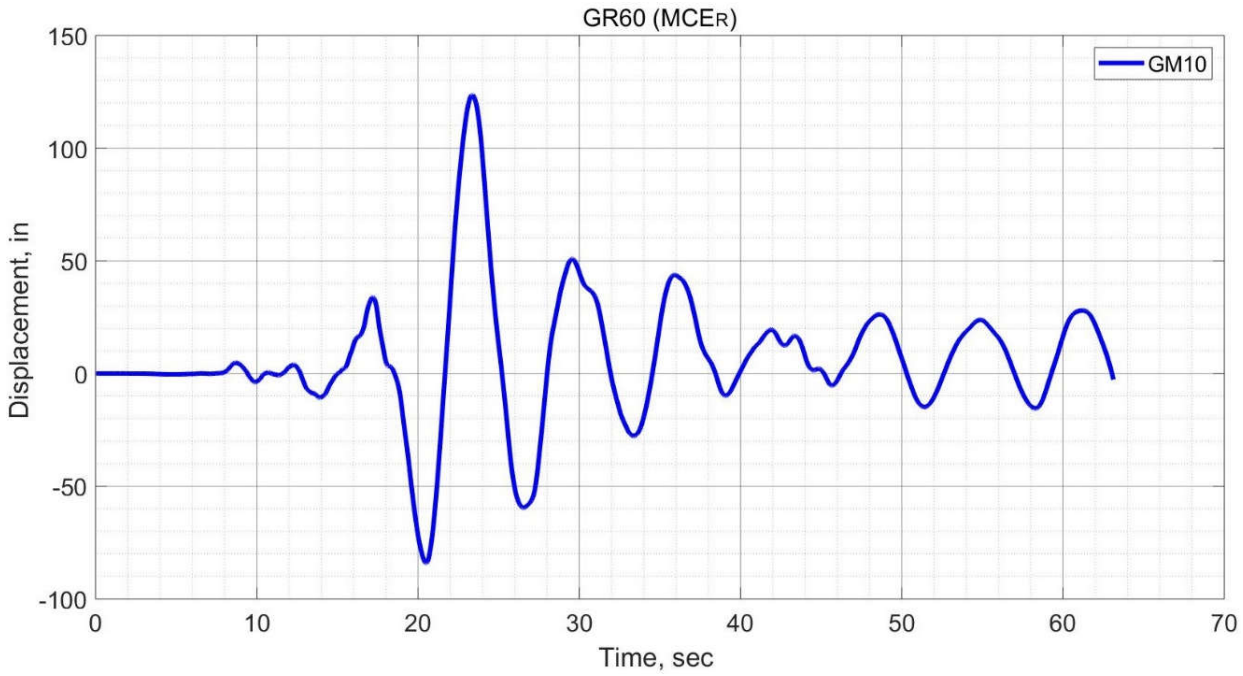

Figure 7.35 Time History for Peak Roof Displacement for X-direction (Case 1 – MCER).

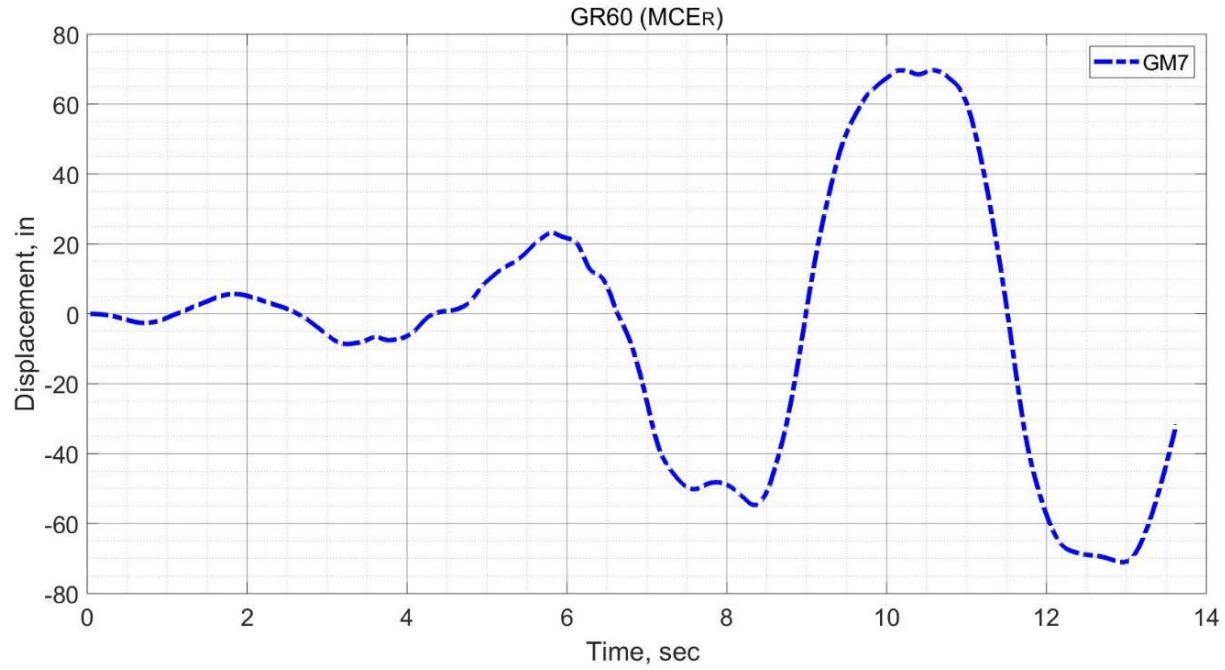

Figure 7.36 Time History for Peak Roof Displacement for Y-direction (Case 1 – MCER).

7.3.2 Element Level

As mentioned in Section 7.2.2, the TBI guidelines require categorizing the actions in all structural members as force-based actions or deformation-based actions for the evaluation process. For the MCER shaking level, it is crucial to mention that the TBI guidelines require using the mean value from all analyses for evaluation with the acceptance criteria for force-based actions, while using the maximum value from all analyses for deformation-based actions. In addition, for both actions the TBI guidelines require using the maximum value from all analyses to evaluate with the acceptance criteria to ensure that all calculated demands from any analysis are within the acceptable range of the model. In the subsections below, the elements of the seismic force resisting system with their actions are presented and evaluated using the acceptance criteria of the TBI guidelines.

7.3.2.1 Core Wall Response

7.3.2.1.1 Core Wall Force-Based Action

The TBI guidelines specify that shear force in the core walls of tall buildings is a force-based action. To evaluate the shear demands of core walls, the TBI guidelines require that the shear force demands satisfy the following equations:

$$1.925 \times V_{mean} \leq V_{exp} \quad \textbf{(7-8)}$$

V_{mean} is the mean value of the maximum shear demands from all ground motions. V_{exp} is described in Equation (7-2).

Figure 7.37 shows the core wall shear forces over the building height and the limiting (V_{exp}) as in Equation (7-8). The shear demands in the core wall satisfy Equation (7-8) as required by the

TBI guidelines. In addition, the shear force demands vary approximately in a linear manner with the height of the building. A small increase in the shear force demands in the y-direction was noticed compared with demands in the x-direction. As shown in Figure 7.37, considering that the maximum demand of the shear force in the core wall was also within the acceptable limits, all analyses produced an acceptable response and all results are within the acceptable modeling range. The maximum observed shear force demand was 13390 kips for y-direction, while 11070 kips in x-direction. A change in the shear response of the core wall was noticed at the twentieth story due to the wall thickness changing from 24 in. to 18 in.

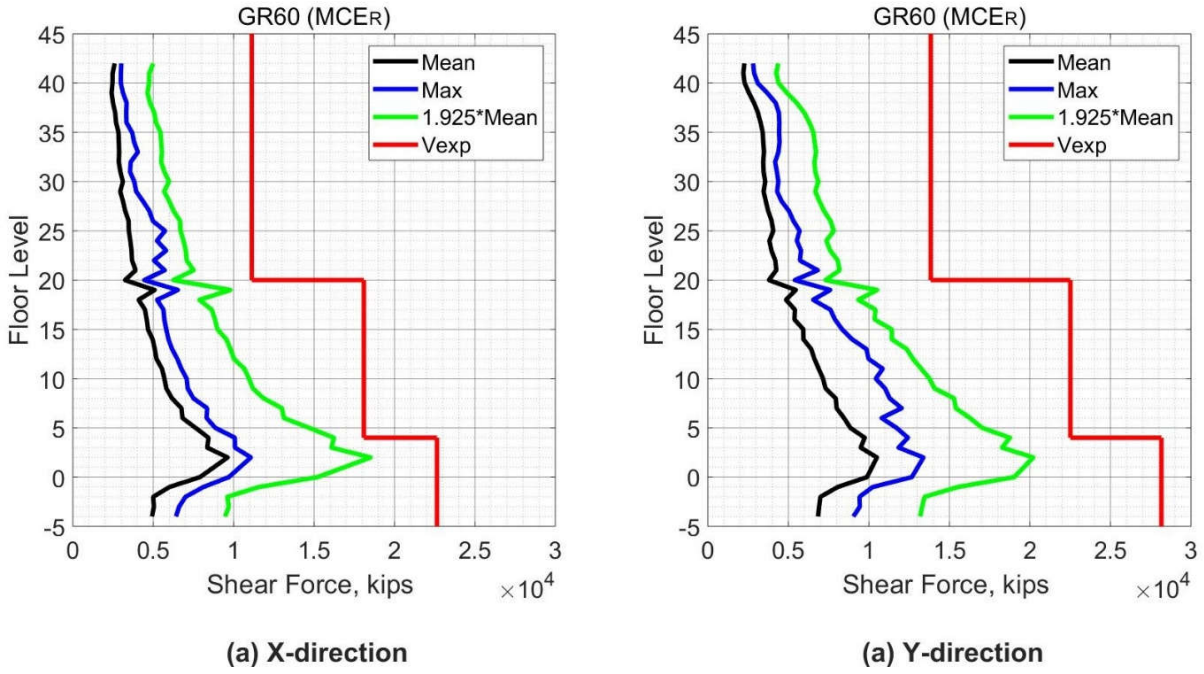

Figure 7.37 Shear Forces in Core Wall (Case 1 – MCER).

7.3.2.1.2 Core Wall Deformation-Based Action

As stated in Section 7.2.2.1.2, the TBI guidelines specify the tensile strain in the reinforcing steel and concrete compression strain as deformation-based actions for shear walls. The TBI guidelines require that the maximum strain demands in the steel bars and concrete should be less than the acceptable limits. Therefore, the strain demands in the reinforcing steel and concrete were monitored during the analyses on all edges of the core wall. The strain was determined by using the vertical displacement (Δz) of the nodes of the core wall edges as described in Section 7.2.2.1.2. The TBI guidelines recommend using 0.05 and 0.003 as acceptable limits for tensile strains in reinforcing bars and compression strains in concrete, respectively for MCER level.

Figures 7.38 to 7.41 show that the maximum tensile strain in the core wall reinforcement is 0.015, which is below the acceptable limit of 0.05. However, the reinforcing bars experienced yielding for all stories from ground story to the thirty second story. The core wall below the ground level did not experience yielding because of the effect of the podium's levels. The maximum tensile strain of reinforcing bars in the core wall occurred at the first story above the podium. A change in the tensile strain was noticed at the twentieth story due to the wall thickness changing from 24 in. to 18 in.

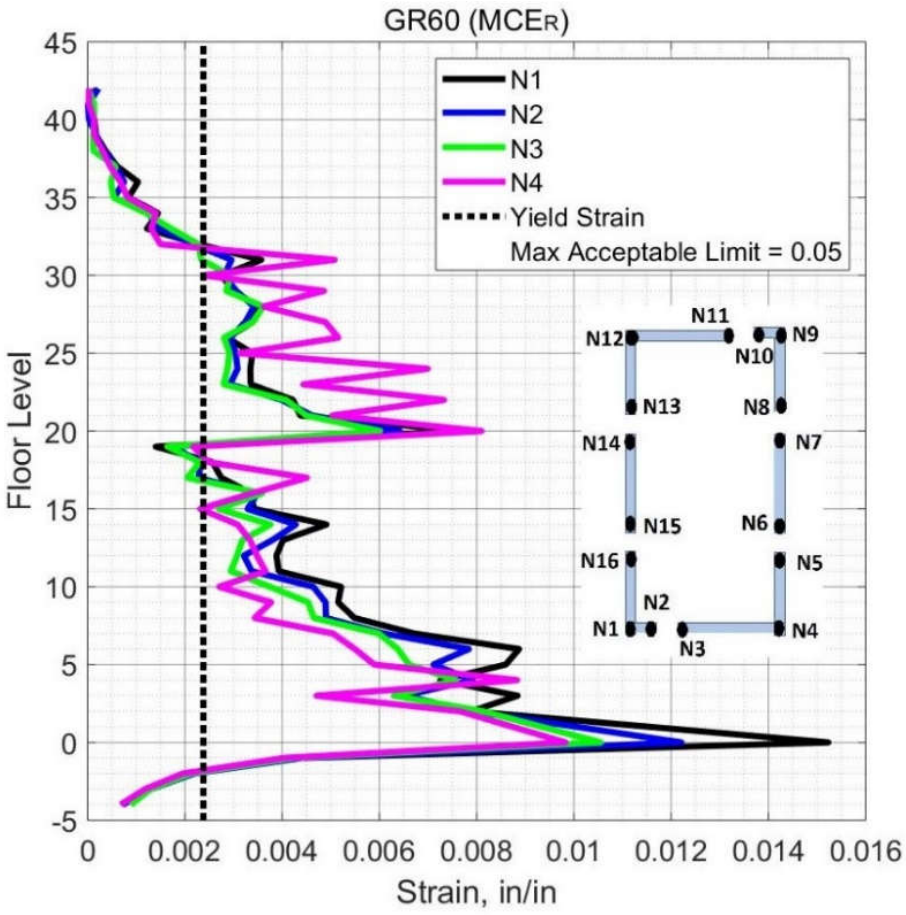

Figure 7.38 Peak Tensile Strain in Steel Bars in Core Wall Edges N1-N4 (Case 1 – MCER).

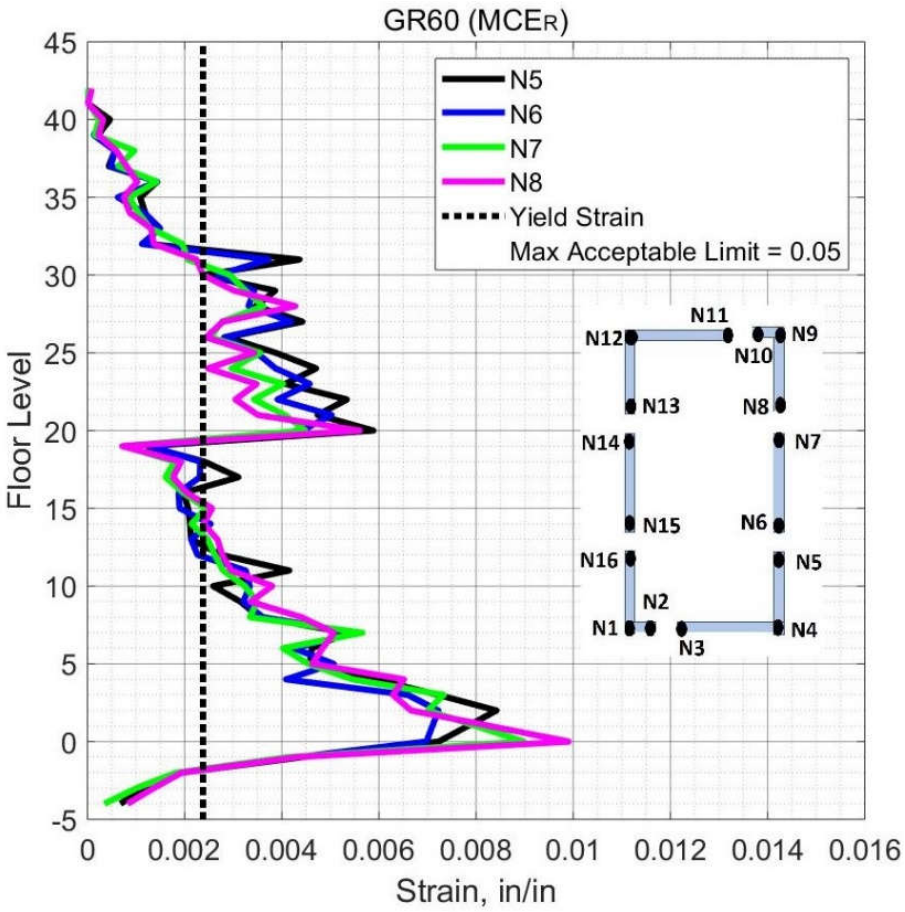

Figure 7.39 Peak Tensile Strain in Steel Bars in Core Wall Edges N5-N8 (Case 1 – MCER).

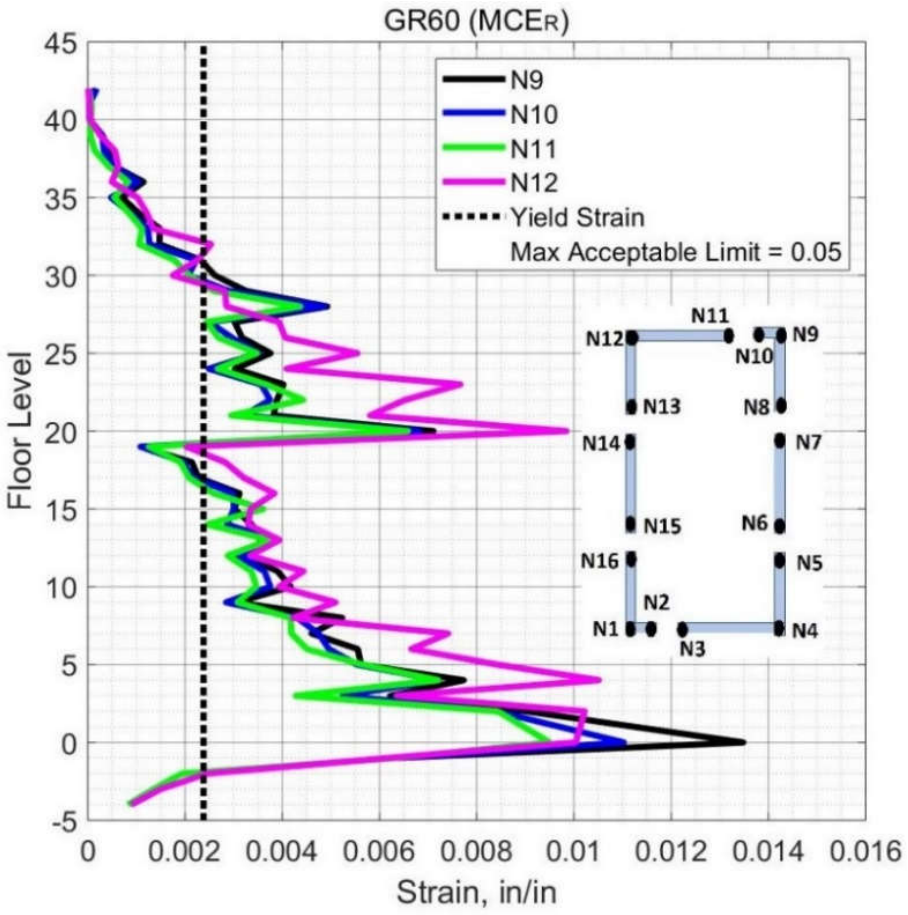

Figure 7.40 Peak Tensile Strain in Steel Bars in Core Wall Edges N9-N12 (Case 1 – MCER).

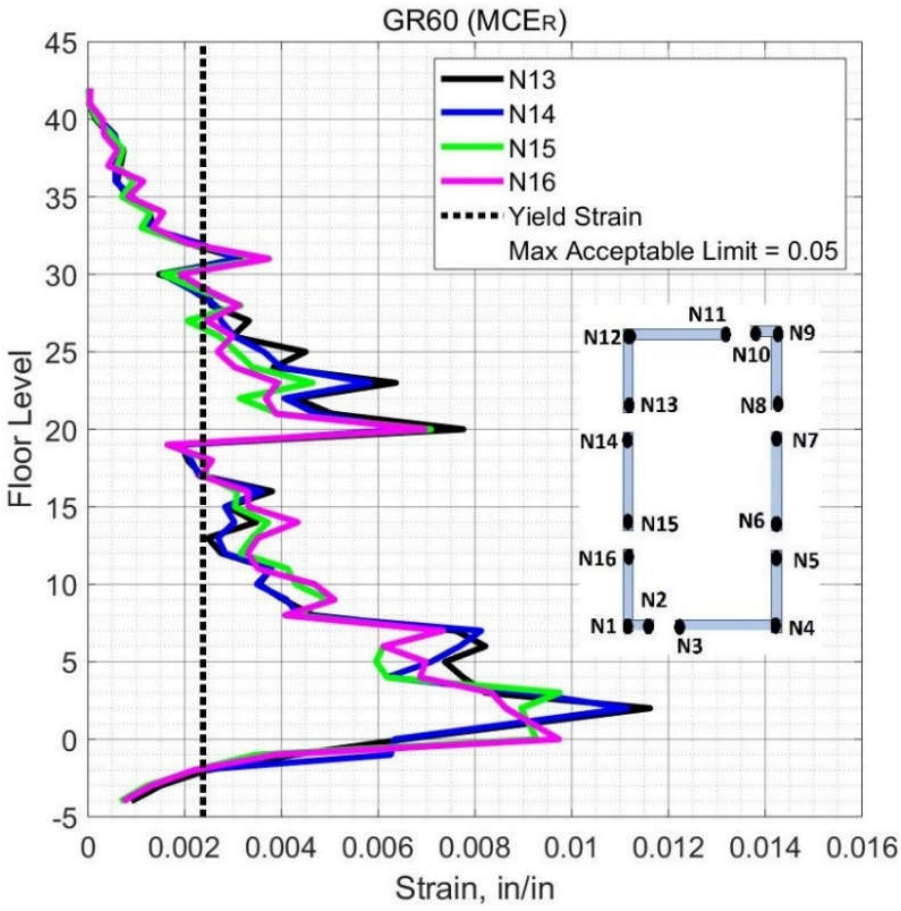

Figure 7.41 Peak Tensile Strain in Steel Bars in Core Wall Edges N13-N16 (Case 1 – MCER).

Figures 7.42 to 7.45 show the maximum values of the compression strain in the core wall concrete at the wall edges over the building height. The core wall concrete experiences fairly low values of concrete compression strain, below 0.002, for all stories as shown in Figures 7.42 to 7.45. The maximum compression strain of concrete in the core wall occurred at the first story above the podium. A small change in the compression strain was noticed at the twentieth story due to the wall thickness changing from 24 in. to 18 in.

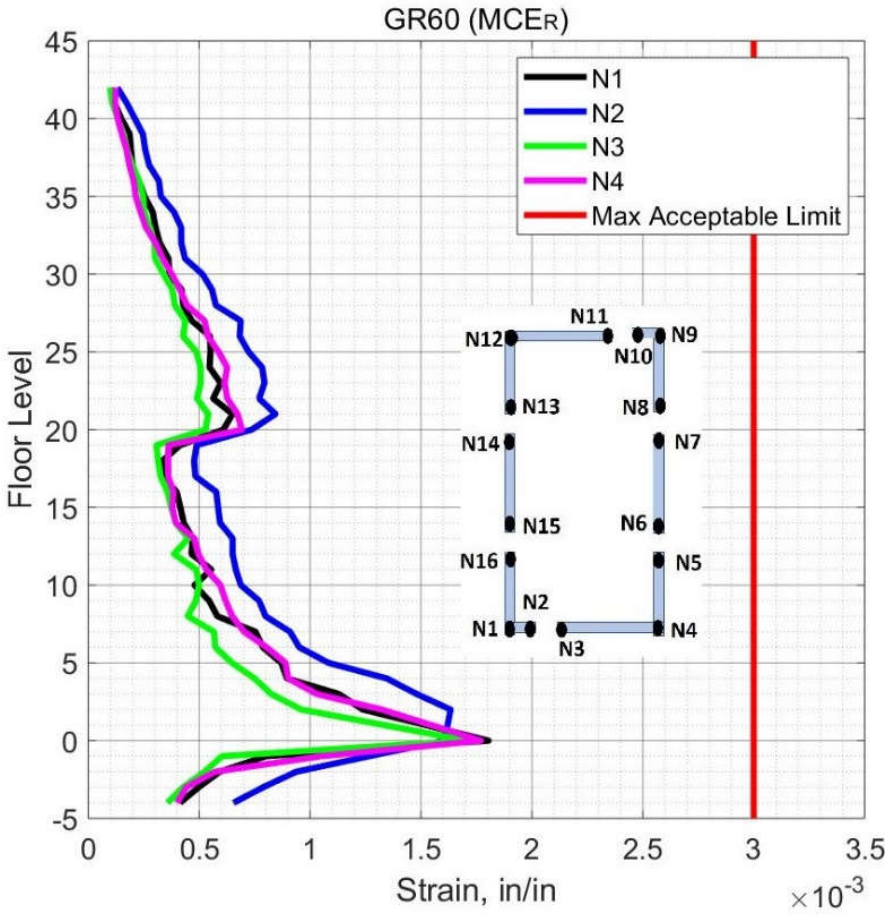

Figure 7.42 Peak Concrete Compression Strain in Core Wall Edges N1-N4 (Case 1 – MCER).

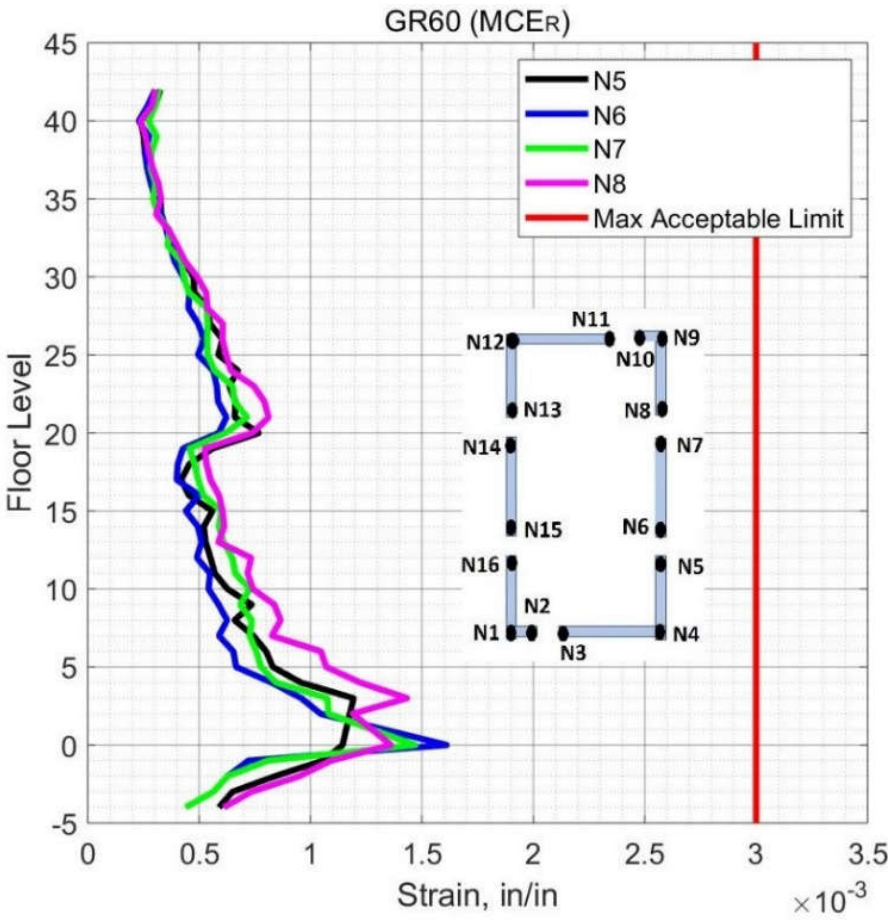

Figure 7.43 Peak Concrete Compression Strain in Core Wall Edges N5-N8 (Case 1 – MCER).

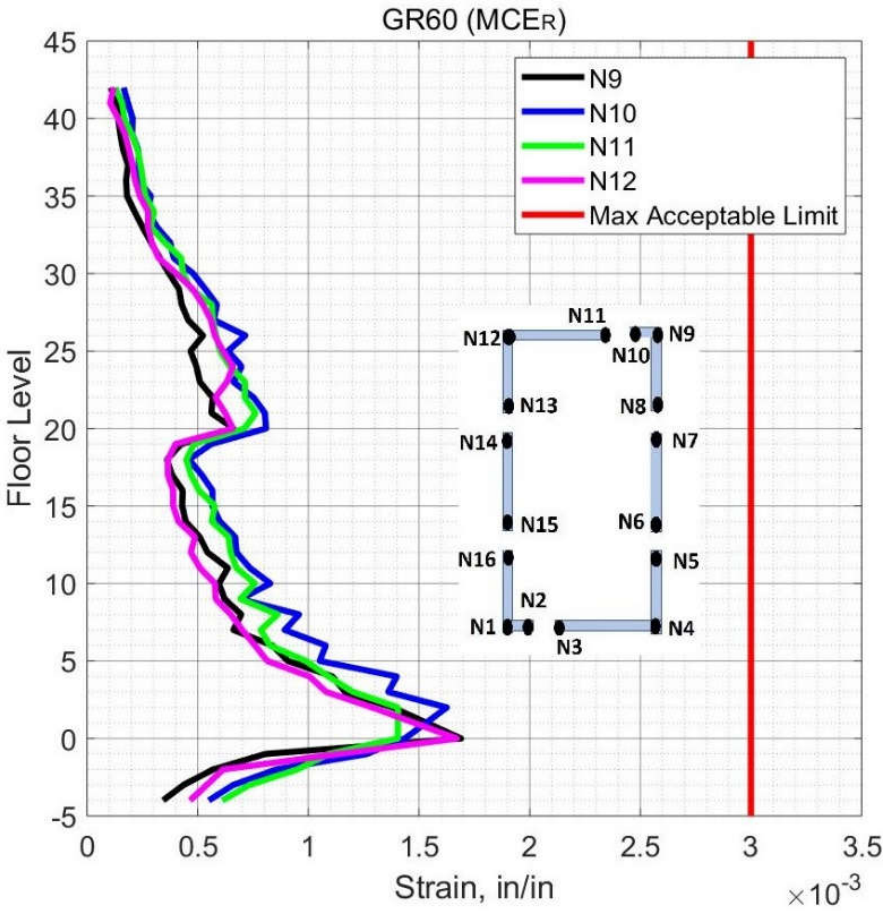

Figure 7.44 Peak Concrete Compression Strain in Core Wall Edges N9-N12 (Case 1 – MCER).

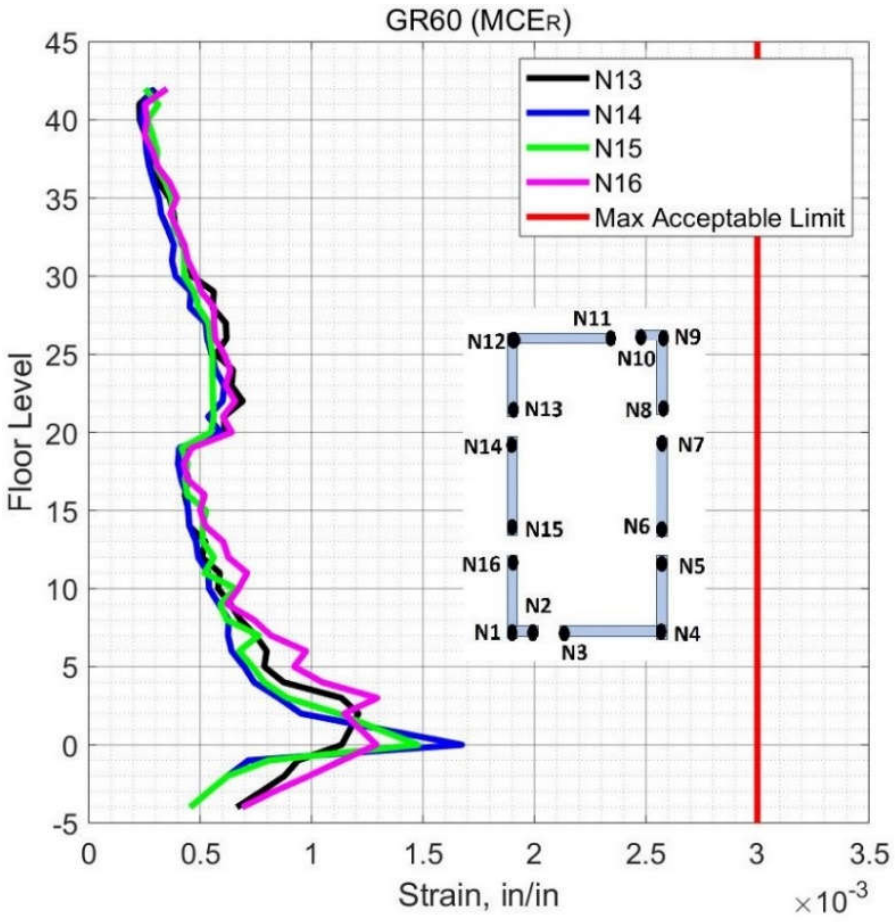

Figure 7.45 Peak Concrete Compression Strain in Core Wall Edges N13-N16 (Case 1 – MCER).

7.3.2.1.3 Coupling Beams

As stated in Section 7.2.2.1.3, the rotation is the deformation based-action for coupling beams with diagonal reinforcing. The rotation demand of all the coupling beams was monitored during all the analyses. To determine the acceptable capacity of coupling beams rotation for the MCER level, the TBI guidelines recommend using the acceptance criteria of ASCE 41 for Collapse Prevention level or the test data if available. The maximum allowable rotation is 0.05 according to the ASCE 41. The same fragility curves, that provided by A study by (Naish 2010) and used in

Section 7.2.2.1.3, will be utilized to examine the performance of the coupling beams in the MCER shaking level.

Figure 7.46 (a) shows the mean and maximum values of the rotation of coupling beams with a 1.7 aspect ratio (coupling beams in the x-direction), over the building height. The peak value of the rotation is 0.02 which is below the allowable limit of 0.05. The results indicate that coupling beams experienced yielding of steel reinforcement according to the data in Figure 7.18. In addition, the coupling beams are expected to have a damage state (DSI), which means that the coupling beams need minor repair. However, the rotation demands of coupling beams satisfy the requirement of the TBI guidelines for MCER level.

Figure 7.46 (b) shows the mean and maximum values of the rotation of coupling beams with a 2.1 aspect ratio (coupling beams in the y-direction), over the building height. The peak value of the rotation is 0.025 which is below the allowable limit of 0.05. The results indicate that coupling beams experience yielding of steel reinforcement according to the data in Figure 7.19. In addition, the coupling beams are expected to have a damage state (DSI), which means that the coupling beams need minor repair. However, the rotation demands of coupling beams satisfy the requirement of the TBI guidelines for MCER level.

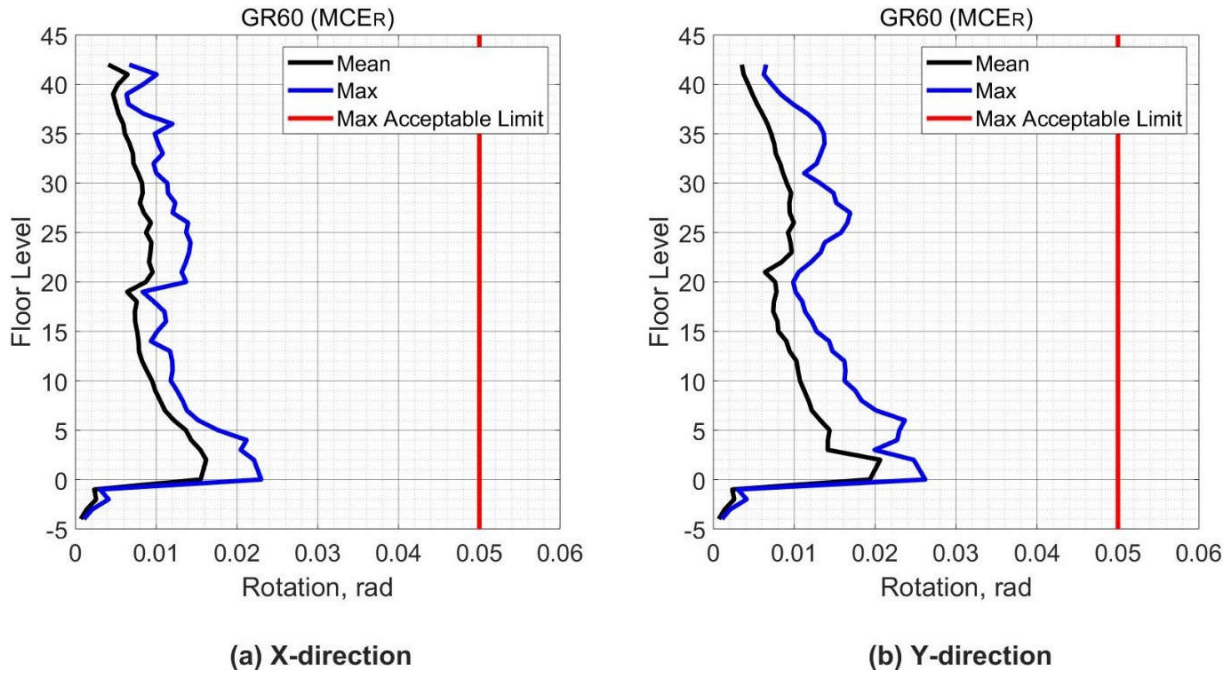

Figure 7.46 Rotation Demand in Coupling Beams (Case 1 – MCER).

7.3.2.2 Special Moment Frame Response

7.3.2.2.1 Beam Force-Based Action

The TBI guidelines specify the shear in the beams of special moment frames as a force-based action. For evaluation of a force based-action in a structural element for MCER level, the TBI guidelines provide the following equations:

$$Q_{final} \leq Q_{exp} \tag{7-9}$$

$$Q_{final} = (1.7 + 0.3S_{ms})D + 1.5L + 1.925I_e(Q_T - Q_{ns}) \tag{7-10}$$

Where:

Q_{final}	Final demand of the force based-action, see Equation (7-10)
Q_{exp}	Expected capacity of the force-based action in the structural element from the ACI 318-14 equations when using the expected material strengths.
S_{ms}	Spectral response acceleration at the short period after site class adjustment as defined in ASCE 71-16
D	Dead load effects.
L	Live load effect
I_e	Seismic importance factor as defined in ASCE 7-16.
Q_T	Mean value of the force based-action from all the ground motions in the suite.
Q_{ns}	Value of the force based-action from non-seismic loads.

As mentioned above, the TBI guidelines specify that the shear force in the beams is a force based-action. Consequently, the expected shear capacity of the beams, Q_{exp}, is calculated using the equation from ACI 318-14 (Equation (7-5)). To evaluate the shear action in beams, Equation (7-9) will be as follows:

$$V_{final} \leq V_{exp} \quad \textbf{(7-11)}$$

V_{final} is the shear force demands in beams calculated from Equation (7-10) ($V_{final} = Q_{final}$). V_{exp} is calculated by using Equation (7-5). It is important to note that the contribution of concrete in shear strength of beams is not considered to be more conservative.

Figure 7.47 shows the shear force demands in the beams of the special moment frame over the building height. In the legend of Figure 7.47, the results noted as "Mean" represent the mean value of the maximum shear force in the beams at each floor level from all ground motions analyses, while the results noted as "Max" represent the maximum shear force in the beams obtained from all analyses. In addition, the values shown as "Vfinal" and "Vexp" in the legend were obtained by using Equations (7-10) and (7-5), respectively. As shown in Figure 7.47, the main conclusion is that shear force demands in special moment frame beams meet the requirements of the TBI guidelines by satisfying Equation (7-11). In addition, the maximum shear force demands (350 kips) obtained from all ground motions are within the acceptable limits of the expected shear capacity (667 kips) of the beams. Consequently, all analyses produced an acceptable response based on the maximum shear force demands in the beams.

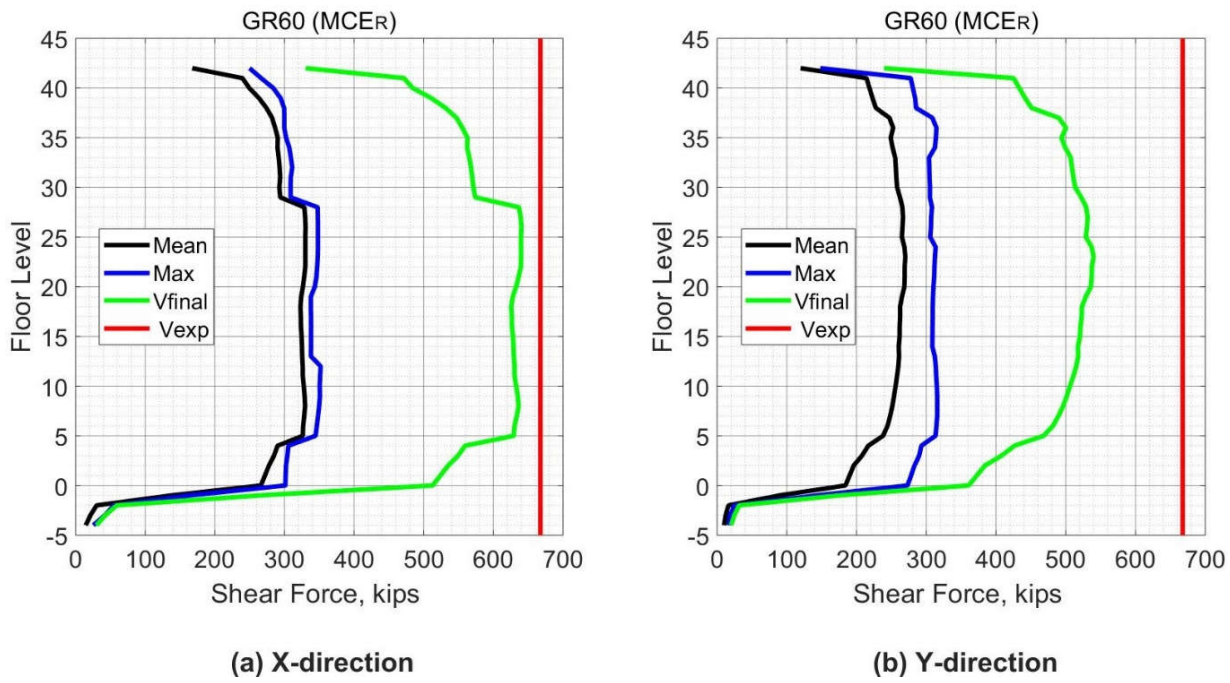

Figure 7.47 Peak Shear Force in Beams (Case 1 – MCER).

7.3.2.2.2 Beam Deformation-Based Action

As stated in Section 7.2.2.2.2, the deformation-based action for beams is the plastic rotation of the beam chord. Due to the use of the fiber section for modeling the beam cross-sections, the tensile strains in the longitudinal reinforcing bars in beams were also monitored as another indicator for flexural demands on the beams. To calculate the plastic rotation demands in the beams and columns of special moment frame in the MCER level, the same procedure used in Section 7.2.2.2.2 will be applied. The procedure requires monitoring the section curvature at each time during each analysis.

To calculate the acceptable limit of rotation capacity of beams and columns, TBI guidelines permit using the acceptance criteria of ASCE 41 for Collapse Prevention level. For the acceptable limit of tensile strain in the reinforcing bars, both TBI guidelines and ASCE 41 give 0.05 as a maximum acceptable tensile strain limit.

Figure 7.48 shows the mean and the maximum tensile strain demands in the longitudinal reinforcement of the beams at each floor level. The maximum tensile strain demands (0.027) are within the acceptable limit (0.05). In addition, reinforcing bars in beams oriented in the x-direction experienced more tensile strain (0.027) compared to beams oriented in the y-direction (0.009). The expected yield strain of Grade 60 is 0.0024. Figure 7.48 depicts that all beams in levels above the main podium experienced yielding of reinforcing bars.

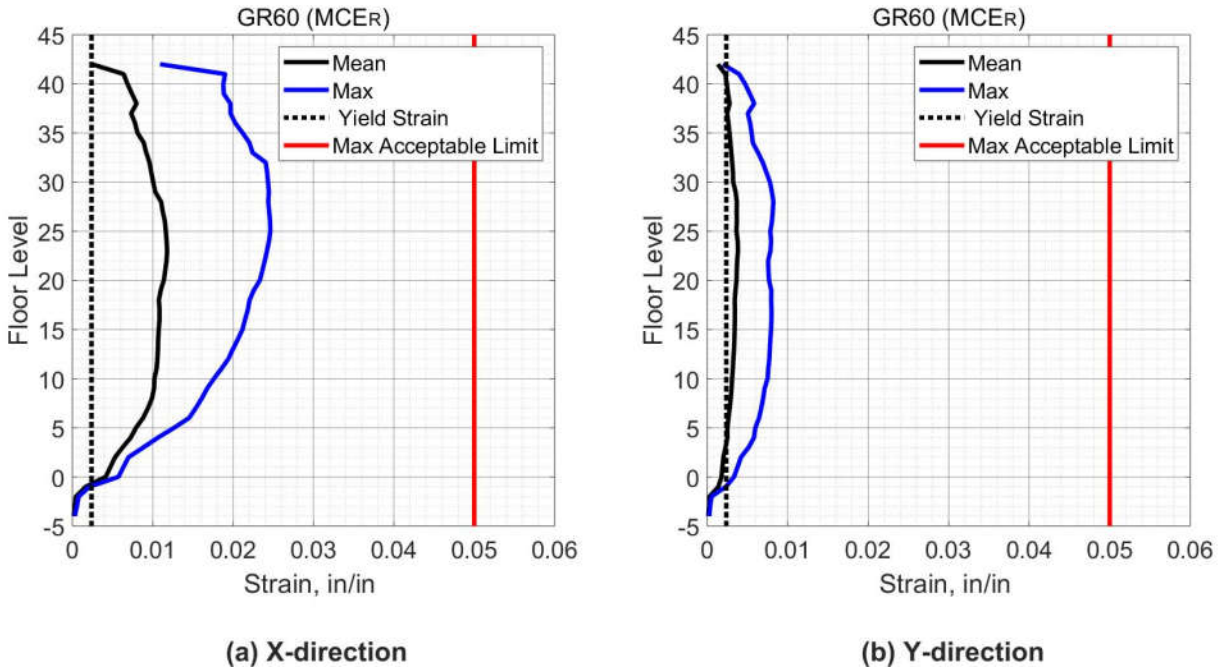

Figure 7.48 Peak Tensile Strain in Reinforcing bars in Beams (Case 1 – MCER).

Figure 7.49 shows the mean and the maximum plastic rotation demands in the beams at each floor level. The plastic rotation demand was approximately 0.030 rad which is below the acceptable limits of 0.045 of ASCE 41 for the beams. A consistent finding with the tensile strain demands is observed in which beams oriented in the x-direction experienced more rotation

demands compared with beams in the y-direction. Based on the strain and plastic rotation results, the deformation-based actions in the beams satisfy the requirement of TBI guidelines.

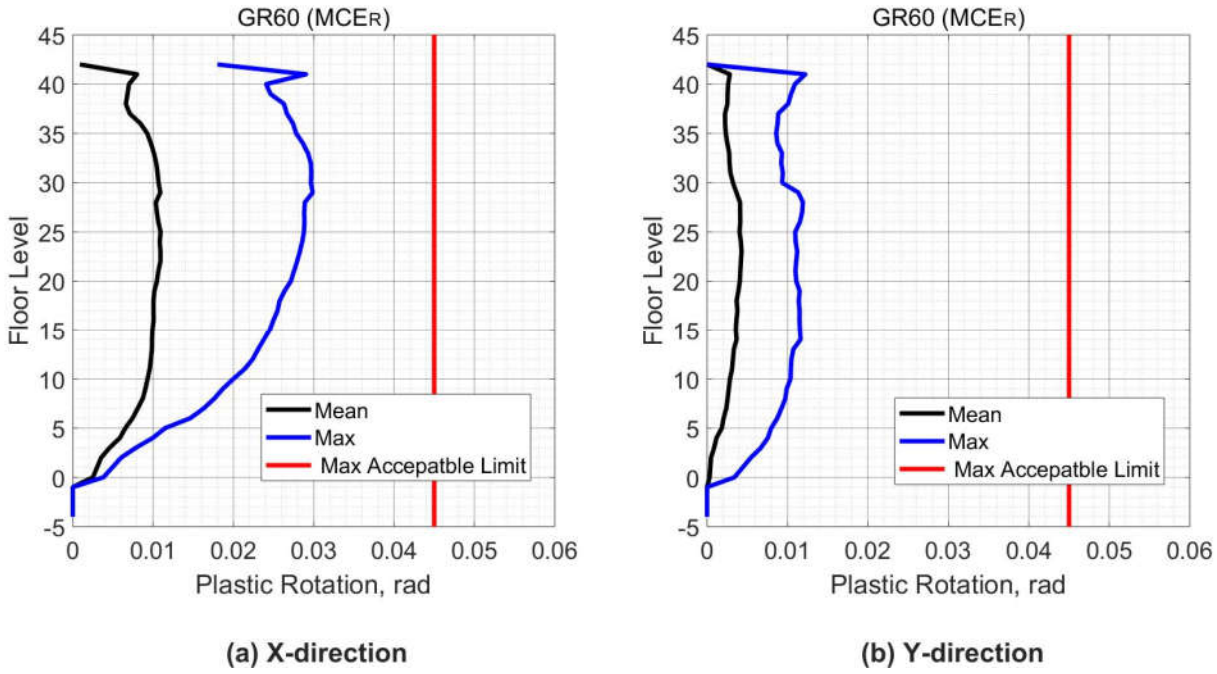

Figure 7.49 Plastic Rotation in Beams (Case 1 - MCER).

7.3.2.2.3 Columns Force-based Action

The same equations and procedure used in evaluating the shear forces demands in beams in Section 7.3.2.2.1 were applied to evaluate the shear force demands in the columns of the special moment frames. In the legend of Figures 7.50 through 7.53, the results noted as "Mean" represent the mean value of the shear force in the columns from all ground motions analyses while the results noted as "Max" represent the maximum shear force obtained from all analyses. In addition, results with "Vfinal" and "Vexp" in the legend represent the parameters in Equation (7-11) for the columns. As shown in Figures 7.50 to 7.53, the shear force demands in the columns are within the

limits of the TBI guidelines, by satisfying equation (7-11). The maximum shear demands obtained from all analyses are also within the acceptable limits (shear force capacity). Therefore, all analyses produced acceptable responses when considering the shear force demands of the columns. In contrast with the shear force demands of the core wall, the shear forces in the columns were more uniform with building height.

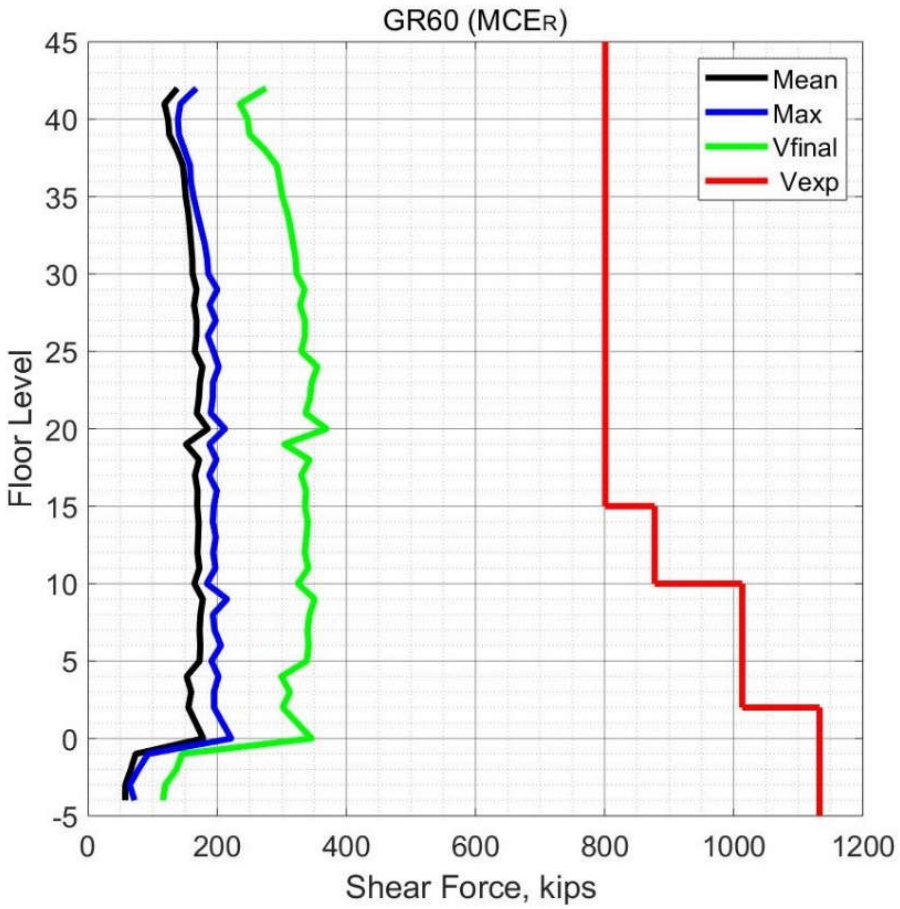

Figure 7.50 Peak Shear Force in Corner Columns (Case 1 – MCER).

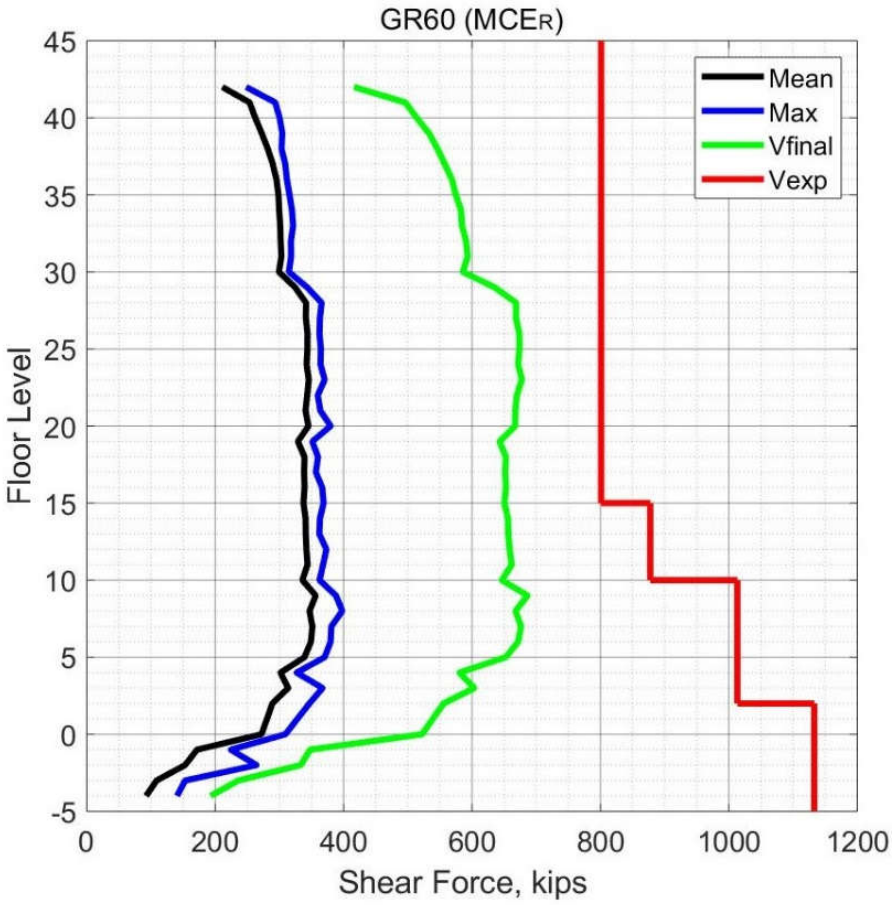

Figure 7.51 Peak Shear Force in Interior Columns X-direction (Case 1 – MCER).

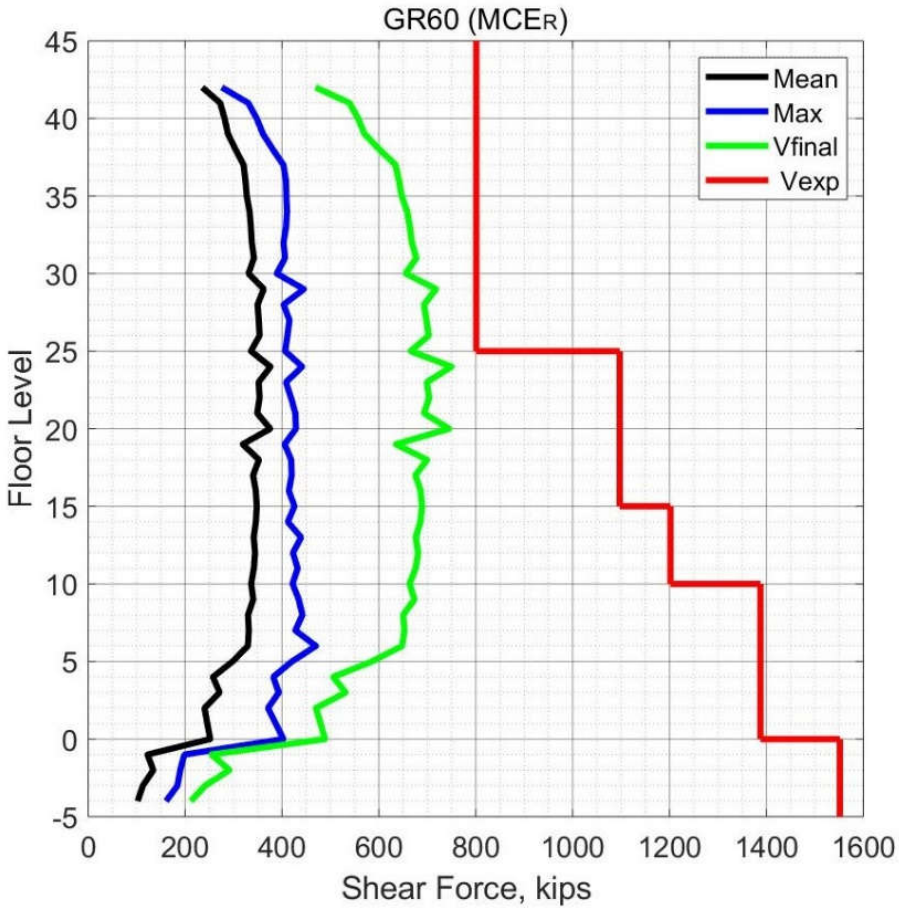

Figure 7.52 Peak Shear Force in Columns on Grid B and E (Case 1 – MCER).

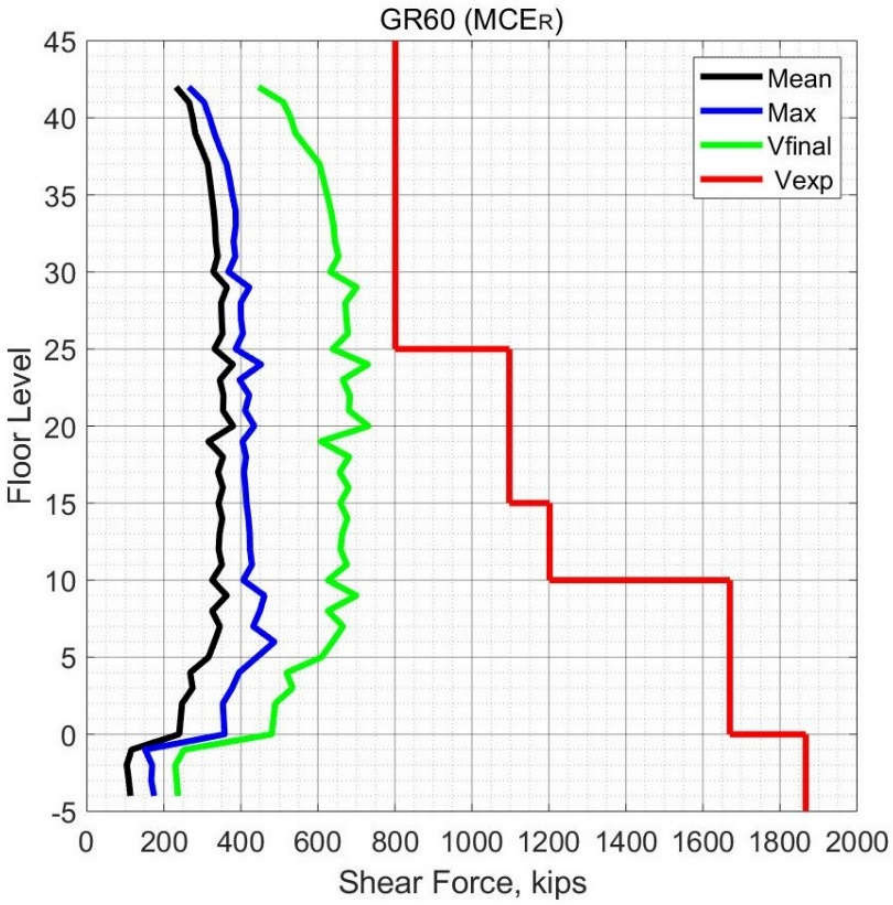

Figure 7.53 Peak Shear Force in Columns on Grid C.5 (Case 1 – MCER).

7.3.2.2.4 Column Deformation-Based Action

The deformation-based action for columns is the plastic rotation of the columns' chords. To satisfy the requirement of TBI guidelines, the maximum plastic rotation demands in the columns from all ground motions in the suite should be less than the rotation capacity of the columns. To calculate the plastic rotation demands on the columns, the same procedure and equations that used for determining beams demands in Section 7.2.2.2.2 (Equation (7-6) and (7-7)), were utilized for the columns. To calculate the acceptable limit of columns rotation capacity, the TBI guidelines permit using the acceptance criteria of ASCE 41 for the collapse

prevention level. In addition, modeling the columns cross sections by the fiber section provides a means to monitor the tensile strains in the longitudinal reinforcing bars in the columns. The tensile strain in reinforcing bars of columns reflects the combined effect of axial and moment demands on columns. The maximum value of the tensile strain in the columns' longitudinal bars and the mean value from all ground motion in the suite are depicted in Figure 7.54. The maximum tensile strain demands (0.0023) did not exceed the expected yield strain (0.0024) which means no plastic hinges formed in the columns. In other words, columns did not experience plastic rotations. As mentioned, the preferable design approach is that plastic hinges form in the beams and the columns stay elastic as possible. The behavior of non-yielding columns in the case study building is a preferable behavior in seismic application.

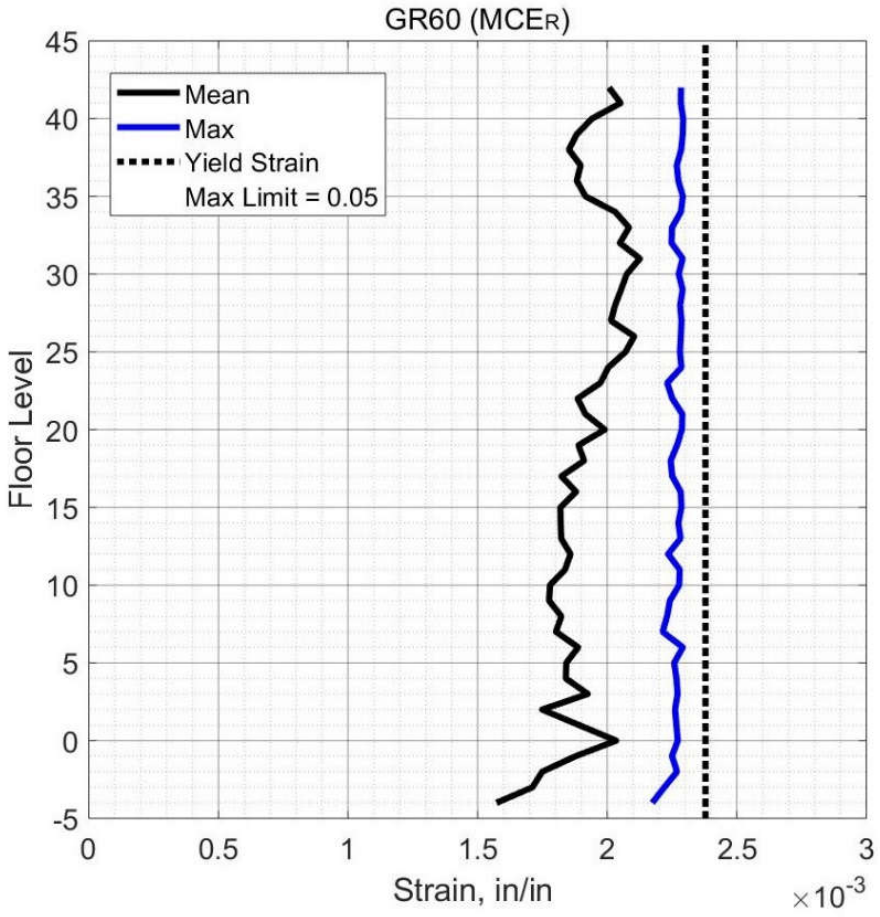

Figure 7.54 Peak Tensile Strain in Reinforcing Bars in Columns (Case 1 – MCER).

7.3.2.3 Contribution of Core Wall and Frame in Dual System

As mentioned previously, the seismic force resisting system (SFRS) of the case study building is a dual system that consists of the core wall and the special moment frame. To better understand the behavior of the dual system, the contribution of its components in resisting the story shear force is depicted in Figure 7.55 for the x- and y-directions, respectively. Figure 7.56 shows the contribution percentage of the shear forces for the core wall and the frame over the building height. The frame contribution is approximately constant over the building height, while the core wall contribution varies linearly. The frame contribution in the lower stories is approximately one-

third of the story shear, while in the upper stories the frame contribution is about one-half of the total story shear.

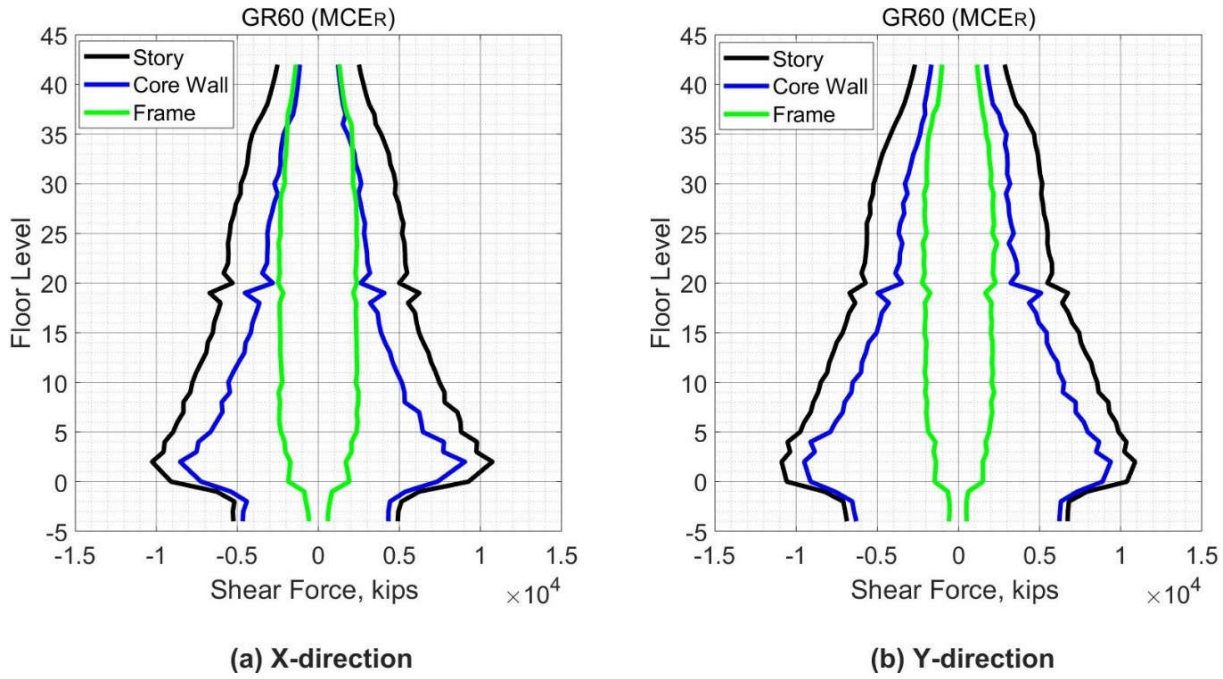

Figure 7.55 Shear Force Contribution of Core Wall & Frame (Case 1 – MCER).

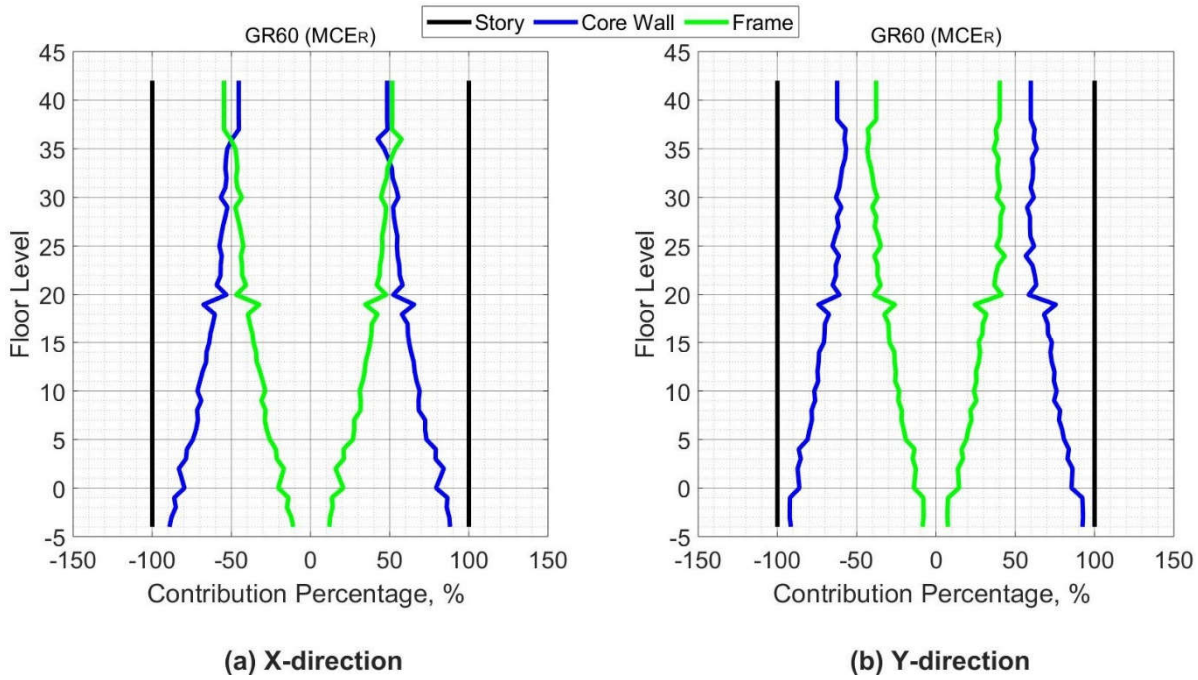

Figure 7.56 Contribution Percentage of Core wall & Frame Shear Force (Case 1 – MCER).

CHAPTER VIII

CASE 2 – GRADE 80 REINFORCEMENT RESULTS

8.1 INTRODUCTION

Case 2 consists of the study building reinforced with high strength reinforcing steel bars in all structural members. ASTM A706 Grade 80 reinforcement was used in the seismic force resisting system (SFRS) in both the core wall and the special moment frames. In this case, the cross-section dimensions of all the structural members were the same as in the case 1, however the area of reinforcement in all members was 0.8 times the area of reinforcement in the case reinforced with the conventional steel bars (case 1). The minimum reinforcing ratio for columns of the special moment frame was 0.01 times the column cross section, while for concrete core wall the minimum ratio was 0.0025 as recommended by (NEHRP, 2014). In the following sections, the response of the case study building reinforced with reduced amount of reinforcement (Grade 80) will be examined and checked with the TBI guidelines acceptance criteria for both SLE and MCER levels. The procedures and equations that used to calculate the structural demand parameters in the previous Chapter (case 1), will be applied for determining the response demands for this case for both SLE and MCER levels.

8.2 SLE LEVEL

The same ground motions used in the SLE in case 1 were used for the SLE analyses of case 2. The results of seven analyses are presented and compared with the acceptance criteria of the TBI guidelines. According to the TBI guidelines, first, the mean value of the response parameters from all ground motions in the suite should be checked with the acceptance criteria. Second, the TBI guidelines do not require checking the maximum response parameters from all ground

motions in this level. However, the maximum response parameters will also be presented to examine the performance of the case study building in more depth.

8.2.1 Global Response

8.2.1.1 Drift Ratio

Figure 8.1 shows the mean and the maximum values of the drift ratios from all analyses over the building height. The mean peak interstory drift from the seven analyses was very close to 0.0047 in the x-direction and approximately 0.0030 in the y-direction, where both values were within the acceptable limit of the TBI guidelines of 0.0050. Figures 8.2 and 8.3 show the peak drift ratios from all ground motions over the building height.

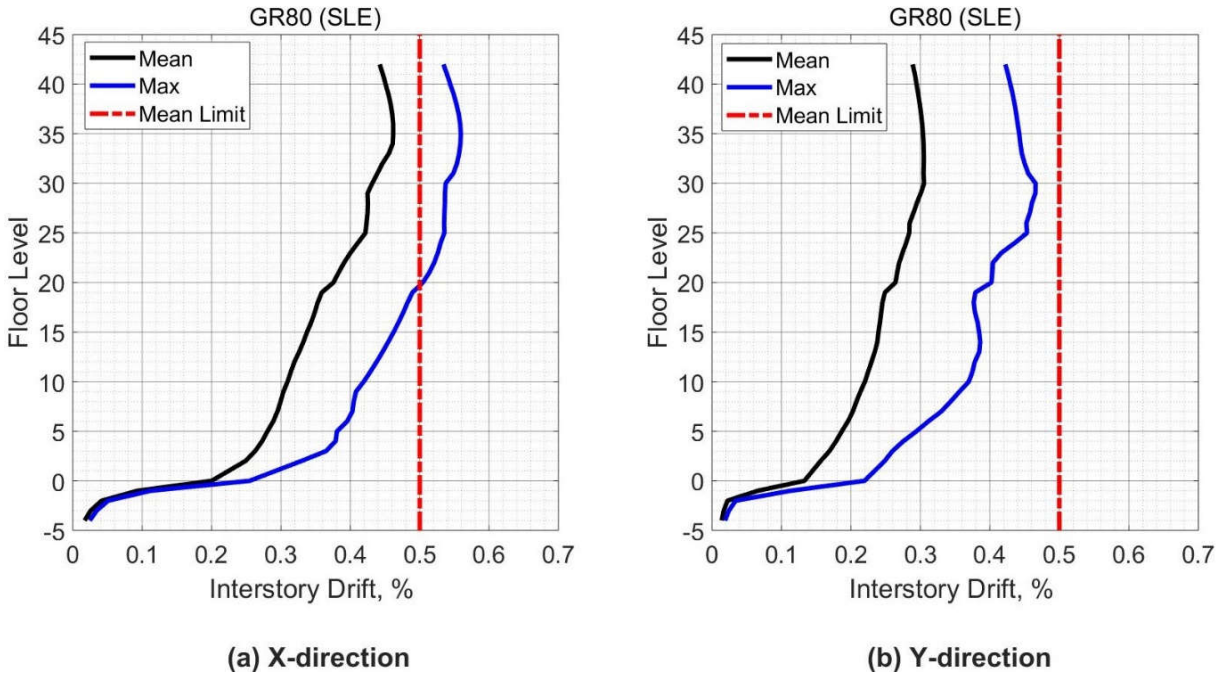

Figure 8.1 Peak Interstory Drift (Case 2 – SLE).

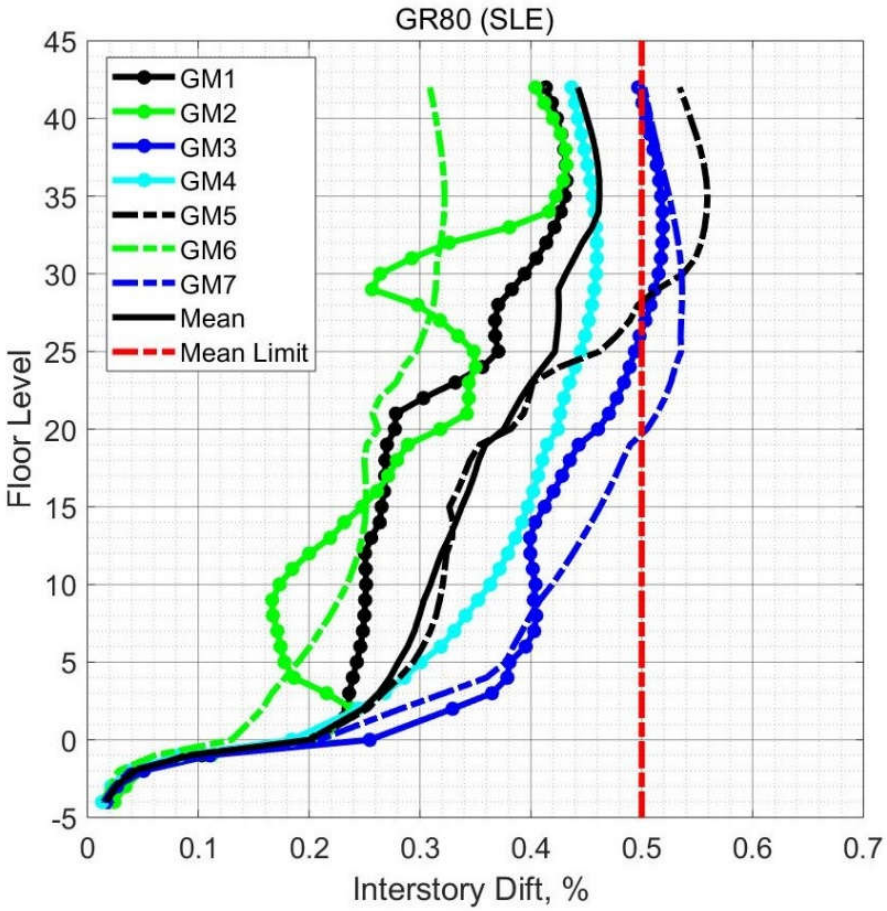

Figure 8.2 Peak Interstory Drift from All Ground Motions for X-direction (Case 2 -SLE).

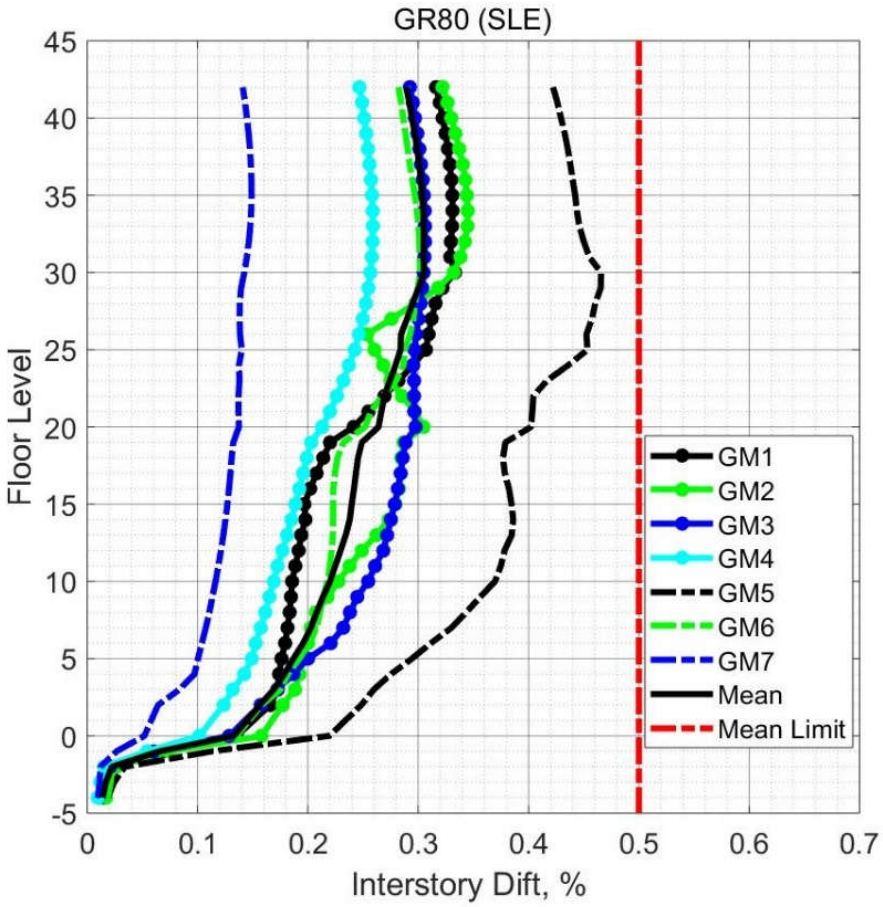

Figure 8.3 Peak Interstory Drift from All Ground Motions for Y-direction (Case 2-SLE).

8.2.1.2 Displacement

As in Section 7.2.1.2, Figure 8.4 depicts the mean value of the displacement of each story at the same time step that the roof experiences a maximum displacement value.

Figures 8.5 and 8.6 show the time history of the roof displacement in the x-direction and y-direction, respectively from a ground motion at which the displacement demand of the roof was the highest one among other ground motions. During the seventh ground motion, the roof experienced a maximum displacement in the x-direction while during the fifth ground motion the maximum roof displacement in the y-direction was observed.

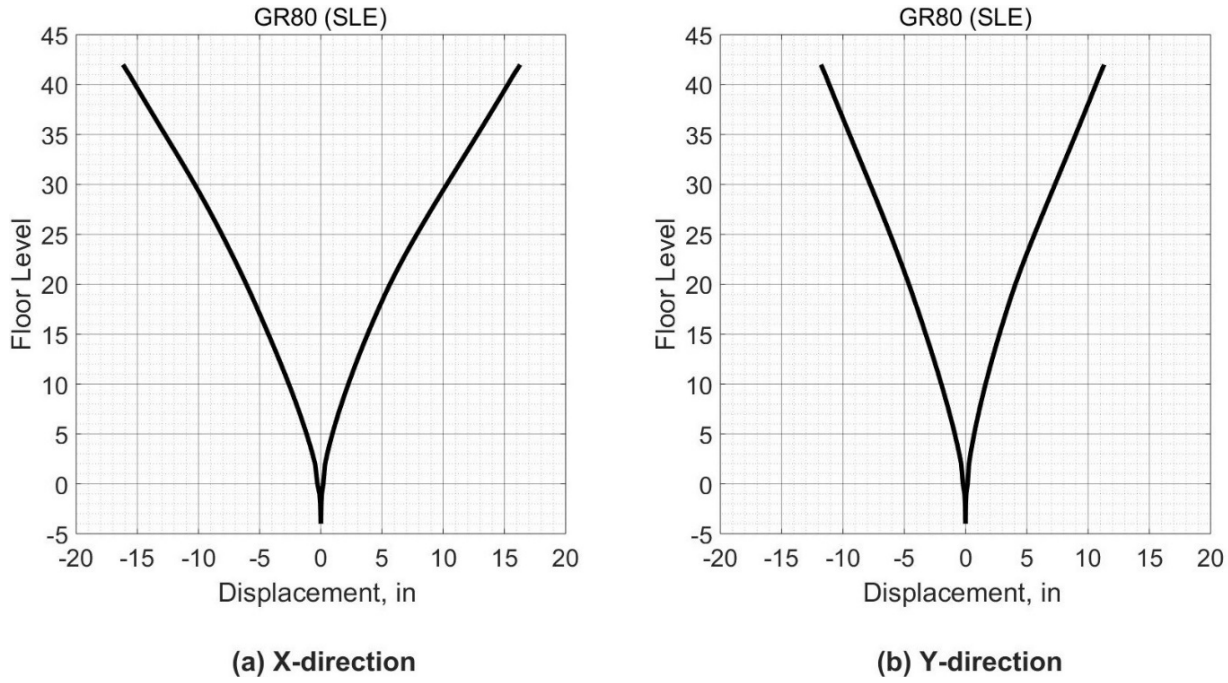

Figure 8.4 Floors Displacement Synchronous with Peak Roof Displacement (Case 2 - SLE).

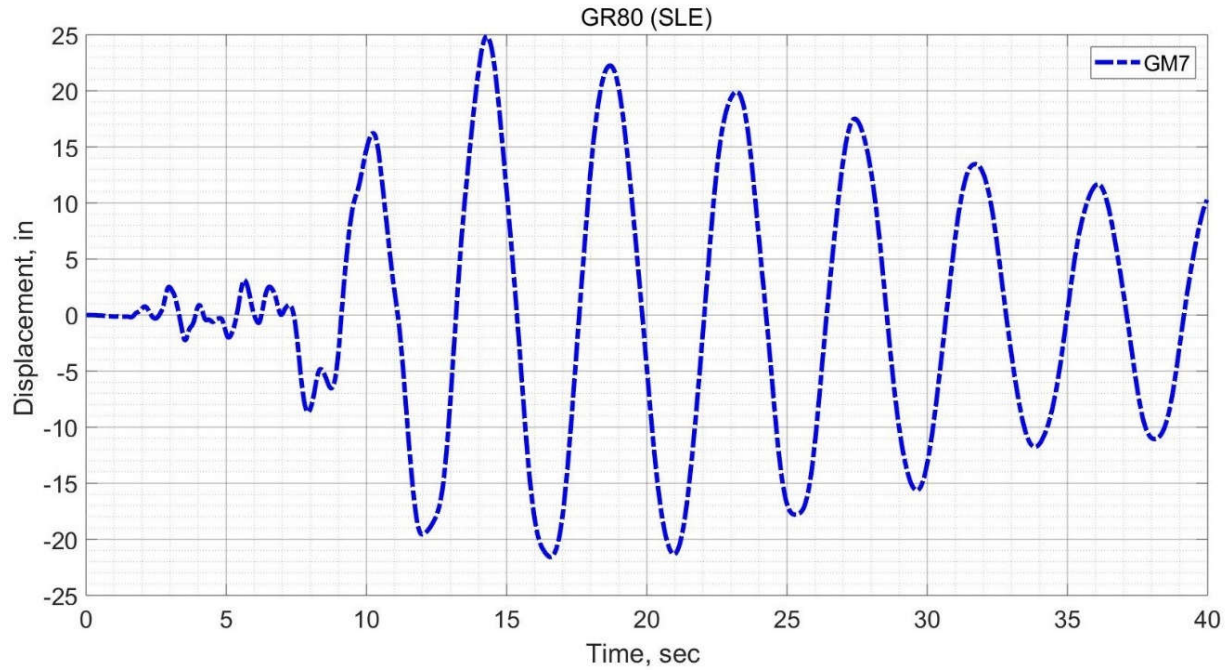

Figure 8.5 Time History for Peak Roof Displacement for X-direction (Case 2 – SLE).

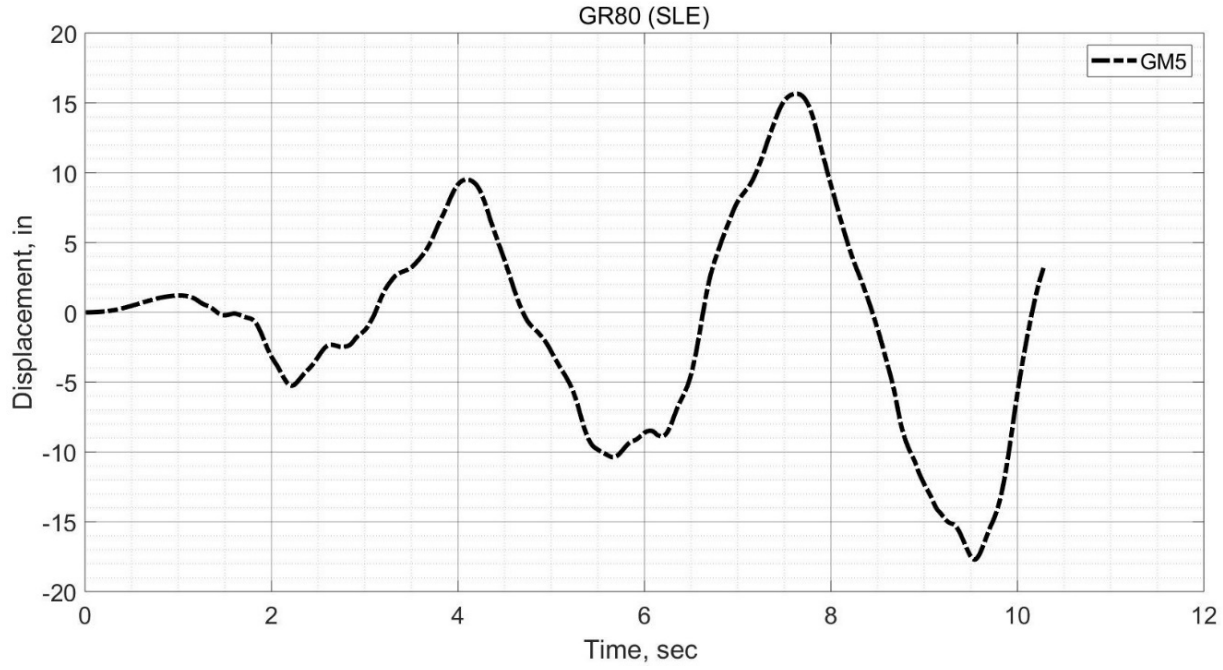

Figure 8.6 Time History for Peak Roof Displacement for Y-direction (Case 2 – SLE).

8.2.2 Element Level

As stated in Section 7.2.2, the TBI guidelines require using only the mean value from all analyses for evaluation with the acceptance criteria for both the force and deformation based-actions in this level. The maximum response parameters for both actions will also be presented to examine the response of the case study building in more depth. In the subsections below, the elements of the seismic force resisting system with their actions are presented and evaluated using the acceptance criteria of the TBI guidelines.

8.2.2.1 Core Wall Response

8.2.2.1.1 Core Wall Force-Based Action

The TBI guidelines specify that the shear force in the core walls of tall buildings is a force-based action. To evaluate the shear demands of core walls, the TBI guidelines required that the

shear force demands satisfy the Equation (7-1). Figure 8.7 shows the core wall shear forces over the building height and the values of $\phi Vexp$. The shear demands in the core wall satisfy Equation (7-1) as required by the TBI guidelines. In addition, the shear force demands varied approximately in a linear manner with the height of the building. For the mean response, the demand was approximately the same in both the x- and y-directions. The peak shear force of the mean values was 6536 kips, and 6747 kips, for x and y-direction, respectively. The maximum response was also less than the limit of the mean response.

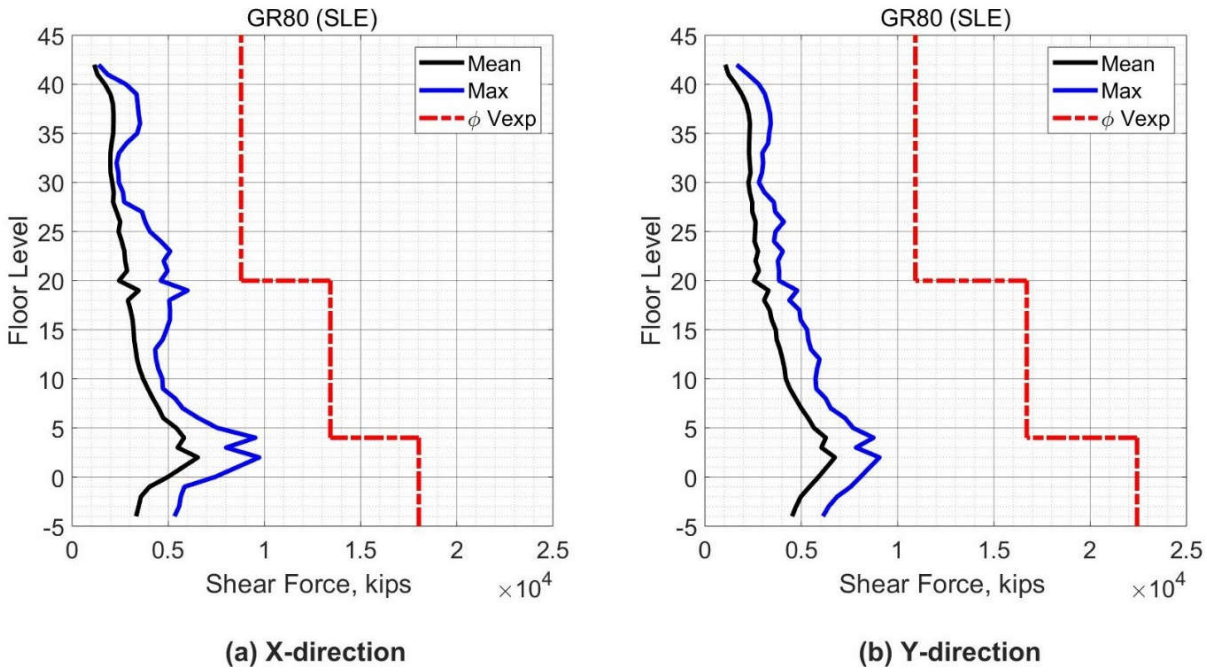

Figure 8.7 Shear Forces in Core Wall (Case 2 – SLE).

8.2.2.1.2 Core Wall Deformation-Based Actions

Figures 8.8 to 8.11 show the mean values of the maximum tensile strain in the core wall reinforcement steel at locations shown in Figure 7.9 over the building height. The TBI guidelines

consider the yielding of steel bars as damage that should be avoided in the SLE shaking level. The maximum tensile strain in the steel bars in the core wall edges was 0.002, which is below the expected yield strain of Grade 80 (0.0029). The steel reinforcement in the core wall do not experience yielding strain, therefore the requirements of the TBI guidelines are satisfied.

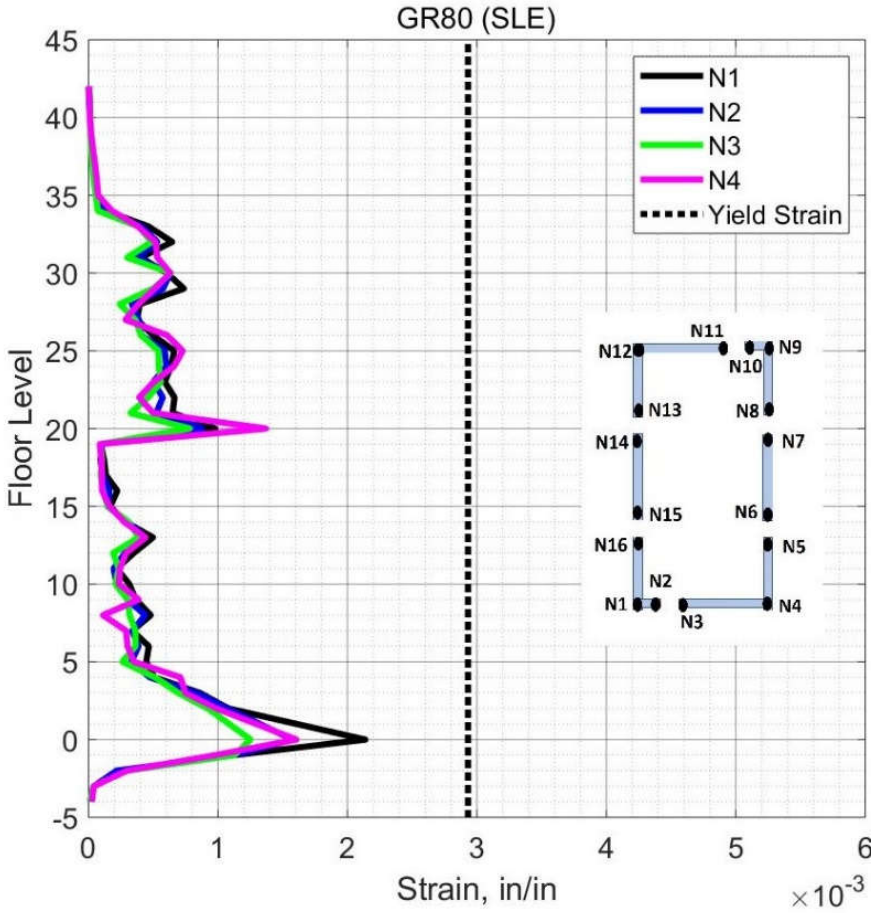

Figure 8.8 Mean Tensile Strain in Steel Bars in Core Wall Edges N1-N4 (Case 2 – SLE).

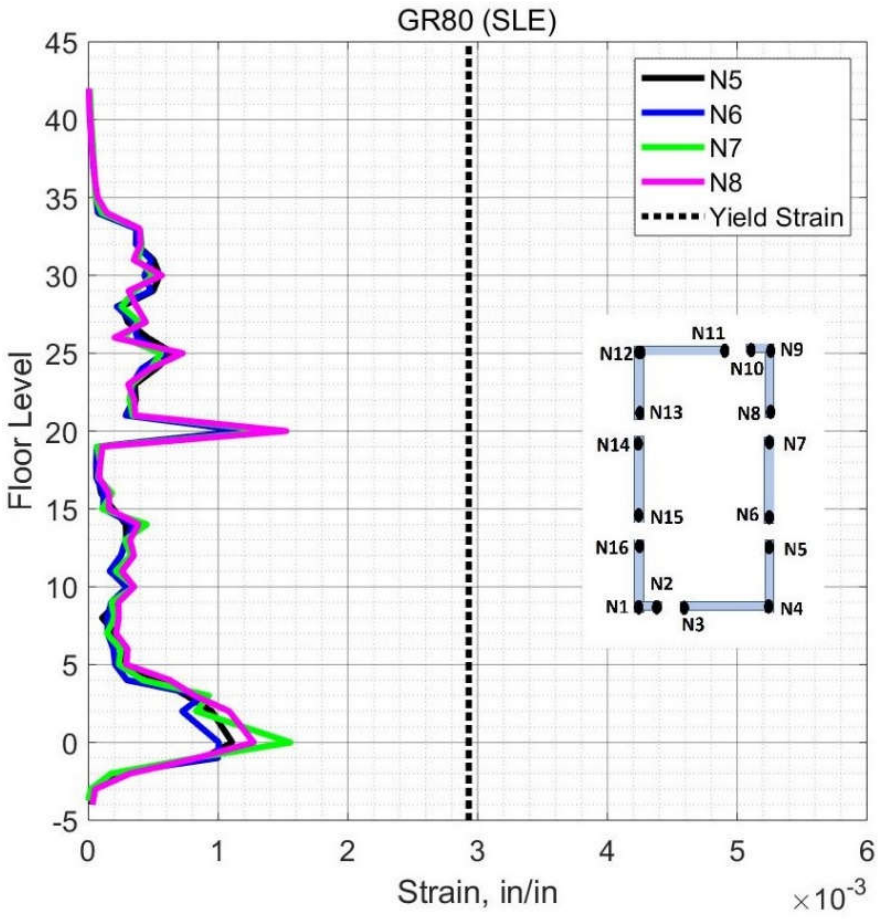

Figure 8.9 Mean Tensile Strain in Steel Bars in Core Wall Edges N5-N8 (Case 2 – SLE).

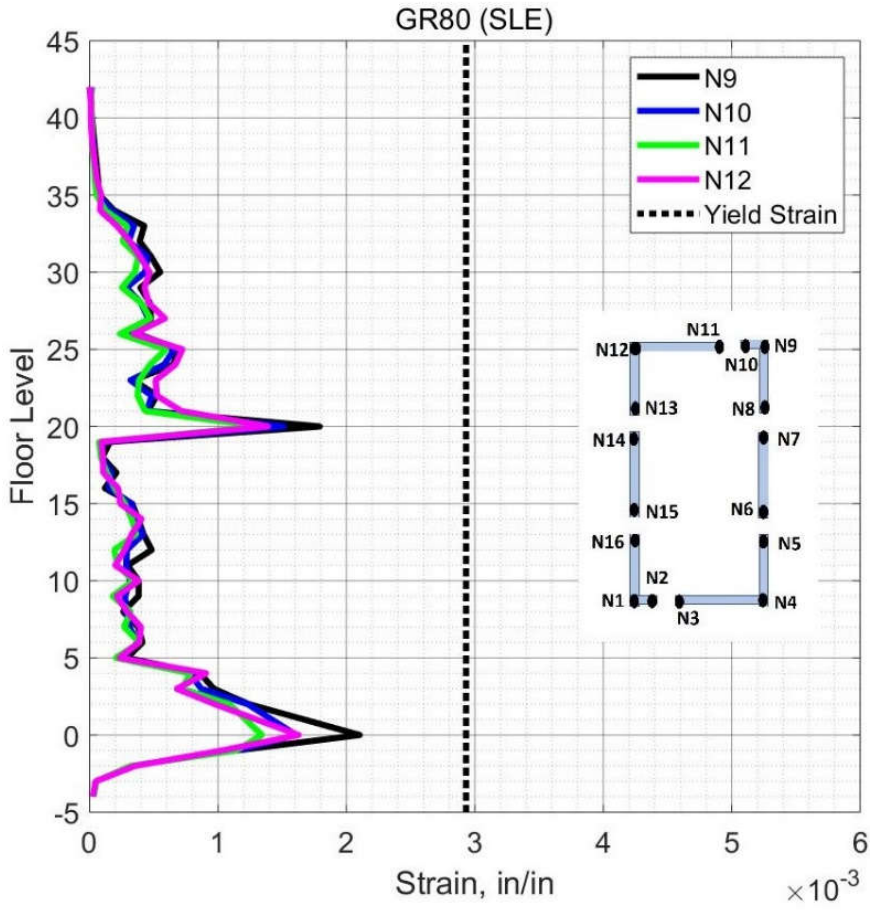

Figure 8.10 Mean Tensile Strain in Steel Bars in Core Wall Edges N9-N12 (Case 2 – SLE).

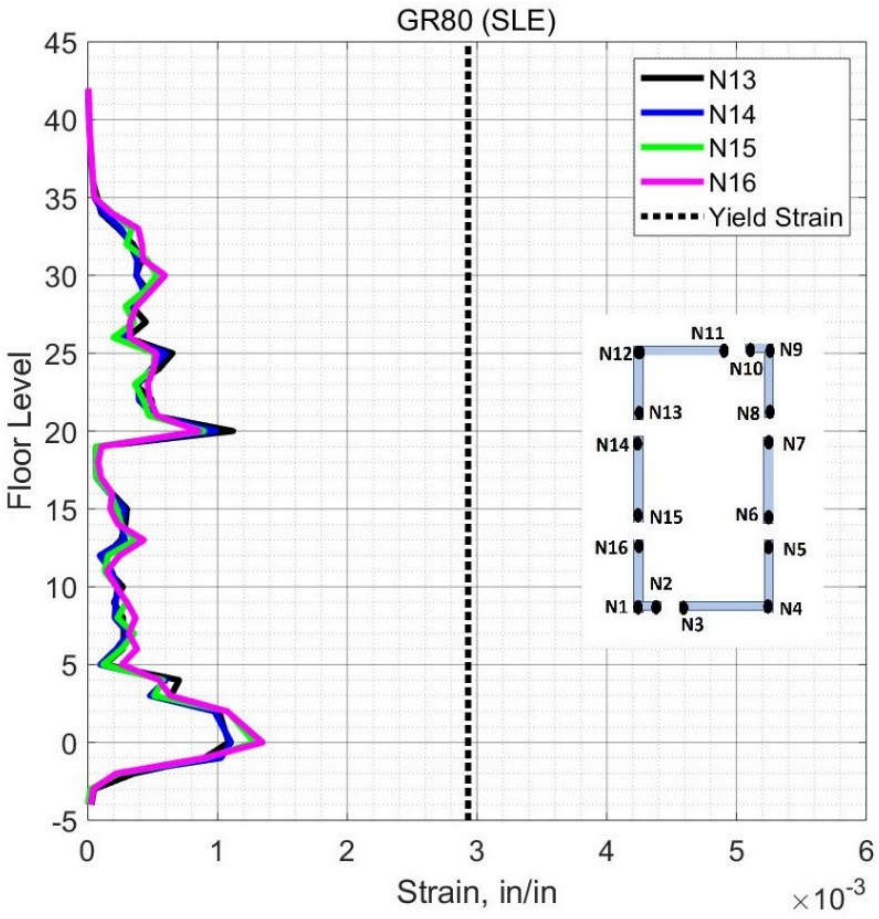

Figure 8.11 Mean Tensile Strain in Steel Bars in Core Wall Edges N13-N16 (Case 2 – SLE).

Figures 8.12 to 8.15 show the mean values of the maximum compression strain in the core wall concrete at locations shown in Figure 7.9 over the building height. The TBI guidelines consider the cracking of concrete as damage that should be avoided in the SLE shaking level. The concrete compression strain in the core wall was very low (< 0.00075), therefore the requirements of the TBI guidelines are satisfied.

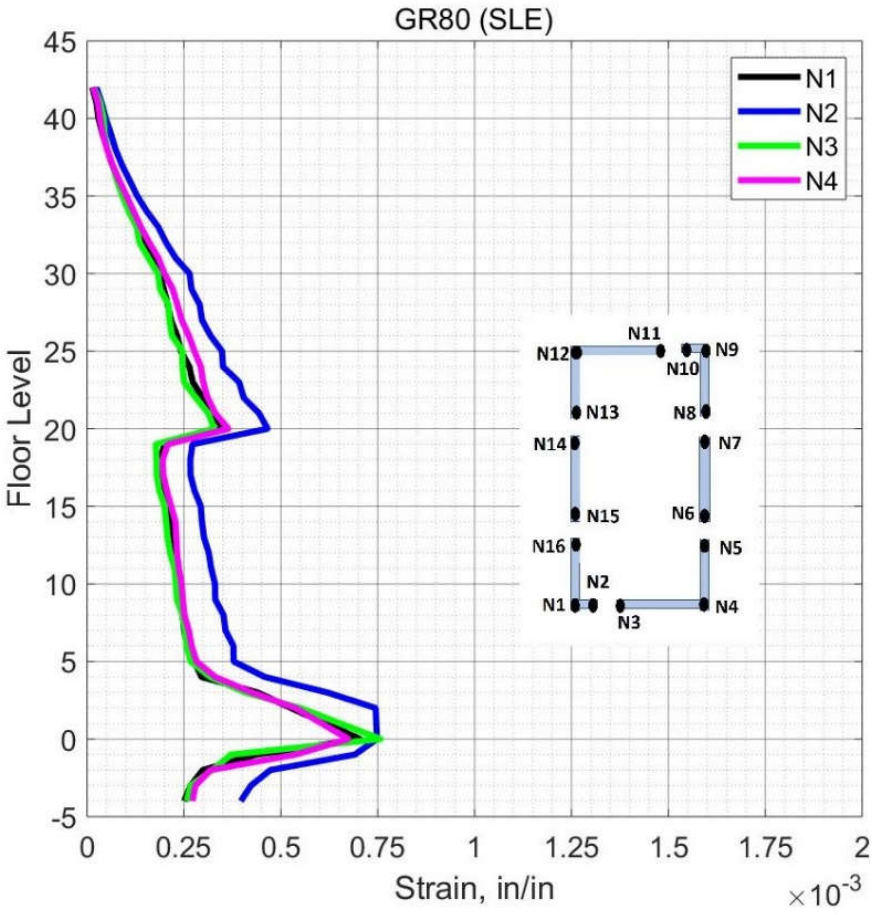

Figure 8.12 Mean Concrete Compression Strain in Core Wall Edges N1-N4 (Case 2 – SLE).

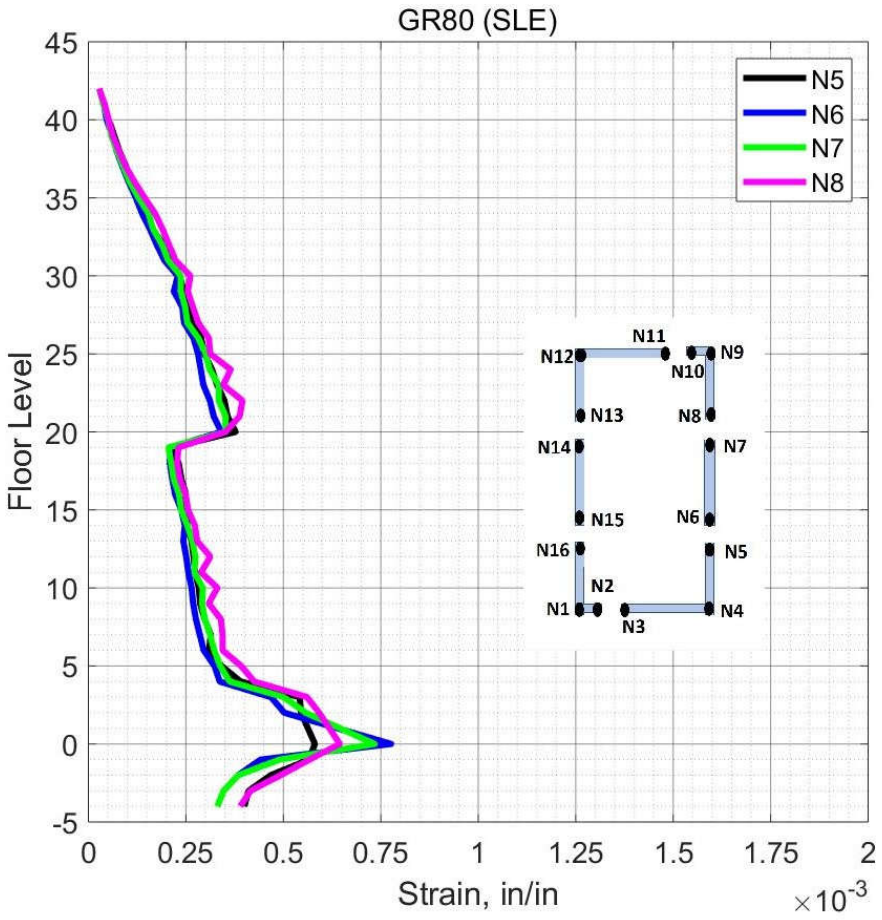

Figure 8.13 Mean Concrete Compression Strain in Core Wall Edges N5-N8 (Case 2 – SLE).

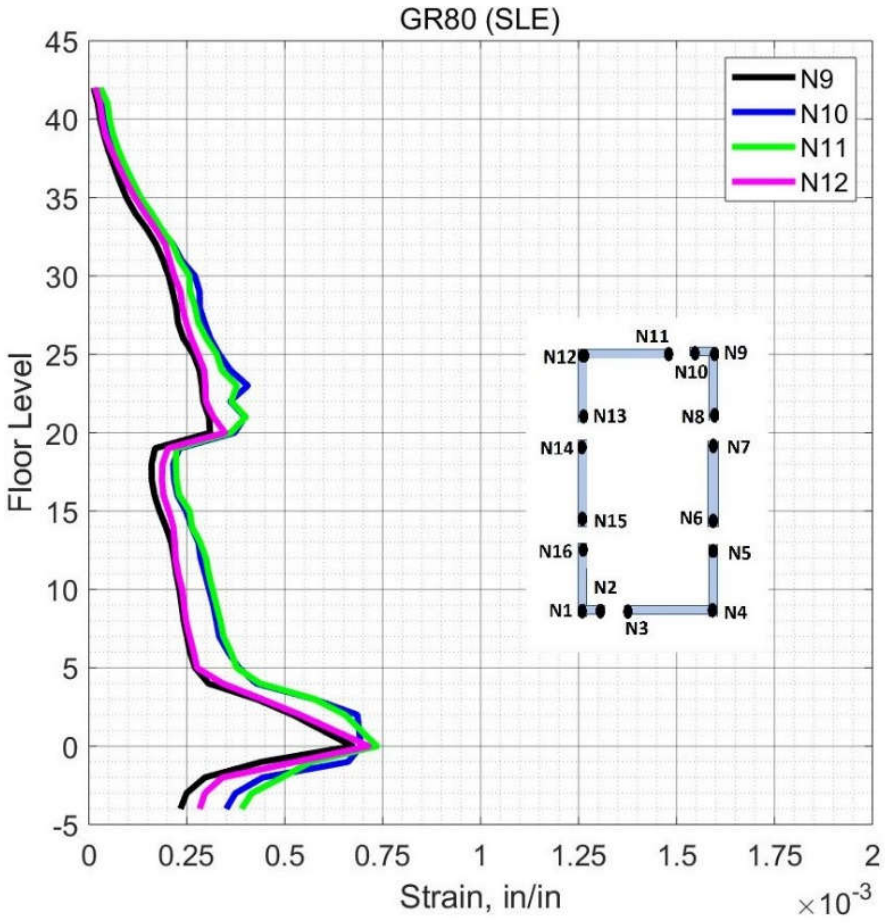

Figure 8.14 Mean Concrete Compression Strain in Core Wall Edges N9-N14 (Case 2 – SLE).

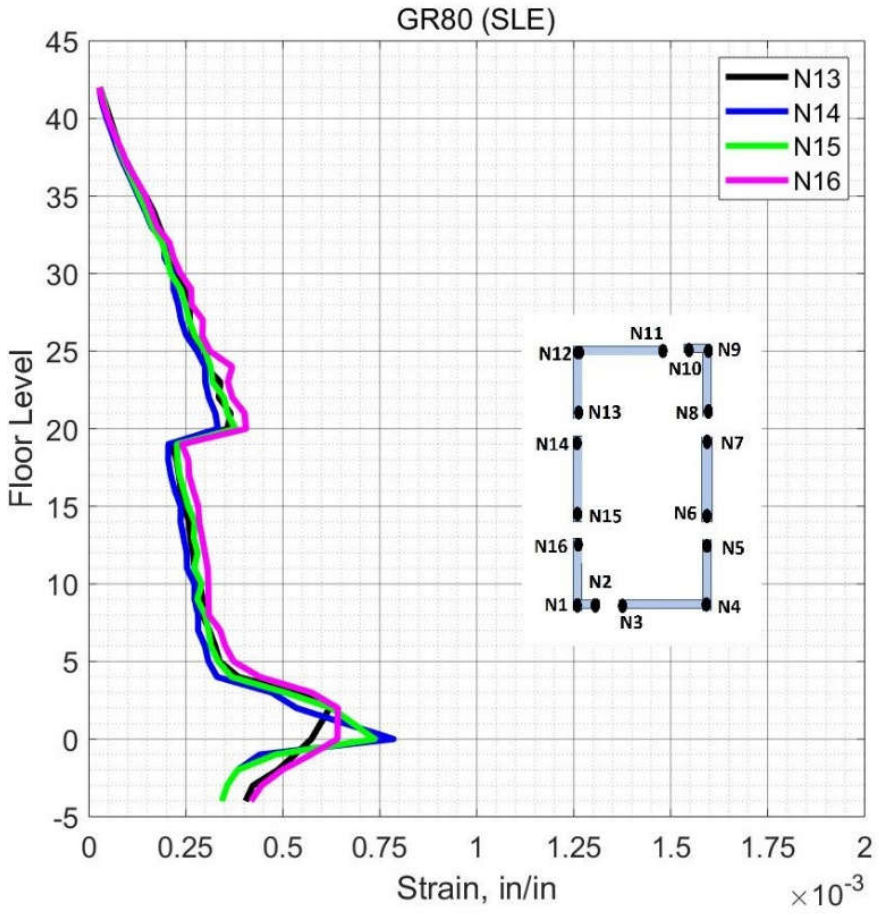

Figure 8.15 Mean Concrete Compression Strain in Core Wall Edges N13-N16 (Case 2 – SLE).

8.2.2.1.3 Coupling Beams

Figure 8.16 (a) shows the mean and maximum values of the rotation of coupling beams with a 1.7 aspect ratio (coupling beams in the x-direction), over the building height. The peak value of the mean rotation is 0.0015 which indicate that coupling beams do not experience yielding of steel reinforcement according to the data in Figure 7.18. In addition, the rotation demands are below the allowable limit of ASCE 41 (0.0060). Therefore, the rotation demands of coupling beams satisfy the requirement of the TBI guidelines.

Figure 8.16 (b) shows the mean and maximum values of the rotation of coupling beams with a 2.1 aspect ratio (coupling beams in the y-direction), over the building height. The peak value of the mean rotation is 0.0015 which indicate that coupling beams do not experience yielding of steel reinforcement according to the data in Figure 7.19. In addition, the rotation demand is below the allowable limit of ASCE 41 (0.0060). Therefore, the rotation demands of coupling beams satisfy the requirement of the TBI guidelines.

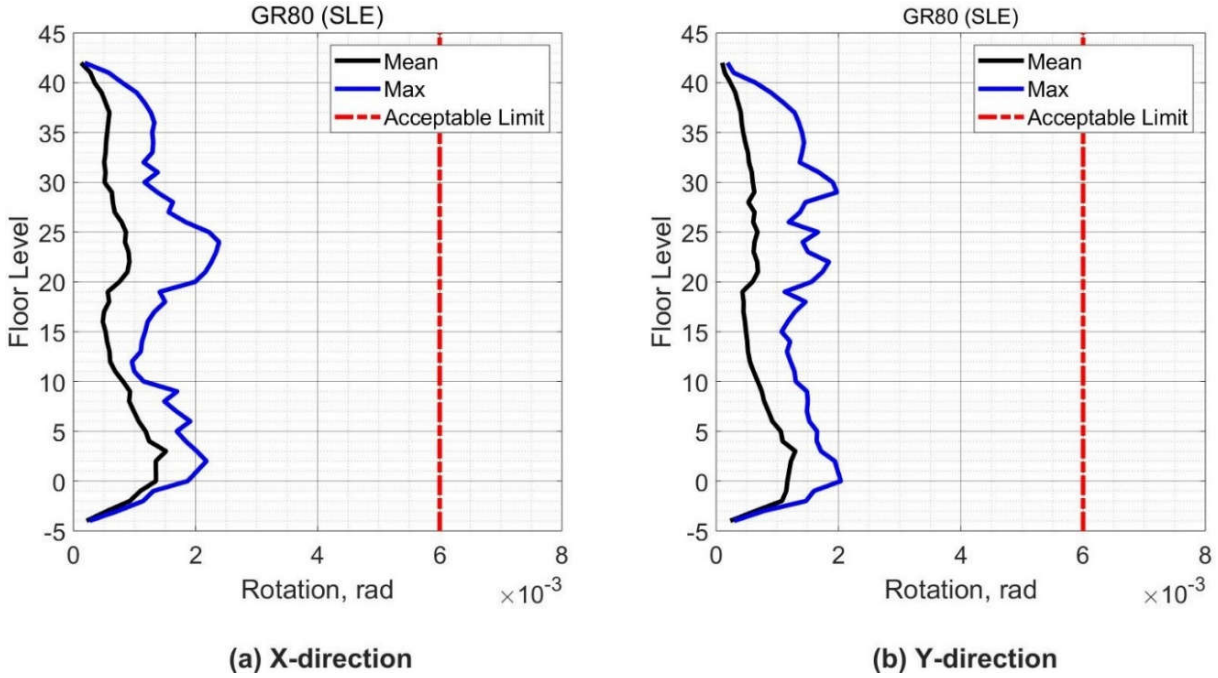

Figure 8.16 Rotation Demand in Coupling Beams (Case 2 – SLE).

8.2.2.2 Special Moment Frame Response

8.2.2.2.1 Beam Force-Based Action

The TBI guidelines specify the shear forces in the beams of special moment frames as a force-based action. The shear demands should satisfy Equation (7-1). The expected shear strength

(V_{exp}) of beams or columns is calculated by using Equation (7-5) from ACI 318-14. Figure 8.17 shows the mean and the maximum values of beams shear forces from all ground motions over the building height and the limiting values of ($\phi Vexp$). In addition, the mean shear force demands in the beams of the special moment frame satisfy the requirements of the TBI guidelines by satisfying Equation (7-1). A slight increase in shear forces demands for the beams in the x-direction is noticed compared with beams in the y-direction. In general, the maximum shear demand in the beams was 200 kips while the reduced shear capacity of the beams was 500 kips.

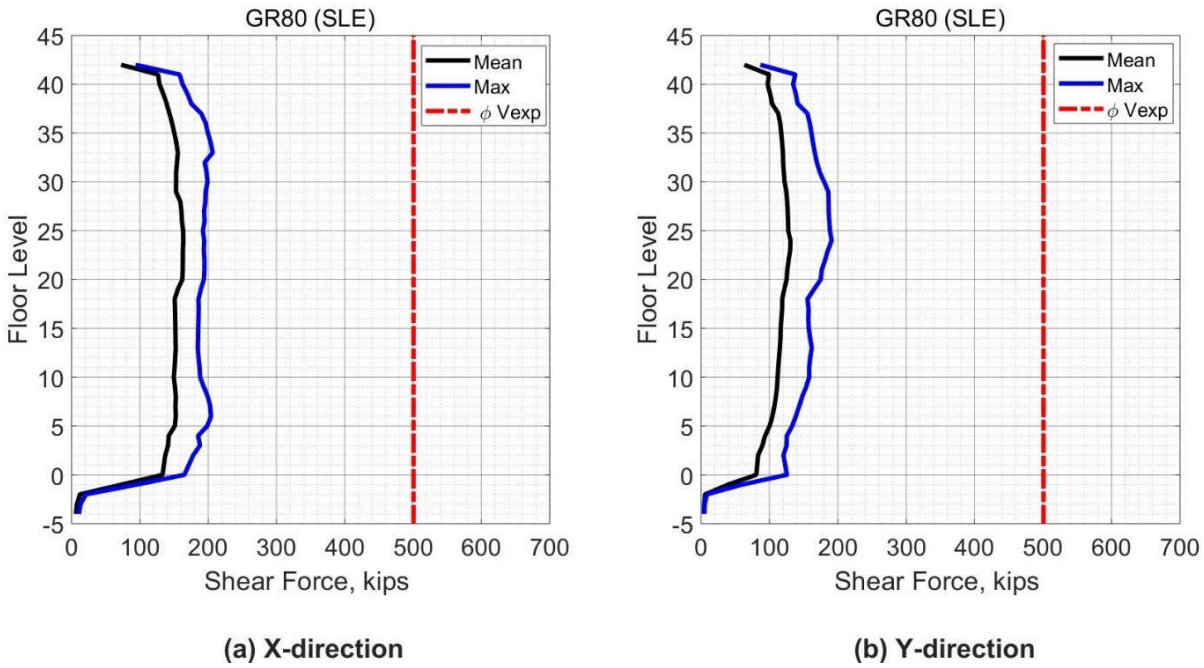

Figure 8.17 Peak Shear Force in Beams (Case 2 – SLE).

8.2.2.2.2 Beam Deformation-Based Action

Figure 8.18 shows the mean and maximum tensile strain demands in the longitudinal reinforcement in the beams sections that are in the beam ends over the building height. The TBI

guidelines consider the yielding of steel bars as damage that should be avoided in the SLE shaking level. The mean tensile strain of the steel reinforcement in all beams (0.0015) do not exceed the expected yield strain of Grade 80 (0.0029 in/in), therefore the requirements of the TBI guidelines are satisfied. A small increase in the tensile strain of the reinforcing bars in the beams oriented in the x-direction is noticed compared with the beams oriented in the y-direction. No yielding of the steel bars in the beams means that the beams do not experience plastic rotation.

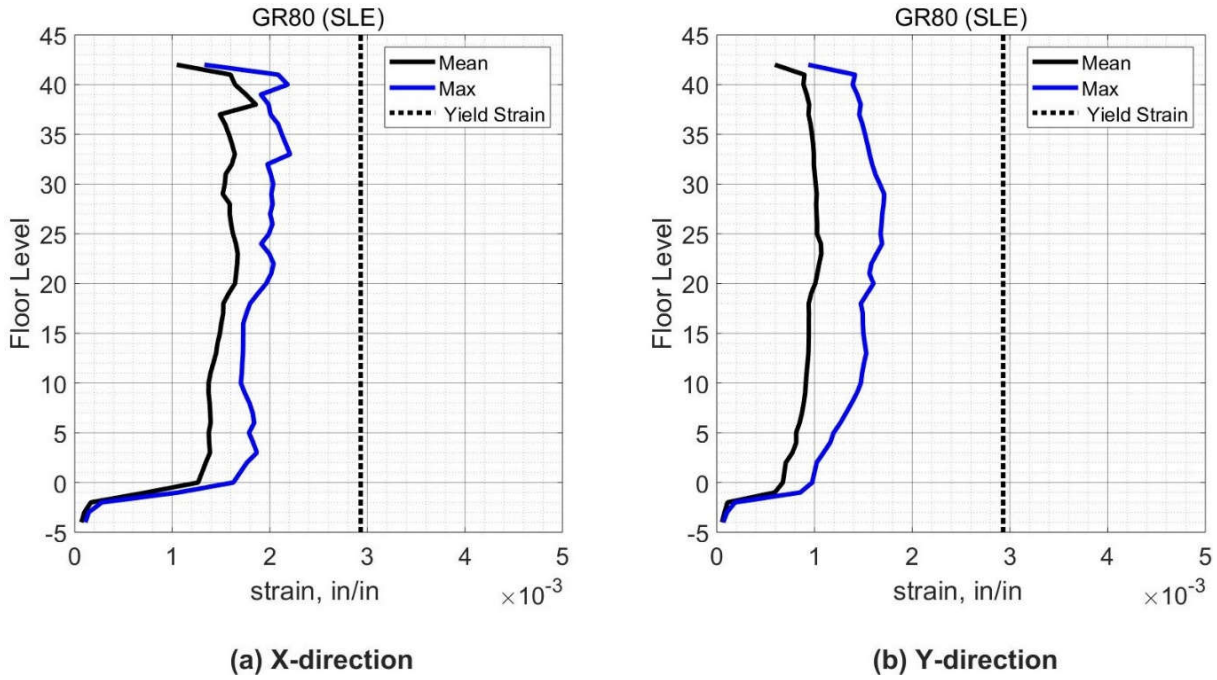

Figure 8.18 Peak Tensile Strain in Reinforcing bars in Beams (Case 2 – SLE).

8.2.2.2.3 Columns Force-Based Action

Figures 8.19 to 8.22 show the mean and maximum values of the shear forces from all analyses in the building columns and the limiting values of ($\phi Vexp$) over the building height. The shear forces in the columns satisfies the requirements of the TBI guidelines by satisfying Equation

(7-1).

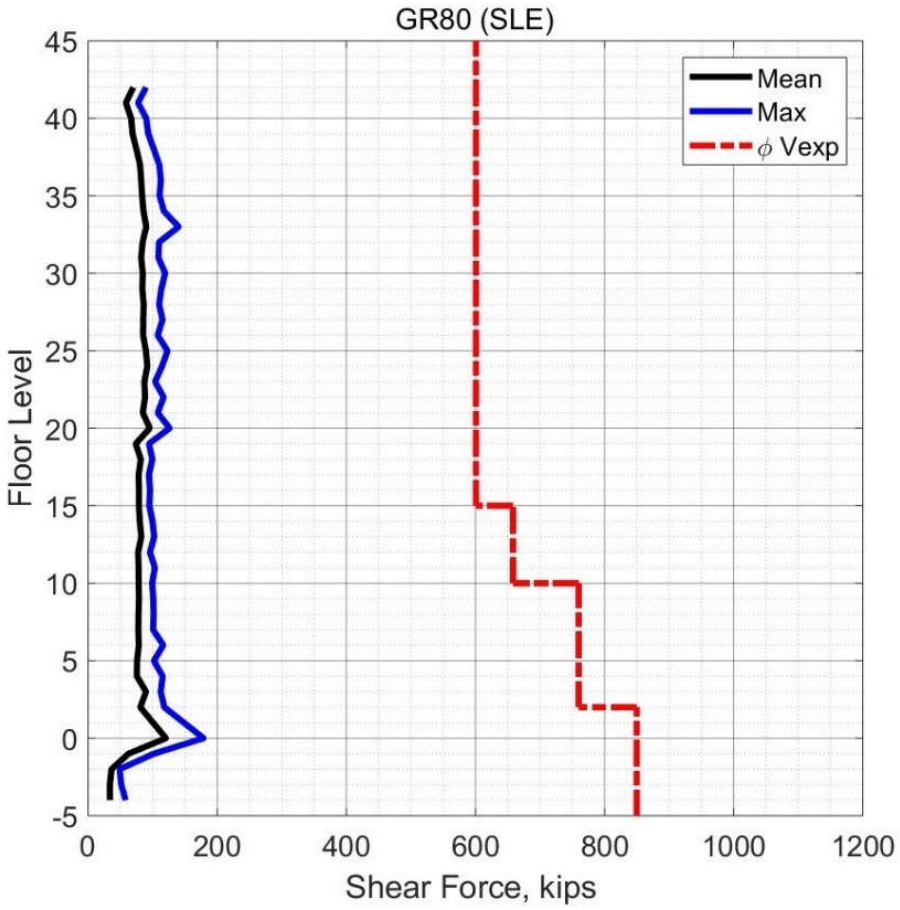

Figure 8.19 Peak Shear Force in Corner Columns (Case 2 – SLE).

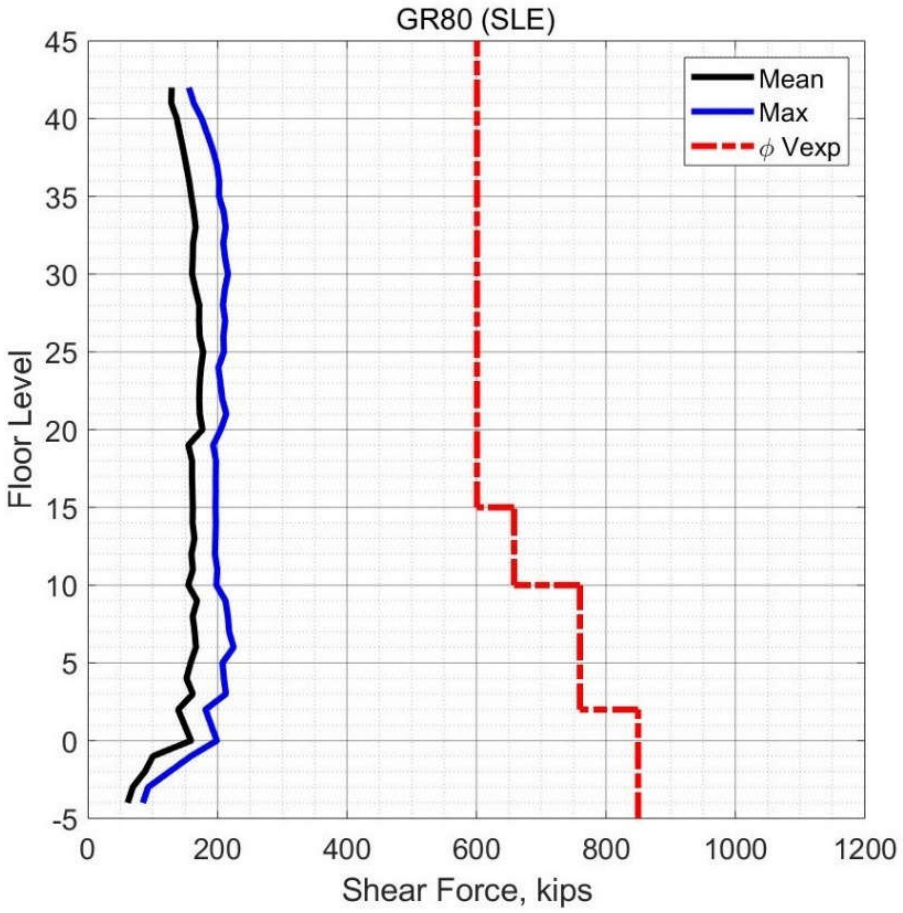

Figure 8.20 Peak Shear Force in Interior Columns X-direction (Case 2 – SLE).

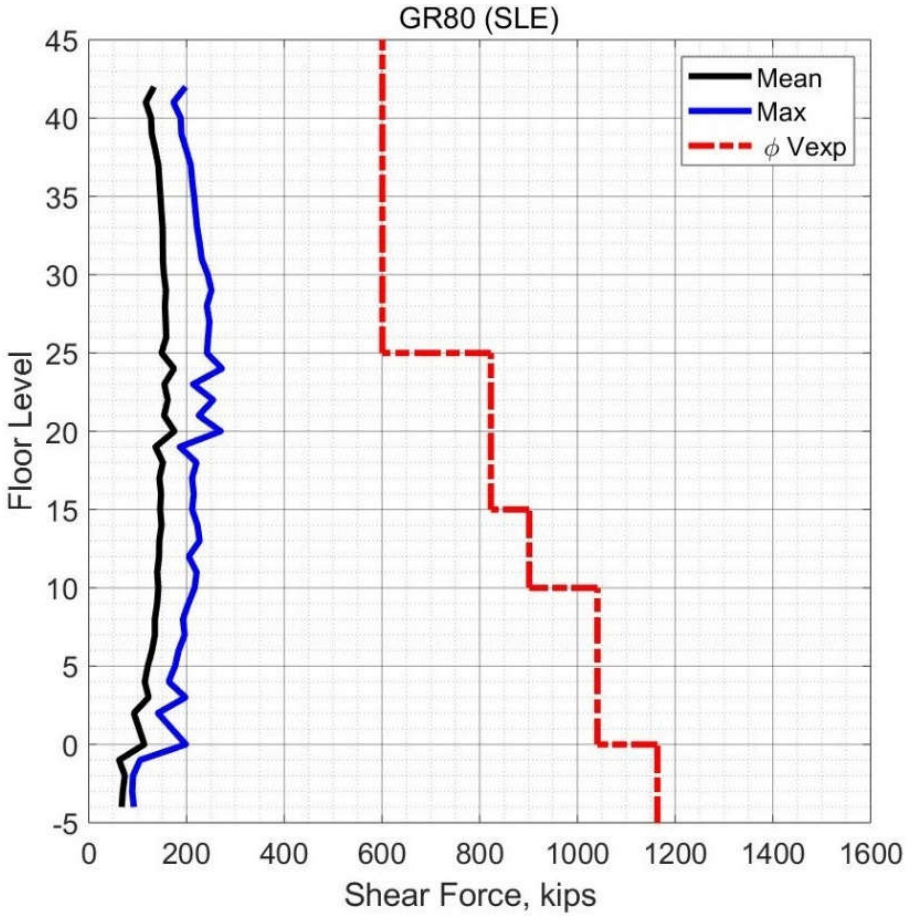

Figure 8.21 Peak Shear Force in Columns on Grid B and E (Case 2 – SLE).

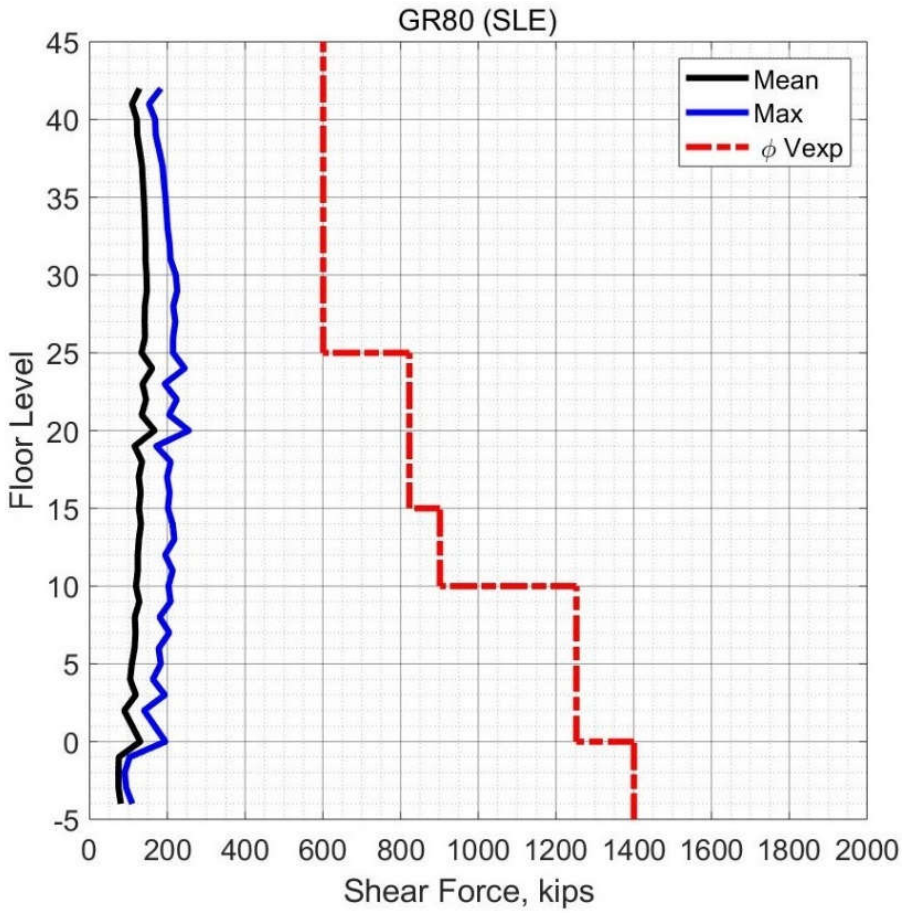

Figure 8.22 Peak Shear Force in Columns on Grid C.5 (Case 2 – SLE).

8.2.2.2.4 Column Deformation-Based Action

Figure 8.23 shows the maximum value of the tensile strain in the longitudinal bars in the columns and the mean value from all ground motion in the suite over the building height. The TBI guidelines consider the yielding of steel bars as damage that should be avoided in the SLE shaking level. The tensile strain demands did not exceed the expected yield strain which means no damage could be expected in the columns. Consequently, there is no plastic rotation in all the columns for this shaking level. Depending on the results of the tensile strain of the reinforcing bars, the columns satisfy the requirements of the TBI guidelines.

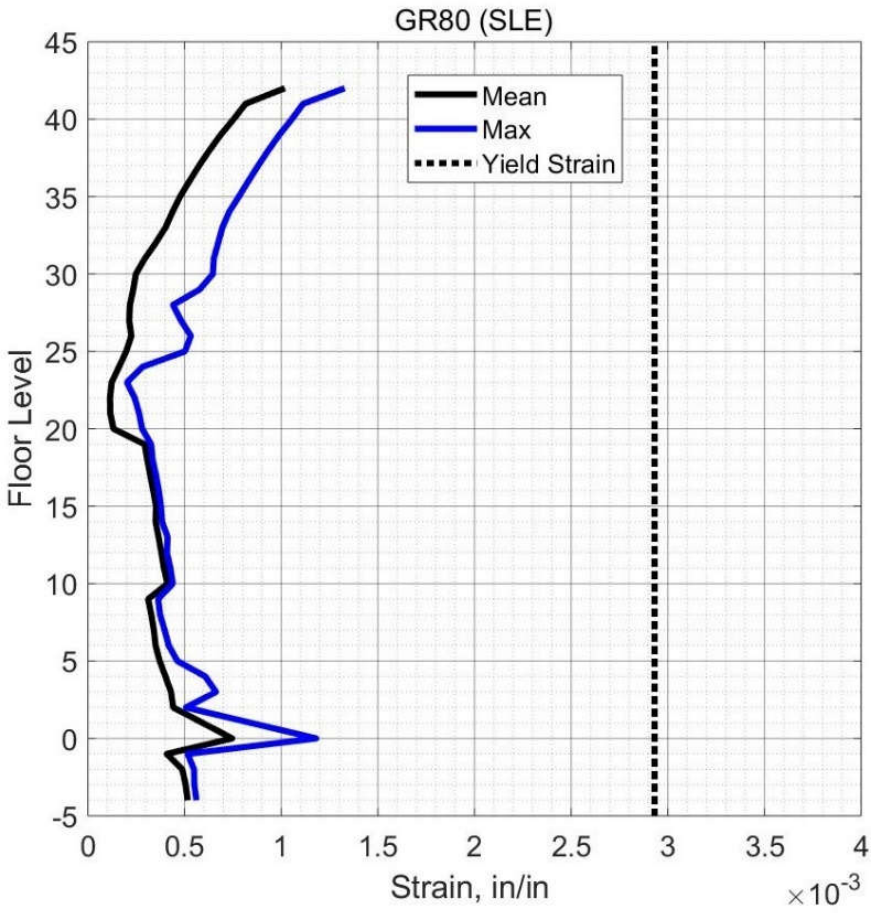

Figure 8.23 Peak Tensile Strain in Reinforcing Bars in Columns (Case 2 – SLE).

8.2.2.3 Contribution of Core Wall and Frame in Dual System

To better understand the behavior of the dual system, the contribution of its components in resisting the story shear force is depicted in Figure 8.24. Figure 8.25 shows the contribution percentage of the shear forces for the core wall and the frame over the building height. The frame contribution is approximately constant over the building height, while the core wall contribution varies linearly. In general, the core wall contributes more than 80% of the total story shear for the lower stories and 50% for the upper stories.

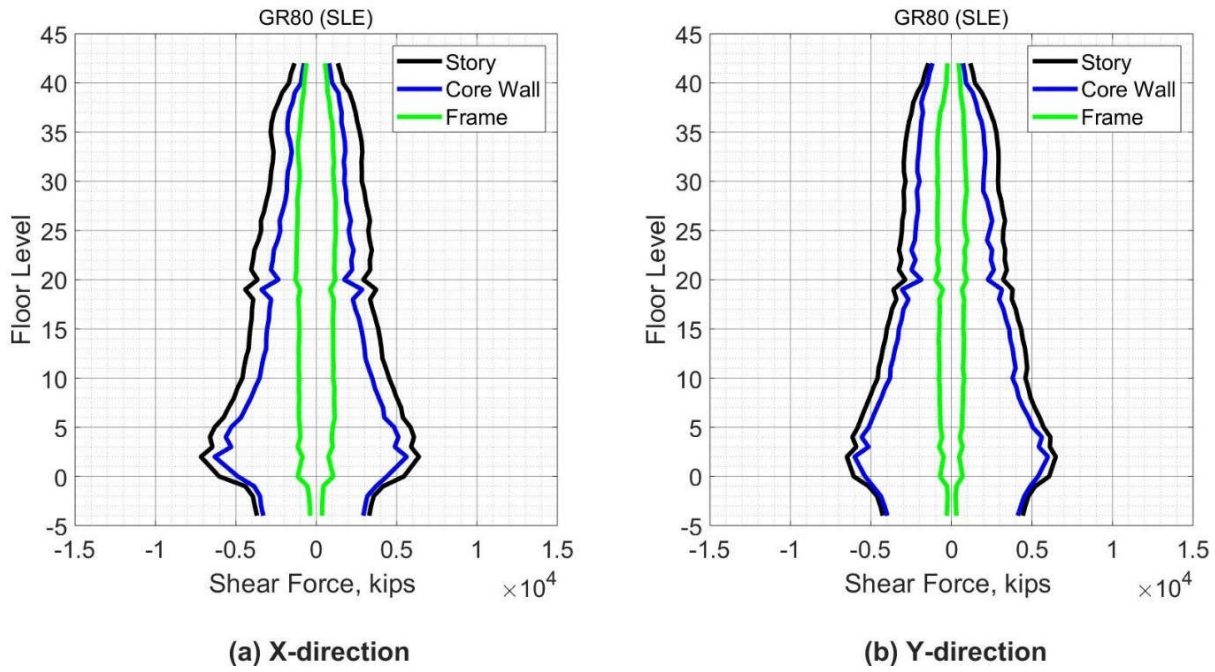

Figure 8.24 Shear Force Contribution of Core Wall & Frame (Case 2 – SLE).

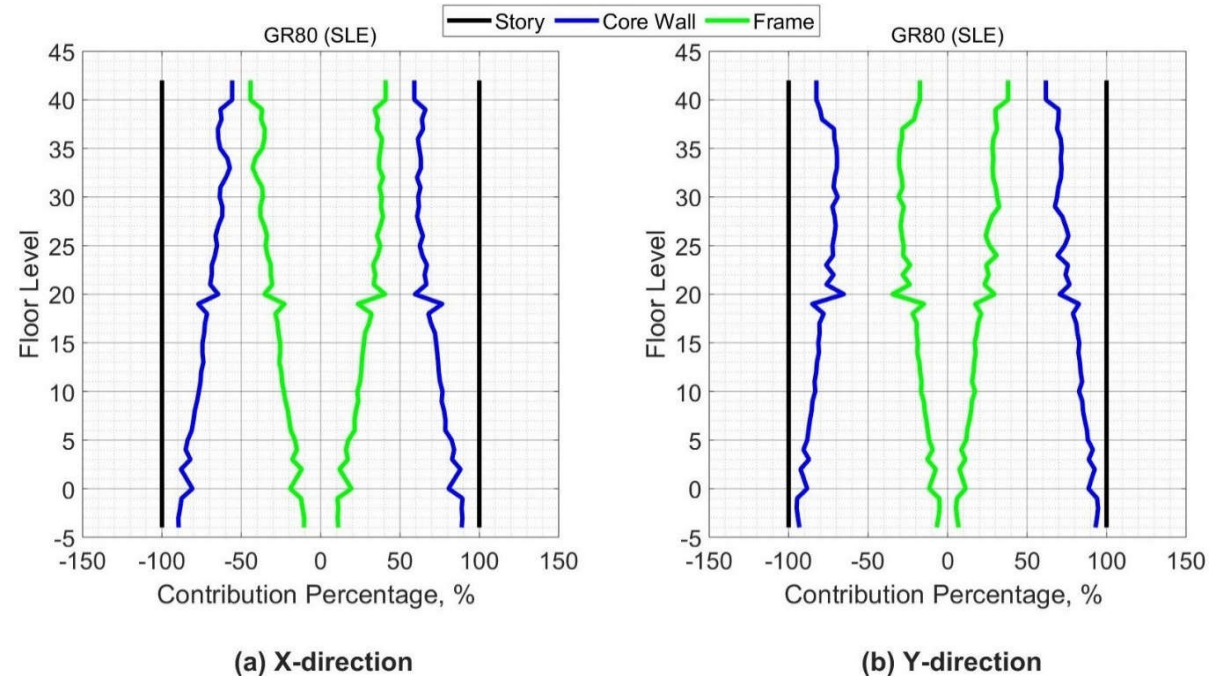

Figure 8.25 Contribution Percentage of Core wall & Frame Shear Force (Case 2 – SLE).

8.3 MCER LEVEL

The same ground motions used in the MCER in case 1 were used for the MCER analyses of the case 2. As stated in Section 7.3, the results of eleven analyses are represented and compared with the acceptance criteria of the TBI guidelines. According to the TBI guidelines, first, the mean value of the response parameters from all ground motions in the suite should be checked with the acceptance criteria. Second, the maximum response parameters from all ground motions should be checked to ensure that no unacceptable response was produced by any ground motion from the suite. All the response parameters were calculated by the same procedures that were described in Section 7.2.

8.3.1 Global Response

8.3.1.1 Drift Ratio

Figure 8.26 shows the mean and the maximum values of the interstory drift ratios from all the ground motions analyses over the building height. The mean interstory drift from the eleven analyses was very close to 0.022 in the x-direction and approximately 0.012 in the y-direction, where both values were within the acceptable limit of TBI guidelines of 0.030. In addition, the maximum interstory drift was 0.030 and 0.0180 for the x- and y-directions, respectively. The maximum values of drift ratios were also within the acceptable limit of TBI guidelines (0.045), which indicates that no unacceptable response was produced when considering the drift ratios. Figures 8.27 and 8.28 depict the maximum drift ratios form each considered ground motion over the building height.

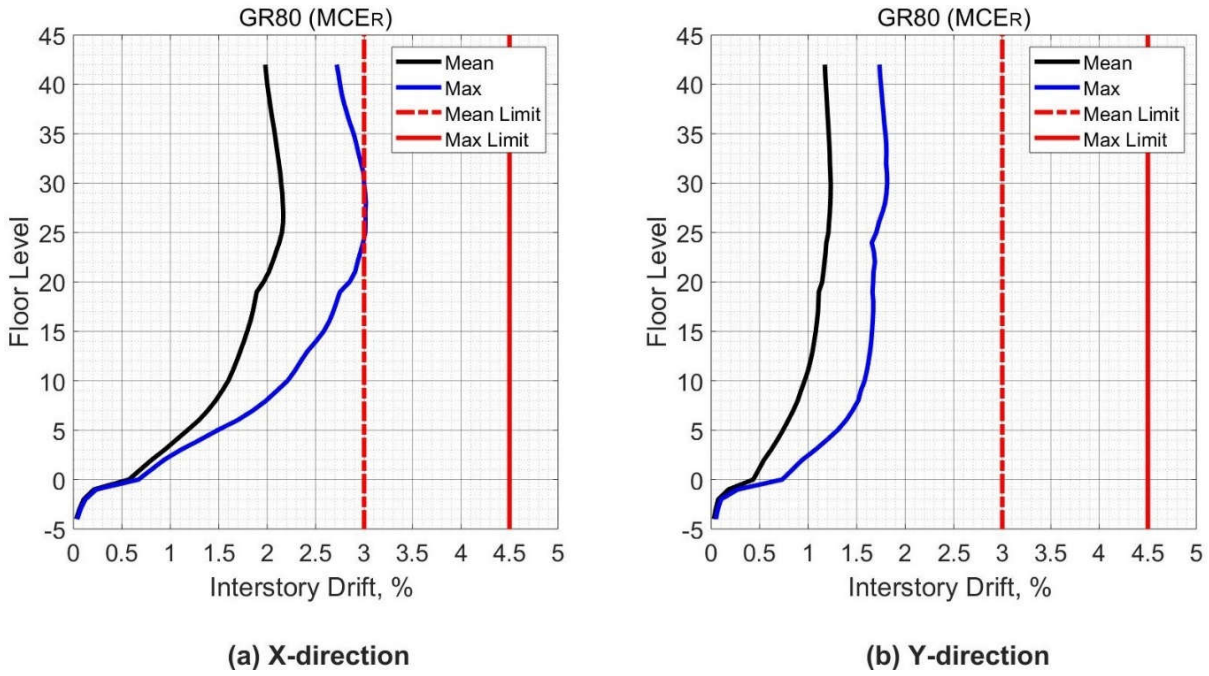

Figure 8.26 Peak Interstory Drift (Case 2 – MCER).

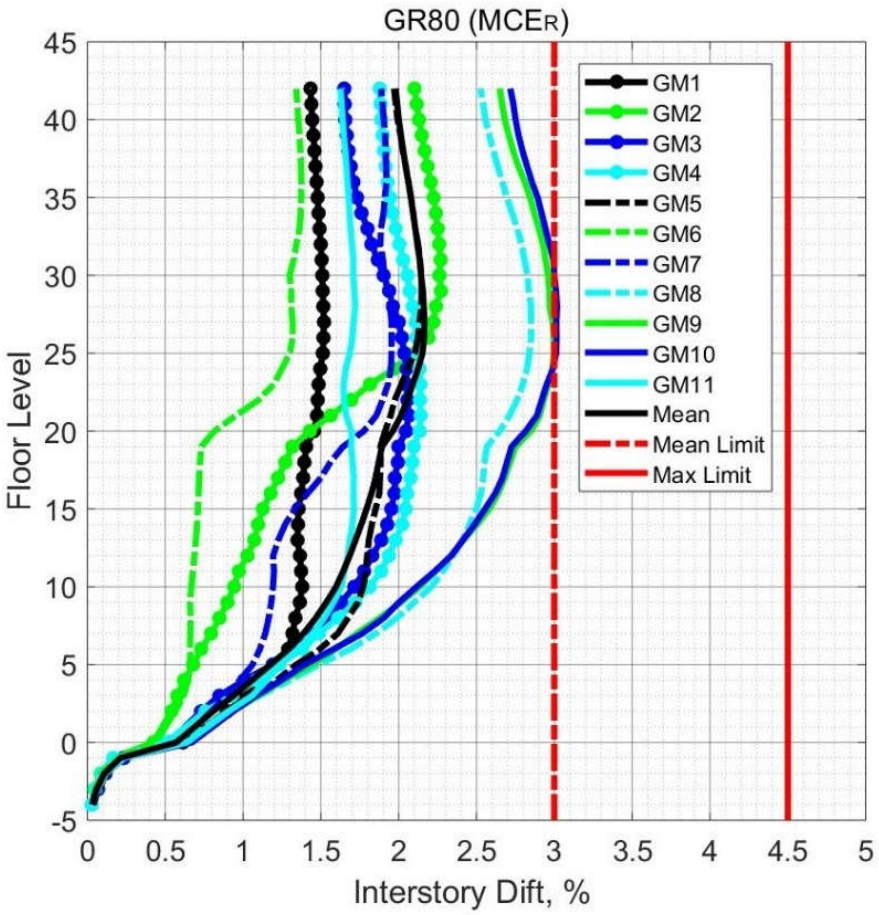

Figure 8.27 Peak Interstory Drift from All Ground Motions for X-direction (Case 2 - MCER).

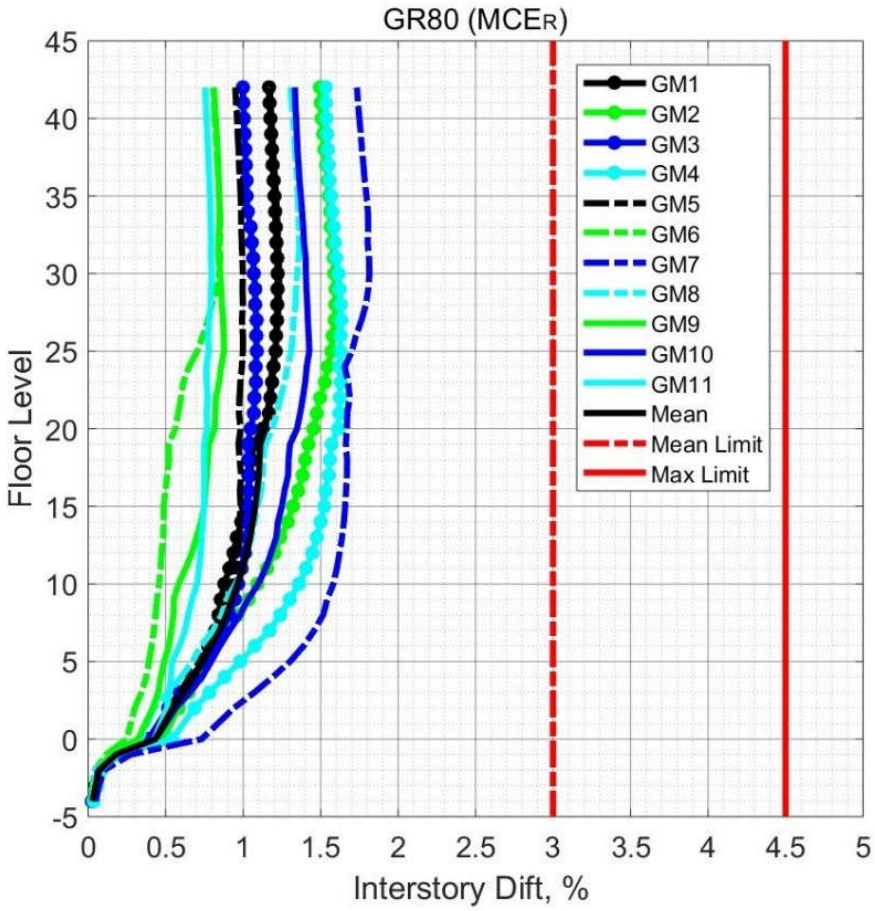

Figure 8.28 Peak Interstory Drift from All Ground Motions for Y-direction (Case 2 - MCER).

8.3.1.2 Residual Drift Ratio

Figure 8.29 shows that the maximum of the mean values of the residual drift was 0.0075 in the x- direction and 0.0035 in the y-direction where both values are below the TBI limit (0.0100). In addition, the maximum residual drift ratio obtained from all analyses was 0.0115, which is below the limit of the TBI guidelines for residual drift ratios (0.0150). Consequently, no unacceptable response was produced from any ground motion when considering the values of the residual drift ratio.

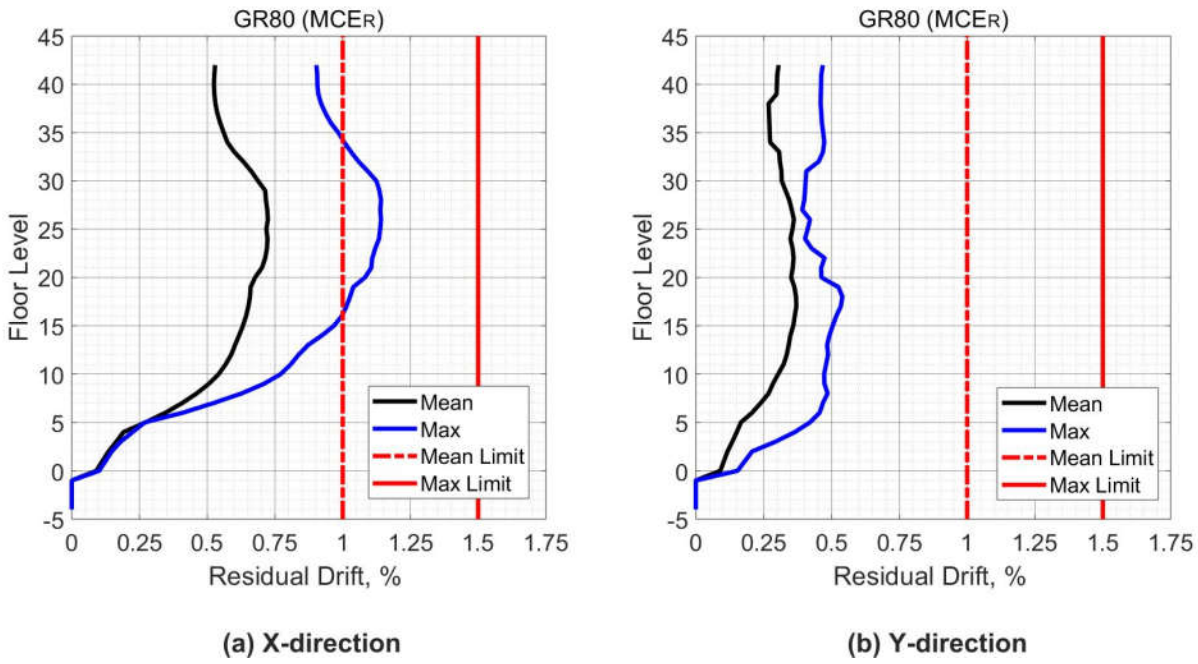

Figure 8.29 Peak Residual Drift (Case 2 – MCER).

8.3.1.3 Displacement

Figure 8.30 depicts the mean value of the displacement of each story at the same time step that the roof experienced a maximum displacement value. The mean displacement of the roof was 80 in. and 50 in. for x and y-direction, respectively.

Figures 8.31 and 8.32 show the time history of the roof displacement in the x-direction and y-direction, respectively from a ground motion at which the displacement demand of the roof was the highest one among other ground motions. During the ninth ground motion, the roof experienced a maximum displacement in the x-direction while during the seventh ground motion the maximum roof displacement in the y-direction was observed.

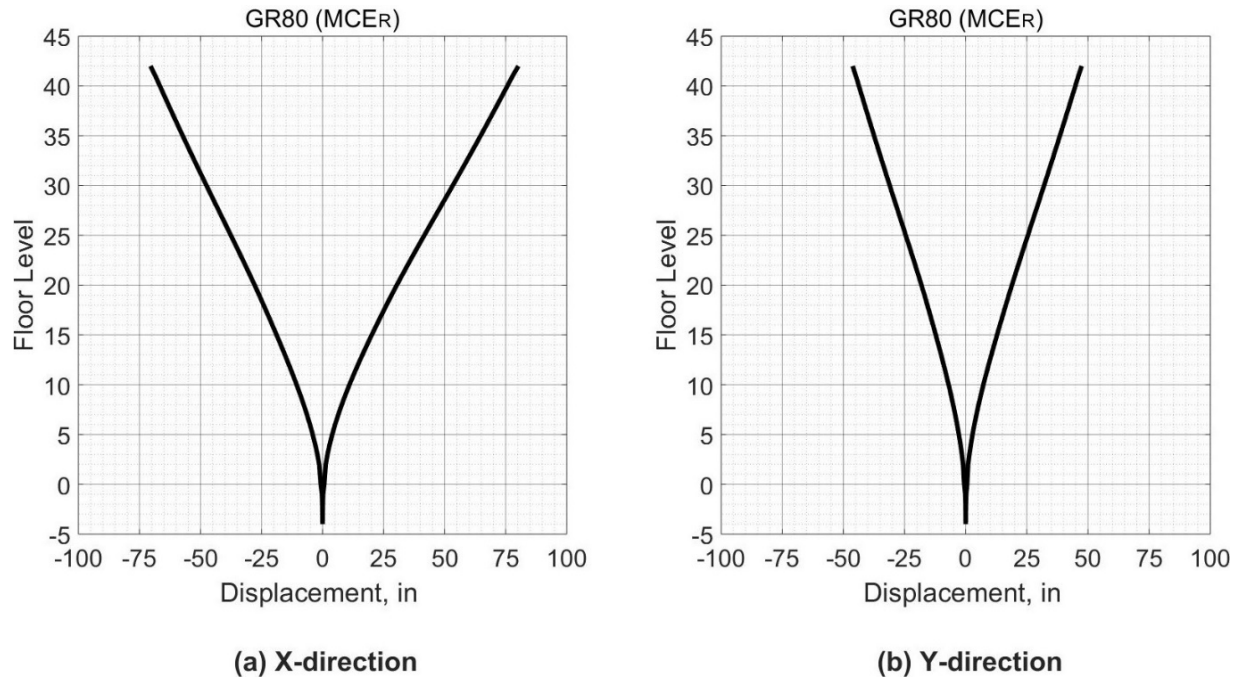

Figure 8.30 Floors Displacement Synchronous with Peak Roof Displacement (Case 2 - MCER).

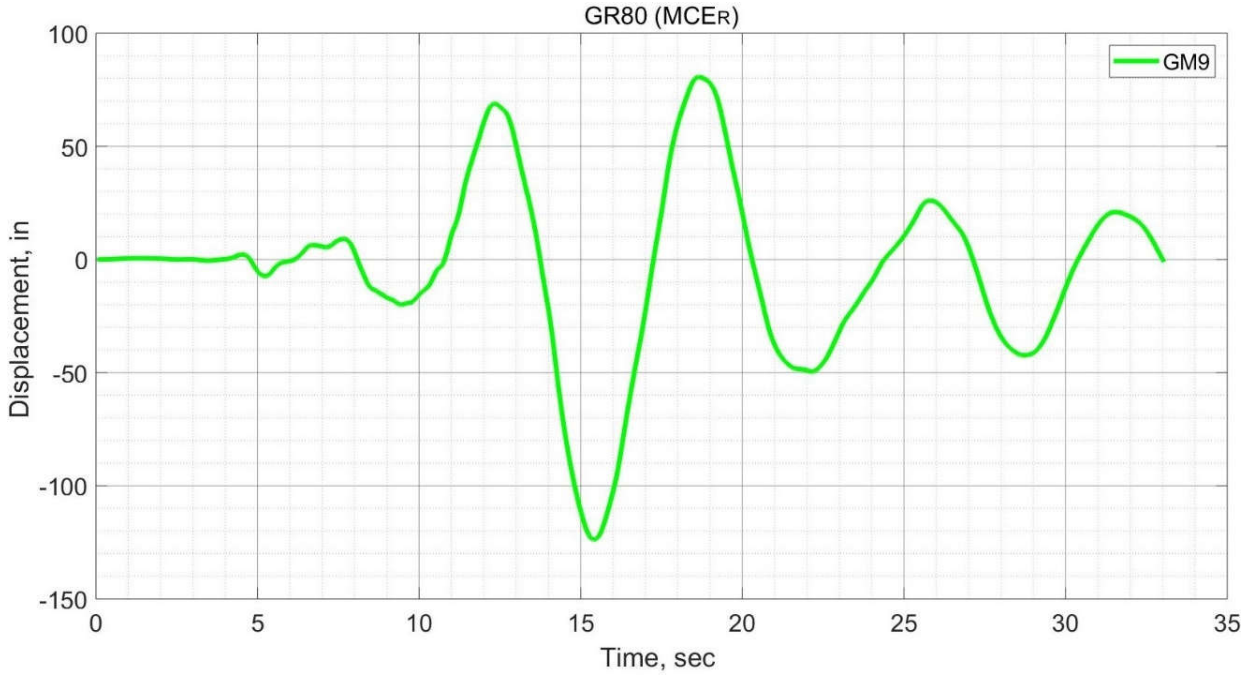

Figure 8.31 Time History for Peak Roof Displacement for X-direction (Case 2 – MCER).

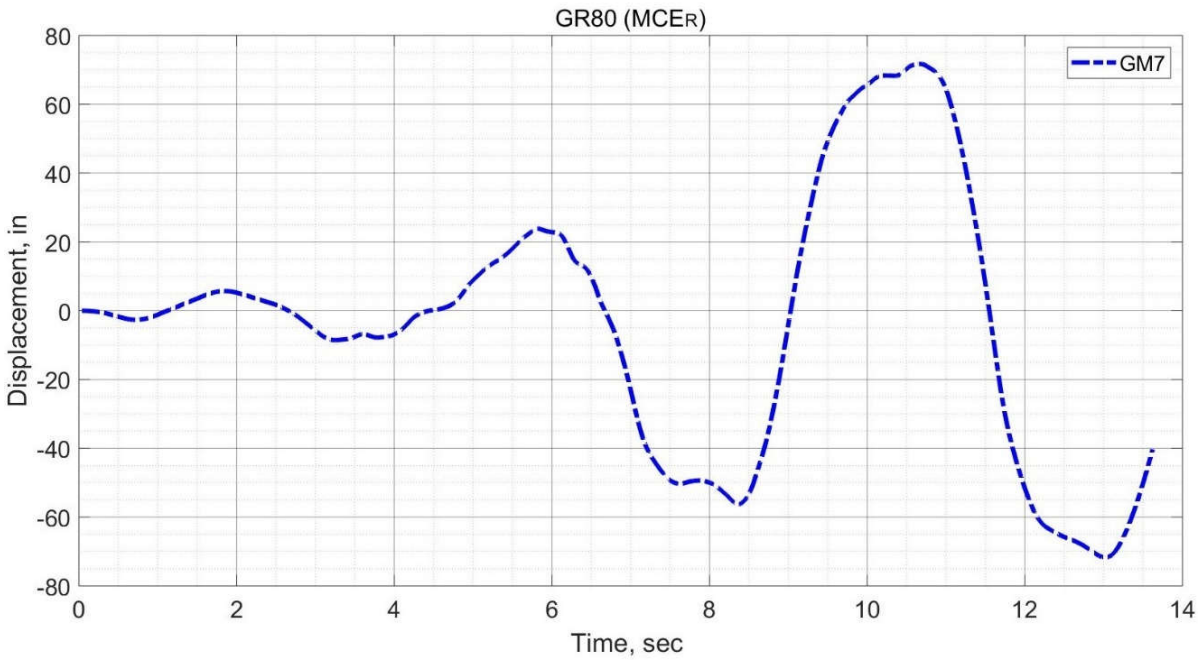

Figure 8.32 Time History for Peak Roof Displacement for Y-direction (Case 2 – MCER).

8.3.2 Element Level

As mentioned in Section 7.3.2, For the MCER shaking level, the TBI guidelines require using the mean value from all analyses for evaluation with the acceptance criteria for force-based actions, while using the maximum value from all analyses for deformation-based actions. In addition, for both actions the TBI guidelines require using the maximum value from all analyses to evaluate with the acceptance criteria to ensure that all calculated demands from any analysis are within the acceptable range of the model. In the subsections below, the elements of the seismic force resisting system with their actions are presented and evaluated using the acceptance criteria of the TBI guidelines.

8.3.2.1 Core Wall Response

8.3.2.1.1 Core Wall Force-Based Action

To evaluate the shear demands of core walls, the TBI guidelines required that the shear force demands satisfy Equation (7-8). Figure 8.33 shows the core wall shear forces over the building height and the limiting (*Vexp*) as in Equation (7-8). The shear demands in the core wall satisfy Equation (7-8) as required by the TBI guidelines. In addition, the shear force demands varied approximately in a linear manner with the height of the building. A small increase in the shear force demands in the y-direction was noticed compared with demands in the x-direction. The maximum observed shear demand was 13044 kips for y-direction, while 11104 kips in x-direction. A change in the shear response of the core wall was noticed at the twentieth story due to the wall thickness changing from 24 in. to 18 in. As shown in Figure 8.33, considering that the maximum demand of the shear force in the core wall was also within the acceptable limits, all analyses produced an acceptable response and all results are within the acceptable modeling range.

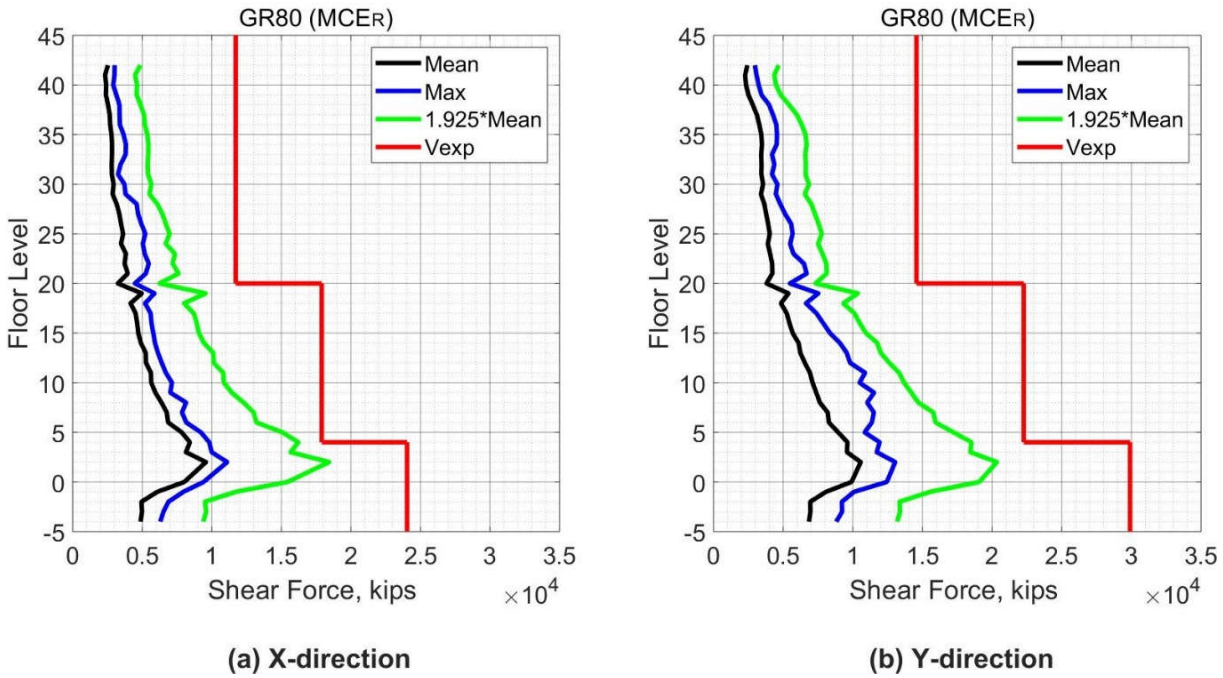

Figure 8.33 Shear Forces in Core Wall (Case 2 – MCER).

8.3.2.1.2 Core Wall Deformation-Based Action

As stated in Section 7.2.2.1.2, the tensile strain in the reinforcing steel and concrete compression strain were monitored during the analyses on all edges of the core wall. The strain was determined by using the vertical displacement (Δz) of the nodes of the core wall edges. Figures 8.34 to 8.37 show that the maximum tensile strain in the core wall reinforcement is 0.016, which is below the acceptable limit of 0.05. The maximum tensile strain in the longitudinal reinforcement of the core wall is far below the minimum requirements for the fracture elongation (total elongation) of Grade 80 (0.12) according to the ASTM A 706. In addition, the maximum tensile strain demand is below 75% of the uniform elongation of Grade 80 (0.088) (Drit Sokoli & Ghannoum, 2016). For seismic applications, the reliable maximum tensile strain for reinforcing bars is 75% of the uniform elongation (NEHRP, 2014). However, the reinforcing bars experienced

yielding for all stories from ground story to the thirtieth story. The core wall below the ground level did not experience yielding because of the effect of the podium's levels.

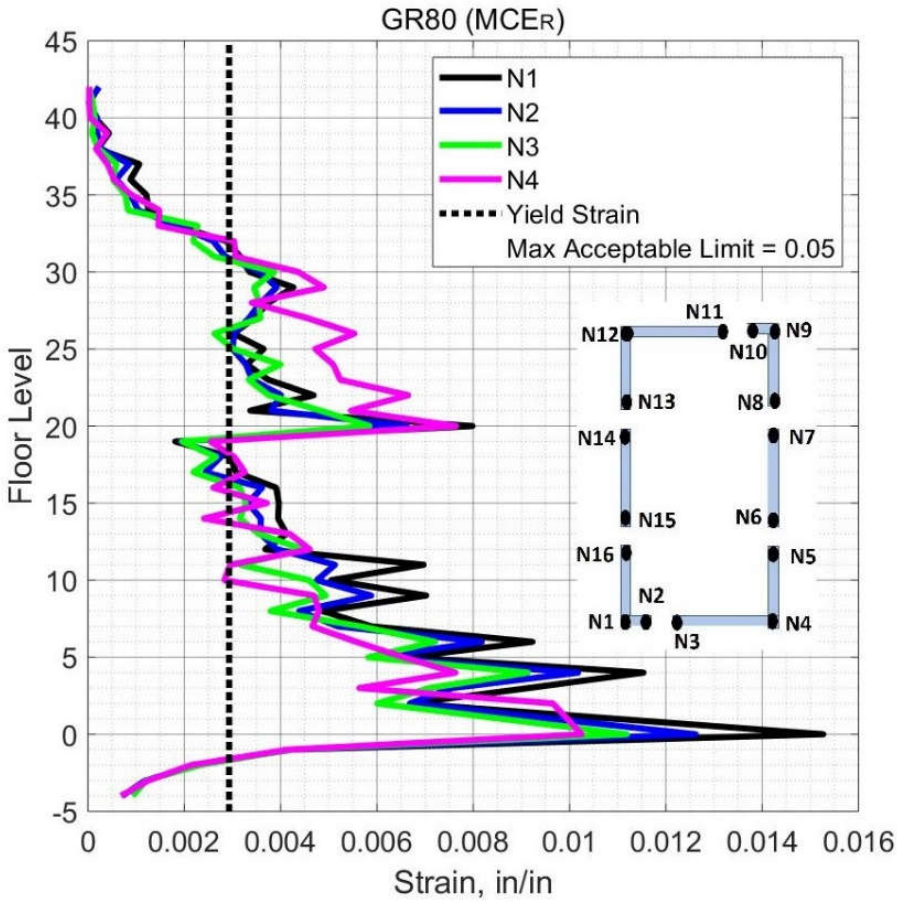

Figure 8.34 Peak Tensile Strain in Steel Bars in Core Wall Edges N1-N4 (Case 2 – MCER).

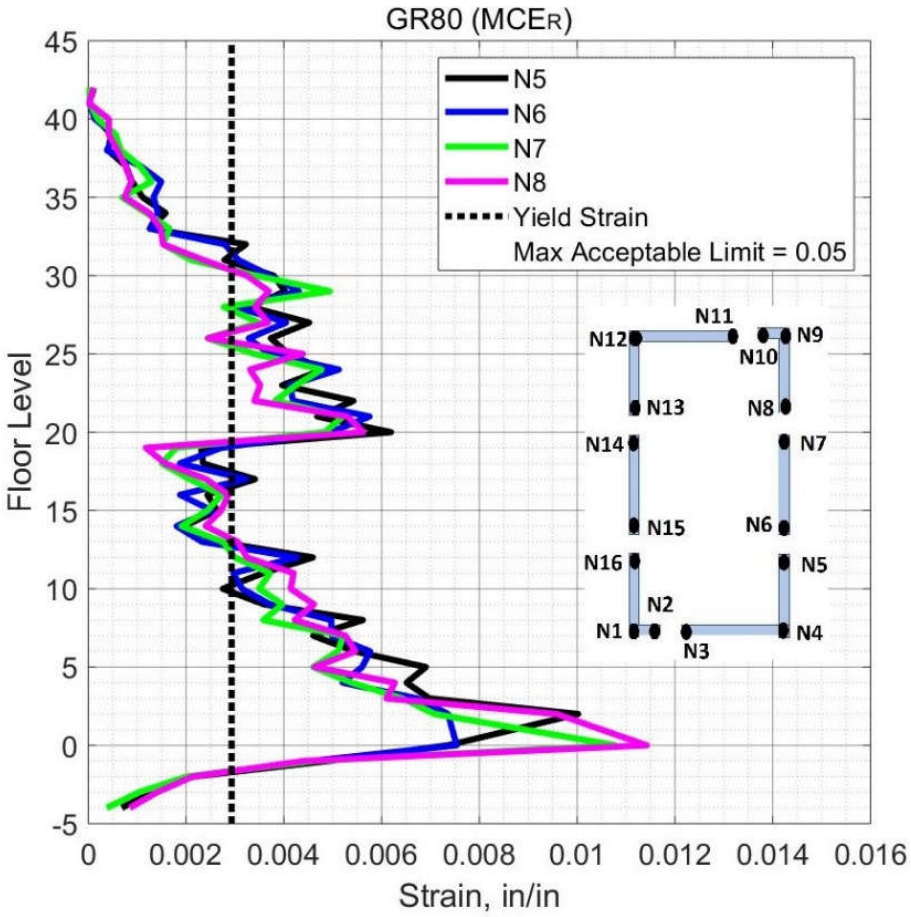

Figure 8.35 Peak Tensile Strain in Steel Bars in Core Wall Edges N5-N8 (Case 2 – MCER).

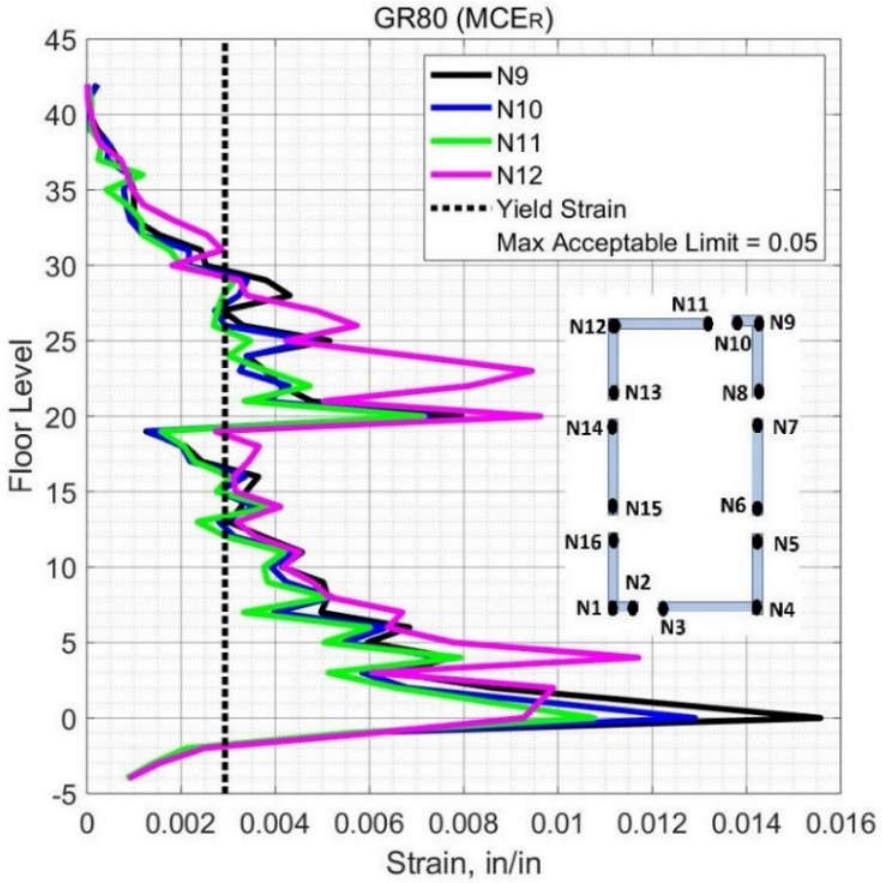

Figure 8.36 Peak Tensile Strain in Steel Bars in Core Wall Edges N9-N12 (Case 2 – MCER).

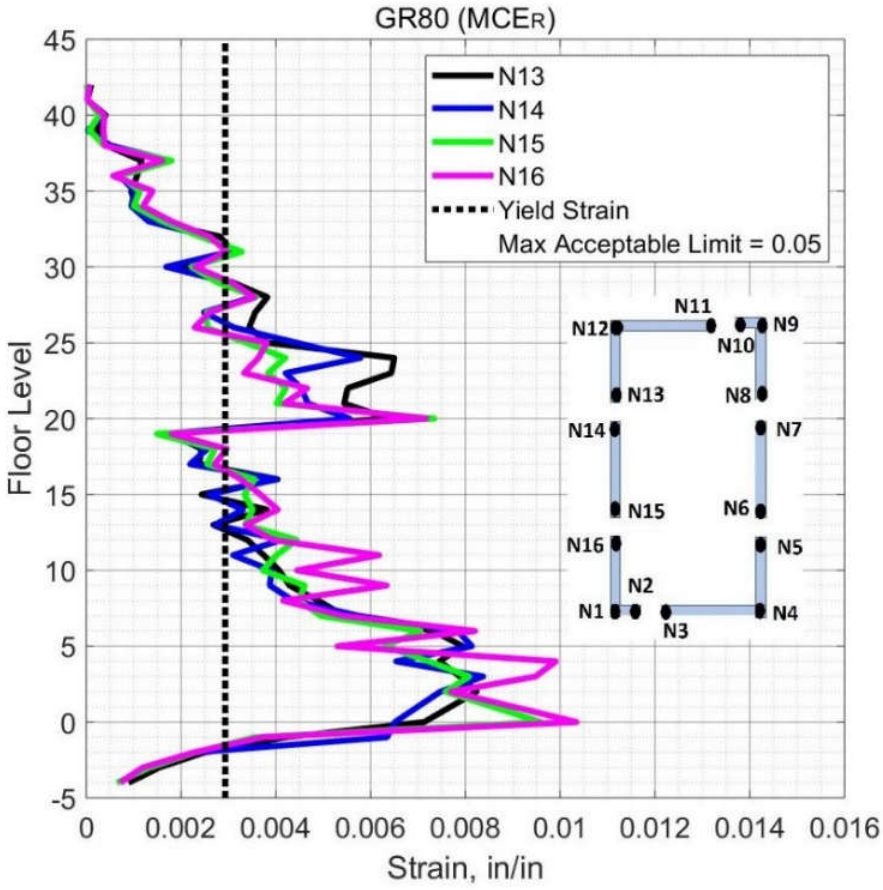

Figure 8.37 Peak Tensile Strain in Steel Bars in Core Wall Edges N13-N16 (Case 2 – MCER).

Figures 8.38 to 8.41 show the maximum values of the compression strain in the core wall concrete at the wall edges over the building height. The core wall concrete experiences low values of concrete compression strain, below 0.002, for all stories.

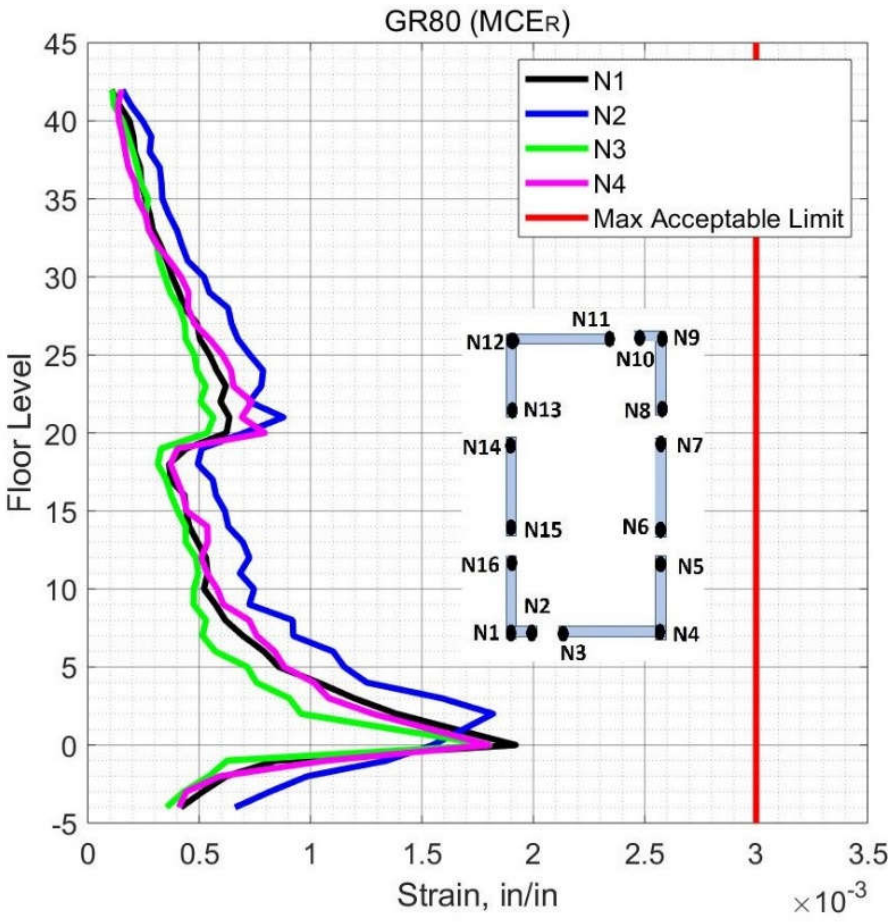

Figure 8.38 Peak Concrete Compression Strain in Core Wall Edges N1-N4 (Case 2 – MCER).

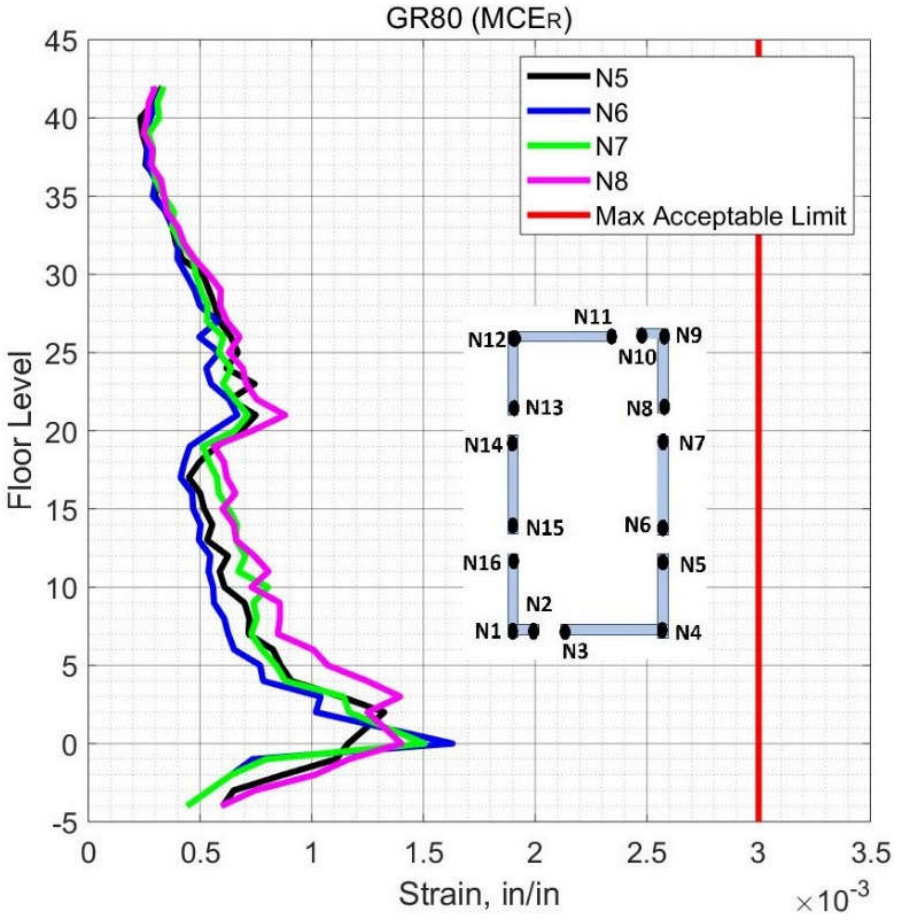

Figure 8.39 Peak Concrete Compression Strain in Core Wall Edges N5-N8 (Case 2 – MCER).

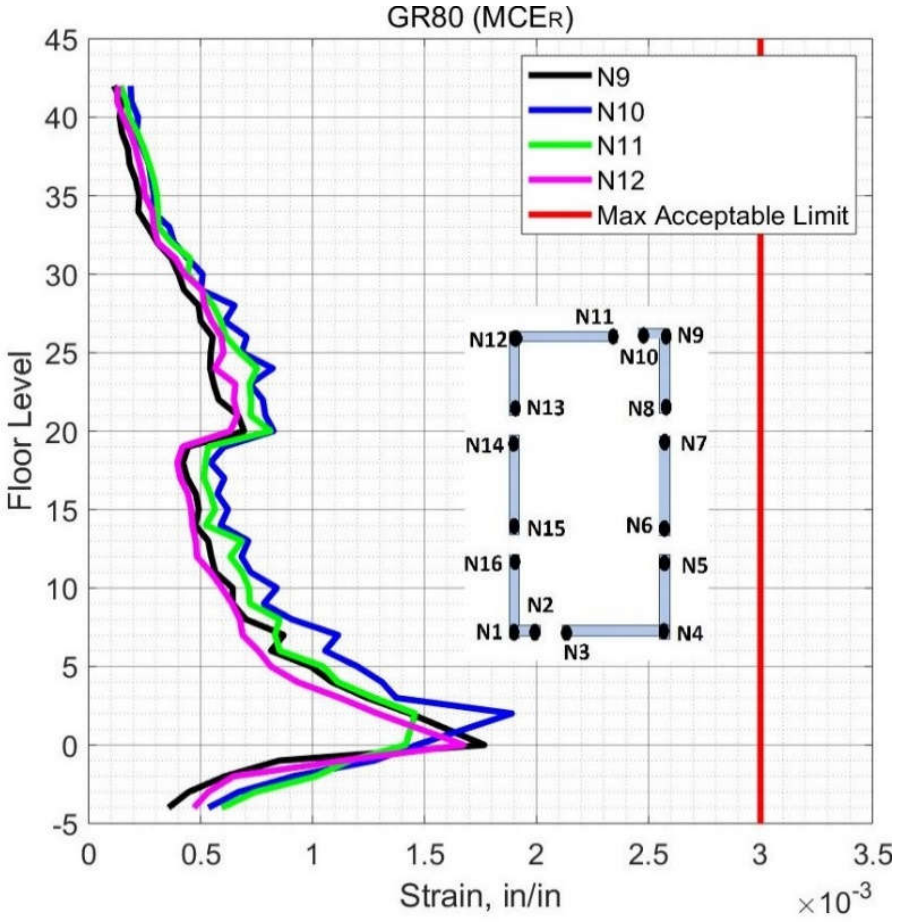

Figure 8.40 Peak Concrete Compression Strain in Core Wall Edges N9-N12 (Case 2 – MCER).

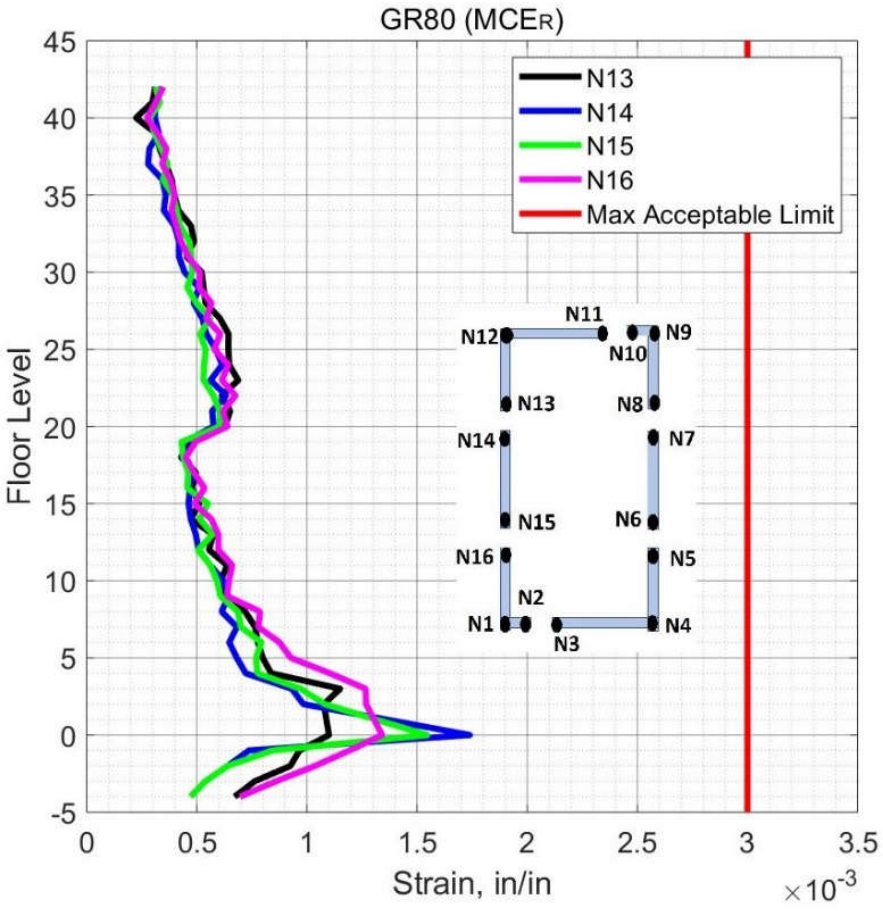

Figure 8.41 Peak Concrete Compression Strain in Core Wall Edges N13-N16 (Case 2 – MCER).

8.3.2.1.3 Coupling Beams

Figure 8.42 (a) shows the mean and maximum values of the rotation of coupling beams with a 1.7 aspect ratio (coupling beams in the x-direction), over the building height. The peak value of the rotation is 0.025 which is below the allowable limit of 0.050. The results indicate that coupling beams do experience yielding of steel reinforcement according to the data in Figure 7.18. In addition, the coupling beams expected to have a damage state (DSI), which means that the

coupling beams need minor repair. However, the rotation demands of coupling beams satisfy the requirement of the TBI guidelines for MCER level.

Figure 8.42 (b) shows the mean and maximum values of the rotation of coupling beams with a 2.1 aspect ratio (coupling beams in the y-direction), over the building height. The peak value of the rotation is 0.03 which is below the allowable limit of 0.05. The results indicate that coupling beams do experience yielding of steel reinforcement according to the data in Figure 7.19. In addition, the coupling beams expected to have a damage state (DSI), which means that the coupling beams need minor repair. However, the rotation demands of coupling beams satisfy the requirement of the TBI guidelines for MCER level.

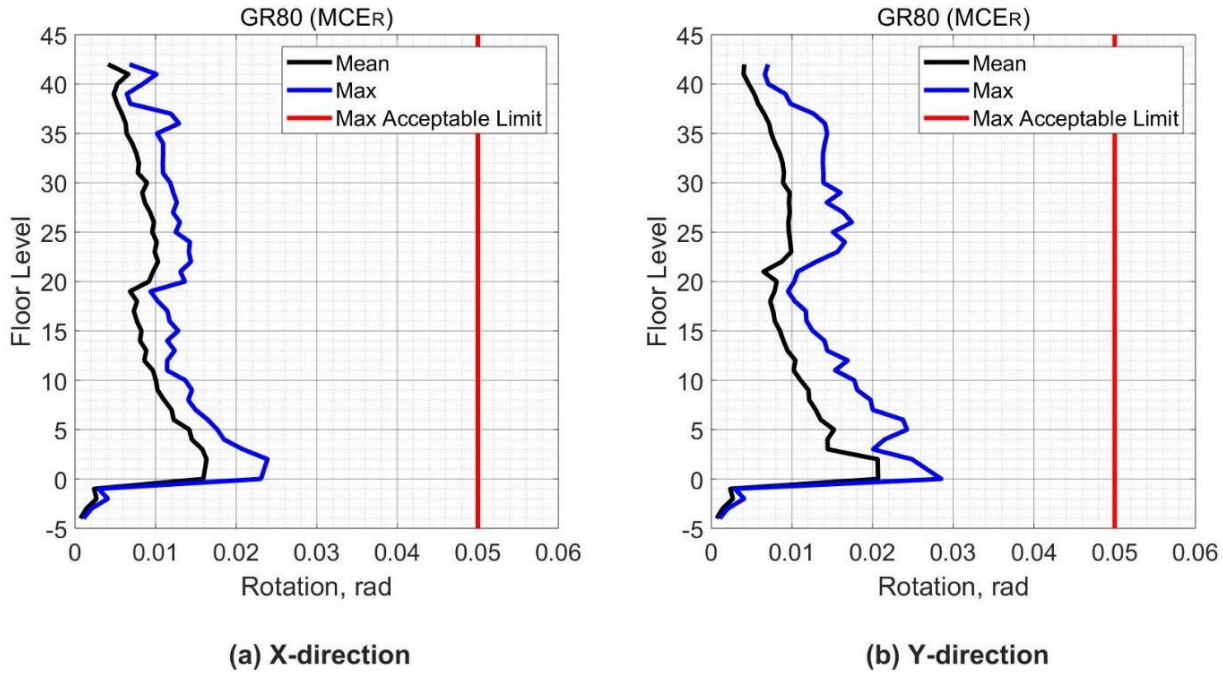

Figure 8.42 Rotation Demand in Coupling Beams (Case 2 – MCER).

8.3.2.2 Special Moment Frame Response

8.3.2.2.1 Beam Force-Based Action

As stated in Section 7.3.2.2.1, To evaluate the shear action in the beams, Equation (7-11) will be applied. Figure 8.43 shows the shear force demands in the beams of the special moment frame over the building height. In the legend of Figure 8.43, the results noted as “Mean” represent the mean value of the maximum shear force in the beams at each floor level from all ground motions analyses, while the results noted as “Max” represent the maximum shear force in the beams obtained from all analyses. In addition, the values shown as “Vfinal” and “Vexp” in the legend were obtained by using Equations (7-10) and (7-5), respectively. As shown in Figure 8.43, the main conclusion is that shear force demands in special moment frame beams meet the requirements of the TBI guidelines by satisfying Equation (7-11). In addition, the maximum shear force demands (335 kips) obtained from all ground motions are within the acceptable limits of the expected shear capacity (667 kips) of the beams. In other words, the maximum shear force demands obtained from all ground motions are within the acceptable limits of the expected shear capacity of the beams. Consequently, all analyses produced an acceptable response based on the shear force demands in the beams.

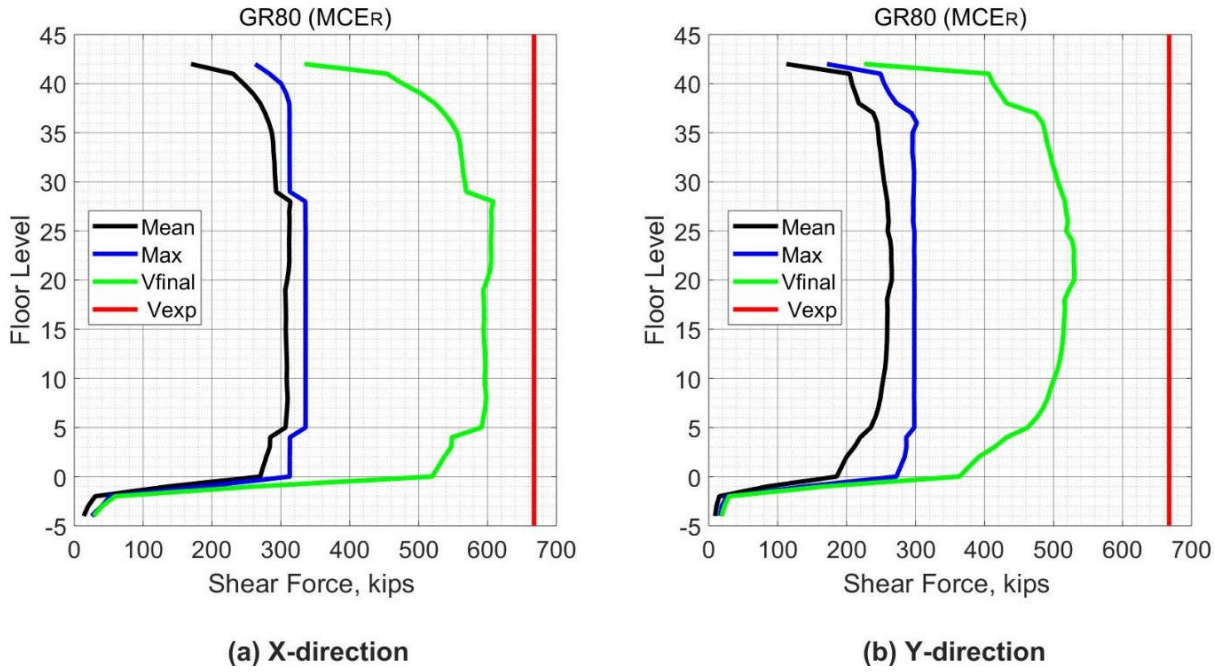

Figure 8.43 Peak Shear Force in Beams (Case 2 – MCER).

8.3.2.2.2 Beam Deformation-Based Action

Figure 8.44 shows the mean and the maximum tensile strain demands in the longitudinal reinforcement of the beams at each floor level. The maximum tensile strain demands (0.03) are within the acceptable limit (0.05). In addition, reinforcing bars in beams oriented in the x-direction experienced more tensile strain (0.03) compared to beams oriented in the y-direction (0.012). According to the ASTM A 706, the minimum requirements for the fracture elongation (total elongation) of Grade 80 is 0.12 which is higher than the measured tensile strain of 0.03. The maximum tensile strain demand for the beam longitudinal bars (0.03) is below the uniform elongation of Grade 80 (0.088) (Drit Sokoli & Ghannoum, 2016). In addition, for seismic application, the reliable maximum tensile strain for reinforcing bars is 75% of the uniform elongation (NEHRP, 2014). The maximum tensile strain demand is below the 75% of its uniform

elongation for case GR80. Considering the tensile strain results of the reinforcing bars in the beams, Grade 80 could be a valuable option for reinforcing the beams of special moment frame. Considering the expected yield strain for Grade 80 is 0.0029, so all beams in the levels above the main podium experienced yielding of reinforcing bars when considering the maximum demands for both directions.

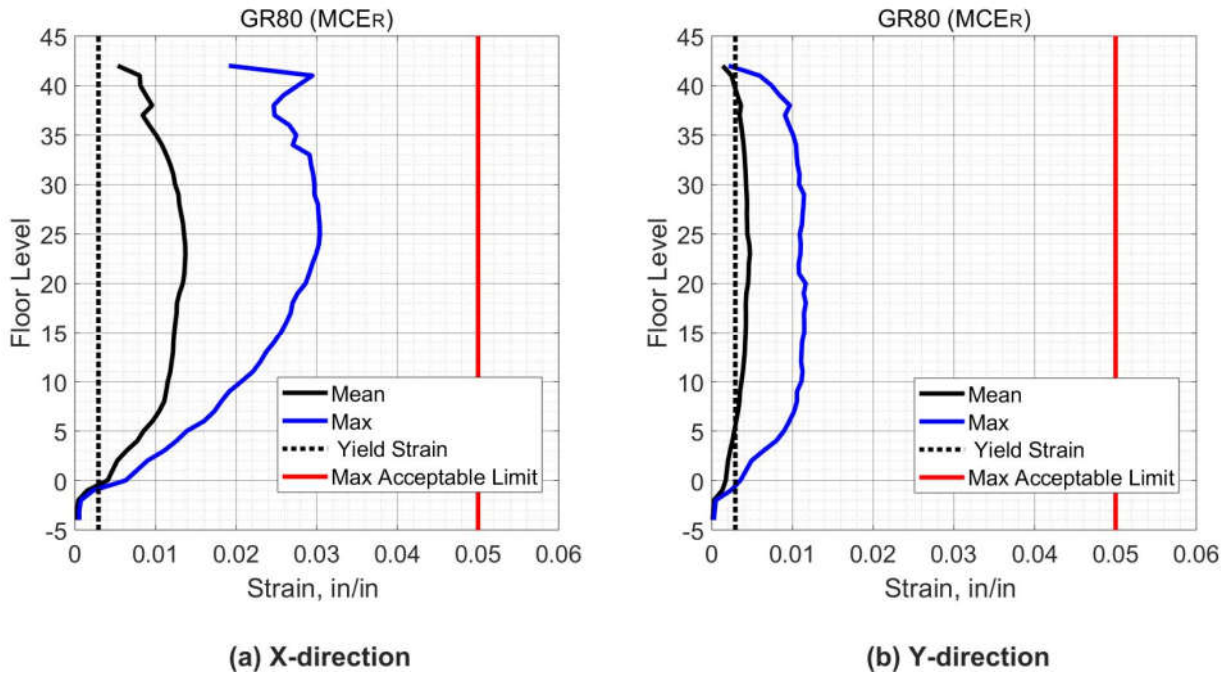

Figure 8.44 Peak Tensile Strain in Reinforcing bars in Beams (Case 2 – MCER).

Figure 8.45 shows the mean and the maximum plastic rotation demands in the beams at each floor level. The plastic rotation demand was approximately 0.03 rad which is below the acceptable limits of 0.045 of ASCE 41. A consistent finding with the tensile strain demands is observed in which beams oriented in the x-direction experienced more rotation demands compared with beams in the y-direction.

Based on the strain and plastic rotation results, the deformation-based actions in the beams satisfy the requirement of TBI guidelines.

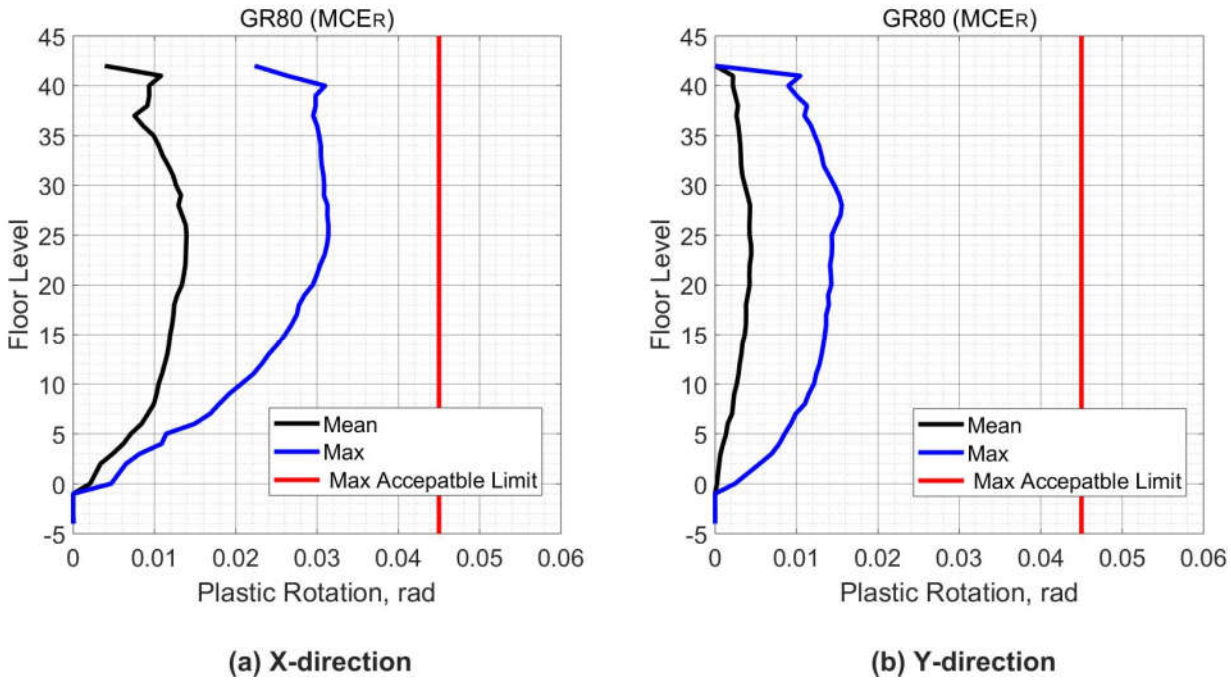

Figure 8.45 Plastic Rotation in Beams (Case 2 - MCER).

8.3.2.2.3 Columns Force-Based Action

In the legend of Figures 8.46 through 8.49, the results noted as "Mean" represent the mean value of the shear force in the columns from all ground motions analyses while the results noted as "Max" represent the maximum shear force obtained from all analyses. In addition, results with "Vfinal" and "Vexp" in the legend represent the parameters in Equation (7-11) for the columns. The shear force demands in the columns are within the limits of the TBI guidelines, by satisfying equation (7-11). The maximum shear demands obtained from all analyses are also within the acceptable limits. Therefore, all analyses produced acceptable responses when considering the

shear force demands of the columns. In contrast with the shear force demands of the core wall, the shear forces were more uniform with building height.

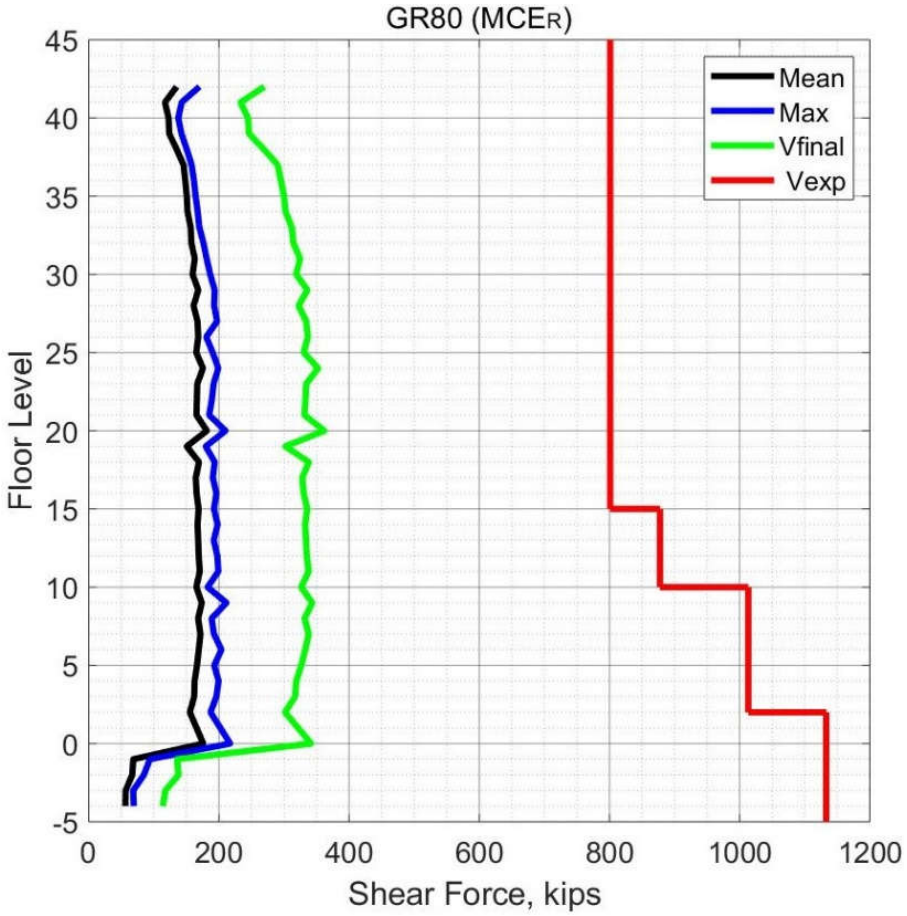

Figure 8.46 Peak Shear Force in Corner Columns (Case 2 – MCER).

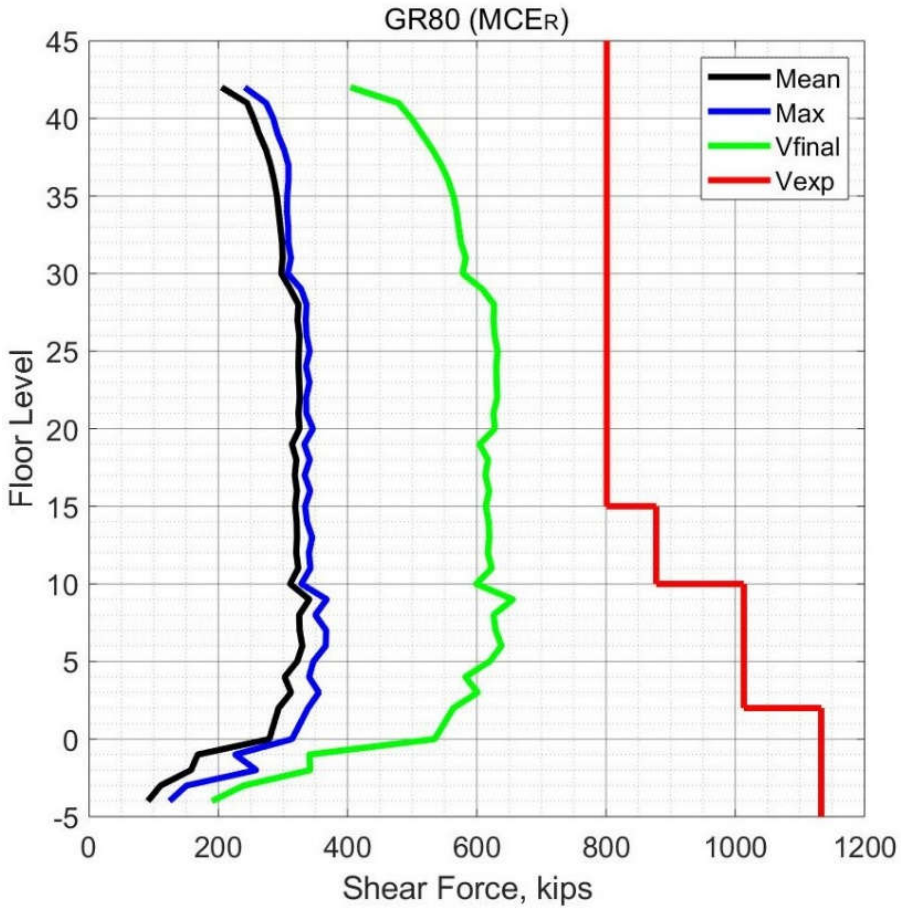

Figure 8.47 Peak Shear Force in Interior Columns X-direction (Case 2 – MCER).

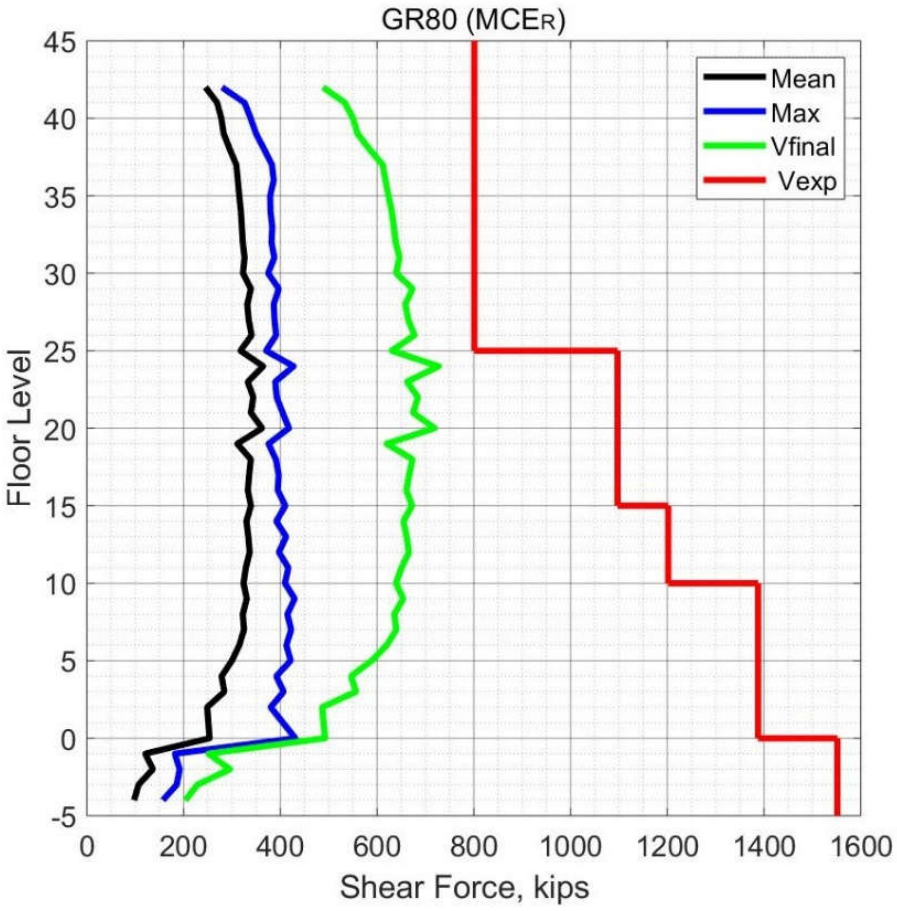

Figure 8.48 Peak Shear Force in Columns on Grid B and E (Case 2 – SLE).

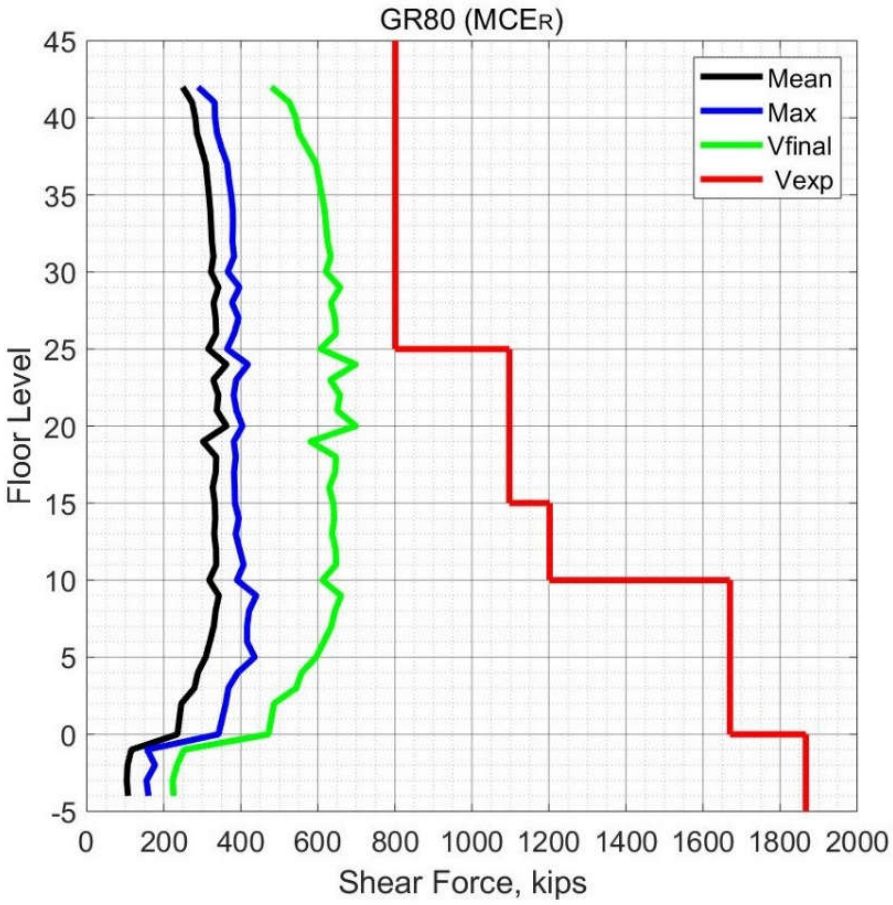

Figure 8.49 Peak Shear Force in Columns on Grid C.5 (Case 2 – MCER).

8.3.2.2.4 Column Deformation-Based Action

The maximum value of the tensile strain in the columns' longitudinal bars and the mean value from all ground motion in the suite are depicted in Figure 8.50. The maximum tensile strain demands (0.0027) did not exceed the expected yield strain of Grade 80 (0.0029), which means no plastic hinges formed in the columns. In other words, columns did not experience plastic rotations. As mention previously, the behavior of non-yielding columns is one of the preferable design approaches for seismic applications where most plastic rotation demands form in the beams.

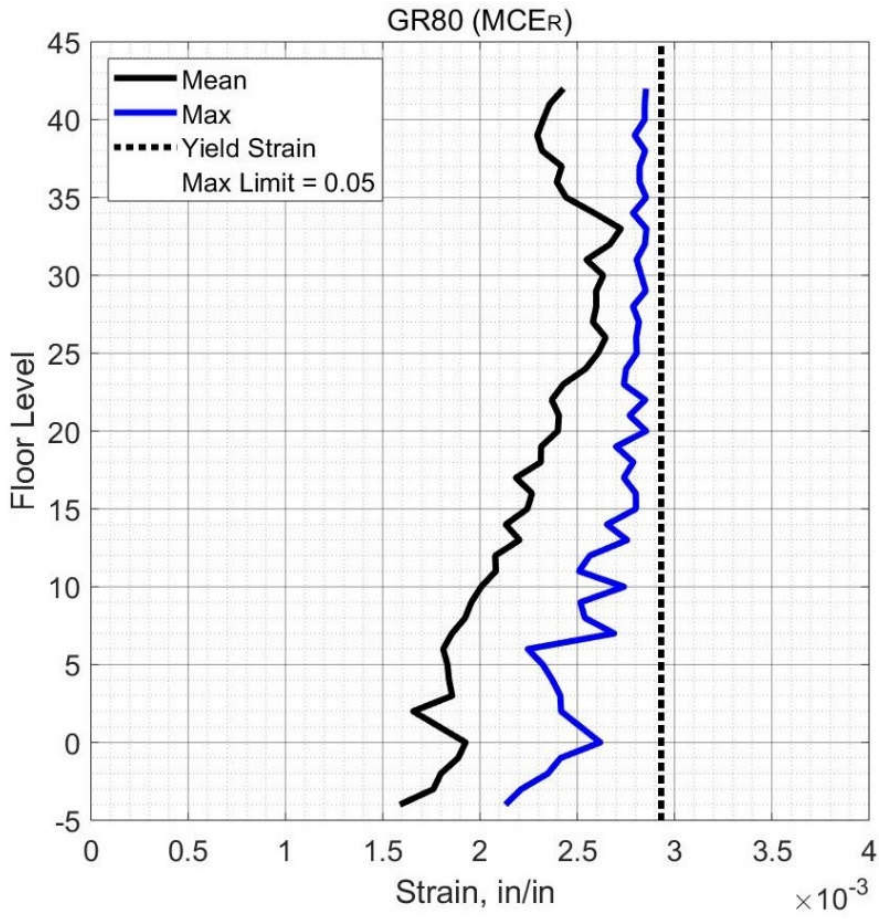

Figure 8.50 Peak Tensile Strain in Reinforcing Bars in Columns (Case 2 – MCER).

8.3.2.3 Contribution of Core Wall and Frame in Dual System

The contribution of the components of the dual system in resisting the story shear force is depicted in Figure 8.51 for the x- and y-directions, respectively. Figure 8.52 shows the contribution percentage of the shear forces for the core wall and the frame over the building height. The frame contribution is approximately constant over the building height, while the core wall contribution varies linearly. The frame contribution in the lower stories is approximately one-third of the story shear, while in the upper stories the frame contribution is about one-half of the total story shear.

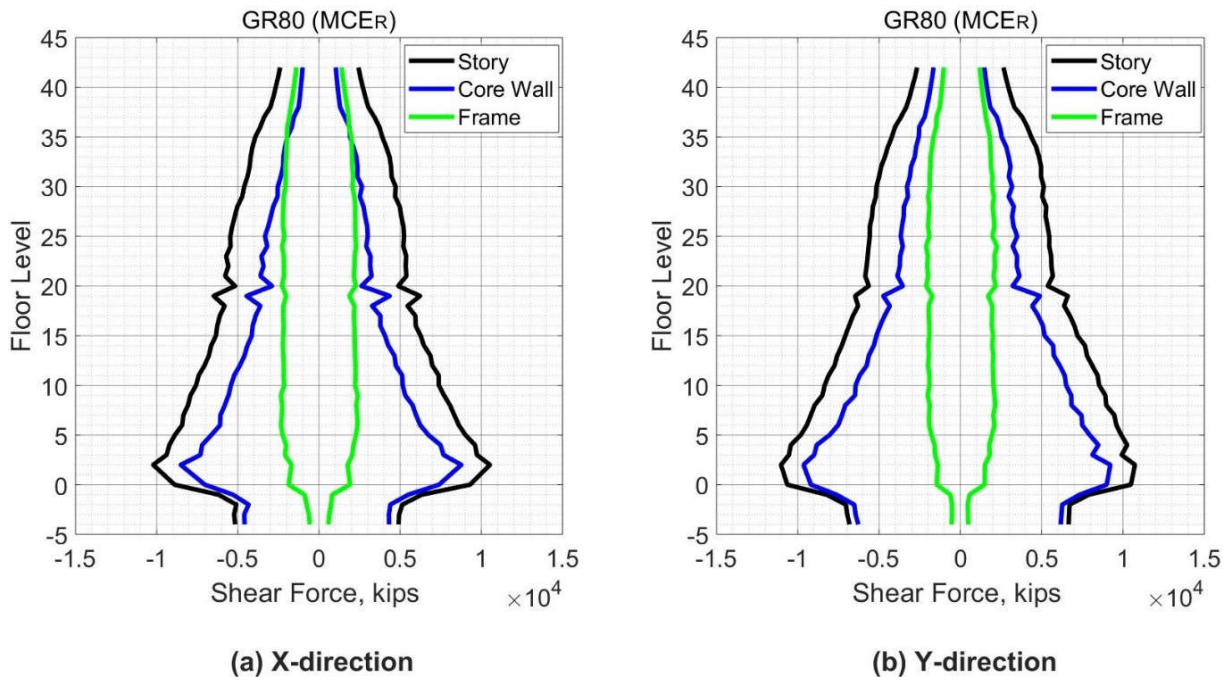

Figure 8.51 Shear Force Contribution of Core Wall & Frame (Case 2 – MCER).

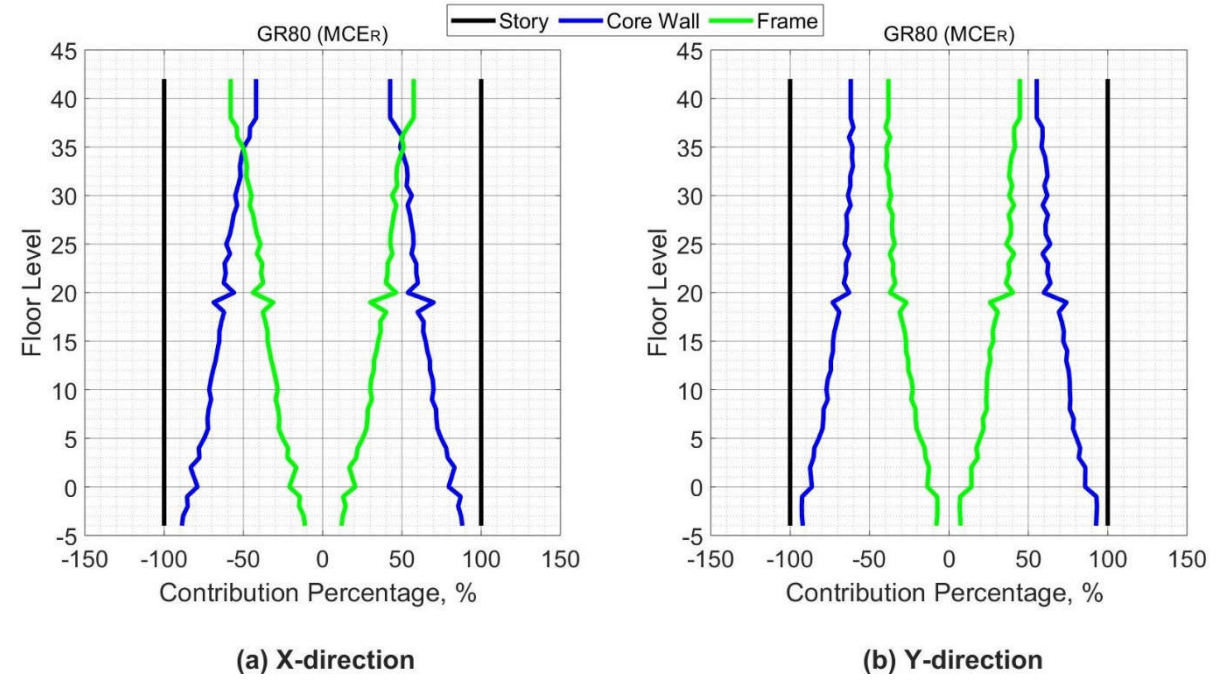

Figure 8.52 Contribution Percentage of Core wall & Frame Shear Force (Case 2 – MCER).

CHAPTER IX

CASE 3 – GRADE 100 REINFORCEMENT RESULTS

9.1 INTRODUCTION

Case 3 consists of the study building reinforced with high strength reinforcing steel bars in all structural members. ASTM A1305 Grade 100 reinforcement was used in the seismic force resisting system (SFRS) in both the core wall and the special moment frames. In this case, the cross-section dimensions of all the structural members were the same as in the case 1, however the area of reinforcement in all members was 0.6 times the area of reinforcement in the case reinforced with the conventional steel bars (case 1). The minimum reinforcing ratio for columns of the special moment frame was 0.01 times the column cross section, while for concrete core wall the minimum ratio was 0.0025, as recommended by ((NEHRP, 2014). In the following sections, the response of the case study building reinforced with reduced amount of reinforcement (Grade 100) will be examined and checked with the TBI guidelines acceptance criteria for both SLE and MCER levels. The procedures and equations that used to calculate the structural demand parameters in the previous Chapter (case 1), will be applied for determining the response demands for this case for both SLE and MCER levels.

9.2 SLE LEVEL

The same ground motions used in the SLE in case 1 were used for the SLE analyses of case 3. The results of seven analyses are represented and compared with the acceptance criteria of the TBI guidelines. According to the TBI guidelines, first, the mean value of the response parameters from all ground motions in the suite should be checked with the acceptance criteria. Second, the TBI guidelines do not require checking the maximum response parameters from all ground

motions in this level. However, the maximum response parameters will also be presented to examine the performance of the case study building in more depth.

9.2.1 Global Response

9.2.1.1 Drift Ratio

Figure 9.1 shows the mean and the maximum values of the drift ratios from all analyses over the building height. The mean peak interstory drift from the seven analyses was very close to 0.0047 in the x-direction and approximately 0.0030 in the y-direction, where both values were within the acceptable limit of the TBI guidelines of 0.0050. Figures 9.2 and 9.3 show the peak drift ratios from all ground motions over the building height.

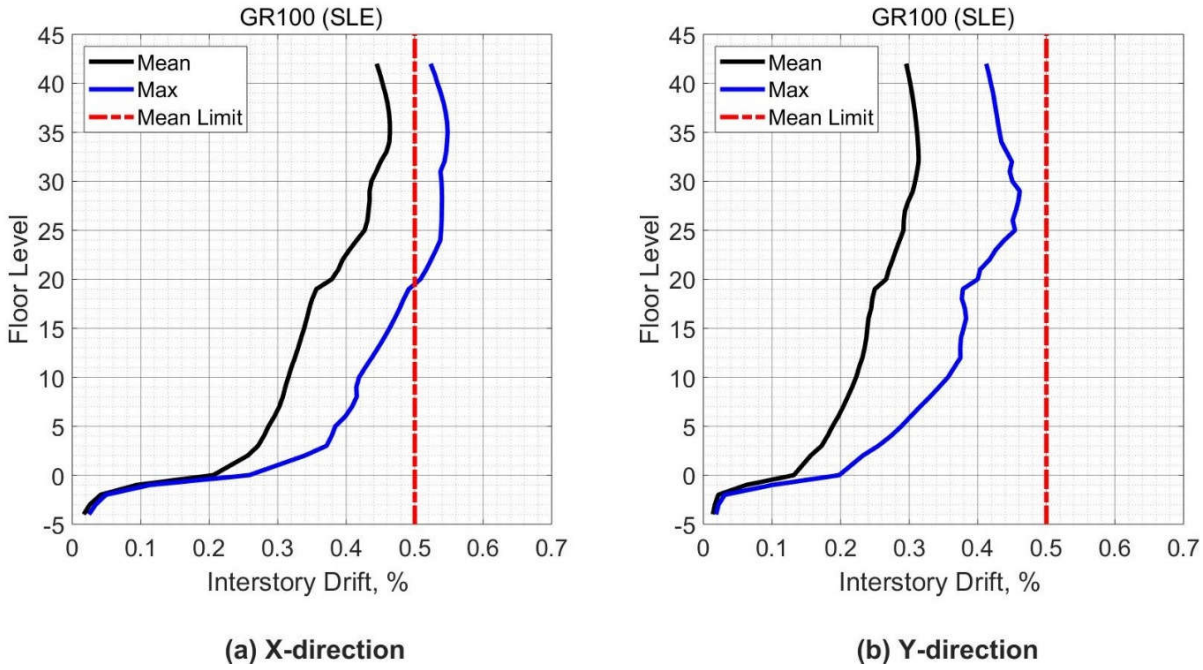

Figure 9.1 Peak Interstory Drift (Case 3 – SLE).

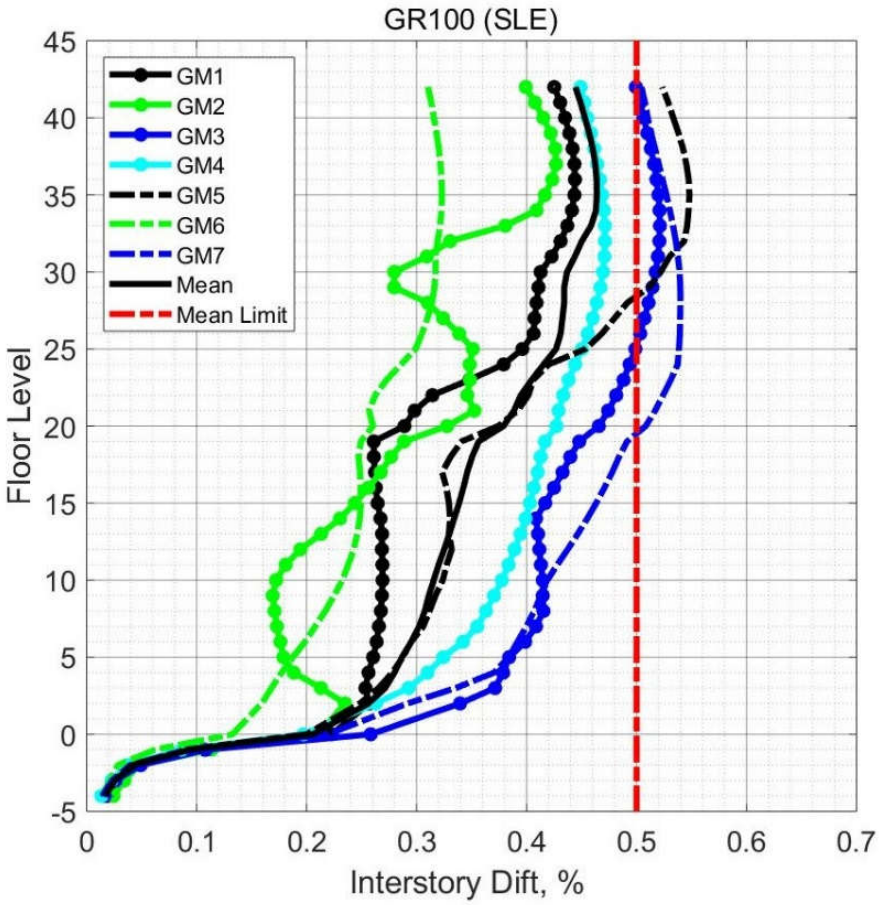

Figure 9.2 Peak Interstory Drift from All Ground Motions for X-direction (Case 3 -SLE).

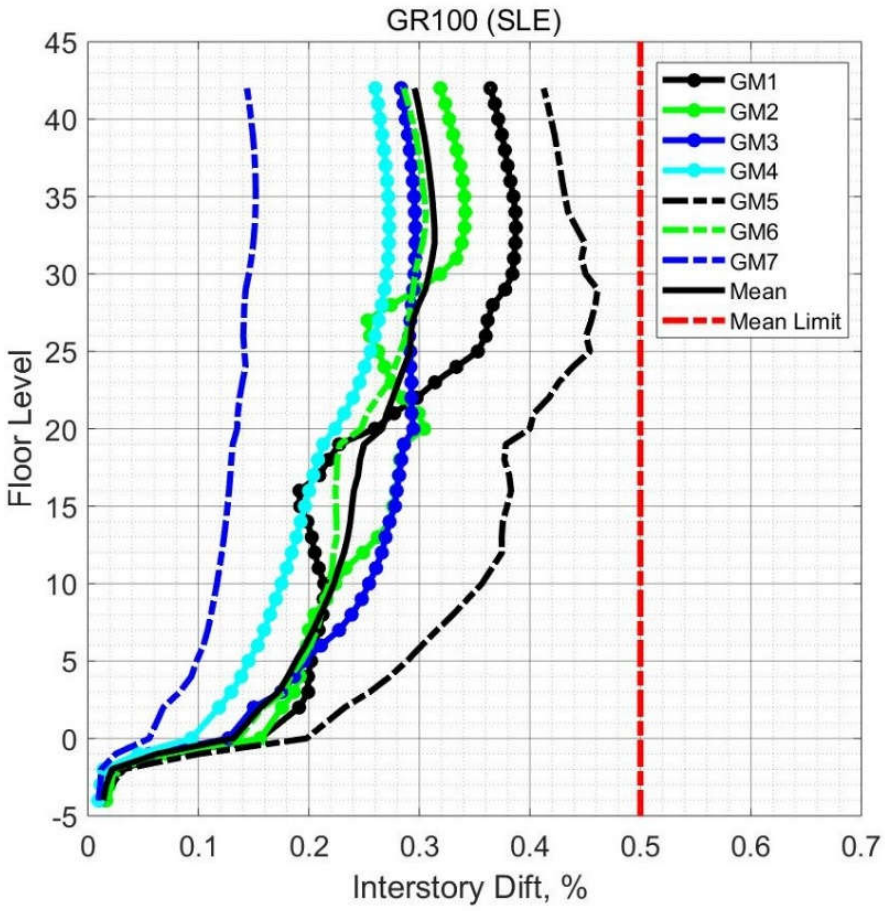

Figure 9.3 Peak Interstory Drift from All Ground Motions for Y-direction (Case 3 -SLE).

9.2.1.2 Displacement

As in Section 7.2.1.2, Figure 9.4 depicts the mean value of the displacement of each story at the same time step that the roof experiences a maximum displacement value.

Figures 9.5 and 9.6 show the time history of the roof displacement in the x-direction and y-direction, respectively from a ground motion at which the displacement demand of the roof was the highest one among other ground motions. During the seventh ground motion, the roof experience a maximum displacement in the x-direction while during the fifth ground motion the maximum roof displacement in the y-direction was observed.

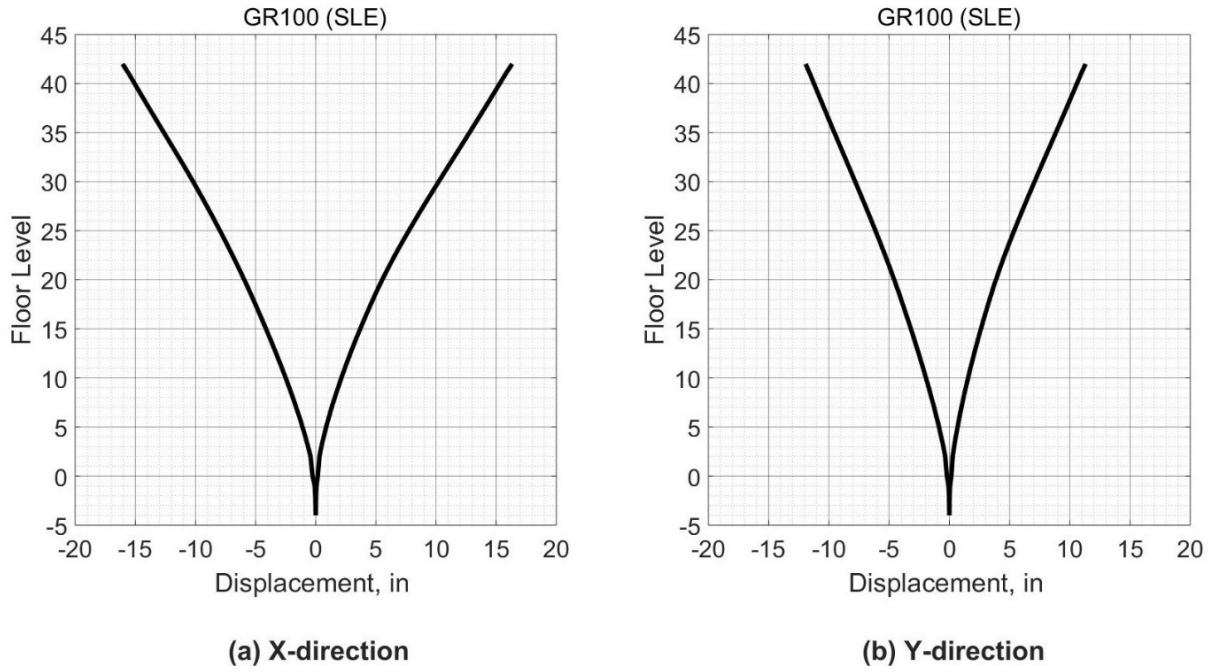

Figure 9.4 Floors Displacement Synchronous with Peak Roof Displacement (Case 3 - SLE).

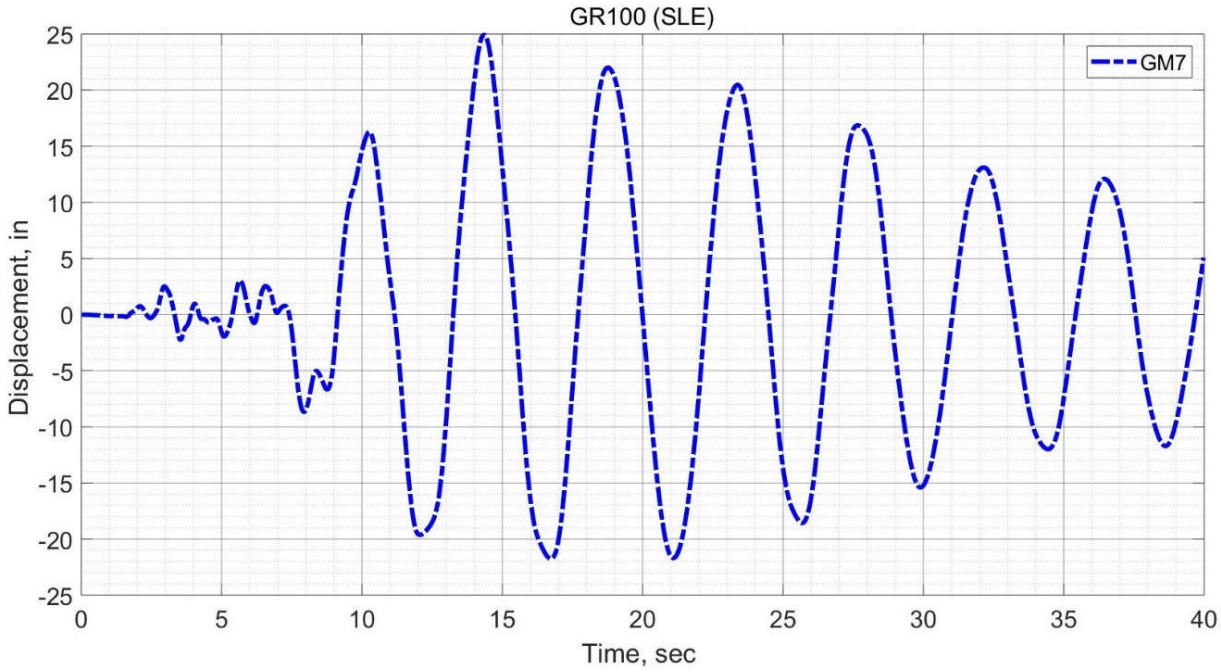

Figure 9.5 Time History for Peak Roof Displacement for X-direction (Case 3 – SLE).

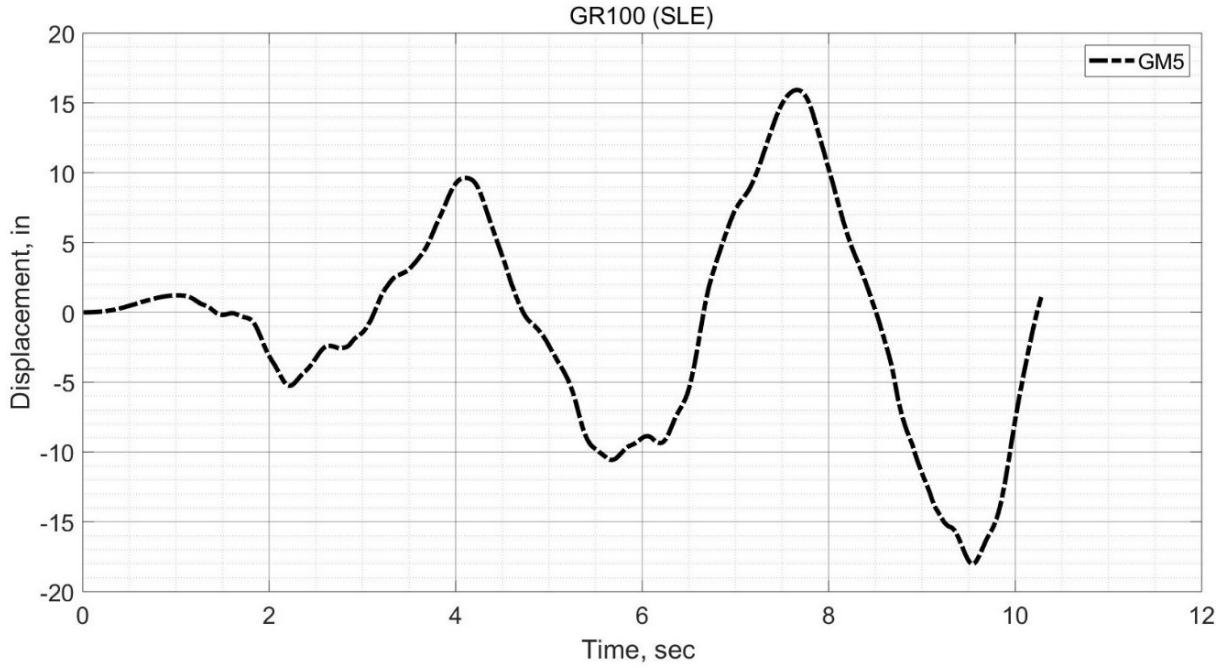

Figure 9.6 Time History for Peak Roof Displacement for Y-direction (Case 3 – SLE).

9.2.2 Element Level

As stated in Section 7.2.2, the TBI guidelines require using only the mean value from all analyses for evaluation with the acceptance criteria for both the force and deformation based-actions in this level. The maximum response parameters for both actions will also be presented to examine the response of the case study building in more depth. In the subsections below, the elements of the seismic force resisting system with their actions are presented and evaluated using the acceptance criteria of the TBI guidelines.

9.2.2.1 Core Wall Response

9.2.2.1.1 Core Wall Force-Based Action

The TBI guidelines specify that shear in the core walls of tall buildings is a force-based action. To evaluate the shear demands of core walls, the TBI guidelines required that the shear

force demands satisfy the Equation (7-1). Figure 9.7 shows the core wall shear forces over the building height and the values of $\phi Vexp$. The shear demands in the core wall satisfy Equation (7-1) as required by the TBI guidelines. In addition, the shear force demands varied approximately in a linear manner with the height of the building. For the mean response, the demand was approximately the same in both the x- and y-directions. The peak shear force of the mean values was 6638 kips, and 6682 kips, for x and y-direction, respectively. The maximum response was also less than the limit of the mean response.

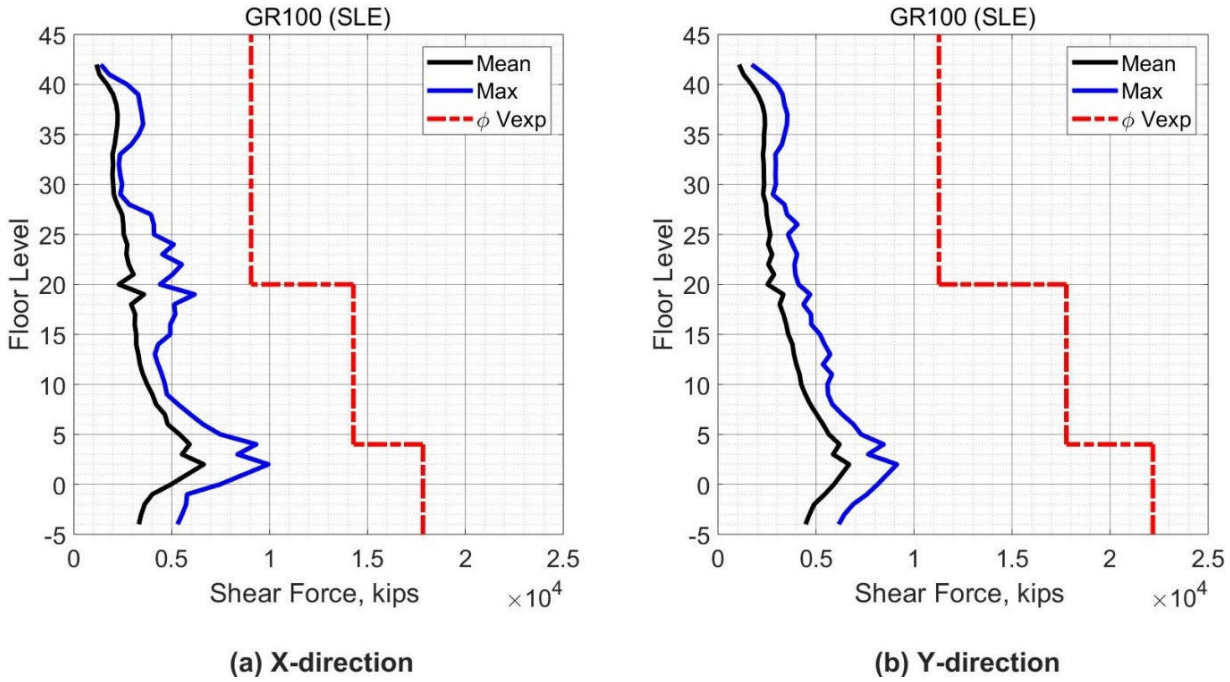

Figure 9.7 Shear Forces in Core Wall (Case 3 – SLE).

9.2.2.1.2 Core Wall Deformation-Based Actions

Figures 9.8 to 9.11 show the mean values of the maximum tensile strain in the core wall reinforcement steel at locations shown in Figure 7.6 over the building height. The TBI guidelines consider the yielding of steel bars as damage that should be avoided in the SLE shaking level. The

maximum tensile strain in the steel bars in the core wall edges was 0.002, which is below the expected yield strain of Grade 100 (0.004). The steel reinforcement in the core wall do not experience yielding strain, therefore the requirements of the TBI guidelines are satisfied.

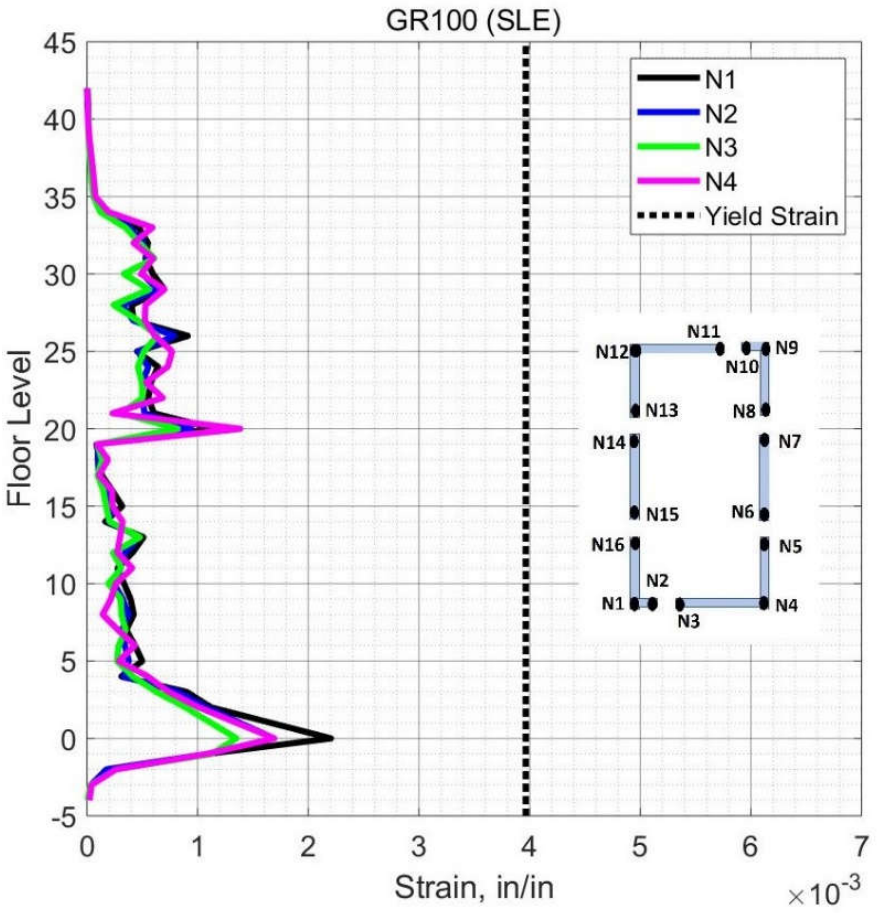

Figure 9.8 Mean Tensile Strain in Steel Bars in Core Wall Edges N1-N4 (Case 3 – SLE).

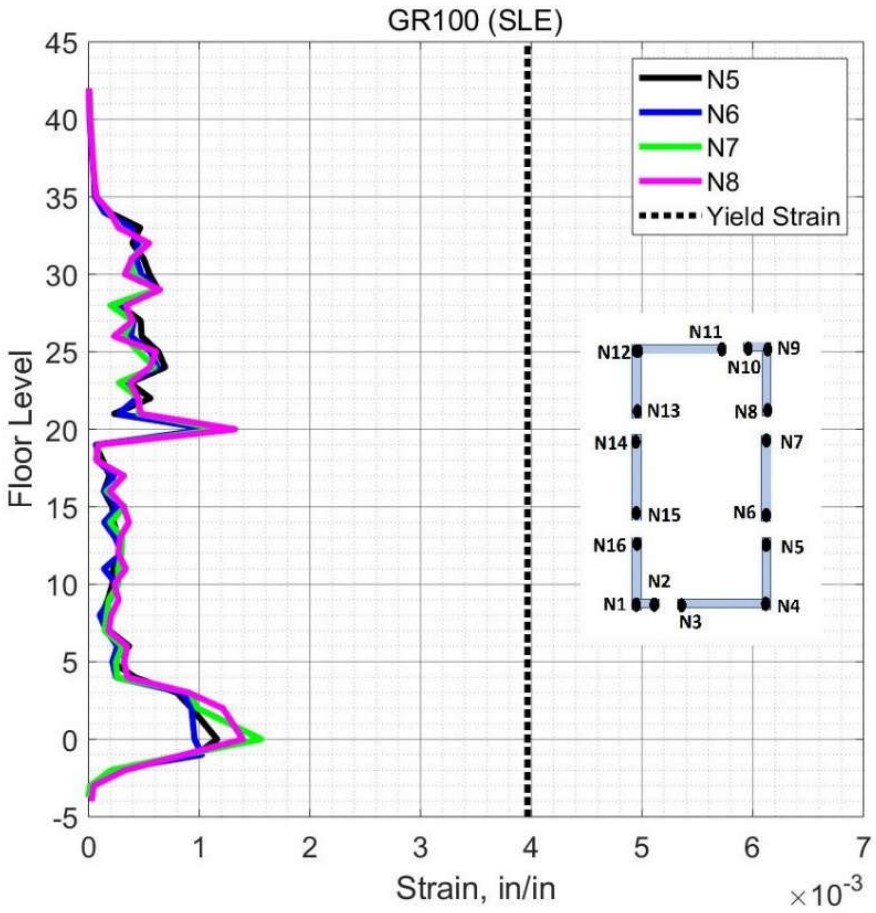

Figure 9.9 Mean Tensile Strain in Steel Bars in Core Wall Edges N5-N8 (Case 3 – SLE).

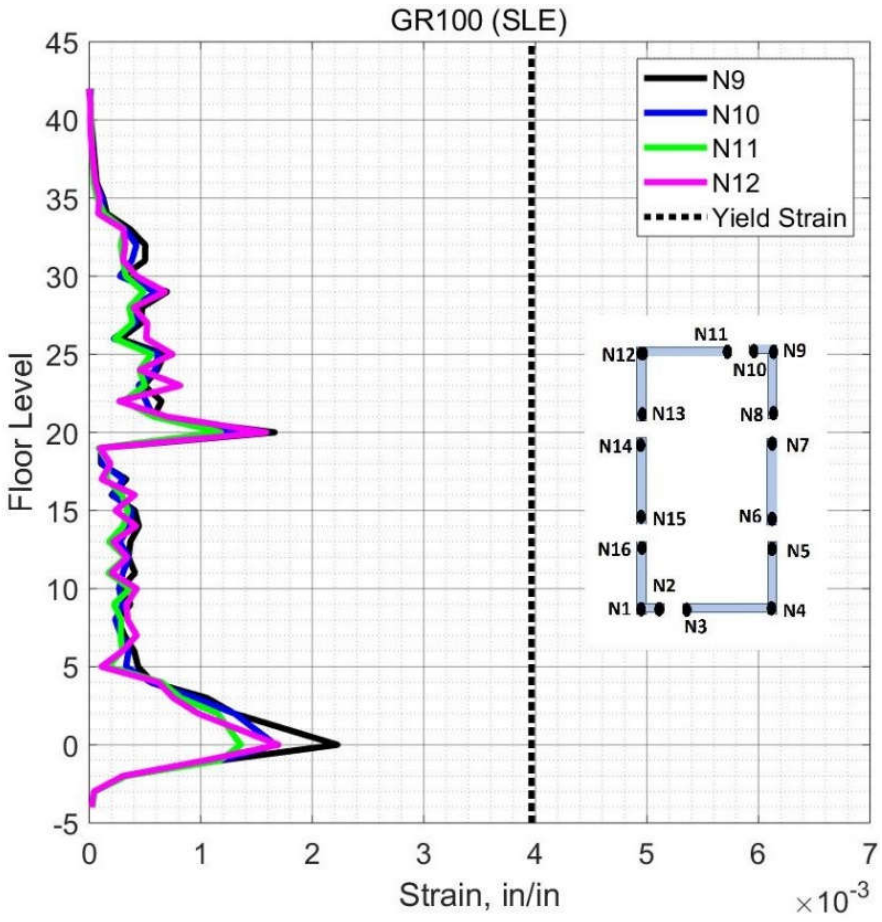

Figure 9.10 Mean Tensile Strain in Steel Bars in Core Wall Edges N9-N12 (Case 3 – SLE).

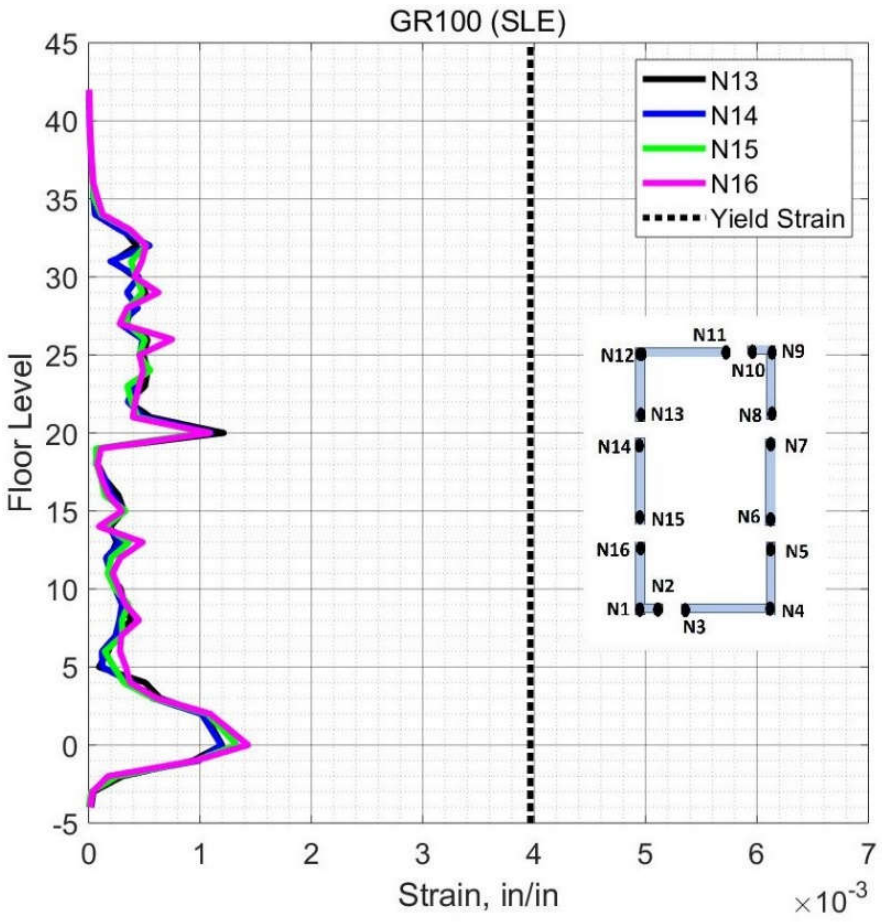

Figure 9.11 Mean Tensile Strain in Steel Bars in Core Wall Edges N13-N16 (Case 3 – SLE).

Figures 9.12 to 9.15 show the mean values of the maximum compression strain in the core wall concrete at locations shown in Figure 7.6 over the building height. The TBI guidelines consider the cracking of concrete as damage that should be avoided in the SLE shaking level. The concrete compression strain in the core wall was very low (< 0.00075), therefore the requirements of the TBI guidelines are satisfied.

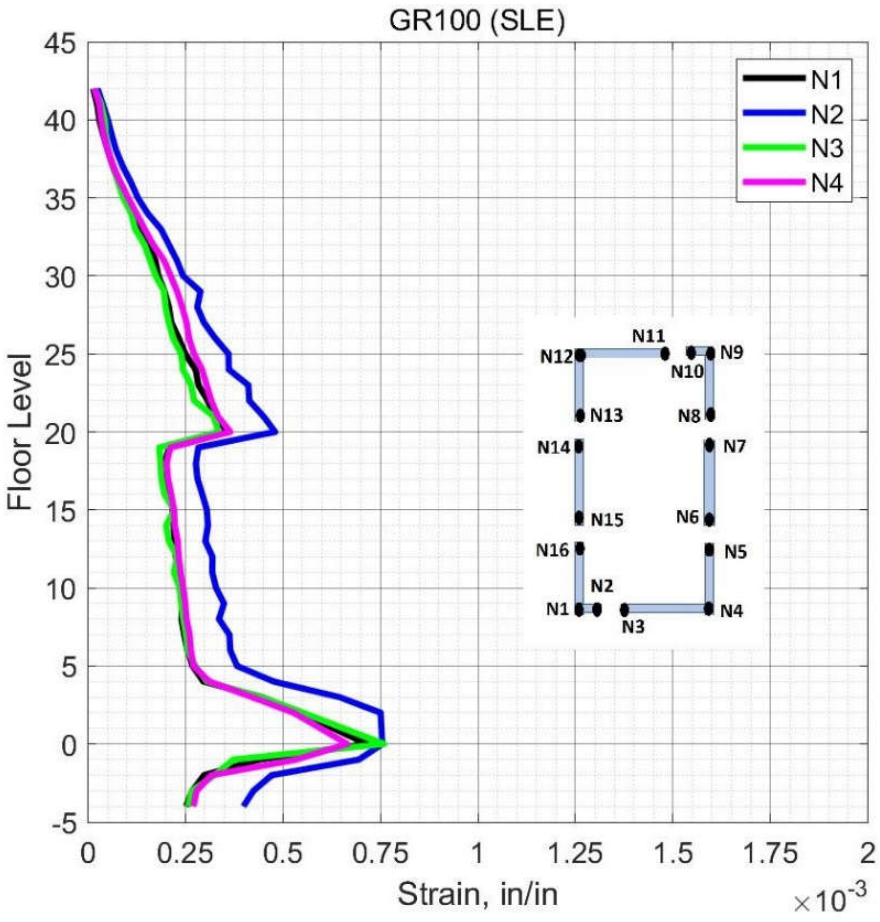

Figure 9.12 Mean Concrete Compression Strain in Core Wall Edges N1-N4 (Case 3 – SLE).

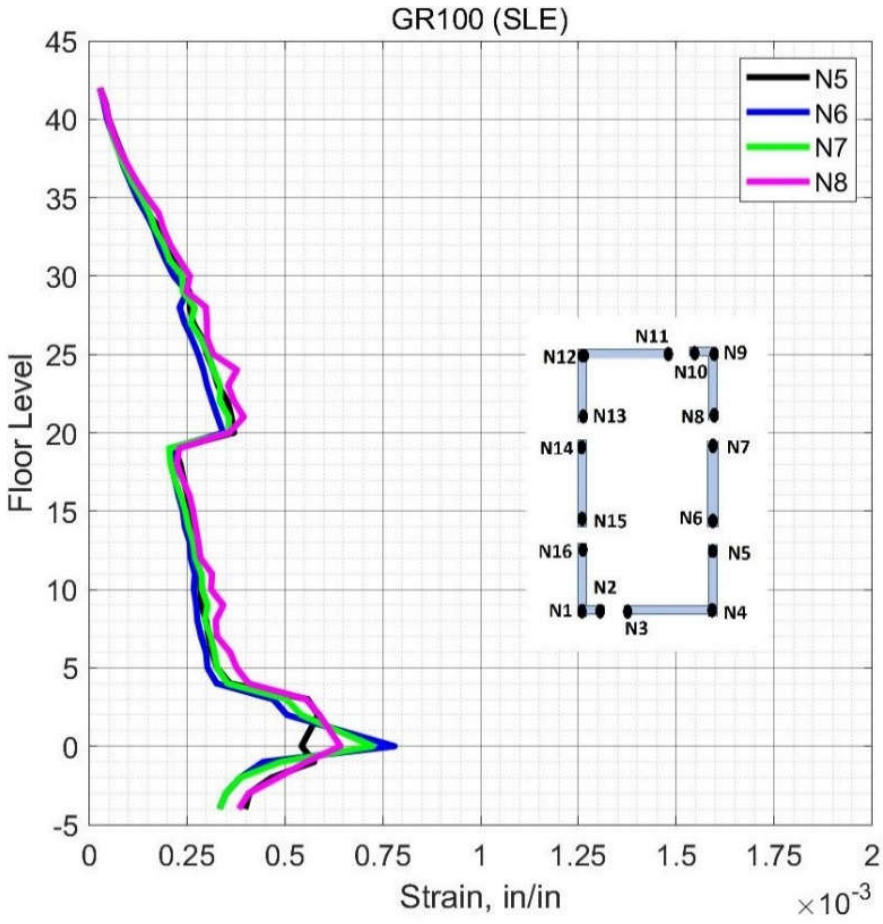

Figure 9.13 Mean Concrete Compression Strain in Core Wall Edges N5-N8 (Case 3 – SLE).

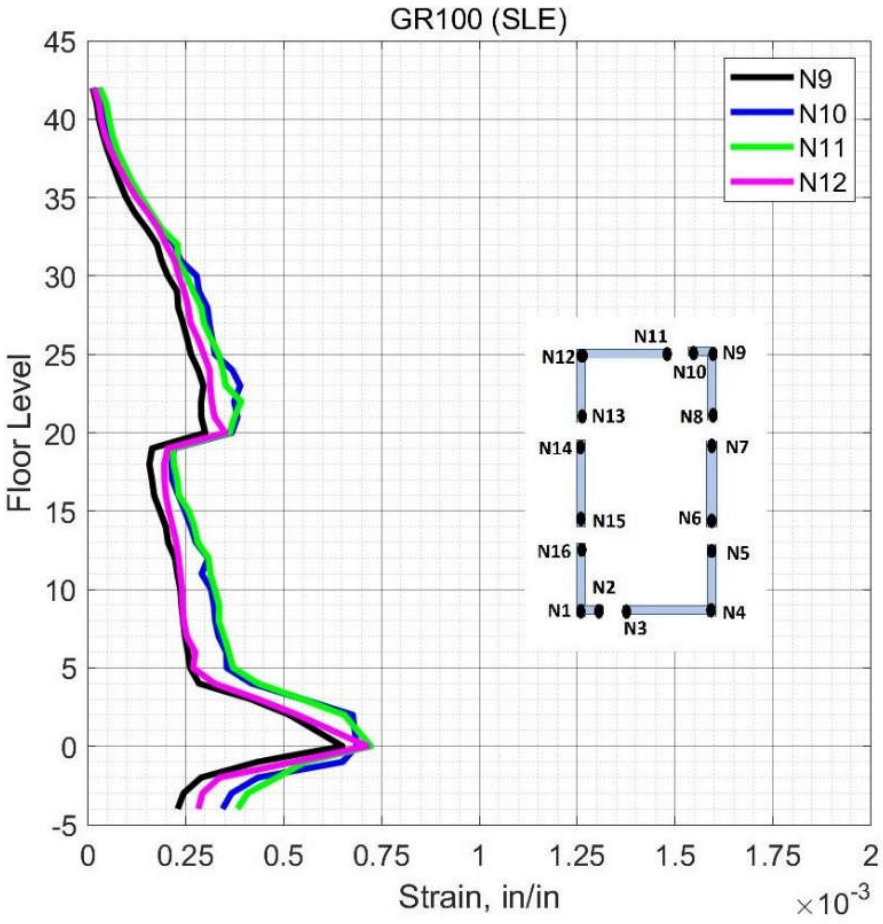

Figure 9.14 Mean Concrete Compression Strain in Core Wall Edges N9-N12 (Case 3 – SLE).

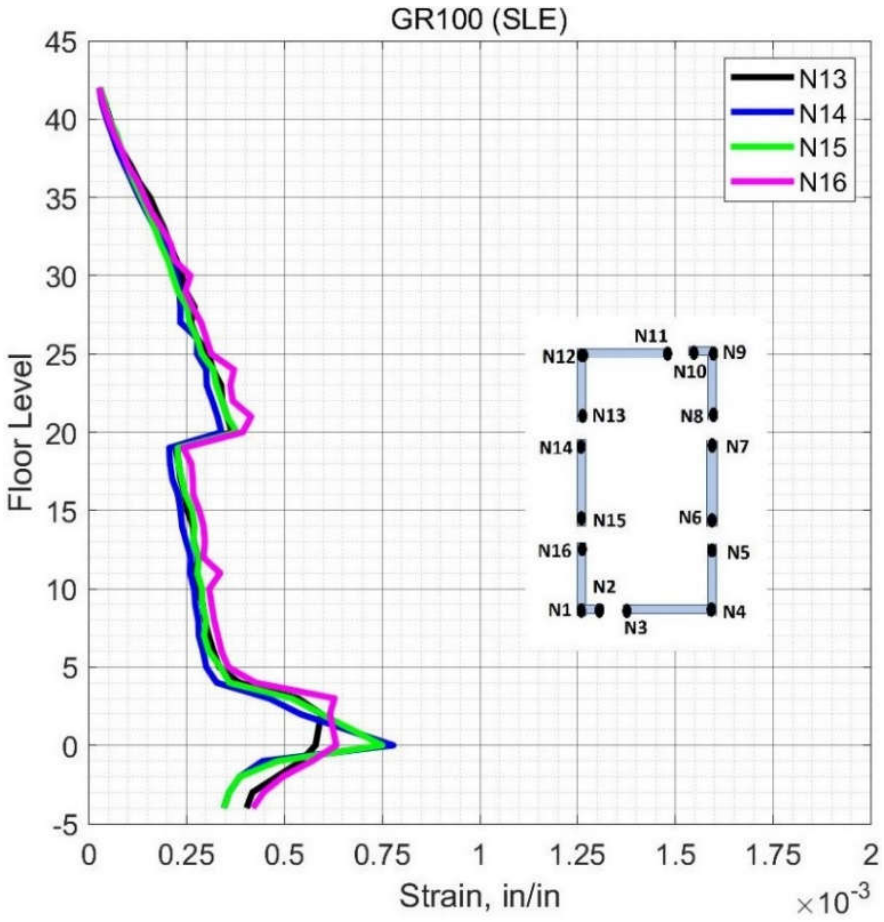

Figure 9.15 Mean Concrete Compression Strain in Core Wall Edges N13-N16 (Case 3 – SLE).

9.2.2.1.3 Coupling Beams

Figure 9.16 (a) shows the mean and maximum values of the rotation of coupling beams with a 1.7 aspect ratio (coupling beams in the x-direction), over the building height. The peak value of the mean rotation is 0.0016 which indicate that coupling beams do not experience yielding of steel reinforcement according to the data in Figure 7.18. In addition, the rotation demands are below the allowable limit of ASCE 41 (0.0060). Therefore, the rotation demands of coupling beams satisfy the requirement of the TBI guidelines.

Figure 9.16 (b) shows the mean and maximum values of the rotation of coupling beams with a 2.1 aspect ratio (coupling beams in the y-direction), over the building height. The peak value of the mean rotation is 0.0012 which indicate that coupling beams do not experience yielding of steel reinforcement according to the data in Figure 7.19. In addition, the rotation demands are below the allowable limit of ASCE 41 (0.0060). Therefore, the rotation demands of coupling beams satisfy the requirement of the TBI guidelines.

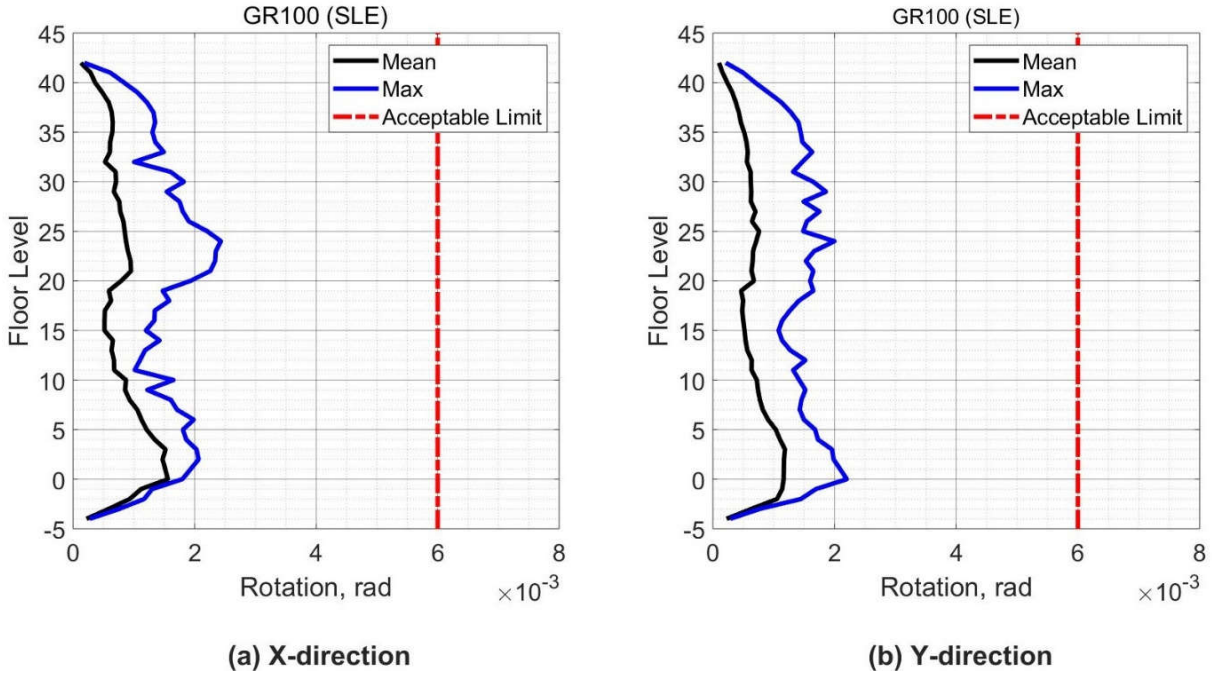

Figure 9.16 Rotation Demand in Coupling Beams (Case 3 – SLE).

9.2.2.2 Special Moment Frame Response

9.2.2.2.1 Beam Force-Based Action

The TBI guidelines specify the shear in the beams of special moment frames as a force-based action. The shear demands should satisfy Equation (7-1). The expected shear strength (V_{exp})

of beams or columns is calculated by using Equation (7-5) from ACI 318-14. Figure 9.17 shows the mean and the maximum values of beams shear forces from all ground motions over the building height and the limiting values of ($\phi Vexp$). In addition, the mean shear force demands in the beams of the special moment frame satisfy the requirements of the TBI guidelines by satisfying Equation (7-1). A slight increase in shear forces demands for the beams in the x-direction is noticed compared with beams in the y-direction. The maximum shear demand in the beams was 200 kips while the reduced shear capacity of the beams was 500 kips.

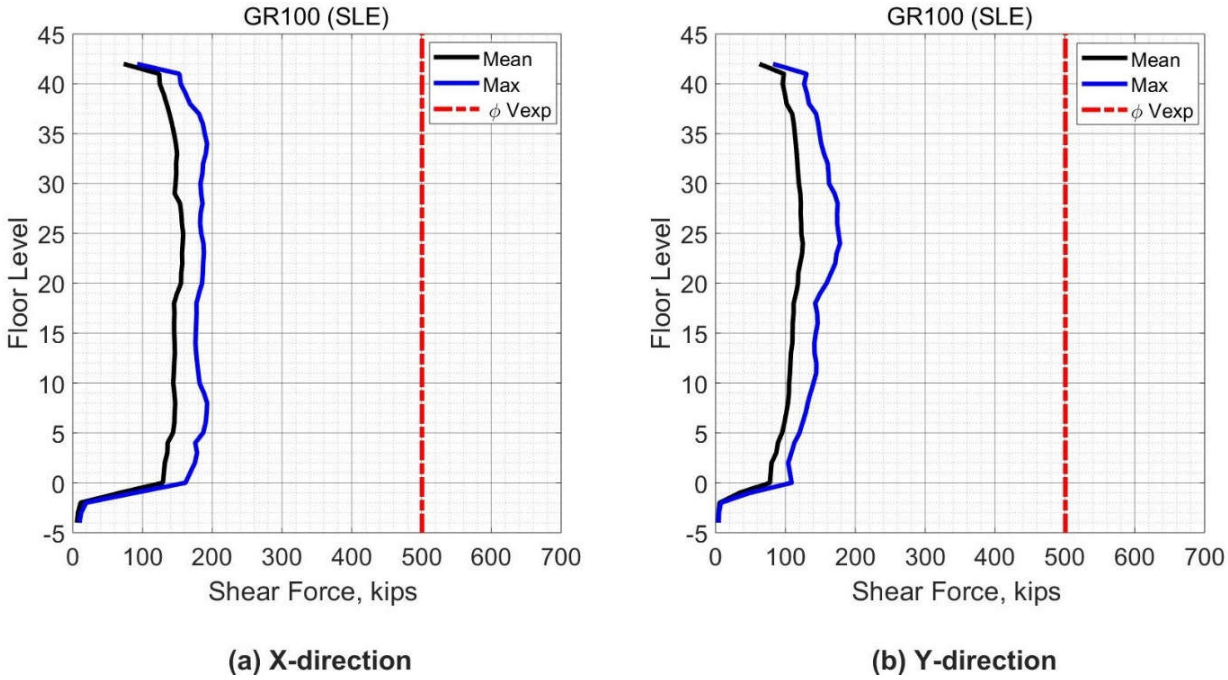

Figure 9.17 Peak Shear Force in Beams (Case 2 – SLE).

9.2.2.2.2 Beam Deformation-Based Action

Figure 9.18 shows the mean and maximum tensile strain demands in the longitudinal reinforcement in the beams sections that are in the beam ends over the building height. The TBI

guidelines consider the yielding of steel bars as damage that should be avoided in the SLE shaking level. The mean tensile strain of the steel reinforcement in all beams do not exceed the expected yield strain of Grade 100 (0.004 in/in), therefore the requirements of the TBI guidelines are satisfied. An increase in the tensile strain of the reinforcing bars in the beams oriented in the x-direction is noticed compared with the beams oriented in the y-direction. No yielding of the steel bars in the beams means that the beams do not experience plastic rotation.

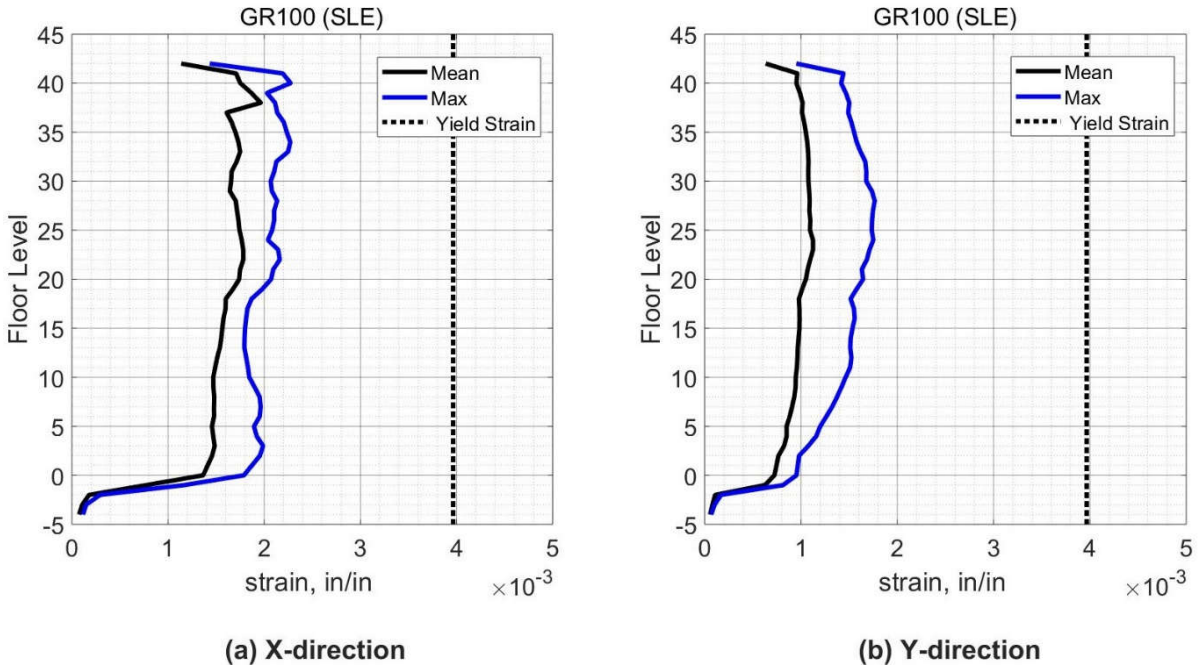

Figure 9.18 Peak Tensile Strain in Reinforcing bars in Beams (Case 3 – SLE).

9.2.2.2.3 Columns Force-Based Action

Figures 9.19 to 9.22 show the mean and maximum values of the shear forces from all analyses in the building columns and the limiting values of ($\phi Vexp$) over the building height. The

shear forces in the columns satisfies the requirements of the TBI guidelines by satisfying Equation (7-1).

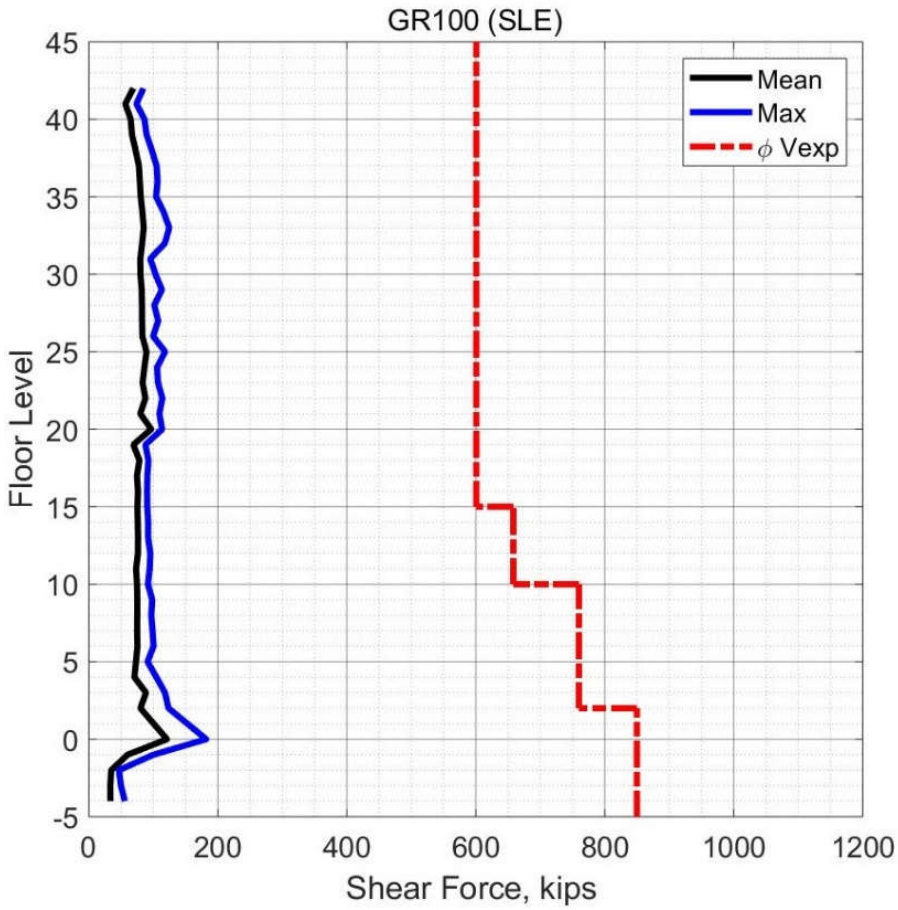

Figure 9.19 Peak Shear Force in Corner Columns (Case 3 – SLE).

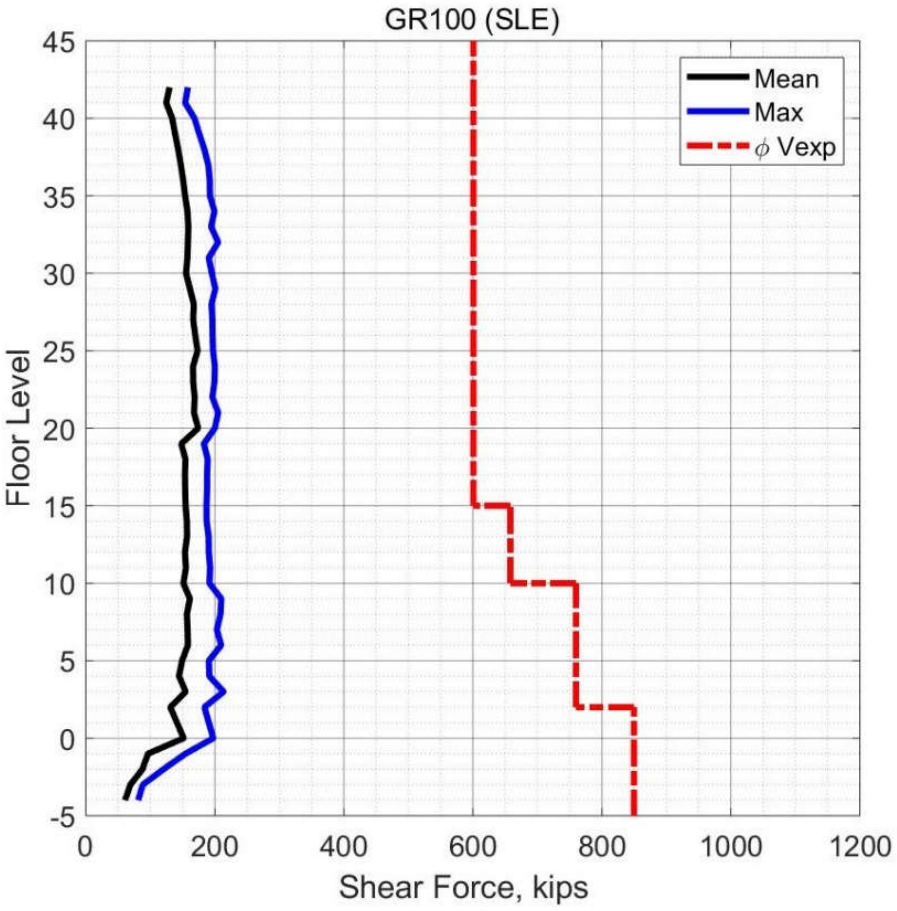

Figure 9.20 Peak Shear Force in Interior Columns X-direction (Case 3 – SLE).

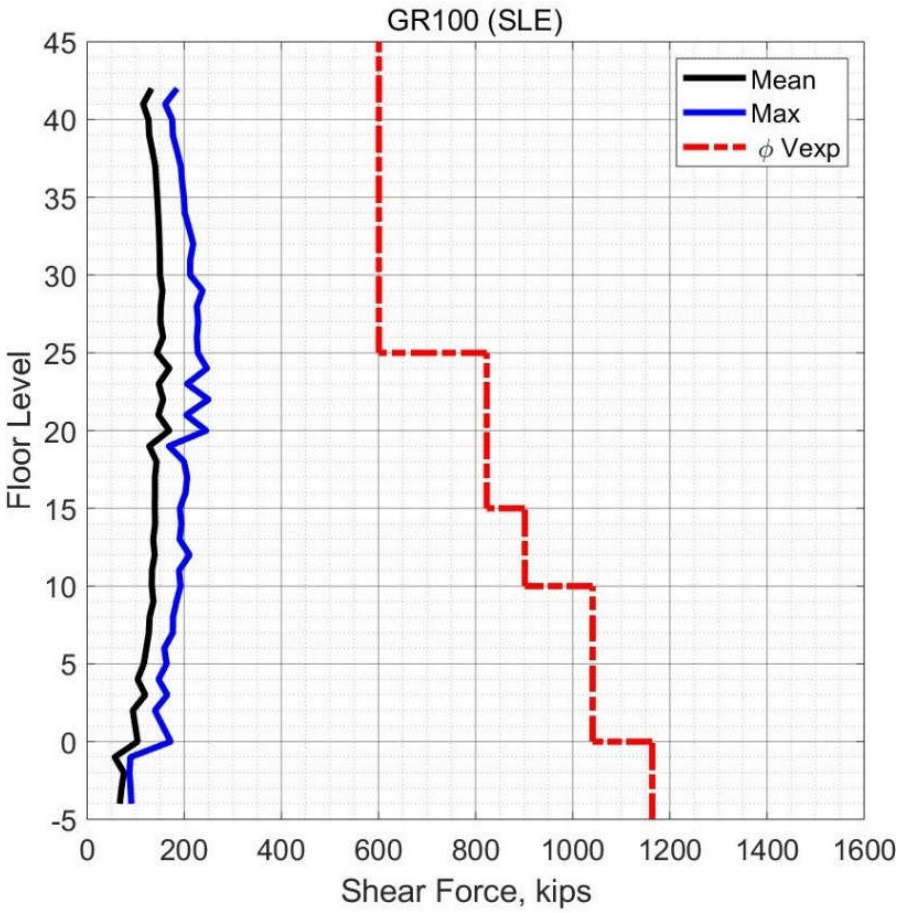

Figure 9.21 Peak Shear Force in Columns on Grid B and E (Case 3 – SLE).

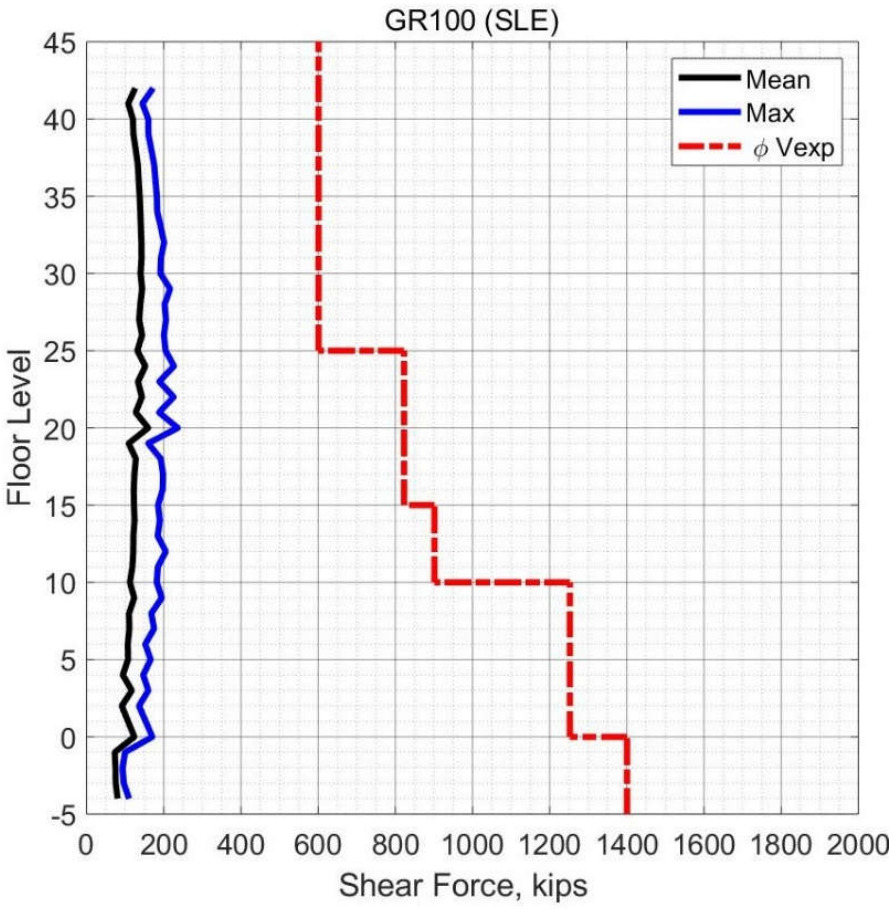

Figure 9.22 Peak Shear Force in Columns on Grid C.5 (Case 3 – SLE).

9.2.2.2.4 Column Deformation-Based Action

Figure 9.23 shows the maximum value of the tensile strain in the longitudinal bars in columns and the mean value from all ground motion in the suite over the building height. The TBI guidelines consider the yielding of steel bars as damage that should be avoided in the SLE shaking level. The tensile strain demands did not exceed the expected yield strain of Grade 100 which means no damage could be expected in the columns. Consequently, there is no plastic rotation in all the columns for this shaking level. Depending on the results of the tensile strain of the reinforcing bars, the columns satisfy the requirements of the TBI guidelines.

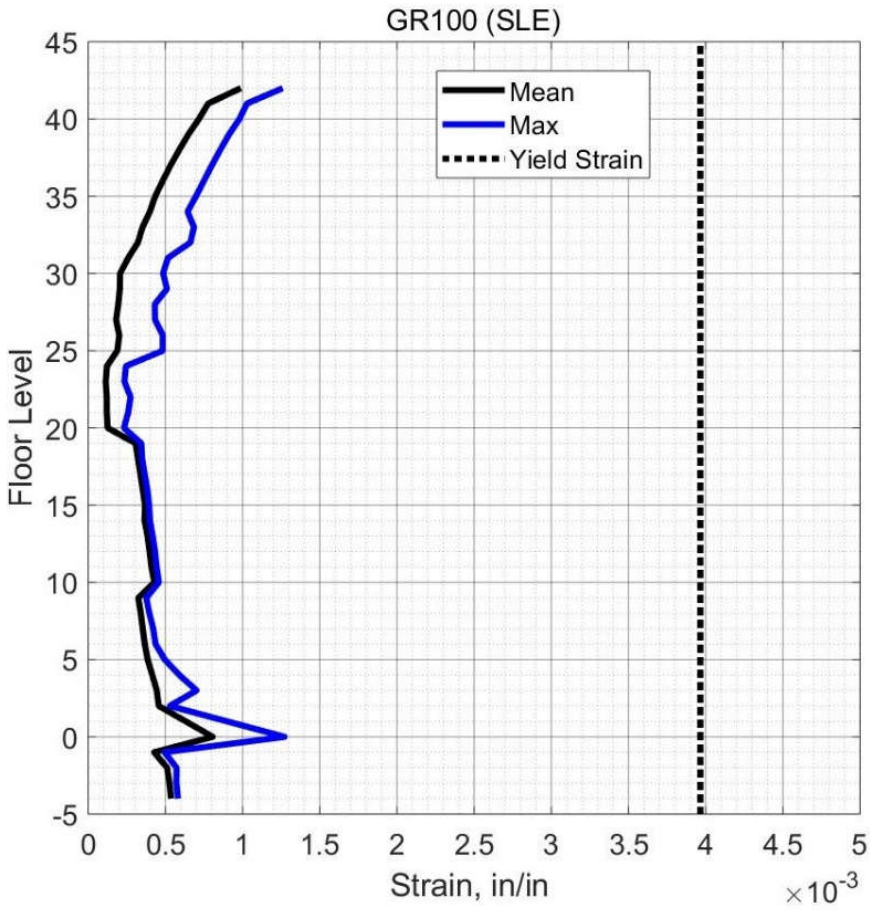

Figure 9.23 Peak Tensile Strain in Reinforcing Bars in Columns (Case 3 – SLE).

9.2.2.3 Contribution of Core Wall and Frame in Dual System

To better understand the behavior of the dual system, the contribution of its components in resisting the story shear force is depicted in Figure 9.24. Figure 9.25 shows the contribution percentage of the shear forces for the core wall and the frame over the building height. The frame contribution is approximately constant over the building height, while the core wall contribution varies linearly. In general, the core wall contributes more than 80% of the total story shear for the lower stories and 50% for the upper stories.

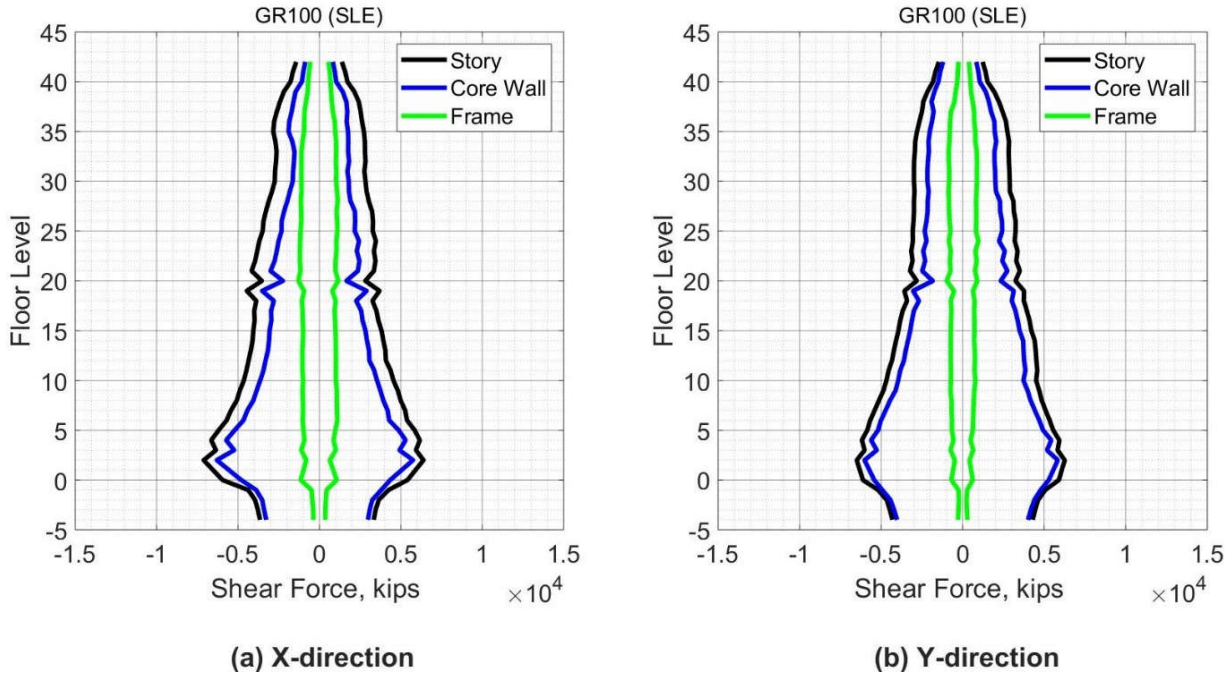

Figure 9.24 Shear Force Contribution of Core Wall & Frame (Case 3 – SLE).

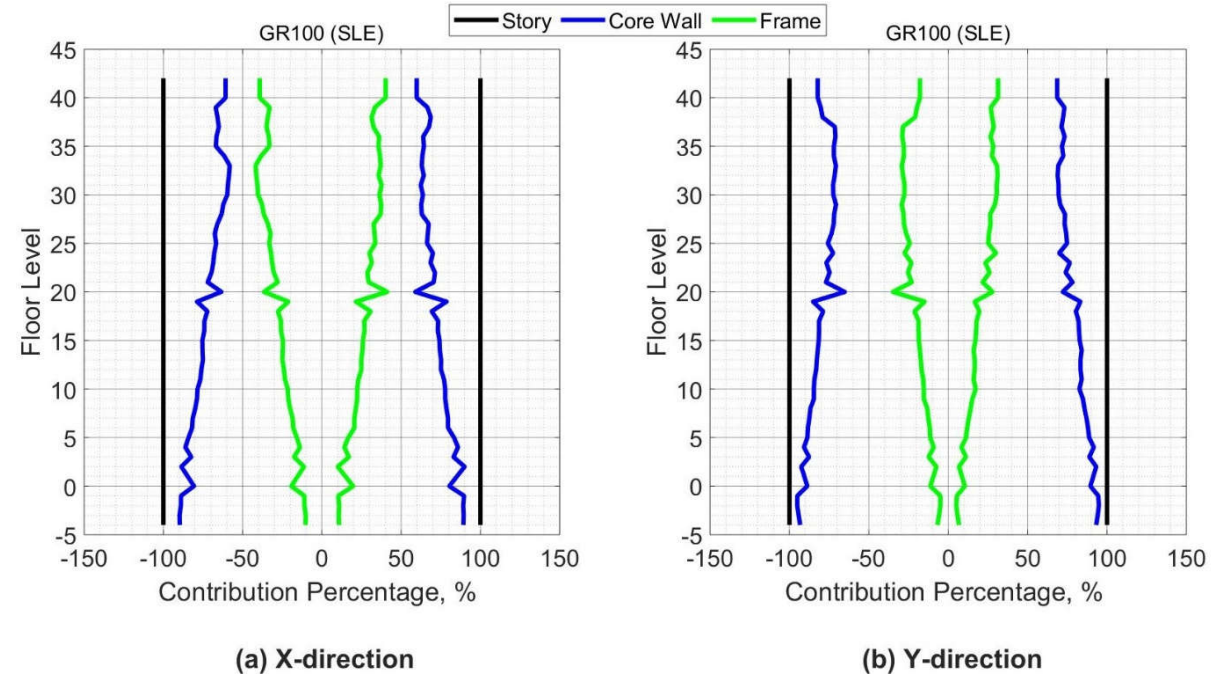

Figure 9.25 Contribution Percentage of Core wall & Frame Shear Force (Case 3 – SLE).

9.3 MCER LEVEL

The same ground motions used in the MCER in case 1 were used for the MCER analyses of case 3. As stated in Section 7.3, the results of eleven analyses are represented and compared with the acceptance criteria of the TBI guidelines. According to the TBI guidelines, first, the mean value of the response parameters from all ground motions in the suite should be checked with the acceptance criteria. Second, the maximum response parameters from all ground motions should be checked to ensure that no unacceptable response was produced by any ground motion from the suite. All the response parameters were calculated by the same procedures that were described in Section 7.2.

9.3.1 Global Response

9.3.1.1 Drift Ratio

Figure 9.26 shows the mean and the maximum values of the interstory drift ratios from all the ground motions analyses over the building height. The mean interstory drift from the eleven analyses was very close to 0.022 in the x-direction and approximately 0.013 in the y-direction, where both values were within the acceptable limit of TBI guidelines of 0.030. In addition, the maximum interstory drift was 0.030 and 0.020 for the x- and y-directions, respectively. The maximum values of drift ratios were also within the acceptable limit of TBI guidelines (0.045), which indicates that no unacceptable response was produced when considering the drift ratios. Figures 9.27 and 9.28 depict the maximum drift ratios form each considered ground motion over the building height.

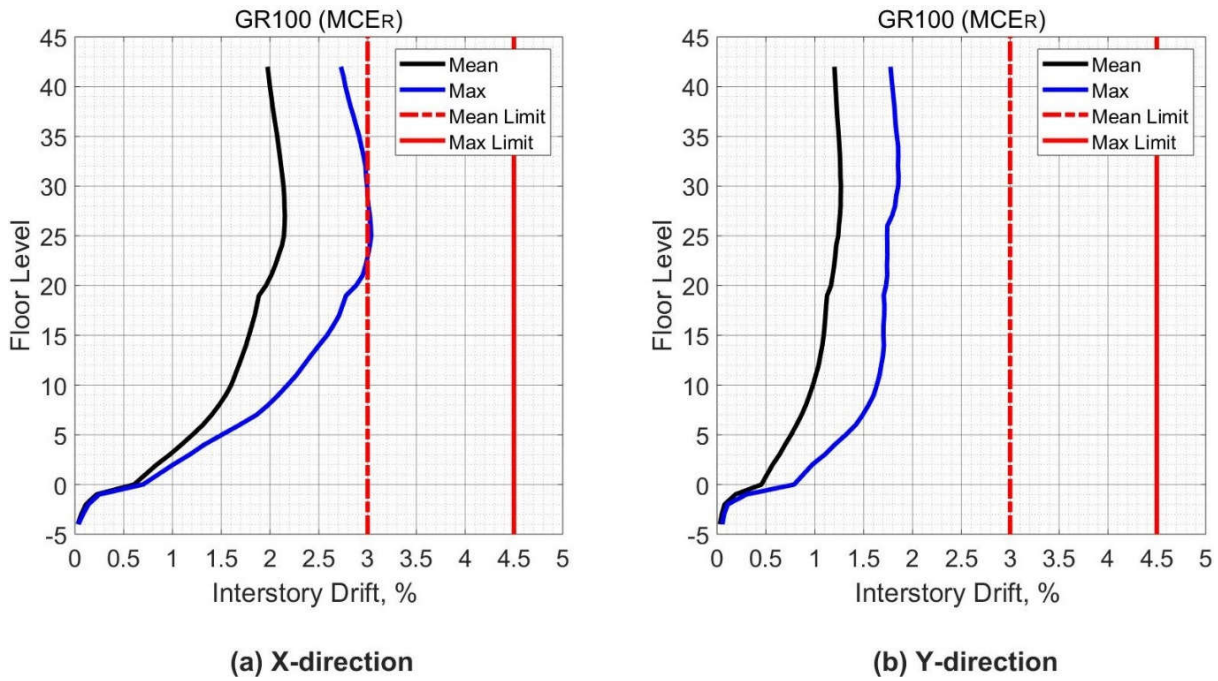

Figure 9.26 Peak Interstory Drift (Case 3 – MCER).

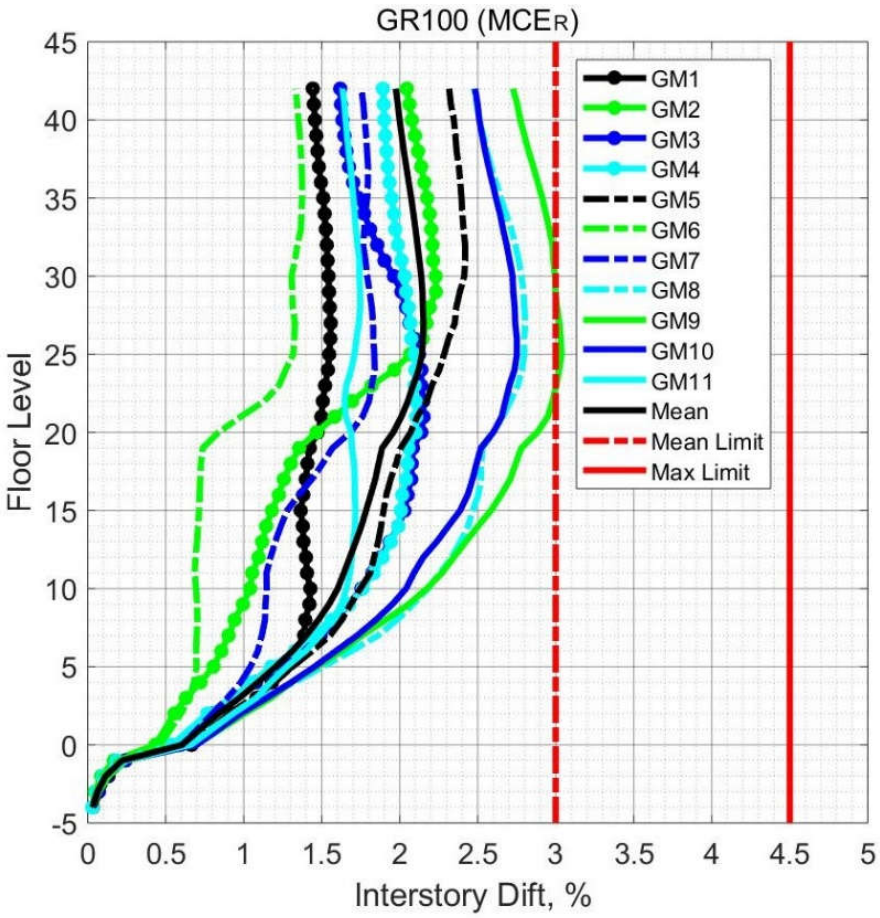

Figure 9.27 Peak Interstory Drift from All Ground Motions for X-direction (Case 3 - MCER).

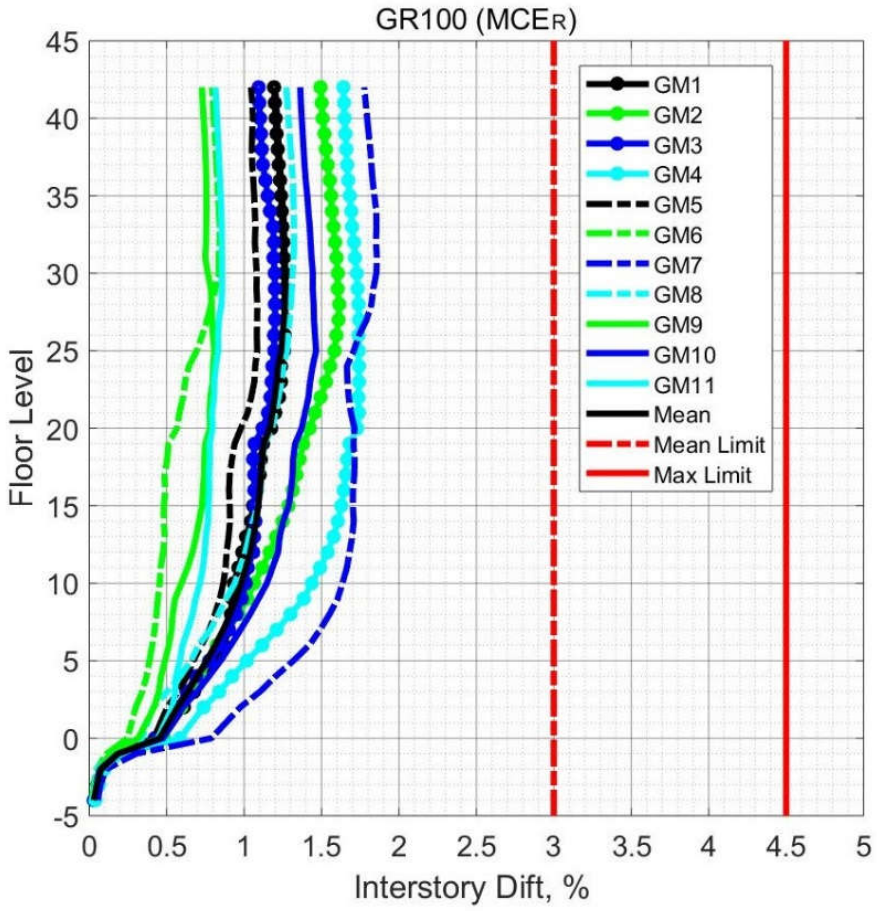

Figure 9.28 Peak Interstory Drift from All Ground Motions for X-direction (Case 3 - MCER).

9.3.1.2 Residual Drift Ratio

Figure 9.29 shows that the maximum of the mean values of the residual drift was 0.0070 in the x- direction and 0.0040 in the y-direction where both values are below the TBI limit (0.0100). In addition, the maximum residual drift ratio obtained from all analyses was 0.0115, which is below the limit of the TBI guidelines for residual drift ratios (0.0150). Consequently, no unacceptable response was produced from any ground motion when considering the values of the residual drift ratio.

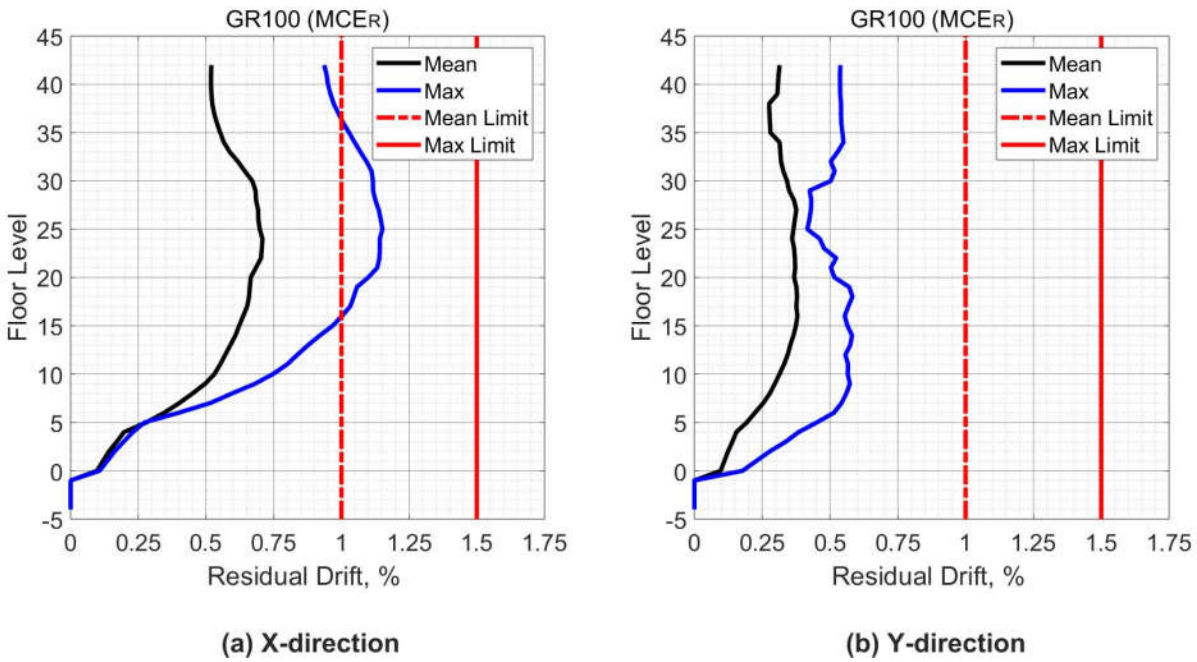

Figure 9.29 Peak Residual Drift (Case 3 – MCER).

9.3.1.3 Displacement

Figure 9.30 depicts the mean value of the displacement of each story at the same time step that the roof experiences a maximum displacement value. The mean displacement of the roof was 75 in and 50 in for x and y-direction, respectively.

Figures 9.31 and 9.32 show the time history of the roof displacement in the x-direction and y-direction, respectively from a ground motion at which the displacement demand of the roof was the highest one among other ground motions. During the ninth ground motion, the roof experience a maximum displacement in the x-direction while during the fourth ground motion the maximum roof displacement in the y-direction was observed.

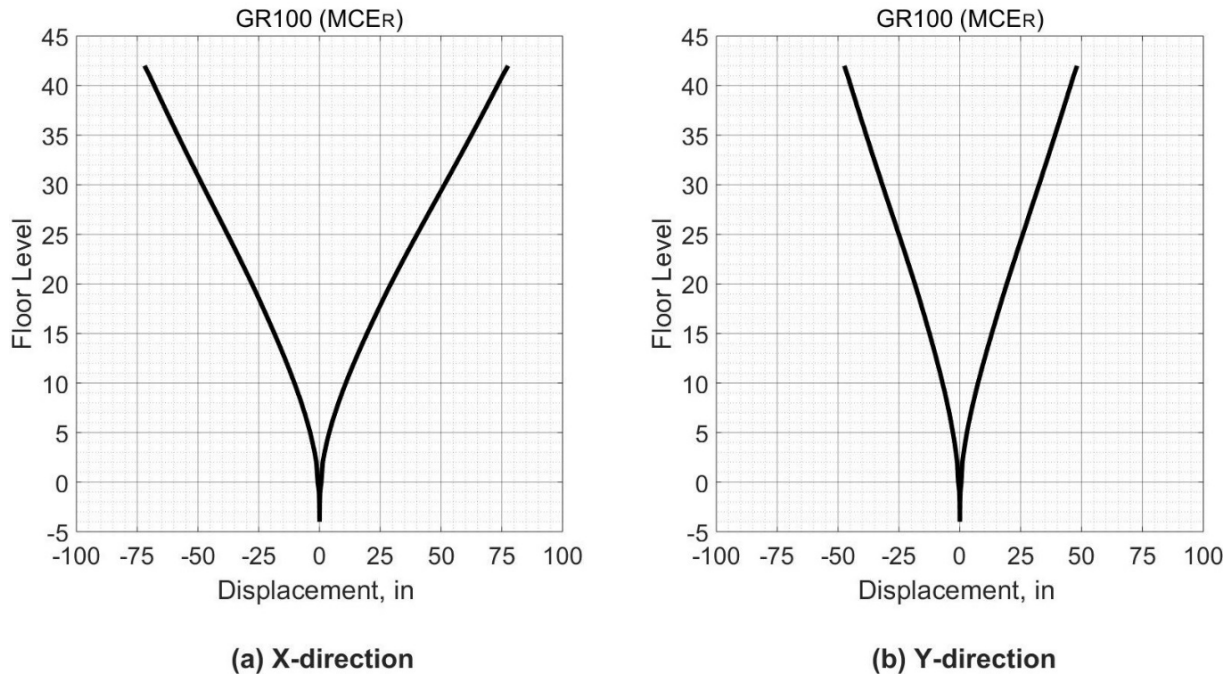

Figure 9.30 Floors Displacement Synchronous with Peak Roof Displacement (Case 3 - MCER).

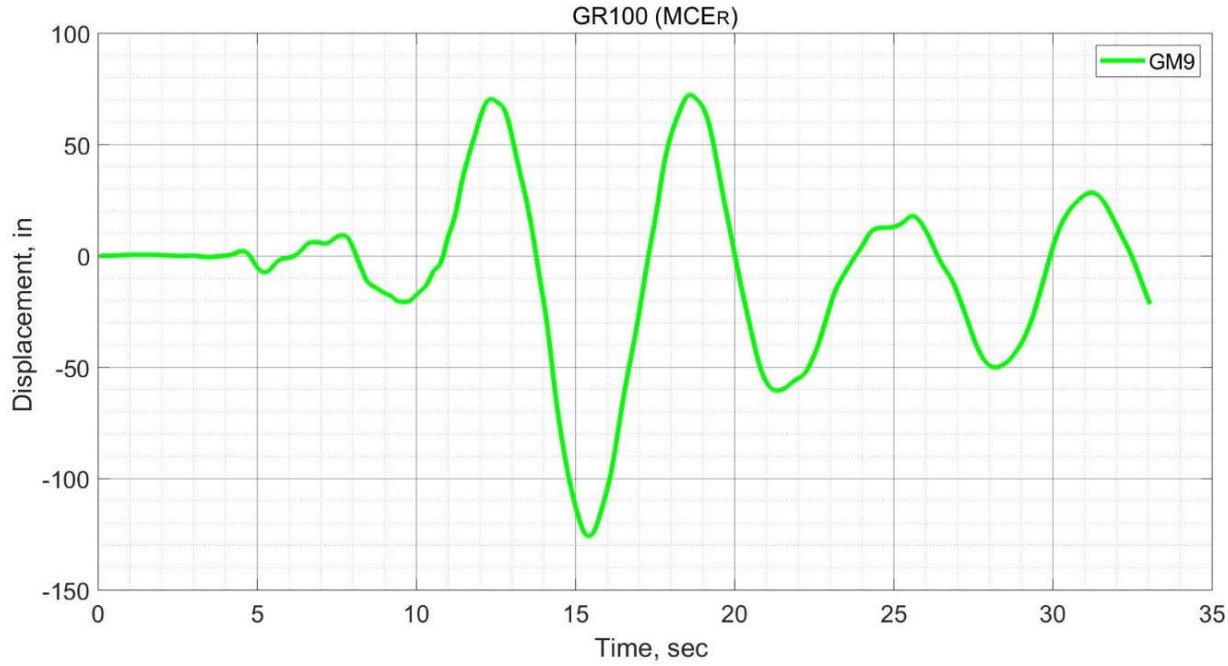

Figure 9.31 Time History for Peak Roof Displacement for X-direction (Case 3 – MCER).

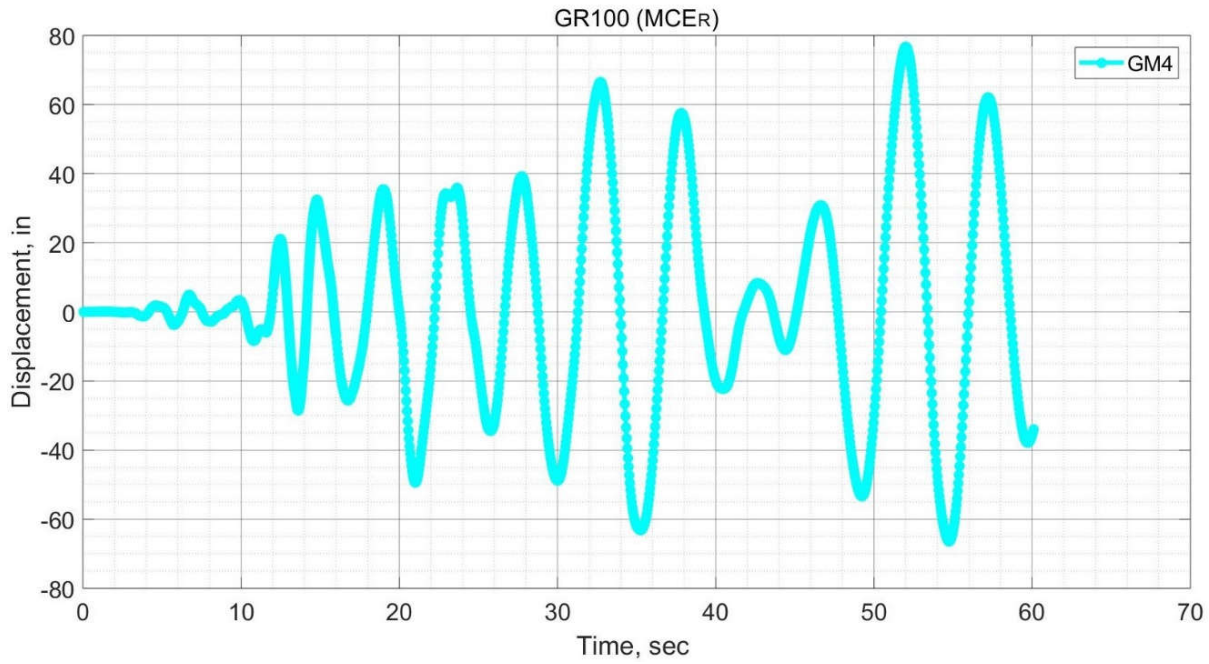

Figure 9.32 Time History for Peak Roof Displacement for Y-direction (Case 3 – MCER).

9.3.2 Element Level

As mentioned in Section 7.3.2, For the MCER shaking level, the TBI guidelines require using the mean value from all analyses for evaluation with the acceptance criteria for force-based actions, while using the maximum value from all analyses for deformation-based actions. In addition, for both actions the TBI guidelines require using the maximum value from all analyses to evaluate with the acceptance criteria to ensure that all calculated demands from any analysis are within the acceptable range of the model. In the subsections below, the elements of the seismic force resisting system with their actions are presented and evaluated using the acceptance criteria of the TBI guidelines.

9.3.2.1 Core Wall Response

9.3.2.1.1 Core Wall Force-Based Action

To evaluate the shear demands of core walls, the TBI guidelines required that the shear force demands satisfy Equation (7-8). Figure 9.33 shows the core wall shear forces over the building height and the limiting (*Vexp*) as in Equation (7-8). The shear demands in the core wall satisfy Equation (7-8) as required by the TBI guidelines. In addition, the shear force demands varied approximately in a linear manner with the height of the building. A change in the shear response of the core wall was noticed at the twentieth story due to the wall thickness changing from 24 in. to 18 in. A small increase in the shear force demands in the y-direction was noticed compared with demands in the x-direction. The maximum observed shear demand was 13506 kips for y-direction, while 11442 kips in x-direction. As shown in Figure 9.33, considering that the maximum demand of the shear force in the core wall was also within the acceptable limits, all analyses produced an acceptable response and all results are within the acceptable modeling range.

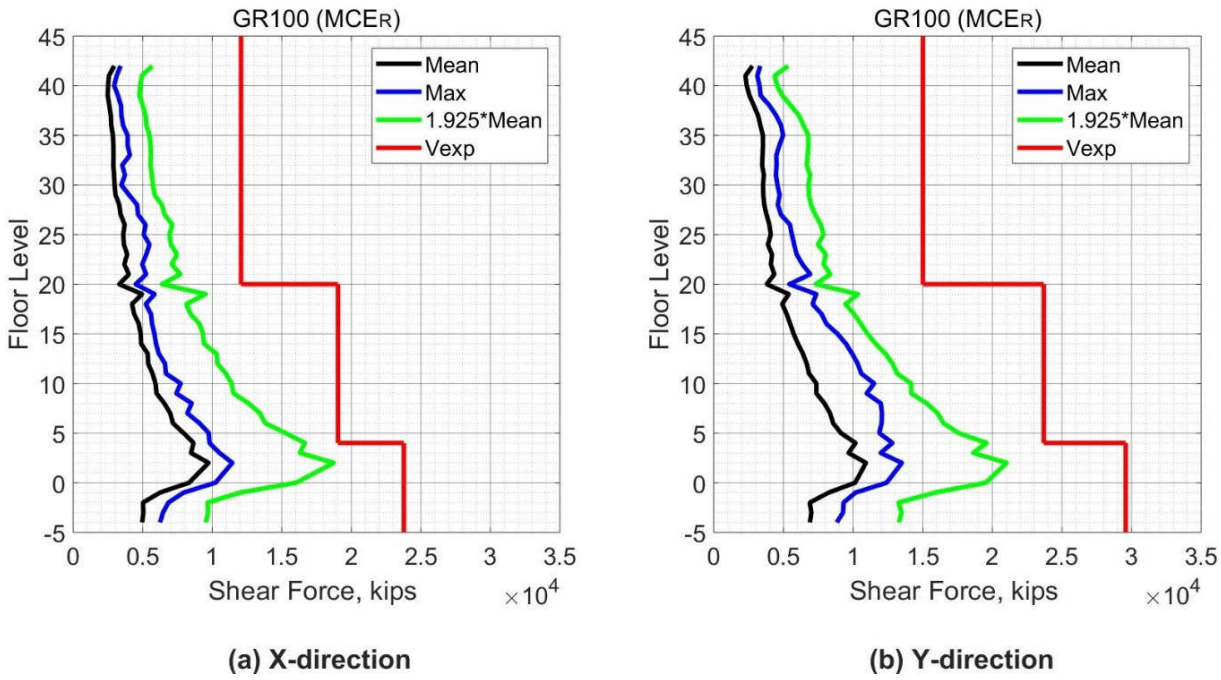

Figure 9.33 Shear Forces in Core Wall (Case 3 – MCER).

9.3.2.1.2 Core Wall Deformation-Based Action

As stated in Section 7.2.2.1.2, the tensile strain in the reinforcing steel and concrete compression strain were monitored during the analyses on all edges of the core wall. The strain was determined by using the vertical displacement (Δz) of the nodes of the core wall edges. Figures 9.34 to 9.37 show that the maximum tensile strain in the core wall reinforcement is 0.016, which is below the acceptable limit of 0.05. The maximum tensile strain demand in reinforcing bars of the core wall was 0.016 which is below the minimum fracture elongation (0.07) as specified by ASTM 1035 for Grades 100 and 120. The uniform elongation of Grades 100 is approximately 0.045 (NEHRP, 2014). Grade 100 could be a valuable option for reinforcing the special walls when considering that the maximum tensile strain demands are below the limit of 75% of the uniform elongation. The reinforcing bars experienced yielding for all stories from ground story to the tenth

story, and stories above the twentieth up to thirtieth story. The core wall below the ground level did not experience yielding because of the effect of the podium's levels.

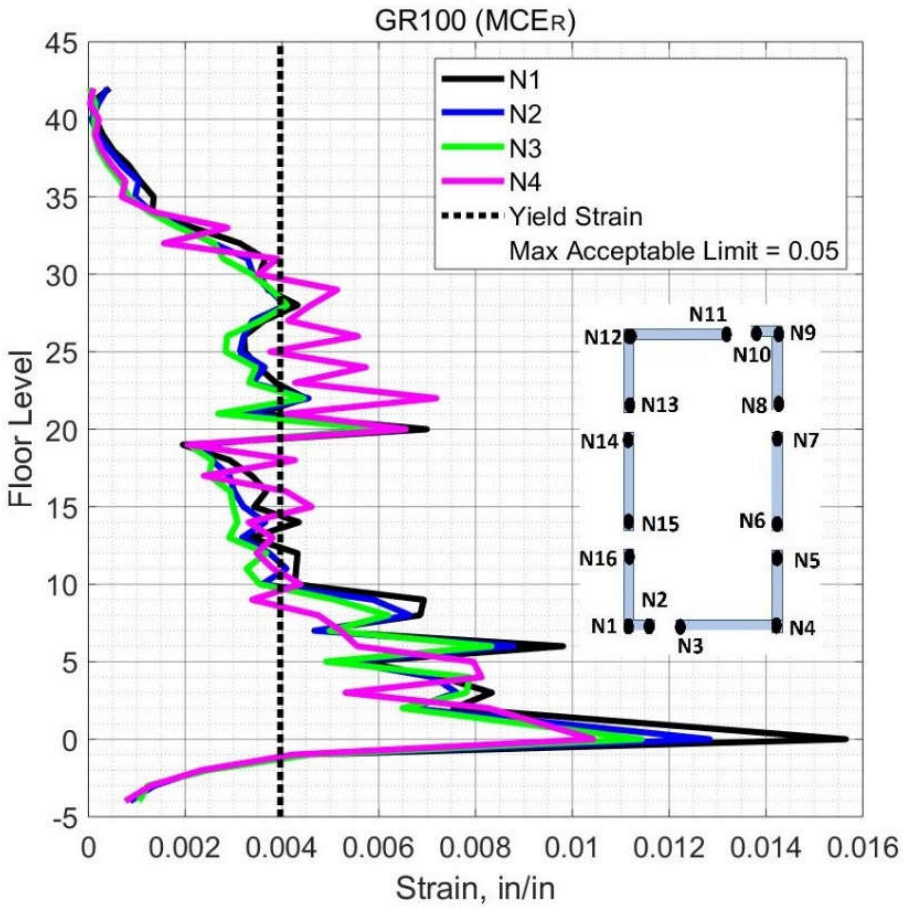

Figure 9.34 Peak Tensile Strain in Steel Bars in Core Wall Edges N1-N4 (Case 3 – MCER).

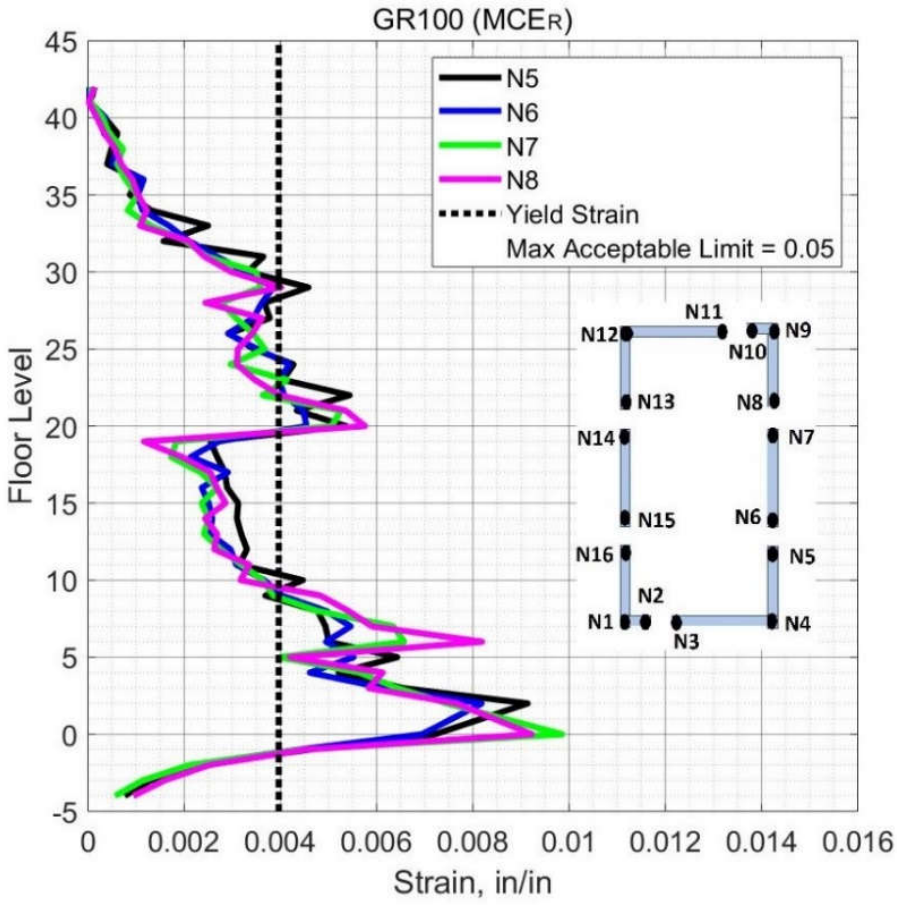

Figure 9.35 Peak Tensile Strain in Steel Bars in Core Wall Edges N5-N8 (Case 3 – MCER).

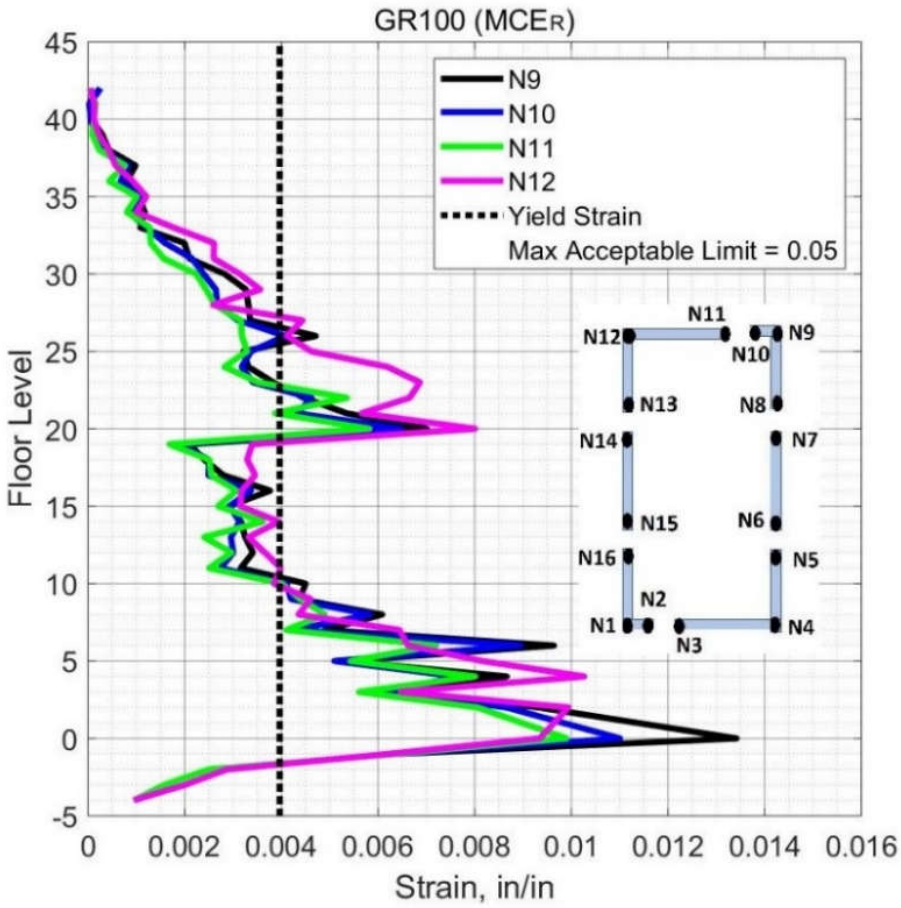

Figure 9.36 Peak Tensile Strain in Steel Bars in Core Wall Edges N9-N12 (Case 3 – MCER).

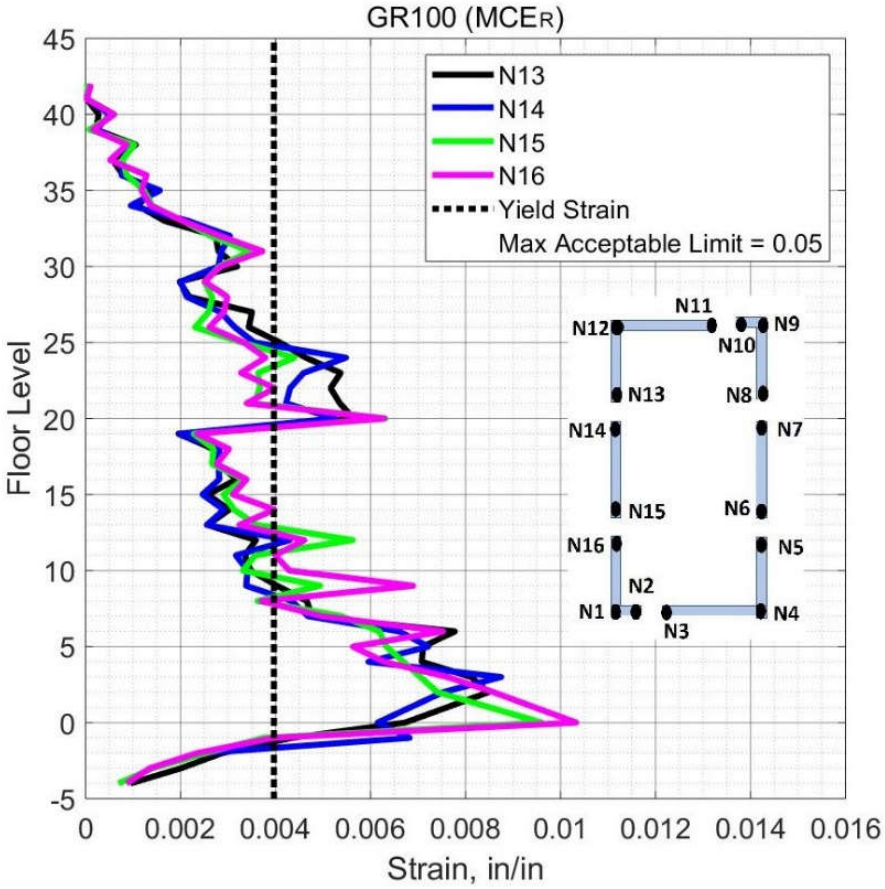

Figure 9.37 Peak Tensile Strain in Steel Bars in Core Wall Edges N13-N16 (Case 3 – MCER).

Figures 9.38 to 9.41 show the maximum values of the compression strain in the core wall concrete at the wall edges over the building height. The core wall concrete experiences low values of concrete compression strain, below 0.002, for all stories.

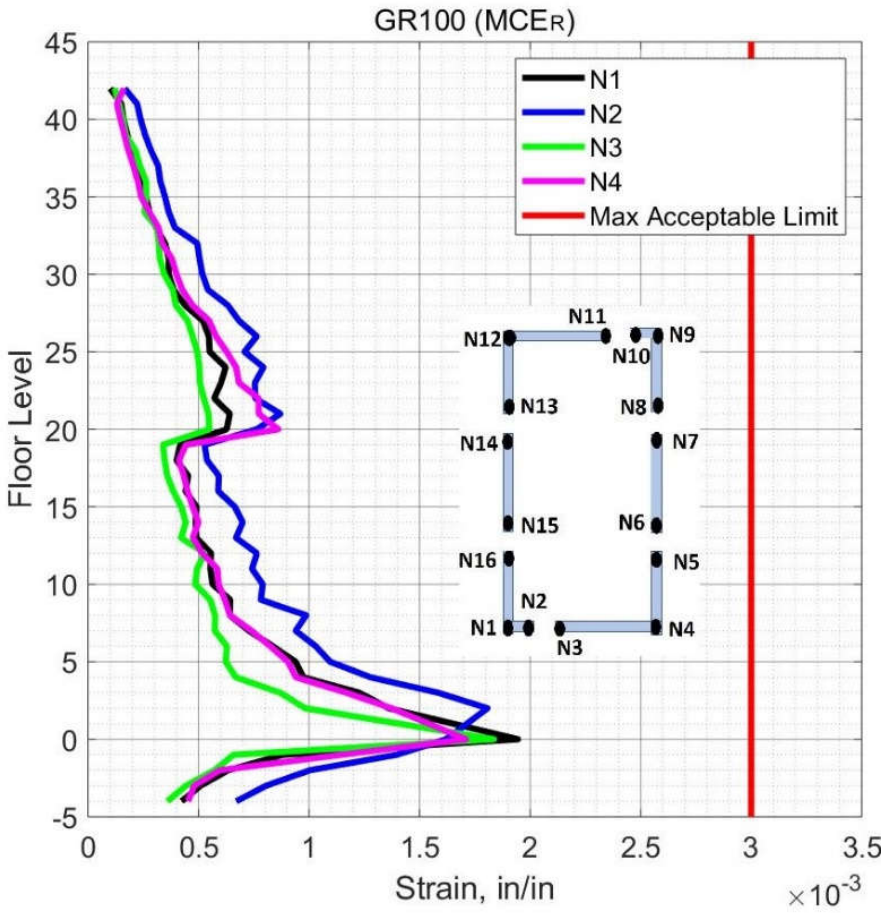

Figure 9.38 Peak Concrete Compression Strain in Core Wall Edges N1-N4 (Case 3 – MCER).

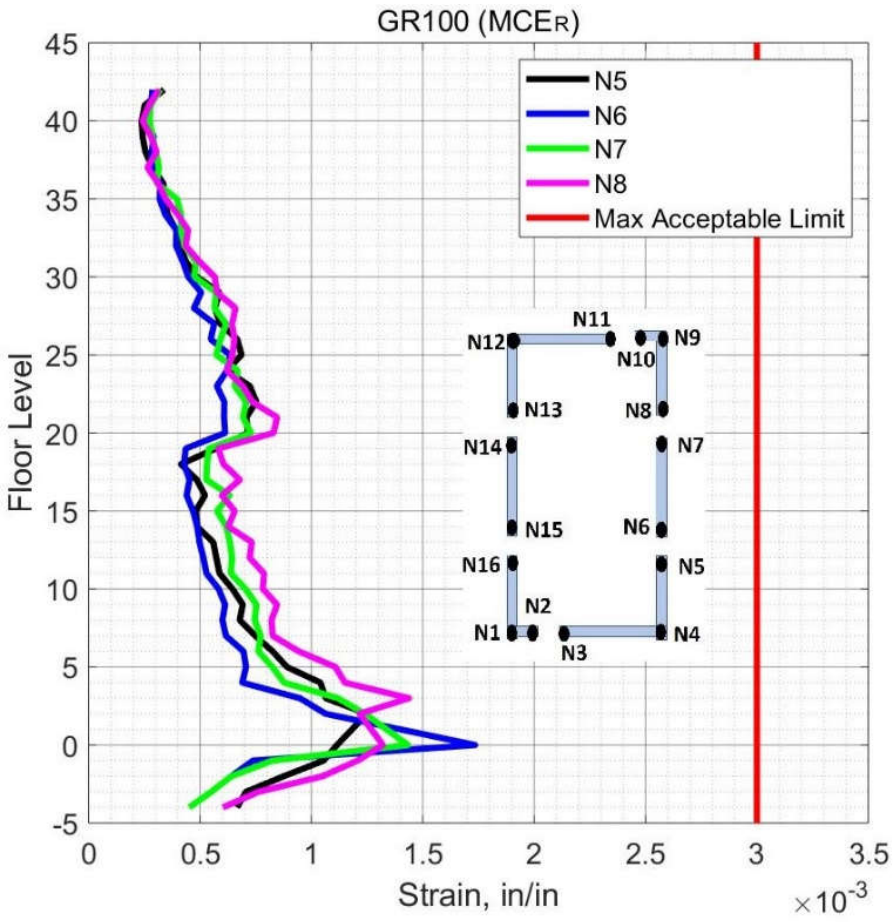

Figure 9.39 Peak Concrete Compression Strain in Core Wall Edges N5-N8 (Case 3 – MCER).

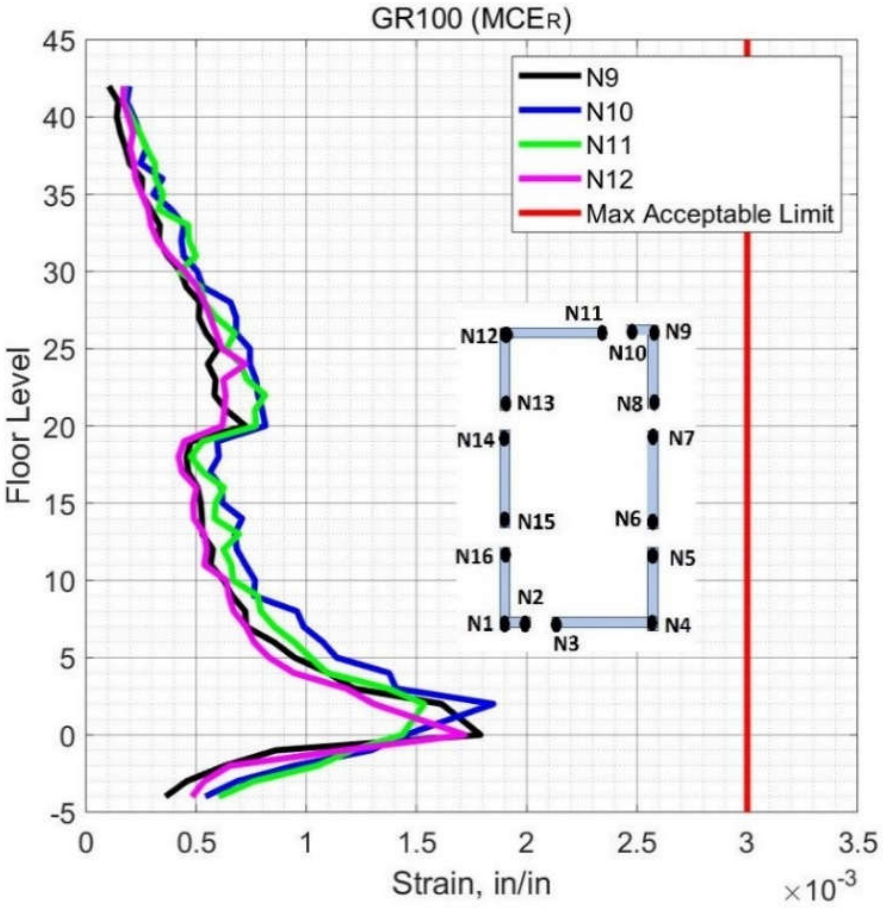

Figure 9.40 Peak Concrete Compression Strain in Core Wall Edges N9-N12 (Case 3 – MCER).

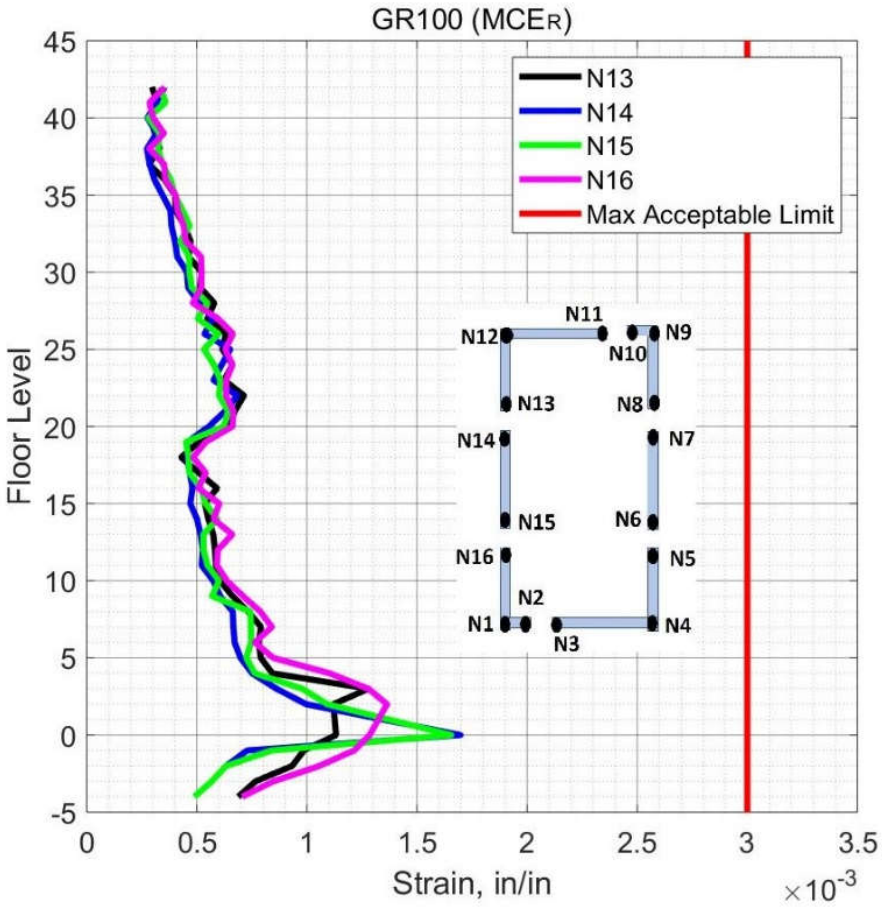

Figure 9.41 Peak Concrete Compression Strain in Core Wall Edges N13-N16 (Case 3 – MCER).

9.3.2.1.3 Coupling Beams

Figure 9.42 (a) shows the mean and maximum values of the rotation of coupling beams with a 1.7 aspect ratio (coupling beams in the x-direction), over the building height. The peak value of the rotation is 0.027 which is below the allowable limit of 0.050 of ASCE 41. The results indicate that coupling beams do experience yielding of steel reinforcement according to the data in Figure 7.18. In addition, the coupling beams expected to have a damage state (DSI), which means that the coupling beams need minor repair. However, the rotation demands of coupling

beams satisfy the requirement of the TBI guidelines for MCER level.

Figure 9.42 (b) shows the mean and maximum values of the rotation of coupling beams with a 2.1 aspect ratio (coupling beams in the y-direction), over the building height. The peak value of the rotation is 0.030 which is below the allowable limit of 0.050. The results indicate that coupling beams do experience yielding of steel reinforcement according to the data in Figure 7.19. In addition, the coupling beams expected to have a damage state (DSI), which means that the coupling beams need minor repair. However, the rotation demands of coupling beams satisfy the requirement of the TBI guidelines for MCER level.

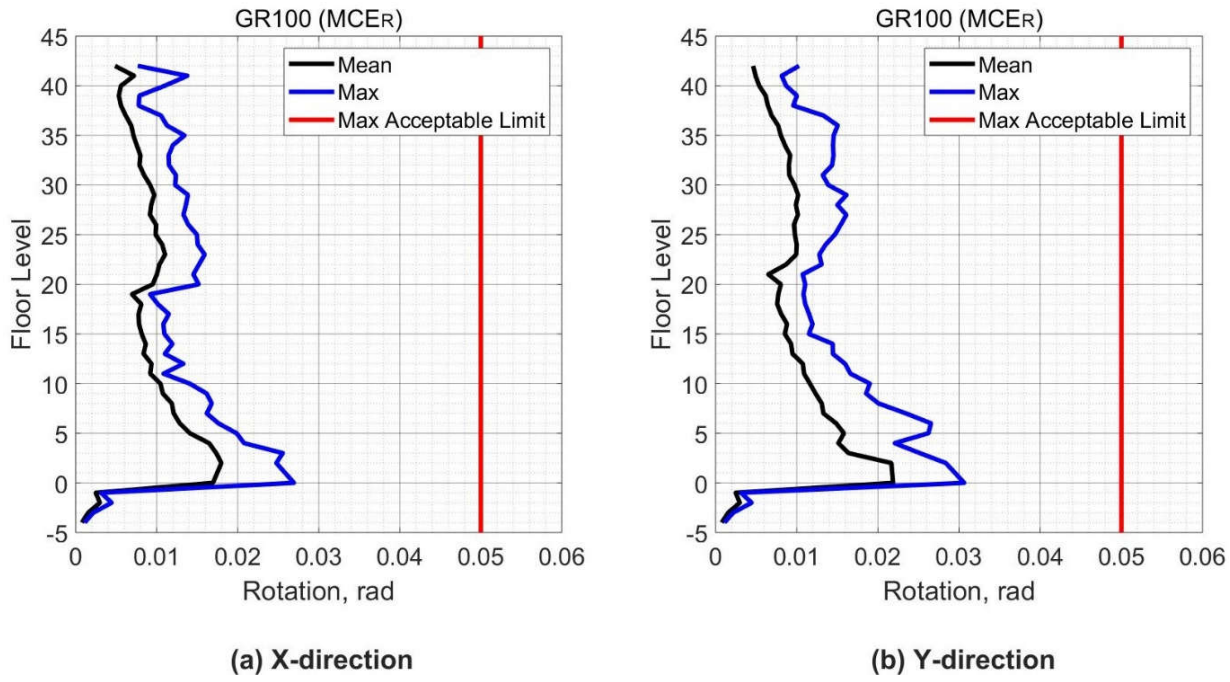

Figure 9.42 Rotation Demand in Coupling Beams (Case 3 – MCER).

9.3.2.2 Special Moment Frame Response

9.3.2.2.1 Beam Force-Based Action

As stated in Section 7.3.2.2.1, To evaluate the shear action in the beams, Equation (7-11) will be applied. Figure 9.43 shows the shear force demands in the beams of the special moment frame over the building height. In the legend of Figure 9.43, the results noted as “Mean” represent the mean value of the maximum shear force in the beams at each floor level from all ground motions analyses, while the results noted as “Max” represent the maximum shear force in the beams obtained from all analyses. In addition, the values shown as “Vfinal” and “Vexp” in the legend were obtained by using Equations (7-10) and (7-5), respectively. As shown in Figure 9.43, the main conclusion is that shear force demands in special moment frame beams meet the requirements of the TBI guidelines by satisfying Equation (7-11). In addition, the maximum shear force demands (365 kips) obtained from all ground motions are within the acceptable limits of the expected shear capacity (667 kips) of the beams. In other words, the maximum shear force demands obtained from all ground motions are within the acceptable limits of the expected shear capacity of the beams. Consequently, all analyses produced an acceptable response based on the shear force demands in the beams.

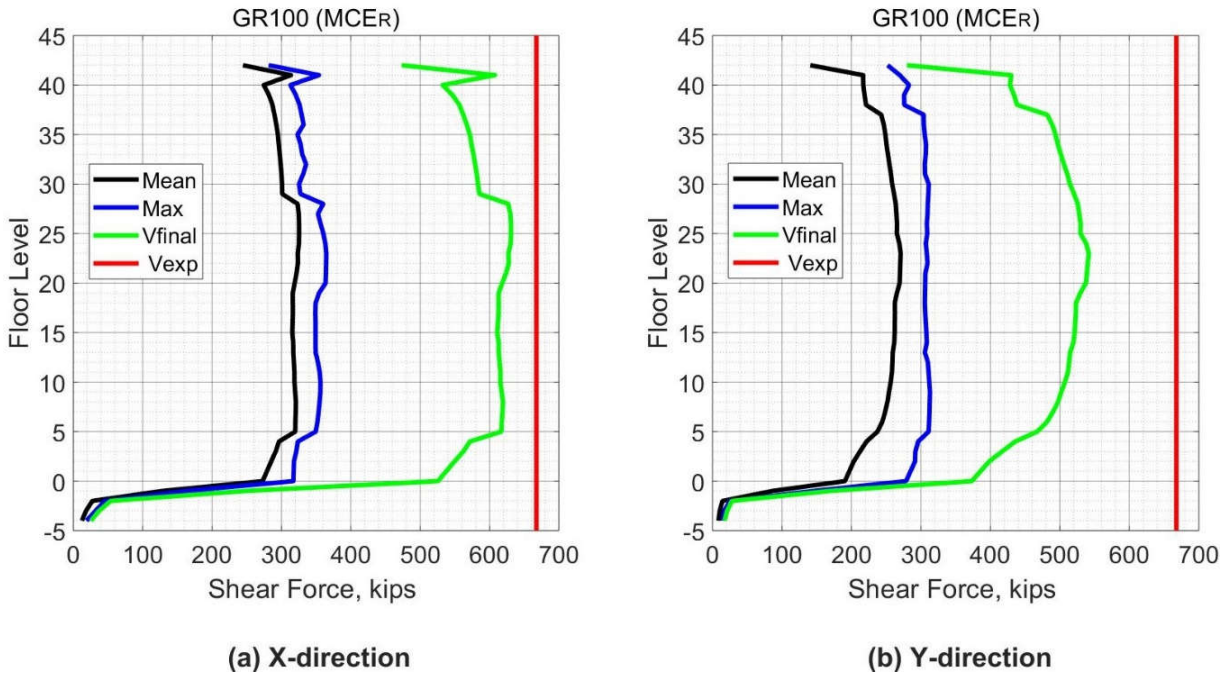

Figure 9.43 Peak Shear Force in Beams (Case 3 – MCER).

9.3.2.2.2 Beam Deformation-Based Action

Figure 9.44 shows the mean and the maximum tensile strain demands in the longitudinal reinforcement of the beams at each floor level. The maximum tensile strain demands (0.033) are within the acceptable limit (0.050). In addition, reinforcing bars in beams oriented in the x-direction experienced more tensile strain (0.033) compared to beams oriented in the y-direction (0.015). The maximum tensile strain demands in the beams are below the minimum fracture elongation 0.07 of ASTM 1035 for Grades 100 and 120. The uniform elongation of Grades 100 and 120 is approximately 0.045 (NEHRP, 2014). The maximum tensile strain demands are below the limit of 75% of the uniform elongation. Considering the results of the tensile strain of the reinforcing bars in the beams, Grade 100 could be a valuable reinforcing material for beams of the special moment frame. The expected yield strain for Grade 100 is 0.004, so all beams in the levels

above the main podium experienced yielding of reinforcing bars when considering the maximum demands for both directions.

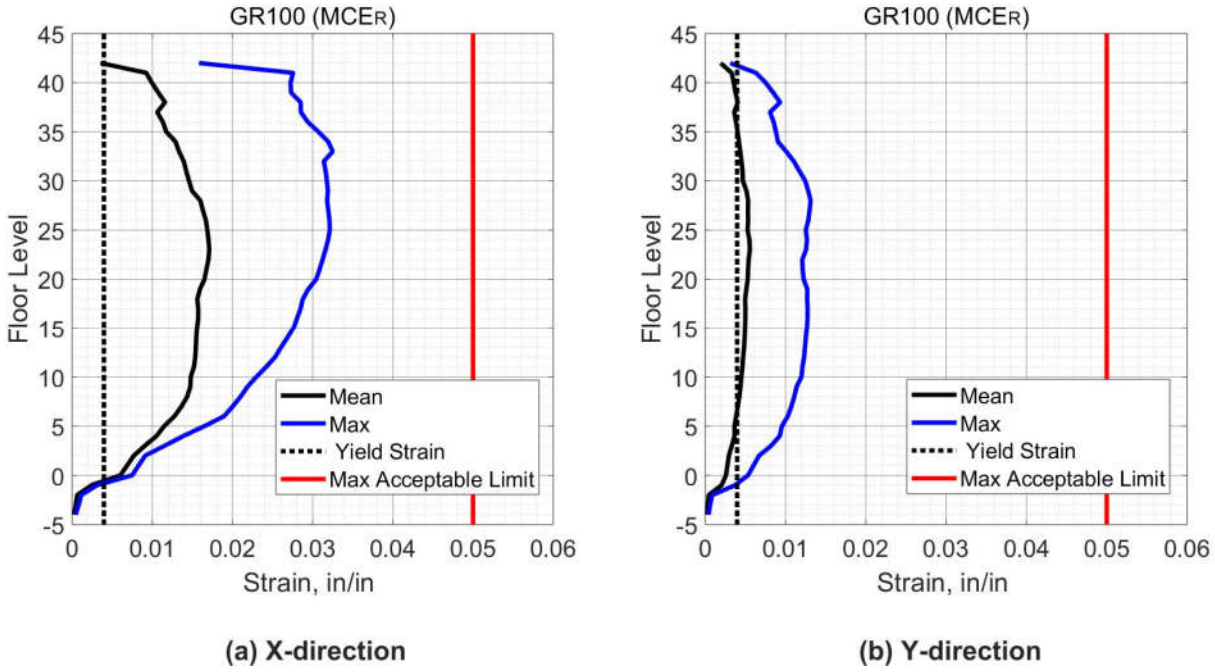

Figure 9.44 Peak Tensile Strain in Reinforcing bars in Beams (Case 3 – MCER).

Figure 9.45 shows the mean and the maximum plastic rotation demands in the beams at each floor level. The plastic rotation demand was approximately 0.03 rad which is below the acceptable limits of 0.045 of ASCE 4. A consistent finding with the tensile strain demands is observed in which beams oriented in the x-direction experienced more rotation demands compared with beams in the y-direction. Based on the strain and plastic rotation results, the deformation-based actions in the beams satisfy the requirement of TBI guidelines.

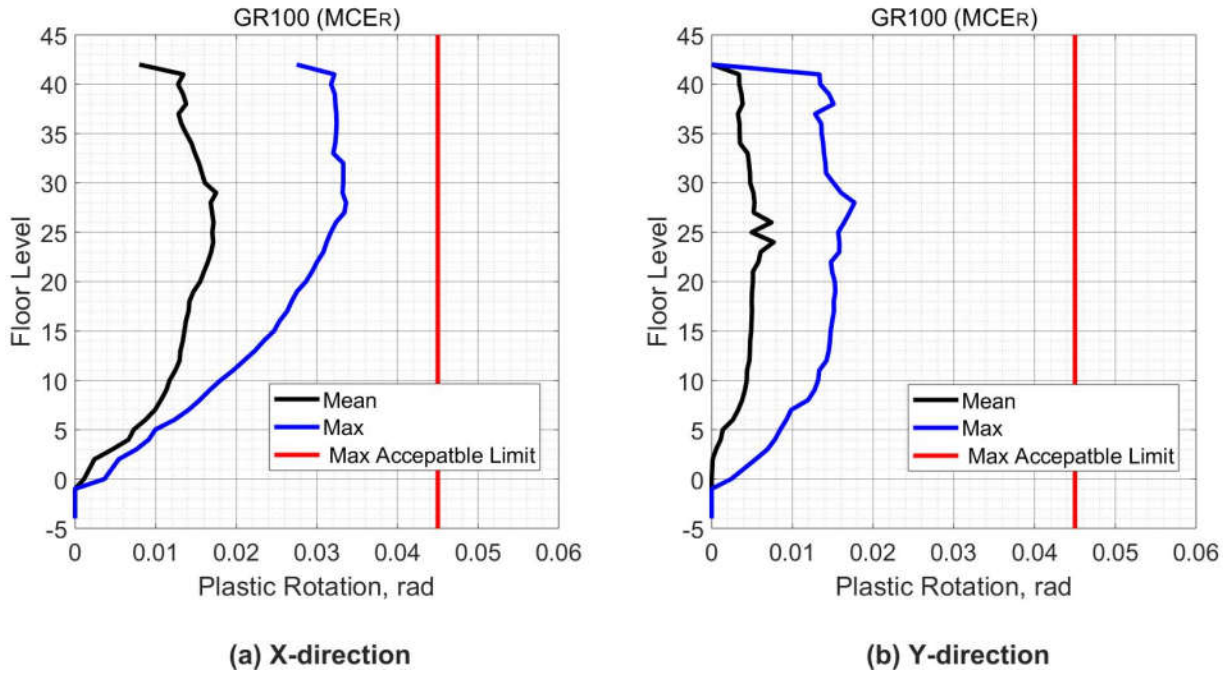

Figure 9.45 Plastic Rotation in Beams (Case 3 - MCER).

9.3.2.2.3 Columns Force-Based Action

In the legend of Figures 9.46 through 9.49, the results noted as "Mean" represent the mean value of the shear force in the columns from all ground motions analyses while the results noted as "Max" represent the maximum shear force obtained from all analyses. In addition, results with "Vfinal" and "Vexp" in the legend represent the parameters in Equation (7-11) for the columns. The shear force demands in the columns are within the limits of the TBI guidelines, by satisfying equation (7-11). The maximum shear demands obtained from all analyses are also within the acceptable limits. Therefore, all analyses produced acceptable responses when considering the shear force demands of the columns. In contrast with the shear force demands of the core wall, the shear forces were more uniform with building height.

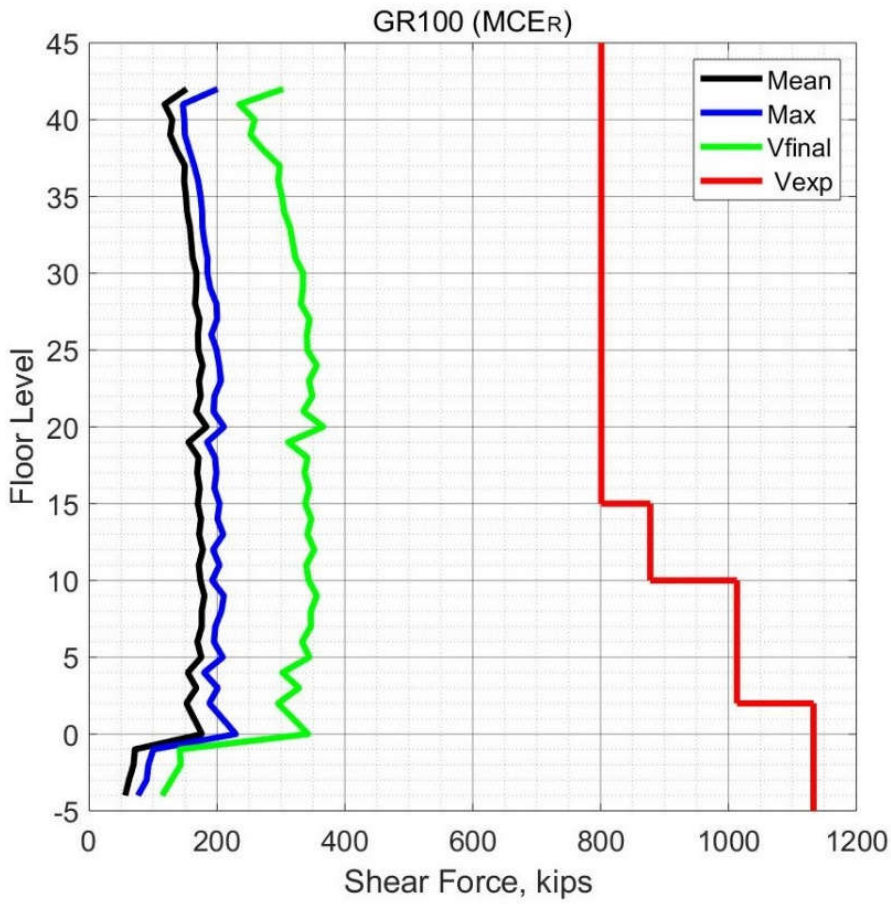

Figure 9.46 Peak Shear Force in Corner Columns (Case 3 – MCER).

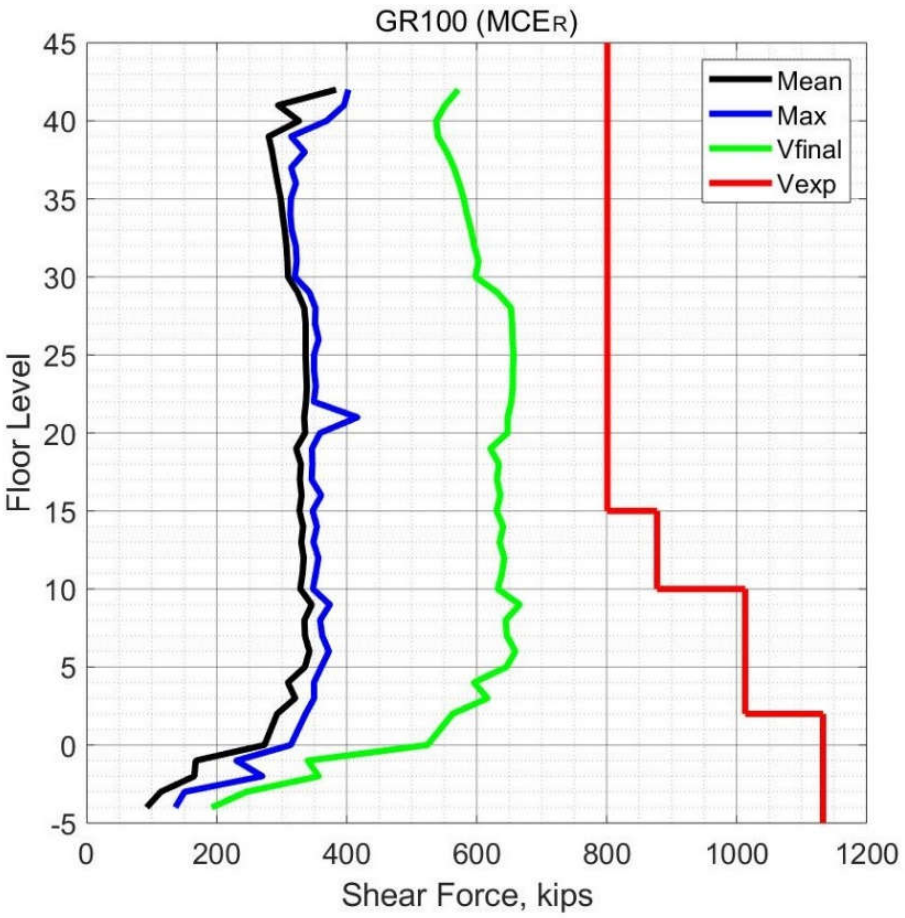

Figure 9.47 Peak Shear Force in Interior Columns X-direction (Case 3 – MCER).

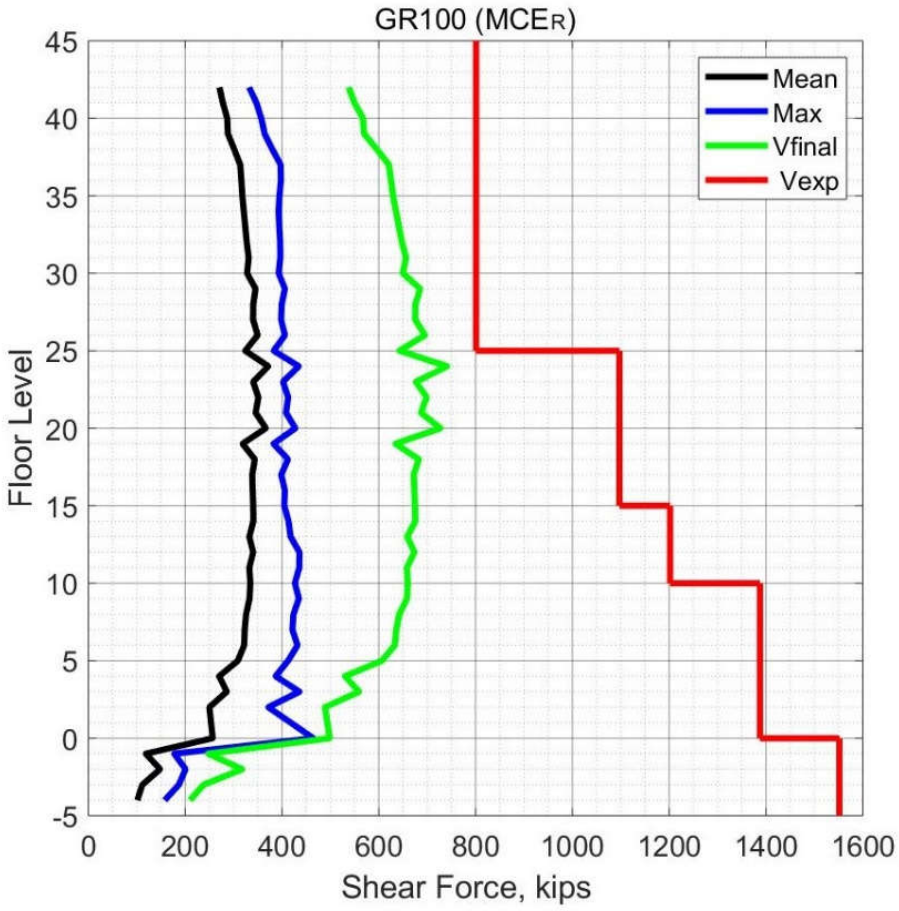

Figure 9.48 Peak Shear Force in Columns on Grid B and E (Case 3 – SLE).

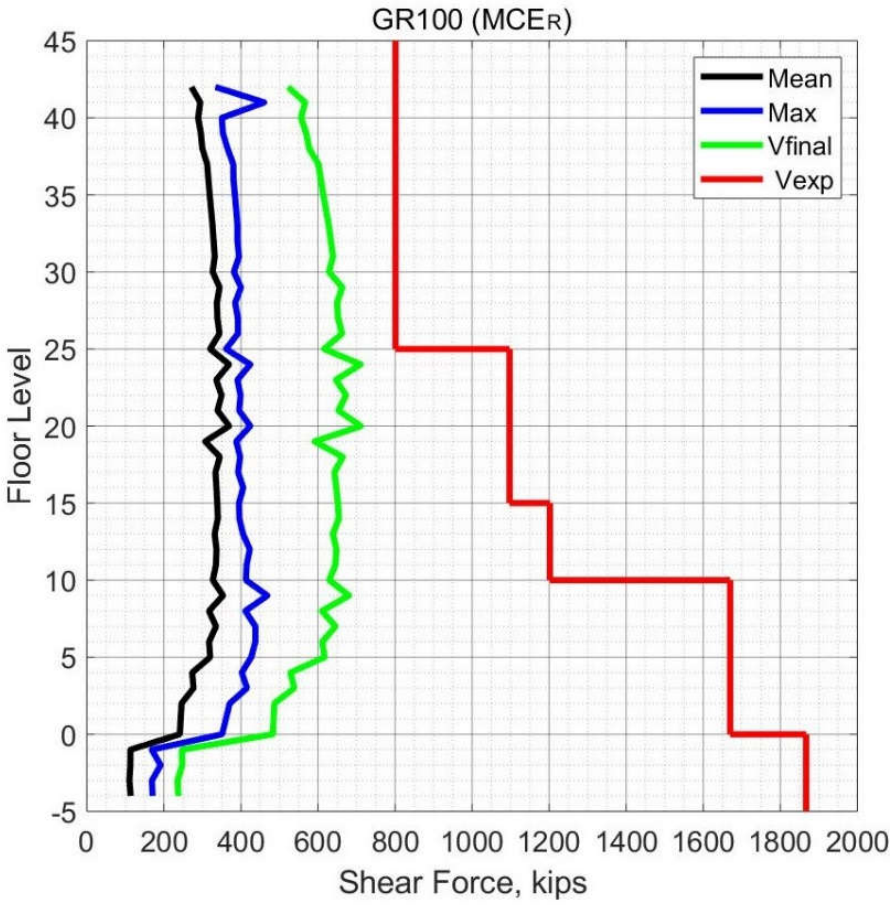

Figure 9.49 Peak Shear Force in Columns on Grid C.5 (Case 3 – MCER).

9.3.2.2.4 Column Deformation-Based Action

The maximum value of the tensile strain in the columns' longitudinal bars and the mean value from all ground motion in the suite are depicted in Figure 9.50. The maximum tensile strain demands (0.0035) did not exceed the yield strain (0.0040) which means no plastic hinges formed in the columns. In other words, columns did not experience plastic rotations. As mention previously, the behavior of non-yielding columns is one of the preferable design approaches for seismic applications where most plastic rotation demands form in the beams.

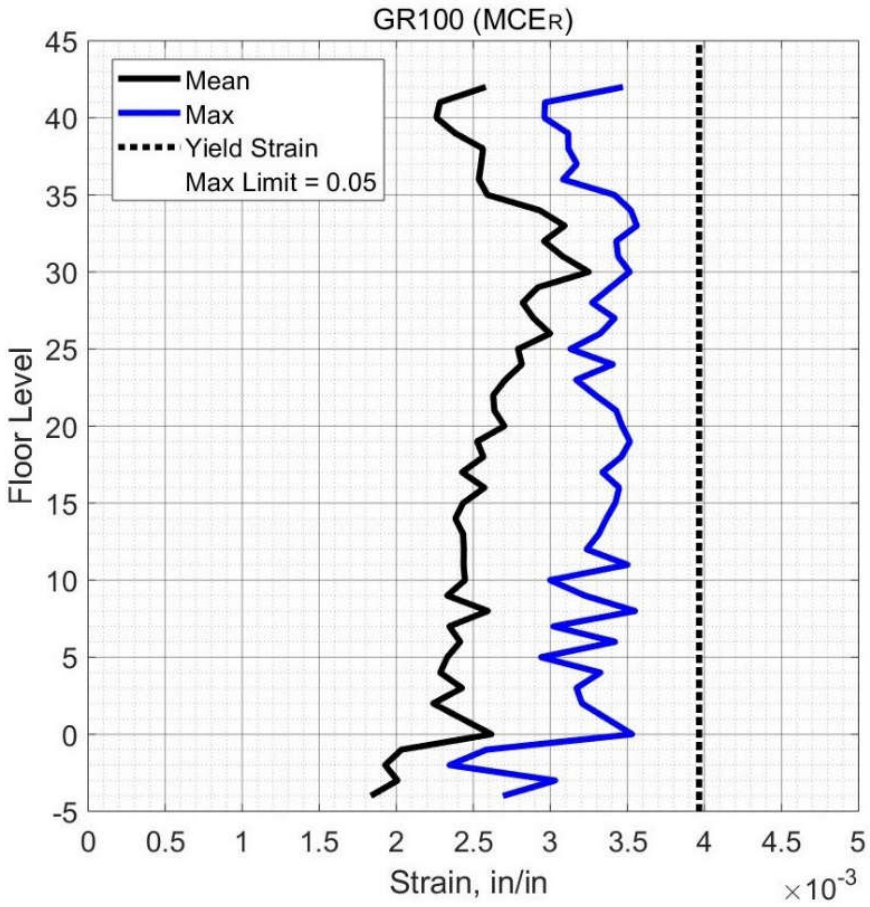

Figure 9.50 Peak Tensile Strain in Reinforcing Bars in Columns (Case 3 – MCER).

9.3.2.3 Contribution of Core Wall and Frame in Dual System

The contribution of the components of the dual system in resisting the story shear force is depicted in Figure 9.51 for the x- and y-directions, respectively. Figure 9.52 shows the contribution percentage of the shear forces for the core wall and the frame over the building height. The frame contribution is approximately constant over the building height, while the core wall contribution varies linearly. The frame contribution in the lower stories is approximately 20% of the story shear, while in the upper stories the frame contribution is about one-half of the total story shear.

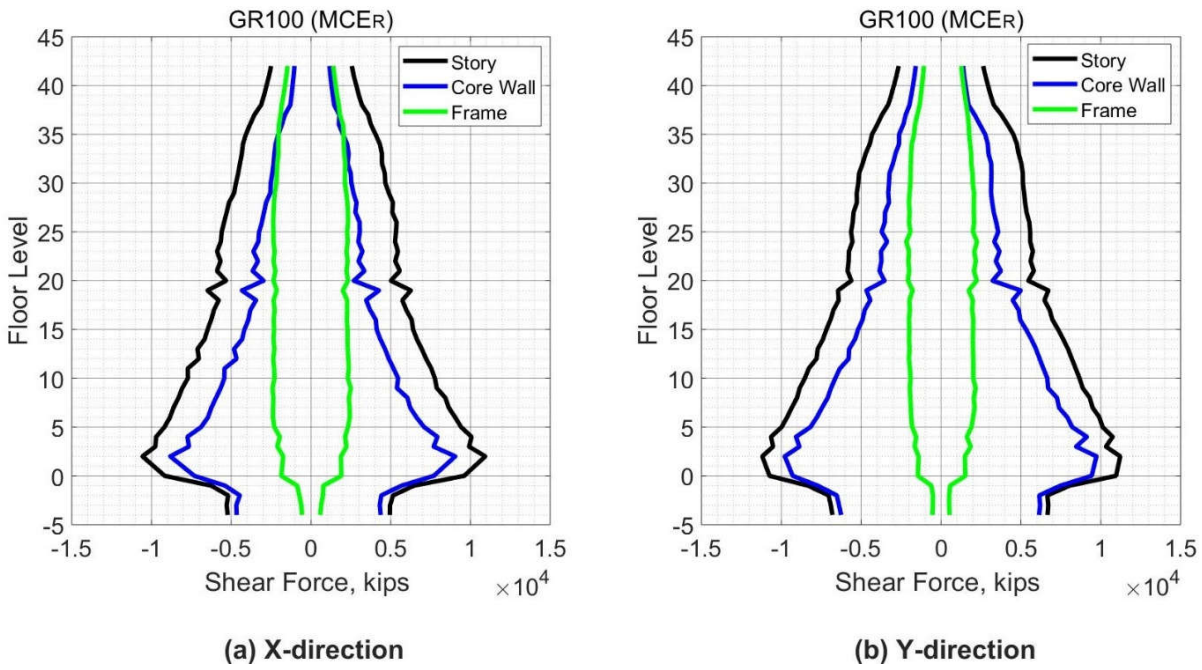

Figure 9.51 Shear Force Contribution of Core Wall & Frame (Case 3 – MCER).

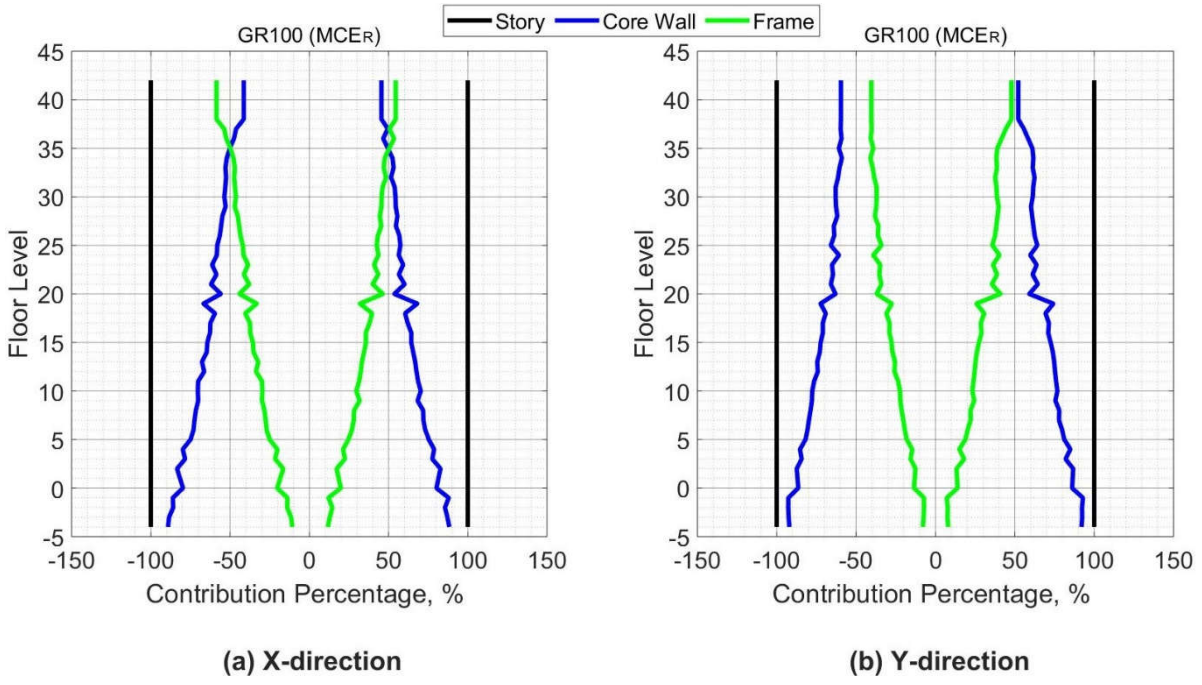

Figure 9.52 Contribution Percentage of Core wall & Frame Shear Force (Case 3 – MCER).

CHAPTER X

CASE 4 – GRADE 120 REINFORCEMENT RESULTS

10.1 INTRODUCTION

Case 4 consists of the study building reinforced with high strength reinforcing steel bars in all structural members. ASTM A1305 Grade 120 reinforcement was used in the seismic force resisting system (SFRS) in both the core wall and the special moment frames. In this case, the cross-section dimensions of all the structural members were the same as in the case 1, however the area of reinforcement in all members was 0.5 times the area of reinforcement in the case reinforced with the conventional steel bars (case 1). The minimum reinforcing ratio for columns of the special moment frame was 0.01 times the column cross section, while for concrete core wall the minimum ratio was 0.0025, as recommended by ((NEHRP, 2014). In the following sections, the response of the case study building reinforced with reduced amount of reinforcement (Grade 120) will be examined and checked with the TBI guidelines acceptance criteria for both SLE and MCER levels. The procedures and equations that used to calculate the structural demand parameters in the previous Chapter (case 1), will be applied for determining the response demands for this case for both SLE and MCER levels.

10.2 SLE LEVEL

The same ground motions used in the SLE in case 1 were used for the SLE analyses of case 4. The results of seven analyses are represented and compared with the acceptance criteria of the TBI guidelines. According to the TBI guidelines, first, the mean value of the response parameters from all ground motions in the suite should be checked with the acceptance criteria. Second, the TBI guidelines do not require checking the maximum response parameters from all ground

motions in this level. However, the maximum response parameters will also be presented to examine the performance of the case study building in more depth.

10.2.1 Global Response

10.2.1.1 Drift Ratio

Figure 10.1 shows the mean and the maximum values of the drift ratios from all analyses over the building height. The mean peak interstory drift from the seven analyses was very close to 0.0047 in the x-direction and approximately 0.0030 in the y-direction, where both values were within the acceptable limit of the TBI guidelines of 0.0050. Figures 10.2 and 10.3 show the peak drift ratios from all ground motions over the building height.

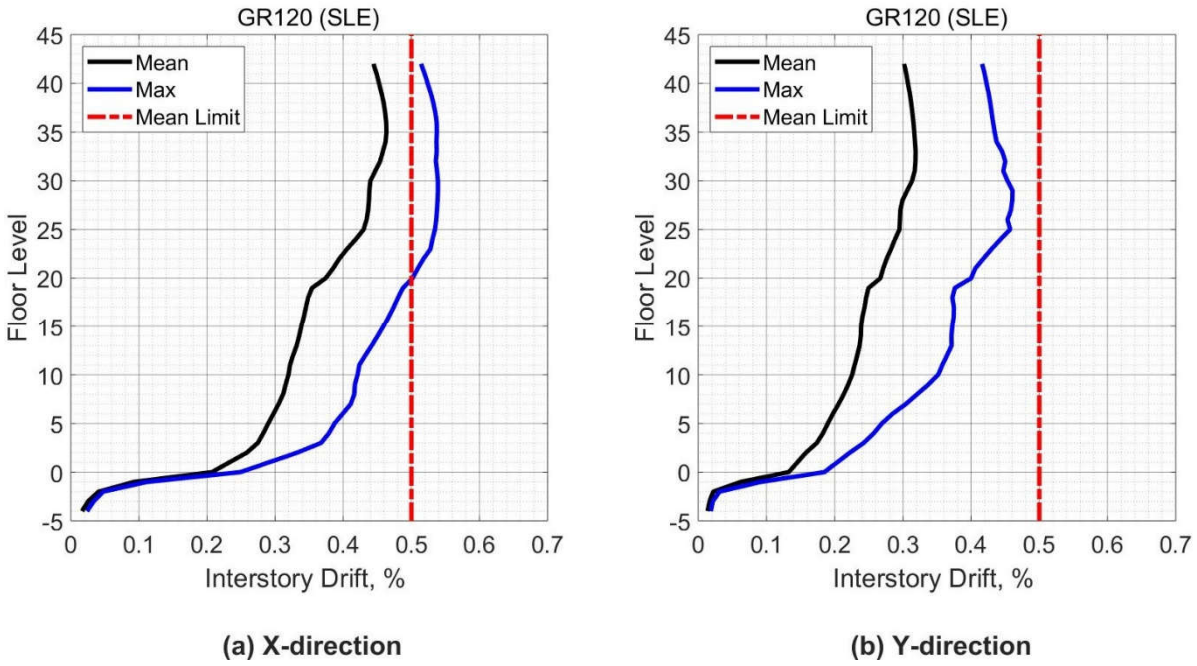

Figure 10.1 Peak Interstory Drift (Case 4 – SLE).

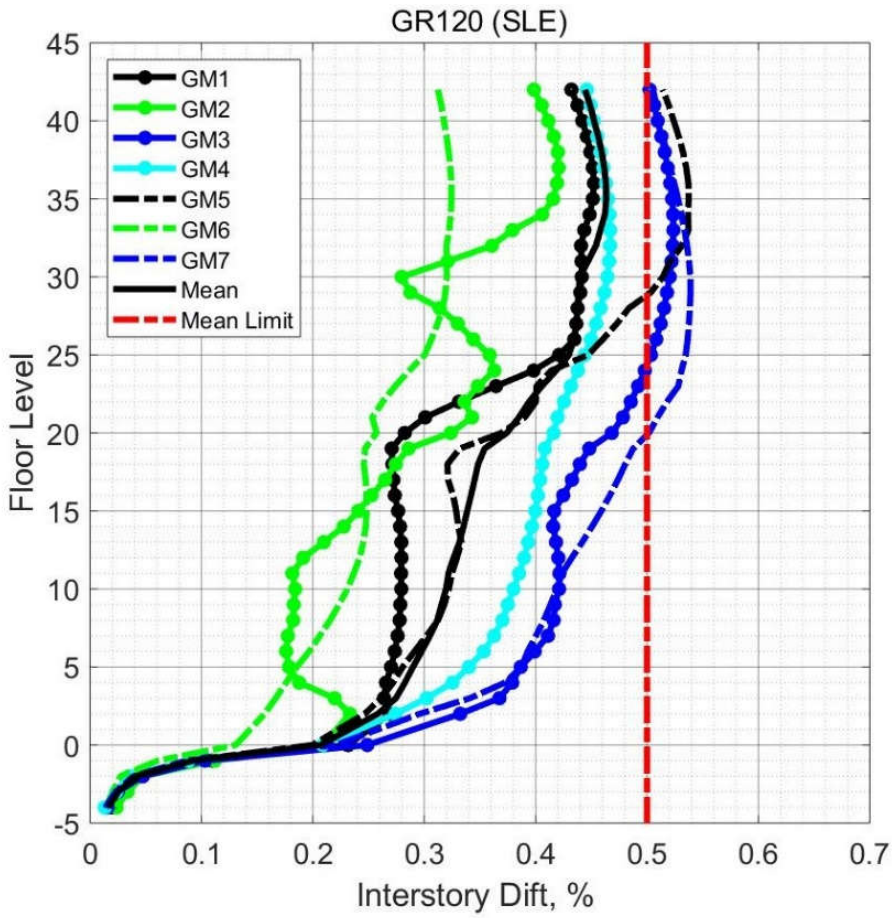

Figure 10.2 Peak Interstory Drift from All Ground Motions for X-direction (Case 4 -SLE).

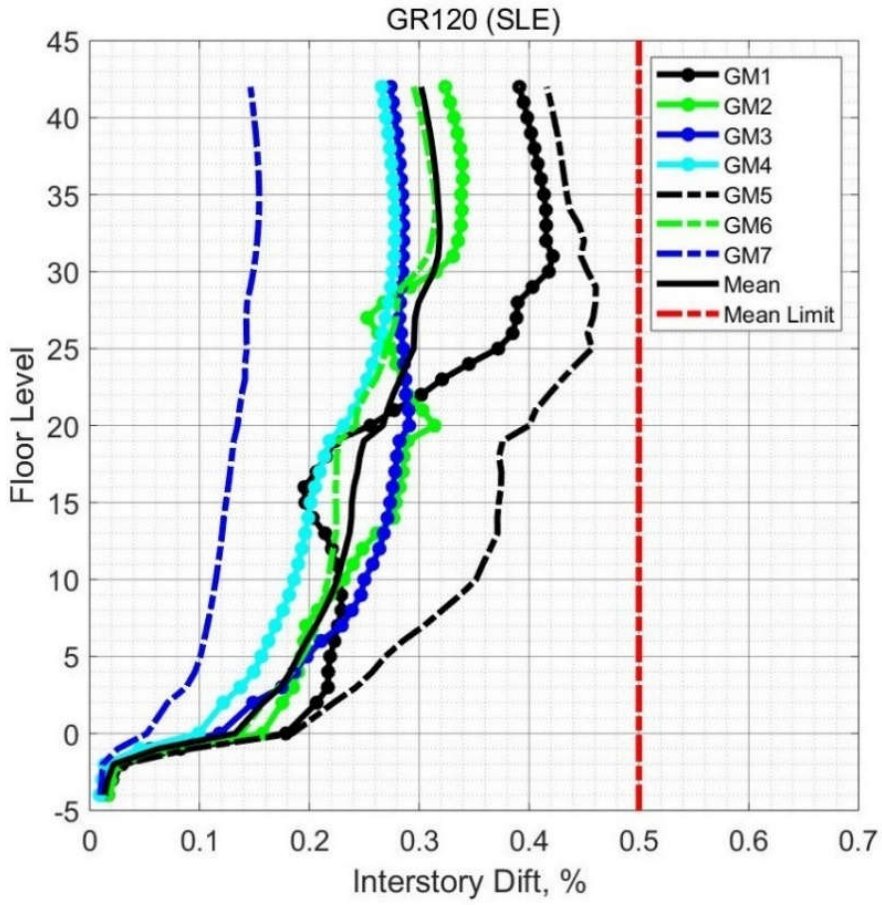

Figure 10.3 Peak Interstory Drift from All Ground Motions for Y-direction (Case 4 -SLE).

10.2.1.2 Displacement

As in Section 7.2.1.2, Figure 10.4 depicts the mean value of the displacement of each story at the same time step that the roof experiences a maximum displacement value.

Figures 10.5 and 10.6 show the time history of the roof displacement in the x-direction and y-direction, respectively from a ground motion at which the displacement demand of the roof was the highest one among other ground motions. During the seventh ground motion, the roof experience a maximum displacement in the x-direction while during the fifth ground motion the maximum roof displacement in the y-direction was observed.

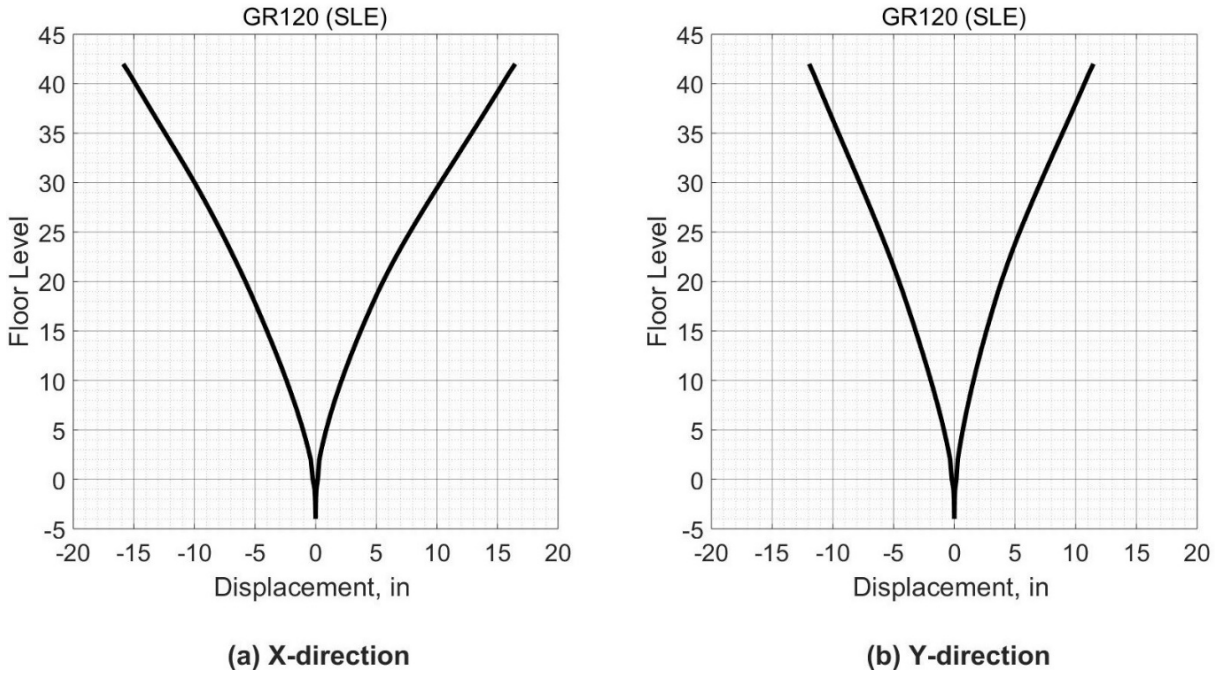

Figure 10.4 Floors Displacement Synchronous with Peak Roof Displacement (Case 4 - SLE).

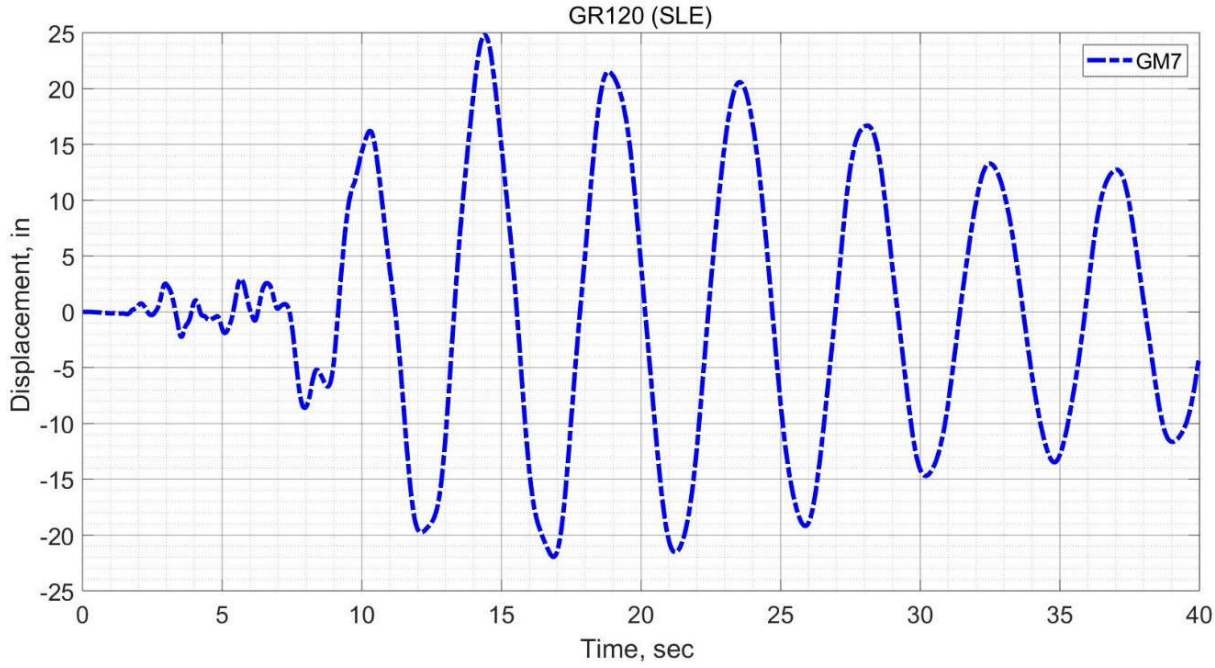

Figure 10.5 Time History for Peak Roof Displacement for X-direction (Case 4 – SLE).

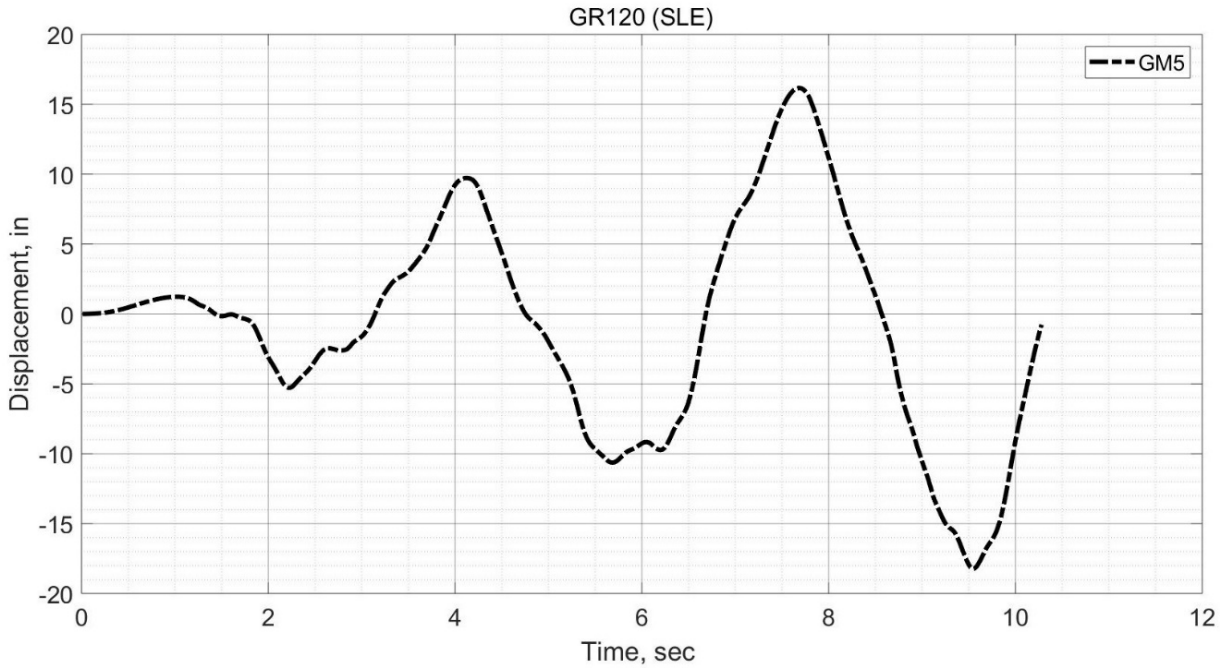

Figure 10.6 Time History for Peak Roof Displacement for Y-direction (Case 4 – SLE).

10.2.2 Element Level

As stated in Section 7.2.2, the TBI guidelines require using only the mean value from all analyses for evaluation with the acceptance criteria for both the force and deformation based-actions in this level. The maximum response parameters for both actions will also be presented to examine the response of the case study building in more depth. In the subsections below, the elements of the seismic force resisting system with their actions are presented and evaluated using the acceptance criteria of the TBI guidelines.

10.2.2.1 Core Wall Response

10.2.2.1.1 Core Wall Force-Based Action

The TBI guidelines specify that shear in the core walls of tall buildings is a force-based action. To evaluate the shear demands of core walls, the TBI guidelines required that the shear

force demands satisfy the Equation (7-1). Figure 10.7 shows the core wall shear forces over the building height and the values of $\phi Vexp$. The shear demands in the core wall satisfy Equation (7-1) as required by the TBI guidelines. In addition, the shear force demands varied approximately in a linear manner with the height of the building. For the mean response, the demand was approximately the same in both the x- and y-directions. The peak shear force of the mean values was 6566 kips, and 6613 kips, for x and y-direction, respectively. The maximum response was also less than the limit of the mean response.

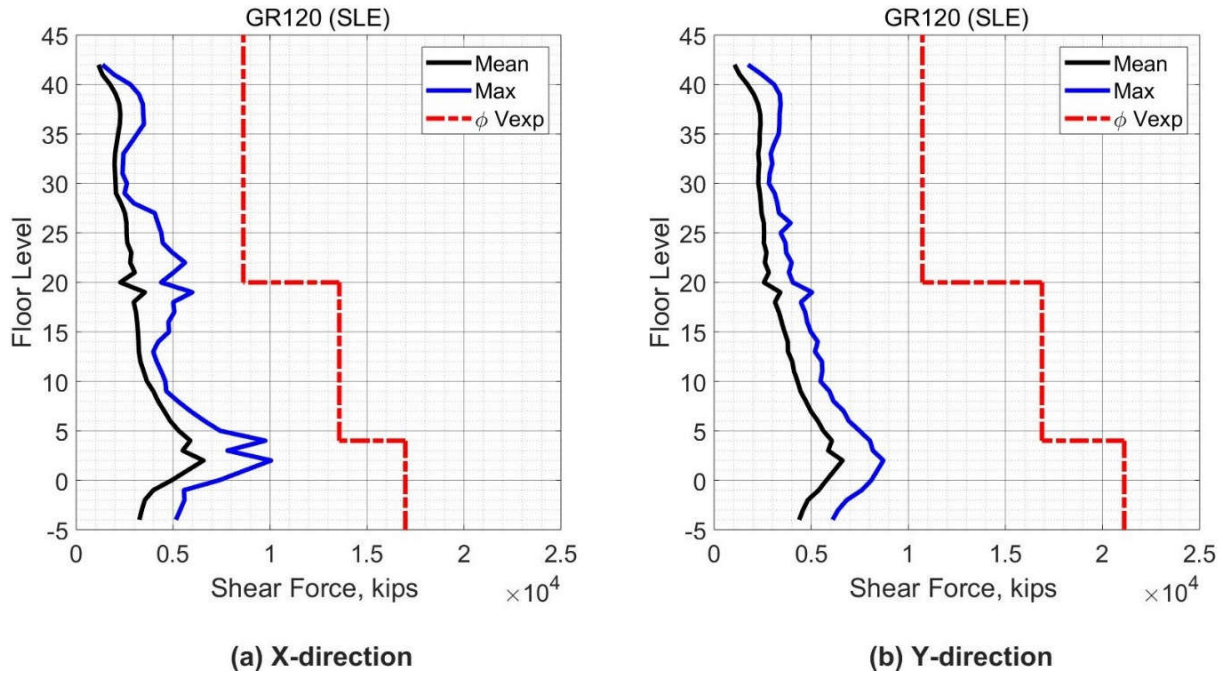

Figure 10.7 Shear Forces in Core Wall (Case 4 – SLE).

10.2.2.1.2 Core wall deformation-Based actions

Figures 10.8 to 10.11 show the mean values of the maximum tensile strain in the core wall reinforcement steel at locations shown in Figure 7.6 over the building height. The TBI guidelines

consider the yielding of steel bars as damage that should be avoided in the SLE shaking level. The maximum tensile strain in the steel bars in the core wall edges was 0.002, which is below the expected yield strain of Grade 120 (0.0048). The steel reinforcement in the core wall do not experience yielding strain, therefore the requirements of the TBI guidelines are satisfied.

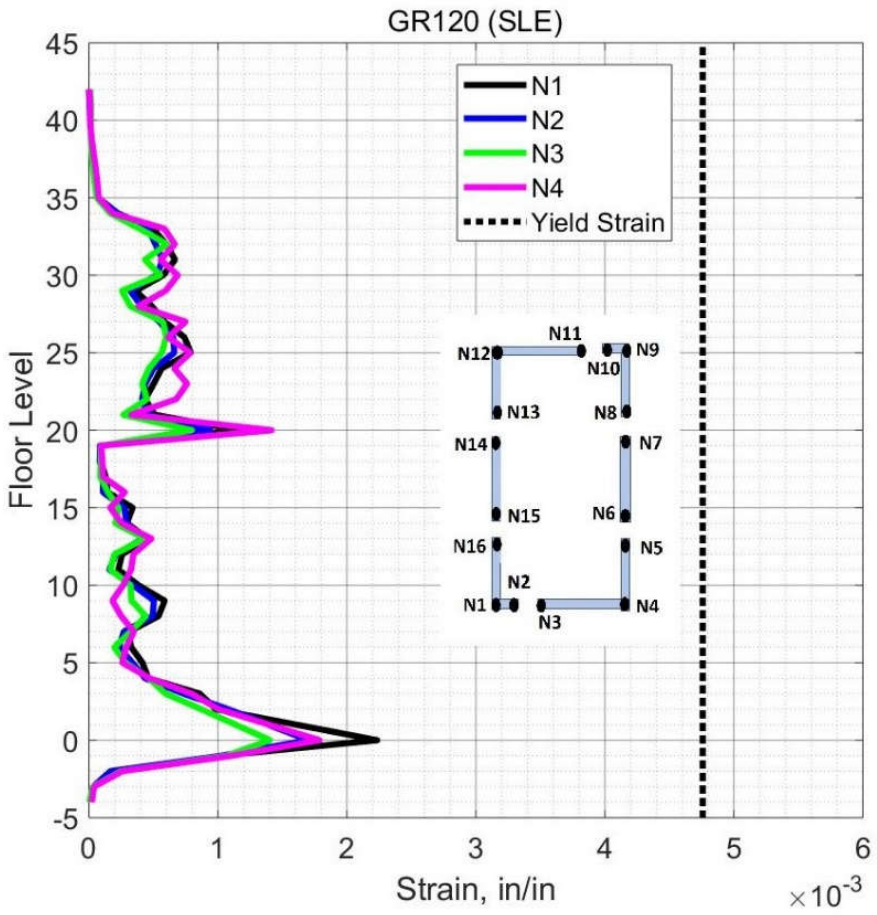

Figure 10.8 Mean Tensile Strain in Steel Bars in Core Wall Edges N1-N4 (Case 4 – SLE).

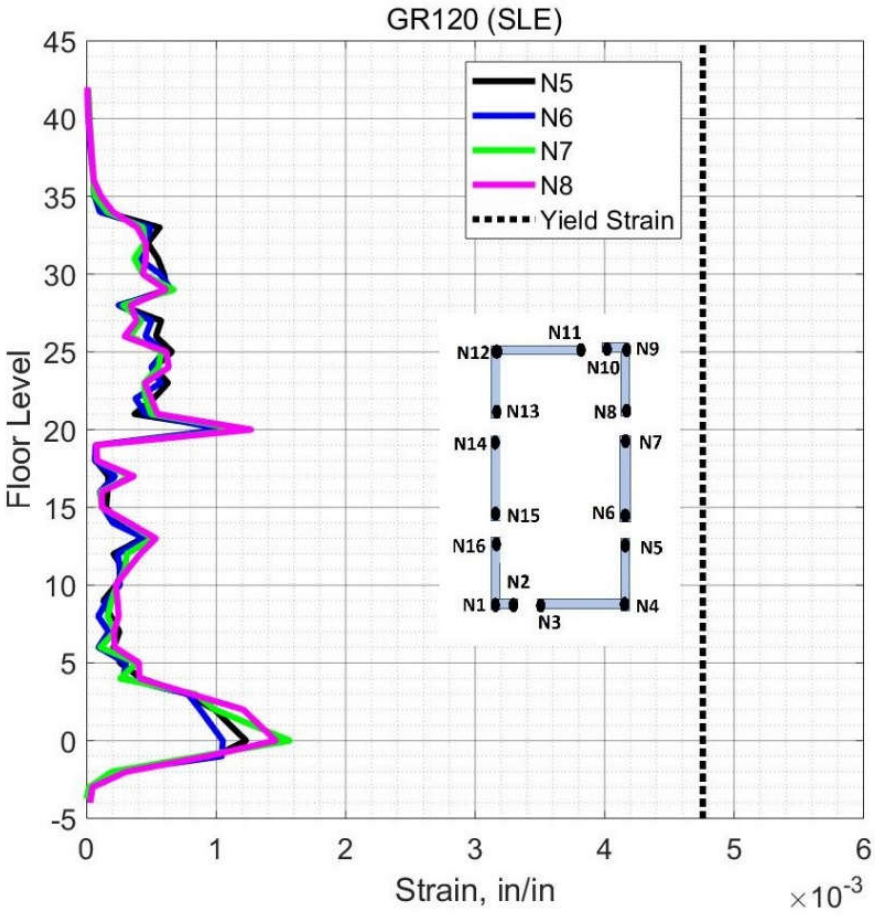

Figure 10.9 Mean Tensile Strain in Steel Bars in Core Wall Edges N5-N8 (Case 4 – SLE).

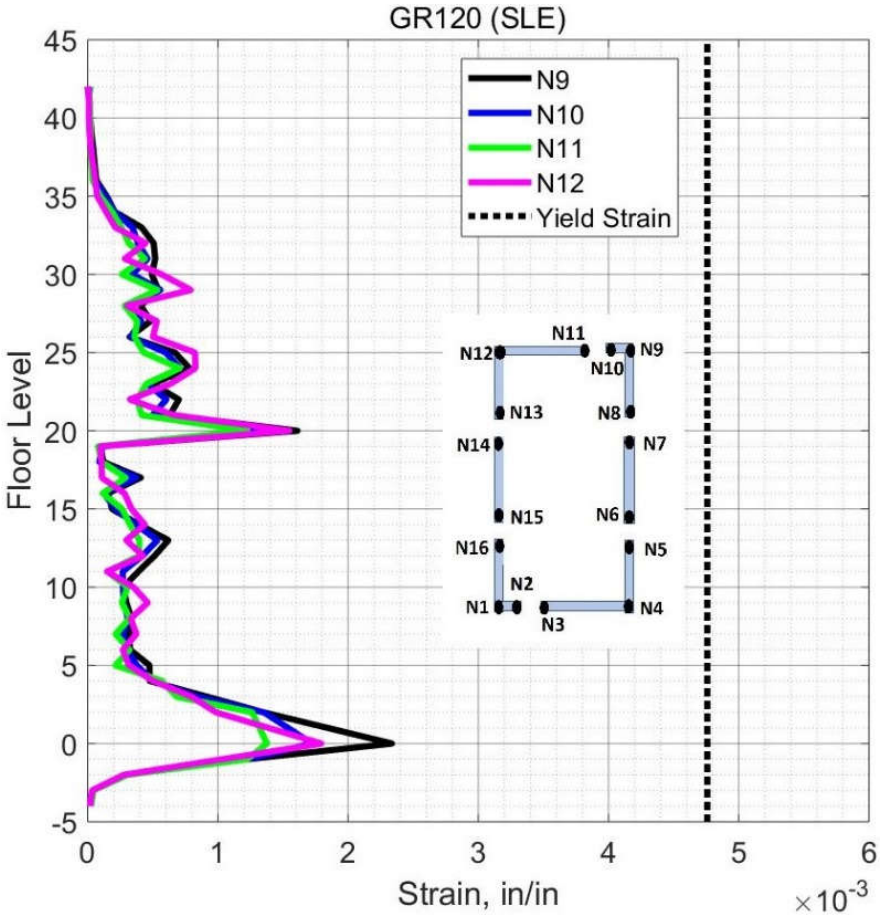

Figure 10.10 Mean Tensile Strain in Steel Bars in Core Wall Edges N9-N12 (Case 4 – SLE).

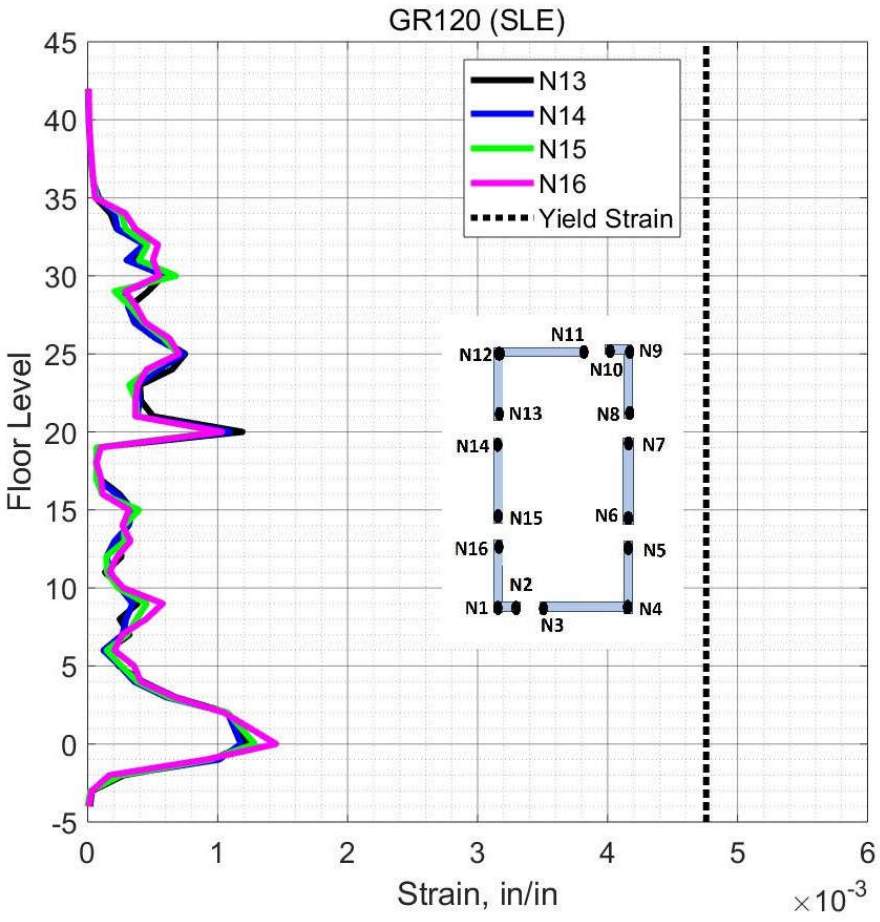

Figure 10.11 Mean Tensile Strain in Steel Bars in Core Wall Edges N13-N16 (Case 4 – SLE).

Figures 10.12 to 10.15 show the mean values of the maximum compression strain in the core wall concrete at locations shown in Figure 7.6 over the building height. The TBI guidelines consider the cracking of concrete as damage that should be avoided in the SLE shaking level. The concrete compression strain in the core wall was very low (< 0.00075), therefore the requirements of the TBI guidelines are satisfied.

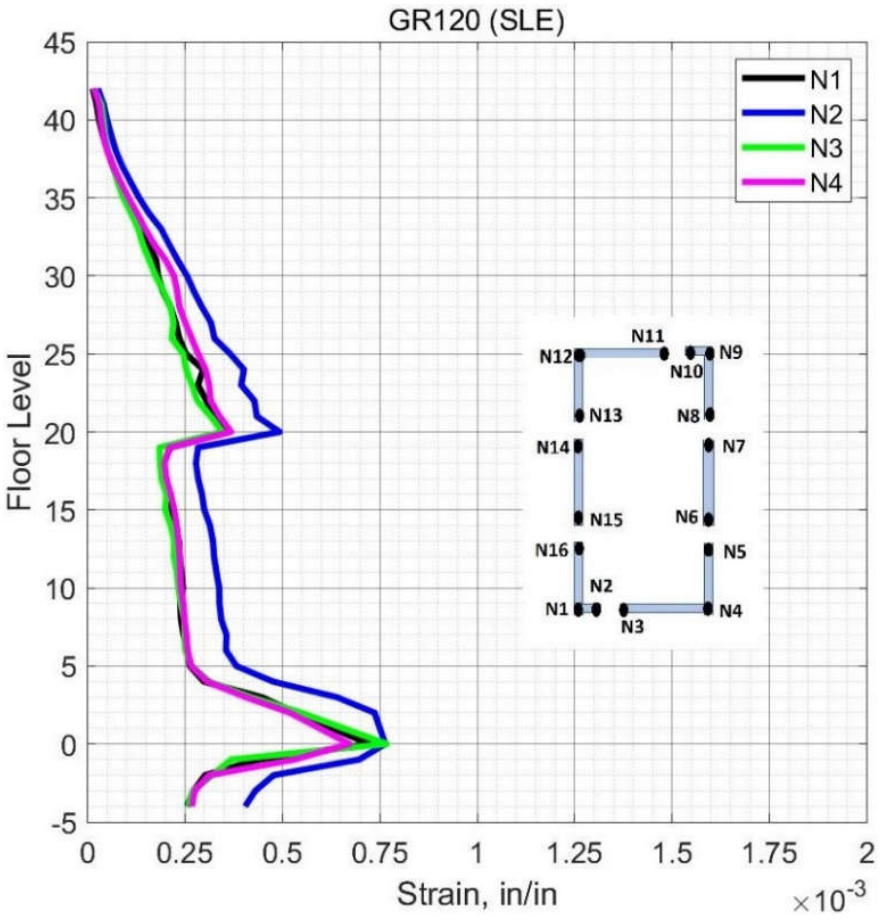

Figure 10.12 Mean Concrete Compression Strain in Core Wall Edges N1-N4 (Case 4 – SLE).

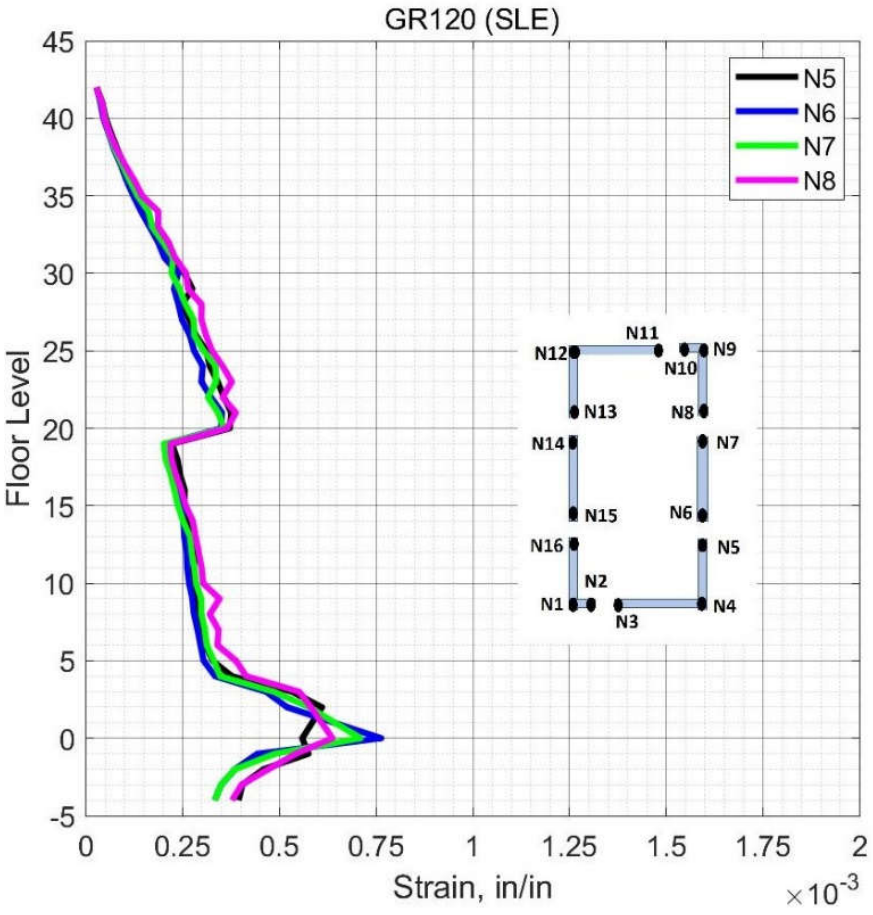

Figure 10.13 Mean Concrete Compression Strain in Core Wall Edges N5-N8 (Case 4 – SLE).

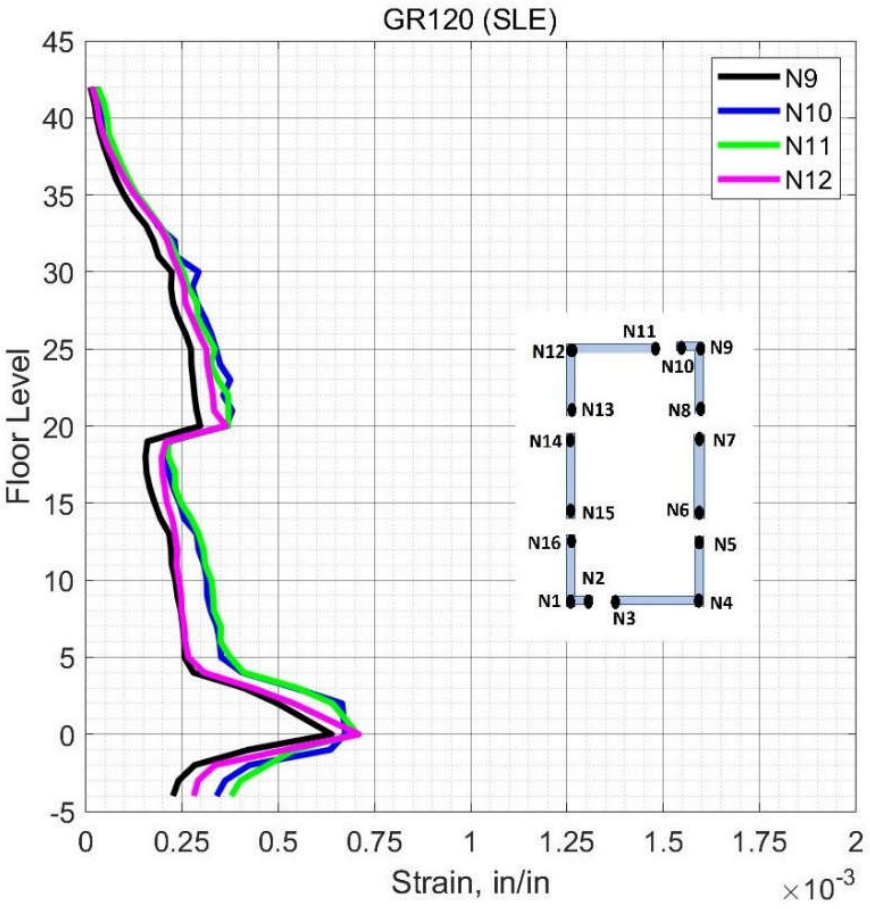

Figure 10.14 Mean Concrete Compression Strain in Core Wall Edges N9-N12 (Case 4 – SLE).

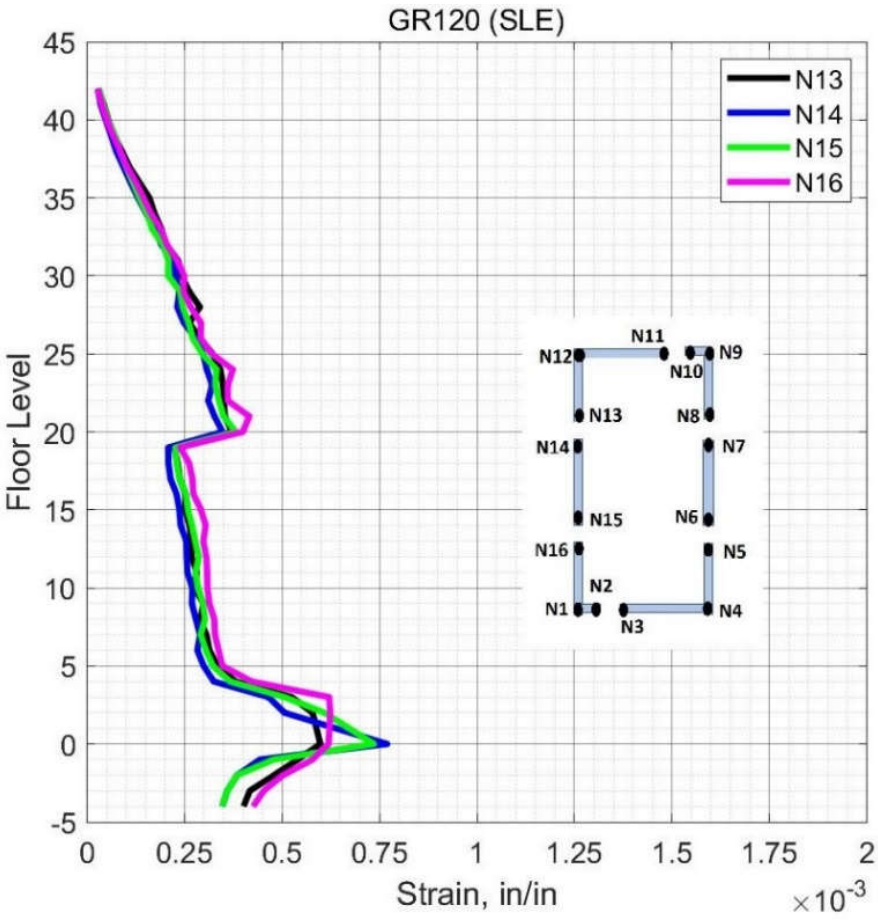

Figure 10.15 Mean Concrete Compression Strain in Core Wall Edges N13-N16 (Case 4 – SLE).

10.2.2.1.3 Coupling Beams

Figure 10.16 (a) shows the mean and maximum values of the rotation of coupling beams with a 1.7 aspect ratio (coupling beams in the x-direction), over the building height. The peak value of the mean rotation is 0.0015 which indicate that coupling beams do not experience yielding of steel reinforcement according to the data in Figure 7.18. In addition, the rotation demands are below the allowable limit of ASCE 41 (0.0060). Therefore, the rotation demands of coupling beams satisfy the requirement of the TBI guidelines.

Figure 10.16 (b) shows the mean and maximum values of the rotation of coupling beams with a 2.1 aspect ratio (coupling beams in the y-direction), over the building height. The peak value of the mean rotation is 0.0012 which indicate that coupling beams do not experience yielding of steel reinforcement according to the data in Figure 7.19. In addition, the rotation demands are below the allowable limit of ASCE 41 (0.0060). Therefore, the rotation demands of coupling beams satisfy the requirement of the TBI guidelines.

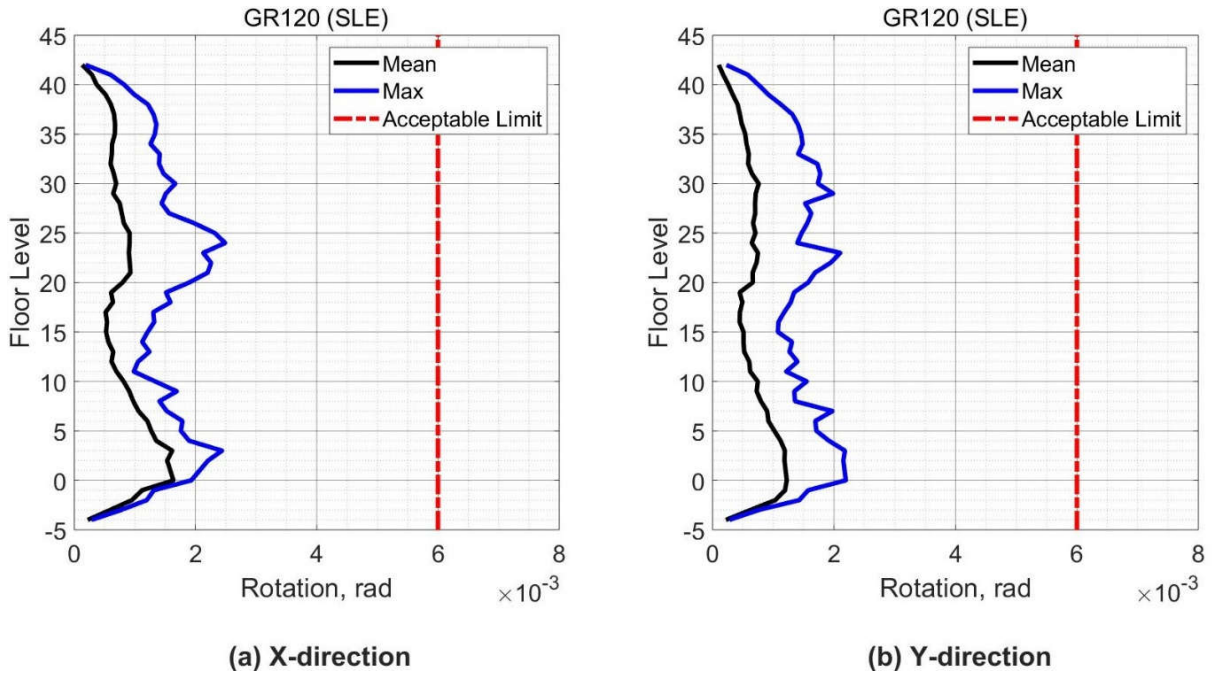

Figure 10.16 Rotation Demand in Coupling Beams (Case 4 – SLE).

10.2.2.2 Special Moment Frame Response

10.2.2.2.1 Beam Force-Based Action

The TBI guidelines specify the shear in the beams of special moment frames as a force-based action. The shear demands should satisfy Equation (7-1). The expected shear strength (V_{exp})

of beams or columns is calculated by using Equation (7-5) from ACI 318-14. Figure 10.17 shows the mean and the maximum values of beams shear forces from all ground motions over the building height and the limiting values of ($\phi Vexp$). In addition, the mean shear force demands in the beams of the special moment frame satisfy the requirements of the TBI guidelines by satisfying Equation (7-1). A slight increase in shear forces demands for the beams in the x-direction is noticed compared with beams in the y-direction. The maximum shear demand in the beams was 200 kips while the reduced shear capacity of the beams was 500 kips.

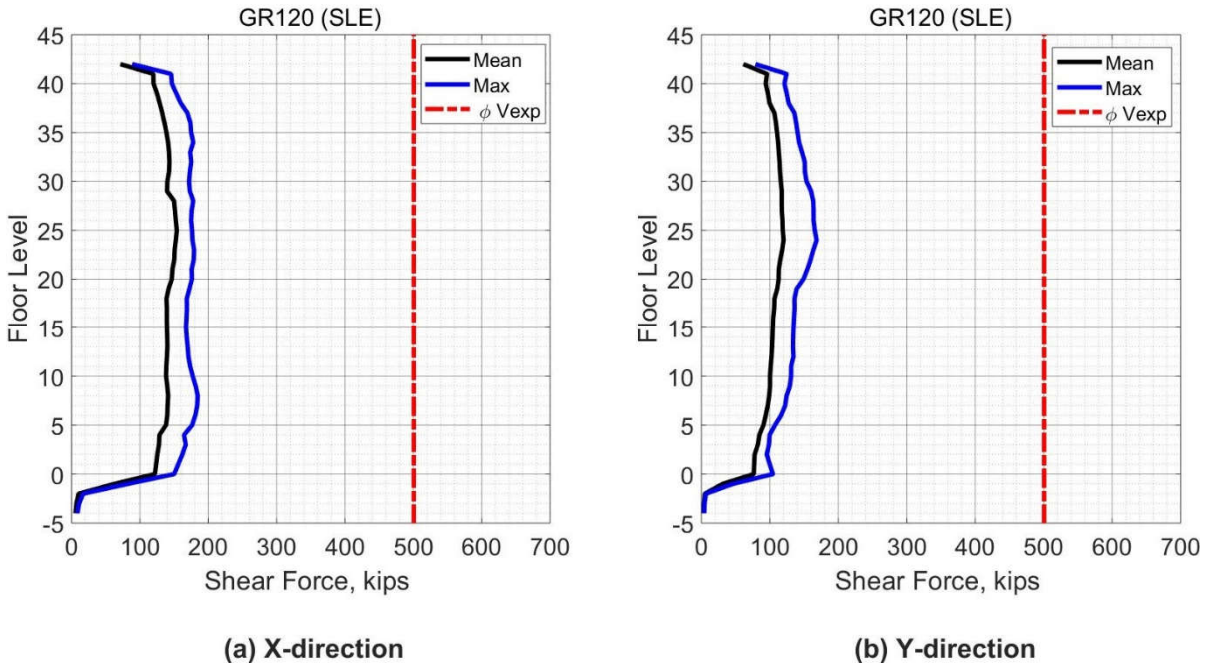

Figure 10.17 Peak Shear Force in Beams (Case 4 – SLE).

10.2.2.2.2 Beam Deformation-Based Action

Figure 10.18 shows the mean and maximum tensile strain demands in the longitudinal reinforcement in the beams sections that are in the beam ends over the building height. The TBI

guidelines consider the yielding of steel bars as damage that should be avoided in the SLE shaking level. The mean tensile strain of the steel reinforcement in all beams do not exceed the expected yield strain of Grade 120 (0.0048 in/in), therefore the requirements of the TBI guidelines are satisfied. A small increase in the tensile strain of the reinforcing bars in the beams oriented in the x-direction is noticed compared with the beams oriented in the y-direction. No yielding of the steel bars in the beams means that the beams do not experience plastic rotation.

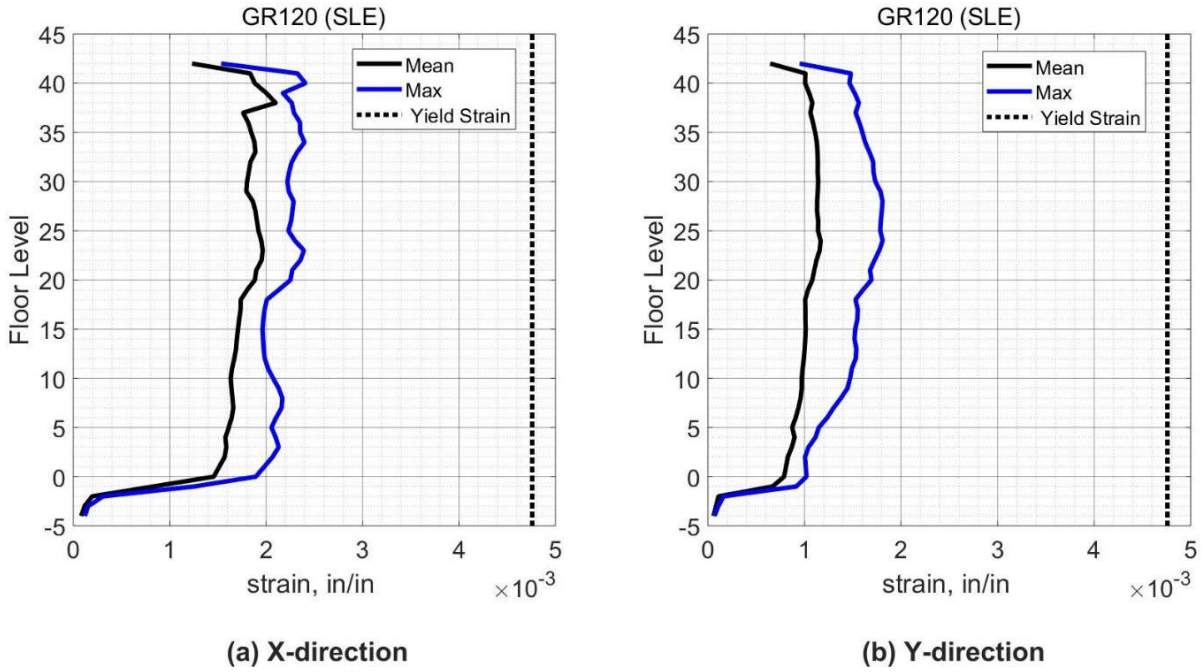

Figure 10.18 Peak Tensile Strain in Reinforcing bars in Beams (Case 4 – SLE).

10.2.2.2.3 Columns Force-Based Action

Figures 10.19 to 10.22 show the mean and maximum values of the shear forces from all analyses in the building columns and the limiting values of ($\phi Vexp$) over the building height. The

shear forces in the columns satisfies the requirements of the TBI guidelines by satisfying Equation (7-1).

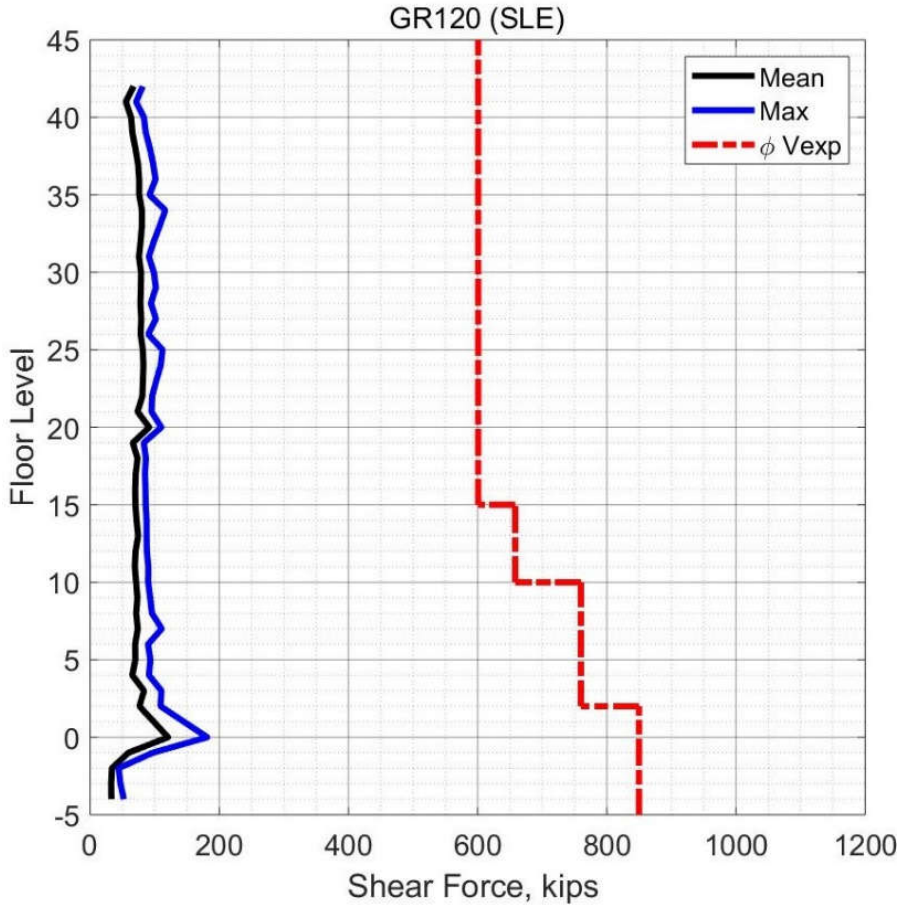

Figure 10.19 Peak Shear Force in Corner Columns (Case 4 – SLE).

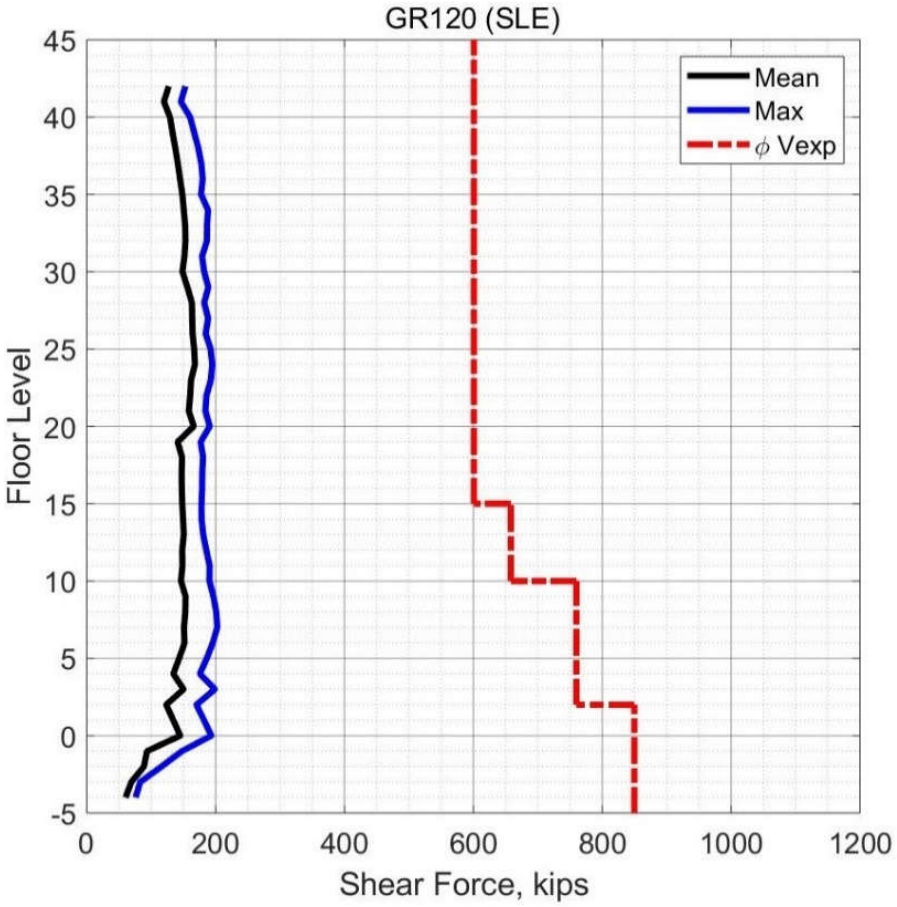

Figure 10.20 Peak Shear Force in Interior Columns X-direction (Case 4 – SLE).

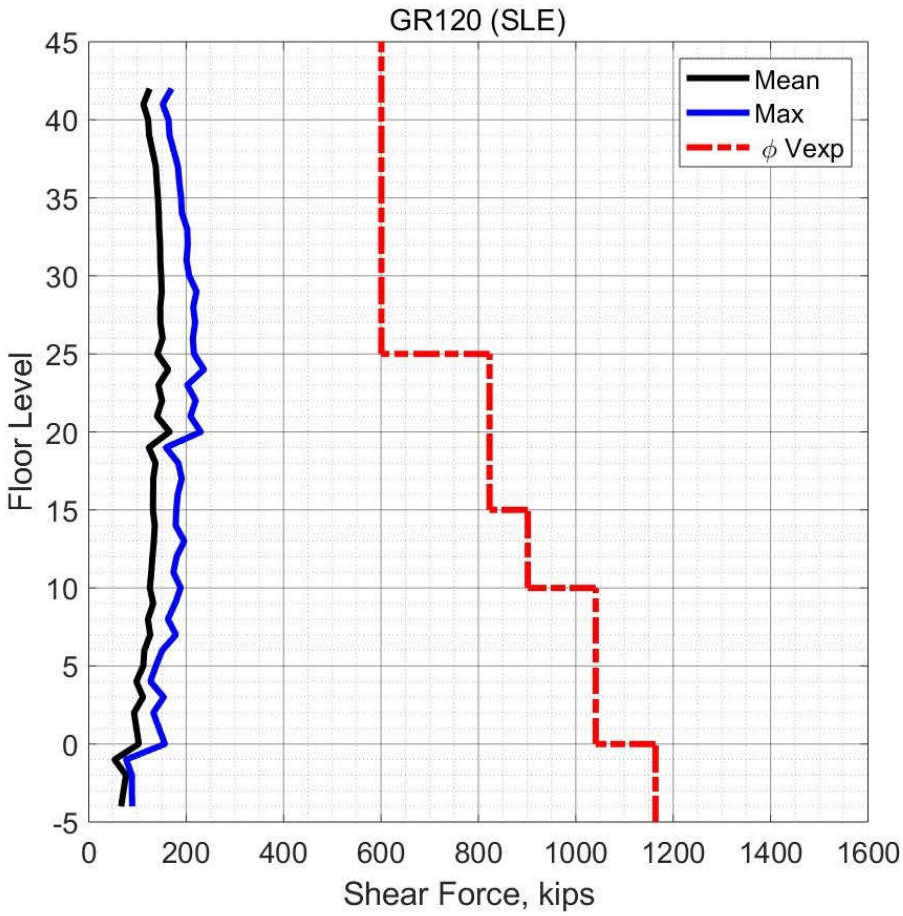

Figure 10.21 Peak Shear Force in Columns on Grid B and E (Case 4 – SLE).

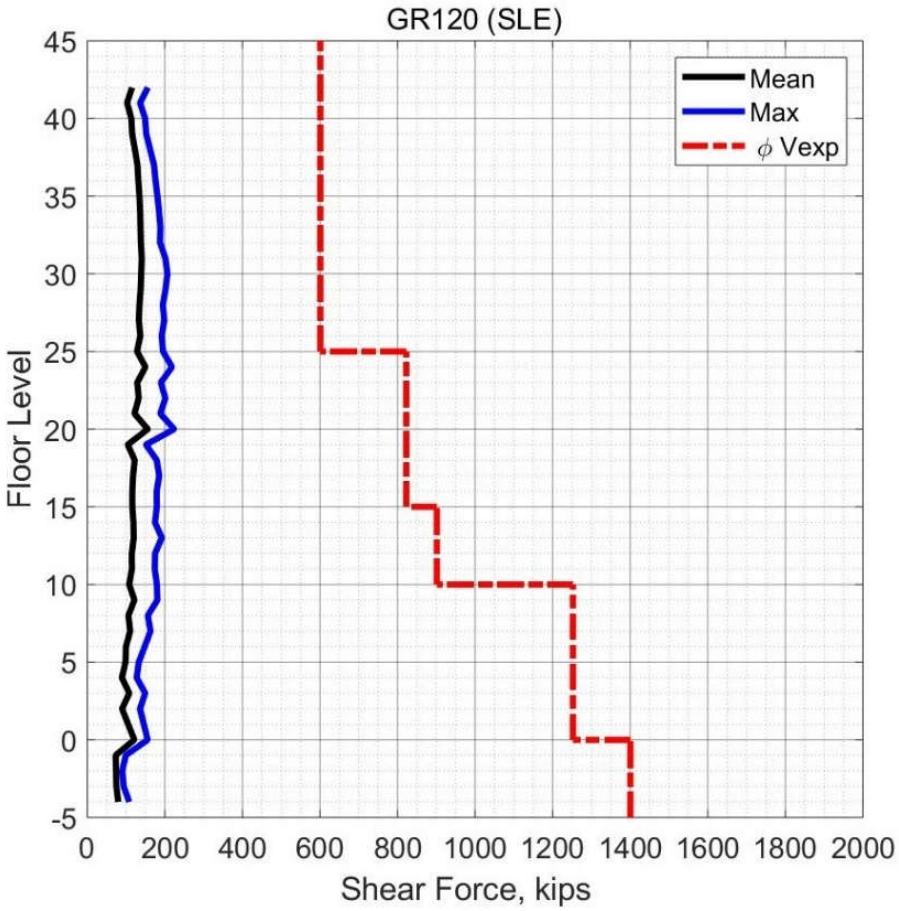

Figure 10.22 Peak Shear Force in Columns on Grid C.5 (Case 4 – SLE).

10.2.2.2.4 Column Deformation-Based Action

Figure 10.23 shows the maximum value of the tensile strain in the longitudinal bars in columns and the mean value from all ground motion in the suite over the building height. The TBI guidelines consider the yielding of steel bars as damage that should be avoided in the SLE shaking level. The tensile strain demands did not exceed the expected yield strain which means no damage could be expected in the columns. Consequently, there is no plastic rotation in all the columns for this shaking level. depending on the results of the tensile strain of the reinforcing bars, the columns satisfy the requirements of the TBI guidelines.

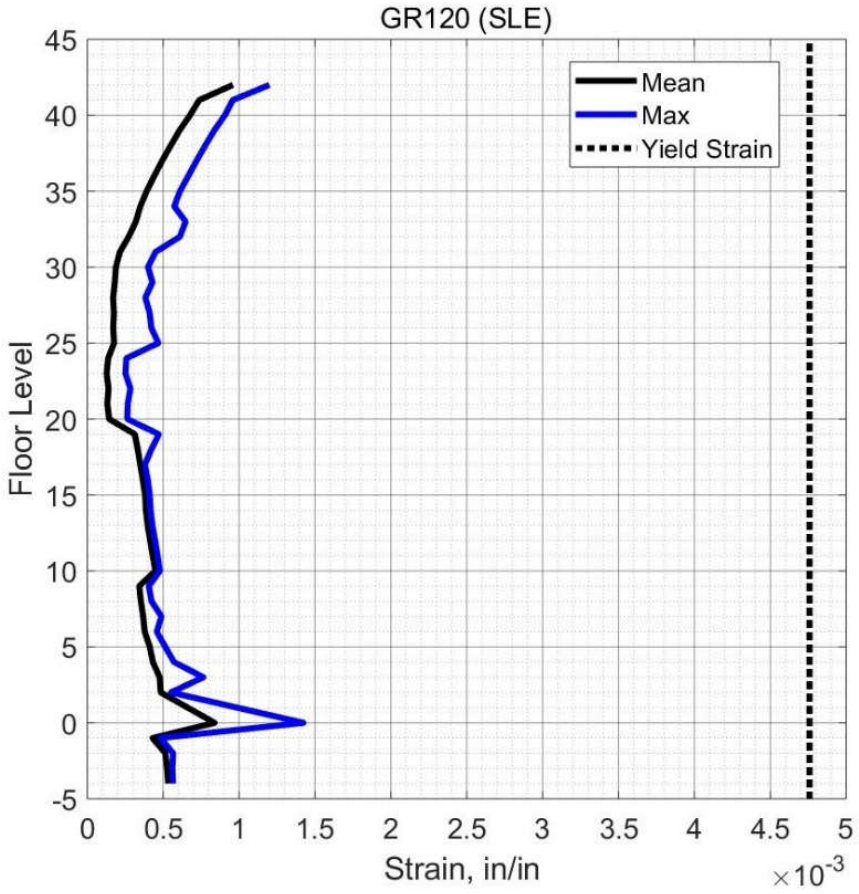

Figure 10.23 Peak Tensile Strain in Reinforcing Bars in Columns (Case 4 – SLE).

10.2.2.3 Contribution of Core Wall and Frame in Dual System

To better understand the behavior of the dual system, the contribution of its components in resisting the story shear force is depicted in Figure 10.24. Figure 10.25 shows the contribution percentage of the shear forces for the core wall and the frame over the building height. The frame contribution is approximately constant over the building height, while the core wall contribution varies linearly. In general, the core wall contributes more than 80% of the total story shear for the lower stories and 50% for the upper stories.

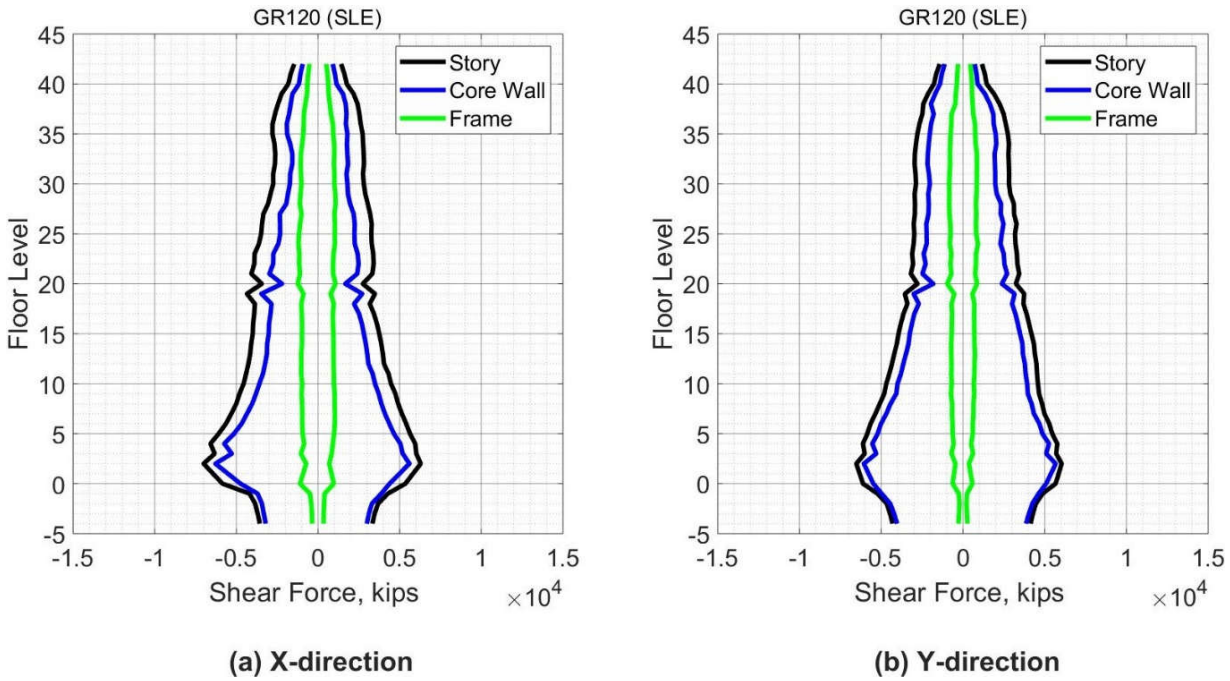

Figure 10.24 Shear Force Contribution of Core Wall & Frame (Case 4 – SLE).

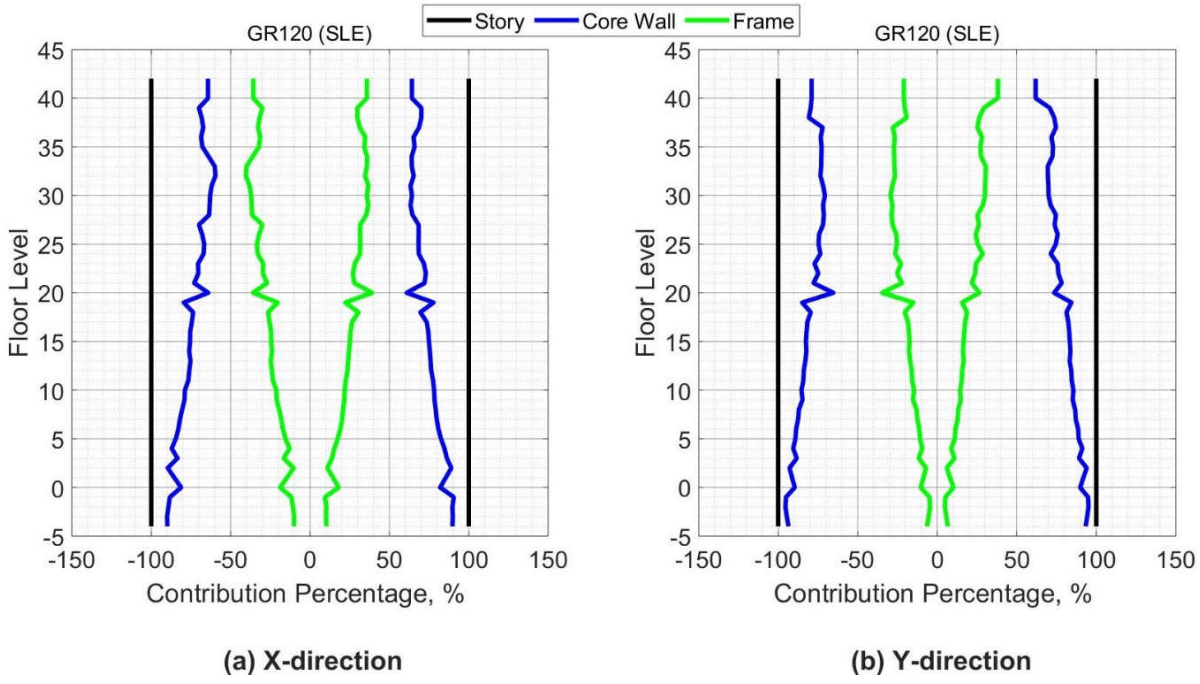

Figure 10.25 Contribution Percentage of Core wall & Frame Shear Force (Case 4 – SLE).

10.3 MCER LEVEL

The same ground motions used in the MCER in case 1 were used for the MCER analyses of case 4. As stated in Section 7.3, the results of eleven analyses are represented and compared with the acceptance criteria of the TBI guidelines. According to the TBI guidelines, first, the mean value of the response parameters from all ground motions in the suite should be checked with the acceptance criteria. Second, the maximum response parameters from all ground motions should be checked to ensure that no unacceptable response was produced by any ground motion from the suite. All the response parameters were calculated by the same procedures that were described in Section 7.2.

10.3.1 Global Response

10.3.1.1 Drift Ratio

Figure 10.26 shows the mean and the maximum values of the interstory drift ratios from all the ground motions analyses over the building height. The mean interstory drift from the eleven analyses was very close to 0.022 in the x-direction and approximately 0.012 in the y-direction, where both values were within the acceptable limit of TBI guidelines of 0.030. In addition, the maximum interstory drift was slightly more than 0.030 and 0.020 for the x- and y-directions, respectively. The maximum values of drift ratios were also within the acceptable limit of TBI guidelines (0.045), which indicates that no unacceptable response was produced when considering the drift ratios. Figures 10.27 and 10.28 depict the maximum drift ratios form each considered ground motion over the building height.

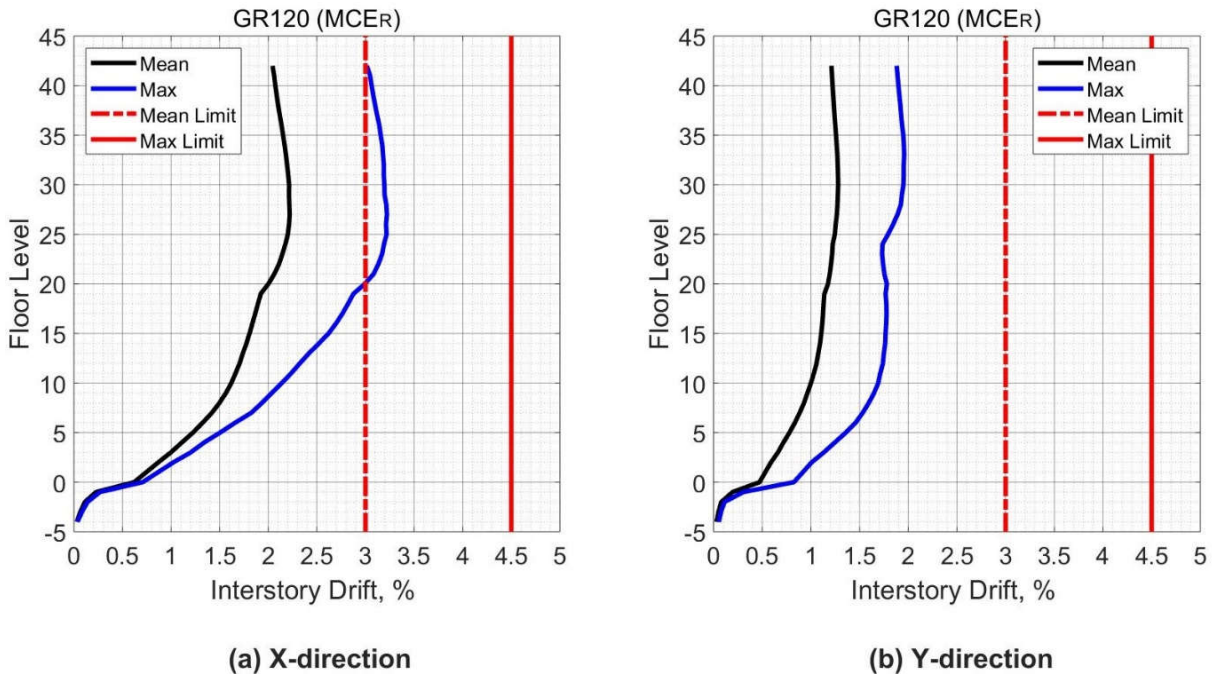

Figure 10.26 Peak Interstory Drift (Case 4 – MCER).

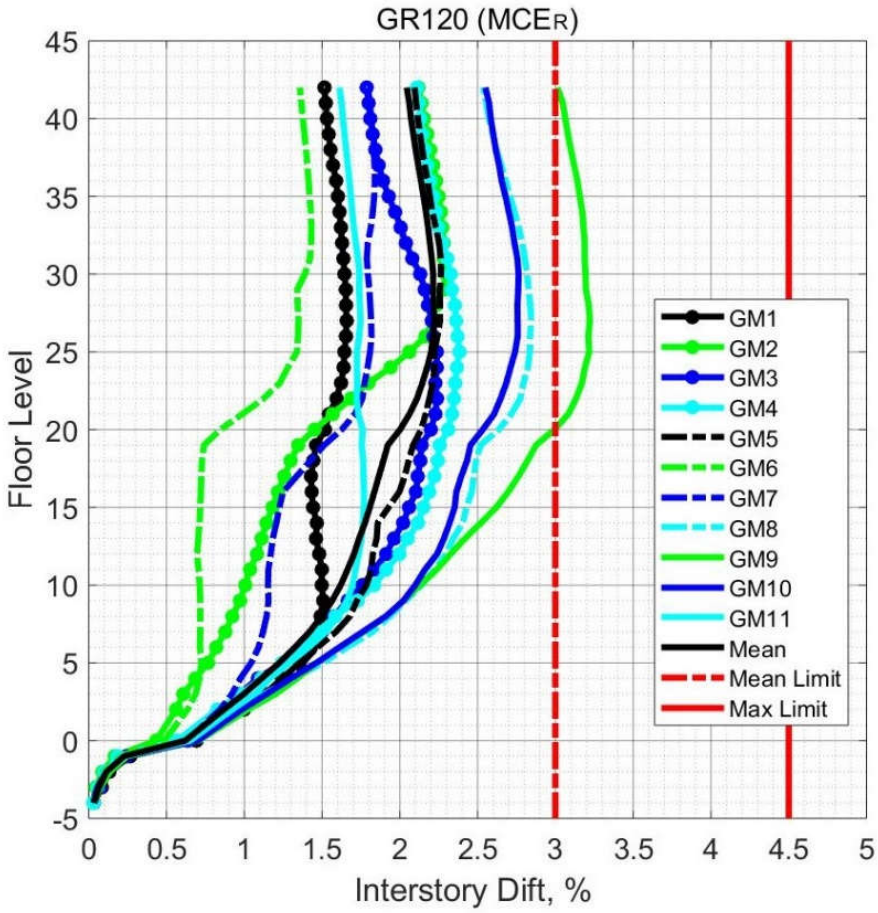

Figure 10.27 Peak Interstory Drift from All Ground Motions for X-direction (Case 4 - MCER).

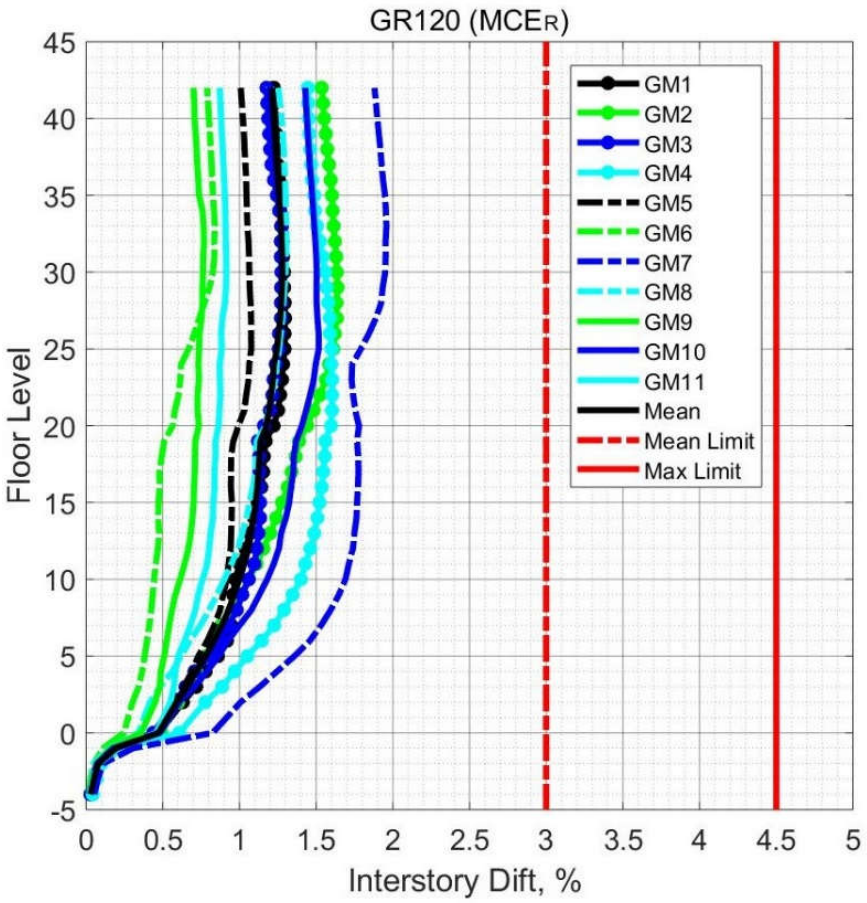

Figure 10.28 Peak Interstory Drift from All Ground Motions for Y-direction (Case 4 - MCER).

10.3.1.2 Residual Drift Ratio

Figure 10.29 shows that the maximum of the mean values of the residual drift was 0.0075 in the x- direction and 0.0040 in the y-direction where both values are below the TBI limit (0.0100). In addition, the maximum residual drift ratio obtained from all analyses was 0.0125, which is below the limit of the TBI guidelines for residual drift ratios (0.0150). Consequently, no unacceptable response was produced from any ground motion when considering the values of the residual drift ratio.

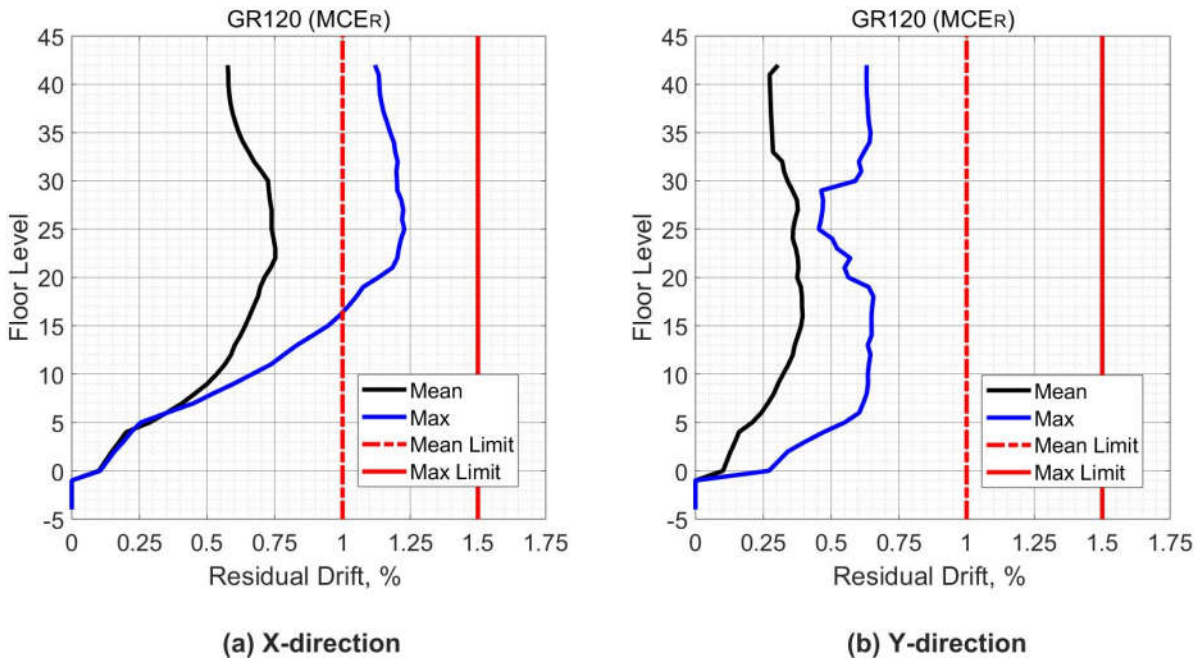

Figure 10.29 Peak Residual Drift (Case 4 – MCER).

10.3.1.3 Displacement

Figure 10.30 depicts the mean value of the displacement of each story at the same time step that the roof experiences a maximum displacement value. The mean displacement of the roof was 80 in and 50 in for x and y-direction, respectively.

Figures 10.31 and 10.32 show the time history of the roof displacement in the x-direction and y-direction, respectively from a ground motion at which the displacement demand of the roof was the highest one among other ground motions. During the ninth ground motion, the roof experience a maximum displacement in the x-direction while during the seventh ground motion the maximum roof displacement in the y-direction was observed.

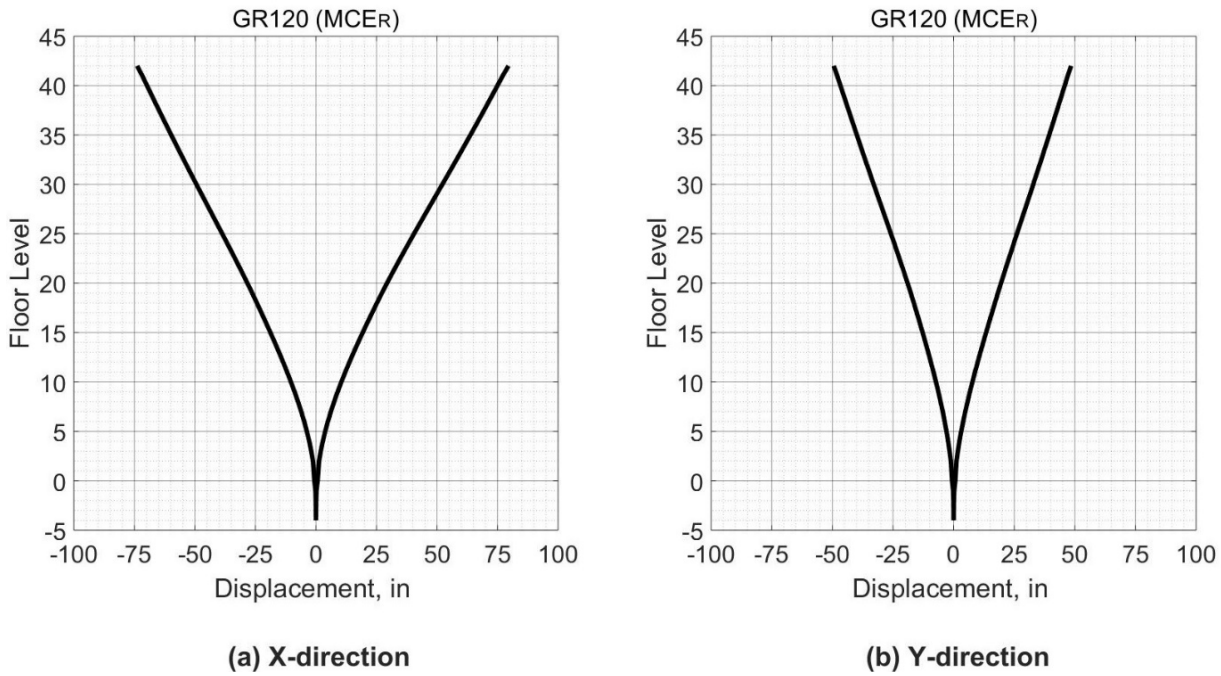

Figure 10.30 Floors Displacement Synchronous with Peak Roof Displacement (Case 4 - MCER).

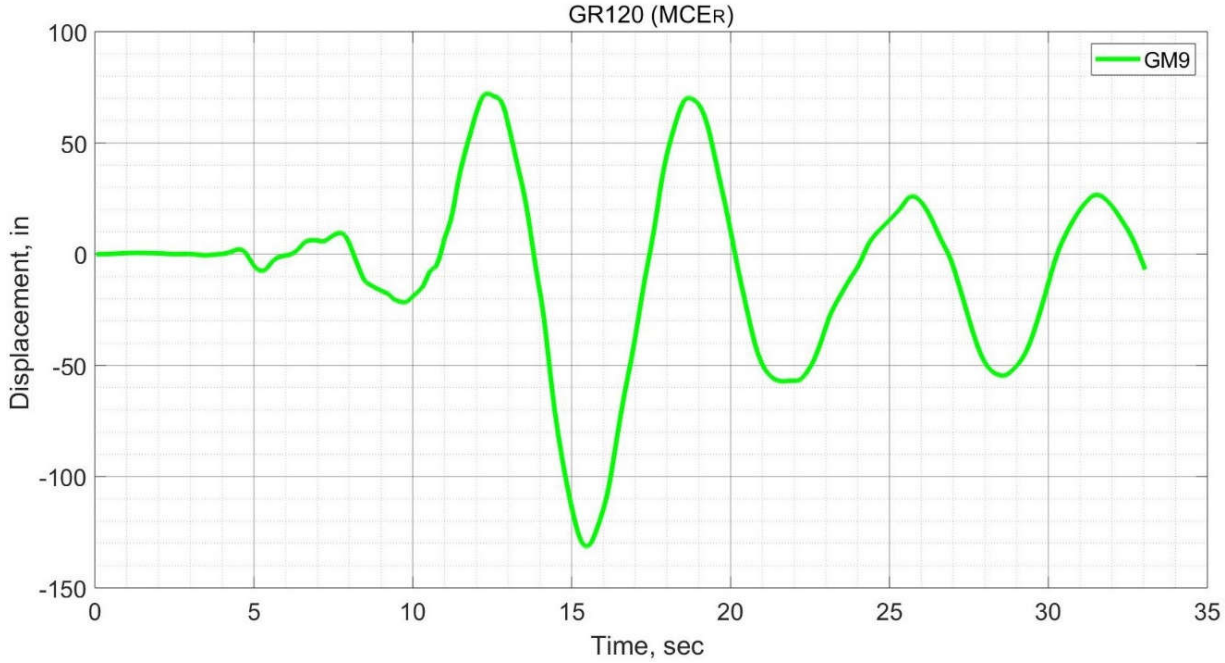

Figure 10.31 Time History for Peak Roof Displacement for X-direction (Case 4 – MCER).

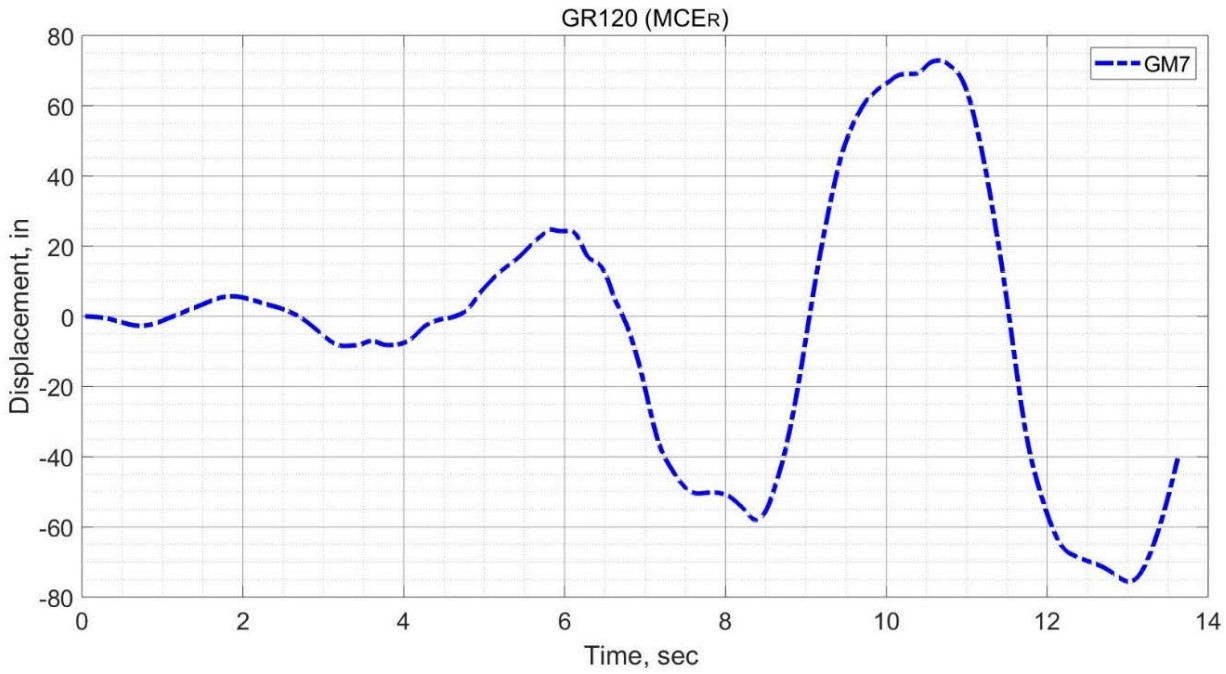

Figure 10.32 Time History for Peak Roof Displacement for Y-direction (Case 4 – MCER).

10.3.2 Element Level

As mentioned in Section 7.3.2, For the MCER shaking level, the TBI guidelines require using the mean value from all analyses for evaluation with the acceptance criteria for force-based actions, while using the maximum value from all analyses for deformation-based actions. In addition, for both actions the TBI guidelines require using the maximum value from all analyses to evaluate with the acceptance criteria to ensure that all calculated demands from any analysis are within the acceptable range of the model. In the subsections below, the elements of the seismic force resisting system with their actions are presented and evaluated using the acceptance criteria of the TBI guidelines.

10.3.2.1 Core Wall Response

10.3.2.1.1 Core Wall Force-Based Action

To evaluate the shear demands of core walls, the TBI guidelines required that the shear force demands satisfy Equation (7-8). Figure 10.33 shows the core wall shear forces over the building height and the limiting (*Vexp*) as in Equation (7-8). The shear demands in the core wall satisfy Equation (7-8) as required by the TBI guidelines. In addition, the shear force demands varied approximately in a linear manner with the height of the building. A small increase in the shear force demands in the y-direction was noticed compared with demands in the x-direction. The maximum observed shear demand was 13482 kips for y-direction, while 12550 kips in x-direction. A change in the shear response of the core wall was noticed at the twentieth story due to the wall thickness changing from 24 in. to 18 in. As shown in Figure 10.33, considering that the maximum demand of the shear force in the core wall was also within the acceptable limits, all analyses produced an acceptable response and all results are within the acceptable modeling range.

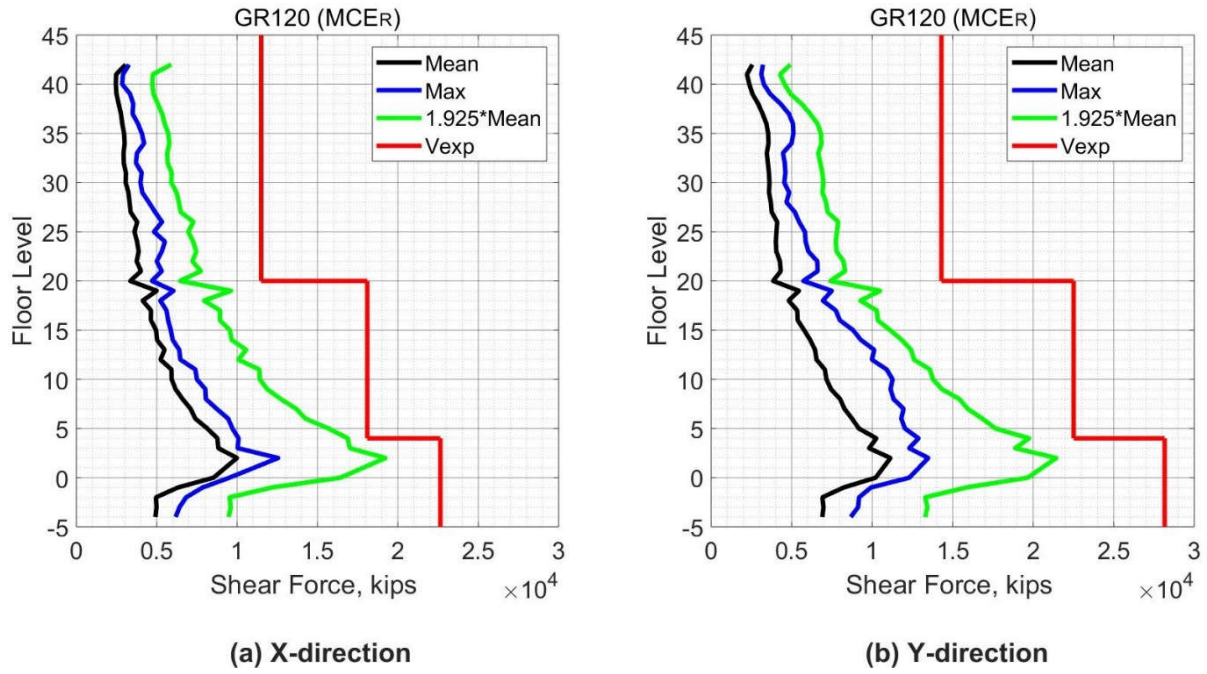

Figure 10.33 Shear Forces in Core Wall (Case 4 – MCER).

10.3.2.1.2 Core Wall Deformation-Based Action

As stated in Section 7.2.2.1.2, the tensile strain in the reinforcing steel and concrete compression strain were monitored during the analyses on all edges of the core wall. The strain was determined by using the vertical displacement (Δz) of the nodes of the core wall edges. Figures 9.34 to 9.37 show that the maximum tensile strain in the core wall reinforcement is 0.014, which is below the acceptable limit of 0.05. The maximum tensile strain demand in reinforcing bars of the core wall was 0.014 which is below the minimum fracture elongation (0.07) as specified by ASTM 1035 for Grades 100 and 120. The uniform elongation of Grades 100 is approximately 0.045 (NEHRP, 2014). Grade 120 could be a valuable option for reinforcing the special walls when considering that the maximum tensile strain demands are below the limit of 75% of the uniform elongation. The reinforcing bars experienced yielding for all stories from ground story to the tenth

story, and stories above the twentieth story up to twenty third story only. The core wall below the ground level did not experience yielding because of the effect of the podium's levels.

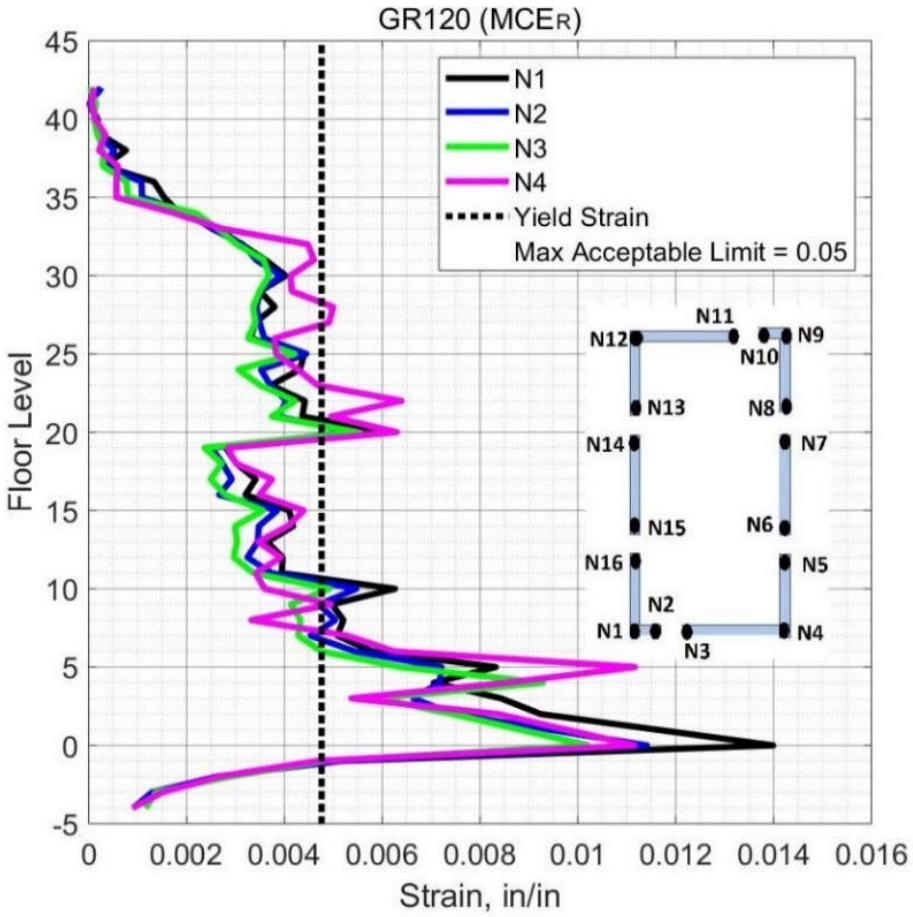

Figure 10.34 Peak Tensile Strain in Steel Bars in Core Wall Edges N1-N4 (Case 4 – MCER).

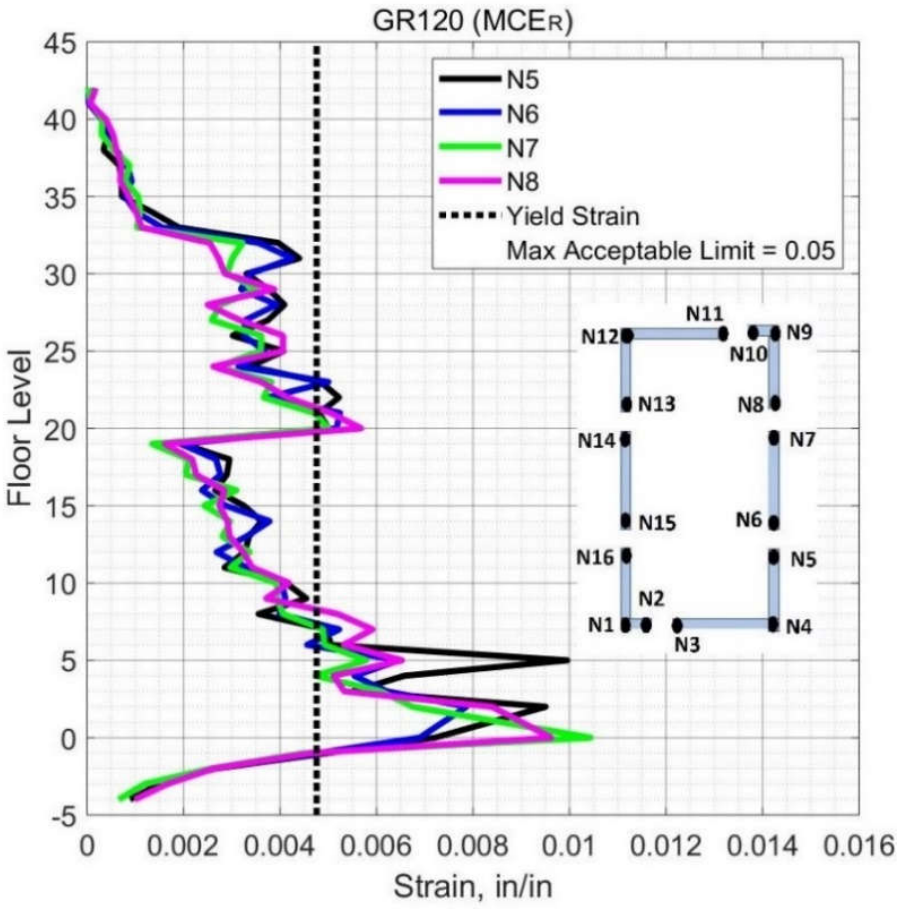

Figure 10.35 Peak Tensile Strain in Steel Bars in Core Wall Edges N5-N8 (Case 4 – MCER).

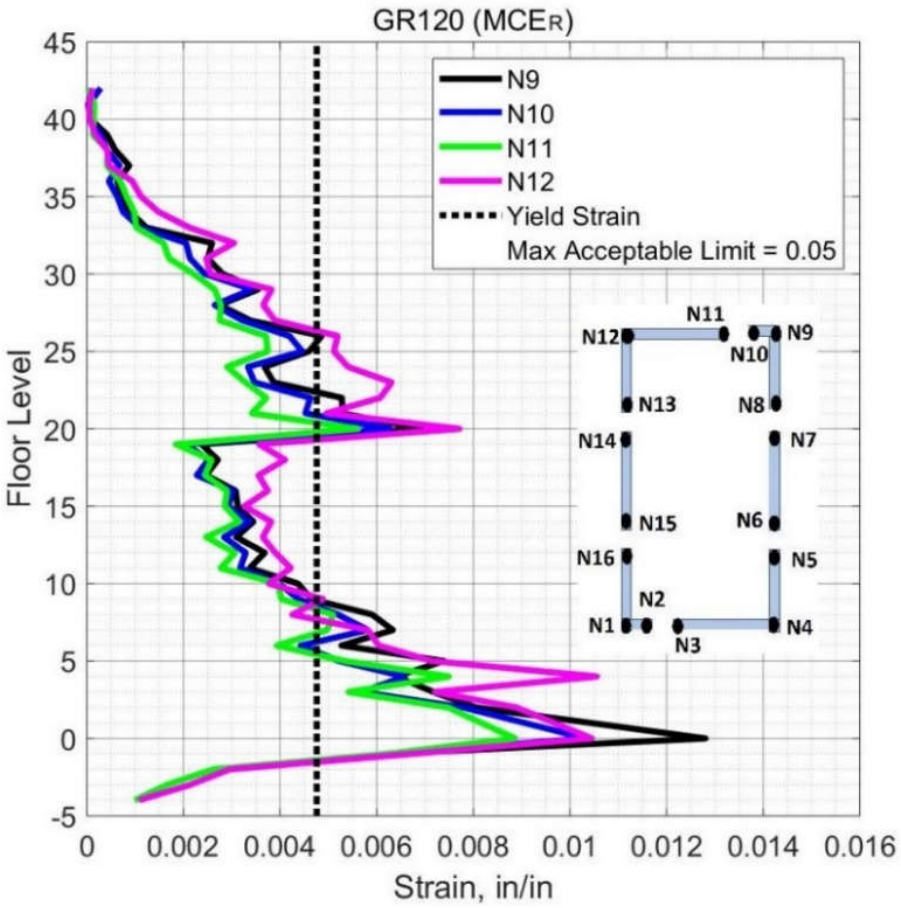

Figure 10.36 Peak Tensile Strain in Steel Bars in Core Wall Edges N9-N12 (Case 4 – MCER).

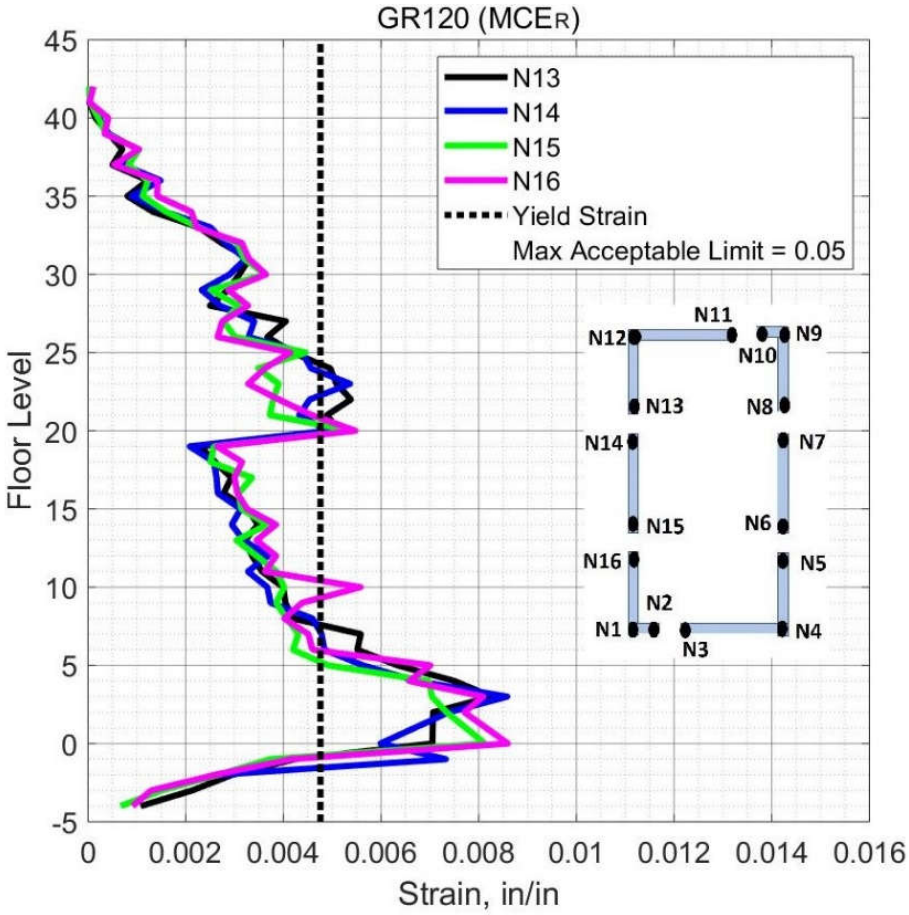

Figure 10.37 Peak Tensile Strain in Steel Bars in Core Wall Edges N13-N16 (Case 4 – MCER).

Figures 10.38 to 10.41 show the maximum values of the compression strain in the core wall concrete at the wall edges over the building height. The core wall concrete experiences low values of concrete compression strain, below 0.002, for all stories.

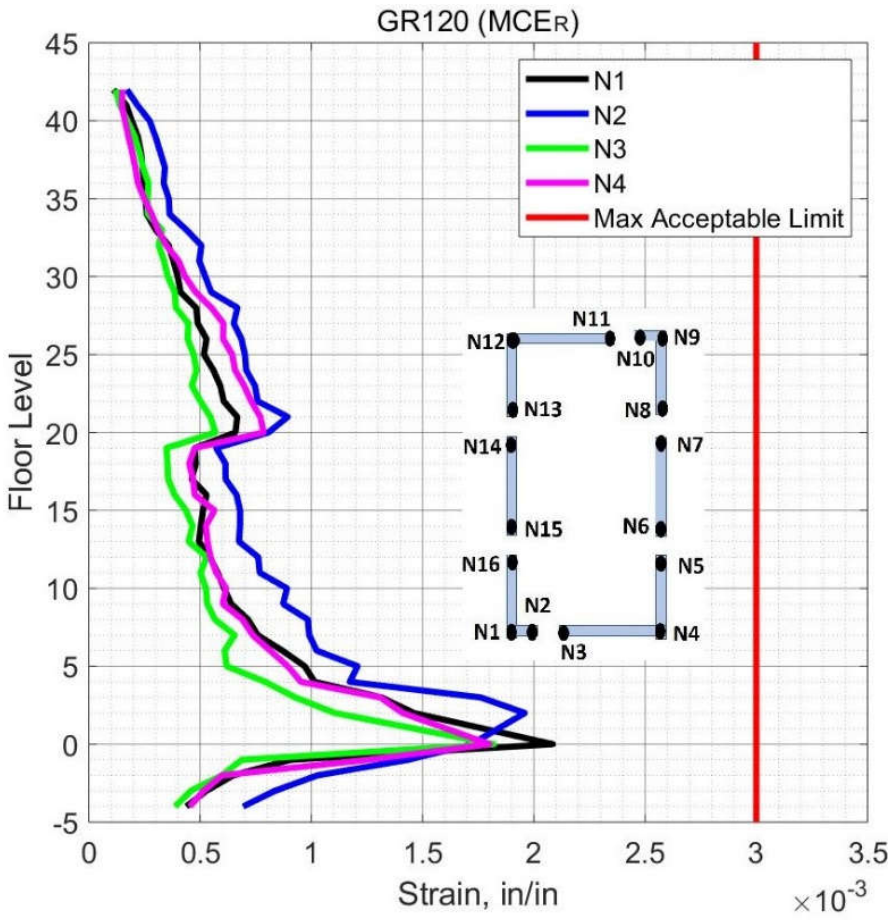

Figure 10.38 Peak Concrete Compression Strain in Core Wall Edges N1-N4 (Case 4 – MCER).

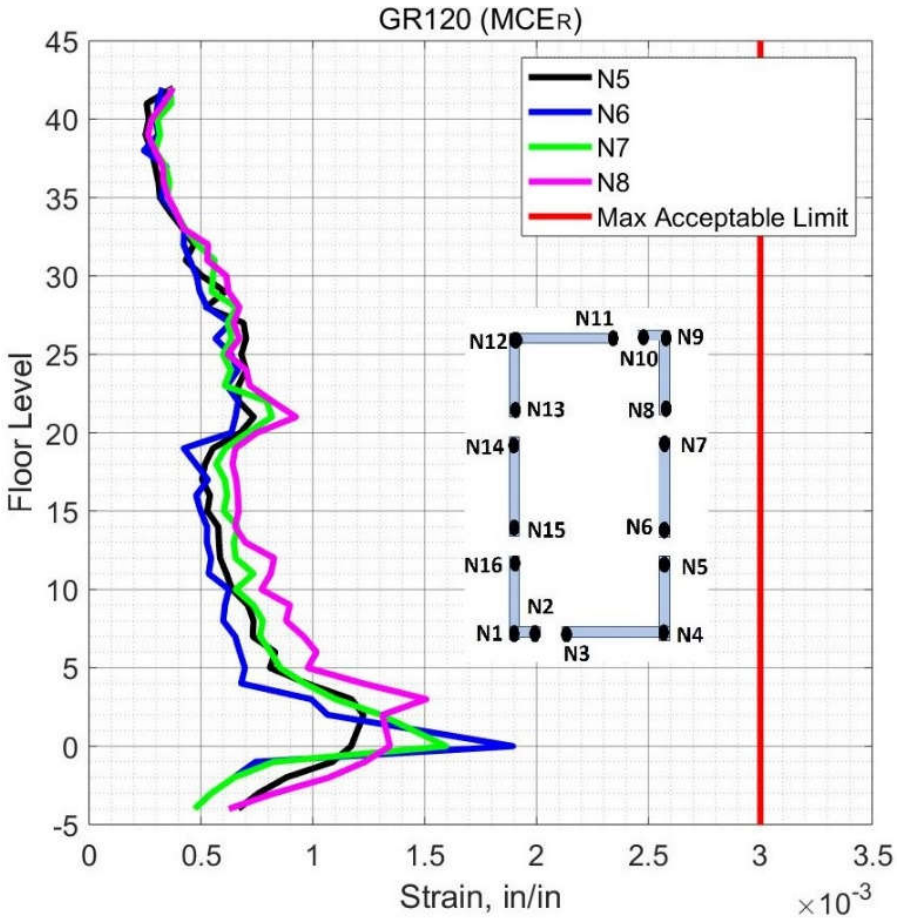

Figure 10.39 Peak Concrete Compression Strain in Core Wall Edges N5-N8 (Case 4 – MCER).

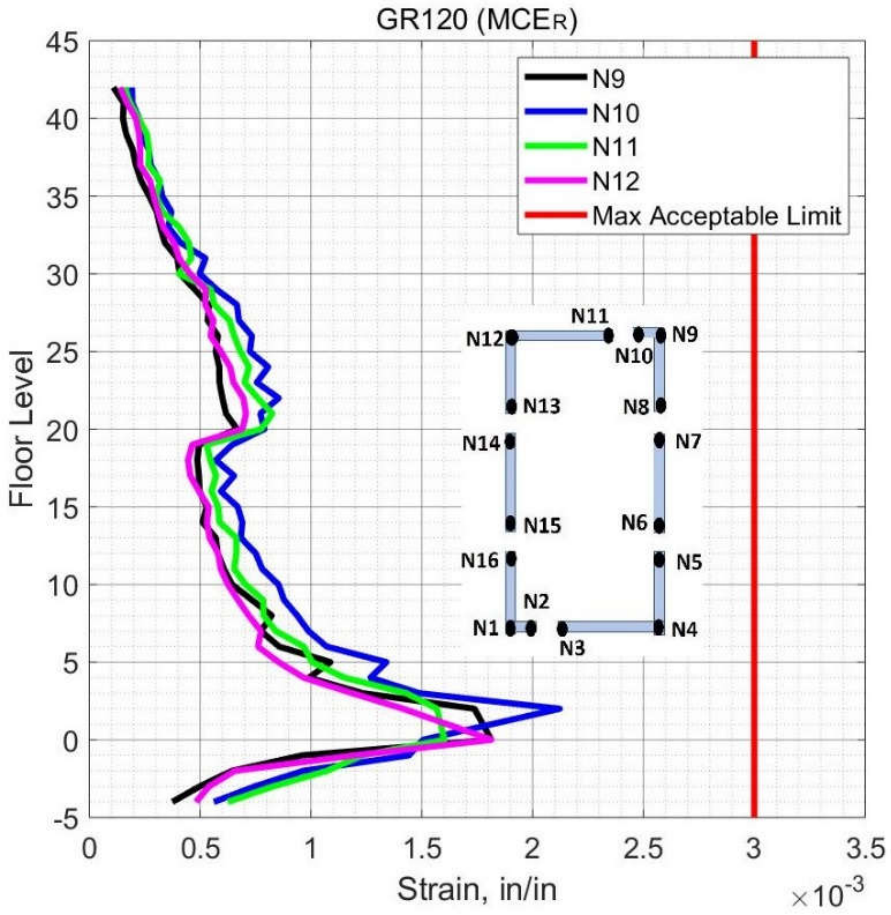

Figure 10.40 Peak Concrete Compression Strain in Core Wall Edges N9-N12 (Case 4 – MCER).

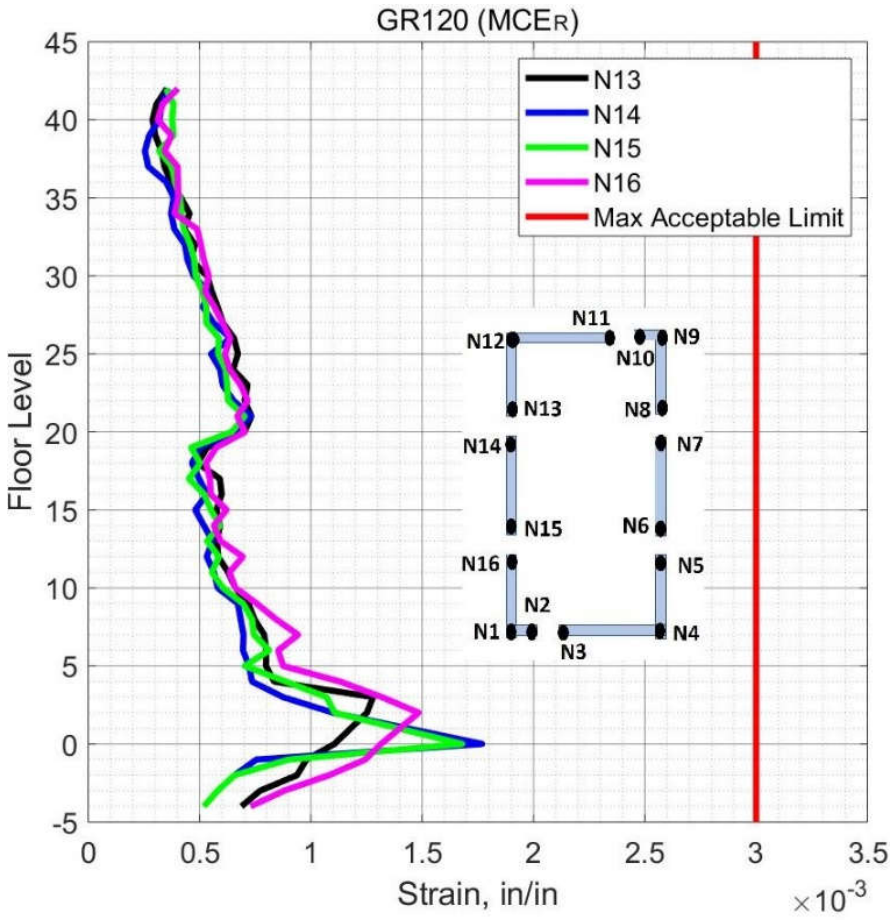

Figure 10.41 Peak Concrete Compression Strain in Core Wall Edges N13-N16 (Case 4 – MCER).

10.3.2.1.3 Coupling Beams

Figure 10.42 (a) shows the mean and maximum values of the rotation of coupling beams with a 1.7 aspect ratio (coupling beams in the x-direction), over the building height. The peak value of the rotation is less than 0.03 which is below the allowable limit of 0.050. The results indicate that coupling beams do experience yielding of steel reinforcement according to the data in Figure 7.18. In addition, the coupling beams expected to have a damage state (DSI), which means that the coupling beams need minor repair. However, the rotation demands of coupling

beams satisfy the requirement of the TBI guidelines for MCER level.

Figure 10.42 (b) shows the mean and maximum values of the rotation of coupling beams with a 2.1 aspect ratio (coupling beams in the y-direction), over the building height. The peak value of the rotation is approximately 0.03 which is below the allowable limit of 0.050. The results indicate that coupling beams do experience yielding of steel reinforcement according to the data in Figure 7.19. In addition, the coupling beams expected to have a damage state (DSI), which means that the coupling beams need minor repair. However, the rotation demands of coupling beams satisfy the requirement of the TBI guidelines for MCER level.

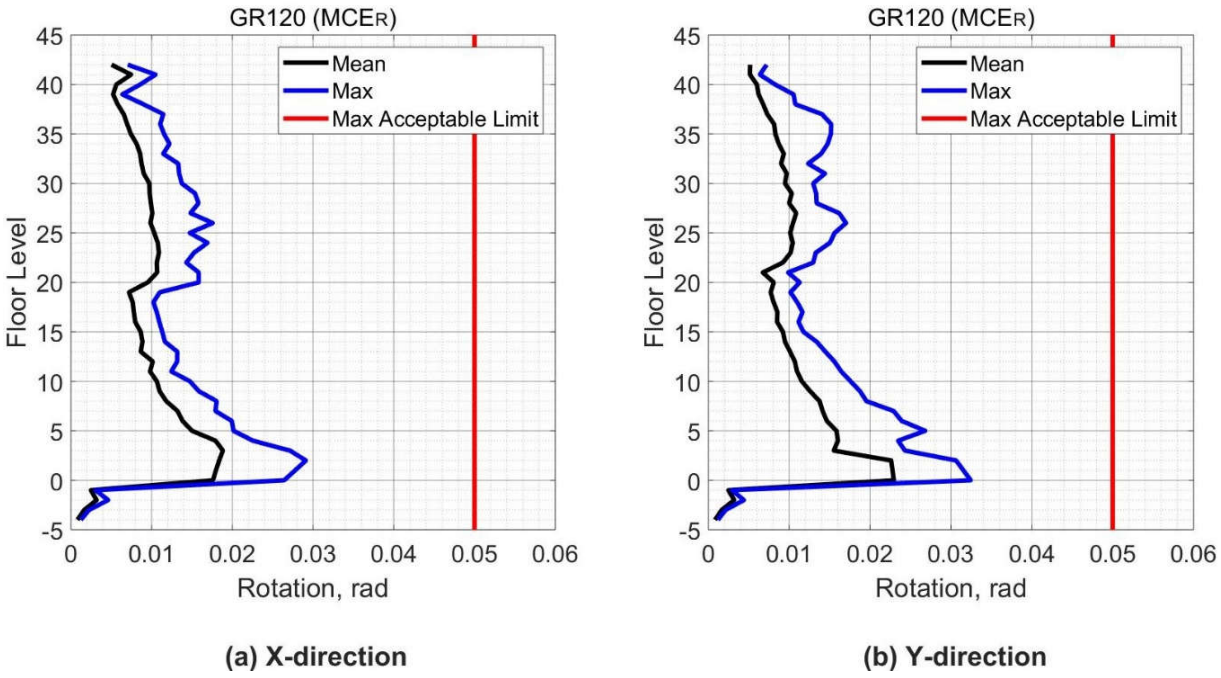

Figure 10.42 Rotation Demand in Coupling Beams (Case 4 – MCER).

10.3.2.2 Special Moment Frame Response

10.3.2.2.1 Beam Force-Based Action

As stated in Section 7.3.2.2.1, To evaluate the shear action in the beams, Equation (7-11) will be applied. Figure 10.43 shows the shear force demands in the beams of the special moment frame over the building height. In the legend of Figure 10.43, the results noted as "Mean" represent the mean value of the maximum shear force in the beams at each floor level from all ground motions analyses, while the results noted as "Max" represent the maximum shear force in the beams obtained from all analyses. In addition, the values shown as "Vfinal" and "Vexp" in the legend were obtained by using Equations (7-10) and (7-5), respectively. As shown in Figure 10.43, the main conclusion is that shear force demands in special moment frame beams meet the requirements of the TBI guidelines by satisfying Equation (7-11). In addition, the maximum shear force demands (360 kips) obtained from all ground motions are within the acceptable limits of the expected shear capacity (667 kips) of the beams. In other words, the maximum shear force demands obtained from all ground motions are within the acceptable limits of the expected shear capacity of the beams. Consequently, all analyses produced an acceptable response based on the shear force demands in the beams.

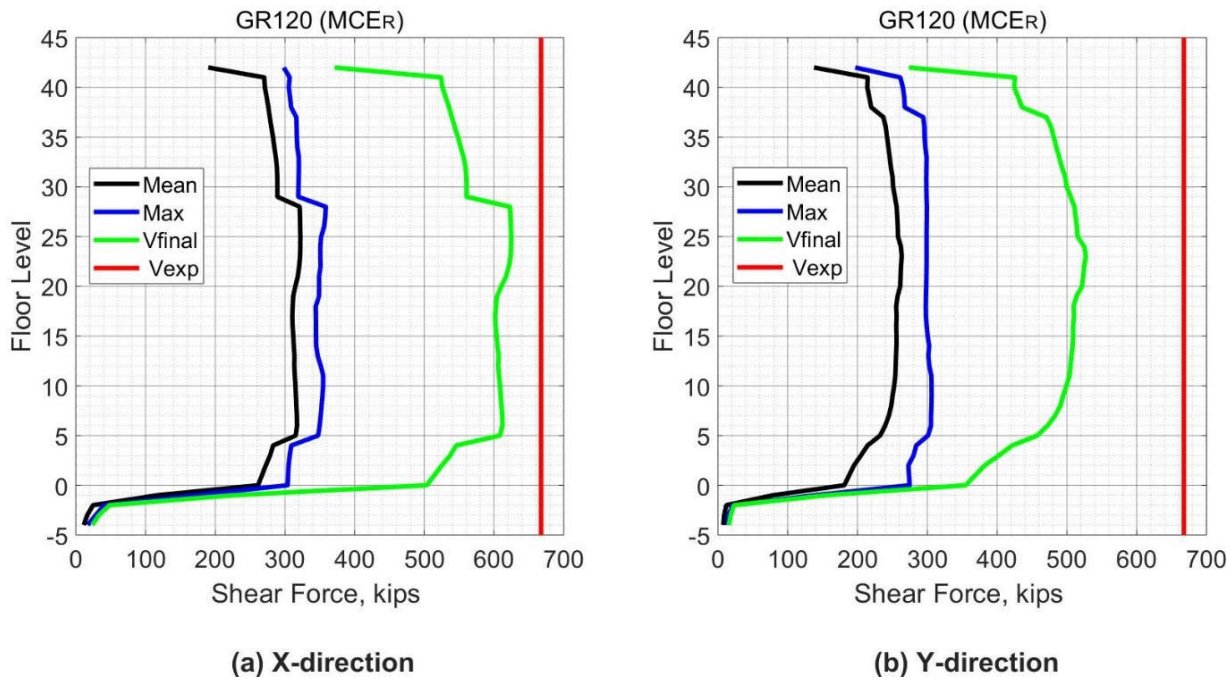

Figure 10.43 Peak Shear Force in Beams (Case 4 – MCER).

10.3.2.2.2 Beam Deformation-Based Action

Figure 10.44 shows the mean and the maximum tensile strain demands in the longitudinal reinforcement of the beams at each floor level. The maximum tensile strain demands (0.035) are within the acceptable limit (0.050). In addition, reinforcing bars in beams oriented in the x-direction experienced more tensile strain (0.035) compared to beams oriented in the y-direction (0.015). The maximum tensile strain demands in the beams are below the minimum fracture elongation 0.07 of ASTM 1035 for Grades 100 and 120. The uniform elongation of Grades 100 and 120 is approximately 0.045 (NEHRP, 2014). The maximum tensile strain demands are below the limit of 75% of the uniform elongation. Considering the results of the tensile strain of the reinforcing bars in the beams, Grade 120 could be a valuable reinforcing material for beams of the special moment frame. The expected yield strain for Grade 120 is 0.0048, so all beams in the levels

above the main podium experienced yielding of reinforcing bars when considering the maximum demands for both directions.

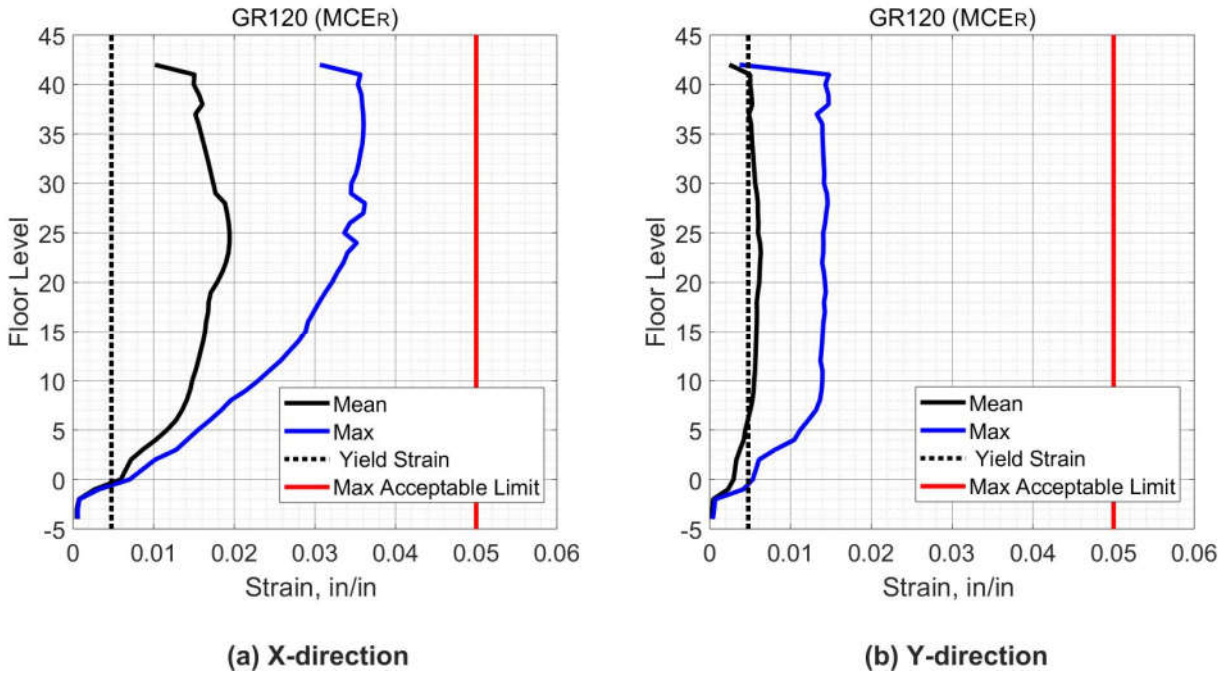

Figure 10.44 Peak Tensile Strain in Reinforcing bars in Beams (Case 4 – MCER).

Figure 10.45 shows the mean and the maximum plastic rotation demands in the beams at each floor level. The plastic rotation demands were within the acceptable limits with a maximum demand of approximately 0.04 rad. A consistent finding with the tensile strain demands is observed in which beams oriented in the x-direction experienced more rotation demands compared with beams in the y-direction. Based on the strain and plastic rotation results, the deformation-based actions in the beams satisfy the requirement of TBI guidelines.

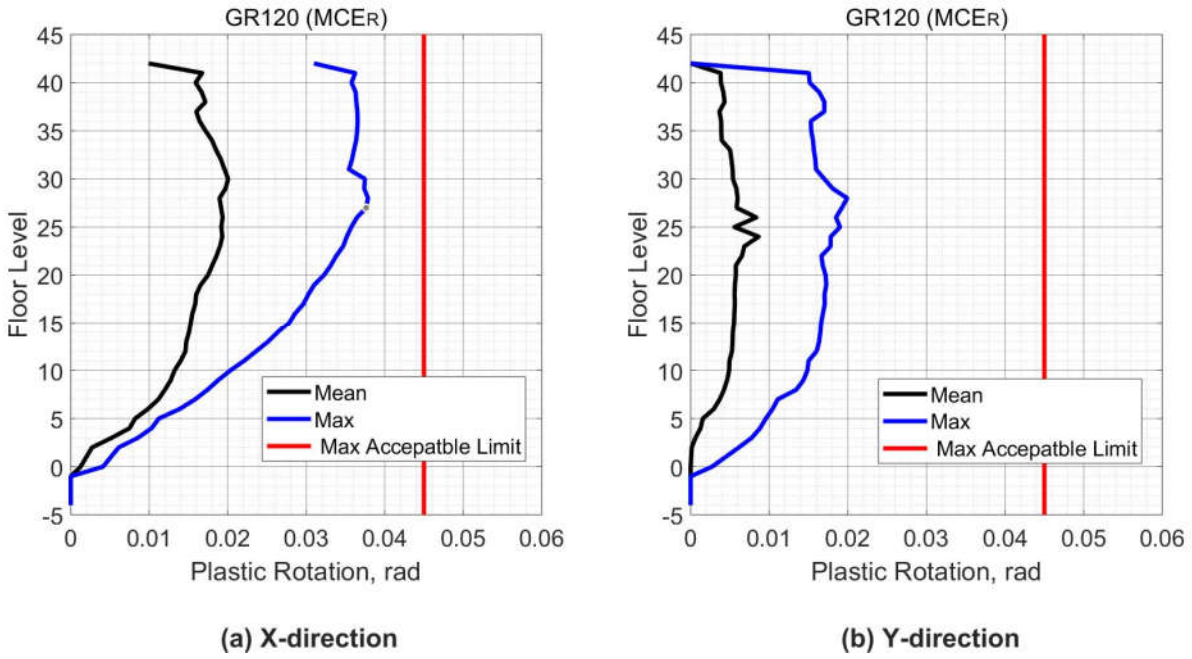

Figure 10.45 Plastic Rotation in Beams (Case 4 - MCER).

10.3.2.2.3 Columns Force-Based Action

In the legend of Figures 10.46 through 10.49, the results noted as "Mean" represent the mean value of the shear force in the columns from all ground motions analyses while the results noted as "Max" represent the maximum shear force obtained from all analyses. In addition, results with "Vfinal" and "Vexp" in the legend represent the parameters in Equation (7-11) for the columns. The shear force demands in the columns are within the limits of the TBI guidelines, by satisfying equation (7-11). The maximum shear demands obtained from all analyses are also within the acceptable limits. Therefore, all analyses produced acceptable responses when considering the shear force demands of the columns. In contrast with the shear force demands of the core wall, the shear forces were more uniform with building height.

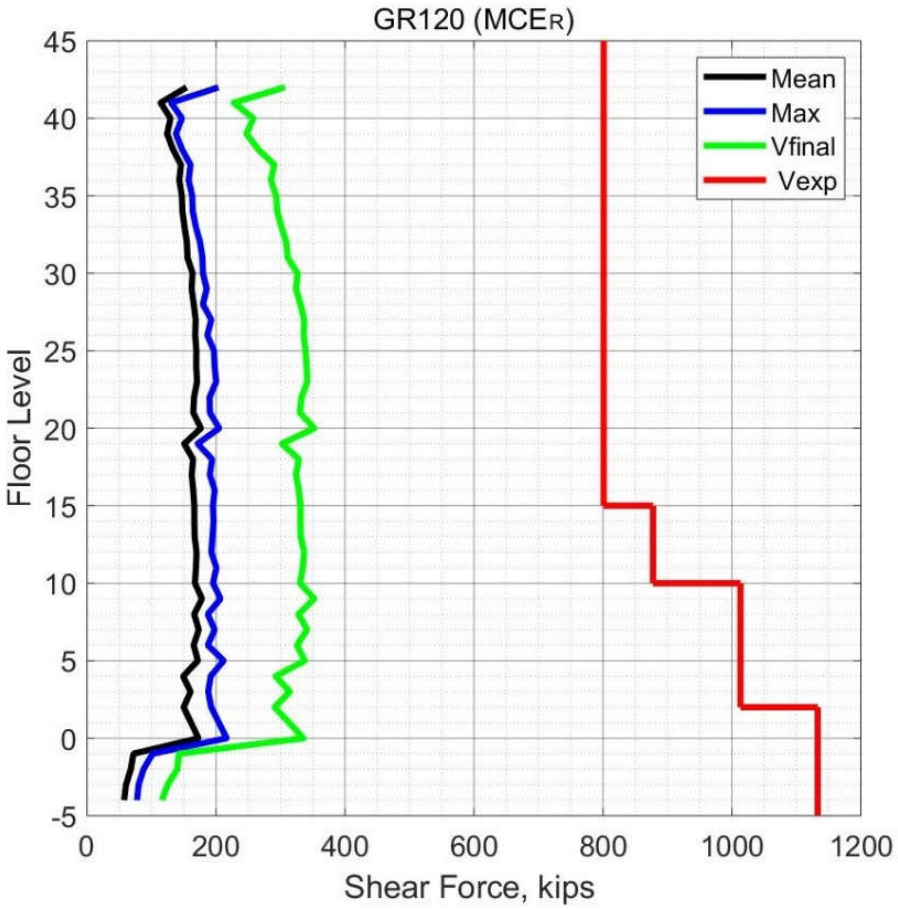

Figure 10.46 Peak Shear Force in Corner Columns (Case 4 – MCER).

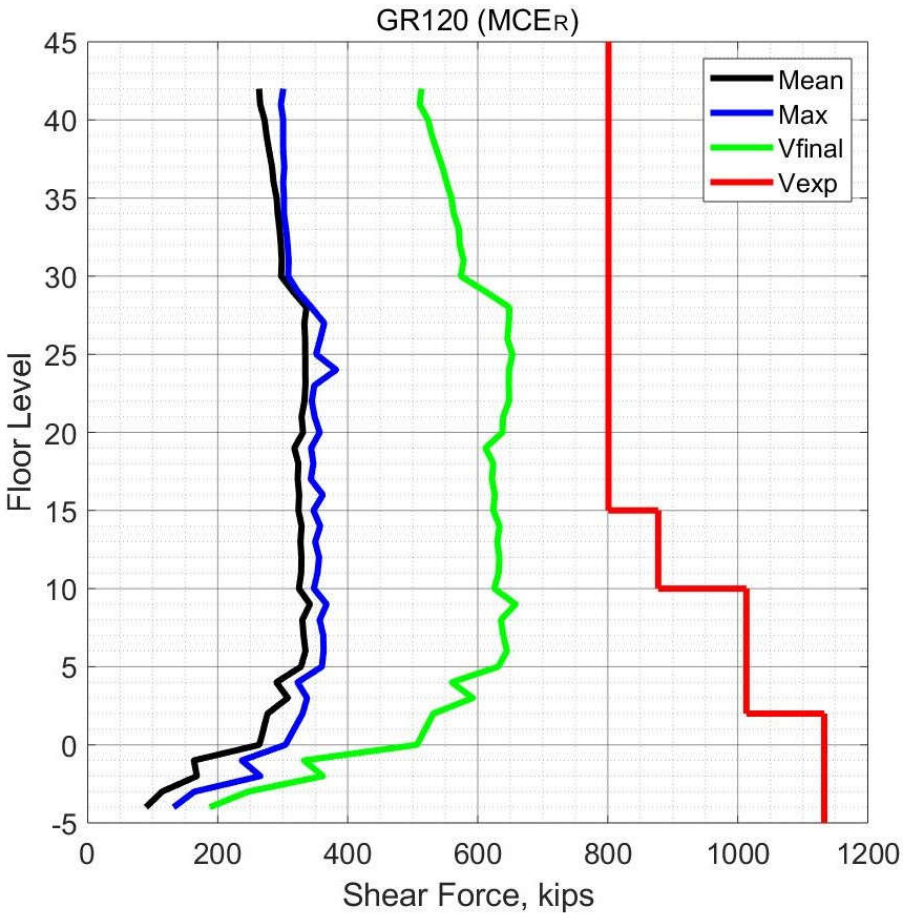

Figure 10.47 Peak Shear Force in Interior Columns X-direction (Case 4 – MCER).

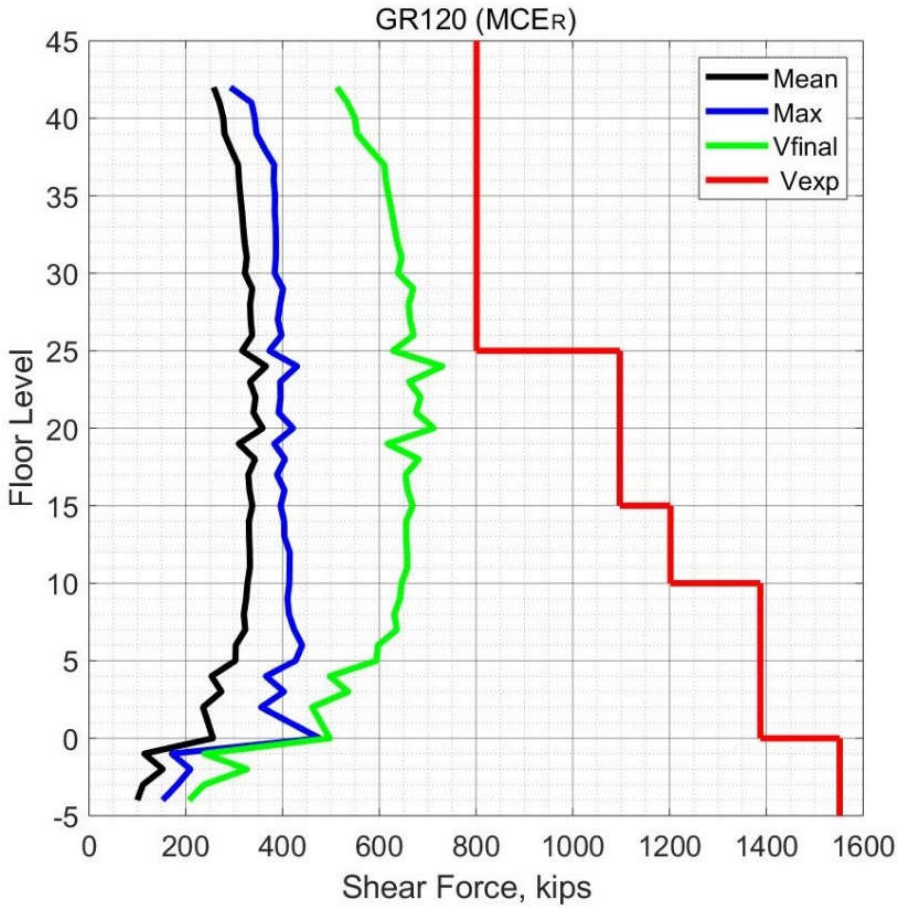

Figure 10.48 Peak Shear Force in Columns on Grid B and E (Case 4 – SLE).

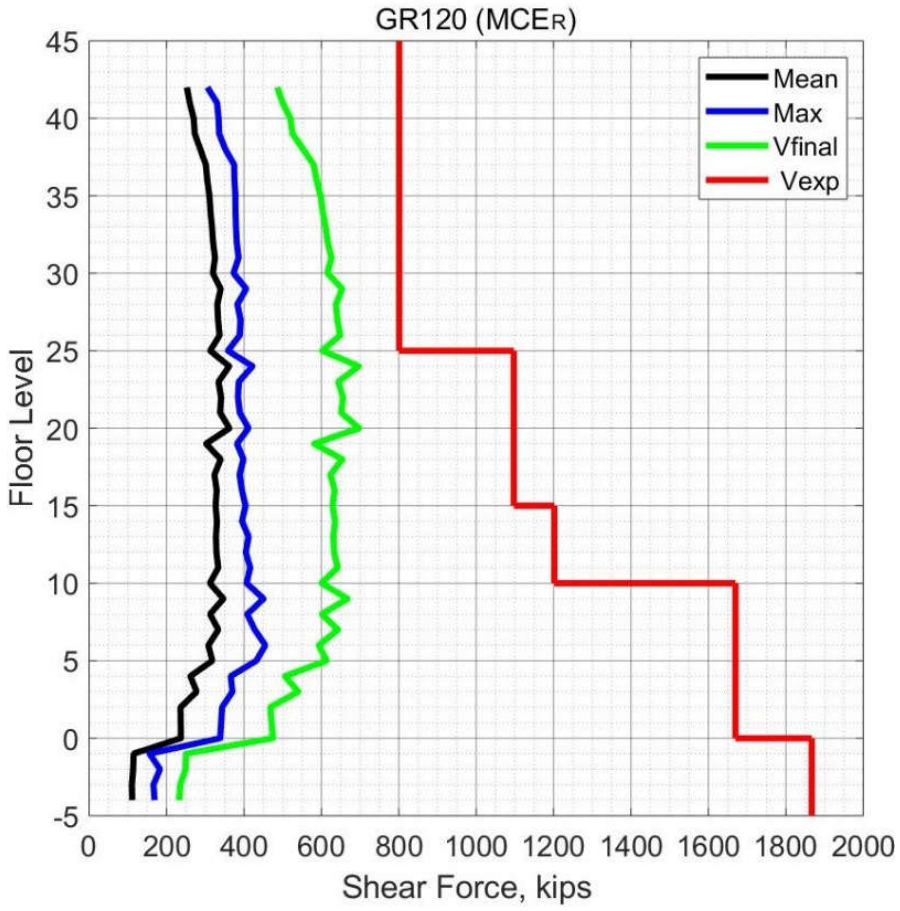

Figure 10.49 Peak Shear Force in Columns on Grid C.5 (Case 4 – MCER).

10.3.2.2.4 Column Deformation-Based Action

The maximum value of the tensile strain in the columns' longitudinal bars and the mean value from all ground motion in the suite are depicted in Figure 10.50. The maximum tensile strain demands (0.0043) did not exceed the expected yield strain of Grade 120 (0.0048), which means no plastic hinges formed in the columns. In other words, columns did not experience plastic rotations. As mention previously, the behavior of non-yielding columns is one of the preferable design approaches for seismic applications where most plastic rotation demands form in the beams.

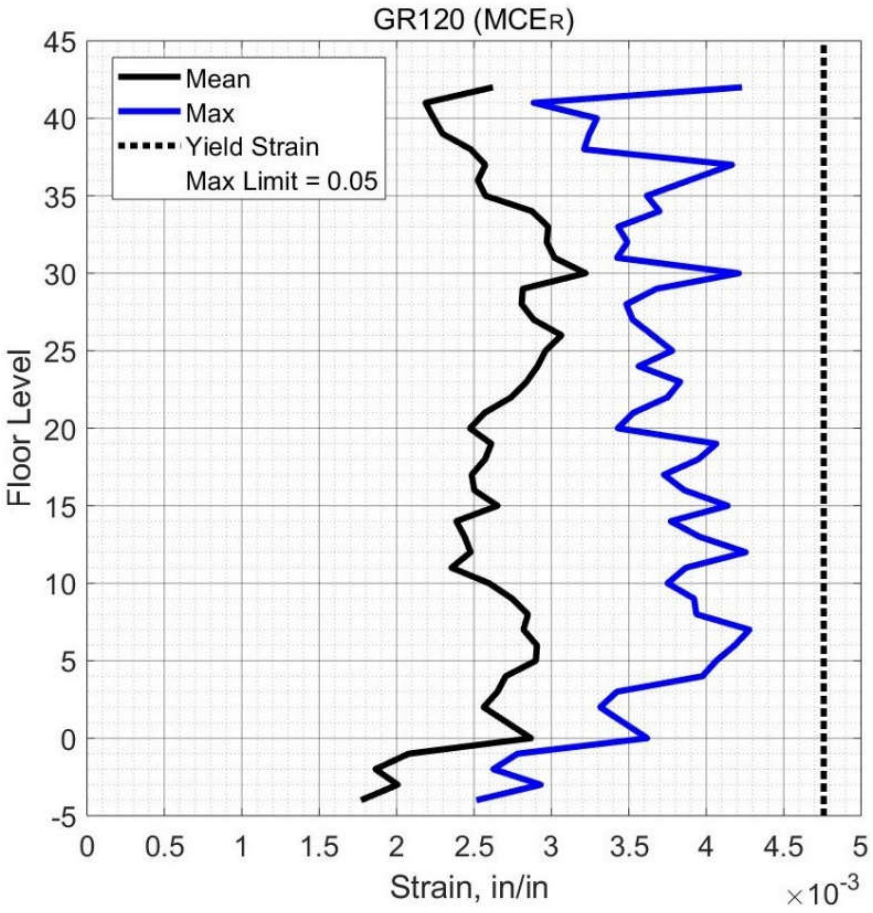

Figure 10.50 Peak Tensile Strain in Reinforcing Bars in Columns (Case 4 – MCER).

10.3.2.3 Contribution of Core Wall and Frame in Dual System

The contribution of the components of the dual system in resisting the story shear force is depicted in Figure 10.51 for the x- and y-directions, respectively. Figure 10.52 shows the contribution percentage of the shear forces for the core wall and the frame over the building height. The frame contribution is approximately constant over the building height, while the core wall contribution varies linearly. The frame contribution in the lower stories is approximately one-third of the story shear, while in the upper stories the frame contribution is about one-half of the total story shear.

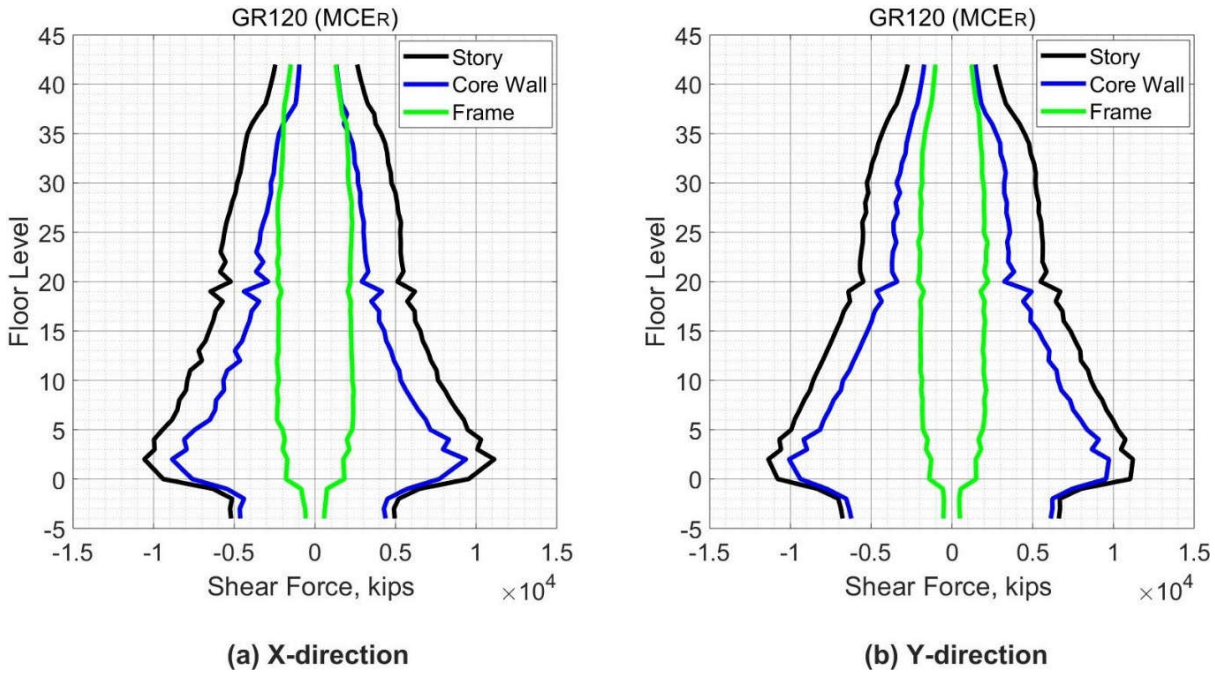

Figure 10.51 Shear Force Contribution of Core Wall & Frame (Case 4 – MCER).

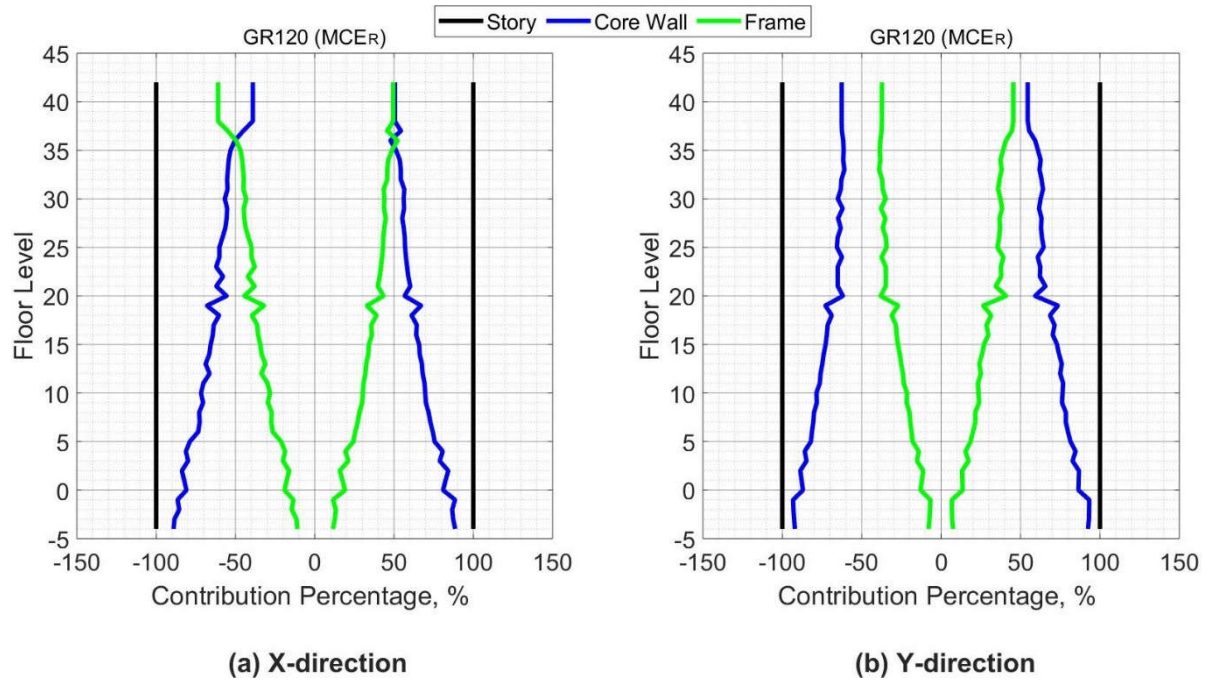

Figure 10.52 Contribution Percentage of Core wall & Frame Shear Force (Case 4 – MCER).

CHAPTER XI

CASE 5 – SHAPE MEMORY ALLOY REINFORCEMENT RESULTS

11.1 INTRODUCTION

Case 5 consists of the study building reinforced with conventional reinforcing steel bars and shape memory alloy bars in the structural members. Due to high cost of SMA bars, they were utilized in the regions where the structural demands are expected to be high and causing considerable amount of yielding of the conventional steel bars. The SMA bars were used as longitudinal reinforcement bars in the plastic hinge regions for all the beams of the special moment frames for all stories above the main podium. In addition, SMA bars were utilized for the vertical reinforcement of the core wall from the base to the thirty second story above the main podium and for the diagonal reinforcement of all coupling beams for all stories above the main podium. For the horizontal reinforcement of the core wall, ASTM A706 Grade 60 was used. For columns, ASTM A706 Grade 60 was used for longitudinal reinforcement for all stories. In this case, the cross-section dimensions of all the structural members were the same as in the case 1, however the area of SMA reinforcement in all members was the same as the area of the conventional reinforcement in the case 1. In the following sections, the response of the case study building reinforced with SMA bars and conventional reinforcing (Grade 60) will be examined and checked with the TBI guidelines acceptance criteria for both SLE and MCER levels. The procedures and equations that used to calculate the structural demand parameters in the previous Chapter (case 1), will be applied for determining the response demands for this case for both SLE and MCER levels.

11.1.1 Boundary Elements of Core Wall for SMA Bars

To calculate the appropriate length of the boundary elements in the core wall the following Equations were used (Moehle 2014).

$$l_{be} \geq \max((c - 0.1l_w), c/2) \quad \textbf{(11-1)}$$

$$c \geq \frac{l_w}{900(\frac{\delta_u}{h_w})} \quad \textbf{(11-2)}$$

Where:

l_{be}	The boundary element length
l_w	The wall length
c	Compression region in the cross section of the wall
h_w	The wall height
δ_u	The top-level design displacement of the wall

The ratio of (*δu/hw)* should not be less than 0.005. Using the 0.005 will also gives the longest length for the boundary elements and was adopted to be more conservative. By using the above equations, the length of the boundary elements for wall piers with length 24.5 ft, 17.5 ft, and 10 ft are 3 ft, 2.2 ft, 1.5 ft, respectively. The selected boundary lengths were 3 ft for all core wall edges to be more conservative and to extend the SMA bars deeper into the wall length. The distance for the longitudinal reinforcement of the core wall up to twentieth story is 14 in., and 18 in. for the other stories. Using four SMA bars inside the three feet boundary element will make the distance 12 in. which is less than the required distance of 14 in. for stories up to twentieth. Using three SMA bars inside the three feet boundary element will make the distance 18 in. which is equal

to the required distance of 18 in. for the upper stories. Figure 11.1 depicts the boundary elements that used for using the SMA bars as longitudinal reinforcing bars instead the conventional steel bars in the core wall. The remaining wall length was reinforced with the conventional steel bars.

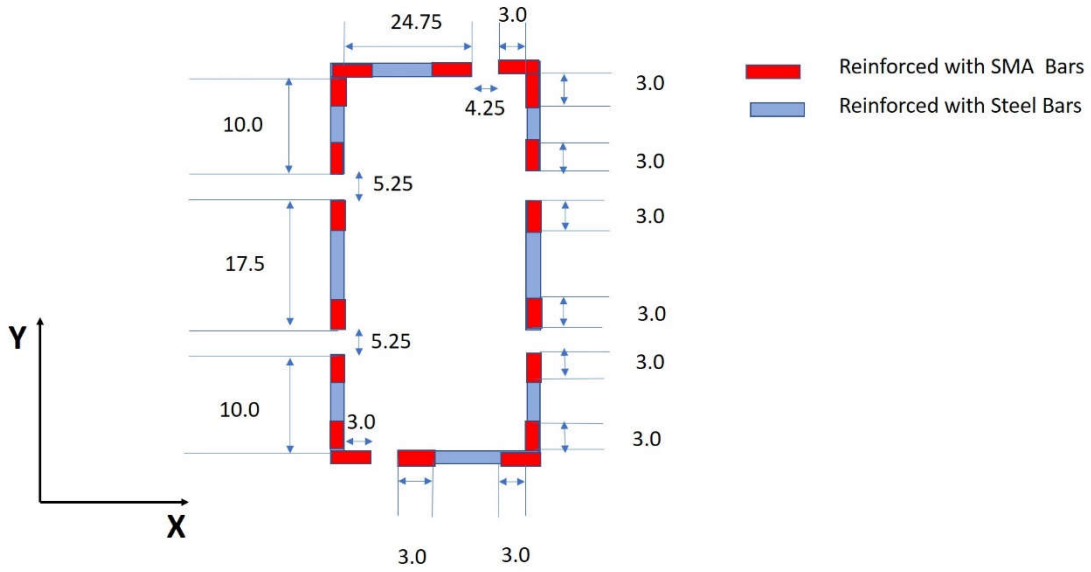

Figure 11.1 Boundary Elements for Core Wall.

11.2 SLE LEVEL

The same ground motions used in the SLE in case 1 were used for the SLE analyses of case 5. The results of seven analyses are represented and compared with the acceptance criteria of the TBI guidelines. According to the TBI guidelines, first, the mean value of the response parameters from all ground motions in the suite should be checked with the acceptance criteria. Second, the TBI guidelines do not require checking the maximum response parameters from all ground motions in this level. However, the maximum response parameters will also be presented to examine the performance of the case study building in more depth.

11.2.1 Global Response

11.2.1.1 Drift Ratio

Figure 11.2 shows the mean and the maximum values of the drift ratios from all analyses over the building height. The mean peak interstory drift from the seven analyses was very close to 0.0047 in the x-direction and approximately 0.0030 in the y-direction, where both values were within the acceptable limit of the TBI guidelines of 0.0050. Figures 11.3 and 11.4 show the peak drift ratios from all ground motions over the building height.

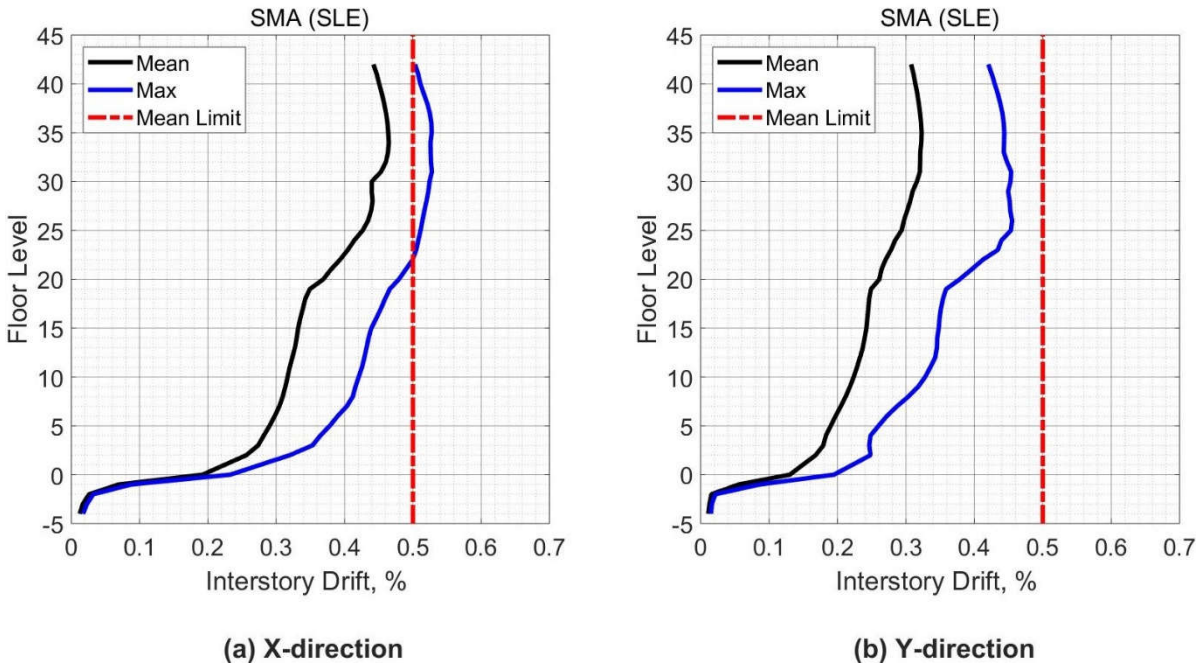

Figure 11.2 Peak Interstory Drift (Case 5 – SLE).

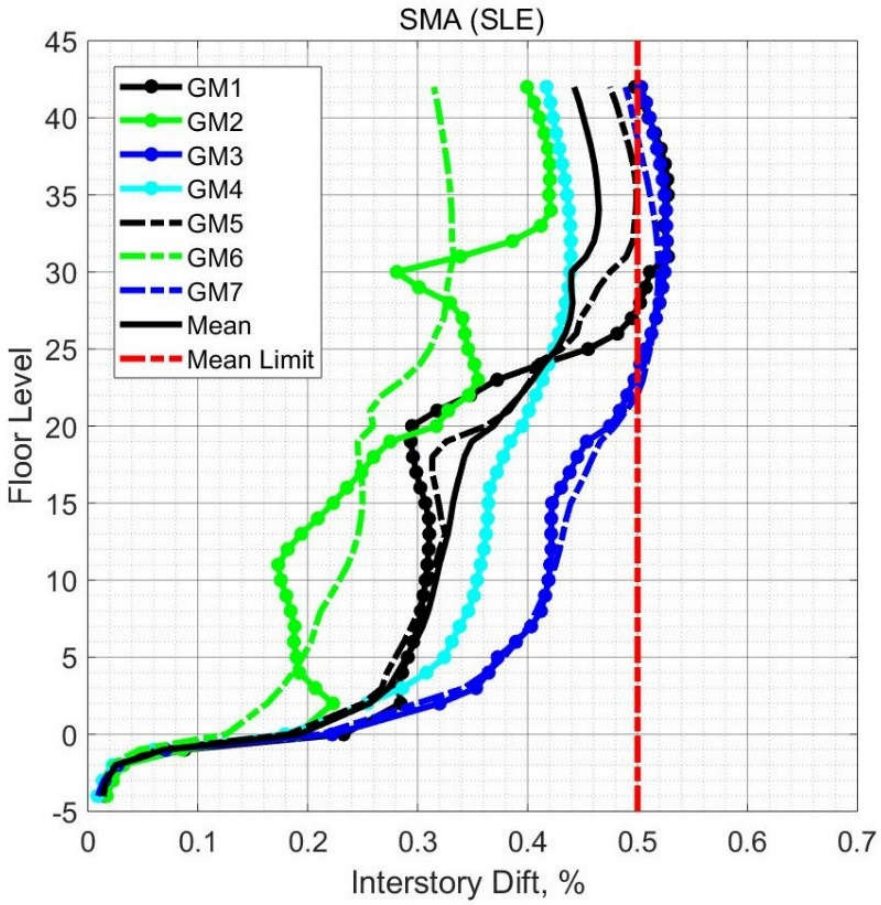

Figure 11.3 Peak Interstory Drift from All Ground Motions for X-direction (Case 5 - SLE).

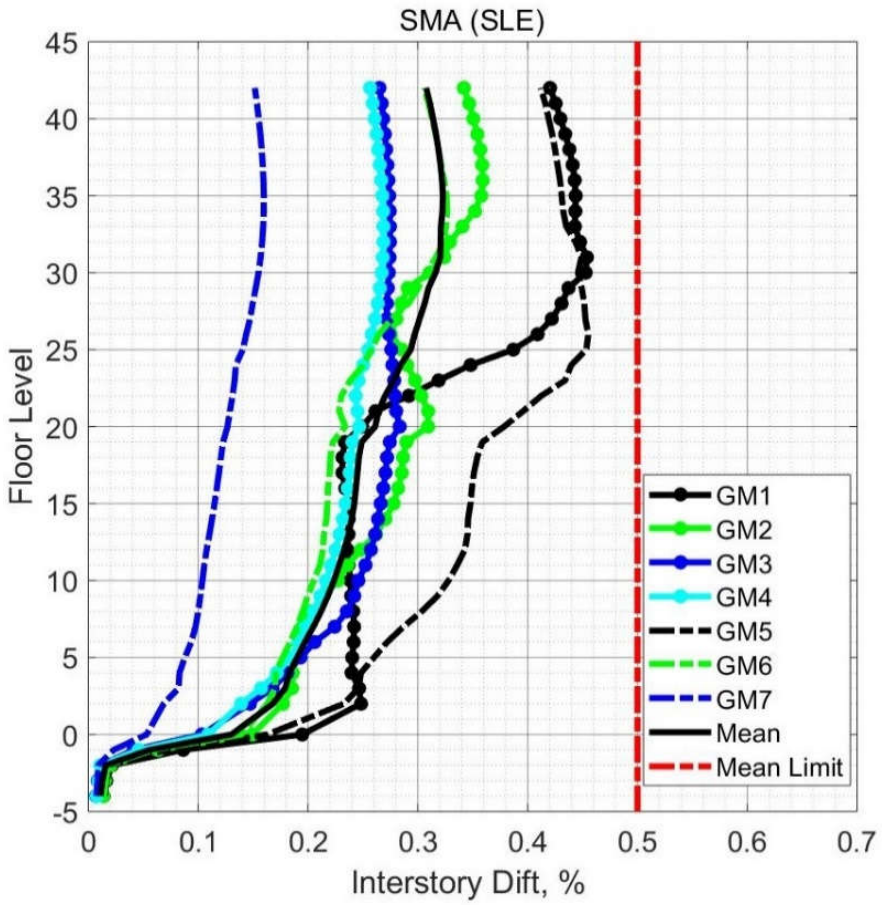

Figure 11.4 Peak Interstory Drift from All Ground Motions for Y-direction (Case 5 - SLE).

11.2.1.2 Displacement

As in Section 7.2.1.2, Figure 11.5 depicts the mean value of the displacement of each story at the same time step that the roof experiences a maximum displacement value.

Figures 11.6 and 11.7 show the time history of the roof displacement in the x-direction and y-direction, respectively from a ground motion at which the displacement demand of the roof was the highest one among other ground motions. During the seventh ground motion, the roof experience a maximum displacement in the x-direction while during the fifth ground motion the maximum roof displacement in the y-direction was observed.

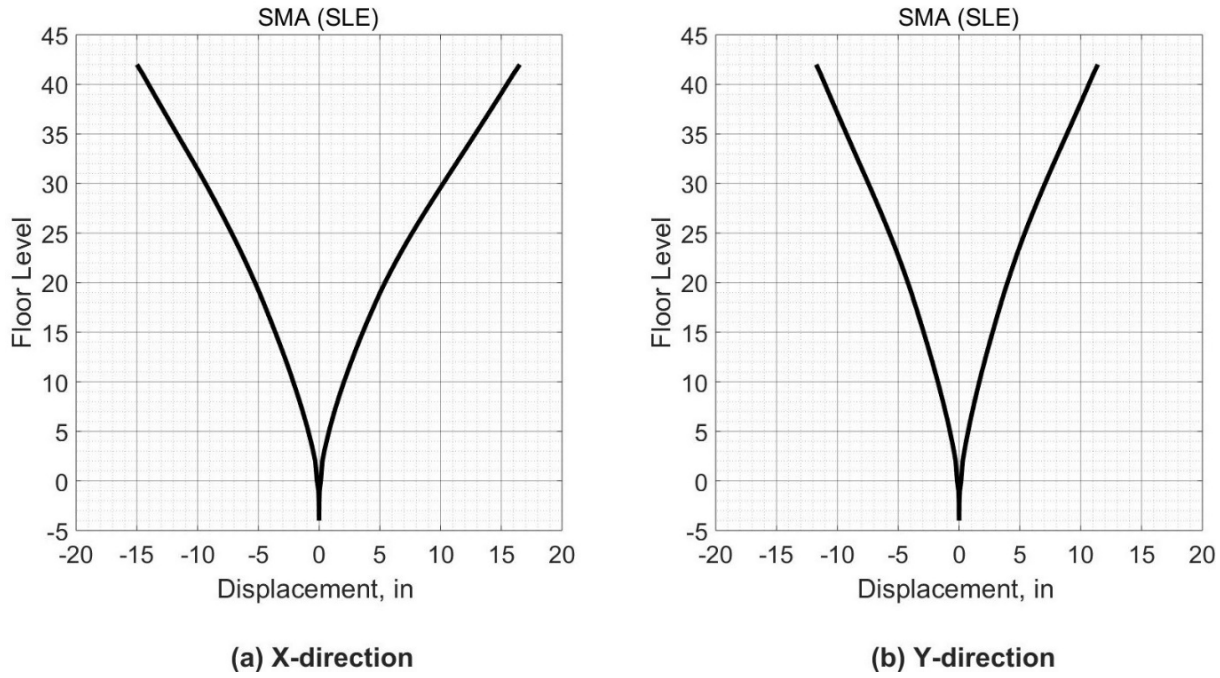

Figure 11.5 Floors Displacement Synchronous with Peak Roof Displacement (Case 1 - SLE).

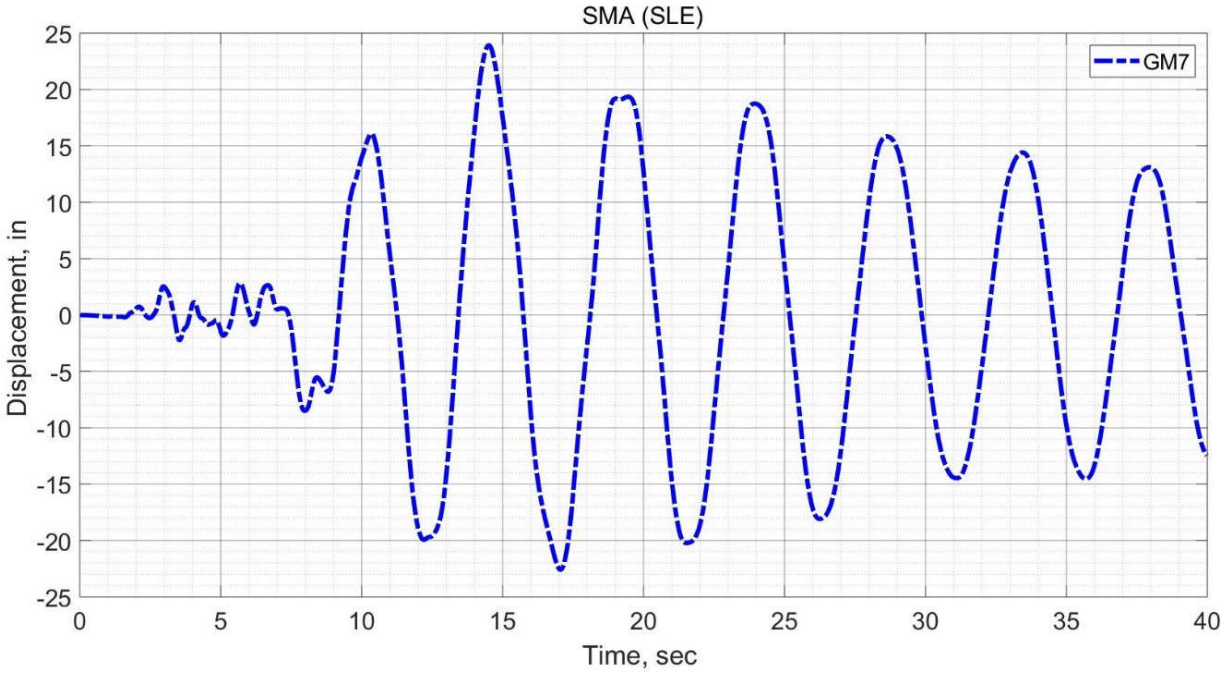

Figure 11.6 Time History For Peak Roof Displacement for X-direction (Case 5 – SLE).

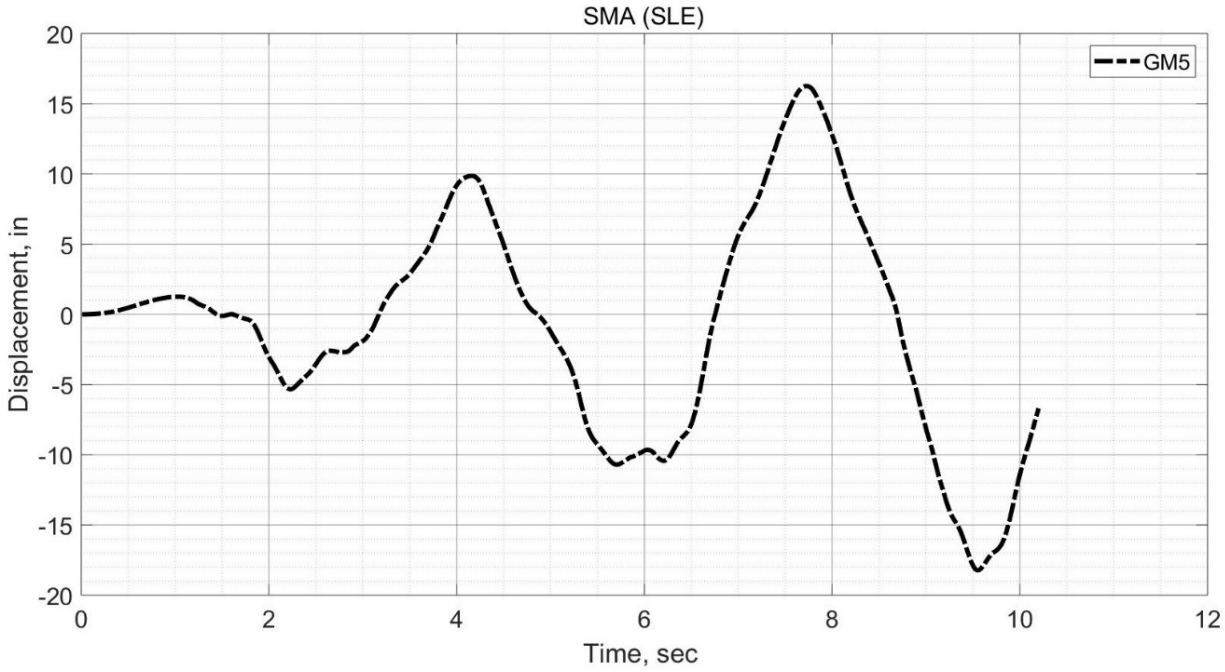

Figure 11.7 Time History for Peak Roof Displacement for Y-direction (Case 5 – SLE).

11.2.2 Element Level

As stated in Section 7.2.2, the TBI guidelines require using only the mean value from all analyses for evaluation with the acceptance criteria for both the force and deformation based-actions in this level. The maximum response parameters for both actions will also be presented to examine the response of the case study building in more depth. In the subsections below, the elements of the seismic force resisting system with their actions are presented and evaluated using the acceptance criteria of the TBI guidelines.

11.2.2.1 Core Wall Response

11.2.2.1.1 Core Wall Force-Based Action

The TBI guidelines specify that shear in the core walls of tall buildings is a force-based action. To evaluate the shear demands of core walls, the TBI guidelines required that the shear

force demands satisfy the Equation (7-1). It is important to mention that the horizontal reinforcement of the core wall was the conventional steel bars leading to the possibility of using Equation (7-1) to calculate the capacity of the wall. Figure 11.8 shows the core wall shear forces over the building height and the values of ($\phi Vexp$). The shear demands in the core wall satisfy Equation (7-1) as required by the TBI guidelines. In addition, the shear force demands varied approximately in a linear manner with the height of the building. For the mean response, the demand was approximately the same in both the x- and y-directions. The peak shear force of the mean values was 6440 kips, and 6570 kips, for x and y-direction, respectively. The maximum response was also less than the limit of the mean response. A change in the shear response of the core wall was noticed at the twentieth story due to the wall thickness changing from 24 in. to 18 in.

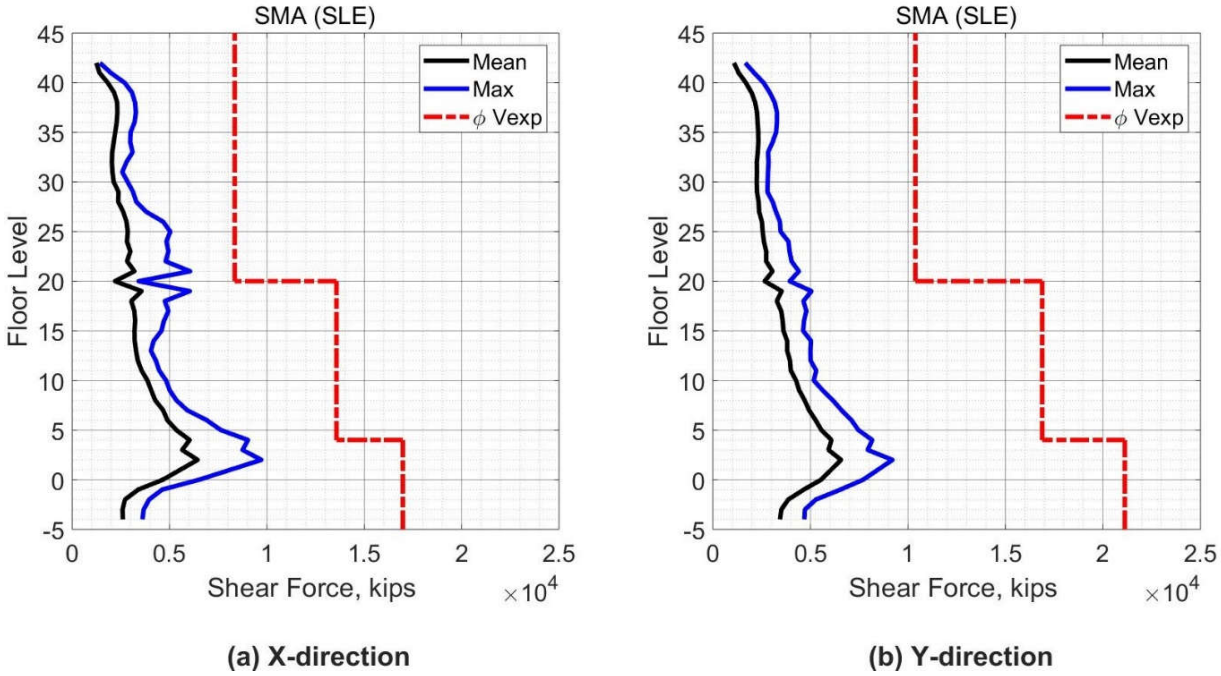

Figure 11.8 Shear Forces in Core Wall (Case 5 – SLE).

11.2.2.1.2 Core Wall Deformation-Based Actions

Figures 11.9 to 11.12 show the mean values of the maximum tensile strain in the core wall reinforcement steel at locations shown in Figure 7.9 over the building height. The TBI guidelines consider the yielding of steel bars as damage that should be avoided in the SLE shaking level. the SMA bars do not actually have a yield limit, however the stress strain relationship of the SMA remains linear till the strain reaches the limit of 0.01. After that, the stress strain relationship has low slope compared with the initial line. Therefore, the strain of 0.01 could be considered as the yield limit for the SMA bars. It is important to note that SMA bars have a capacity to recover 0.06 strain. The tensile strain demands in the SMA bars in the core wall did not exceed 0.003. Consequently, with these values of tensile strain, the SMA bars are still in the linear portion, therefore the requirements of the TBI guidelines are satisfied.

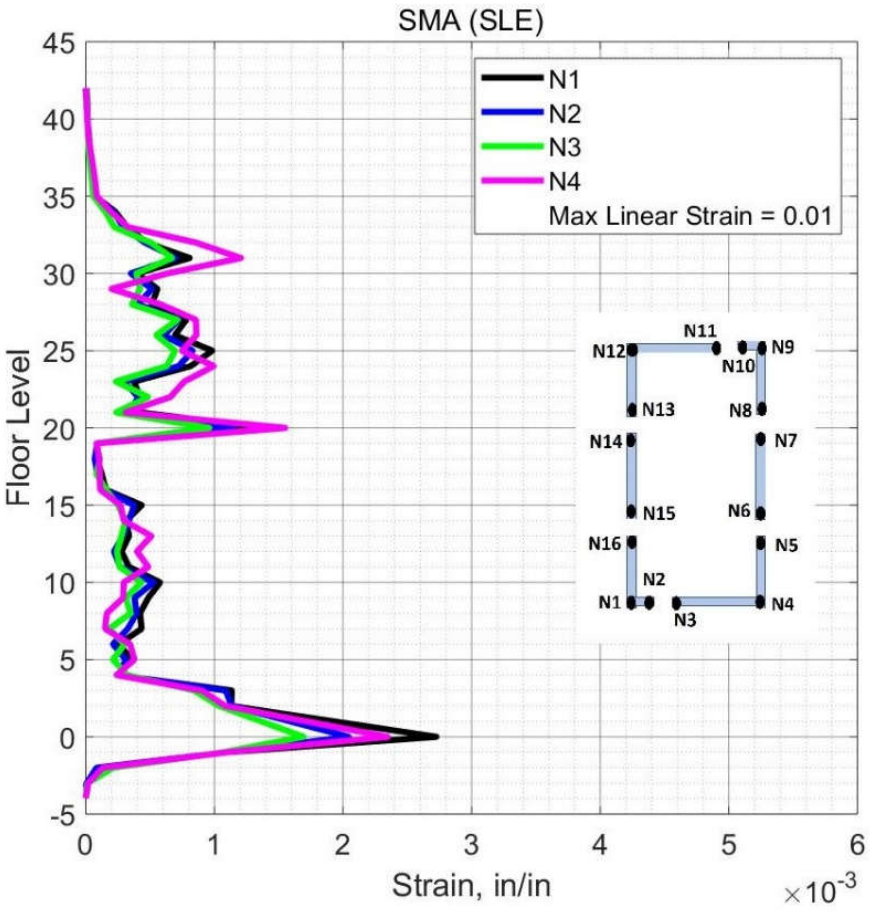

Figure 11.9 Mean Tensile Strain in SMA Bars in Core Wall Edges N1-N4 (Case 5 – SLE).

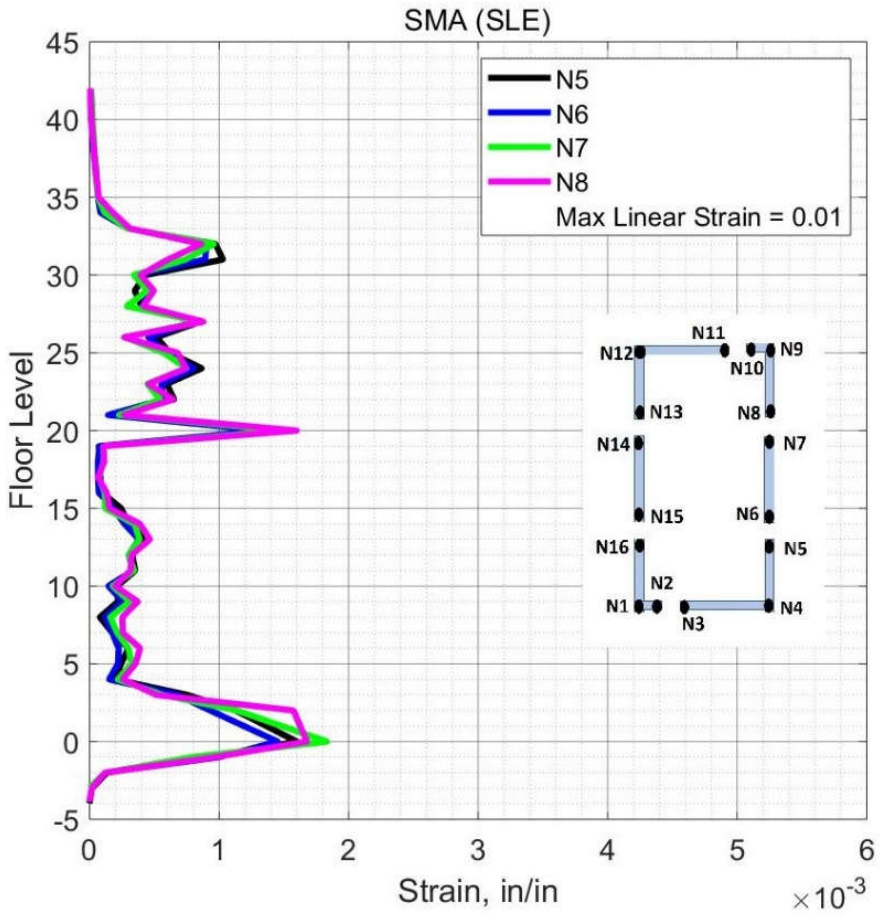

Figure 11.10 Mean Tensile Strain in SMA Bars in Core Wall Edges N5-N8 (Case 5 – SLE).

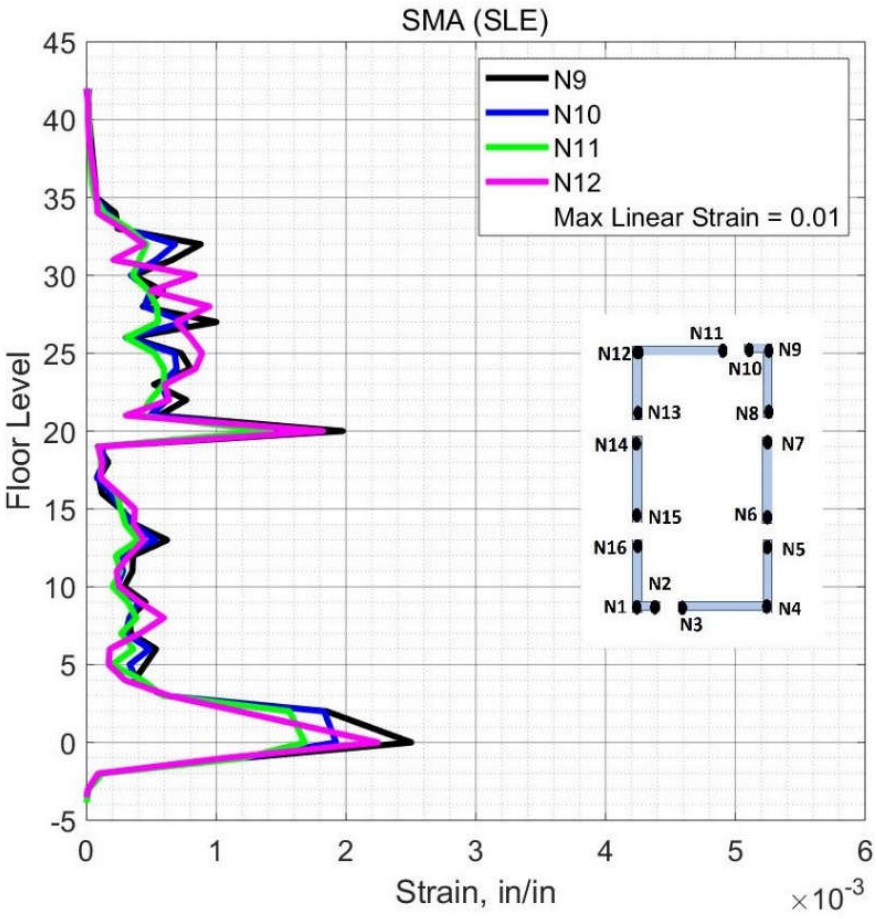

Figure 11.11 Mean Tensile Strain in SMA Bars in Core Wall Edges N9-N12 (Case 5 – SLE).

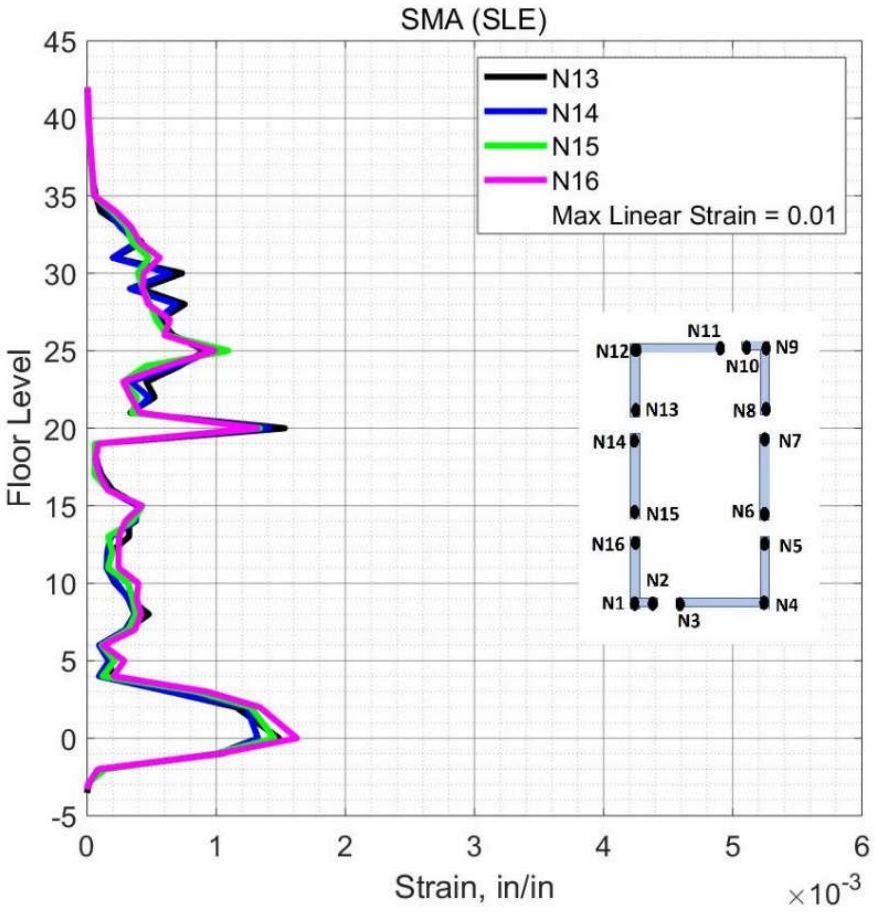

Figure 11.12 Mean Tensile Strain in SMA Bars in Core Wall Edges N13-N16 (Case 5 – SLE).

Figures 11.13 to 11.16 show the mean values of the maximum compression strain in the core wall concrete at locations shown in Figure 7.9 over the building height. The TBI guidelines consider the cracking of concrete as damage that should be avoided in the SLE shaking level. The concrete compression strain in the core wall was very low (< 0.00075), therefore the requirements of the TBI guidelines are satisfied.

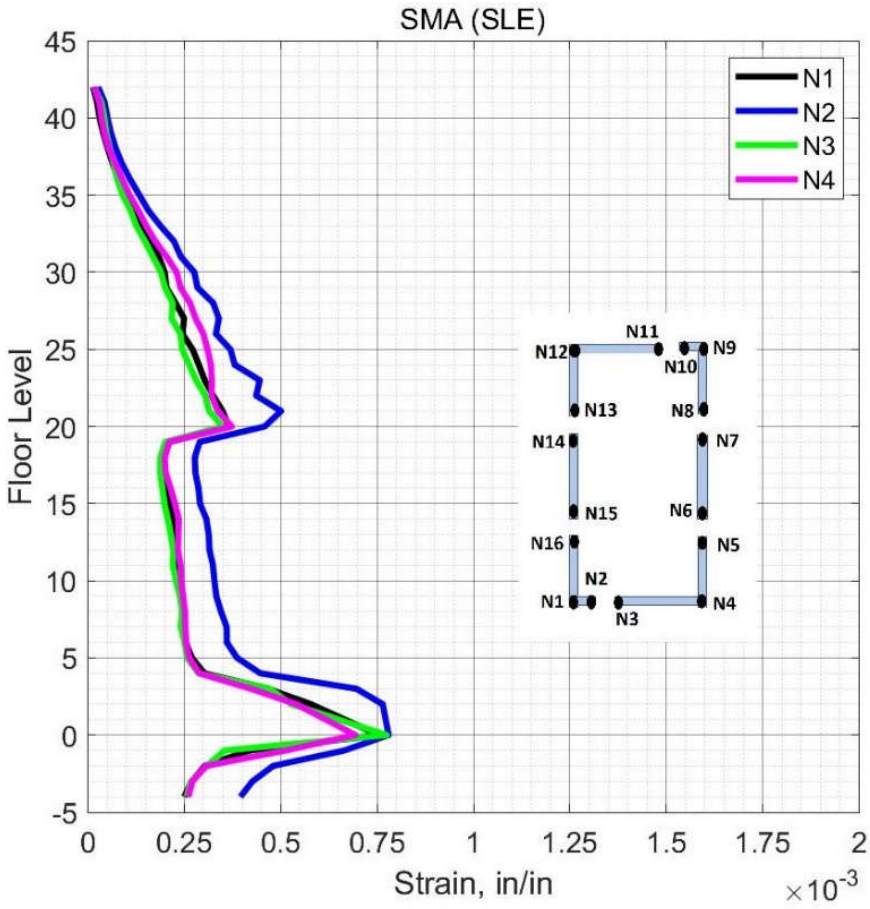

Figure 11.13 Mean Concrete Compression Strain in Core Wall Edges N1-N4 (Case 5 – SLE).

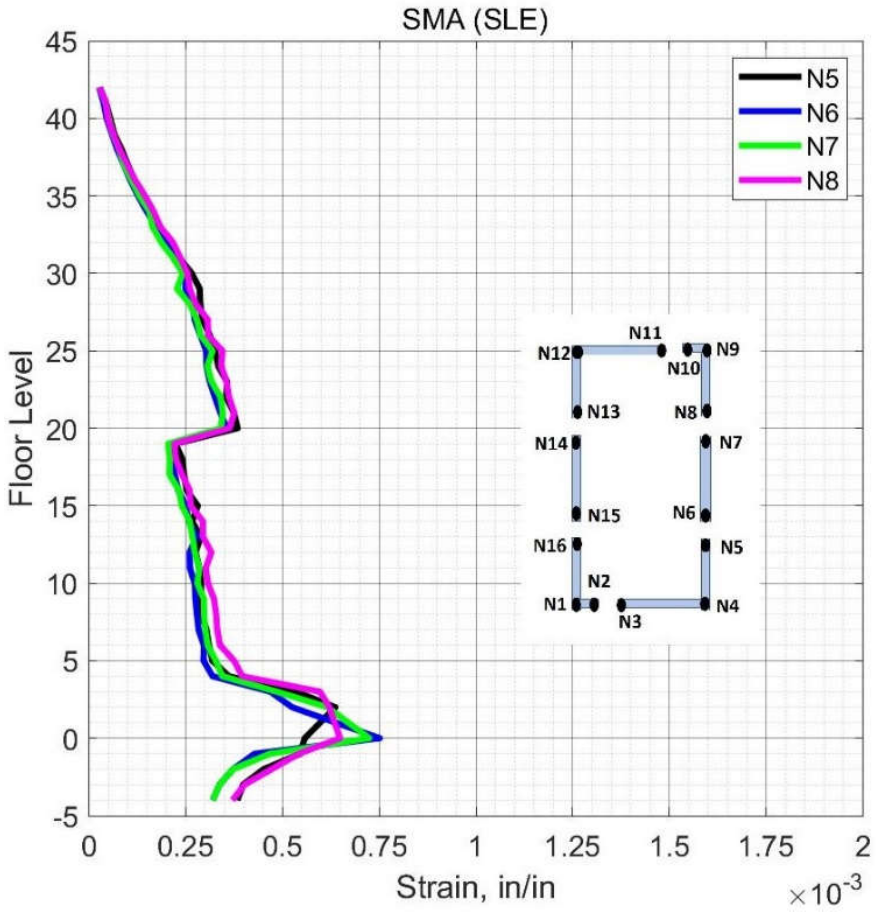

Figure 11.14 Mean Concrete Compression Strain in Core Wall Edges N5-N8 (Case 5 – SLE).

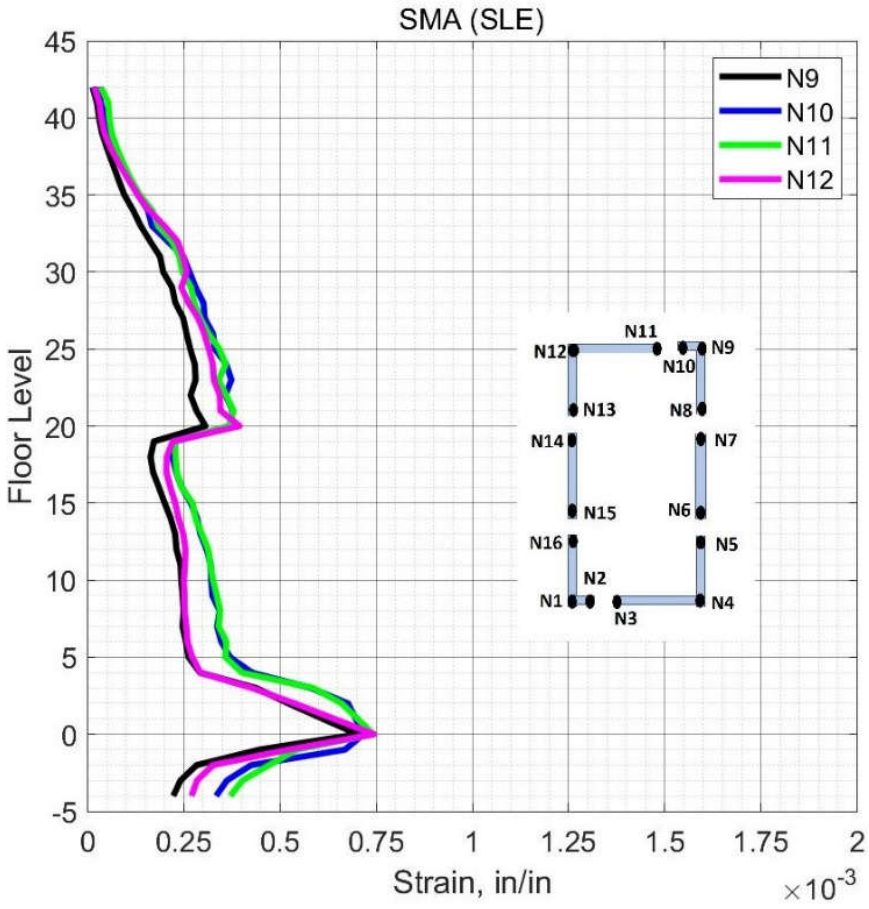

Figure 11.15 Mean Concrete Compression Strain in Core Wall Edges N9-N12 (Case 5 – SLE).

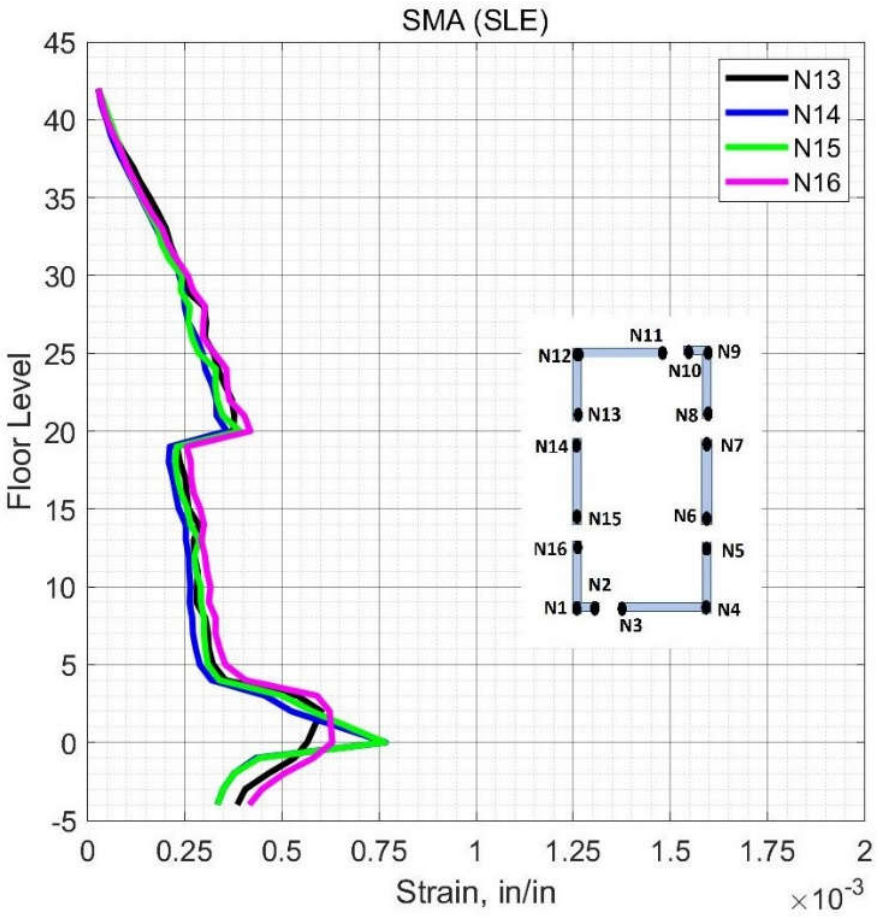

Figure 11.16 Mean Concrete Compression Strain in Core Wall Edges N13-N16 (Case 5 – SLE).

11.2.2.1.3 Coupling Beams

Figure 11.17 (a) shows the mean and maximum values of the rotation of coupling beams with a 1.7 aspect ratio (coupling beams in the x-direction), over the building height. The peak value of the mean rotation is 0.0017 which is below the max allowable limit of 0.006. In addition, considering the data in Figure 7.18, one could conclude that the coupling beams do not experience yielding strain.

Figure 11.17 (b) shows the mean and maximum values of the rotation of coupling beams

with a 2.1 aspect ratio (coupling beams in the y-direction), over the building height. The peak value of the mean rotation is 0.0015 which is below the max allowable limit of 0.006. In addition, considering the data in Figure 7.19, one could conclude that the coupling beams do not experience yielding strain.

In addition, the diagonal reinforcement of SMA bars are capable to recover 0.06 strain. Therefore, the rotation demands of coupling beams satisfy the requirement of the TBI guidelines.

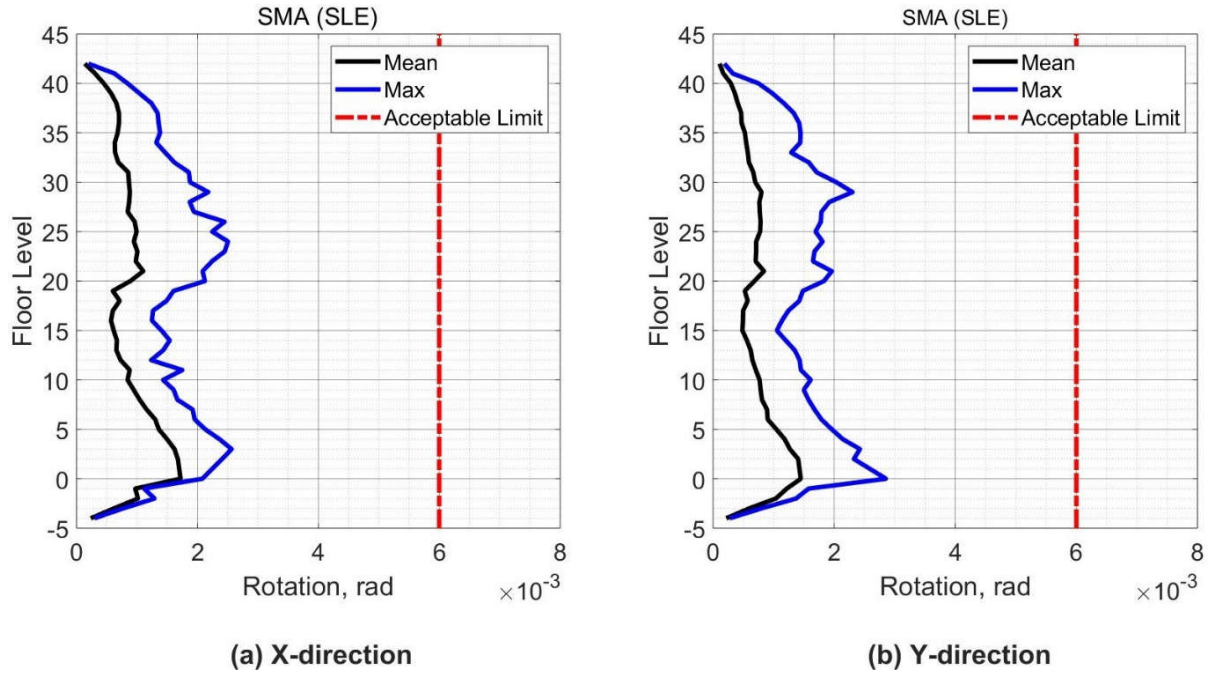

Figure 11.17 Rotation Demand in Coupling Beams (Case 5 – SLE).

11.2.2.2 Special Moment Frame Response

11.2.2.2.1 Beam Force-Based Action

The TBI guidelines specify the shear in the beams of special moment frames as a force-based action. The shear demands should satisfy Equation **(7-1)**. The conventional steel bars were used for the shear reinforcement of the beams and columns of the special moment frame, therefore, the expected shear strength (V_{exp}) of beams or columns could be calculated by using Equation (7-5) from ACI 318-14. Figure 11.18 shows the mean and the maximum values of beams shear forces from all ground motions over the building height and the limiting values of ($\phi Vexp$). In addition, the mean shear force demands in the beams of the special moment frame satisfy the requirements of the TBI guidelines by satisfying Equation **(7-1)**. A slight increase in shear forces demands for the beams in the x-direction is noticed compared with beams in the y-direction. The maximum shear demand in the beams was 200 kips while the reduced shear capacity of the beams was 500 kips.

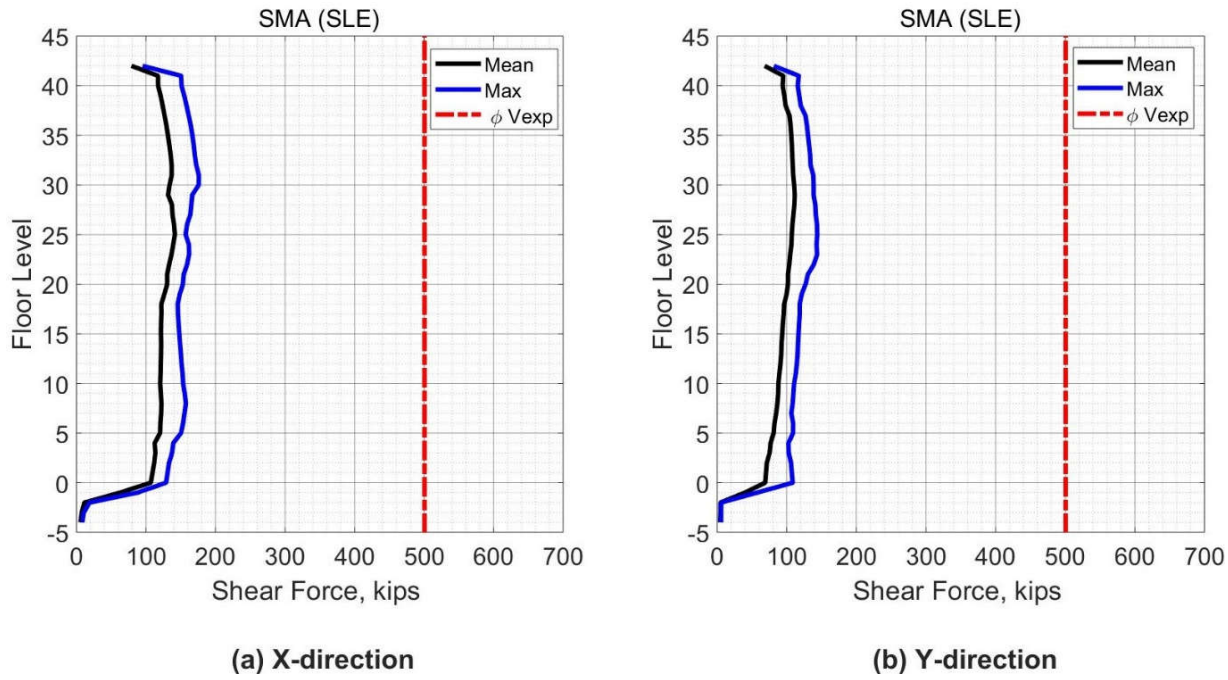

Figure 11.18 Peak Shear Force in Beams (Case 5 – SLE).

11.2.2.2.2 Beam Deformation-Based Action

Figure 11.19 shows the mean and maximum tensile strain demands in the longitudinal reinforcement of SMA bars in the beams sections that are in the beam ends over the building height. The TBI guidelines consider the yielding of steel bars as damage that should be avoided in the SLE shaking level. As stated in Section 11.2.2.1.2, for the SMA bars, the strain limit of 0.01 represents the end of the linear portion in the stress strain relationship. The mean tensile strain of the SMA reinforcement in all beams do not exceed the value of 0.0025, which means that SMA bars are still in the linear portion, therefore, the requirements of the TBI guidelines are satisfied. A small increase in the tensile strain of the reinforcing bars in the beams oriented in the x-direction is noticed compared with the beams oriented in the y-direction. During this level of shaking, the SMA bars in the plastic hinge regions of the beams are still in the linear portion, in other words,

the beams do not experience plastic rotation.

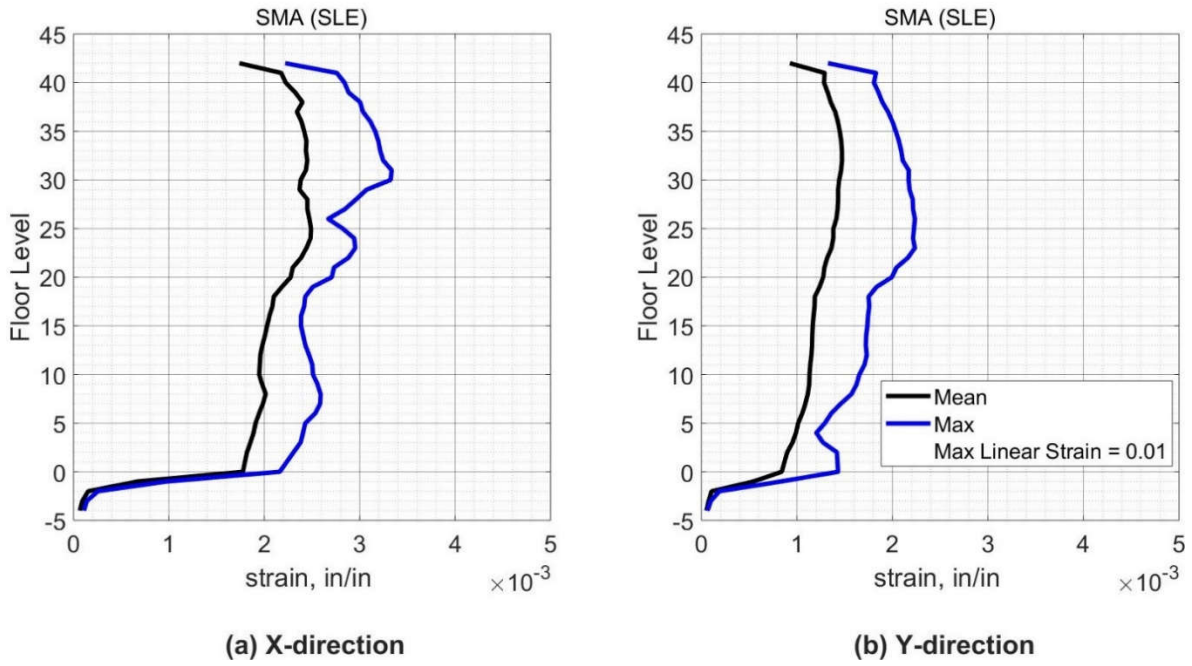

Figure 11.19 Peak Tensile Strain in Reinforcing bars (SMA) in Beams (Case 5 – SLE).

11.2.2.2.3 Columns Force-based Action

As mentioned previously, the conventional steel bars were used for the shear reinforcement of the columns of the special moment frame, therefore, the expected shear strength (V_{exp}) of the columns could be calculated by using Equation (7-5) from ACI 318-14. Figures 11.20 to 11.23 show the mean and maximum values of the shear forces from all analyses in the building columns and the limiting values of ($\phi Vexp$) over the building height. The shear forces in the columns satisfies the requirements of the TBI guidelines by satisfying Equation (7-1).

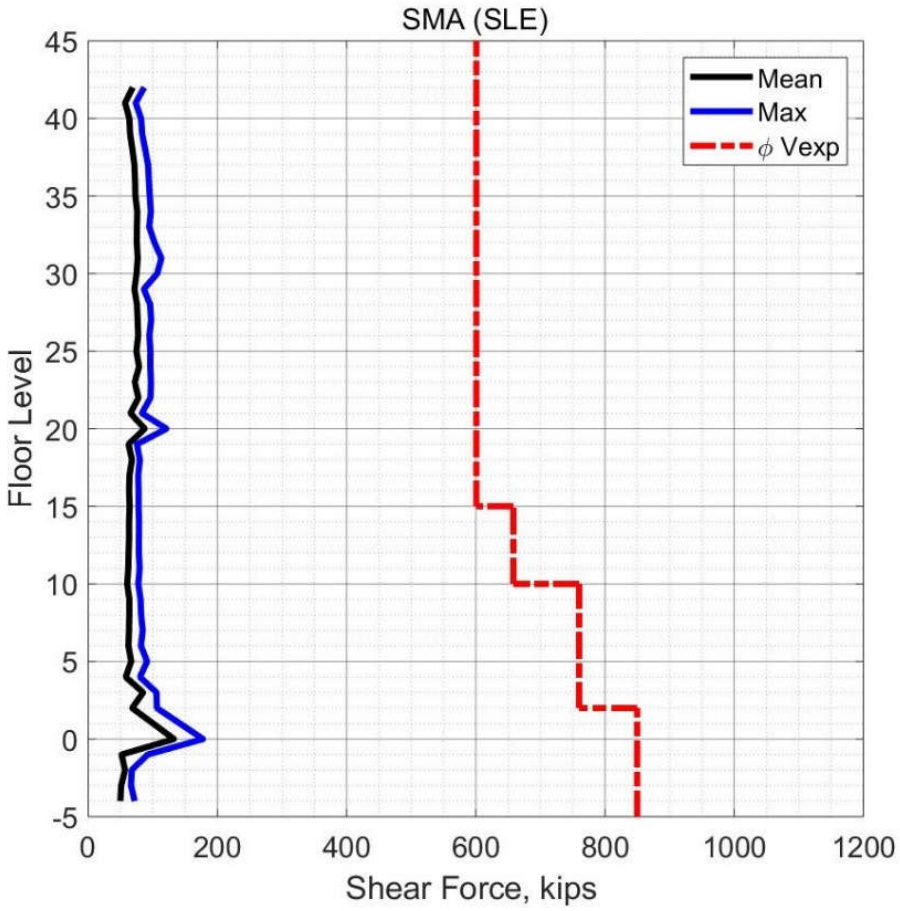

Figure 11.20 Peak Shear Force in Corner Columns (Case 5 – SLE).

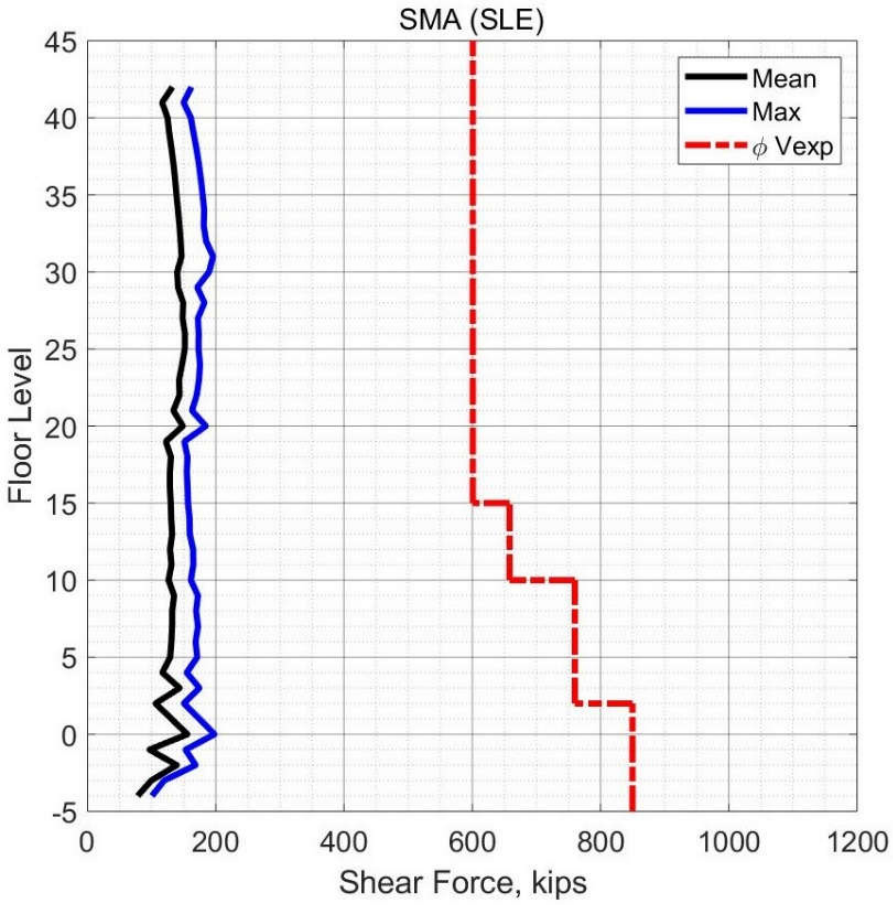

Figure 11.21 Peak Shear Force in Interior Columns X-direction (Case 5 – SLE).

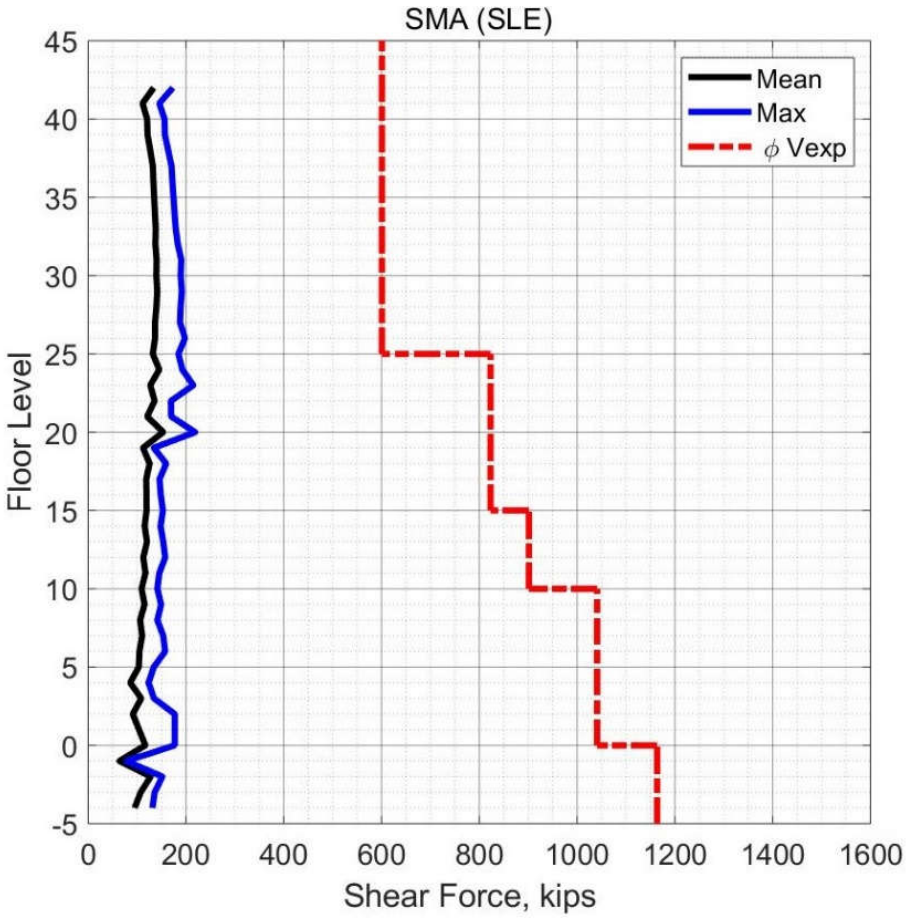

Figure 11.22 Peak Shear Force in Columns on Grid B and E (Case 5 – SLE).

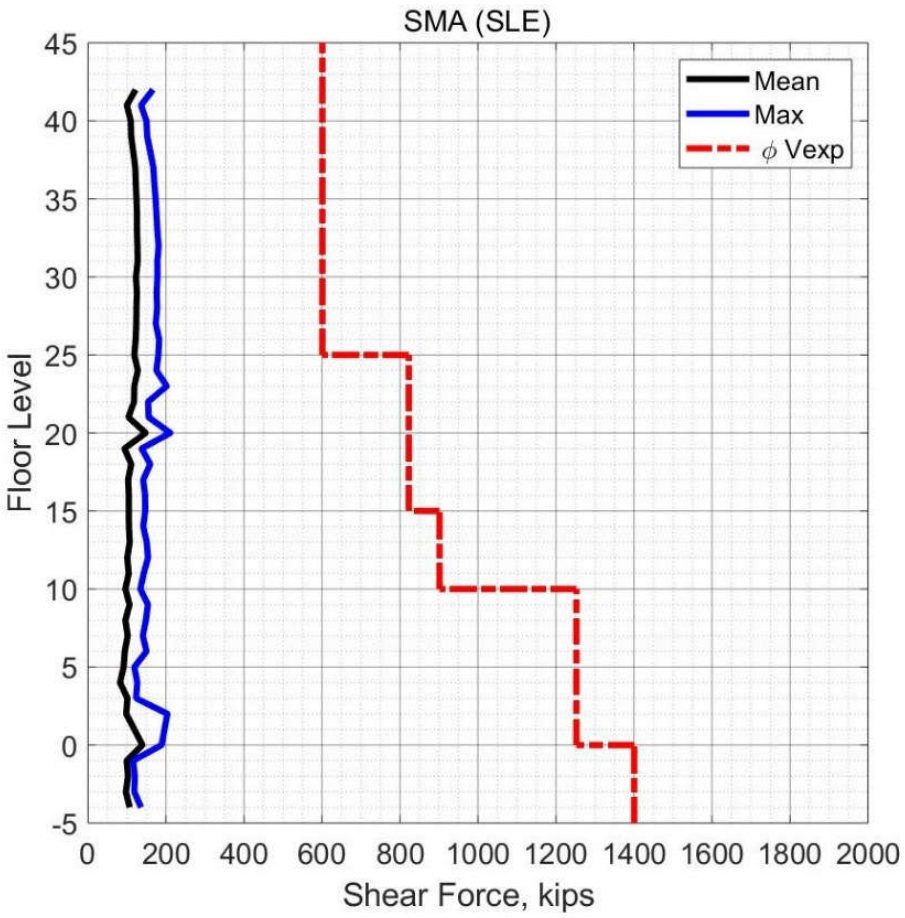

Figure 11.23 Peak Shear Force in Columns on Grid C.5 (Case 5 – SLE).

11.2.2.2.4 Column Deformation-Based Action

Figure 11.24 shows the maximum value of the tensile strain in the longitudinal bars in columns and the mean value from all ground motion in the suite over the building height. The TBI guidelines consider the yielding of steel bars as damage that should be avoided in the SLE shaking level. The tensile strain demands did not exceed the expected yield strain of Grade 60 (0.0024) which means no damage could be expected in the columns. Consequently, there is no plastic rotation in all the columns for this shaking level. depending on the results of the tensile strain of the reinforcing bars, the columns satisfy the requirements of the TBI guidelines.

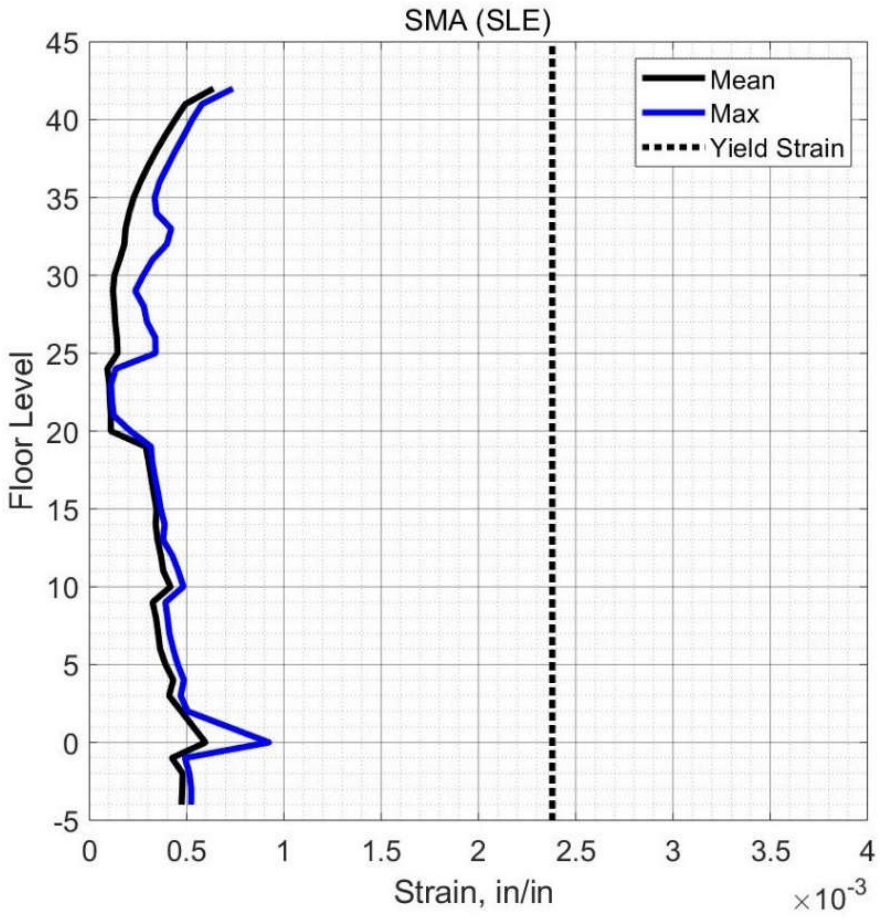

Figure 11.24 Peak Tensile Strain in Reinforcing Bars in Columns (Case 5 – SLE).

11.2.2.3 Contribution of Core Wall and Frame in Dual System

To better understand the behavior of the dual system, the contribution of its components in resisting the story shear force is depicted in Figure 11.25. Figure 11.26 shows the contribution percentage of the shear forces for the core wall and the frame over the building height. The frame contribution is approximately constant over the building height, while the core wall contribution varies linearly. In general, the core wall contributes more than 90% of the total story shear for the lower stories and 50% for the upper stories.

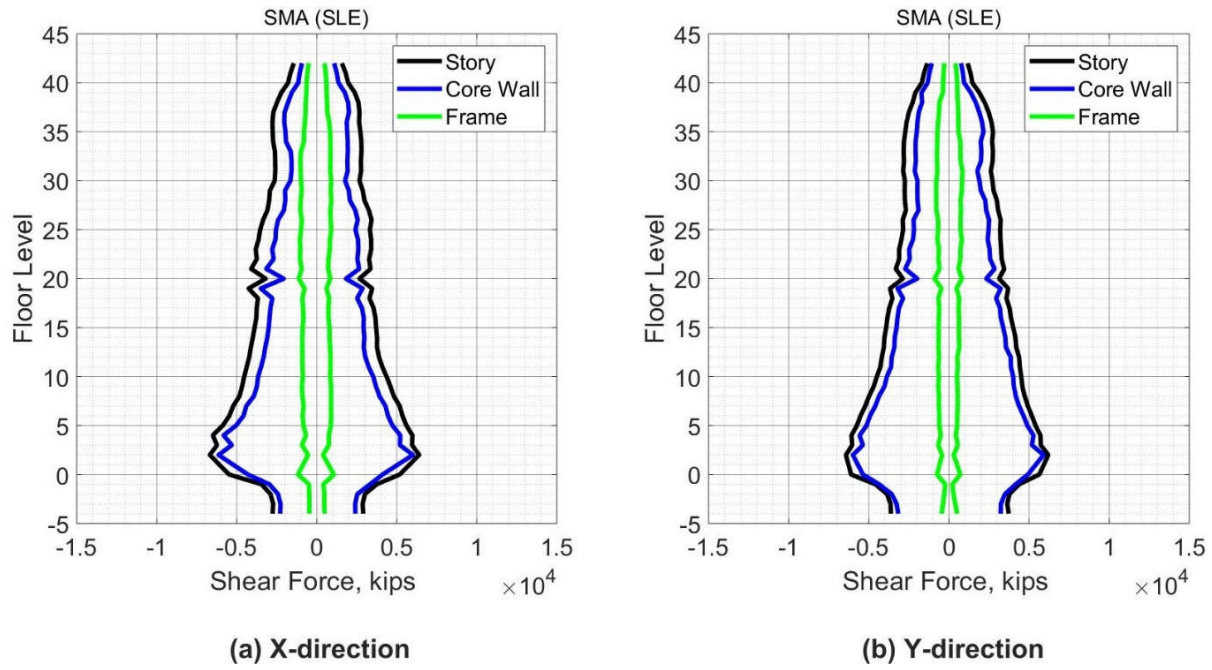

Figure 11.25 Shear Force Contribution of Core Wall & Frame (Case 5 – SLE).

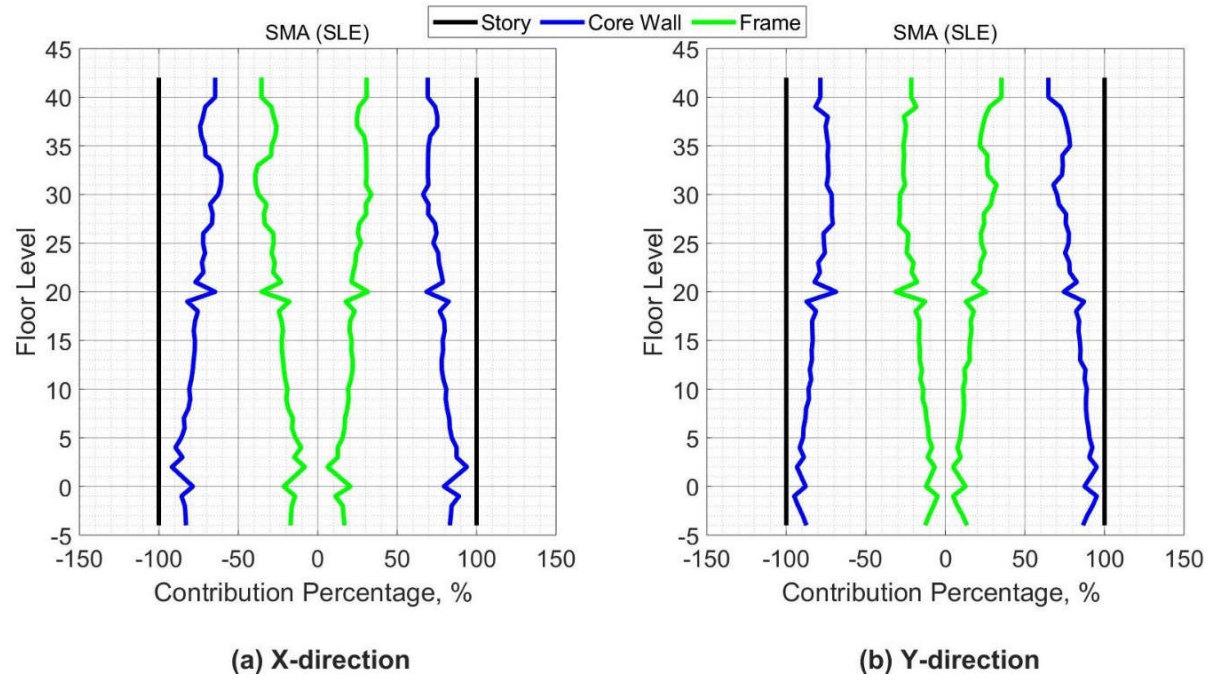

Figure 11.26 Contribution Percentage of Core wall & Frame Shear Force (Case 5 – SLE).

11.3 MCER LEVEL

The same ground motions used in the MCER in case 1 were used for the MCER analyses of case 5. As stated in Section 7.3, the results of eleven analyses are represented and compared with the acceptance criteria of the TBI guidelines. According to the TBI guidelines, first, the mean value of the response parameters from all ground motions in the suite should be checked with the acceptance criteria. Second, the maximum response parameters from all ground motions should be checked to ensure that no unacceptable response was produced by any ground motion from the suite. All the response parameters were calculated by the same procedures that were described in Section 7.2.

11.3.1 Global Response

11.3.1.1 Drift Ratio

Figure 11.27 shows the mean and the maximum values of the interstory drift ratios from all the ground motions analyses over the building height. The mean interstory drift from the eleven analyses was very close to 0.025 in the x-direction and approximately 0.015 in the y-direction, where both values were within the acceptable limit of TBI guidelines of 0.030. In addition, the maximum interstory drift was slightly more than 0.035 and 0.020 for the x- and y-directions, respectively. The maximum values of drift ratios were also within the acceptable limit of TBI guidelines (0.045), which indicates that no unacceptable response was produced when considering the drift ratios. Figures 11.28 and 11.29 depict the maximum drift ratios form each considered ground motion over the building height.

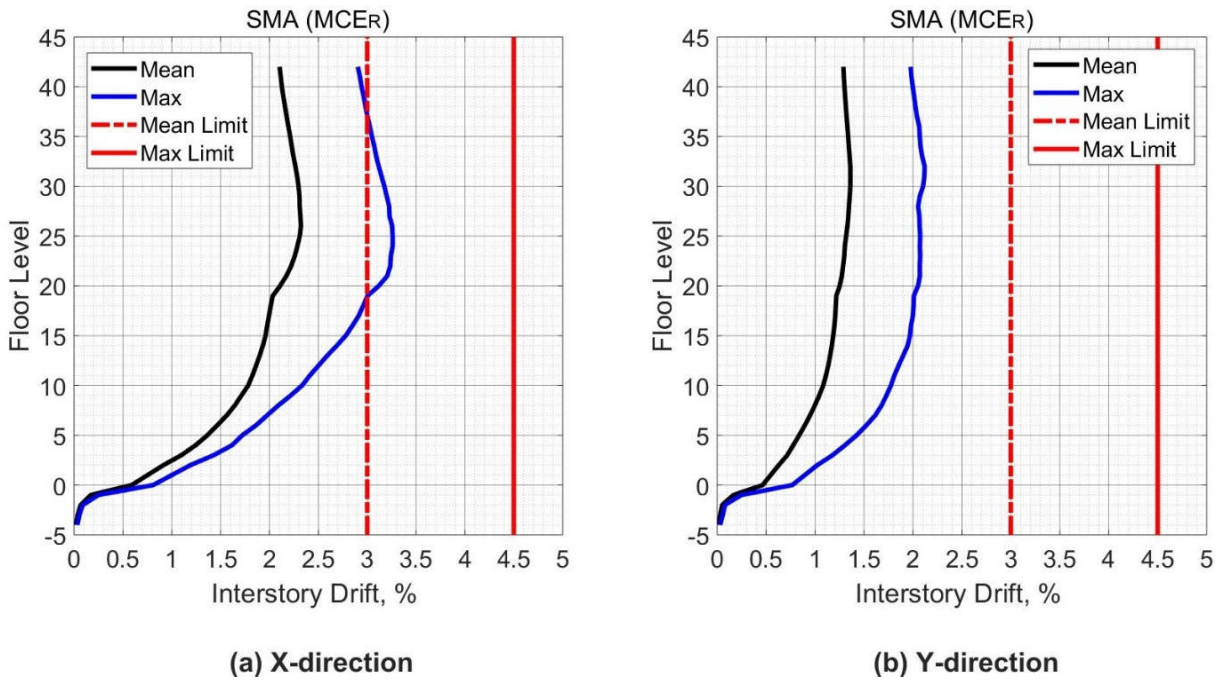

Figure 11.27 Peak Interstory Drift (Case 5 – MCER).

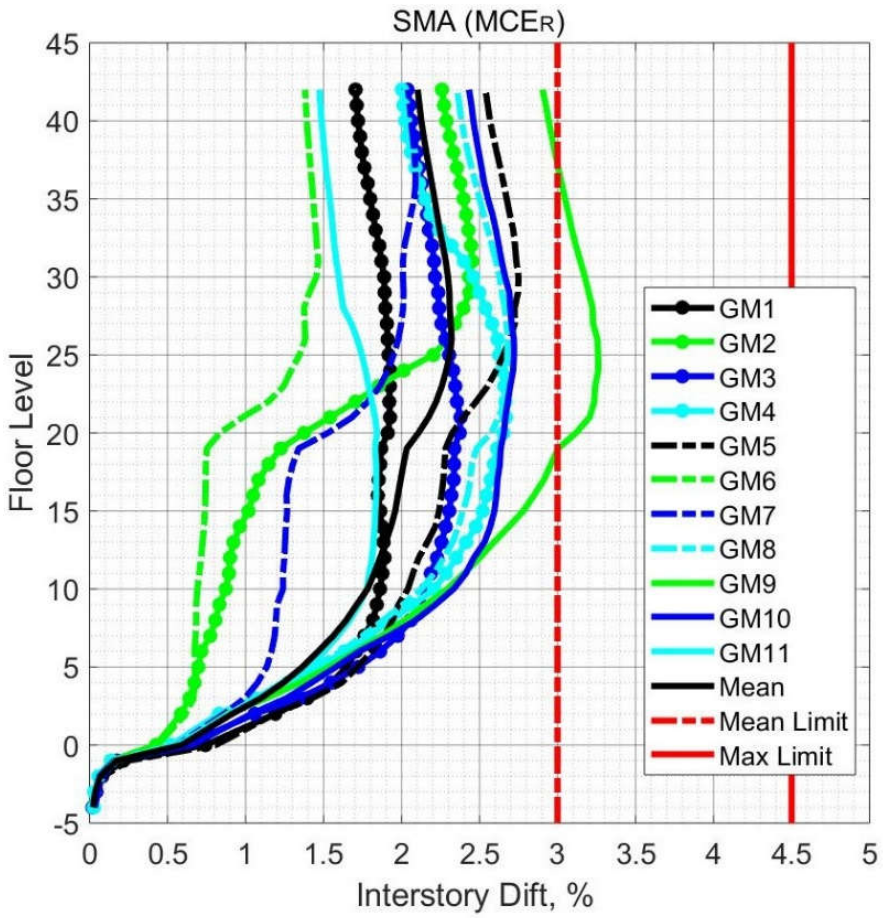

Figure 11.28 Peak Interstory Drift from All Ground Motions for X-direction (Case 5 - MCER).

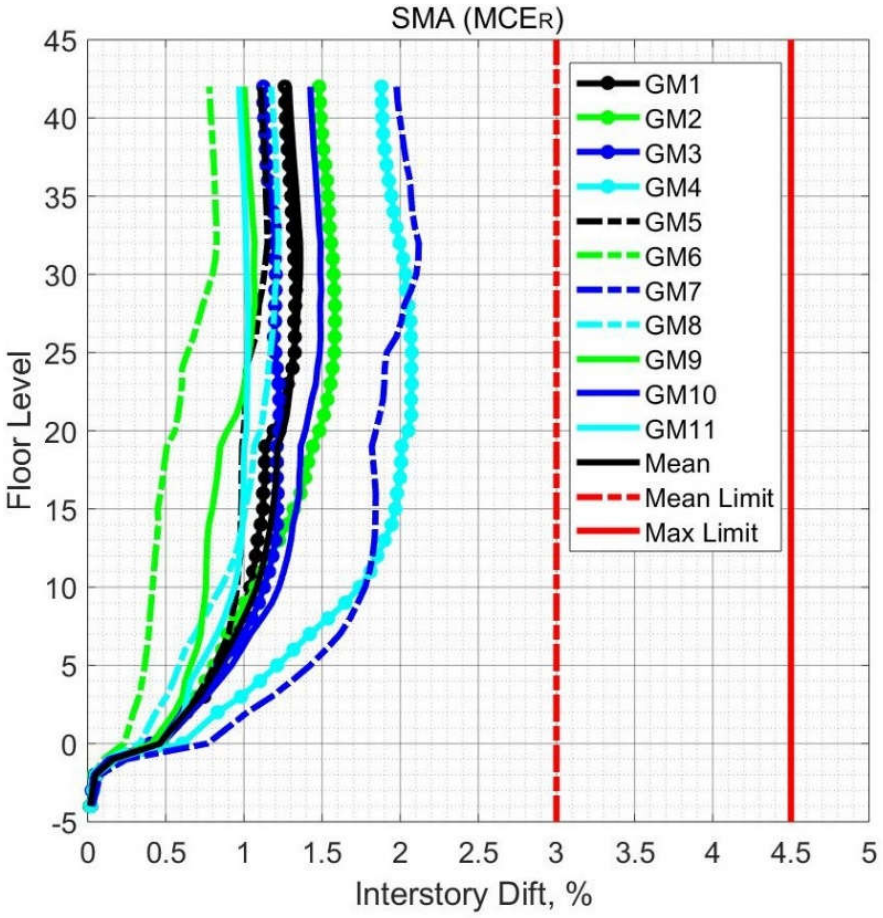

Figure 11.29 Peak Interstory Drift from All Ground Motions for X-direction (Case 5 - MCER).

11.3.1.2 Residual Drift Ratio

The calculations of the residual drift require the story drift at the yield and the maximum drift. SMA bars do not yield like steel bars, however the calculations of residual drift ratio for the SMA case consider the 0.01 stain as a yield point for SMA bars. It is crucial to mention that SMA bars are capable to recover 0.06 strain. When considering the strain of 0.06 as a yield point of the SMA bars, the residual drift for the SMA cases will be approximately zero. Figure 11.30 shows that the maximum of the mean values of the residual drift was 0.0080 in the x- direction and 0.0050

in the y-direction where both values are below the TBI limit (0.0100). In addition, the maximum residual drift ratio obtained from all analyses was slightly more than 0.0125, which is below the limit of the TBI guidelines for residual drift ratios (0.0150). Consequently, no unacceptable response was produced from any ground motion when considering the values of the residual drift ratio.

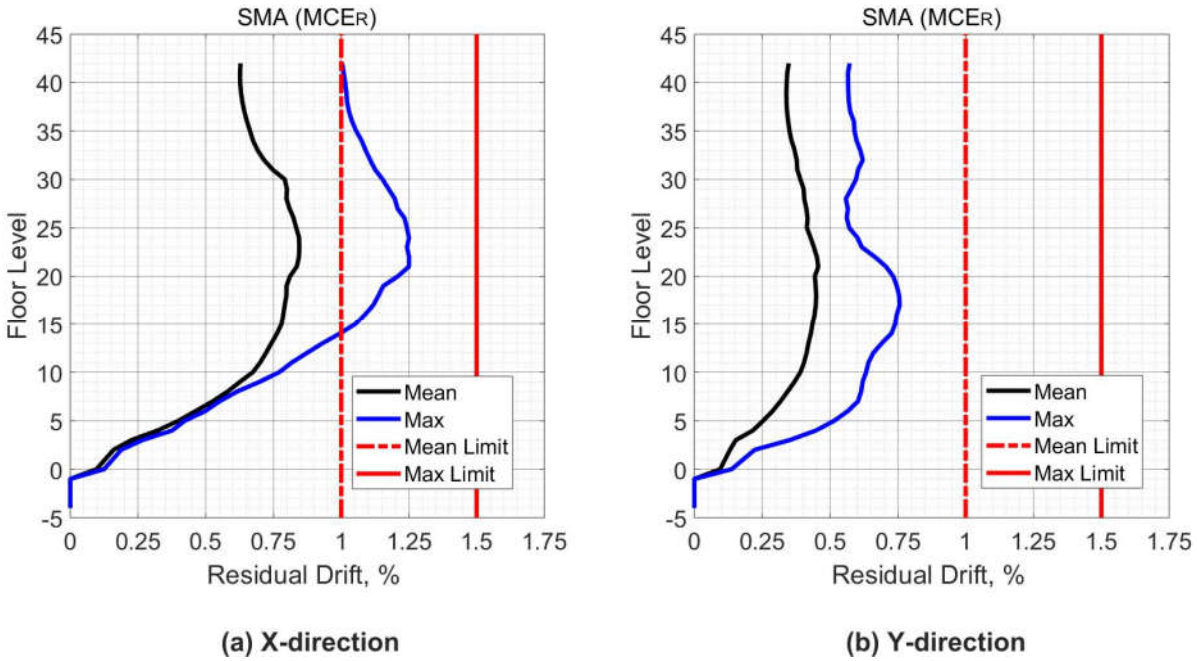

Figure 11.30 Peak Residual Drift (Case 5 – MCER).

11.3.1.3 Displacement

Figure 11.31 depicts the mean value of the displacement of each story at the same time step that the roof experiences a maximum displacement value. The mean displacement of the roof was 85 in and 50 in for x and y-direction, respectively.

Figures 11.32 and 11.33 show the time history of the roof displacement in the x-direction and y-direction, respectively from a ground motion at which the displacement demand of the roof was the highest one among other ground motions. During the ninth ground motion, the roof experience a maximum displacement in the x-direction while during the fourth ground motion the maximum roof displacement in the y-direction was observed.

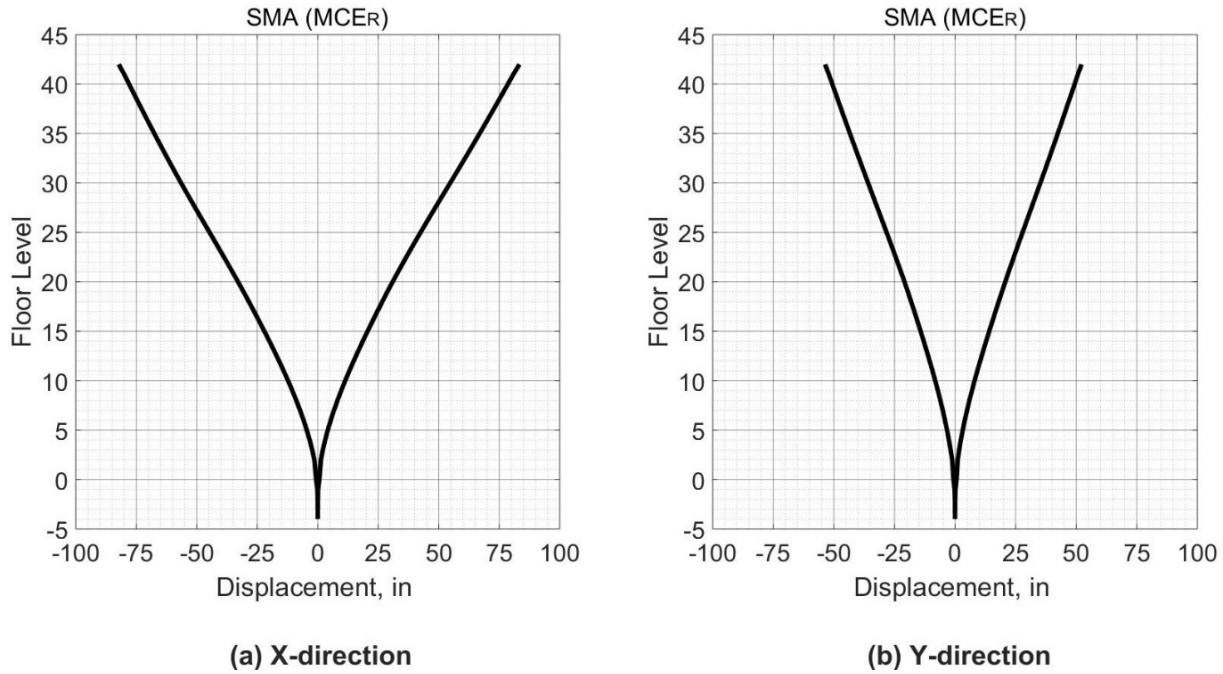

Figure 11.31 Floors Displacement Synchronous with Peak Roof Displacement (Case 5 - MCER).

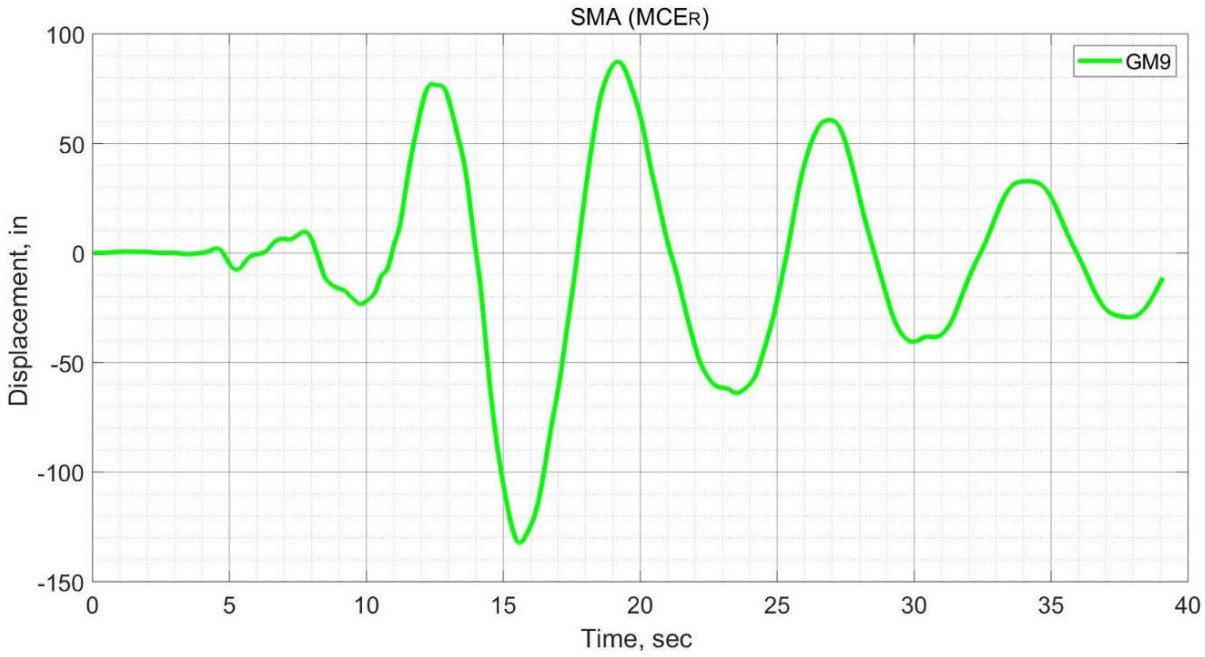

Figure 11.32 Time History for Peak Roof Displacement for X-direction (Case 5 – MCER).

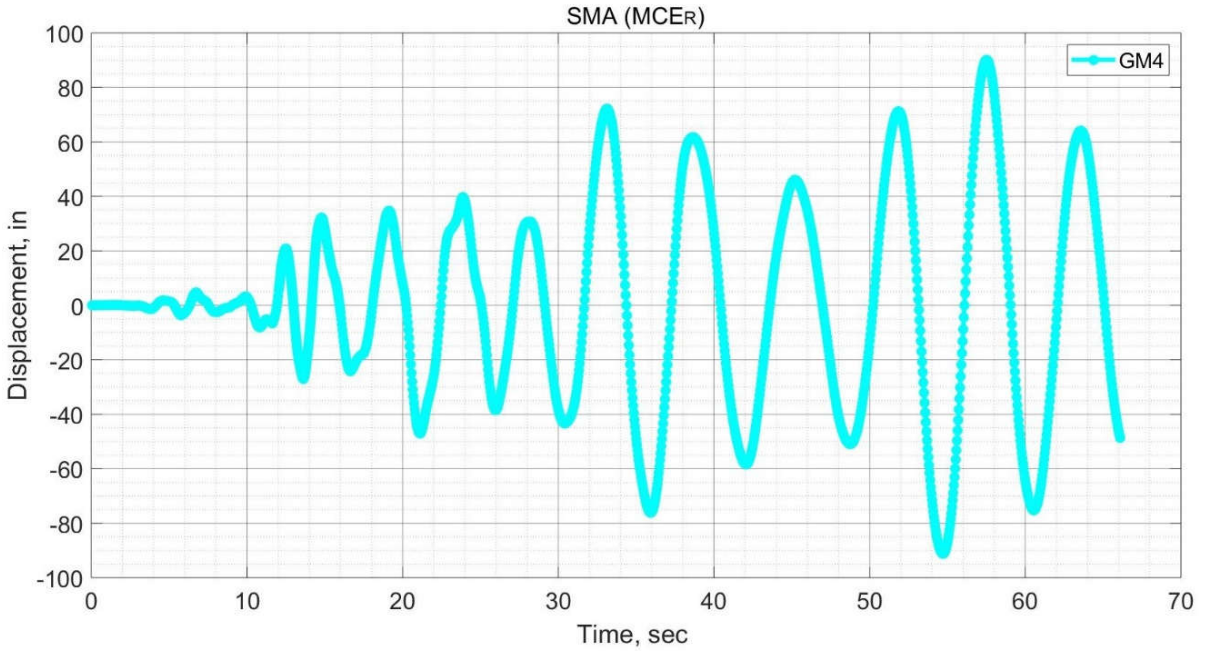

Figure 11.33 Time History for Peak Roof Displacement for Y-direction (Case 5 – MCER).

11.3.2 Element Level

As mentioned in Section 7.3.2, For the MCER shaking level, the TBI guidelines require using the mean value from all analyses for evaluation with the acceptance criteria for force-based actions, while using the maximum value from all analyses for deformation-based actions. In addition, for both actions the TBI guidelines require using the maximum value from all analyses to evaluate with the acceptance criteria to ensure that all calculated demands from any analysis are within the acceptable range of the model. In the subsections below, the elements of the seismic force resisting system with their actions are presented and evaluated using the acceptance criteria of the TBI guidelines.

11.3.2.1 Core Wall Response

11.3.2.1.1 Core Wall Force-Based Action

To evaluate the shear demands of core walls, the TBI guidelines required that the shear force demands satisfy Equation (7-8). As mentioned previously, the horizontal reinforcement of the core wall was the conventional steel bars, therefore applying the code equations for calculating the shear capacity of the wall is possible. Figure 11.34 shows the core wall shear forces over the building height and the limiting (*Vexp*) as in Equation (7-8). The shear demands in the core wall satisfy Equation (7-8) as required by the TBI guidelines. In addition, the shear force demands varied approximately in a linear manner with the height of the building. A small increase in the shear force demands in the y-direction was noticed compared with demands in the x-direction. The maximum observed shear demand was 13670 kips for y-direction, while 12060 kips in x-direction. As shown in Figure 11.34, considering that the maximum demand of the shear force in the core wall was also within the acceptable limits, all analyses produced an acceptable response and all results are within the acceptable modeling range.

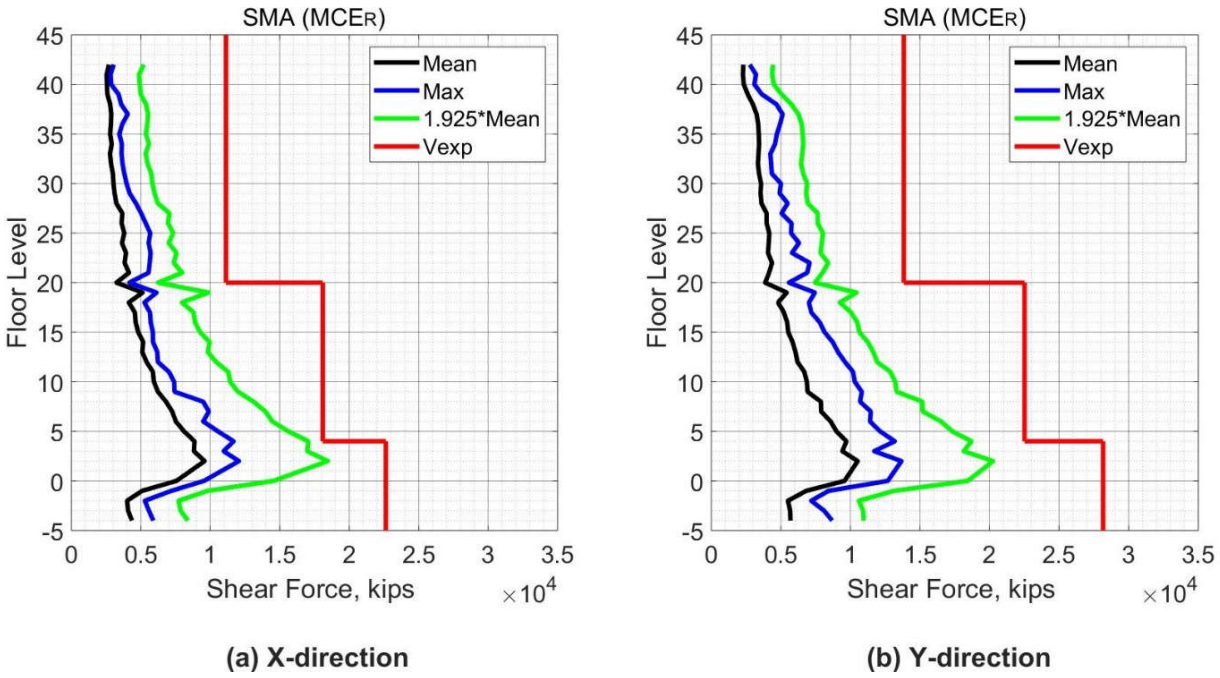

Figure 11.34 Shear Forces in Core Wall (Case 5 – MCER).

11.3.2.1.2 Core Wall Deformation-Based Action

As stated in Section 7.2.2.1.2, the tensile strain in the reinforcing bars and concrete compression strain were monitored during the analyses on all edges of the core wall. The strain was determined by using the vertical displacement (Δz) of the nodes of the core wall edges. Figures 11.35 to 11.38 show that the maximum tensile strain in the core wall reinforcement is 0.016, which is below the recoverable limit of 0.06 of the SMA bars. In other words, the SMA bars are capable to return to its origin shape upon loading remove. Consequently, the TBI guidelines are satisfied due to negligible damage depending on the tensile strain of the wall reinforcement.

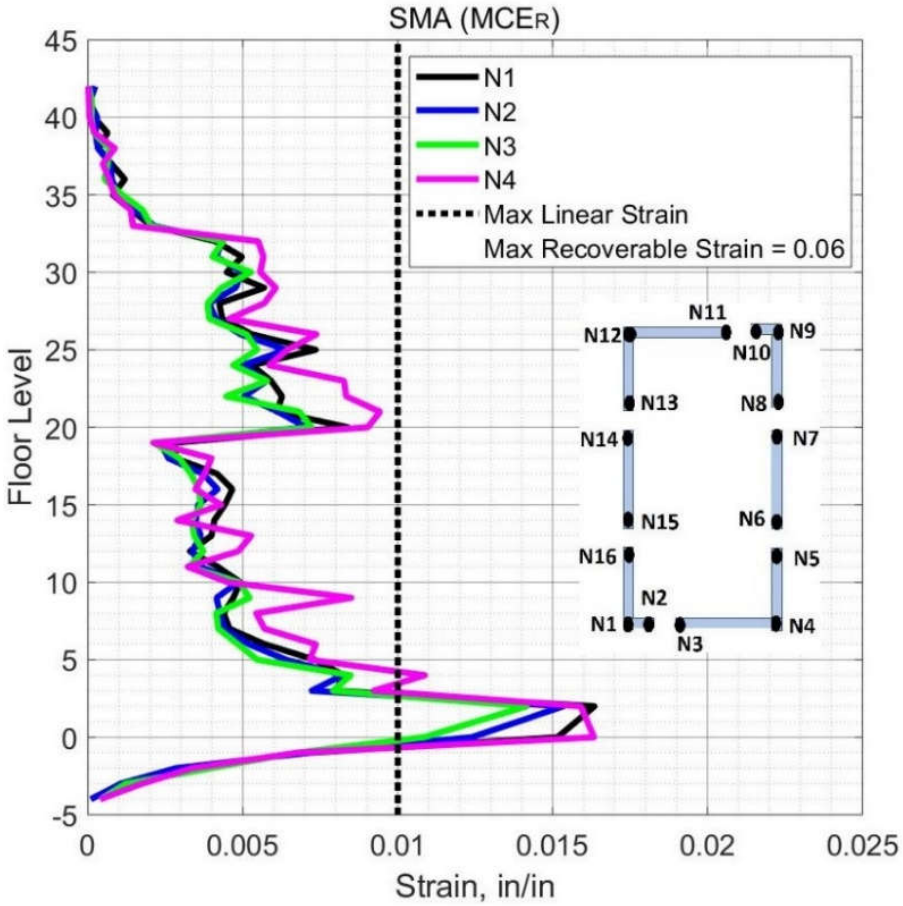

Figure 11.35 Peak Tensile Strain in SMA Bars in Core Wall Edges N1-N4 (Case 5 – MCER).

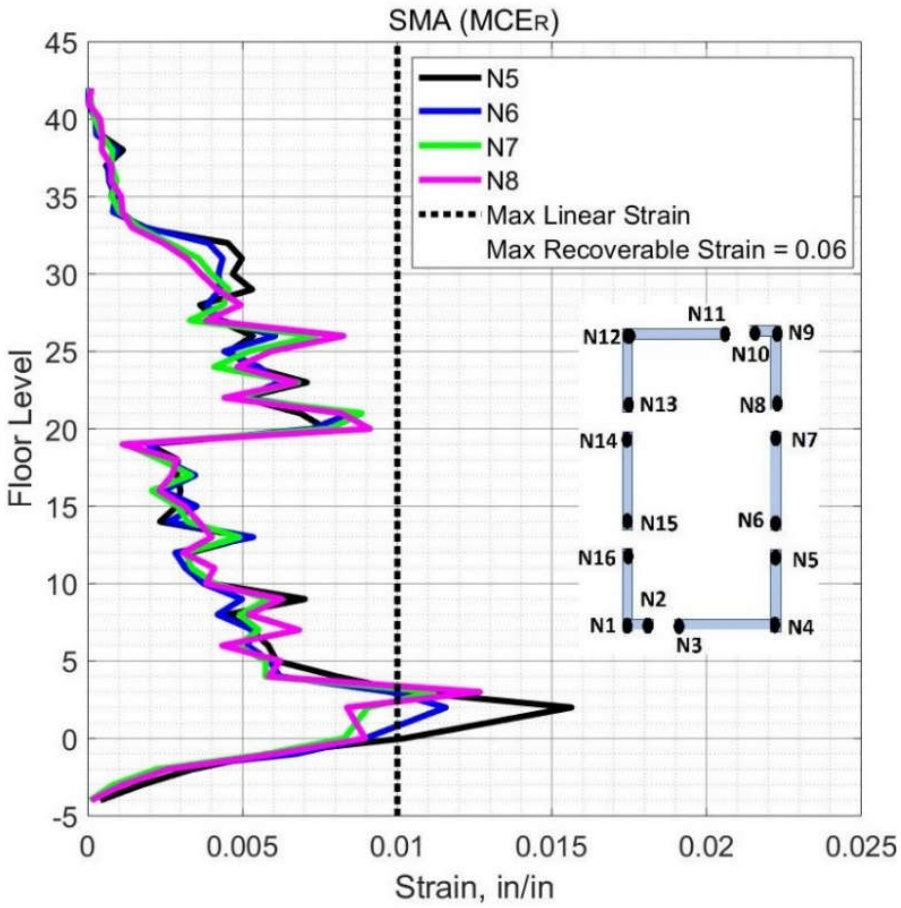

Figure 11.36 Peak Tensile Strain in SMA Bars in Core Wall Edges N5-N8 (Case 5 – MCER).

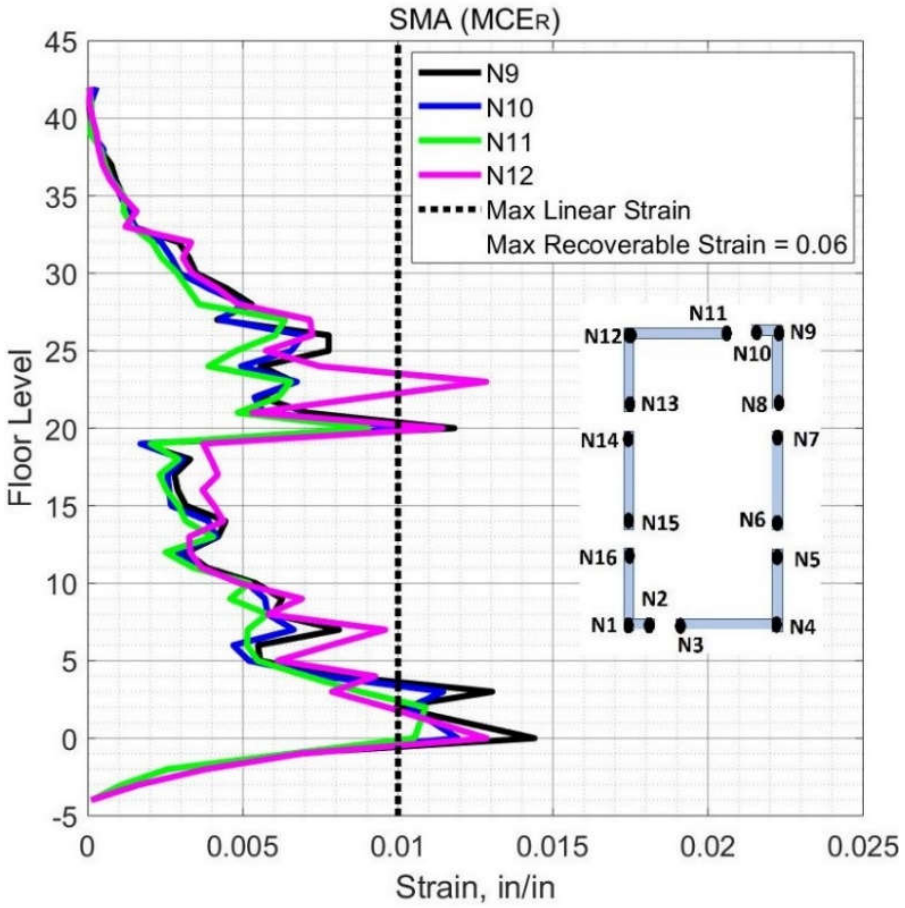

Figure 11.37 Peak Tensile Strain in SMA Bars in Core Wall Edges N9-N12 (Case 5 – MCER).

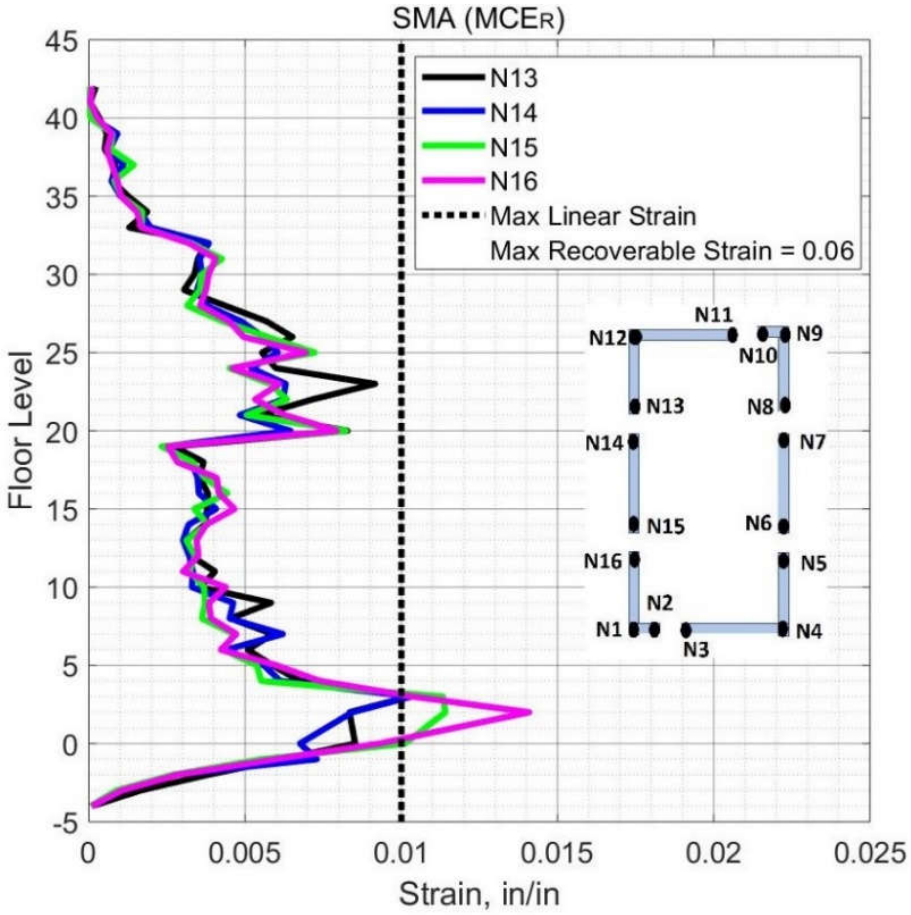

Figure 11.38 Peak Tensile Strain in SMA Bars in Core Wall Edges N13-N16 (Case 5 – MCER).

Figures 11.39 to 11.42 show the maximum values of the compression strain in the core wall concrete at the wall edges over the building height. The core wall concrete experiences low values of concrete compression strain, below 0.0022, for all stories.

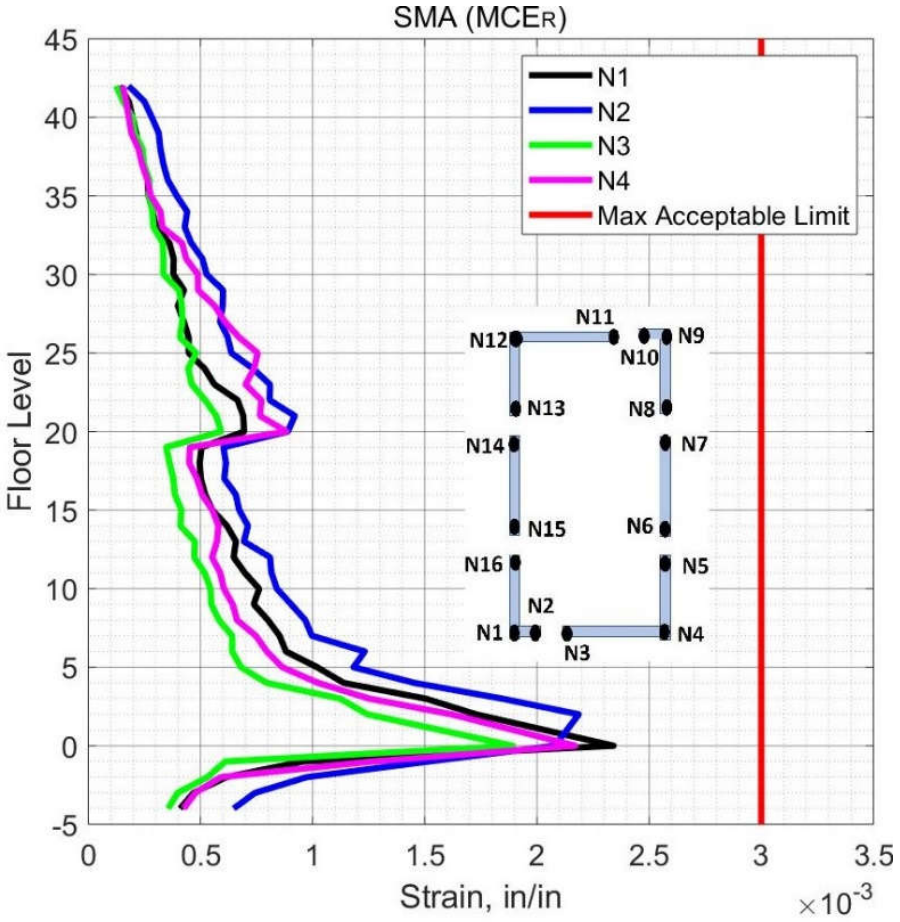

Figure 11.39 Peak Concrete Compression Strain in Core Wall Edges N1-N4 (Case 5 – MCER).

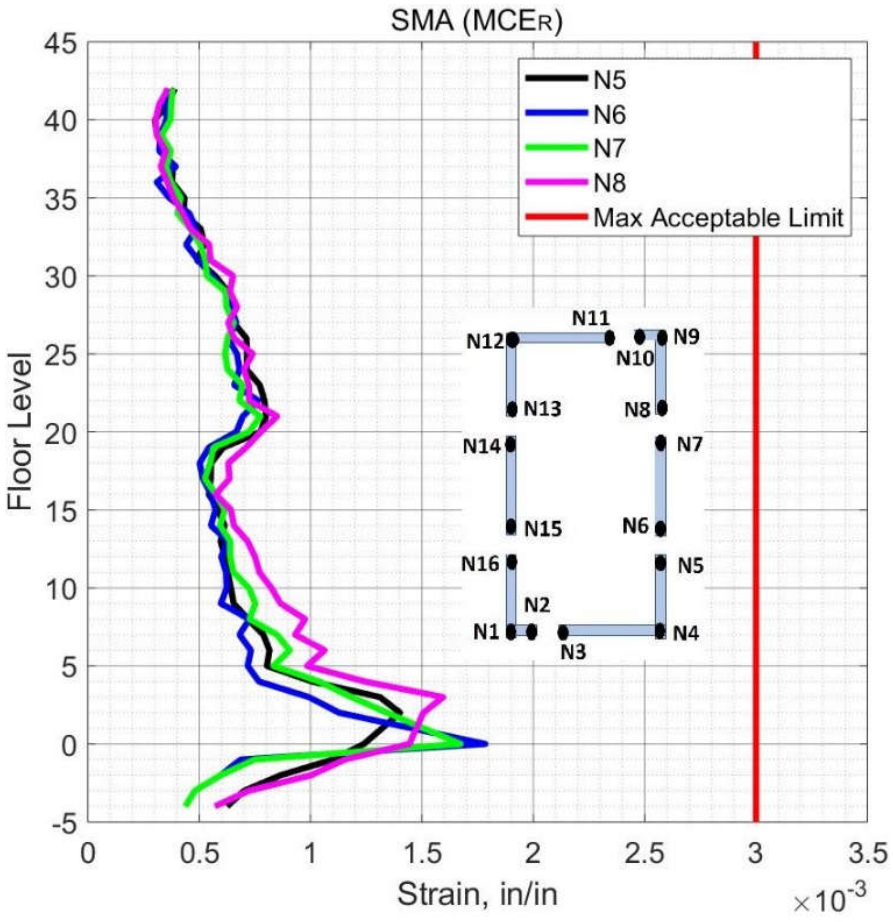

Figure 11.40 Peak Concrete Compression Strain in Core Wall Edges N5-N8 (Case 5 – MCER).

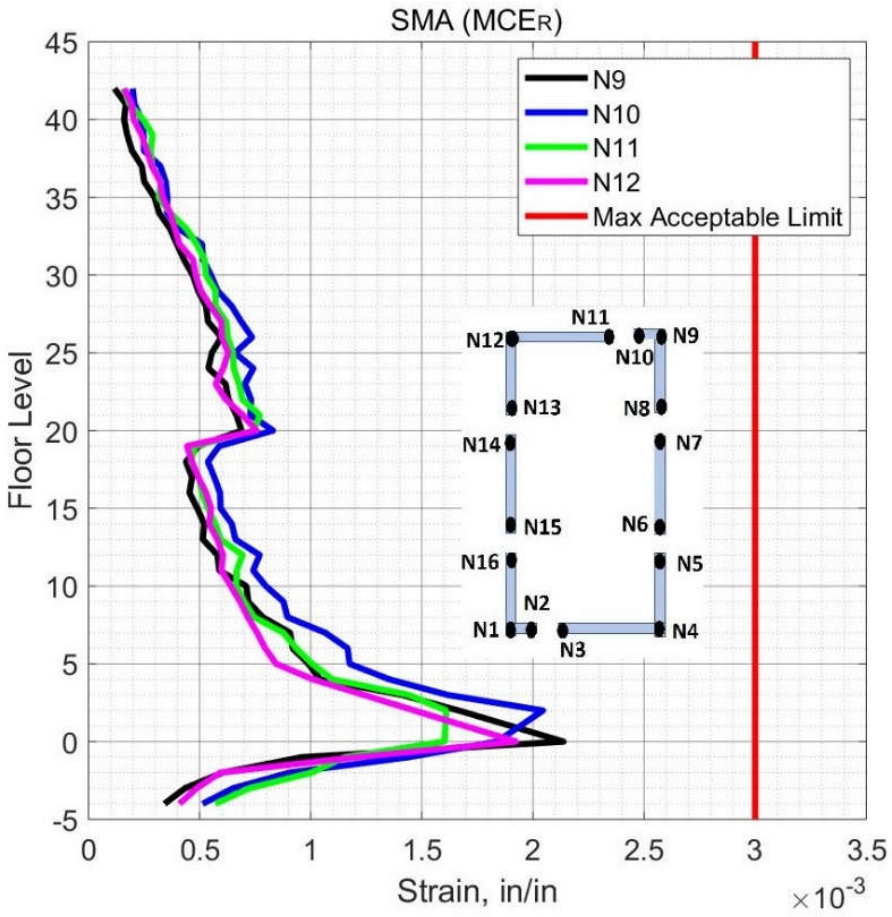

Figure 11.41 Peak Concrete Compression Strain in Core Wall Edges N9-N12 (Case 5 – MCER).

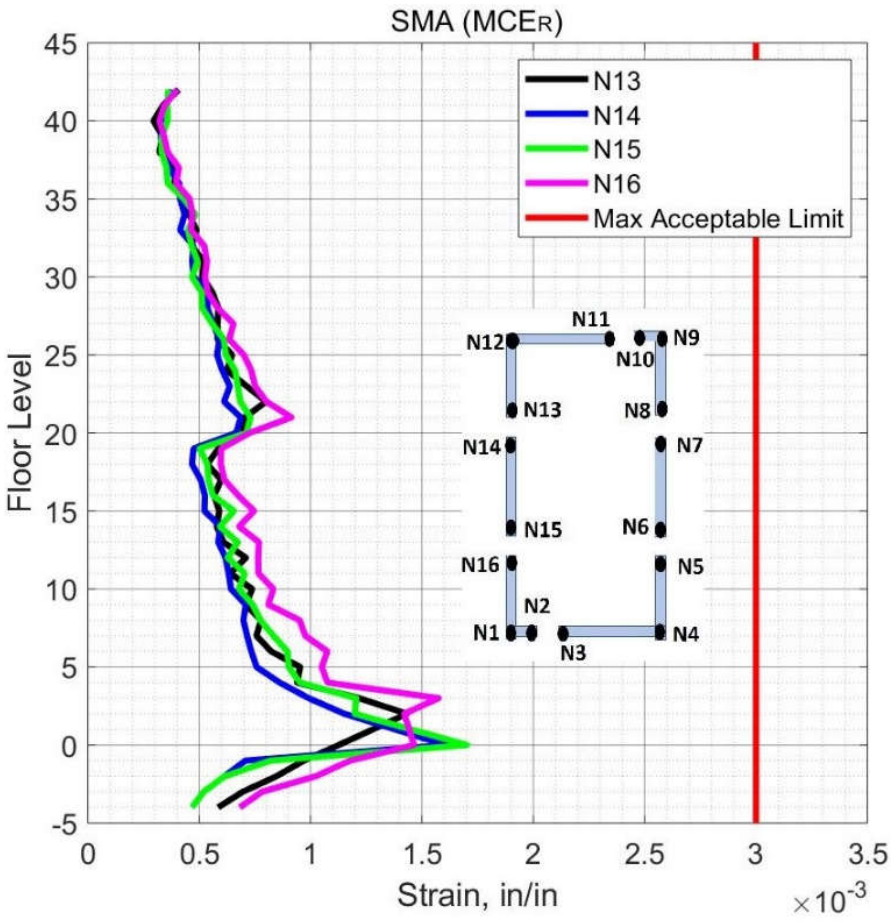

Figure 11.42 Peak Concrete Compression Strain in Core Wall Edges N13-N16 (Case 5 – MCER).

11.3.2.1.3 Coupling Beams

Figure 11.43 (a) shows the mean and maximum values of the rotation of coupling beams with a 1.7 aspect ratio (coupling beams in the x-direction), over the building height. The peak value of the rotation is less than 0.03 which is below the maximum allowable limit of 0.05. In addition, considering the data in Figure 7.18, one could conclude that the coupling beams may experience minor damage. Therefore, the rotation demands of coupling beams satisfy the requirement of the TBI guidelines.

Figure 11.43 (b) shows the mean and maximum values of the rotation of coupling beams with a 2.1 aspect ratio (coupling beams in the y-direction), over the building height. The peak value of the rotation is approximately 0.03 which is below the limit of 0.05. In addition, considering the data in Figure 7.19, one could conclude that the coupling beams may experience minor damage. Therefore, the rotation demands of coupling beams satisfy the requirement of the TBI guidelines.

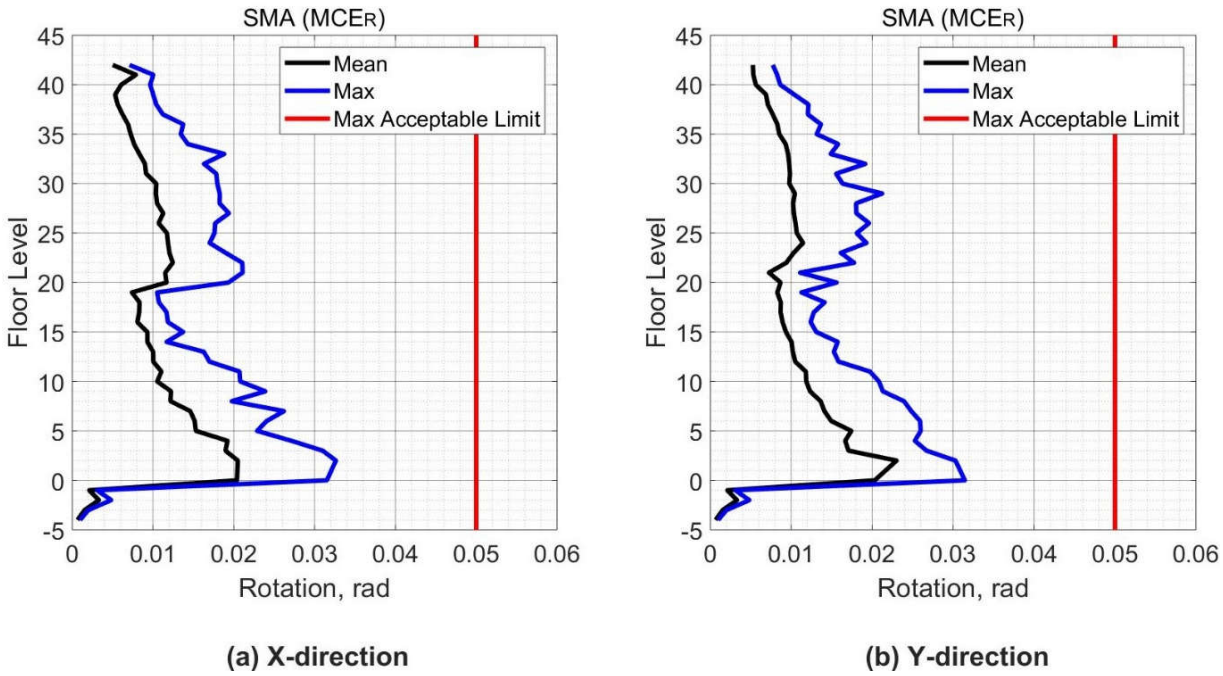

Figure 11.43 Rotation Demand in Coupling Beams (Case 5 – MCER).

11.3.2.2 Special Moment Frame Response

11.3.2.2.1 Beam Force-Based Action

As stated in Section 7.3.2.2.1, To evaluate the shear action in the beams, Equation (7-11) will be applied. Figure 11.44 shows the shear force demands in the beams of the special moment

frame over the building height. In the legend of Figure 11.44, the results noted as “Mean” represent the mean value of the maximum shear force in the beams at each floor level from all ground motions analyses, while the results noted as “Max” represent the maximum shear force in the beams obtained from all analyses. In addition, the values shown as “Vfinal” and “Vexp” in the legend were obtained by using Equations (7-10) and (7-5), respectively. As shown in Figure 11.44, the main conclusion is that shear force demands in special moment frame beams meet the requirements of the TBI guidelines by satisfying Equation (7-11). In addition, the maximum shear force demands (300 kips) obtained from all ground motions are within the acceptable limits of the expected shear capacity (667 kips) of the beams. In other words, the maximum shear force demands obtained from all ground motions are within the acceptable limits of the expected shear capacity of the beams. Consequently, all analyses produced an acceptable response based on the shear force demands in the beams.

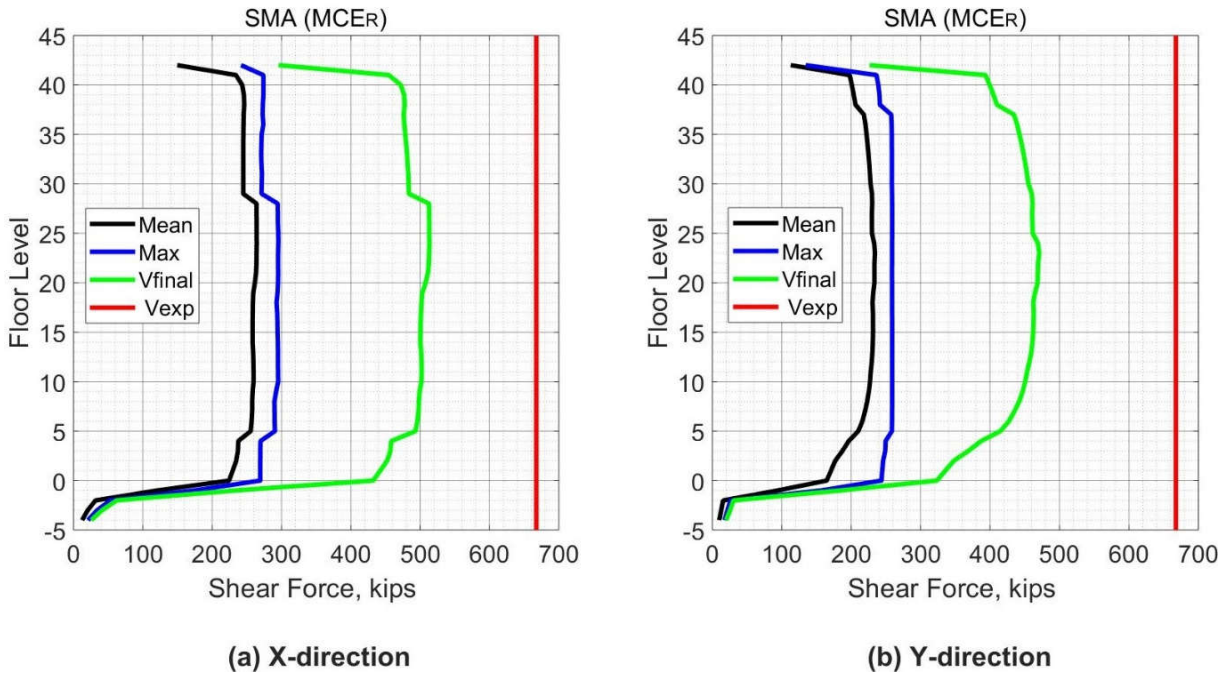

Figure 11.44 Peak Shear Force in Beams (Case 5 – MCER).

11.3.2.2.2 Beam Deformation-Based Action

Figure 11.45 shows the mean and the maximum tensile strain demands in the longitudinal reinforcement of the beams at each floor level. The maximum tensile strain demand (0.03) is below the maximum recoverable limit (0.06) of the SMA bars. In addition, reinforcing bars in beams oriented in the x-direction experienced more tensile strain (0.03) compared to beams oriented in the y-direction (0.01). For the beams oriented in the y-direction, the tensile demand is within the linear limit (0.01) of the SMA. Considering the results of the tensile strain of reinforcement bars in the beams, the bars are capable to return to their origin shapes with negligible residual strain leading to reduce the damage dramatically. Consequently, the TBI guidelines requirements are satisfied.

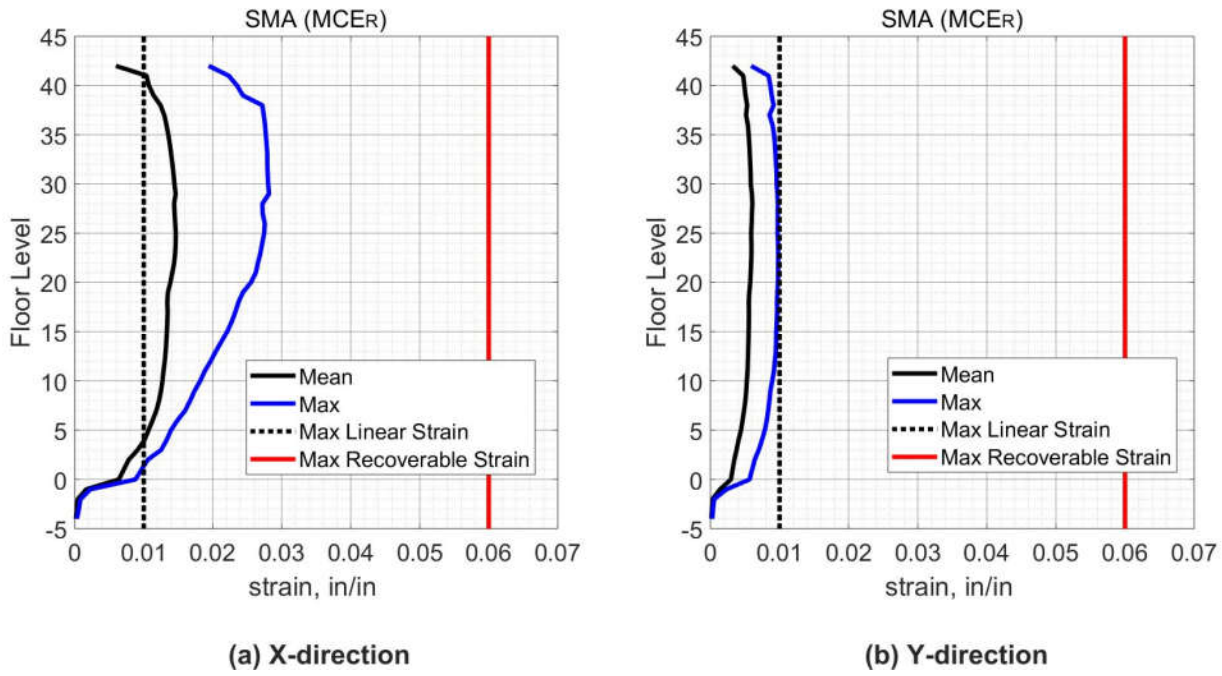

Figure 11.45 Peak Tensile Strain in SMA bars in Beams (Case 5 – MCER).

Whenever the tensile strain of a SMA reinforcing bar reached the linear strain limit (0.01), for the first time, the curvature at that time step was recorded as the yielding curvature. The ultimate curvature is the maximum curvature that the section experiences. After obtaining both yielding and ultimate curvatures, Equation (7-6) was utilized to determine the plastic rotation demands. Figure 11.46 shows the mean and the maximum plastic rotation demands in the beams at each floor level. The plastic rotation demands were within the acceptable limits with a maximum demand of approximately 0.025 rad. The beams in y-direction did not experience plastic rotation. It is essential to mention that the plastic rotation calculations depend on the assumption that SMA bars behave plastically after strain reaches 0.01, however, SMA bars are capable to recover strain up to 0.06. Depending on the results of tensile strain, all beams will recover the strains. Based on the strain and plastic rotation results, the deformation-based actions in the beams satisfy the

requirement of TBI guidelines.

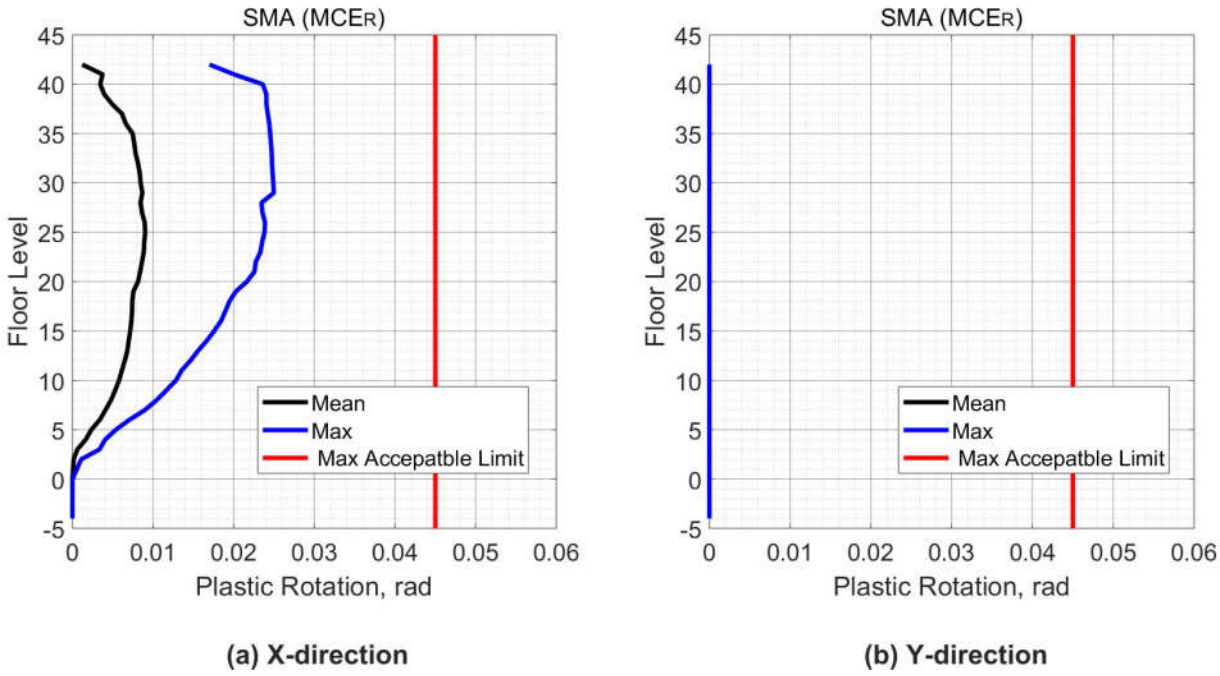

Figure 11.46 Plastic Rotation in Beams (Case 5 - MCER).

11.3.2.2.3 Columns Force-Based Action

In the legend of Figures 11.47 through 11.50, the results noted as "Mean" represent the mean value of the shear force in the columns from all ground motions analyses while the results noted as "Max" represent the maximum shear force obtained from all analyses. In addition, results with "Vfinal" and "Vexp" in the legend represent the parameters in Equation (7-11) for the columns. The shear force demands in the columns are within the limits of the TBI guidelines, by satisfying equation (7-11). The maximum shear demands obtained from all analyses are also within the acceptable limits. Therefore, all analyses produced acceptable responses when considering the

shear force demands of the columns. In contrast with the shear force demands of the core wall, the shear forces were more uniform with building height.

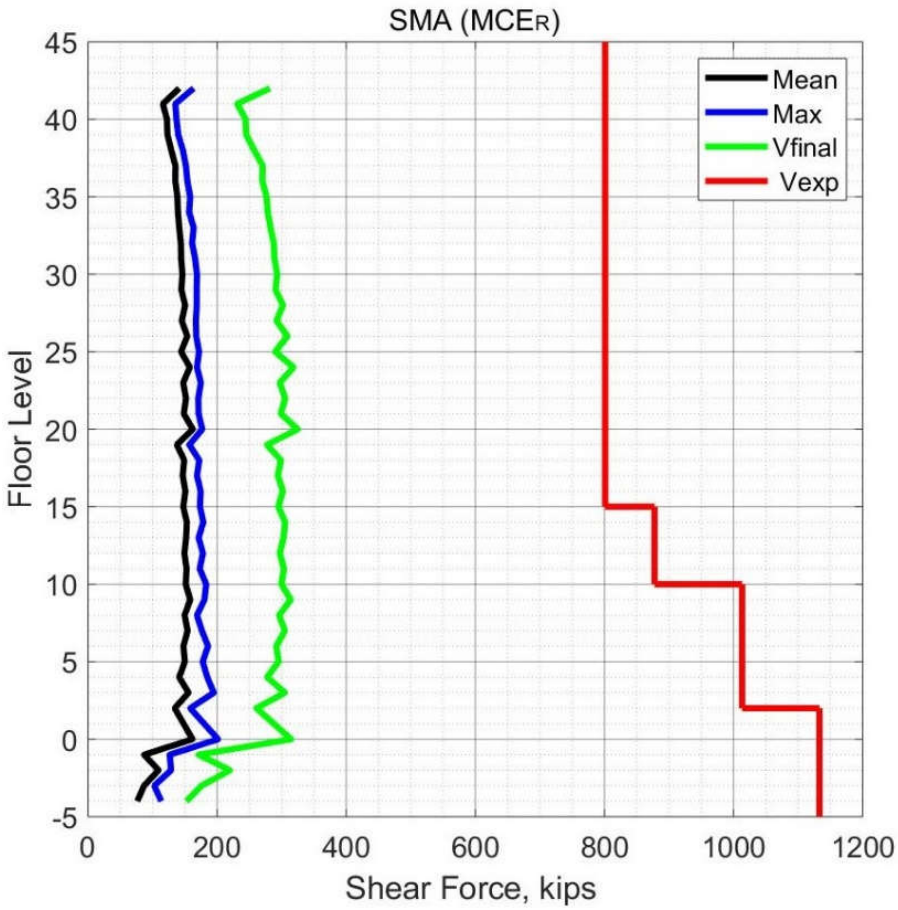

Figure 11.47 Peak Shear Force in Corner Columns (Case 5 – MCER).

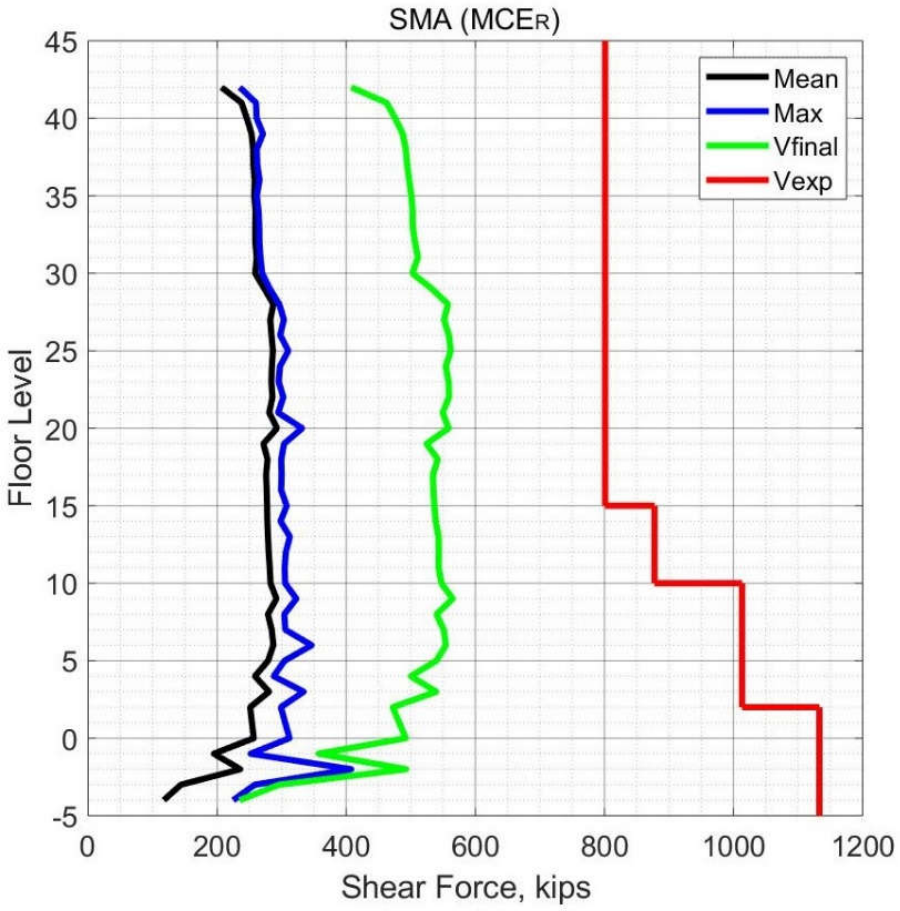

Figure 11.48 Peak Shear Force in Interior Columns X-direction (Case 5 – MCER).

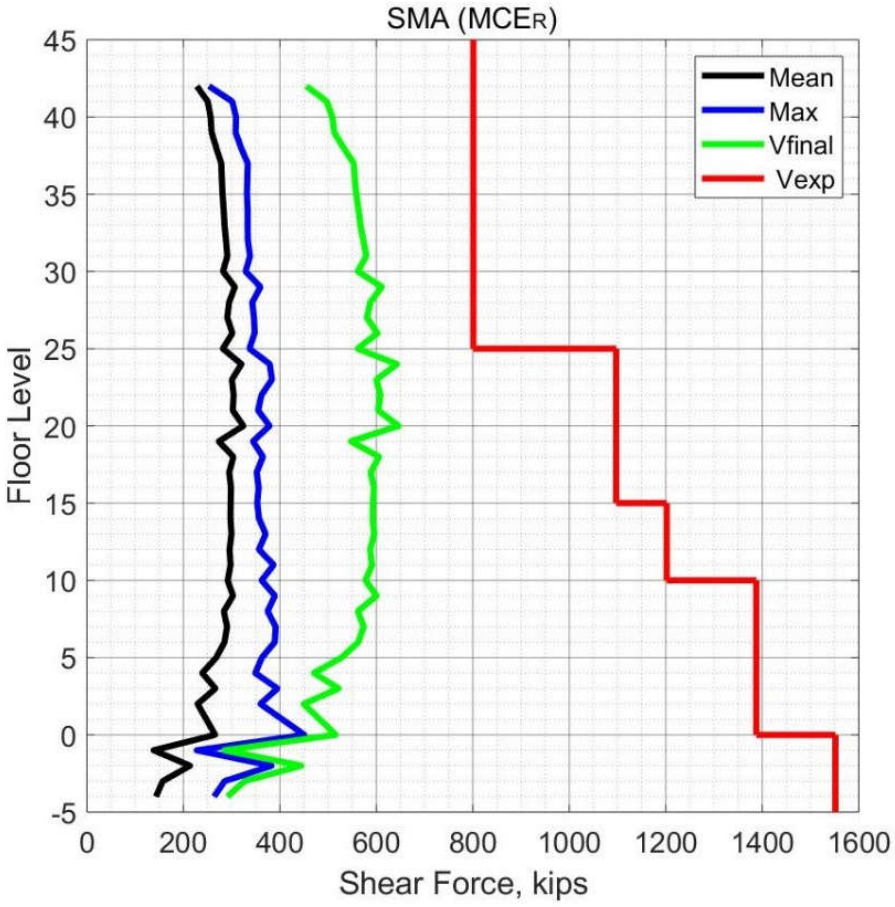

Figure 11.49 Peak Shear Force in Columns on Grid B and E (Case 5 – SLE).

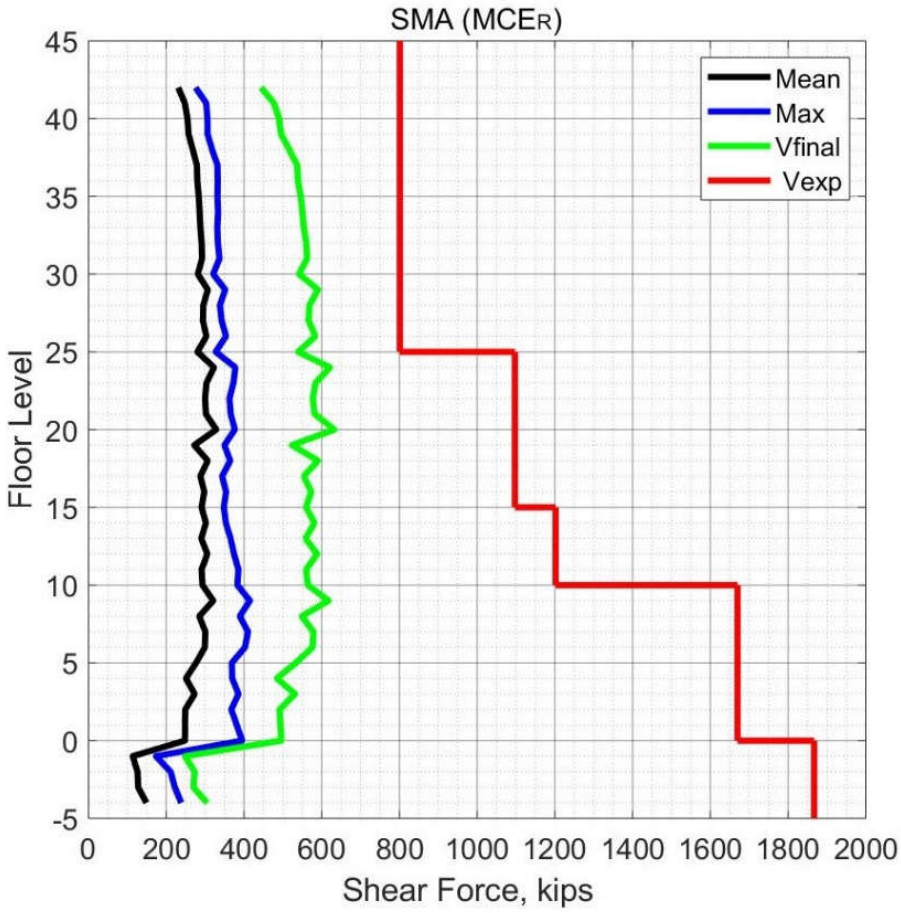

Figure 11.50 Peak Shear Force in Columns on Grid C.5 (Case 5 – MCER).

11.3.2.2.4 Column Deformation-Based Action

The maximum value of the tensile strain in the columns' longitudinal bars and the mean value from all ground motion in the suite are depicted in Figure 11.51. The maximum tensile strain demands (0.0022) did not exceed the expected yield strain of Grade 60 (0.0024) which means no plastic hinges formed in the columns. In other words, columns did not experience plastic rotations. As mention previously, the behavior of non-yielding columns is one of the preferable design approaches for seismic applications where most plastic rotation demands form in the beams.

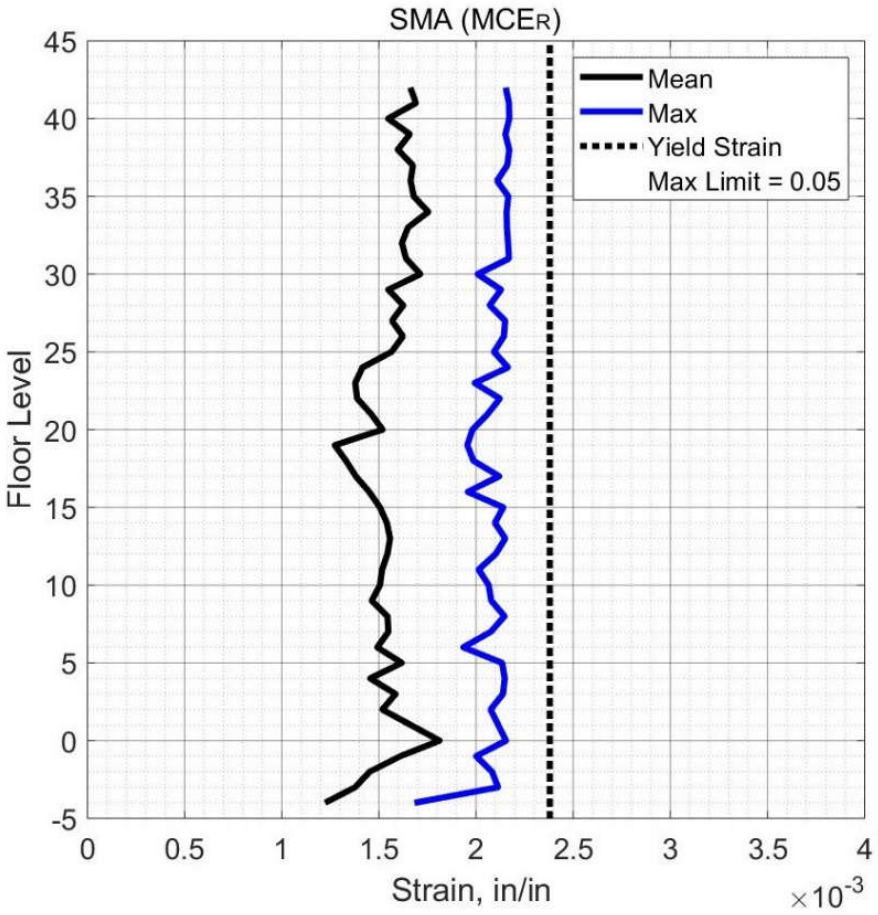

Figure 11.51 Peak Tensile Strain in Reinforcing Bars in Columns (Case 5 – MCER).

11.3.2.3 Contribution of Core Wall and Frame in Dual System

The contribution of the components of the dual system in resisting the story shear force is depicted in Figure 11.52 for the x- and y-directions, respectively. Figure 11.53 shows the contribution percentage of the shear forces for the core wall and the frame over the building height. The frame contribution is approximately constant over the building height, while the core wall contribution varies linearly. The frame contribution in the lower stories is approximately one-third of the story shear, while in the upper stories the frame contribution is about one-half of the total story shear.

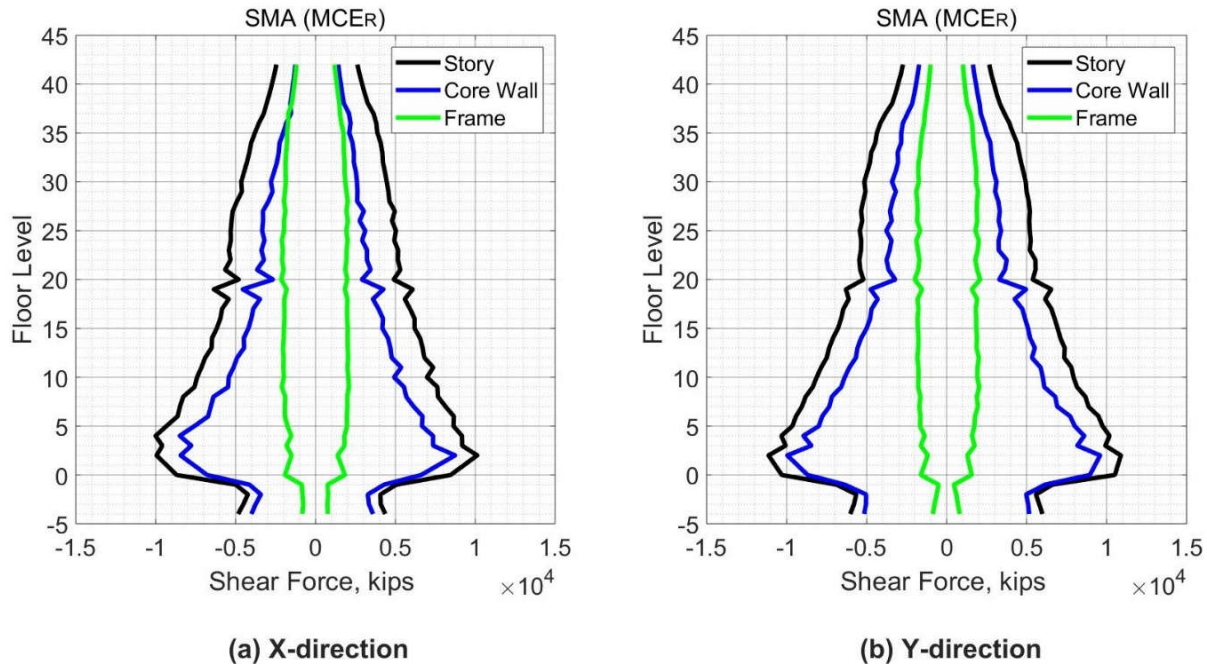

Figure 11.52 Shear Force Contribution of Core Wall & Frame (Case 5 – MCER).

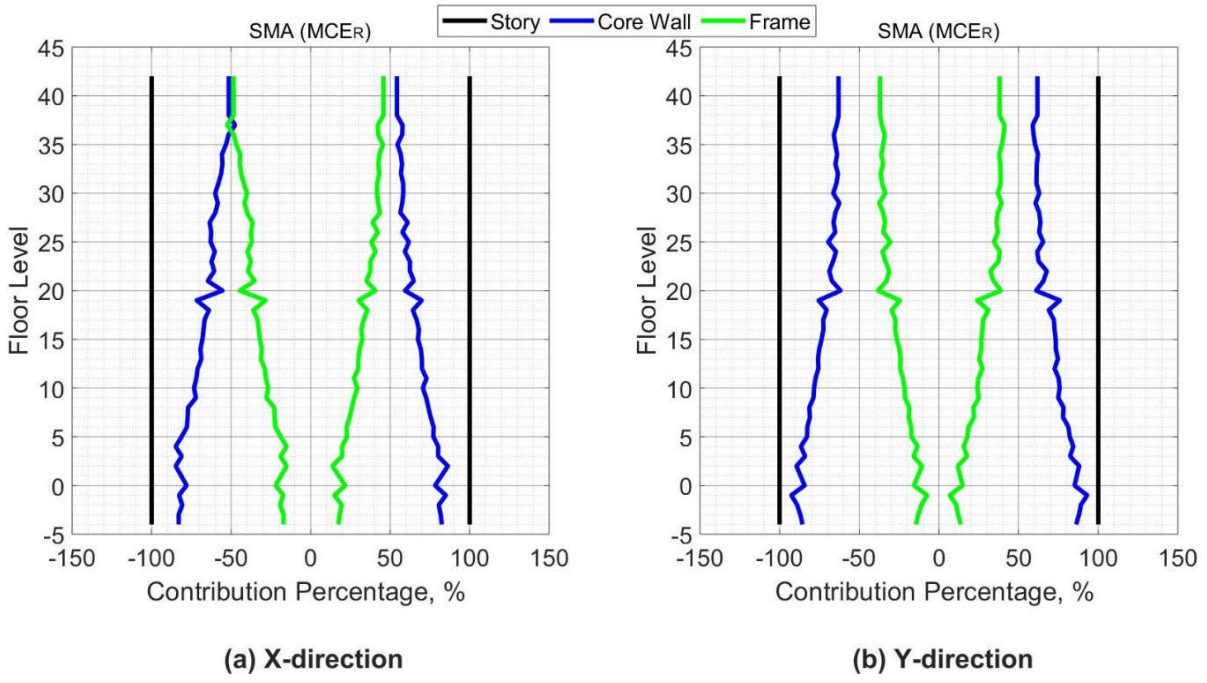

Figure 11.53 Contribution Percentage of Core wall & Frame Shear Force (Case 5 – MCER).

CHAPTER XII

COMPARATIVE STUDY BETWEEN SELECTED CASES

12.1 INTRODUCTION

One of the important questions about using new and different reinforcing materials in concrete structures is whatever the performance of the structures reinforced with these different reinforcing bars is equal or may be better than the performance of the same structures reinforced with the conventional reinforcing bars. Therefore, a comparison between the response parameters of the case study building in the global and elements levels could depict how the performance of the case study building reinforced with high strength steel or shape memory alloy bars differs than the performance of the same building reinforced with conventional steel bars. If the performance of a structure reinforced with a reduced area of high strength reinforcing bars is equivalent to the performance of same structure reinforced with conventional steel bars, then using high strength reinforcement could be a valuable and economic solution.

12.2 REINFORCEMENT STEEL GRADES CASES

The performance of the case study building reinforced with four different grades of reinforcing bars (Grades 60, 80, 100, and 120) will be compared for SLE and MCER shaking levels. A reduced area of reinforcement for high strength steel with the same structural elements' dimensions could be a practical solution for the construction-related problems such as the congestion of reinforcing bars in concrete structures. In addition, a reduced amount of steel reinforcement will lead to reduce the cost, time and labor required for the construction especially in tall buildings.

12.2.1 Global Response

12.2.1.1 Interstory Drift ratio

12.2.1.1.1 SLE Level

Figure 12.1 shows the mean of the peak interstory drift ratios from the seven ground motions for the SLE level. A similar behavior of the drift ratio was noticed for all reinforcement steel grades cases for the SLE shaking level. Figure 12.2 shows the peak interstory drift from the seven ground motions for the case study building reinforced with four reinforcement grades. The peak drift demand is also very close for all cases. The performance of the case study building reinforced with a reduced area of high strength reinforcement could be equivalent to the performance of the same building reinforced with conventional steel bras considering the drift ratio demands.

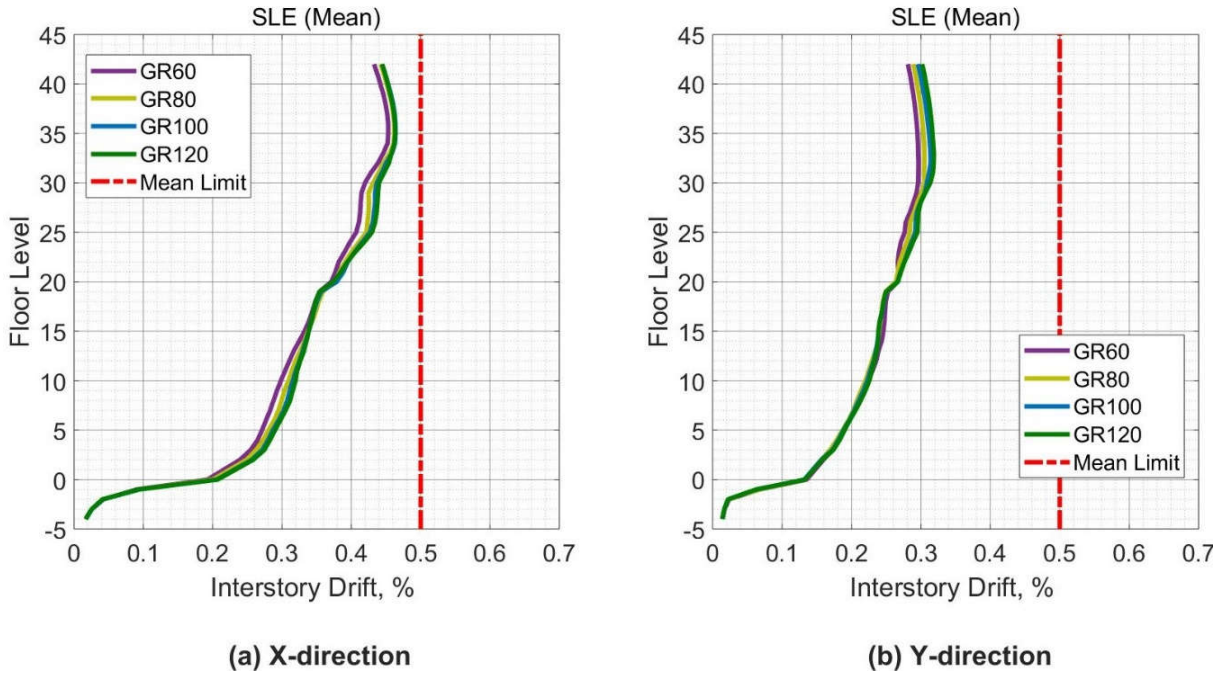

Figure 12.1 Mean of Peak Interstory Drift for Reinforcement Steel Grades Cases (SLE).

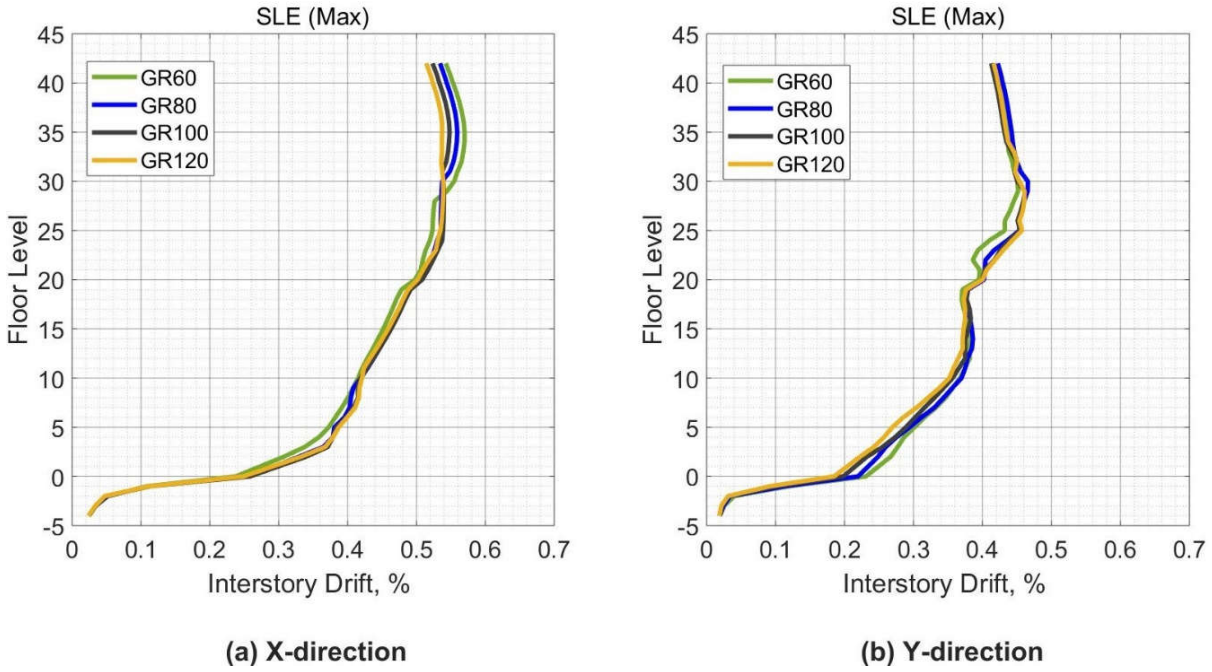

Figure 12.2 Peak Interstory Drift for Reinforcement Steel Grades Cases (SLE).

12.2.1.1.2 MCER Level

Figure 12.3 shows the mean of the peak interstory drift ratios from the eleven ground motions for the MCER level. The drift ratios demand was identical for the case study building reinforced with four different steel grades for the MCER shaking level. Figure 12.4 shows the peak interstory drift from the eleven ground motions for the case study building reinforced with four reinforcement grades. The peak drift demand is also close for all cases with a small increase for the case reinforced with Grade 120 for the upper stories compared with case of Grade 60. For all cases the drift ratio in the x-direction was more than the drift in the y-direction. The maximum drift ratio was within the limit of the mean acceptable drift. The performance of the case study building reinforced with a reduced area of high strength reinforcement and subjected to MCER shaking level could be equivalent to the performance of the same building reinforced with

conventional steel bras considering the drift ratio demands.

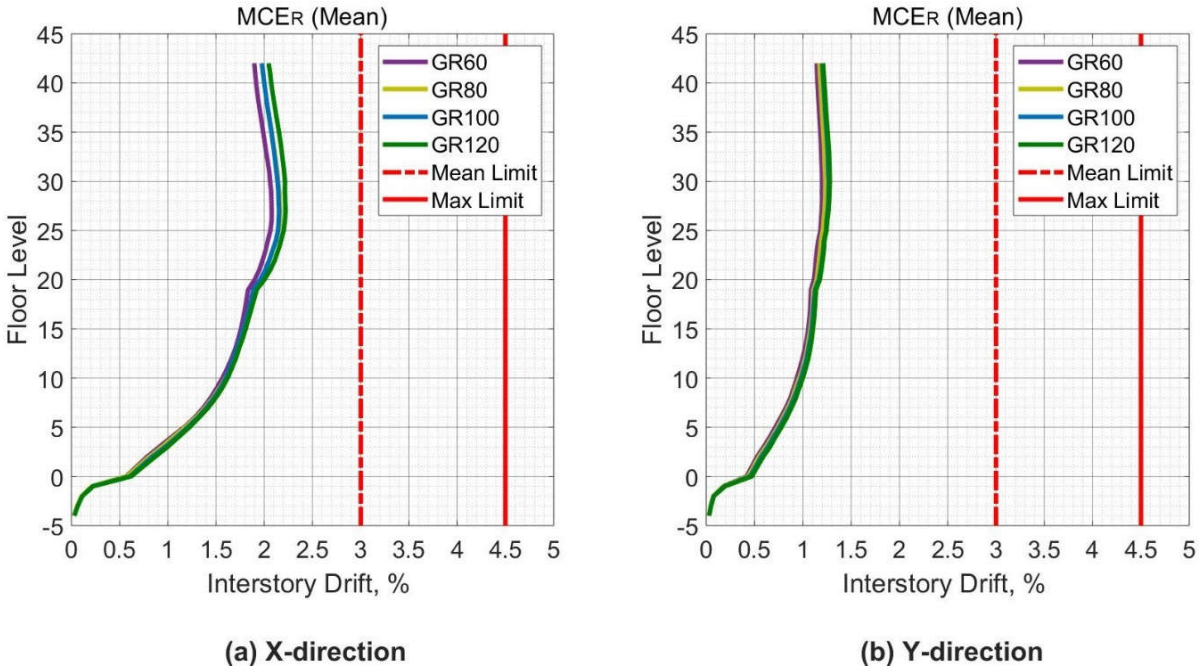

Figure 12.3 Mean of Peak Interstory Drift for Reinforcement Steel Grades Cases (MCER).

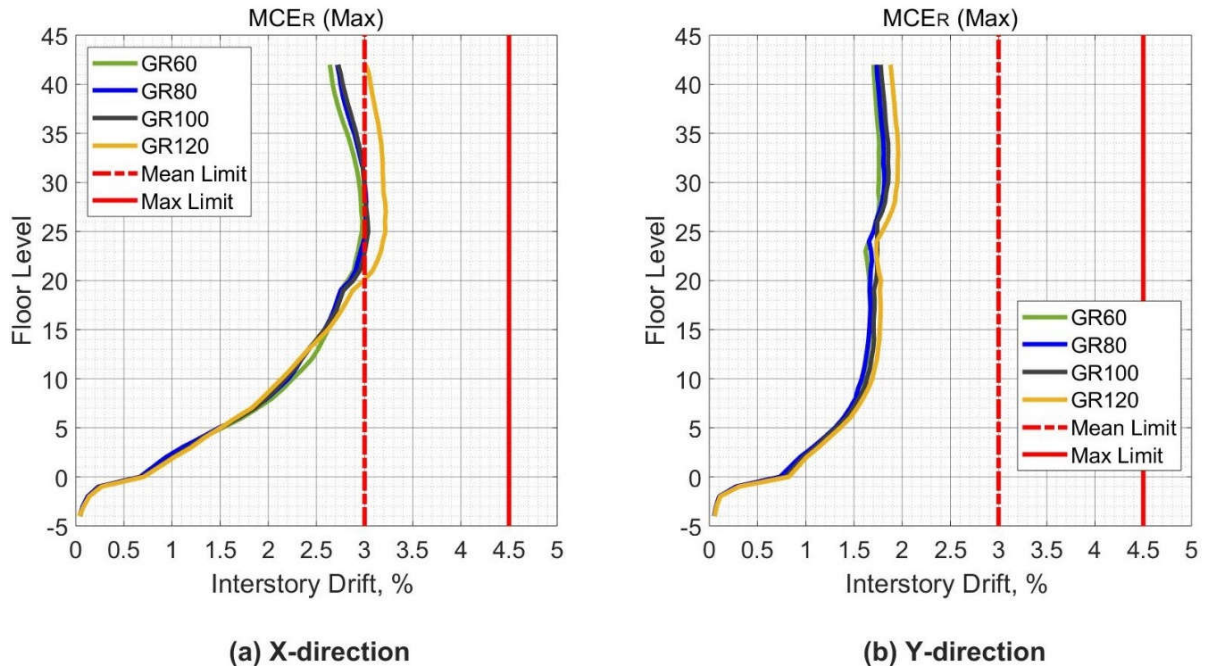

Figure 12.4 Peak Interstory Drift for Reinforcement Steel Grades Cases (MCER).

12.2.1.2 Residual Drift Ratio

12.2.1.2.1 MCER Level

Figure 12.5 shows the mean of the peak residual drift ratios from the eleven ground motions for the MCER level. The drift ratios demand was identical for the case study building reinforced with four different steel grades for the MCER shaking level. The performance of the case study building reinforced with a reduced area of high strength reinforcement and subjected to MCER shaking level could be equivalent to the performance of the same building reinforced with conventional steel bras when considering the residual drift ratio demands.

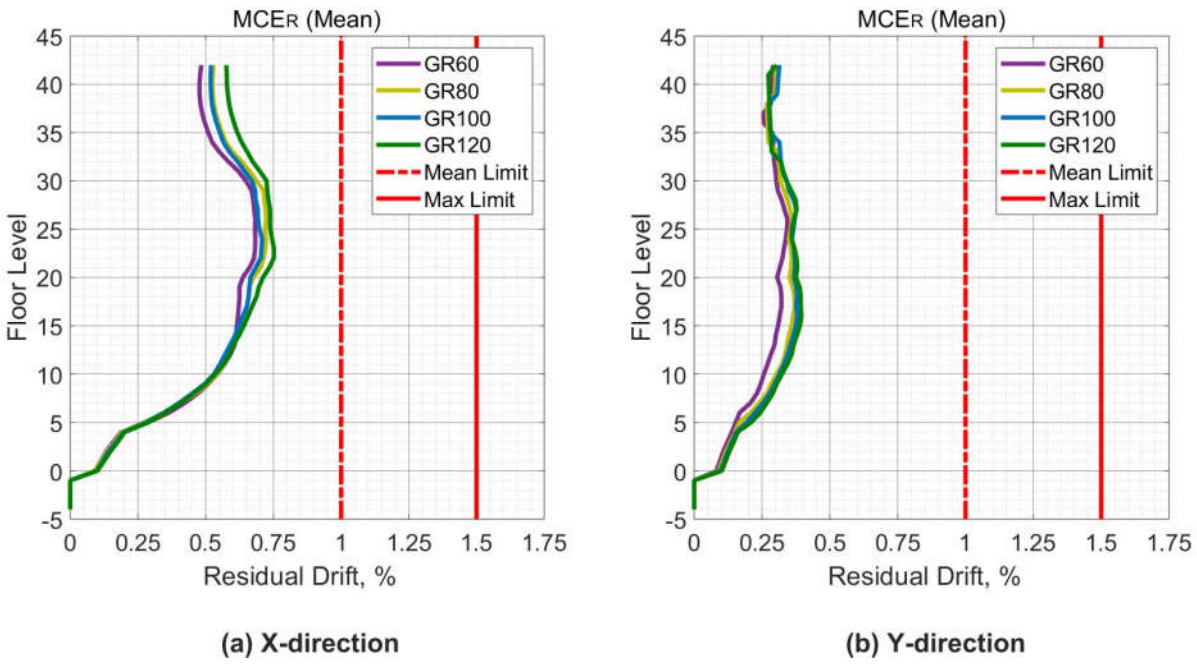

Figure 12.5 Peak Residual Drift for Reinforcement Steel Grades Cases (MCER).

12.2.1.3 Displacement

12.2.1.3.1 SLE Level

The displacement in this section is calculated at each story at the same time step when the roof experiences its maximum displacement. The TBI guidelines do not require checking the displacement demands. Figure 12.6 shows the mean displacement from the seven ground motions for the SLE level. The displacement demand for the case study building reinforced with four different steel grades was identical for the SLE shaking level. Figure 12.7 shows the peak displacement from the seven ground motions for the case study building reinforced with four reinforcement grades. The peak displacement demand is also very close for all cases. The performance of the case study building reinforced with a reduced area of high strength reinforcement could be equivalent to the performance of the same building reinforced with

conventional steel bras when considering the displacement demands.

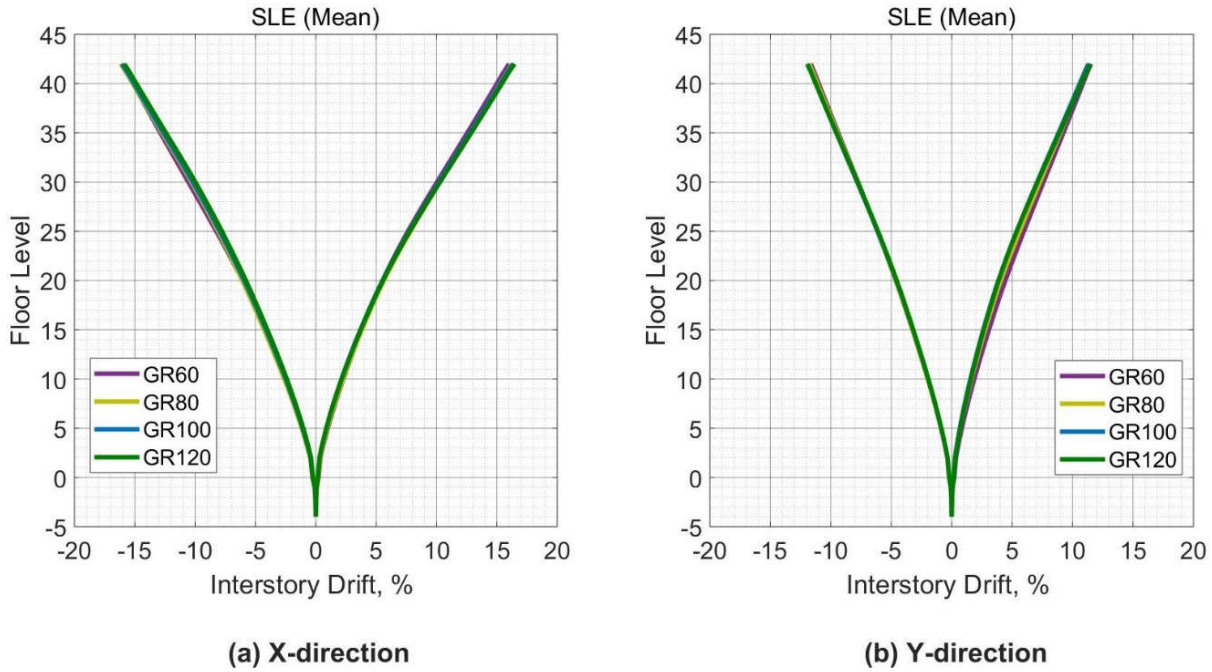

Figure 12.6 Mean of Peak Floors Displacement Synchronous with Peak Roof Displacement for Reinforcement Steel Grades Cases (SLE).

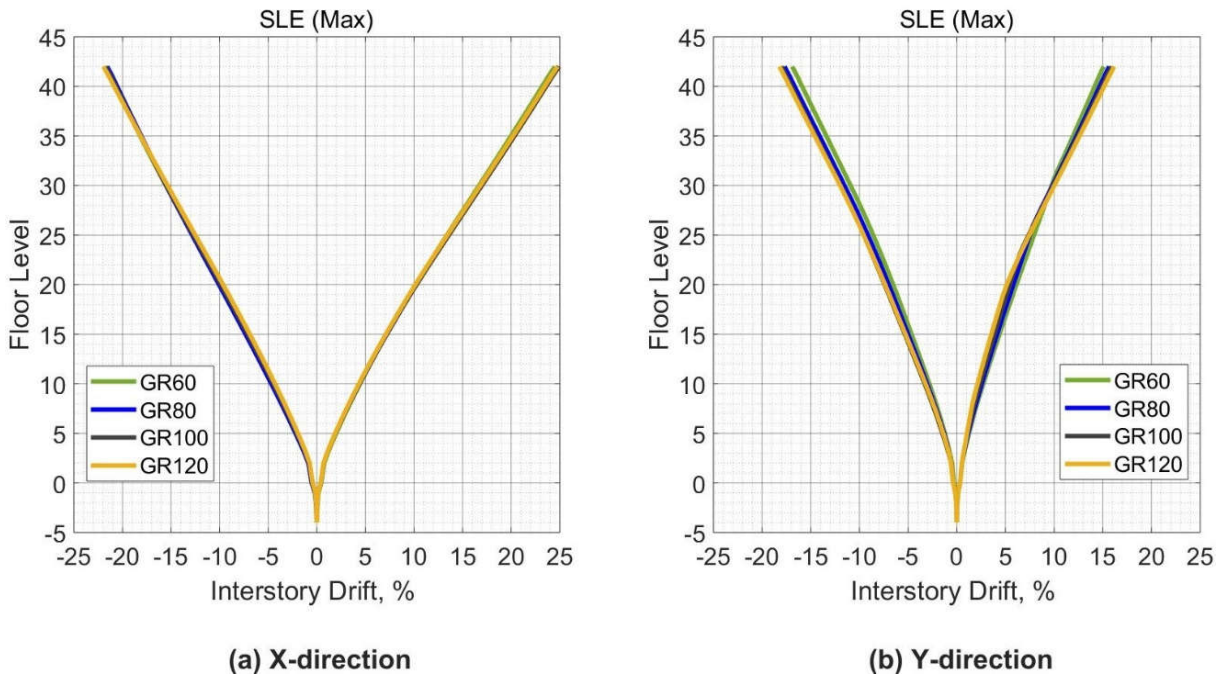

Figure 12.7 Peak Floors Displacement Synchronous with Peak Roof Displacement for Reinforcement Steel Grades Cases (SLE).

12.2.1.3.2 MCER Level

Figure 12.8 shows the mean displacement from the eleven ground motions for the MCER level. The displacement demand was similar for the case study building reinforced with four different steel grades for the MCER shaking level. Figure 12.9 shows the peak displacement from the eleven ground motions for the case study building reinforced with four reinforcement grades. The peak displacement demand was also close for all cases. The performance of the case study building reinforced with a reduced area of high strength reinforcement and subjected to MCER shaking level could be equivalent to the performance of the same building reinforced with conventional steel bras when considering the drift ratio demands.

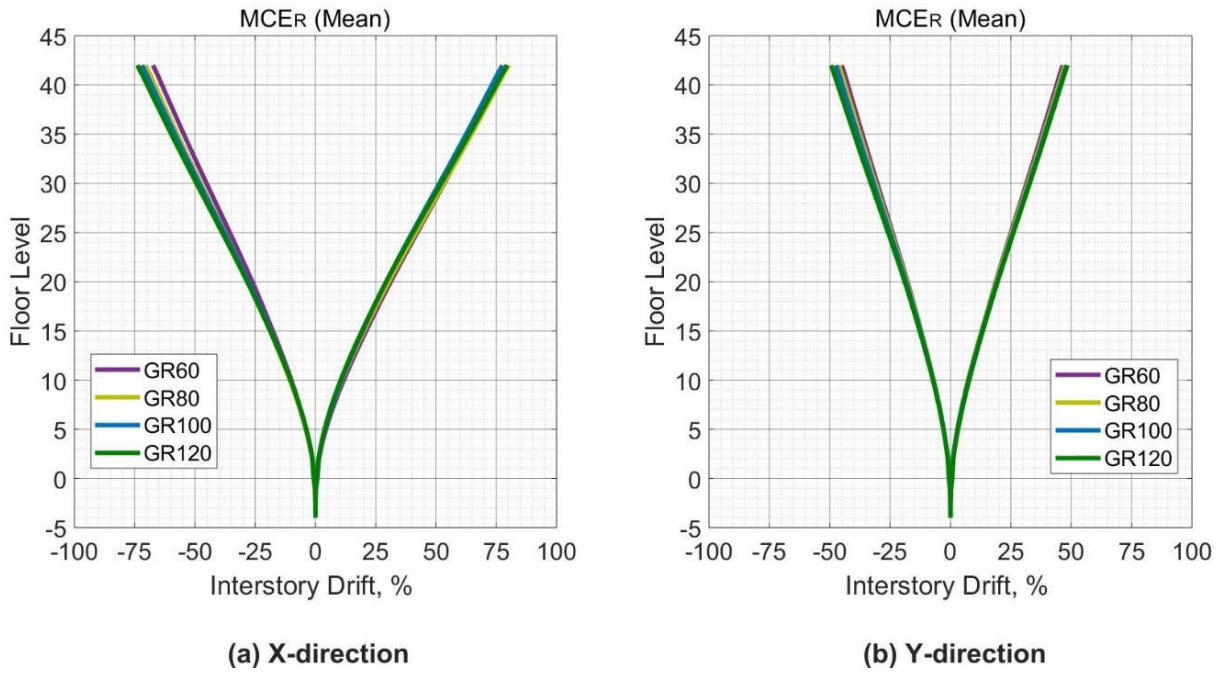

Figure 12.8 Mean of Peak Floors Displacement Synchronous with Peak Roof Displacement for Reinforcement Steel Grades Cases (MCER).

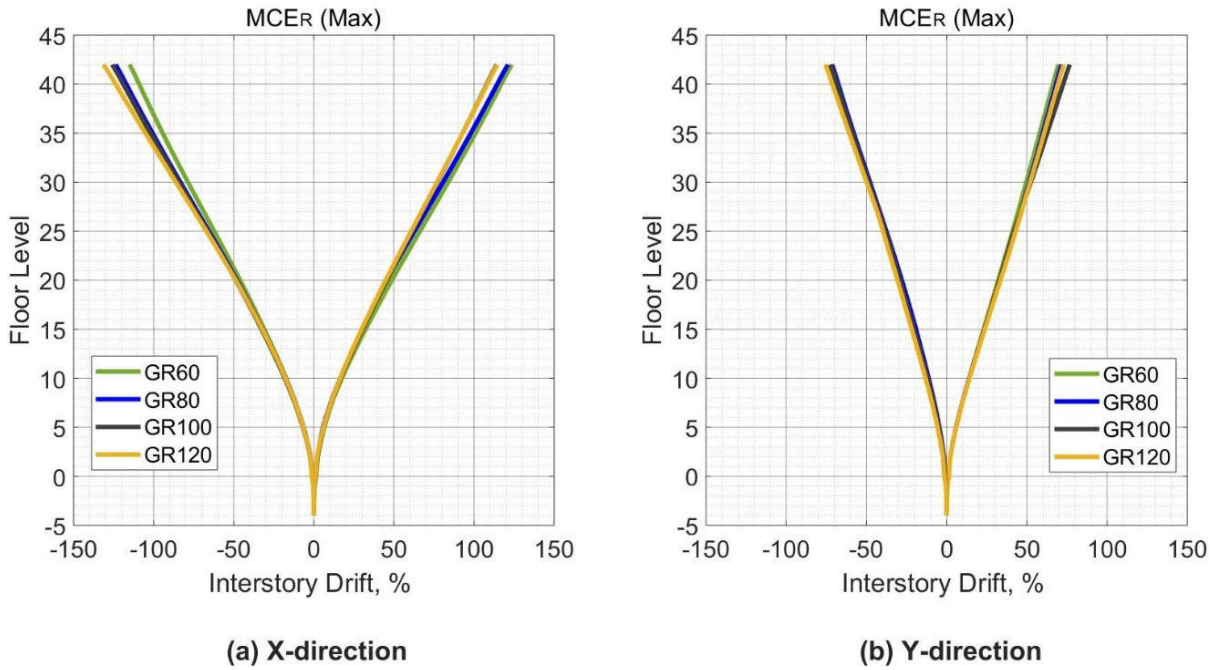

Figure 12.9 Peak Floors Displacement Synchronous with Peak Roof Displacement for Reinforcement Steel Grades Cases (MCER).

12.2.2 Element Level

Both the results of the force-based actions and deformation-based actions will be presented for the reference case and the high strength reinforcement cases. The mean value of the peak response parameters as well as the peak parameters from all analyses will be presented for both the SLE and MCER shaking levels.

12.2.2.1 Core Wall

12.2.2.1.1 SLE Level

Figure 12.10 shows the mean of the peak of the shear force demand in the core wall from the seven ground motions for the SLE level over the building height. The shear force demand was identical for both the reference case and the high strength reinforcement cases for the SLE shaking level. The shear demands experienced some changes near the twentieth story due to the thickness

change of the core wall from 24 in. to 18 in. Figure 12.11 shows the peak shear force demand in the core wall from the seven ground motions over the building height for all cases. The peak shear force demand was also identical for all cases. Depending on the results of the shear response of the core wall, the performance of core wall reinforced with a reduced area of high strength reinforcement is equivalent to the performance of the same wall reinforced with conventional steel bras.

For the deformation-based actions in the core wall, Figure 12.12 depicts the peak of the tensile strain in reinforcing bars in all edges over the building height for SLE level. The tensile strain distribution is approximately the same for all cases, however the maximum tensile strain is 0.002 which is below the expected yielding strain of all used grades. For SLE level, the reinforcing steel bars did not experience yielding. Figure 12.13 depicts the maximum compression strain in the concrete of the core wall edges over the building height. For all cases, the concrete experienced very low compression strain. The apparent similarity in the response of the core wall reflect the equivalent performance between the reference case and the cases reinforced with a reduced area of high strength reinforcement.

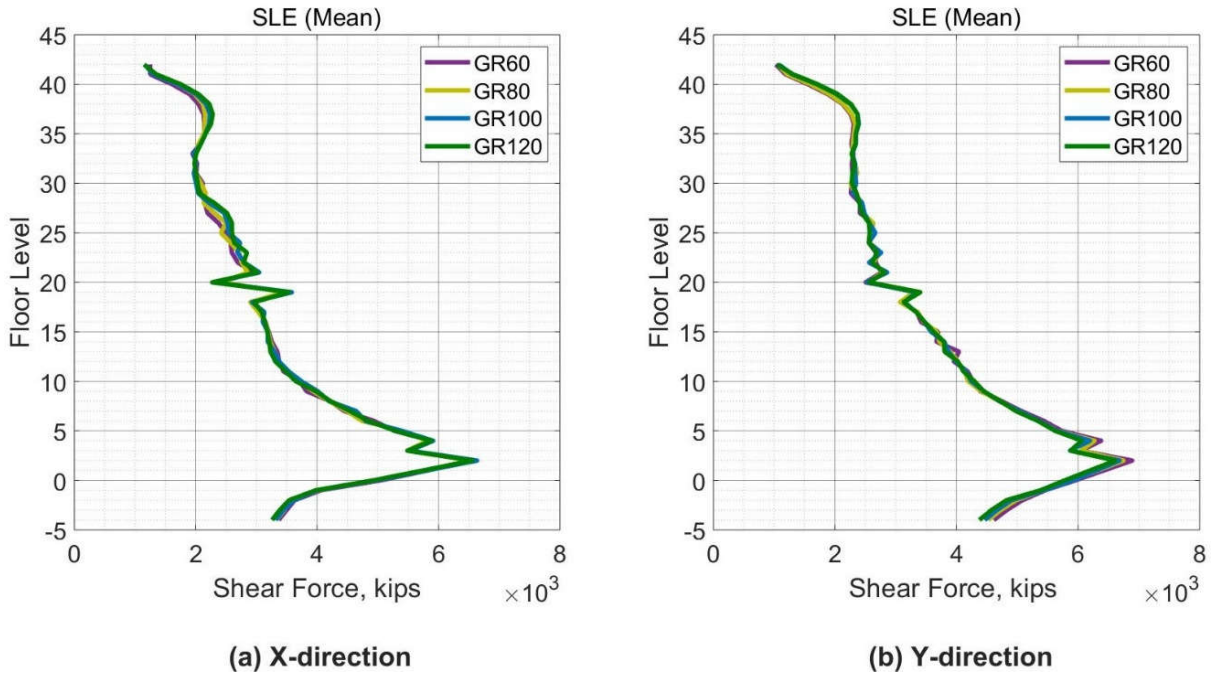

Figure 12.10 Mean of Peak Shear Forces in Core Wall for Reinforcement Steel Grades Cases (SLE).

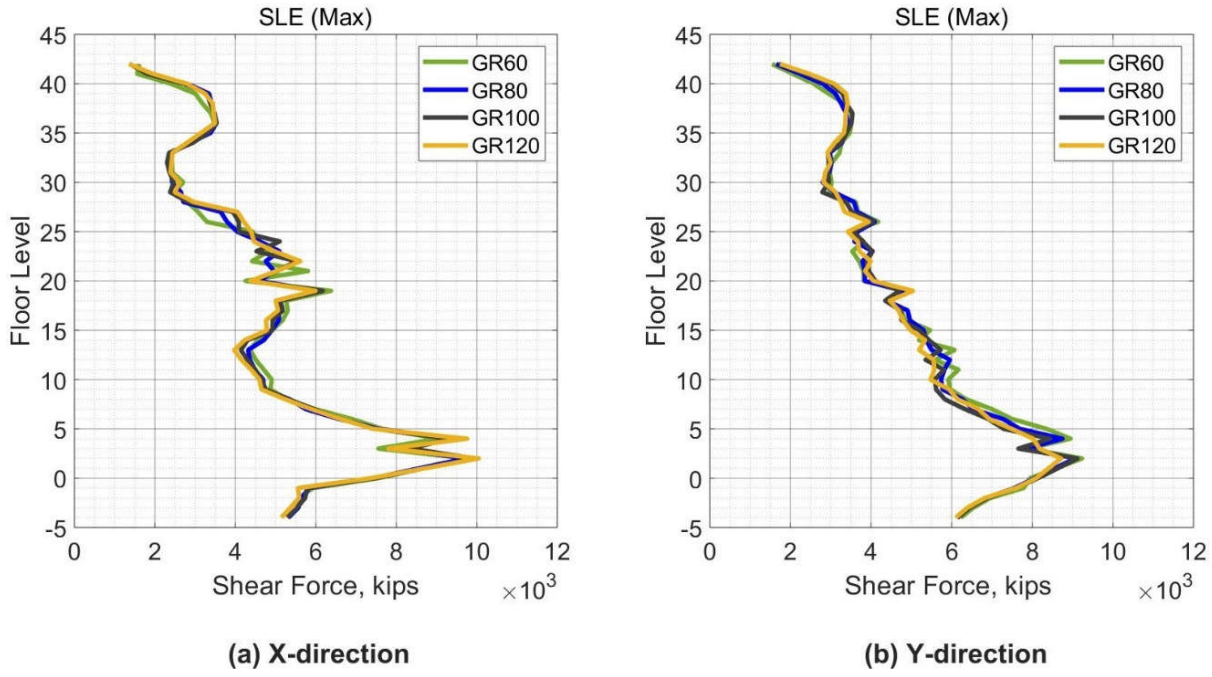

Figure 12.11 Peak Shear Forces in Core Wall for Reinforcement Steel Grades Cases (SLE).

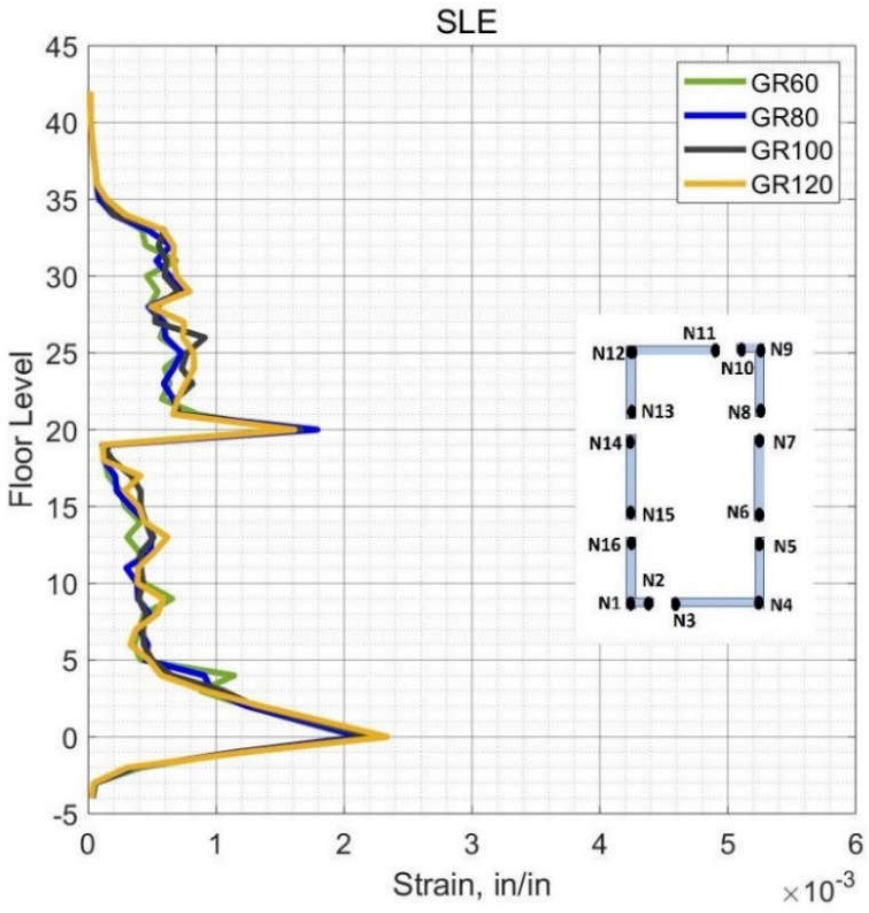

Figure 12.12 Peak of Reinforcement Tensile Strain in Core Wall for Reinforcement Steel Grades Cases (SLE).

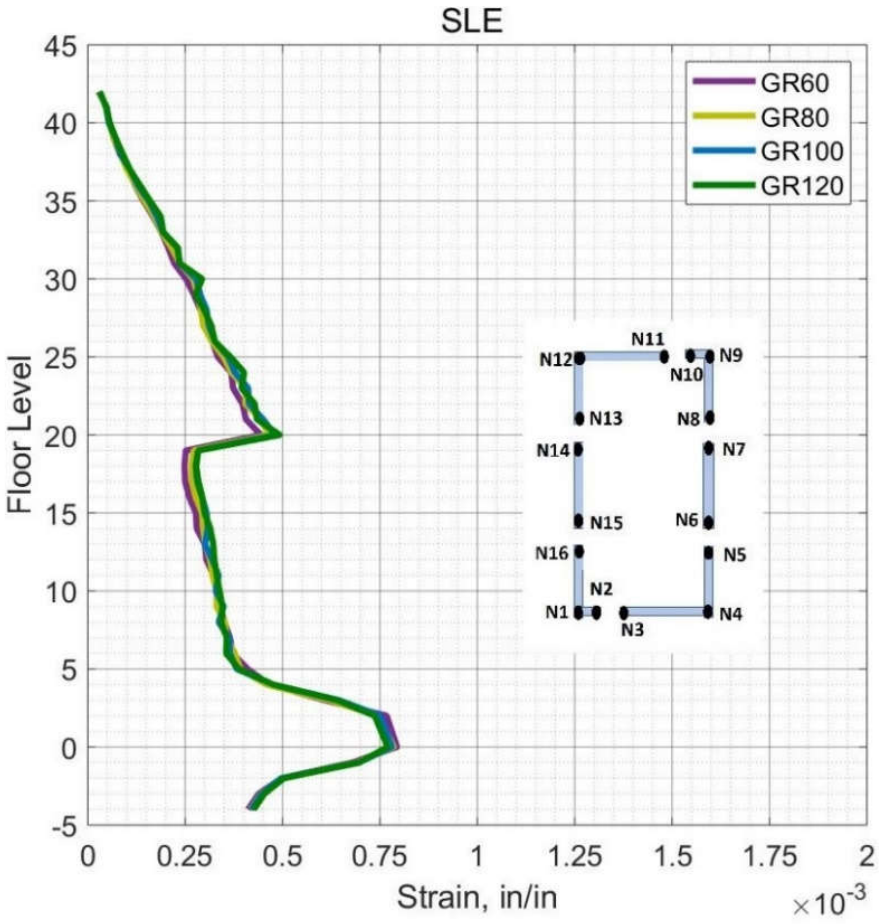

Figure 12.13 Peak of Concrete Compression Strain in Core Wall for Reinforcement Steel Grades Cases (SLE).

12.2.2.1.2 MCER Level

Figure 12.14 shows the mean of the peak shear force demand in the core wall from the eleven ground motions for the MCER level over the building height. The shear force demand in the core wall varies linearly over the building height for all cases. The shear force demand was identical for all cases for the MCER shaking level. The shear demands experienced some variations near the twentieth story due to the thickness change of the core wall from 24 in. to 18 in. Figure 12.15 shows the peak shear force demand in the core wall from the eleven ground motions over

the building height for the case study building reinforced with four reinforcement grades. The peak shear force demands were identical for all cases. Depending on the results of the shear forces response of the core wall, the performance of core wall reinforced with a reduced area of high strength reinforcement is equivalent to the performance of the same wall reinforced with conventional steel bras.

For the deformation-based actions in the core wall, Figure 12.16 depicts the peak of the tensile strain in reinforcing bars in all edges over the building height for MCER level. The tensile strain distribution is approximately the same for all cases, however the maximum tensile strain is 0.016 which indicates that the reinforcing bars in the core wall experienced yielding for all cases. However, the 0.016 tensile strain is still below the maximum acceptable limit of the ASCE 41 of 0.05. For case GR80, the maximum tensile strain in the longitudinal reinforcement of the core wall is far below the minimum requirements for the fracture elongation (total elongation) of Grade 80 (0.12) according to the ASTM A 706. In addition, the maximum tensile strain demand is below 75% of the uniform elongation of Grade 80 (0.088) (Sokoli and Ghannoum, 2016). For seismic applications, the reliable maximum tensile strain for reinforcing bars is 75% of the uniform elongation (NEHRP, 2014). The maximum tensile strain demand in reinforcing bars of the core wall for cases GR100 and GR120 was 0.016. ASTM 1035 for Grades 100 and 120 specifies the minimum fracture elongation 0.07 which is higher than the measured demands for both cases. The uniform elongation of Grades 100 and 120 is approximately 0.045 (NEHRP, 2014). The maximum tensile demands are below the limit of 75% of the uniform elongation for both cases GR100 and GR120 making both steel grades suitable for seismic applications.

Although the tensile strain of the reinforcing bars of the core wall was approximately similar between the refence case and the high strength steel cases, the benefit of using high strength

reinforcement in the core wall is that the reduction in the number of stories that experienced yielding of reinforcing steel. This reduction improves the performance and controls the damage over the core wall height. Figure 12.17 depicts the maximum compression strain in the concrete of the core wall edges over the building height. For all cases, the concrete experienced low compression strain (0.002) which is below the maximum acceptable limit of 0.003. The apparent similarity in the response of the core wall reflect the equivalent performance between the reference case and the cases reinforced with a reduced area of high strength reinforcement. Both the tensile strain and the compression strain showed some variation in the response near the twentieth story due to the thickness change of the core wall from 24 in. to 18 in.

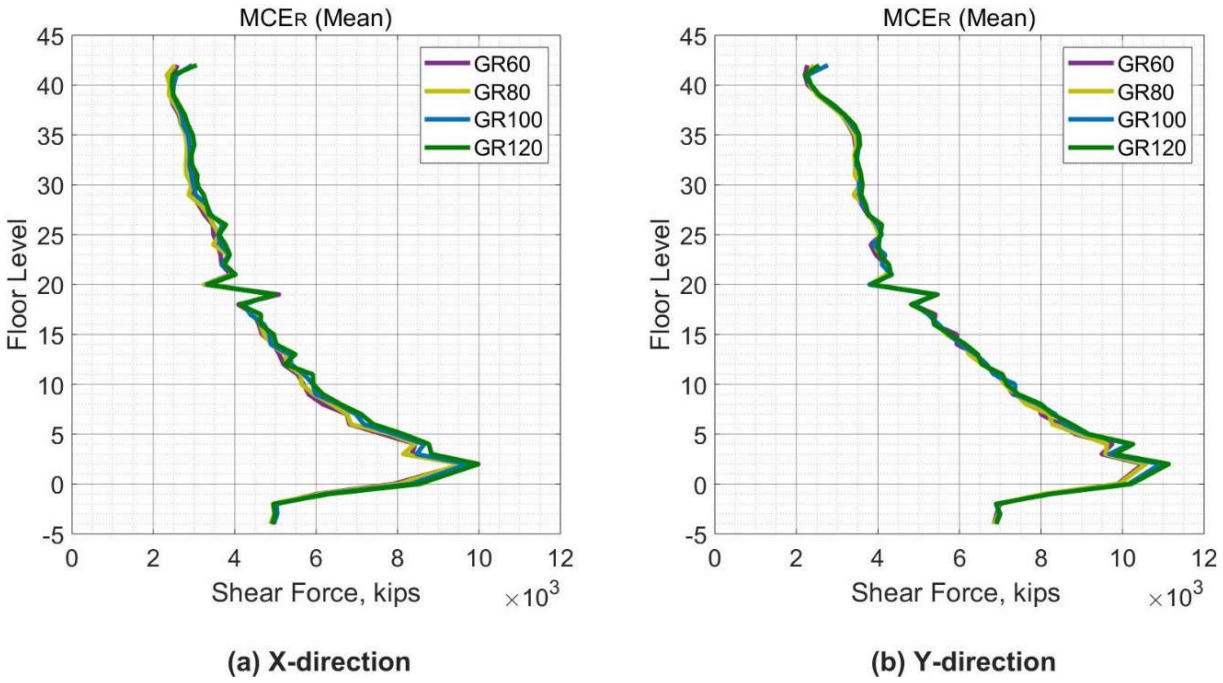

Figure 12.14 Mean of Peak Shear Forces in Core Wall for Reinforcement Steel Grades Cases (MCRE).

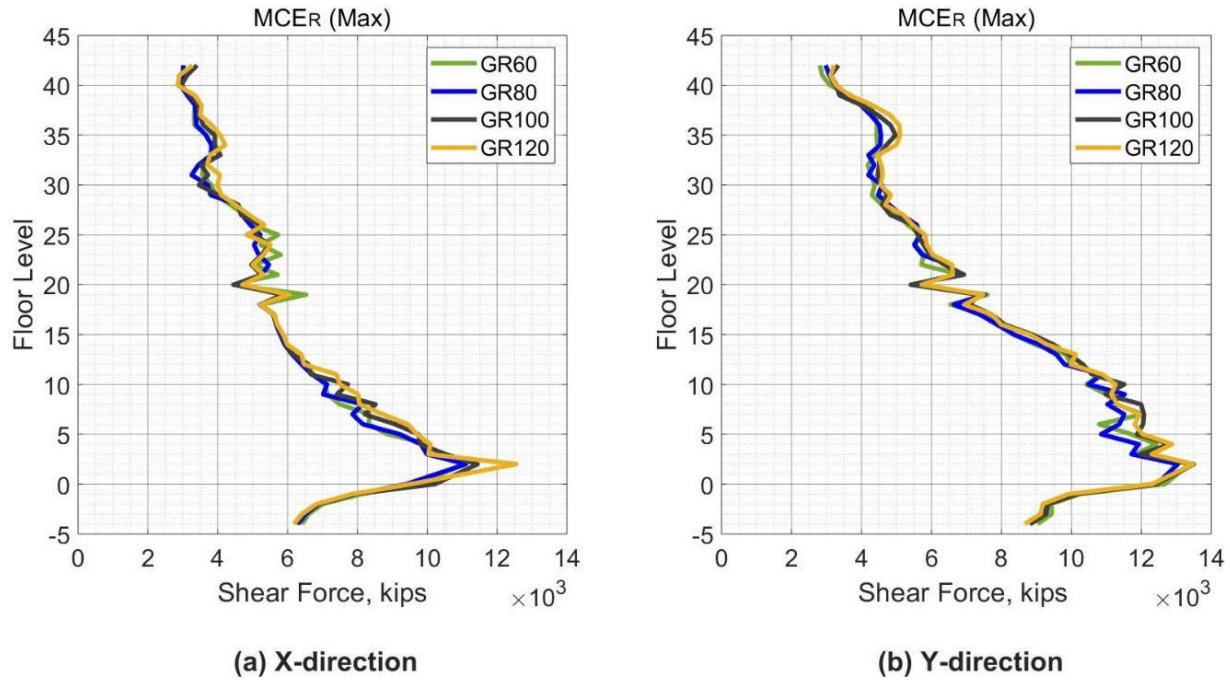

Figure 12.15 Peak Shear Forces in Core Wall for Reinforcement Steel Grades Cases (MCER).

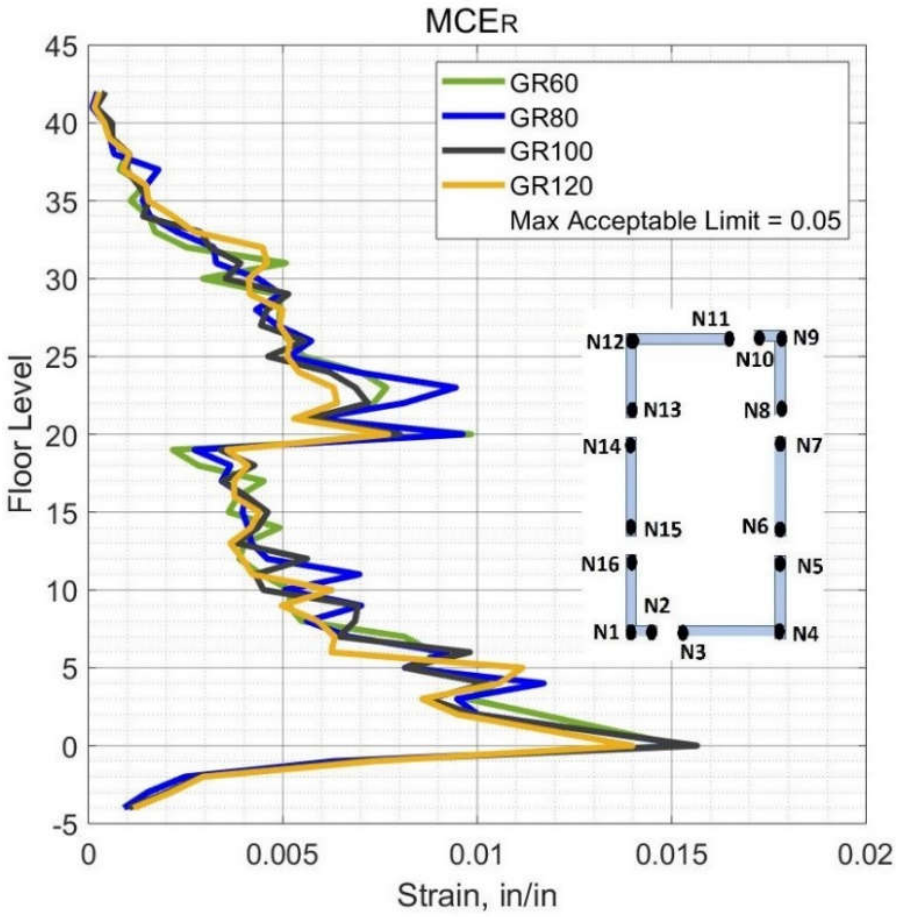

Figure 12.16 Peak of Reinforcement Tensile Strain in Core Wall for Reinforcement Steel Grades Cases (MCER).

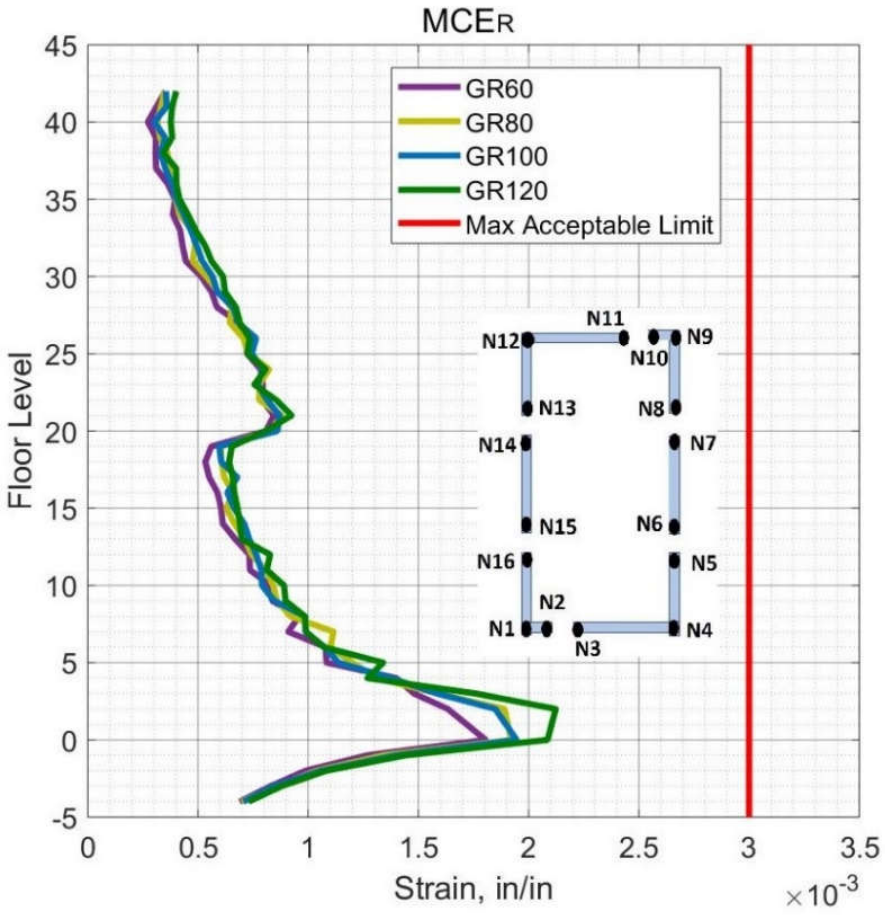

Figure 12.17 Peak of Concrete Compression Strain in Core Wall for Reinforcement Steel Grades Cases (MCER).

12.2.2.2 Coupling Beam

12.2.2.2.1 SLE Level

Figure 12.18 shows the mean of the peak rotation demand in the coupling beams from the seven ground motions for the SLE level over the building height. The rotation demand was identical for all cases for the SLE shaking level. Figure 12.19 shows the peak rotation demand in the core wall from the seven ground motions over the building height for the case study building reinforced with four reinforcement grades. The peak value of the rotation is 0.002 which indicate

that coupling beams did not experience yielding of steel reinforcement according to the data in Figure 7.18. Depending on the results of the rotation demands of the coupling beams, the performance of the coupling beams reinforced with a reduced area of high strength reinforcement is equivalent to the performance of the same beams reinforced with conventional steel bras.

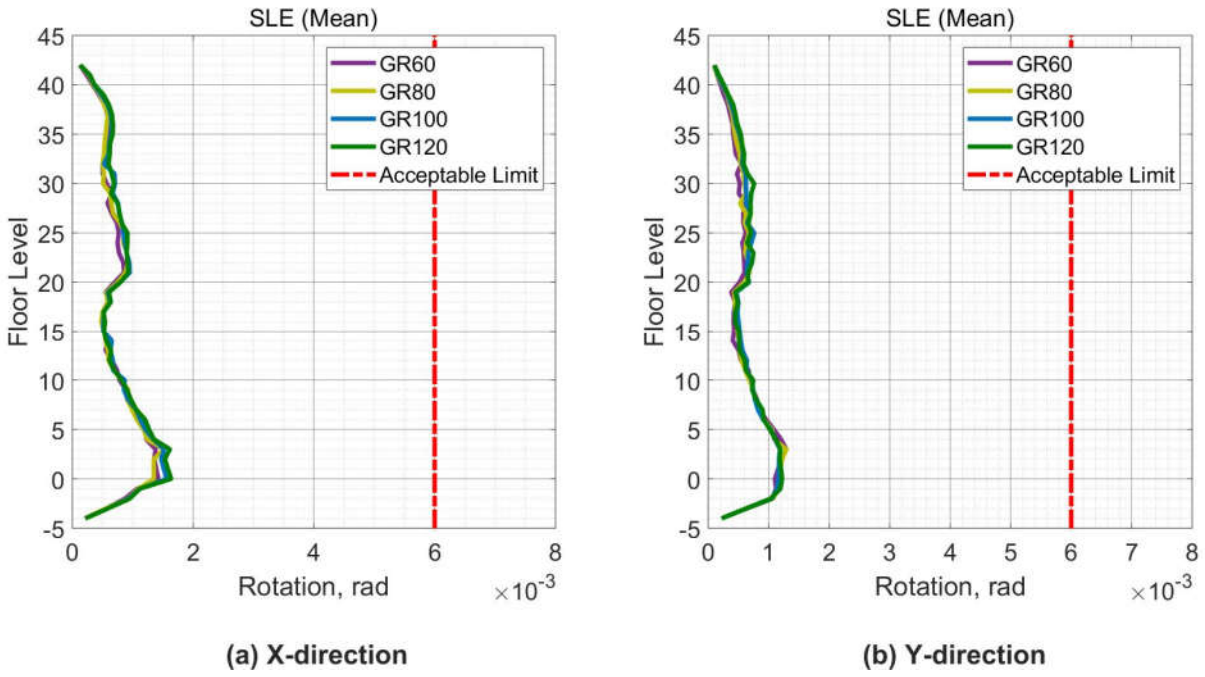

Figure 12.18 Mean of Peak Rotation Demand in Coupling Beams for Reinforcement Steel Grades Cases (SLE).

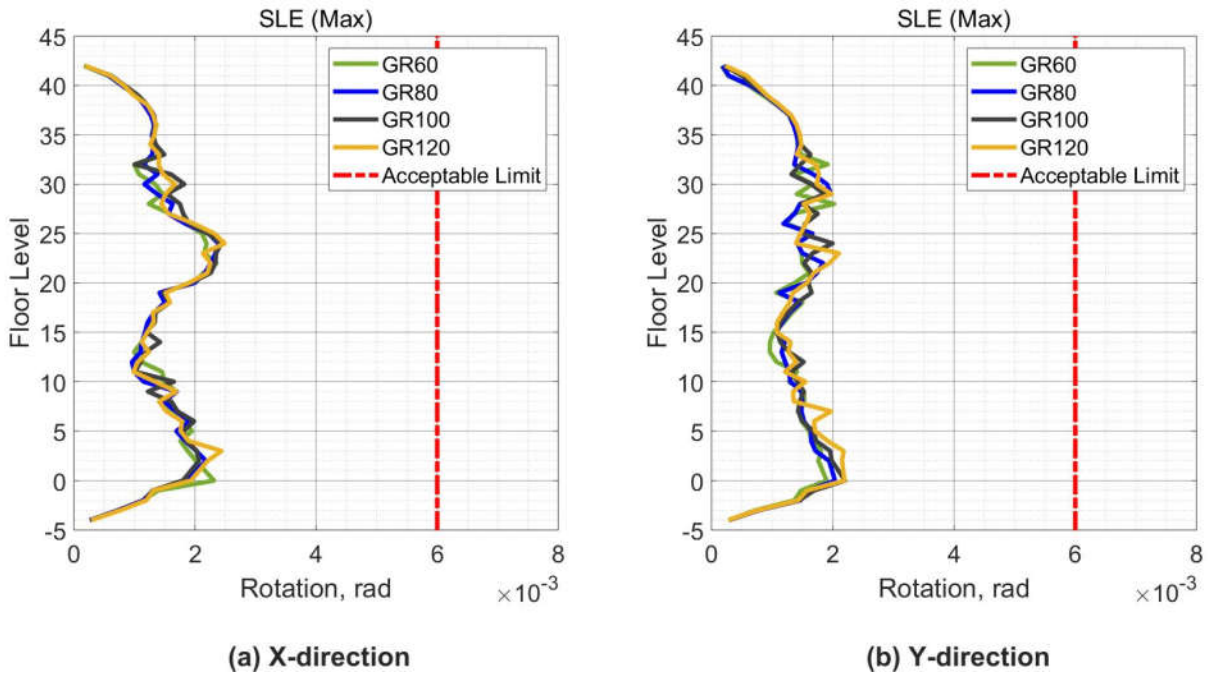

Figure 12.19 Peak Rotation Demand in Coupling Beams for Reinforcement Steel Grades Cases (SLE).

12.2.2.2.2 MCER Level

Figure 12.20 shows the mean of the peak rotation demand in the coupling beams from the eleven ground motions for the MCER level over the building height. The mean rotation demand was similar for the case study building reinforced with four different steel grades for the MCER shaking level. Figure 12.21 shows the peak rotation demand in the core wall from the eleven ground motions over the building height for the case study building reinforced with four reinforcement grades. For the peak rotation demand, the case GR120 showed the highest demand. The peak value of the rotation is 0.03 which indicate that coupling beams experienced yielding of steel reinforcement and minor damage state which means that coupling beams need only minor repair to be functional again according to the data in Figure 7.18. Depending on the results of the rotation demands of the coupling beams, the performance of the coupling beams reinforced with a

reduced area of high strength reinforcement is equivalent and comparable to the performance of the same beams reinforced with conventional steel bras.

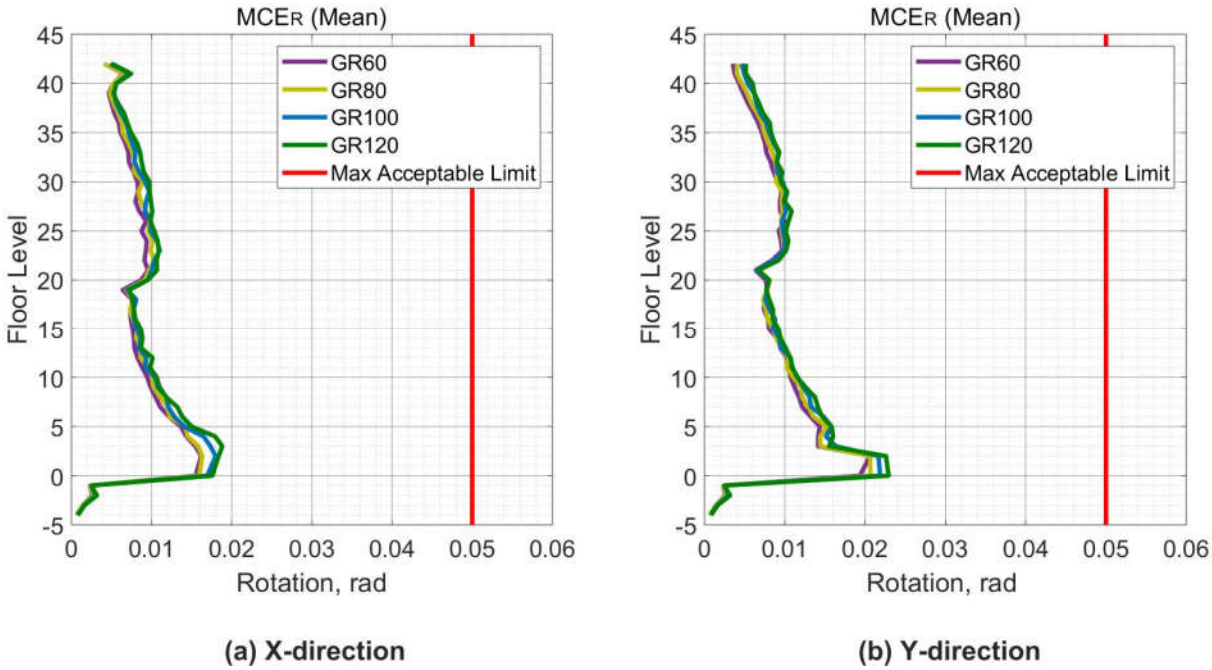

Figure 12.20 Mean of Peak Rotation Demand in Coupling Beams for Reinforcement Steel Grades Cases (MCER).

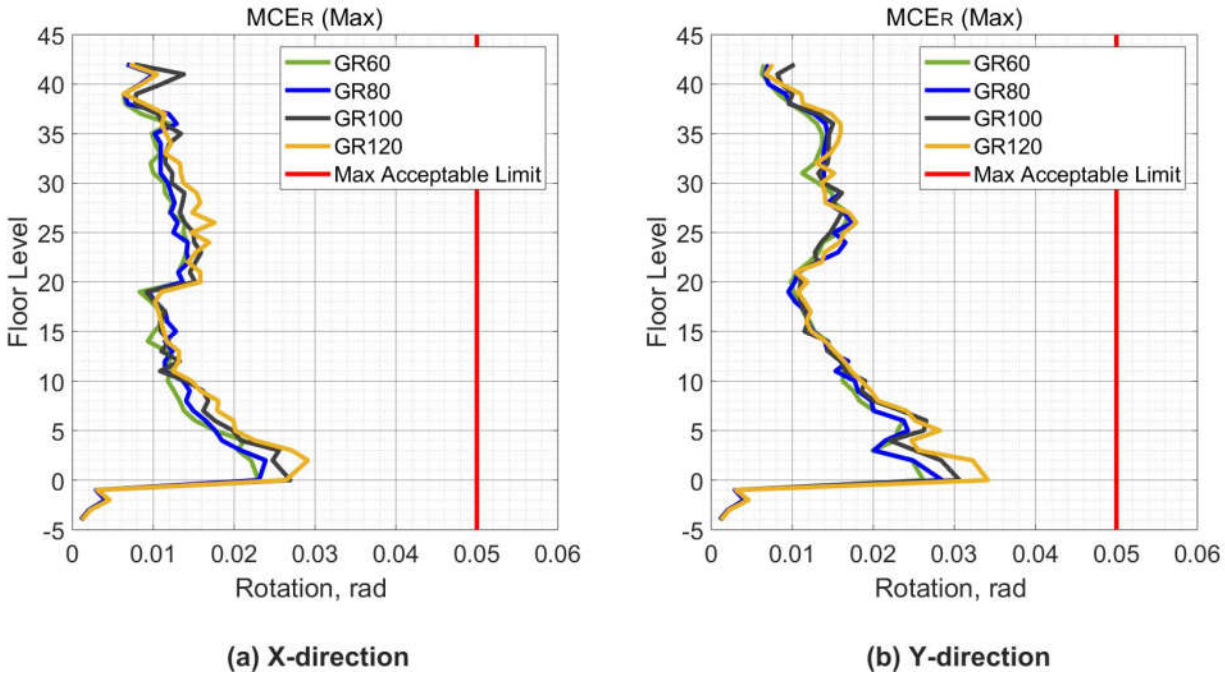

Figure 12.21 Peak Rotation Demand in Coupling Beams for Reinforcement Steel Grades Cases (MCER).

12.2.2.3 Beams

12.2.2.3.1 SLE Level

Figure 12.22 shows the mean of the peak shear force demand in the beams of the special moment frame from the seven ground motions for the SLE level over the building height. The beams shear force demand was similar for the case study building reinforced with four different steel grades for the SLE shaking level. For each case, the shear force demand of the beams was approximately uniform over the building height. Figure 12.23 shows the peak shear force demand in the beams from the seven ground motions over the building height for the case study building reinforced with four reinforcement grades. The peak shear forces demand is less than the reduced shear capacity of the beams for all cases. Depending on the results of the shear response of the beams, the performance of special moment frame beams reinforced with a reduced area of high

strength reinforcement is equivalent to the performance of the same beams reinforced with conventional steel bras.

For the deformation-based actions in the beams, Figure 12.24 depicts the mean of the peak tensile strain in longitudinal reinforcing bars in the beams over the building height for SLE level. A small increase in the mean tensile strain demand was noticed with using a reduced area of high strength reinforcement compared with the conventional bars. Figure 12.25 depicts the peak of the tensile strain in longitudinal reinforcing bars in the beams over the building height for SLE level. The maximum tensile strain is 0.0025 which is below the expected yielding strain of all used grades. For SLE level, the reinforcing steel bars in the beams did not experience yielding. For all cases, the beams responded linearly, and no plastic hinges formed.

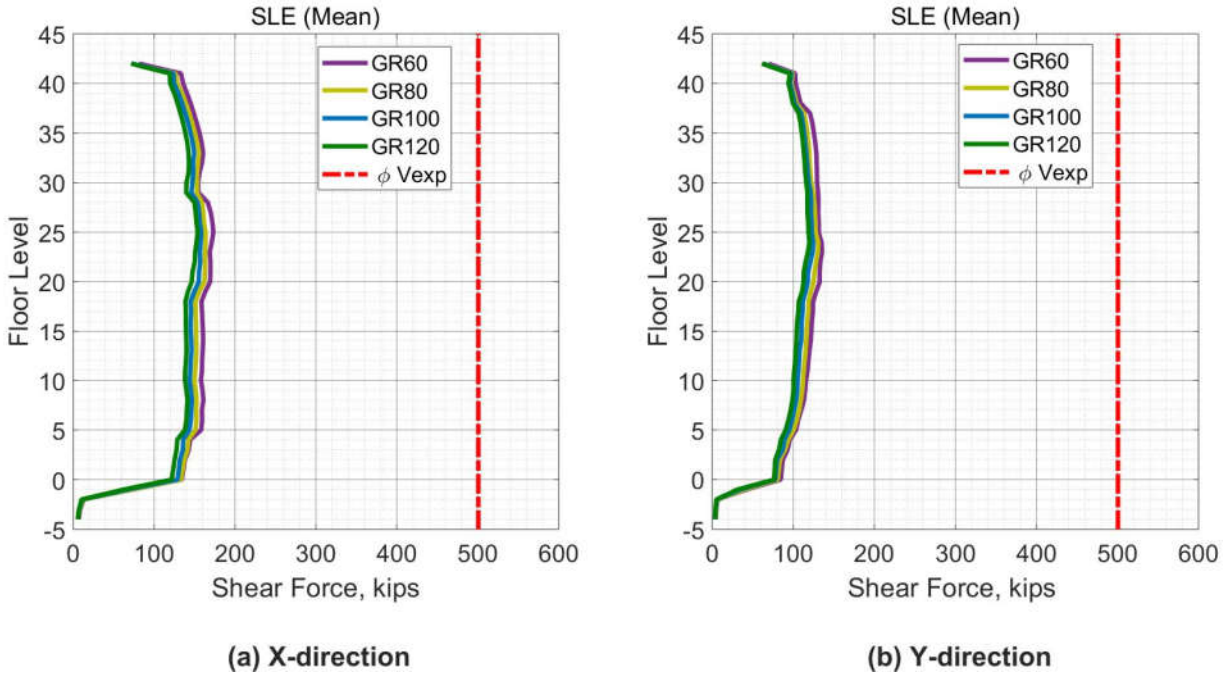

Figure 12.22 Mean of Peak Shear Forces in Beams for Reinforcement Steel Grades Cases (SLE).

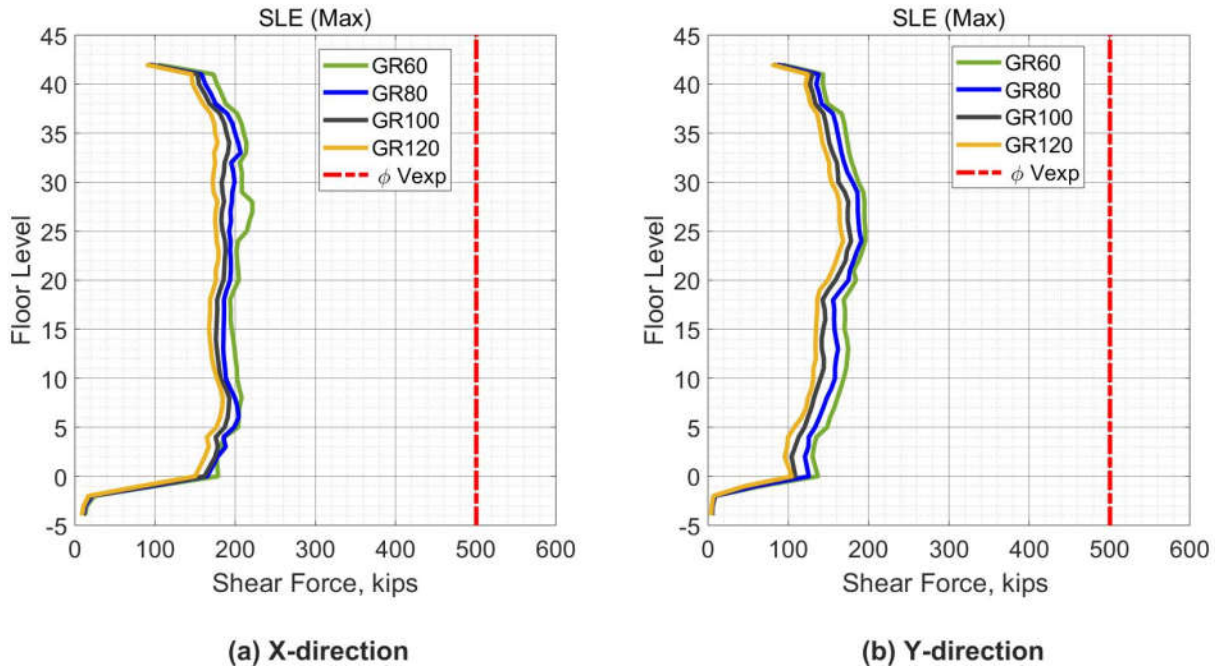

Figure 12.23 Peak Shear Forces in Beams for Reinforcement Steel Grades Cases (SLE).

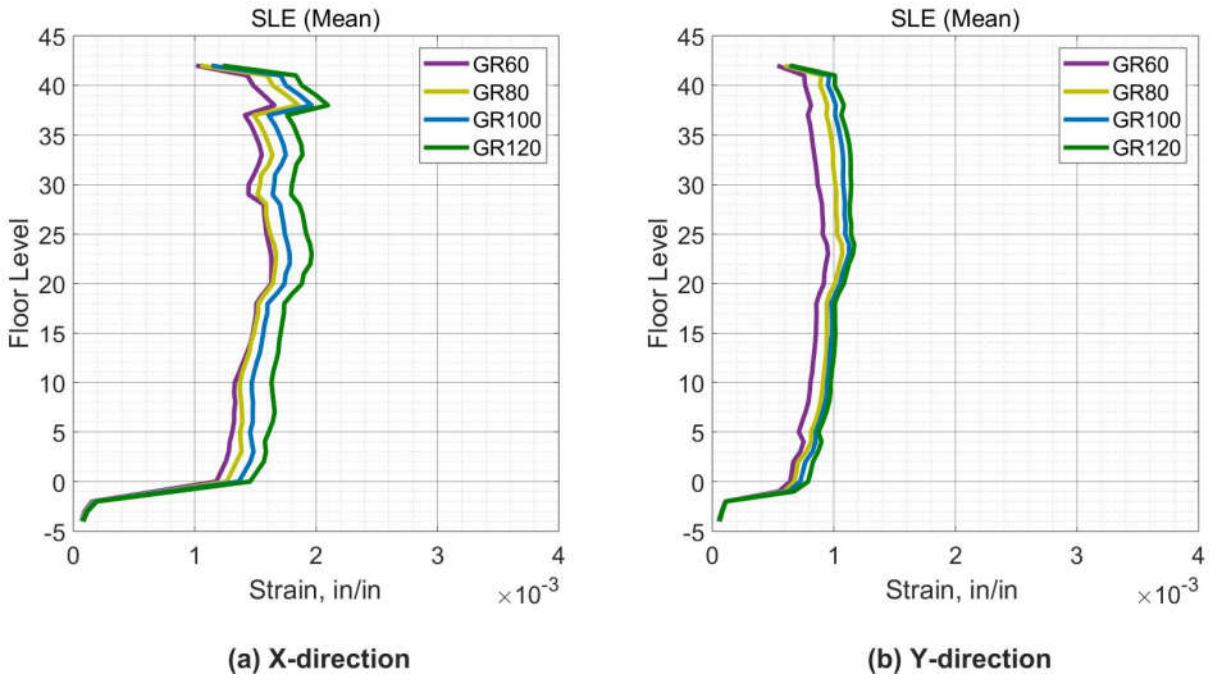

Figure 12.24 Mean of Peak of Reinforcement Tensile Strain in Beams for Reinforcement Steel Grades Cases (SLE).

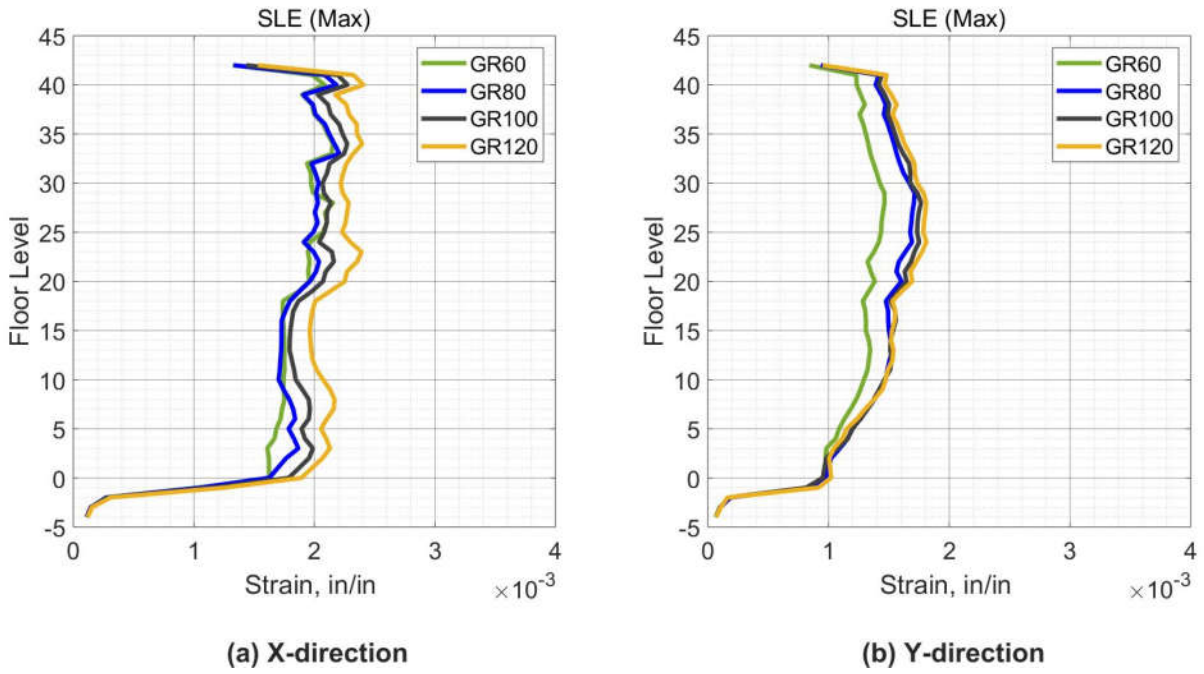

Figure 12.25 Peak of Reinforcement Tensile Strain in Beams for Reinforcement Steel Grades Cases (SLE).

12.2.2.3.2 MCER Level

Figure 12.26 shows the mean of the peak shear force demand in the beams of the special moment frame from the eleven ground motions for the MCER level over the building height. The beams shear force mean demand was identical for the case study building reinforced with four different steel grades for the MCER shaking level. For each case, the shear force demand of the beams was approximately uniform over the building height, however the response showed some variation near the twenty ninth story due to the changing of longitudinal reinforcement area of the beams. Figure 12.27 shows the peak shear force demand in the beams from the eleven ground motions over the building height for the case study building reinforced with four reinforcement grades. The peak shear forces demand is less than the unreduced shear capacity of the beams for all cases. Depending on the results of the shear response of the beams, the performance of special

moment frame beams reinforced with a reduced area of high strength reinforcement is equivalent to the performance of the same beams reinforced with conventional steel bras.

For the deformation-based actions in the beams, Figure 12.28 depicts the mean of the peak tensile strain in longitudinal reinforcing bars in the beams over the building height for MCER level. An increase in the mean tensile strain was noticed with using a reduced area of high strength reinforcement compared with the conventional bars.

Figure 12.29 depicts the peak of the tensile strain in longitudinal reinforcing bars in the beams over the building height for MCER level. The maximum tensile strain for the case GR60 was 0.026 which is below the maximum acceptable limit of 0.05 of ASCE 41. For GR80, the maximum tensile strain in the beams was 0.03. According to the ASTM A 706, the minimum requirements for the fracture elongation (total elongation) of Grade 80 is 0.12 which is higher than the measured tensile strain of 0.03. The maximum tensile strain demand for the beam longitudinal bars (0.03) is below the uniform elongation of Grade 80 (0.088) (Sokoli and Ghannoum, 2016). In addition, for seismic application, the reliable maximum tensile strain for reinforcing bars is 75% of the uniform elongation (NEHRP, 2014). The maximum tensile strain demand is below the 75% of its uniform elongation for case GR80. The maximum tensile strain demands in the beams for cases GR100 and GR120 were 0.033 and 0.036, respectively. ASTM 1035 for Grades 100 and 120 specifies the minimum fracture elongation 0.07 which is higher than the measured demands for both cases. The uniform elongation of Grades 100 and 120 is approximately 0.045 (NEHRP, 2014). The maximum tensile demands are below the limit of 75% of the uniform elongation for both cases GR100 and GR120 making both steel grades suitable for seismic applications. The behavior that high strength steel bars experience more tensile demands compared with conventional bars was observed by some experimental works such as (Tavallali et al. 2014,

Rautenberg 2011, Sokoli and Ghannoum, 2016).

The plastic rotation is an indicator for the flexural demands in the beams. The mean of the peak of the plastic rotation of the beams for MCER level is depicted in Figure 12.30, while the peak plastic rotation is depicted in Figure 12.31. Like the tensile strain results, the plastic rotation showed some increase with the high strength reinforcement compared with conventional bars. However, the maximum plastic rotation for all cases was below the maximum acceptable limit of ACSE 41 (0.045). for high strength reinforcement cases, the range of the maximum rotation demand for the beams was 0.03-0.04. According to the work (Tavallali et al. 2014, Rautenberg 2011, Sokoli and Ghannoum, 2016), cyclic tests were done on beams or columns reinforced with high strength reinforcement up to drift ratio of 5% and the specimens were successfully passed the test with stable hysteric loops.

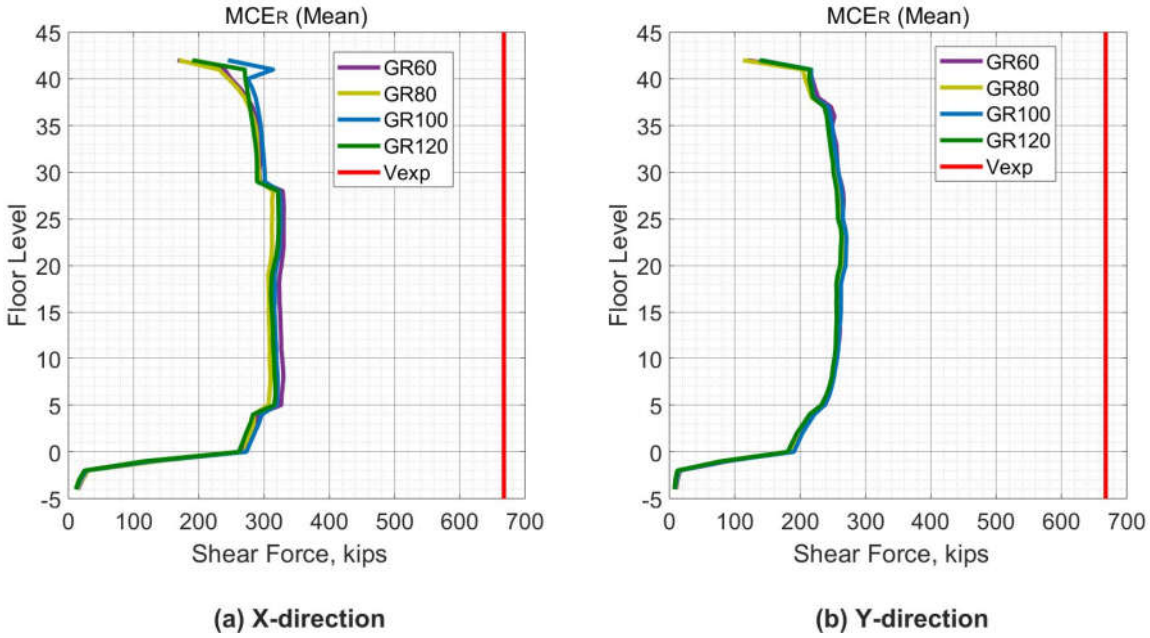

Figure 12.26 Mean of Peak Shear Forces in Beams for Reinforcement Steel Grades Cases (MCER).

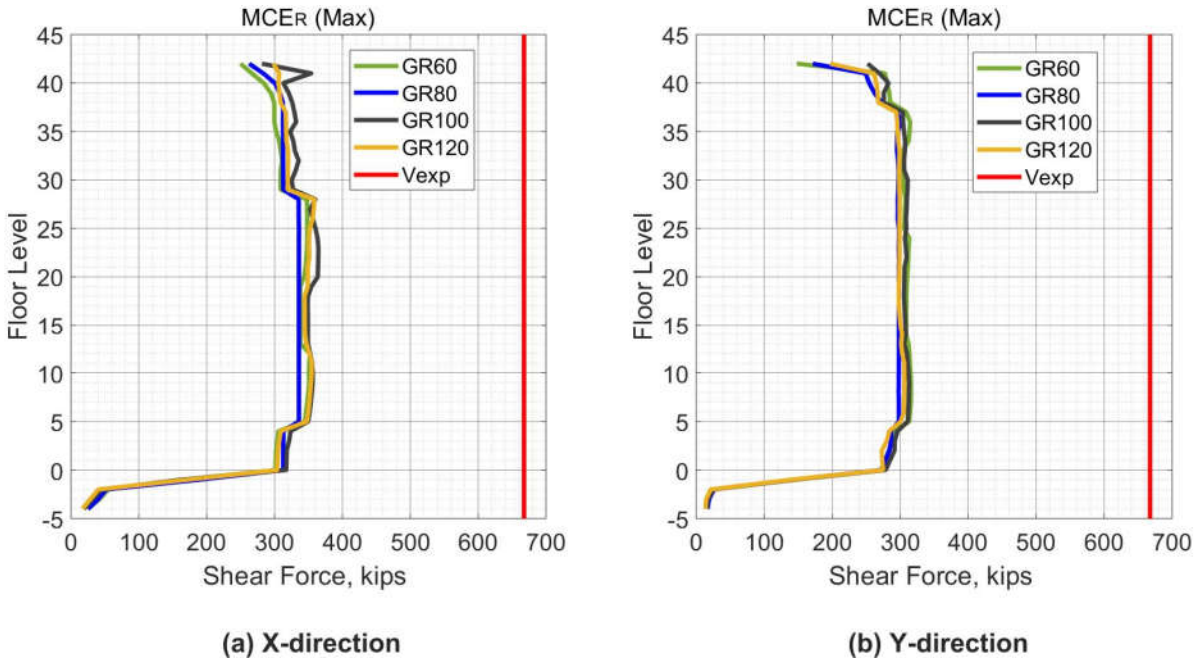

Figure 12.27 Peak Shear Forces in Beams for Reinforcement Steel Grades Cases (MCER).

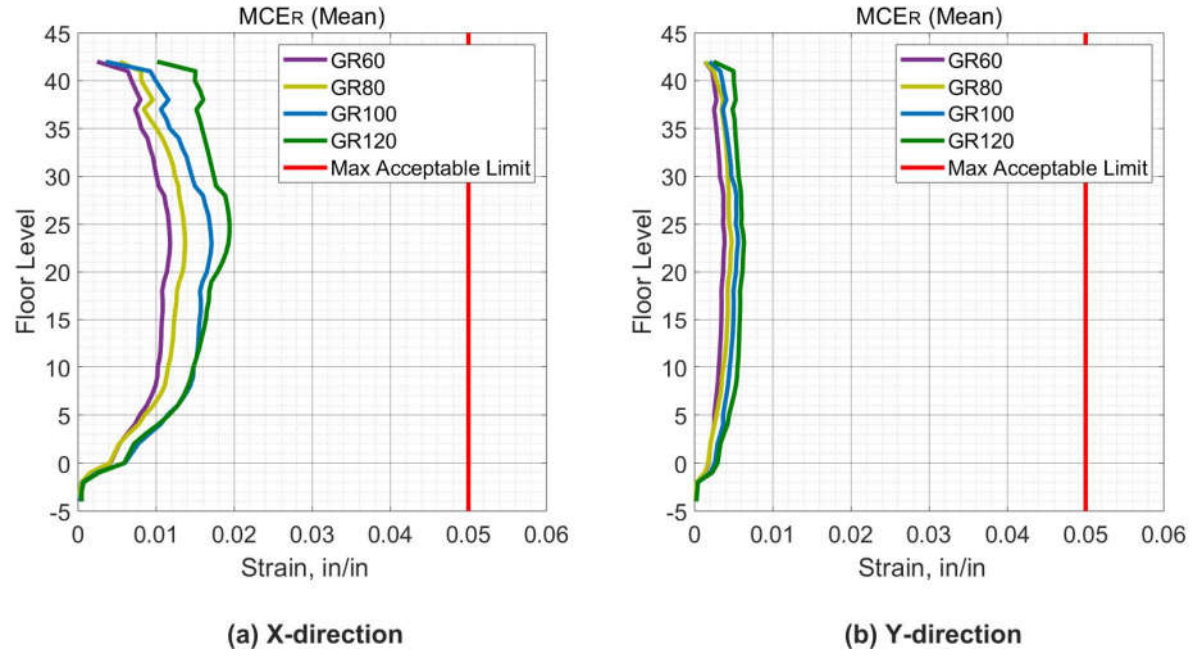

Figure 12.28 Mean of Peak of Reinforcement Tensile Strain in Beams for Reinforcement Steel Grades Cases (MCER).

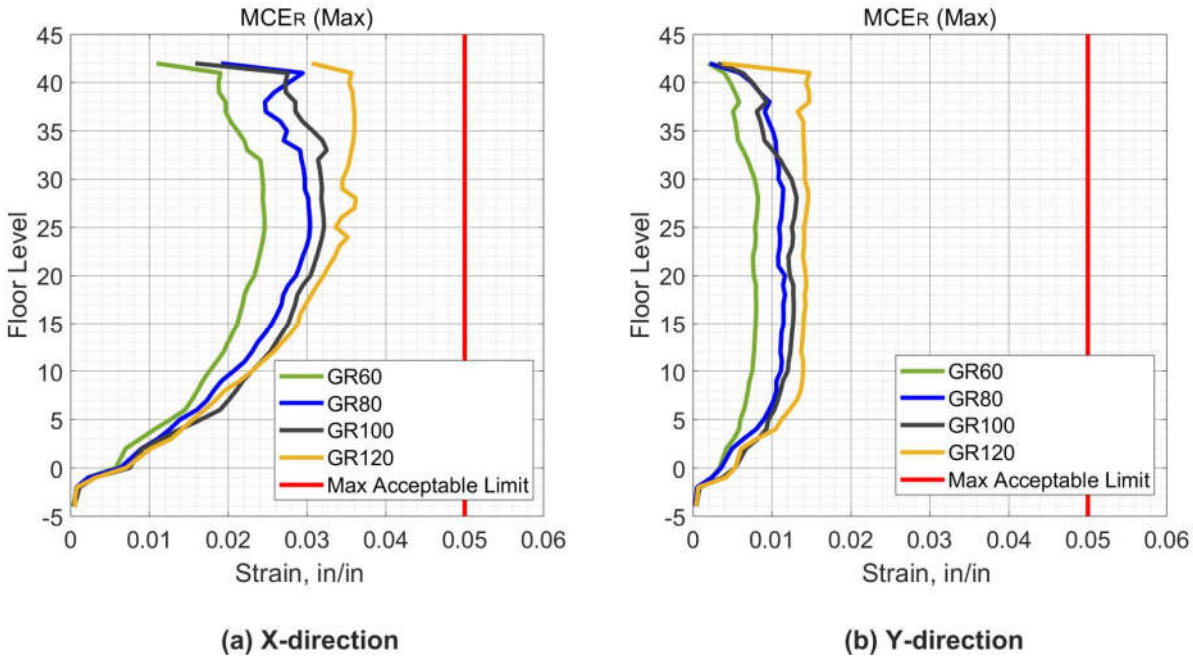

Figure 12.29 Peak of Reinforcement Tensile Strain in Beams for Reinforcement Steel Grades Cases (MCER).

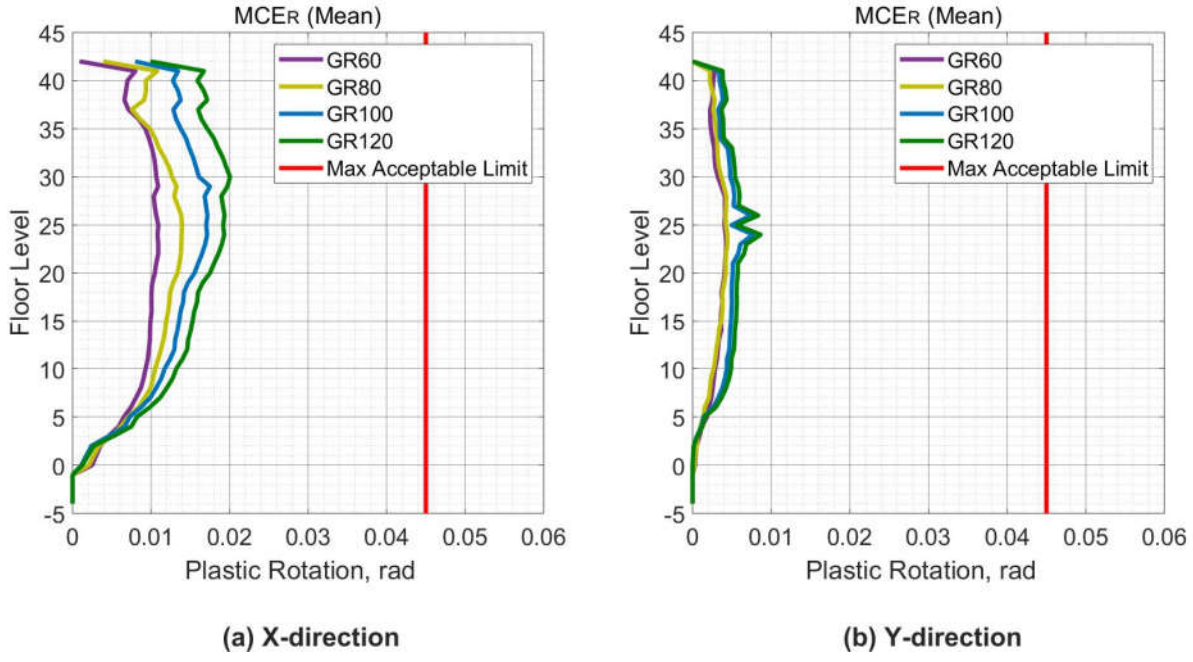

Figure 12.30 Mean of Peak of Beams Plastic Rotation for Reinforcement Steel Grades Cases (MCER).

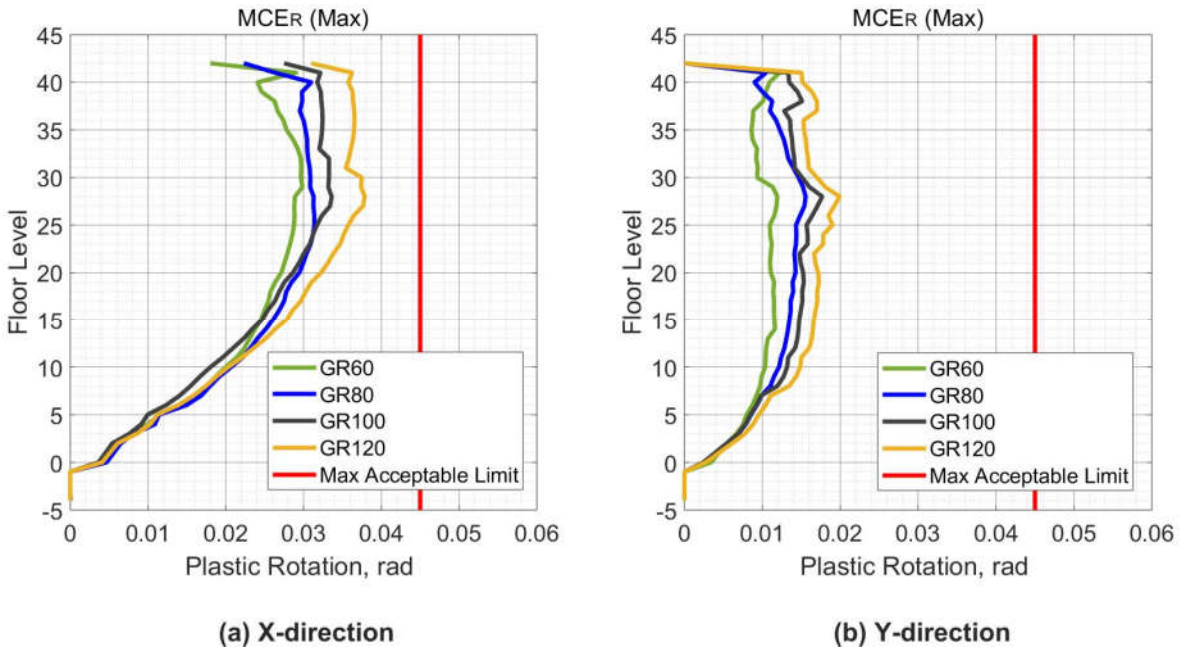

Figure 12.31 Peak of Beams Plastic Rotation for Reinforcement Steel Grades Cases (MCER).

12.2.2.4 Columns

12.2.2.4.1 SLE Level

Figure 12.32 shows the peak of the shear force demand in the columns of the special moment frame from the seven ground motions for the SLE level over the building height. The beams shear force demand was identical for the case study building reinforced with four different steel grades for the SLE shaking level. For each case, the shear force demand of the columns was approximately uniform over the building height. The peak shear forces demand is less than the reduced shear capacity of the columns for all cases. Depending on the results of the shear response of the columns, the performance of special moment frame columns reinforced with a reduced area of high strength reinforcement is equivalent to the performance of the same columns reinforced with conventional steel bras.

For the deformation-based actions in the columns, Figure 12.33 depicts the peak of the tensile strain in longitudinal reinforcing bars in the columns over the building height for SLE level. The maximum tensile strain is 0.0015 which is below the expected yielding strain of all used grades. For SLE level, the reinforcing steel bars in the columns did not experience yielding. No plastic hinge formed in the columns for the SLE level.

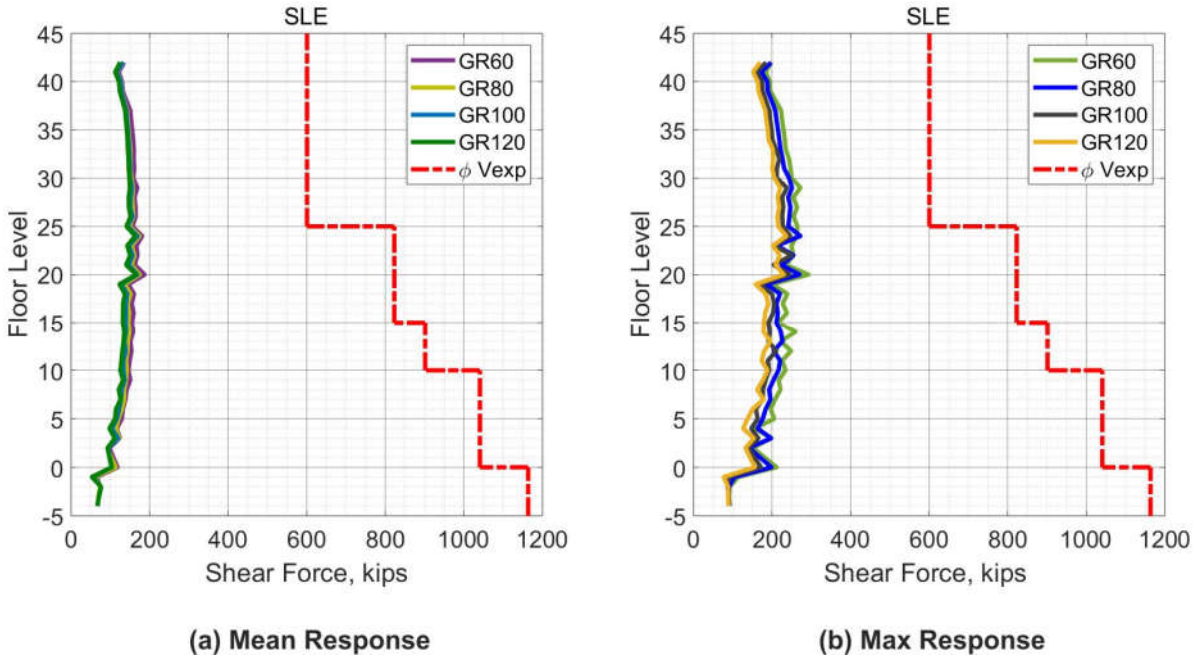

Figure 12.32 Peak Shear Forces in Columns for Reinforcement Steel Grades Cases (SLE).

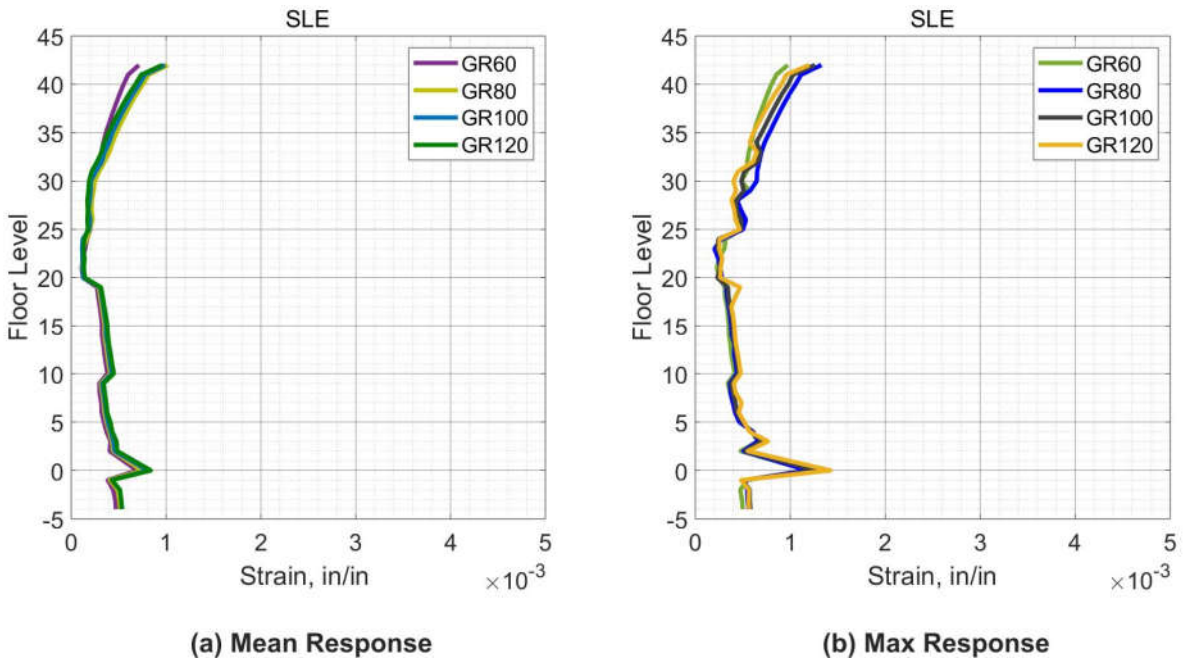

Figure 12.33 Peak of Reinforcement Tensile Strain in Columns for Reinforcement Steel Grades Cases (SLE).

12.2.2.4.2 MCER Level

Figure 12.34 shows the peak of the shear force demand in the columns of the special moment frame from the eleven ground motions for the MCER level over the building height. The columns shear force demand was identical for the case study building reinforced with four different steel grades for the MCER shaking level. For each case, the shear force demand of the columns was approximately uniform over the building height. The peak shear forces demand is less than the unreduced shear capacity of the columns for all cases. Depending on the results of the shear response of the columns, the performance of special moment frame columns reinforced with a reduced area of high strength reinforcement is equivalent to the performance of the same columns reinforced with conventional steel bras.

For the deformation-based actions in the columns, Figure 12.35 depicts the peak of the

tensile strain in longitudinal reinforcing bars in the columns over the building height for MCER level. A small increase in the tensile strain was noticed with using a reduced area of high strength reinforcement compared with the conventional bars. For any case, the maximum tensile strain in the longitudinal bars of the columns did not exceed the expected yield strain of the reinforcement that used for reinforcing the columns. For all cases, the maximum strain (0.0045) is far below the 0.05 limit of the ACSE 41. For all cases, the columns did not experience plastic rotation leading to a preferable response where the columns do not experience plastic hinges while all the hinges form in the beams.

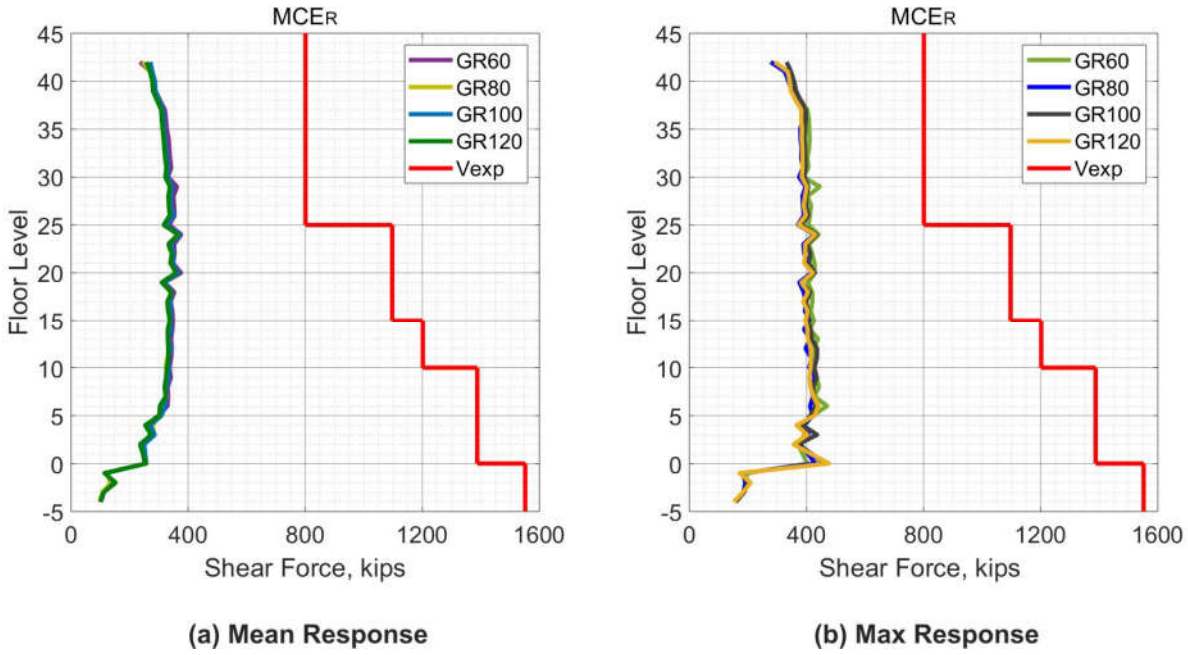

Figure 12.34 Peak Shear Forces in Columns for Reinforcement Steel Grades Cases (MCER).

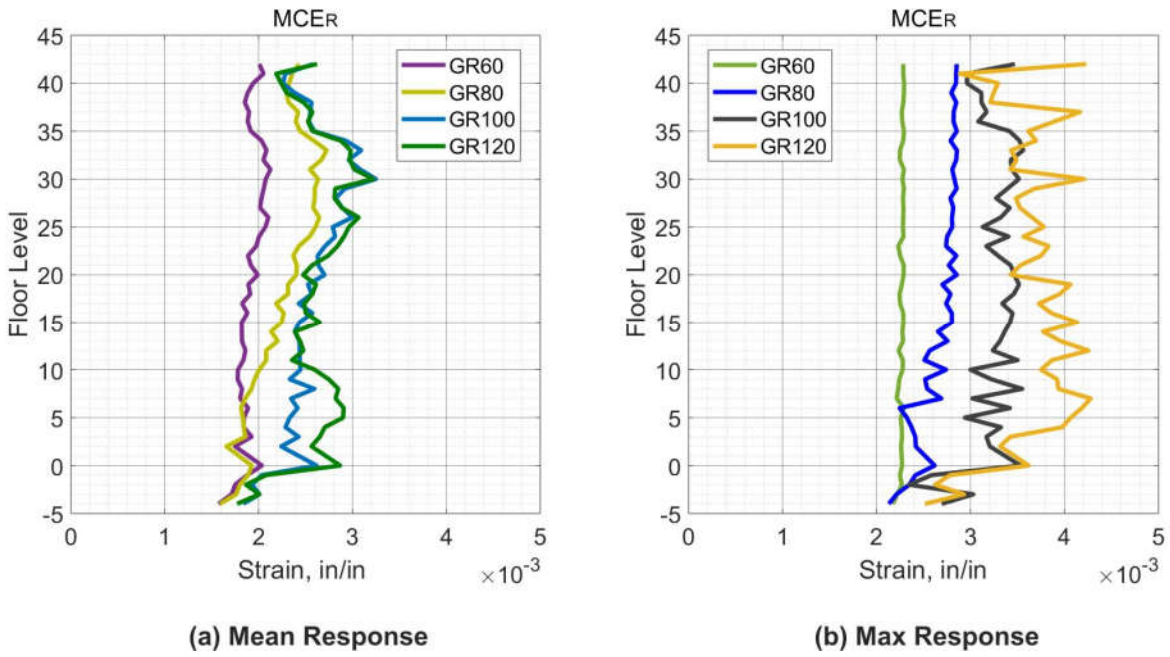

Figure 12.35 Peak of Reinforcement Tensile Strain in Columns for Reinforcement Steel Grades Cases (MCER).

12.3 CONVENTIONAL REINFORCEMENT AND SMA CASES

The response parameters of two cases will be compared. The first case (the reference case) reinforced with conventional steel bars in all members. The other case is the SMA case that reinforced with SMA bars in some specific regions while using the conventional steel bars for the remain regions. The SMA bars were used as longitudinal reinforcing bars in the plastic hinge region in the beams, the boundary elements of the core wall, the diagonal reinforcement of the coupling beams.

12.3.1 Global Response

12.3.1.1 Interstory Drift Ratio

12.3.1.1.1 SLE Level

Figure 12.36 shows the peak interstory drift ratios from the seven ground motions for the

SLE level for the reference case (GR60 case) and the SMA case. The drift ratios demand for both cases was close for the SLE shaking level.

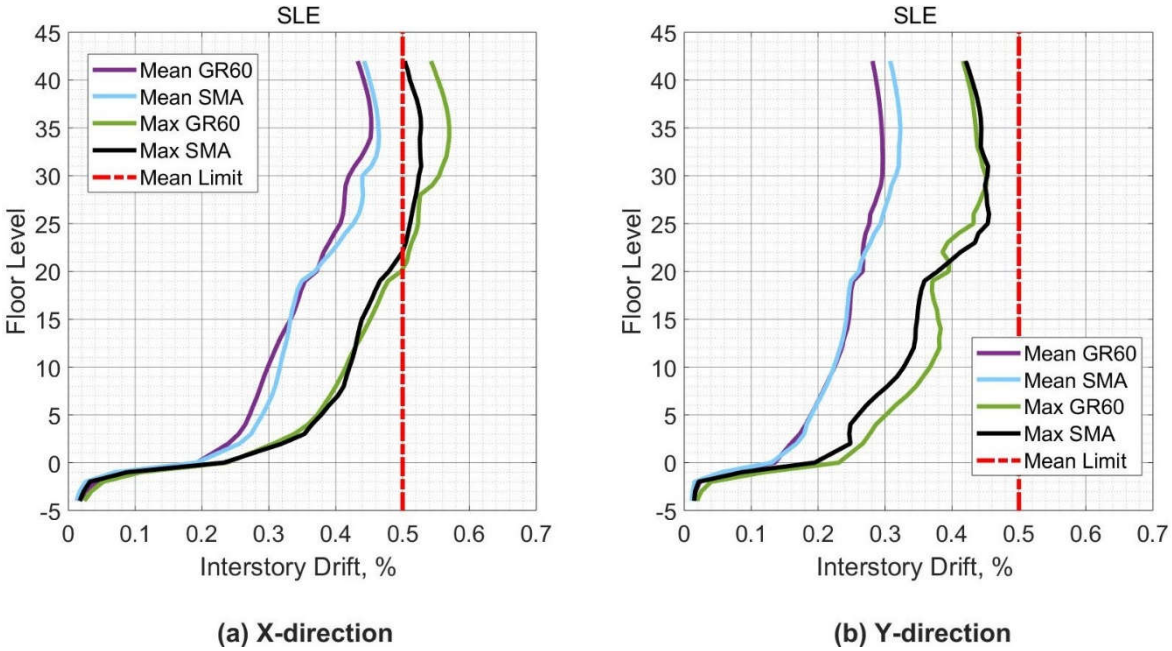

Figure 12.36 Peak Interstory Drift for Conventional Reinforcement and SMA Cases (SLE).

12.3.1.1.2 MCER level

Figure 12.37 shows the peak interstory drift ratios from the eleven ground motions for the MCER level for the GR60 case and the SMA case. An increased drift ratio was noticed for the SMA case due to the low stiffness of the SMA bars compared with the conventional steel bars. However, the drift ratios for both cases are with acceptable limits.

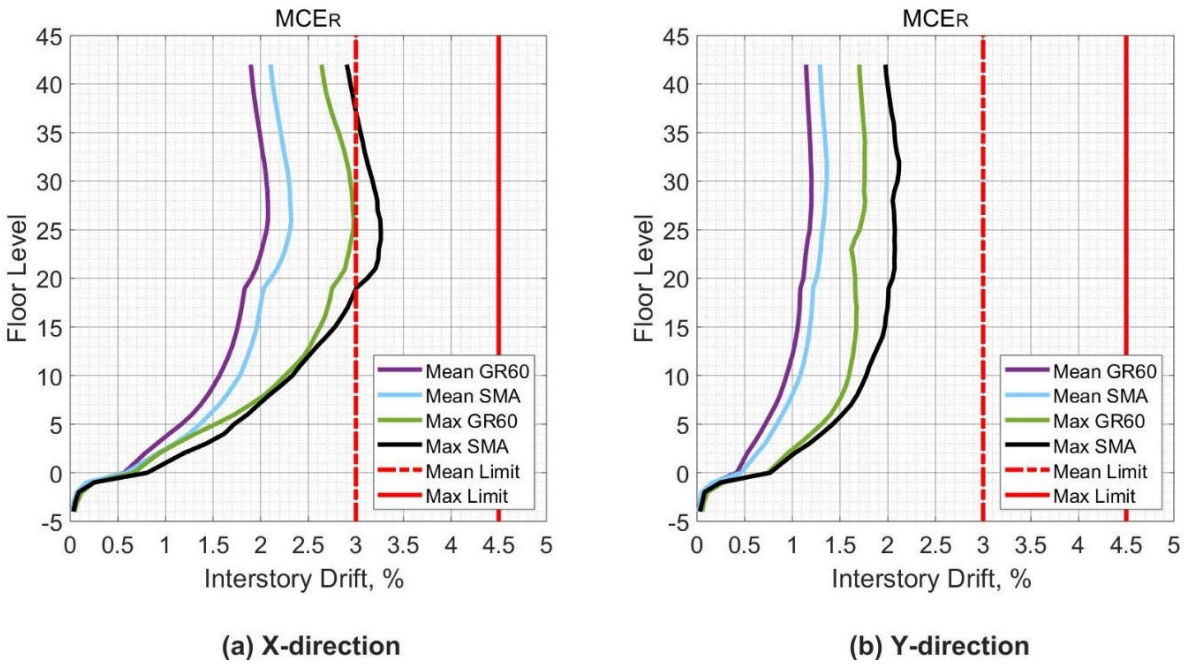

Figure 12.37 Peak Interstory Drift for Conventional Reinforcement and SMA Cases (MCER).

12.3.1.2 Residual Drift Ratio

12.3.1.2.1 MCER Level

Figure 12.38 shows the peak interstory drift ratios from the eleven ground motions for the MCER level for the GR60 case and the SMA case. The calculations of the residual drift require the story drift at the yield and the maximum drift. SMA bars do not yield like steel bars, however the calculations of residual drift ratio for the SMA case consider the 0.01 stain as a yield point for SMA bars. It is crucial to mention that SMA bars are capable to recover 0.06 strain. When considering the strain of 0.06 as a yield point of the SMA bars, the residual drift for the SMA cases will be approximately zero.

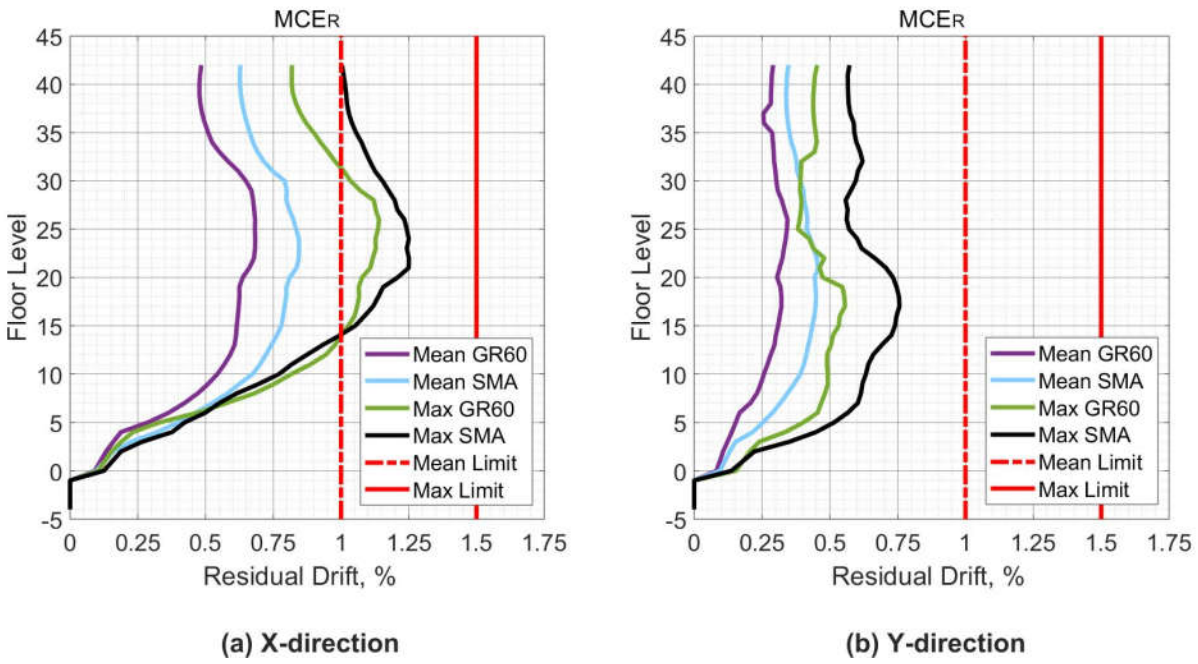

Figure 12.38 Peak Residual Drift for Conventional Reinforcement and SMA Cases (MCER).

12.3.1.3 Displacement

12.3.1.3.1 SLE Level

Figure 12.39 shows the peak displacement from the seven ground motions for the SLE level for the GR60 case and the SMA case. A similar response was noticed for both cases in the SLE shaking level. One explanation is that the case study building responds linearly upon subjected to a load that matching the SLE shaking level, therefore, the building response is not affected significantly by the type of reinforcing materials.

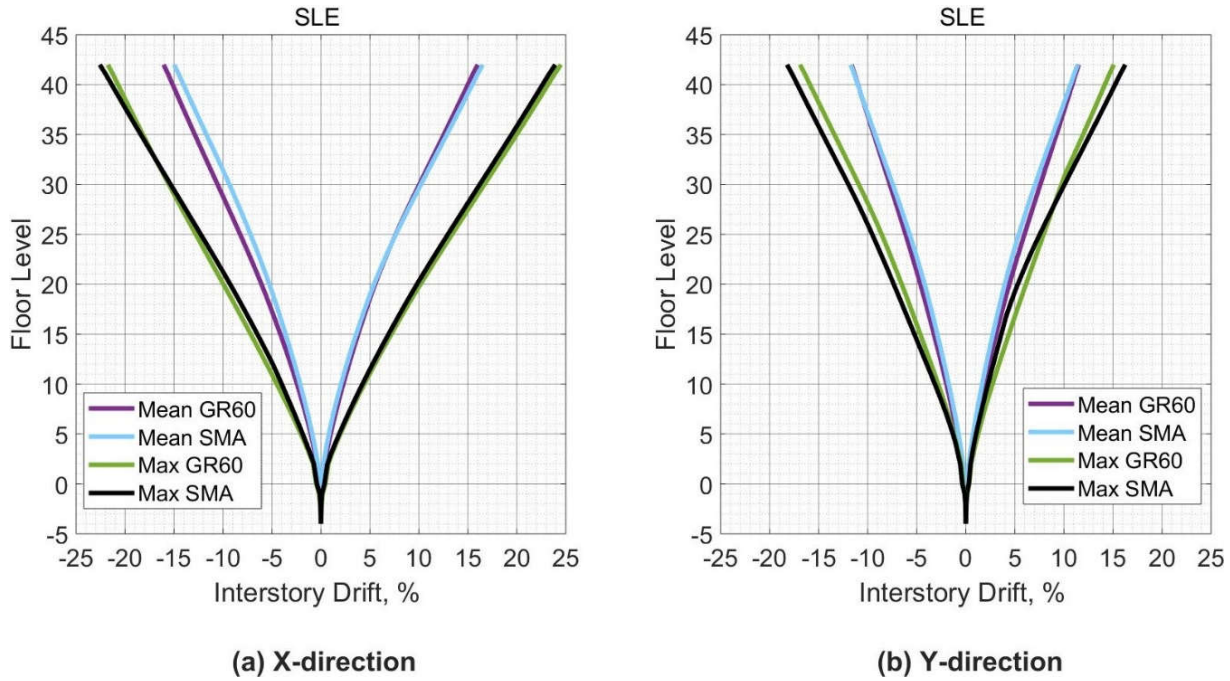

Figure 12.39 Peak Floors Displacement Synchronous with Peak Roof Displacement for Conventional Reinforcement and SMA Cases (SLE).

12.3.1.3.2 MCER Level

Figure 12.40 shows the peak displacement from the eleven ground motions for the MCER level for the GR60 case and the SMA case. The SMA case showed more displacement demands due to the lower stiffness of SMA bars.

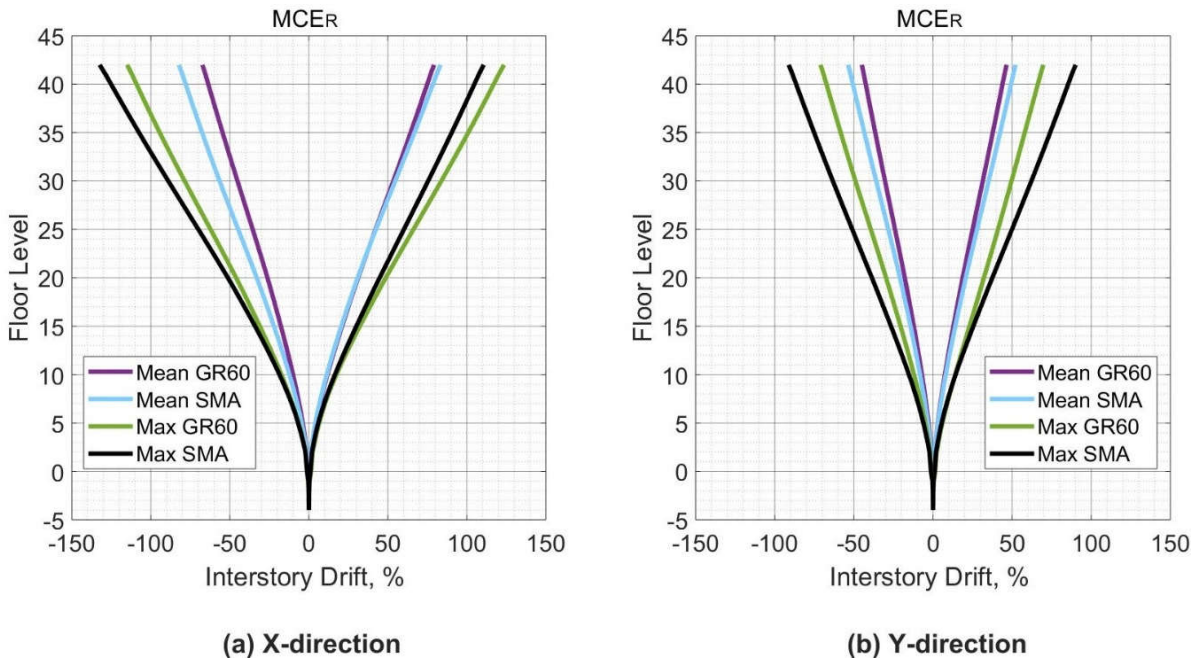

Figure 12.40 Peak Floors Displacement Synchronous with Peak Roof Displacement for Conventional Reinforcement and SMA Cases (MCER).

12.3.2 Element Level

12.3.2.1 Core Wall

12.3.2.1.1 SLE Level

Figure 12.41 shows the peak of the shear force demand in the core wall from the seven ground motions for the SLE level over the building height for both cases. For both cases, the shear force demand was less than the reduced shear capacity of the core wall. The shear force demand for the GR60 and SMA cases was very close in the SLE shaking level. The shear demands experience some changes near the twentieth story due to the thickness change of the core wall from 24 in. to 18 in. in the twentieth story.

For the deformation-based actions in the core wall, Figure 12.42 depicts the peak of the tensile strain in reinforcing bars in all edges over the building height for SLE level. The tensile

strain distribution is approximately the same for both cases with a little increase for the SMA case. However, the maximum tensile strain for GR60 case is 0.002 which is below the expected yielding strain of Grade 60. On the other hand, the maximum strain for SMA case was 0.003 which is below the 0.01 strain that represents the ending limit of the linear portion of the SMA. Figure 12.43 depicts the peak of concrete compression strain in the core wall for both cases over the building height. Very similar strain pattern was obtained for core wall concrete for both cases.

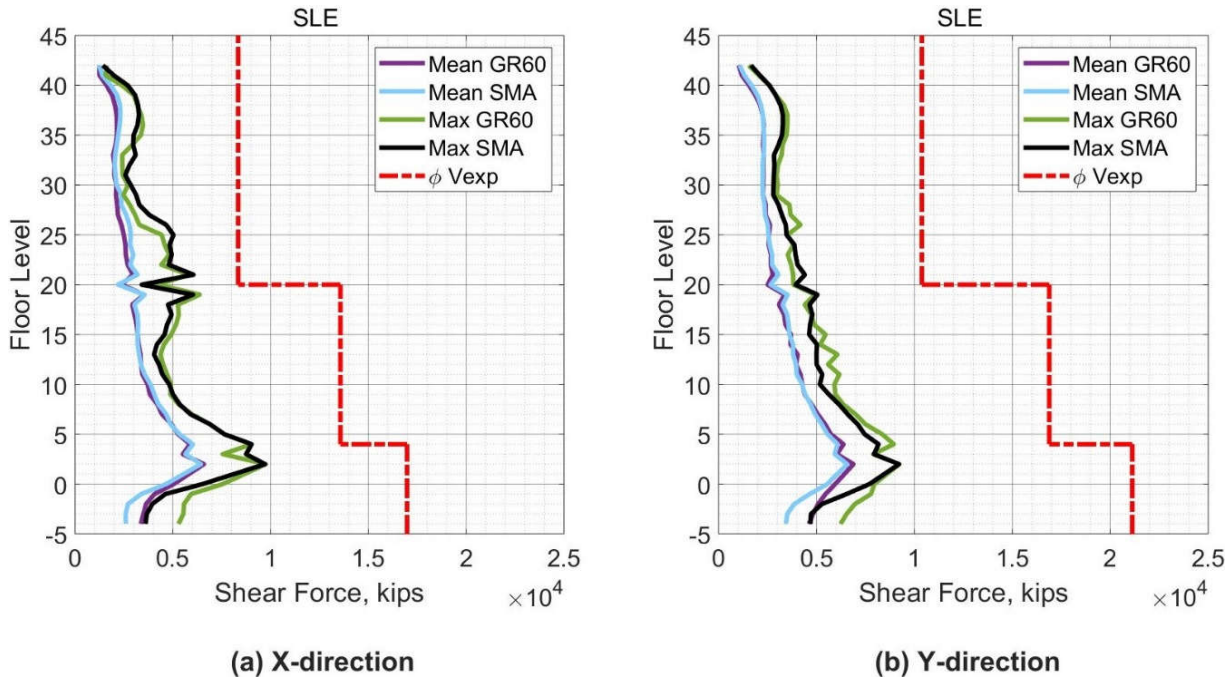

Figure 12.41 Peak Shear Forces in Core Wall for Conventional Reinforcement and SMA Cases (SLE).

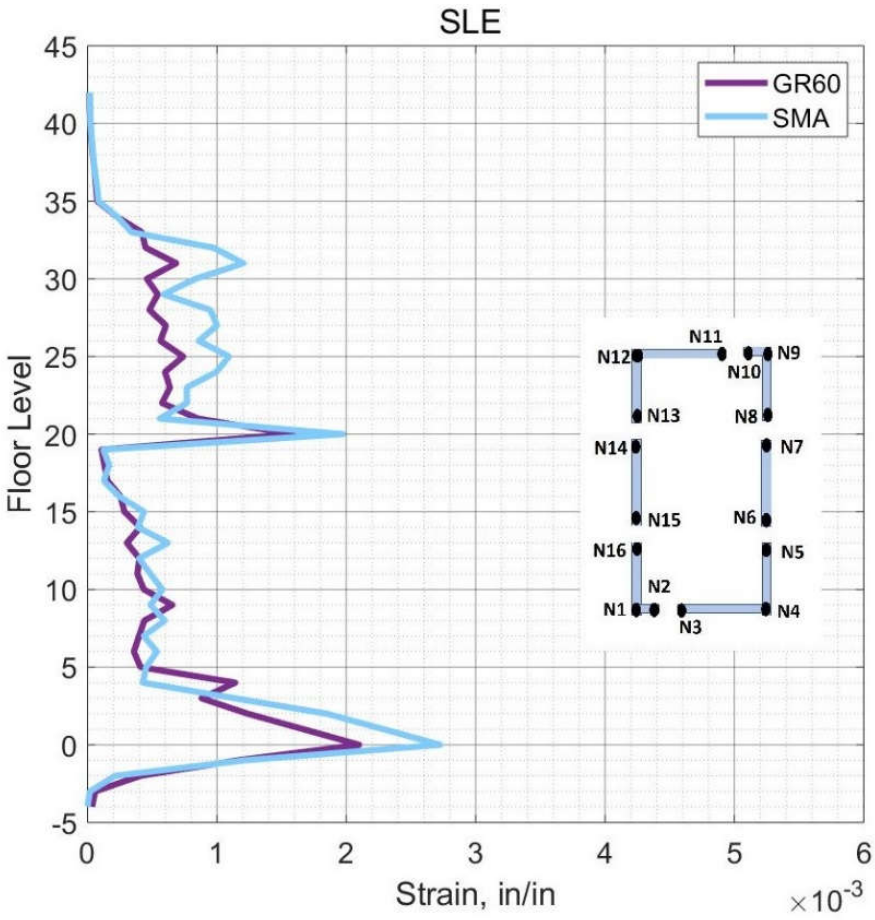

Figure 12.42 Peak of Reinforcement Tensile Strain in Core Wall for Conventional Reinforcement and SMA Cases (SLE).

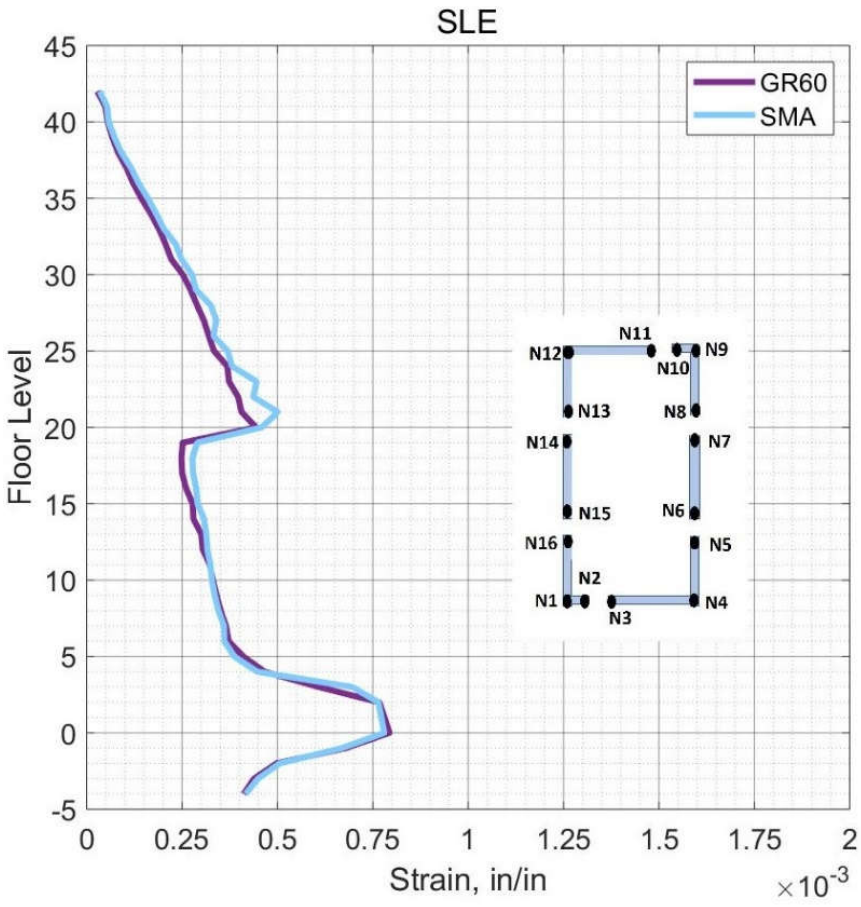

Figure 12.43 Peak of Concrete Compression Strain in Core Wall for Conventional Reinforcement and SMA Cases (SLE).

12.3.2.1.2 MCER Level

Figure 12.44 shows the peak of the shear force demand in the core wall from the eleven ground motions for the MCER level over the building height for both cases. For both cases, the shear force demand was less than the unreduced shear capacity of the core wall. The shear force demand for the GR60 and SMA cases was close in the MCER shaking level. The shear demands experience some changes near the twentieth story due to the thickness change of the core wall from 24 in. to 18 in. in the twentieth story.

For the deformation-based actions in the core wall, Figure 12.45 depicts the peak of the tensile strain in reinforcing bars in all edges over the building height for MCER level. The tensile strain distribution is approximately the same for both cases with an increase for the SMA case especially for stories above the twentieth story up to thirtieth story. However, the maximum tensile strain for GR60 case is 0.015 which is below the maximum acceptable limit of 0.05. On the other hand, the maximum strain for SMA case was 0.016 which is below the 0.06 strain that represents maximum recoverable strain for the SMA. Figure 12.46 depicts the peak of concrete compression strain in the core wall for both cases over the building height. Concrete in SMA cases experienced more compression strain than the case of GR60, however the concrete strain in both cases was below the maximum acceptable strain for concrete 0.003.

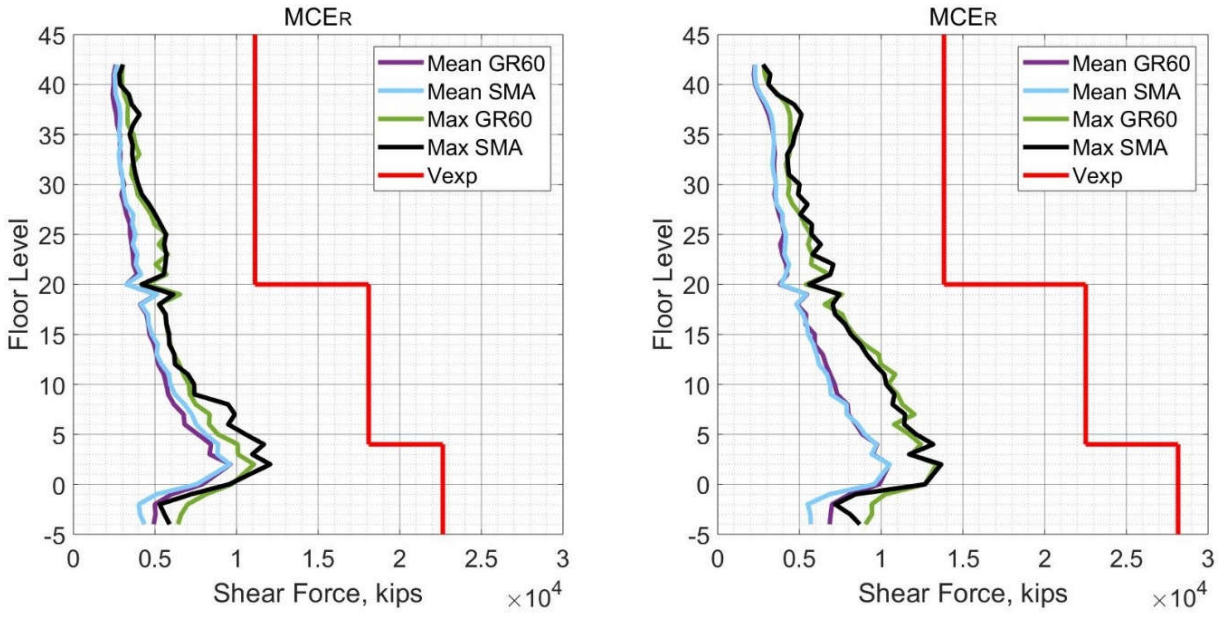

Figure 12.44 Peak Shear Forces in Core Wall for Conventional Reinforcement and SMA Cases (MCER).

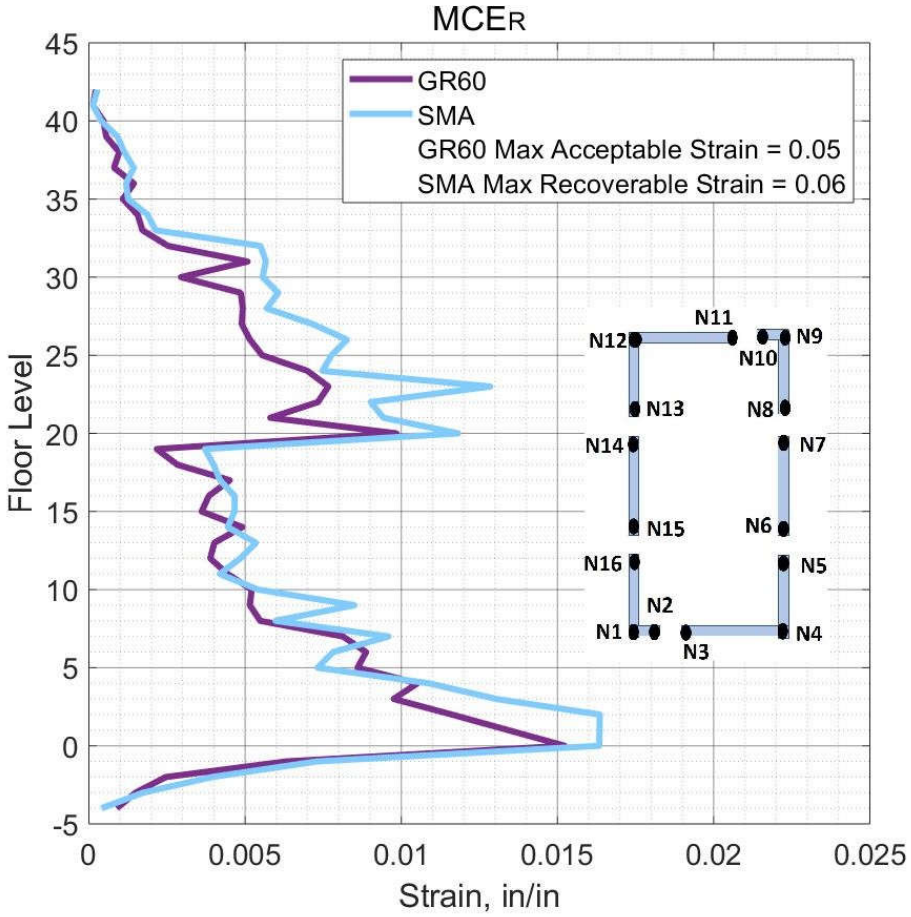

Figure 12.45 Peak of Reinforcement Tensile Strain in Core Wall for Conventional Reinforcement and SMA Cases (MCER).

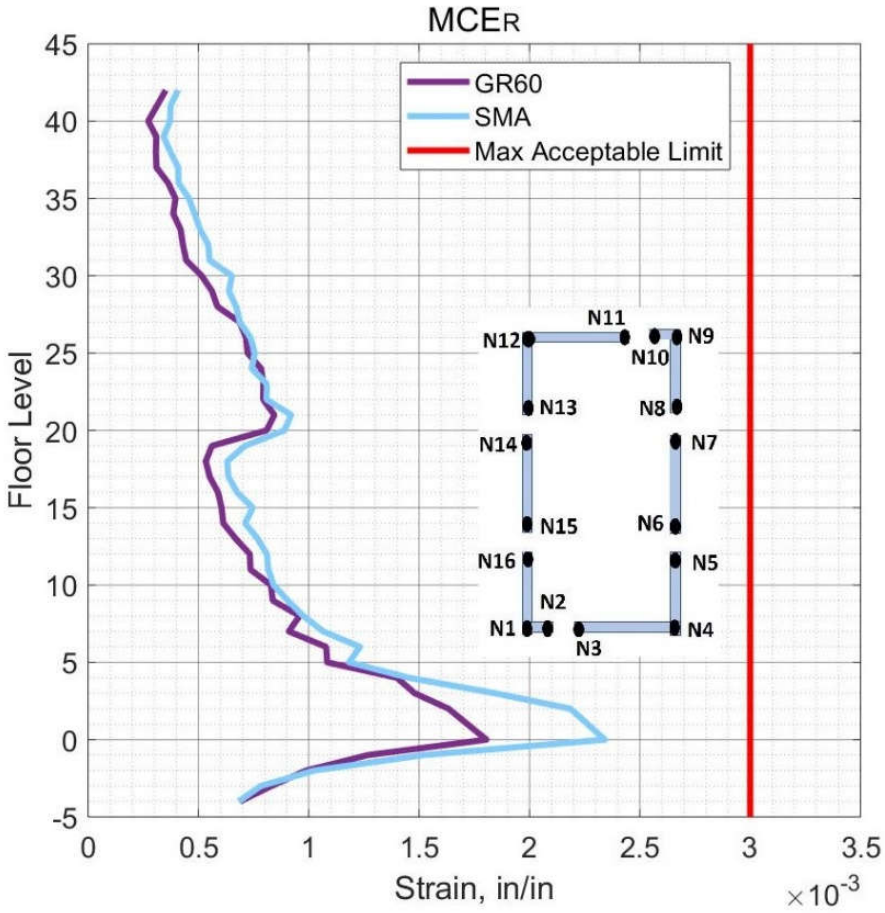

Figure 12.46 Peak of Concrete Compression Strain in Core Wall for Conventional Reinforcement and SMA Cases (MCER).

12.3.2.2 Coupling beam

12.3.2.2.1 SLE Level

Figure 12.47 shows the peak of the rotation demand in the coupling beams from the seven ground motions for the SLE level over the building height for both cases. The peak value of the rotation is 0.0025 which indicate that coupling beams do not experience yielding of steel reinforcement according to the data in Figure 7.18. A similar response was noticed for the coupling beams for both cases which could be explained by that the building responded linearly in the SLE

shaking level.

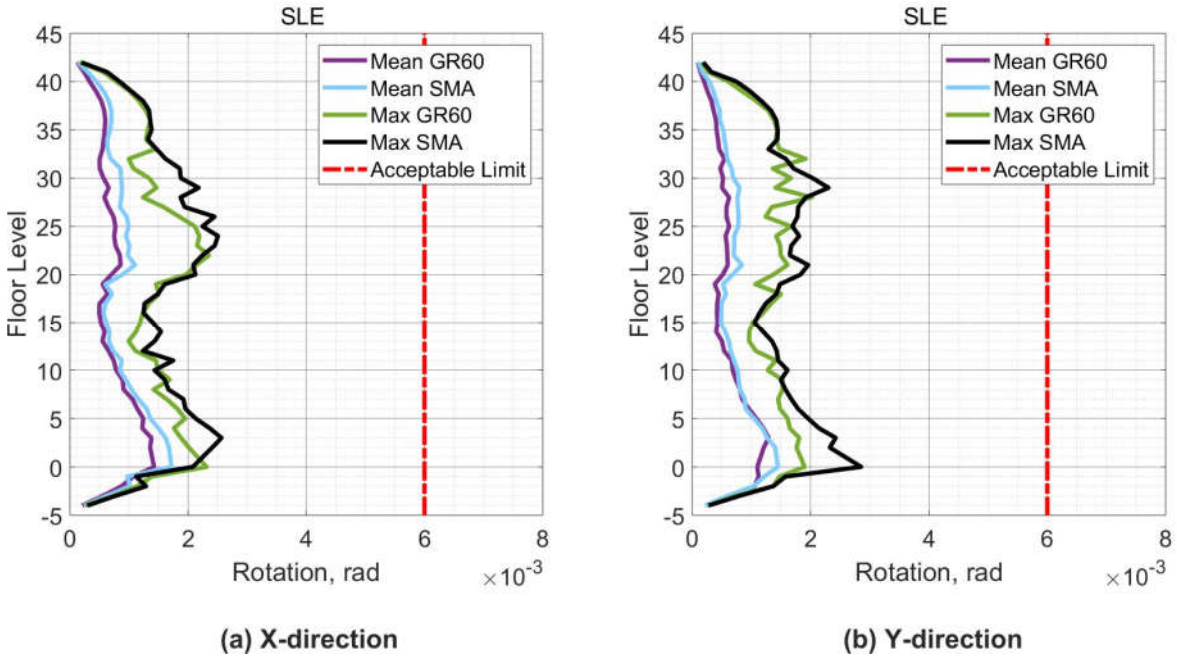

Figure 12.47 Peak Rotation Demand in Coupling Beams for Conventional Reinforcement and SMA Cases (SLE).

12.3.2.2.2 MCER Level

Figure 12.48 shows the peak of the rotation demand in the coupling beams from the eleven ground motions for the MCER level over the building height for both cases. The coupling beams in the SMA case experienced more rotation demands than the GR60 case. For GR60 case, the peak value of the rotation is 0.025 which indicates that coupling beams experience yielding of steel reinforcement and minor damage state according to the data in Figure 7.18. For the SMA case, there is no yielding for the SMA bars, and they have ability to recover strain of 0.06.

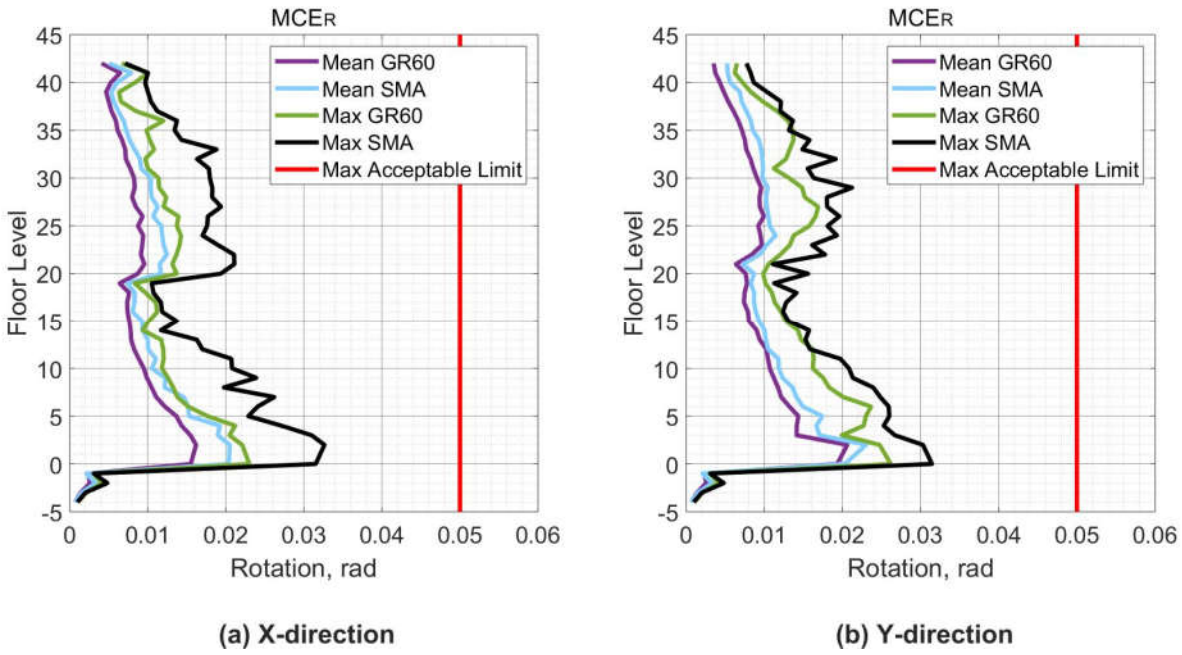

Figure 12.48 Peak Rotation Demand in Coupling Beams for Conventional Reinforcement and SMA Cases (MCER).

12.3.2.3 Beams

12.3.2.3.1 SLE Level

Figure 12.49 shows the peak of the shear force demand in the beams of the special moment frame from the seven ground motions for the SLE level over the building height for both cases. For both cases, the shear force demand of the beams was approximately uniform over the building height. The shear forces demand for the SMA case was less than the shear demand in the beams of the GR60 case. The peak shear forces demand is less than the reduced shear capacity of the beams for both cases.

For the deformation-based actions in the beams, Figure 12.50 depicts the peak of the tensile strain in longitudinal reinforcing bars in the beams over the building height for SLE level. A small increase in the tensile strain was noticed with the SMA case compared with the GR60 case. The

maximum tensile strain for GR60 case is 0.002 which is below the expected yielding strain of Grade 60 (0.0024). On the other hand, the maximum strain for SMA case was 0.0035 which is below the 0.01 strain that represents the ending limit of the linear portion of the SMA. Consequently, no plastic hinges were formed in the beams for both cases.

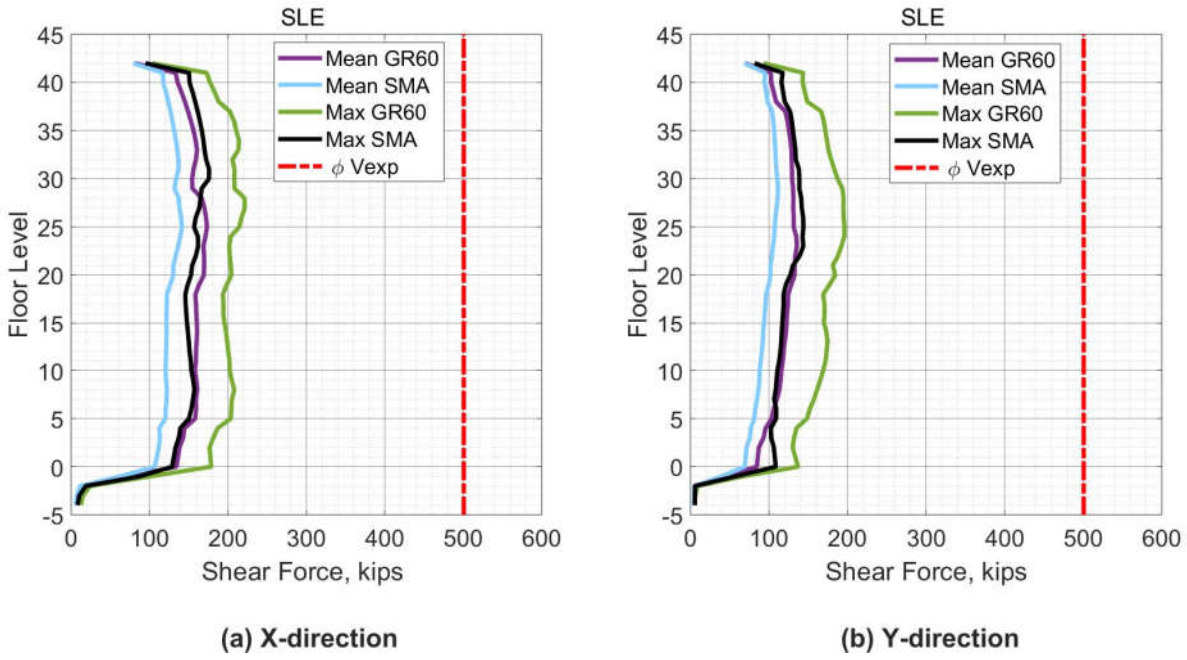

Figure 12.49 Peak Shear Forces in Beams for Conventional Reinforcement and SMA Cases (SLE).

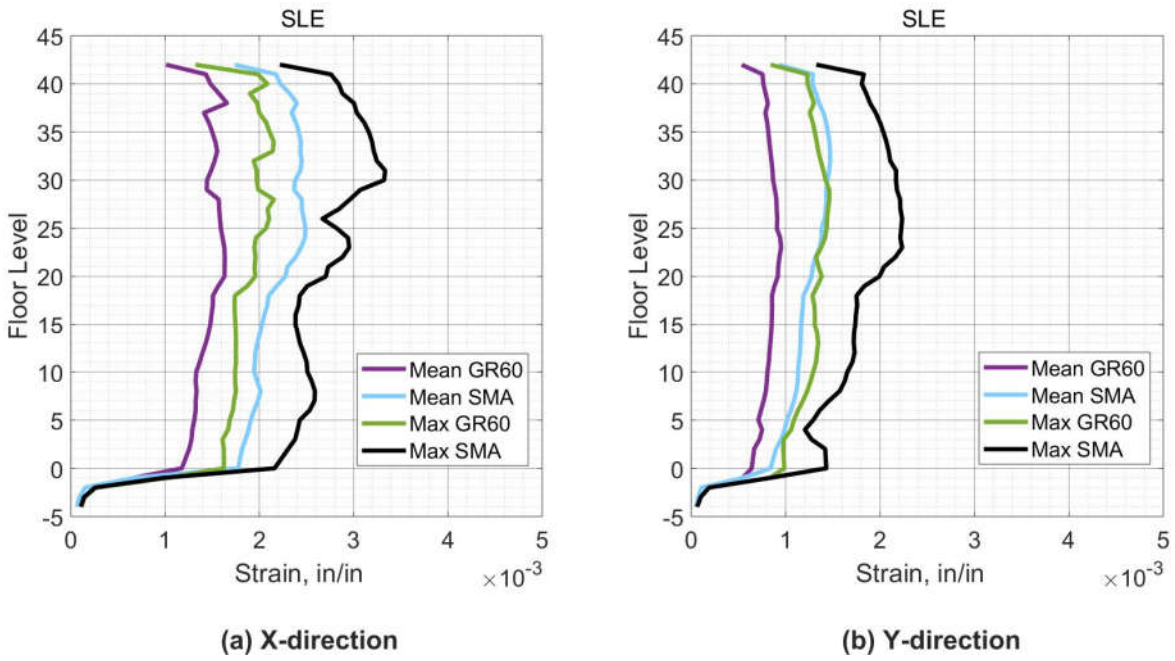

Figure 12.50 Peak of Reinforcement Tensile Strain in Beams for Conventional Reinforcement and SMA Cases (SLE).

12.3.2.3.2 MCER Level

Figure 12.51 shows the peak of the shear force demand in the beams of the special moment frame from the eleven ground motions for the MCER level over the building height for both cases. For both cases, the shear force demand of the beams was approximately uniform over the building height. The shear forces demand for the SMA case was less than the shear demand in the beams of the GR60 case. The peak shear forces demand is less than the unreduced shear capacity of the beams for both cases.

For the deformation-based actions in the beams, Figure 12.52 depicts the peak of the tensile strain in longitudinal reinforcing bars in the beams over the building height for MCER level. The beams in the SMA case experienced more tensile stain than beams in the GR60 case. The maximum tensile strain for GR60 case is less than 0.025 which is below the maximum acceptable

limit of 0.05. On the other hand, the maximum strain for SMA case was 0.03 which is below the 0.06 strain that represents maximum recoverable strain for the SMA. Figure 12.53 depicts the plastic rotation in the beams for both cases over the building height. The calculation of the plastic rotation for the SMA case depend on the idea that SMA bars have a yield point of 0.01 which is not a real yield point, because SMA bars could retain the origin shape even upon subjected to a strain of 0.06. The plastic hinge rotation for the GR60 case is more due to lower yield point compared with SMA case.

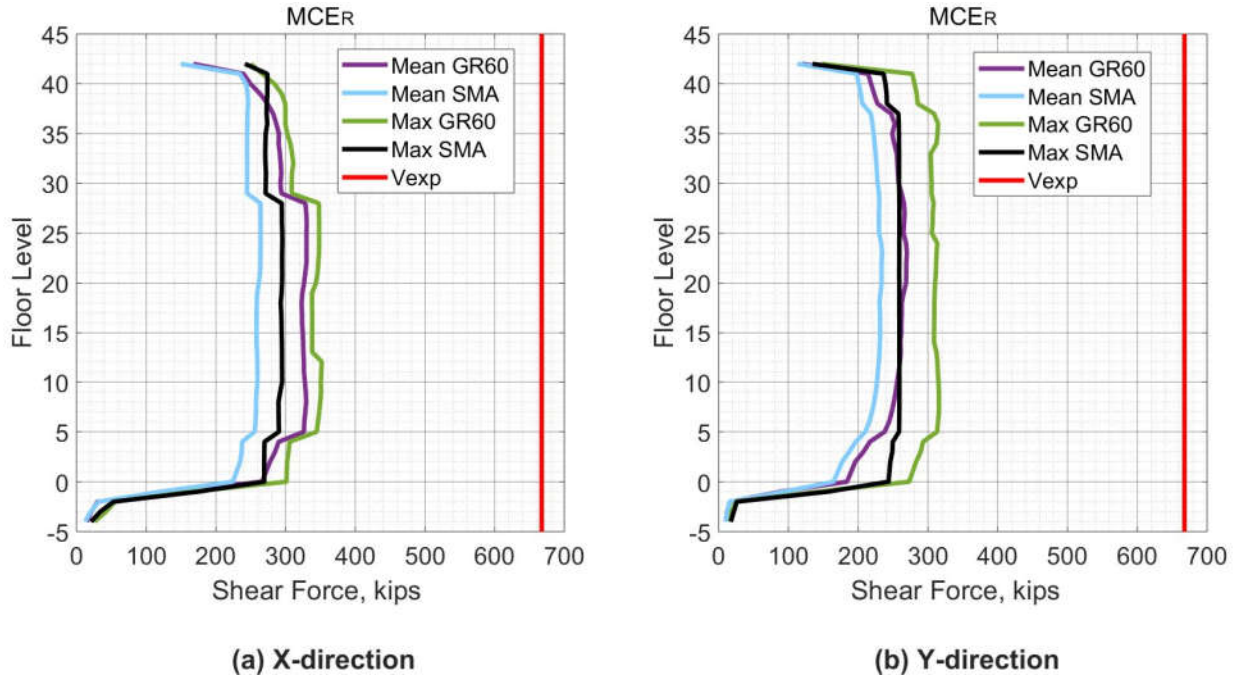

Figure 12.51 Peak Shear Forces in Beams for Conventional Reinforcement and SMA Cases (MCER).

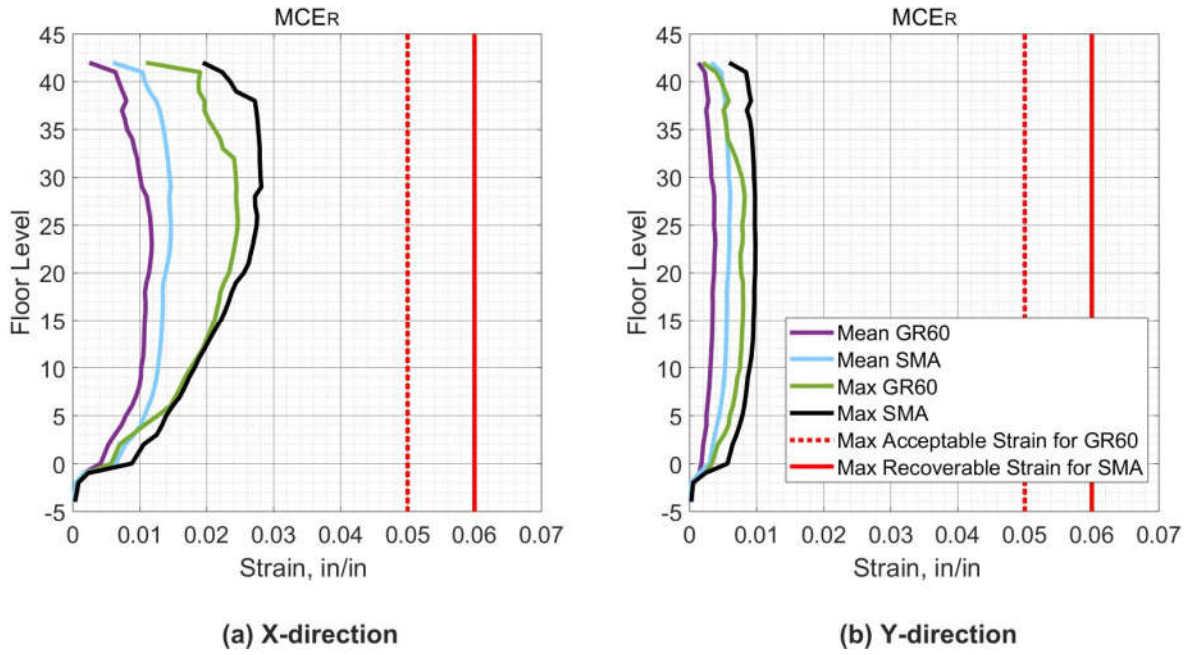

Figure 12.52 Peak of Reinforcement Tensile Strain in Beams for Conventional Reinforcement and SMA Cases (MCER).

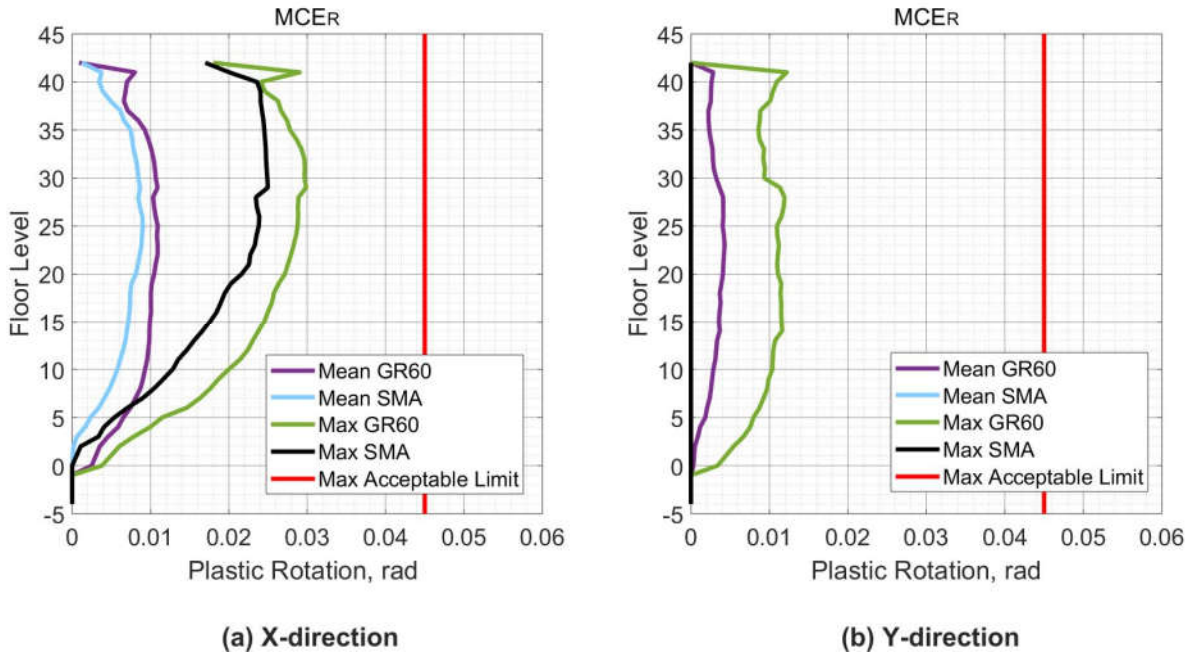

Figure 12.53 Peak of Beams Plastic Rotation for Conventional Reinforcement and SMA Cases (MCER).

12.3.2.4 Columns

12.3.2.4.1 SLE Level

Figure 12.54 shows the peak of the shear force demand in the columns of the special moment frame from the seven ground motions for the SLE level over the building height for both cases. For both cases, the shear force demand of the columns was approximately uniform over the building height. The shear forces demand for the SMA case was less than the shear demand in the columns of the GR60 case. The peak shear forces demand is less than the reduced shear capacity of the columns for both cases.

For the deformation-based actions in the beams, Figure 12.55 depicts the peak of the tensile strain in longitudinal reinforcing bars in the columns over the building height for SLE level for both cases. For both cases, the columns were reinforced with the conventional reinforcing bars. The maximum tensile strain for GR60 case is 0.0015 which is below the expected yielding strain of Grade 60 (0.0024). Consequently, no plastic hinges were formed in the beams for both cases.

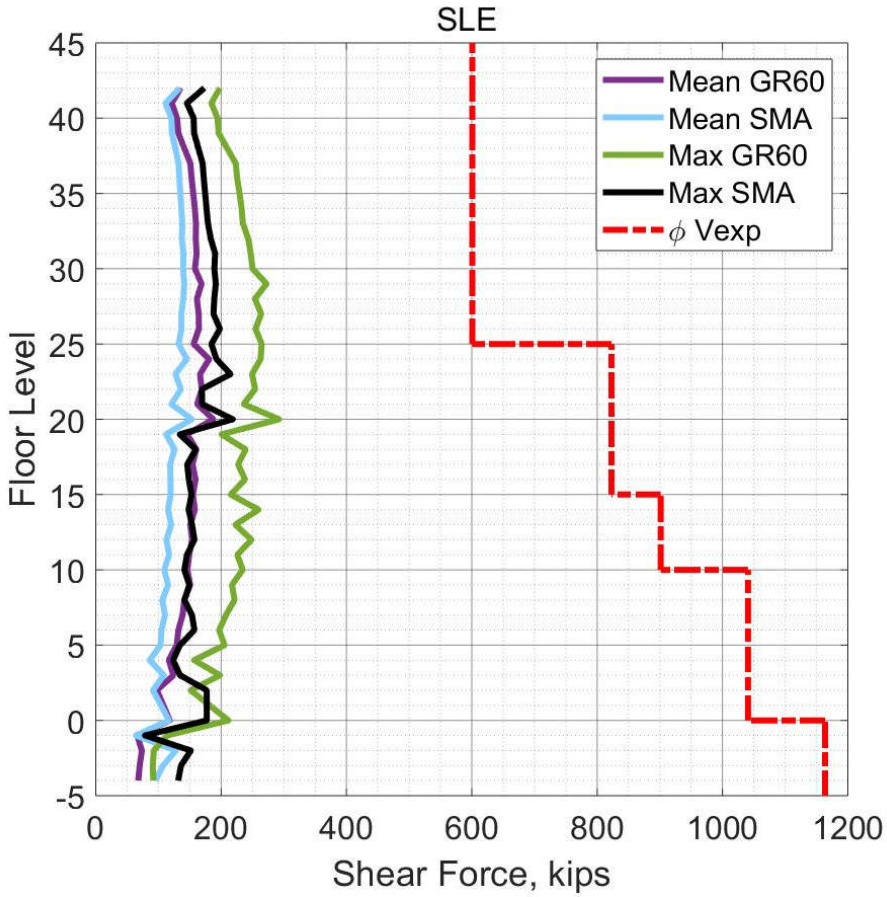

Figure 12.54 Peak Shear Forces in Columns for Conventional Reinforcement and SMA Cases (SLE).

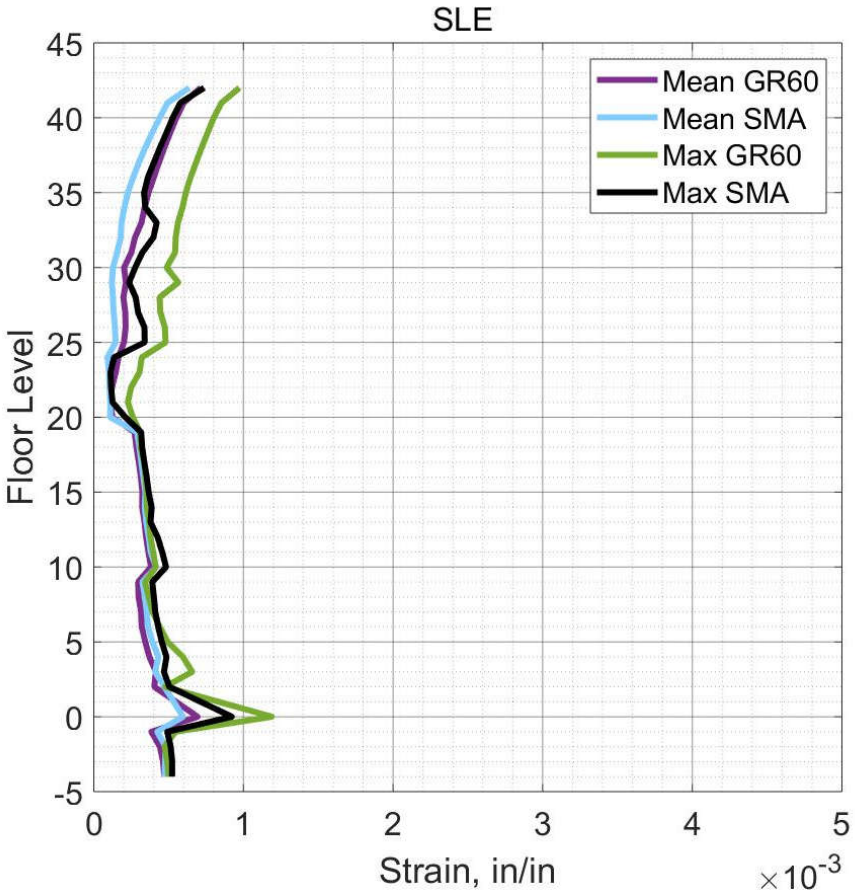

Figure 12.55 Peak of Reinforcement Tensile Strain in Columns for Conventional Reinforcement and SMA Cases (SLE).

12.3.2.4.2 MCER Level

Figure 12.56 shows the peak of the shear force demand in the columns of the special moment frame from the eleven ground motions for the MCER level over the building height for both cases. For both cases, the shear force demand of the columns was approximately uniform over the building height. The peak shear forces demand is less than the unreduced shear capacity of the columns for both cases.

For the deformation-based actions in the beams, Figure 12.57 depicts the peak of the tensile

strain in longitudinal reinforcing bars in the columns over the building height for MCER level for both cases. The maximum tensile strain for both cases is 0.0022 which is below the expected yield strain of grade 60 (0.0024) and below the maximum acceptable limit of 0.05. Consequently, no plastic hinges were formed in the beams for both cases. For both cases, the columns did not experience plastic rotation leading to a preferable response where the columns do not experience plastic hinges while all the hinges form in the beams.

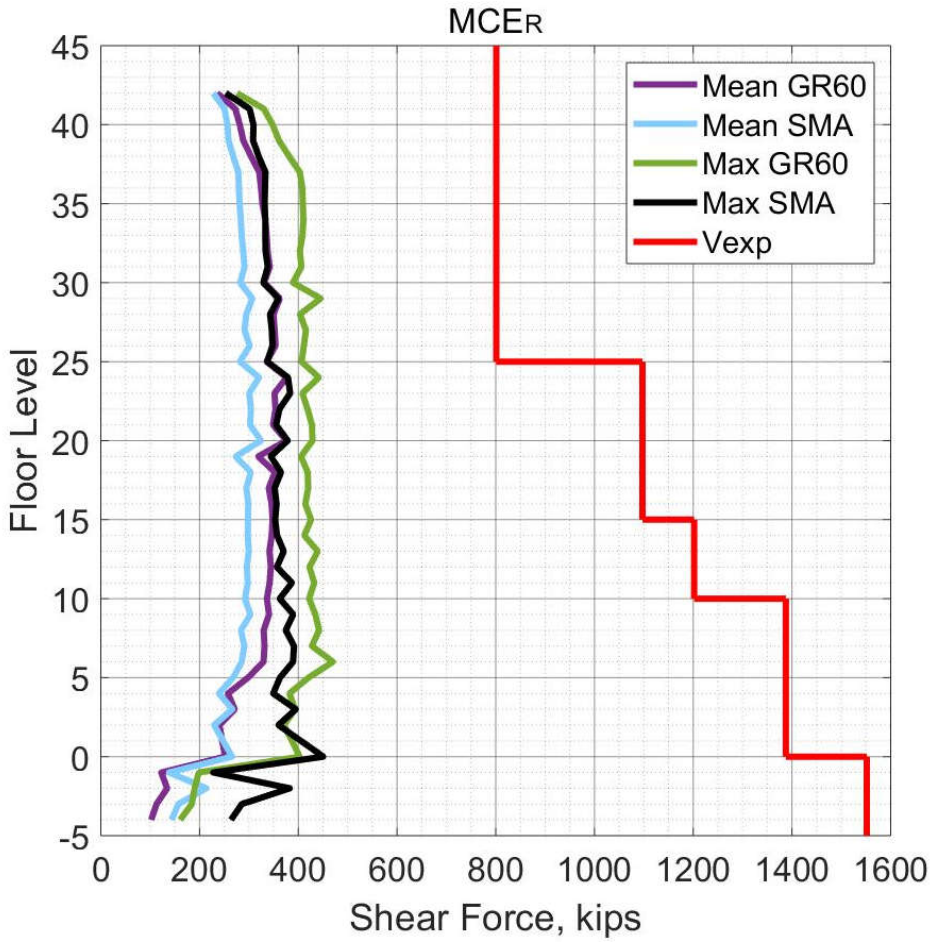

Figure 12.56 Peak Shear Forces in Columns for Conventional Reinforcement and SMA Cases (MCER).

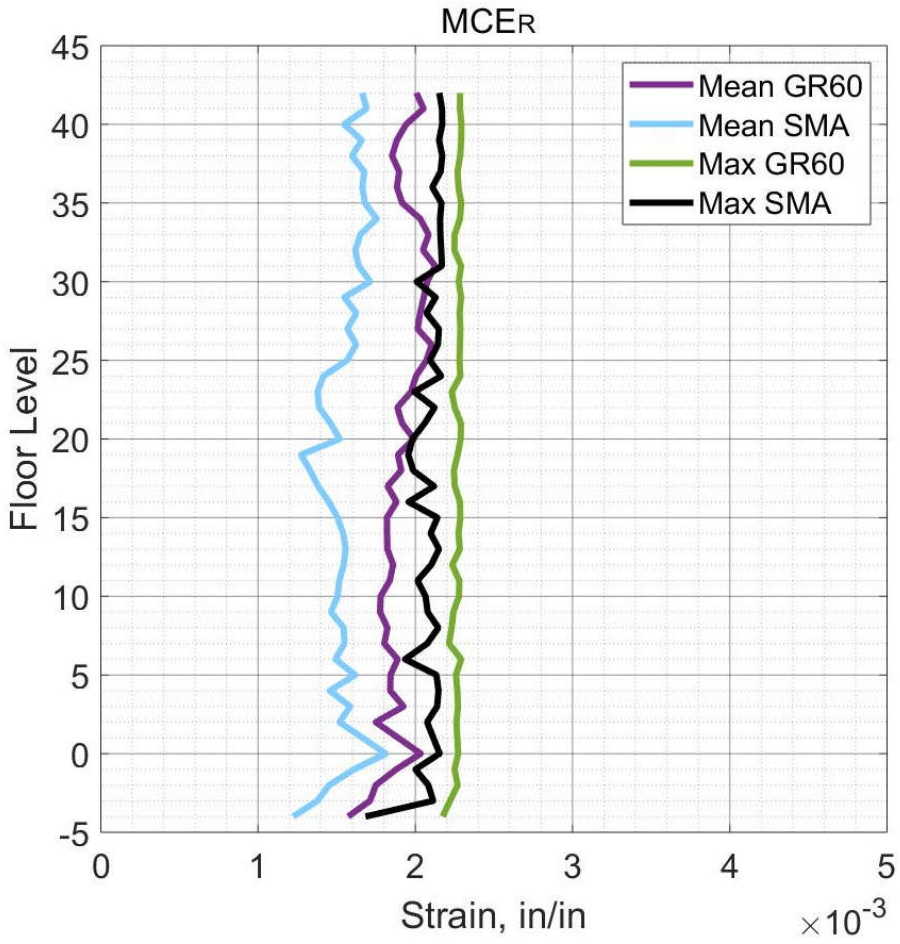

Figure 12.57 Peak of Reinforcement Tensile Strain in Columns for Conventional Reinforcement and SMA Cases (MCER).

CHAPTER XIII

SUMMARY AND CONCLUSION

13.1 SUMMARY

The goal of this study is to investigate the seismic performance of a concrete tall building reinforced with different grades of high strength steel bars and shape memory alloy bars. The TBI guidelines provide the procedure and the acceptance criteria for assessing the seismic performance of tall buildings. The lateral load resisting system of the selected case study (46-story building) consists of a core wall and a special moment frame. After selection of the case study building, the nonlinear model for the case study was prepared by using the elements and materials models that are available in Opensees. According to the requirements of the TBI guidelines, two different suites of ground motions were selected and scaled to match the Service Load Earthquake (SLE) level and the Risk-Targeted Maximum Considered Earthquake (MCER) for the location of the case study building. For each case, seven and eleven dynamic nonlinear analyses were conducted for SLE and MCER levels, respectively. The response parameters were extracted from the analyses and compared with the TBI acceptance criteria.

In the first part of this study, the conventional Grade 60 steel bars selected for the original design (PEER, 2011) were replaced by a reduced area of high strength steel bars. The cases considered include ASTM A706 Grade 80, ASTM A1035 Grade 100, and ASTM A1035 Grade 120. The high strength reinforcing bars were used in both the core wall and the elements of the special moment frame. The global response parameters were determined and compared with the acceptance criteria of the TBI guidelines. In addition, the force-based and deformation-based

actions in the core wall, beams, and columns were determined and compared with the appropriate acceptance criteria.

In the second part of this study, the conventional Grade 60 steel bars were replaced by shape memory alloy bars, but only in specific regions that experience high tensile strain demands based on the analysis for the case of conventional reinforcing bars. The SMA bars were used in the boundary elements of the core wall up to the 32nd story and the plastic hinge regions of the beams for all stories above the main podium. In addition, the SMA bars were used in the diagonal reinforcement of the coupling beams. As in the first part of this study, both the global response parameters and the element level response parameters were determined and checked with the acceptance criteria of the TBI guidelines.

13.2 CONCLUSIONS FOR HIGH STRENGTH REINFORCEMENT CASES

Considering the response parameters presented in Chapters 7 to 10 along with the acceptance criteria of the TBI guidelines, the following conclusion can be drawn.

1. The conventional steel bars can be replaced by a reduced area of high strength reinforcement. The formula for reduction of the area simply depends on the idea that the value of the area of reinforcement times the yield strength is constant and remains same for the reference case reinforced with conventional reinforcement and the cases reinforced with high strength reinforcement.
2. For SLE shaking level, the values for the global response parameter as measured by the interstory drift ratios, were within the acceptable limit of the TBI guidelines (0.005) for all high strength reinforcement cases as well as the reference case. In general, the interstory drift ratio in the x-direction was larger than the interstory drift ratio in the y-direction.

Considering the drift ratio results, all high strength cases satisfied the requirements of the TBI guidelines for the SLE level.

3. All response parameters at the element level are categorized into force-based actions or deformation-based actions. For the SLE shaking level, the shear force is a force-based action that was examined in the core wall, the beams, and the columns according to the TBI guidelines for all cases. For all cases, the mean shear force demand was less than the reduced shear capacity calculated according to the ACI 318-14. In addition, the shear demands were very similar for all cases. The reinforcement tensile strain and the concrete compression strain were examined in all the core wall edges as deformation-based actions. The maximum tensile strain for all cases was less than the expected yield strain of the reinforcing grade, while concrete experiences very low compression strain. The deformation based-action for the special moment frame is the plastic rotation of the beams and the columns. In addition, due to use of the fiber section for simulating the cross-section of the beams and columns, the tensile strain in the longitudinal reinforcing bars could be examined. For SLE level, both the beams and columns did not experience yielding of the longitudinal reinforcement. In other words, the beams and columns did not experience plastic rotations for the SLE shaking level. Finally, all cases satisfy the requirements of the TBI guidelines for the element level for SLE shaking kevel.
4. For the MCER shaking level, the mean value of the peak interstory drift ratios from the eleven analyses were within the limit of the TBI guidelines (0.03) for all cases. In addition, the maximum interstory drift ratios from all analyses also were within the acceptable limit of the TBI guidelines (0.045) for all cases. Considering the drift results, all cases produced an acceptable response. In addition, all analyses for all cases converged.

5. For the MCER shaking level, the force-based action (shear force demand) in all structural elements of the seismic force resisting system of the case study building for all types of reinforcing steel grades satisfy the requirement of the TBI guidelines. In addition, the maximum shear demands from all analyses were less than the shear capacity that is calculated according to the ACI 318-14. So, all analyses are acceptable. According to the TBI guidelines, the maximum response parameters should be used for checking the deformation-based actions for the MCER shaking level. The tensile strain in the reinforcing steel in the core wall edges for all cases was approximately 0.016 which is less than the acceptable limit of 0.05. The concrete experienced very low maximum compression strain of 0.002, which is below the acceptable limit of 0.003. The maximum plastic rotations of the beams were also within the acceptable limit of ASCE 41. In all cases of different steel grades, the columns experienced no yielding of the longitudinal reinforcing bars leading to zero plastic rotation demands in the columns. Finally, all cases satisfy the requirements of the TBI guidelines for the element level for MCER shaking.

Considering the above points, the main conclusion is that replacement the conventional steel bars by a reduced area of high strength reinforcement in concrete tall buildings could introduce a valuable solution to some construction problems such as the congestion of reinforcement. For the case study building, the seismic performance when using high strength reinforcement satisfies the requirement of the TBI guidelines.

13.3 CONCLUSION FOR SHAPE MEMORY ALLOY CASE

One of the challenges for concrete structures to withstand against severe earthquake shaking is permanent deformation in some regions of concrete frames. Residual deformation can lead to detrimental consequences such as high repair cost, longer time for rehabilitation and repair,

and eventual demolition of structures. The main goal of the second part of this study is to evaluate the use of a new and advanced material, shape memory alloy bars, for reinforced concrete structures in order to reduce the permanent deformation and to enhance the seismic performance.

Considering the results of the reference case reinforced with conventional Grade 60 steel bars and the results of the case reinforced with SMA bras in key locations and conventional steel bars in the remaining locations, along with the acceptance criteria of the TBI guidelines, the following conclusion can be drawn.

1. Due to the current high cost of the shape memory alloy bars, the replacement of conventional steel bars by SMA bars was applied only to specific regions in the case study building. The choice of the regions depended on the response of the reference case when subjected to the MCER level demand. The yielding of the conventional steel bars was noticed in the core wall up to 32nd story and in the beams of the special moment frame for all stories above the main podium. In addition, the coupling beams underwent relatively high rotation demands and experienced yielding of diagonal reinforcement. Therefore, the SMA bars were utilized as longitudinal reinforcement in the boundary elements of the core wall and the plastic hinge regions of the beams as well as the coupling beams.
2. For the SLE shaking level, according to the response of the reference case with only conventional reinforcement, the reinforcement in the core wall, the beams, and the columns did not experience yielding of reinforcement. Therefore, the super elastic effect of the SMA bars did not contribute for this shaking level.
3. The response of the SMA case for the global and the element levels satisfied the requirements of the TBI guidelines for the SLE level demand. The response parameters for

the element level evaluation of the SMA case were very close to the response parameters of the reference case.

4. For MCER, the mean of the peak interstory drift ratios from the 11 analyses of the SMA case were within the acceptable limit of the TBI guidelines (0.03). The maximum drift ratios also were within the acceptable limit (0.045). The SMA case produced an acceptable response when considering the drift results.
5. For the MCER level, the shear reinforcement in the core wall and the special moment frame consisted of conventional Grade 60 steel bars, therefore the shear strength equations of ACI 318-14 could be applied. The force-based action (shear force demand) in all structural elements of the lateral load resisting system of the case study building for all types of reinforcing steel grades satisfied the requirement of the TBI guidelines. In addition, the maximum shear demands from all analyses were less than the shear capacity that is calculated according to the ACI 318-14. So, all analyses were acceptable.
6. For the MCER level, the maximum tensile strain in the longitudinal reinforcement of the core wall for the SMA case was 0.016 which is far below the maximum recoverable strain for SMA (0.06). Consequently, the SMA bars could return to their original shape leading to negligible residual strain. The significant reduction in the residual strain is expected to improve the seismic performance of the building.
7. For the MCER level, the maximum tensile strain in the longitudinal reinforcement of the beams was 0.03, which is also below the maximum recoverable strain for SMA (0.06). Consequently, the beams would be able to return to their original shape leading to eliminating or reducing significantly the residual strain. The SMA bars do not have a yield point, however the strain of 0.01 represents the ending of the linear portion of the stress-

stain relationship of SMA. When considering the strain of 0.01 as a yield point for the SMA bars, the plastic rotation of the beams reinforced with SMA in the hinge regions are still within the acceptable limits.

8. For the MCER level, the columns in both the reference case and the SMA case were reinforced with conventional reinforcement. In addition, all the columns in all stories for both cases did not experience yielding of longitudinal reinforcement. So, no plastic rotation is observed in the columns.

Considering the above points, the main conclusion is that utilizing SMA bars as an alternative reinforcement for conventional steel bars could introduce a valuable means for improving the seismic performance of reinforced concrete tall buildings and reducing the residual strain or the damage upon subjecting the structure to severe earthquake shaking.

13.4 RECOMMENDATIONS FOR FUTURE WORKS

Based on the results of the current work some recommendation for future work could be listed

1. More studies will be needed to address the different types of high strength reinforcement that are produced commercially and study the appropriate material model that could be incorporated in a general finite element program.
2. More experimental studies are needed to address the effect of replacing the conventional steel bars by same area of high strength reinforcement on the seismic performance of different structural members.
3. Conduct the same current work on a different case study tall building. The new tall building may have more stories (more than 42 stories), irregular configurations, and different lateral load resisting system such as special moment frame only, etc.

4. Conduct the same current work but changing the members dimensions of the same case study building and using an unreduced area of high strength reinforcement.
5. More studies are needed to address the effect of using high strength concrete with the high strength reinforcement on the seismic performance of tall buildings.
6. Choosing a more intense hazard level (an intensity more than MCER) as a target spectrum to assess the case study building. The reason for choosing a more intense hazard level is to examine the performance of high strength steel bars for more demanding loads.
7. More experimental studies are needed to explore the structural behavior of full-scale specimens for beams, columns, and walls reinforced with SMA bars.

REFERENCES

Abdulridha, A., Palermo, D., Foo, S., and Vecchio, F. J. (2013). "Behavior and Modeling of Superelastic Shape Memory Alloy Reinforced Concrete Beams." *Engineering Structures*, 49, 893-904.

ACI (1956). "Building Code Requirements for Structural Concrete and Commentary." *ACI 318-56*, American Concrete Institute, Farmington Hills, MI.

ACI (1963). "Building Code Requirements for Structural Concrete and Commentary." *ACI 318-63*, American Concrete Institute, Farmington Hills, MI.

ACI (1971). "Building Code Requirements for Structural Concrete and Commentary." *ACI 318-71*, American Concrete Institute, Farmington Hills, MI.

ACI (2005). "Building Code Requirements for Structural Concrete and Commentary." *ACI 318-05*, American Concrete Institute, Farmington Hills, MI.

ACI (2010). "Design Guide for the Use of Astm A1035/A1035m Grade 100 (690) Steel Bars for Structural Concrete." *ACI ITG-6R-10*, American Concrete Institute, Farmington Hills, MI.

ACI (2014). "Building Code Requirements for Structural Concrete and Commentary." *ACI 318-14*, American Concrete Institute, Farmington Hills, MI.

ACI (2019). "Building Code Requirements for Structural Concrete and Commentary." *ACI 318-19*, American Concrete Institute, Farmington Hills, MI.

Alam, M., Youssef, M., and Nehdi, M. (2008). "Analytical Prediction of the Seismic Behaviour of Superelastic Shape Memory Alloy Reinforced Concrete Elements." *Engineering Structures*, 30(12), 3399-3411.

Alam, M. S., Moni, M., and Tesfamariam, S. (2012). "Seismic Overstrength and Ductility of

Concrete Buildings Reinforced with Superelastic Shape Memory Alloy Rebar." *Engineering Structures*, 34, 8-20.

Aoyama, H. (2001). *Design of Modern Highrise Reinforced Concrete Structures*, 1st Ed., World Scientific, Tokyo.

ASCE (2013). "Seismic Evaluation and Retrofit of Existing Buildings." *ASCE/SEI 41-13*, American Society for Civil Engineering, Reston, VA.

ASCE (2016). "Minimum Design Loads for Buildings and Other Structures." *ASCE/SEI 7-16*, American Society for Civil Engineering, Reston, VA.

ASTM (2007). "Standard Test Method for Tension Testing of Nickel-Titanium Superelastic Materials." *ASTM F2516-07*, American Society for Testing and Materials, West Conshohocken, PA.

ASTM (2016a). "Standard Specification for Low –Alloy Steel Deformed and Plain Bars for Concrete Reinforcement." *ASTM A706-16*, American Society for Testing and Materials, West Conshohocken, PA.

ASTM (2016b). "Standard Specification for Deformed and Plain, Low-Carbon, Chromium, Steel Bars for Concrete Reinforcement." *ASTM A1035-16*, American Society for Testing and Materials, West Conshohocken, PA.

ASTM (2017). "Standard Test Methods and Definitions for Mechanical Testing of Steel Products." *ASTM A370-17*, American Society for Testing and Materials, West Conshohocken, PA.

Billah, A. H. M. M., and Alam, M. S. (2016). "Bond Behavior of Smooth and Sand-Coated Shape Memory Alloy (Sma) Rebar in Concrete." *Structures*, 5, 186-195.

Blume, J. A., Newmark, N. M., and Corning, L. H. (1961). *Design of Multistory Reinforced Concrete Buildings for Earthquake Motions*, 1st Ed., Portland Cement Association,

Chicago.

Dazio, A., Beyer, K., and Bachmann, H. (2009). "Quasi-Static Cyclic Tests and Plastic Hinge Analysis of Rc Structural Walls." *Engineering Structures*, 31(7), 1556-1571.

Deierlein, G. G., Reinhorn, A. M., and Willford, M. R. (2010). "Nonlinear Structural Analysis for Seismic Design." NISTGCR - 10-917-5 National Institute of Standards and Technology, Gaithersburg, MD.

FEMA (2009a). "NEHRP Recommended Seismic Provisions for New Buildings and Other Structures " *FEMA P-750*, Federal Emergency Management Agency, Washington, D.C.

FEMA (2009b). "Quantification of Building Seismic Performance Factors." *FEMA P-695*, Federal Emergency Management Agency Washington, D.C.

FEMA (2015). "NEHRP Recommended Seismic Provisions for New Buildings and Other Structures." *P-1050-1*, Federal Emergency Management Agency, Washington, D.C.

Filippou, F. C., Bertero, V. V., and Popov, E. P. (1983). "Effects of Bond Deterioration on Hysteretic Behavior of Reinforced Concrete Joints." UCB/EECR-83/19 Earthqukae Engineering Research Center, University of California, Berkeley, CA.

Gaudenzi, P. (2009). *Smart Structures: Physical Behaviour, Mathematical Modelling and Applications*, 1st Ed., John Wiley & Sons, West Sussex.

Ghassemieh, M., Rezapour, M., and Sadeghi, V. (2016). "Effectiveness of the Shape Memory Alloy Reinforcement in Concrete Coupled Shear Walls." *Journal of Intelligent Material Systems and Structures*, 28(5), 640-652.

Günel, M. H., and Ilgin, H. E. (2014). *Tall Buildings: Structural Systems and Aerodynamic Form*, 1st Ed., Routledge, London.

Haber, Z. B., Saiidi, M. S., and Sanders, D. H. (2014). "Seismic Performance of Precast Columns

with Mechanically Spliced Column-Footing Connections." *ACI Structural Journal*, 111(3), 639-650.

Hognestad, E. (1962). "High-Strength Bars as Concrete Reinforcement, Part 2: Control of Flexural Cracking." *Journal of the PCA Research and Development Laboratories*, 4, 46-63.

ICC-ES (2009). "Acceptance Criteria for Threaded High-Strength Steel Bars for Concrete Reinforcement,." AC 237 International Code Council Evaluation Service, Whittier, CA.

ICC (2016). "International Building Code." International Code Council, Washington, D.C.

Kheyr, A. A., and Naderpour, H. (2007). "Plastic Hinge Rotation Capacity of Reinforced Concrete Beams." *International Journal of Civil Engineering*, 5(1), 30-47.

Lagoudas, D. C. (2008). *Shape Memory Alloys: Modeling and Engineering Applications*, 1st Ed., Springer Science & Business Media, Boston.

LATBSDC (2008). "An Alternative Procedure for Seismic Analysis and Design of Tall Buildings Located in the Los Angeles Region." Los Angeles Tall Buildings Structural Design Council, , Los Angeles, CA.

Lee, H. J., and Chang, C. J. (2017). "High-Strength Reinforcement in Exterior Beam-Column Joints under Cyclic Loading." *ACI Structural Journal*, 114(5), 1325-1338.

Lu, X., Xie, L., Guan, H., Huang, Y., and Lu, X. (2015). "A Shear Wall Element for Nonlinear Seismic Analysis of Super-Tall Buildings Using Opensees." *Finite Elements in Analysis and Design*, 98, 14-25.

Mander, J. B., Priestley, M. J., and Park, R. (1988). "Theoretical Stress-Strain Model for Confined Concrete." *Journal of structural engineering*, 114(8), 1804-1826.

Mazzoni, S., McKenna, F., Scott, M., and Fenves, G. (2006). "Opensees Command Language Manual. Open System for Earthquake Engineering Simulation (Opensees)." Pacific

Earthquake Engineering Research Center, University of California, Berkeley, CA.

Mo, Y.-L. (2013). *Dynamic Behavior of Concrete Structures*, 1st Ed., Elsevier, Tainan.

Moehle, J., Bozorgina, Y., Jayaram, N., Jones, P., Rahnama, M., Shome, N., Tuna, Z., Wallace, J., Yang, T., and Zareian, F. (2011). "Case Studies of the Seismic Performance of Tall Buildings Designed by Alternative Means: Task 12 Report for the Tall Buildings Initiative : Final Report to California Seismic Safety Commission and California Emergency Management Agency." PEER 2011/05 Pacific Earthquake Engineering Research Center, University of California, Berkeley, CA.

Moehle, J. (2008). "Performance-Based Seismic Design of Tall Buildings in the Us." *Proc., 14th World Conference on Earthquake Engineering* Beijing, China.

Moehle, J. (2014). *Seismic Design of Reinforced Concrete Buildings*, 1st Ed., McGraw Hill Professional, Berkeley.

Moehle, J., Mahin, S., and Bozorgnia, Y. (2010). "Modeling and Acceptance Criteria for Seismic Design and Analysis of Tall Buildings." PEER/ATC-72-1 Pacific Earthquake Engineering Research Center, University of California, Berkeley, CA.

Naish, D. A. B. (2010). "Testing and Modeling of Reinforced Concrete Coupling Beams." Ph.D. Dissertation, University of California, Los Angeles, CA.

NEHRP (2014). "Use of High-Strength Reinforcement in Earthquake-Resistant Concrete Structures, National Earthquake Hazard Reduction Program." NIST GCR 14-917-30, National Institute of Standards and Technology, Gaithersburg, MD.

Neuenhofer, A., and Filippou, F. C. (1997). "Evaluation of Nonlinear Frame Finite-Element Models." *Journal of structural engineering*, 123(7), 958-966.

Ozbulut, O. E., Hurlebaus, S., and DesRoches, R. (2011). "Seismic Response Control Using Shape

Memory Alloys: A Review." *Journal of Intelligent Material Systems and Structures*, 22(14), 1531-1549.

Pfund, S. J. (2012). "Cyclic Response of Concrete Beams Reinforced with Astm A1035 Grade-120 Steel Bars." M.S. Thesis, The Pennsylvania State University University Park, PA.

Priestley, M., and Park, R. (1987). "Strength and Ductility of Concrete Bridge Columns under Seismic Loading." *Structural Journal*, 84(1), 61-76.

Rautenberg, J. M. (2011). "Drift Capacity of Concrete Columns Reinforced with High-Strength Steel." Ph.D. Dissertation, Purdue University, West Lafayette, IN.

Saiidi, M. S., and Wang, H. (2006). "Exploratory Study of Seismic Response of Concrete Columns with Shape Memory Alloys Reinforcement." *ACI structural journal*, 103(3), 436.

Shiravand, M., Nashtaee, M., and Veismoradi, S. (2017). "Seismic Assessment of Concrete Buildings Reinforced with Shape Memory Alloy Materials in Different Stories." *The Structural Design of Tall and Special Buildings*, 26(15), 1-13.

Sokoli, D., and Ghannoum, W. M. (2016). "High-Strength Reinforcement in Columns under High Shear Stresses." *ACI Structural Journal*, 113(3), 605-614.

Sokoli, D., Limantono, A., and Ghannoum, M. W. (2017). "Defining Structurally Acceptable Properties of High-Strength Steel Bars through Material and Column Testing, Part Ii: Column Testing Report." CPF Research Grant Agreement# 05-14 The University of Texas at Austin, Austin, TX.

Sugano, S. (2008). "Application of High-Strength and High-Performance Concrete in Seismic Regions." *Proc., 8th HSC/HPC Symposium, Tokyo*Tokyo.

Taucer, F., Spacone, E., and Filippou, F. C. (1991). "A Fiber Beam-Column Element for Seismic Response Analysis of Reinforced Concrete Structures." UCB/EERC-91/17 Earthquake

Engineering research Center, University of California, Berkeley, CA.

Tavallali, H., Lepage, A., Rautenberg, J. M., and Pujol, S. (2014). "Concrete Beams Reinforced with High-Strength Steel Subjected to Displacement Reversals." *ACI Structural Journal*, 111(5), 1037.

Tazarv, M., and Saiidi , M. (2014). "Reinforcing Niti Superelastic Sma for Concrete Structures." *Journal of Structural Engineering*, 141(8), 04014197.

TBI (2010). "Guidelines for Performance-Based Seismic Design of Tall Buildings." 2010/05 Pacific Earthquake Engineering Research Center, University of california, Berkeley, CA.

TBI (2017). "Guidelines for Performance-Based Seismic Design of Tall Buildings." 2017/06 Pacific Earthquake Engineering Research Center, University of California, Berkeley, CA.

Yassin, M. H. M. (1994). "Nonlinear Analysis of Prestressed Concrete Sructures under Monotonic and Cyclic Loads." M.S. Thesis, University of California, Berkeley, CA.

APPENDIX A

Selected Ground Motions

Two sets of ground motions are selected for SLE and MCER levels. There are seven ground motions in the SLE suite and 11 ground motions in the MCER suite. The following figures show the unscaled ground motions in terms of acceleration versus time. The ground motions were taken from the PEER database.

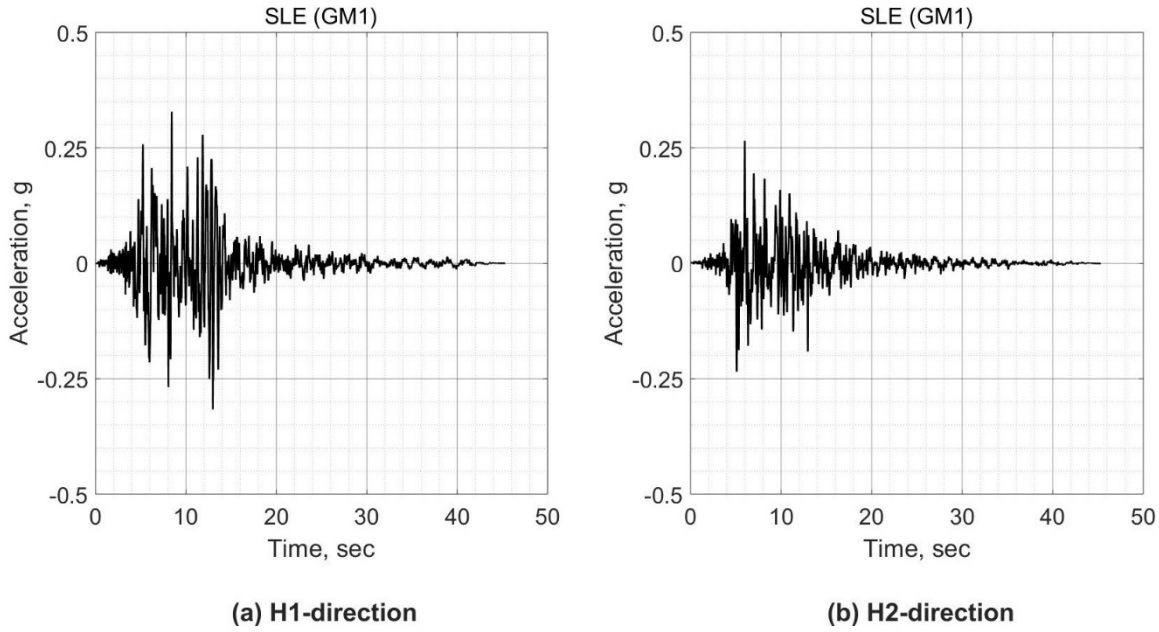

Figure A.1 Two Horizontal Components of the First Ground Motion for SLE.

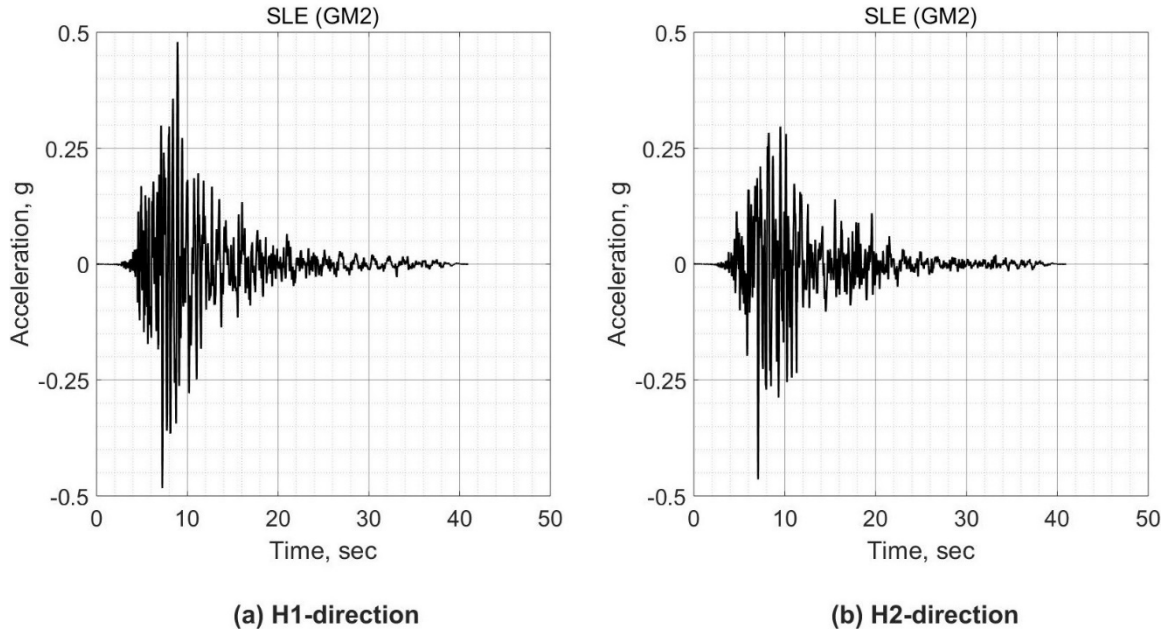

Figure A.2 Two Horizontal Components of the Second Ground Motion for SLE.

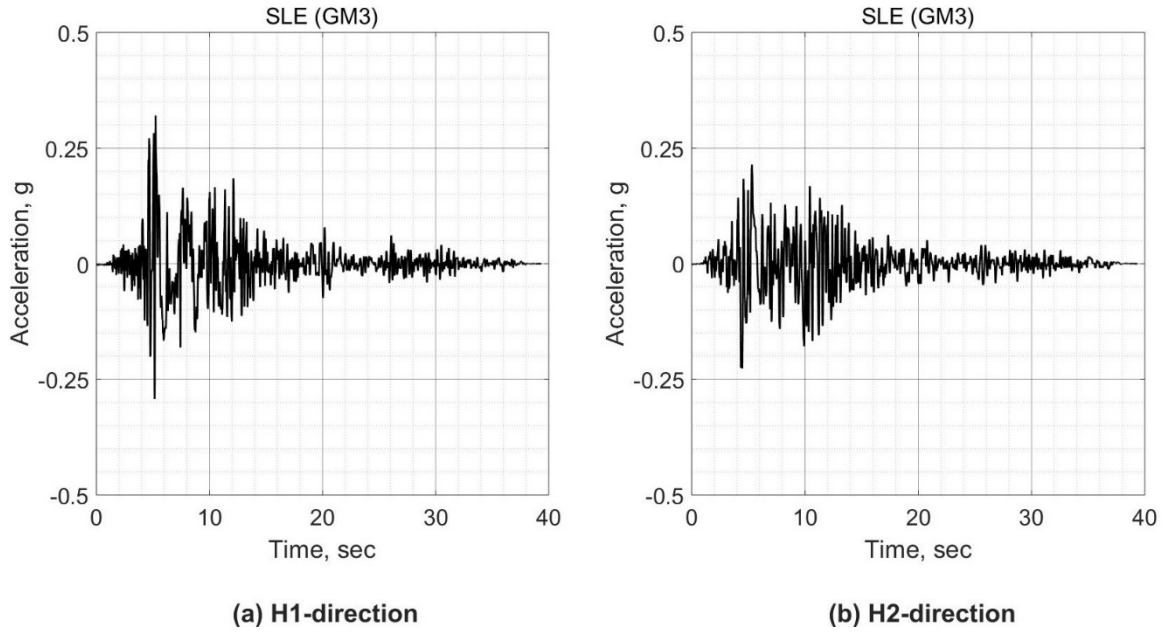

Figure A.3 Two Horizontal Components of the Third Ground Motion for SLE.

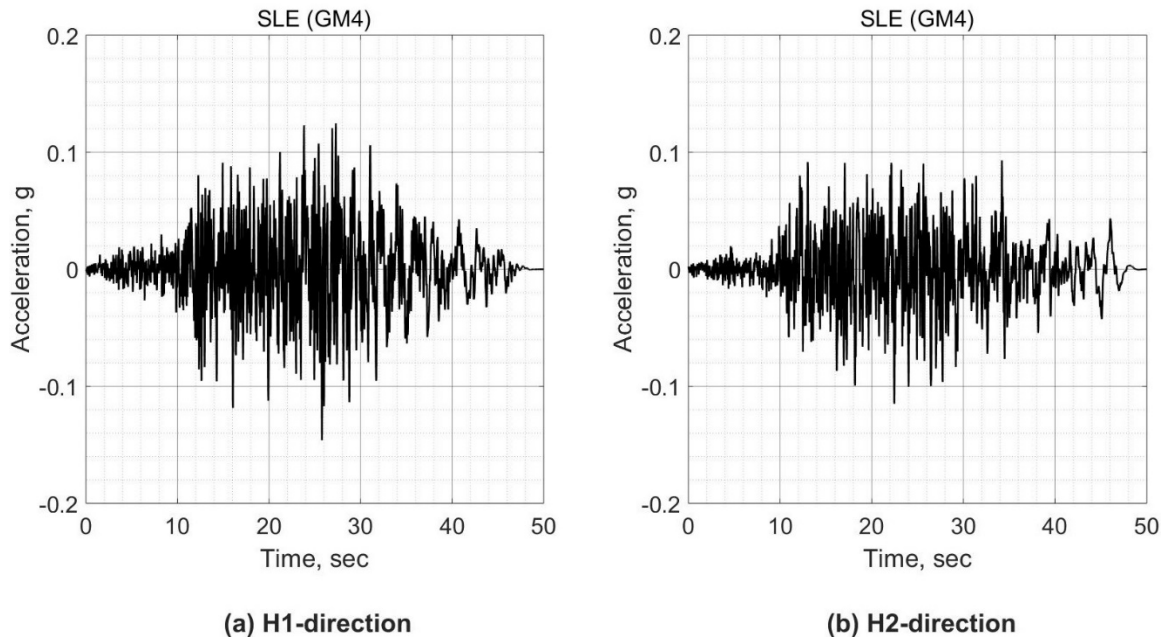

Figure A.4 Two Horizontal Components of the Fourth Ground Motion for SLE.

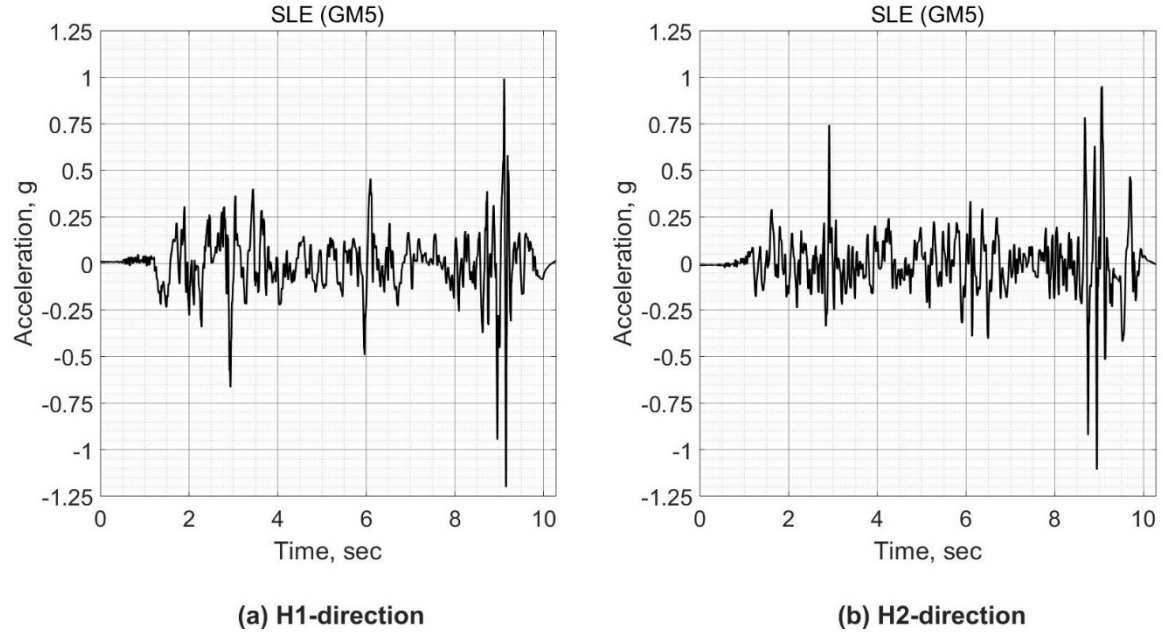

Figure A.5 Two Horizontal Components of the Fifth Ground Motion for SLE.

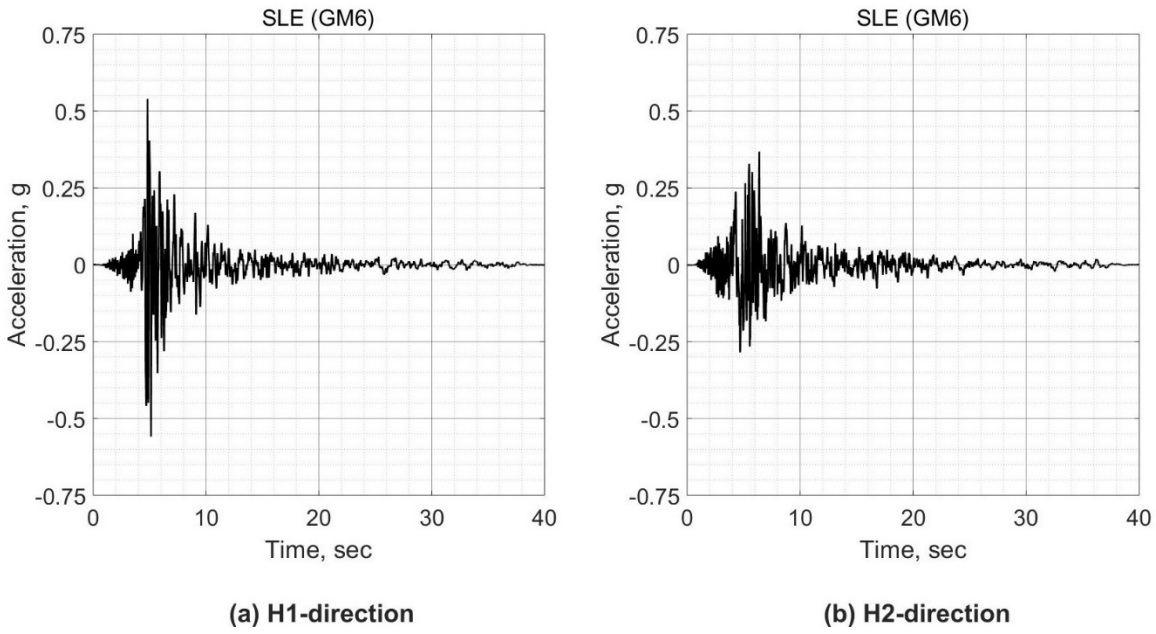

Figure A.6 Two Horizontal Components of the Sixth Ground Motion for SLE.

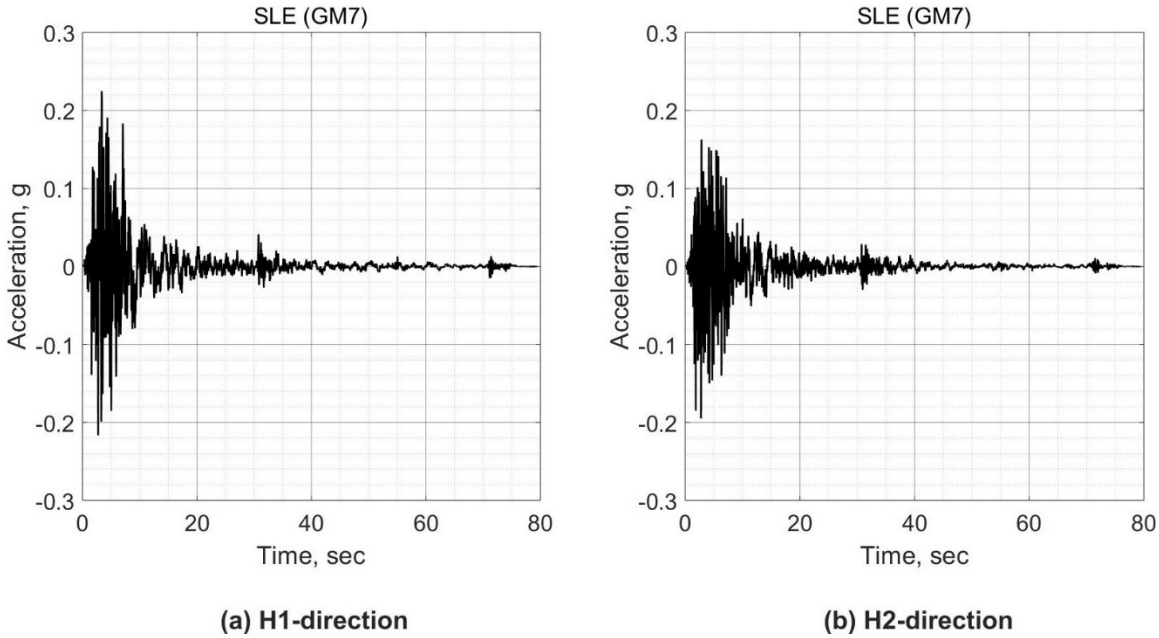

Figure A.7 Two Horizontal Components of the Seventh Ground Motion for SLE.

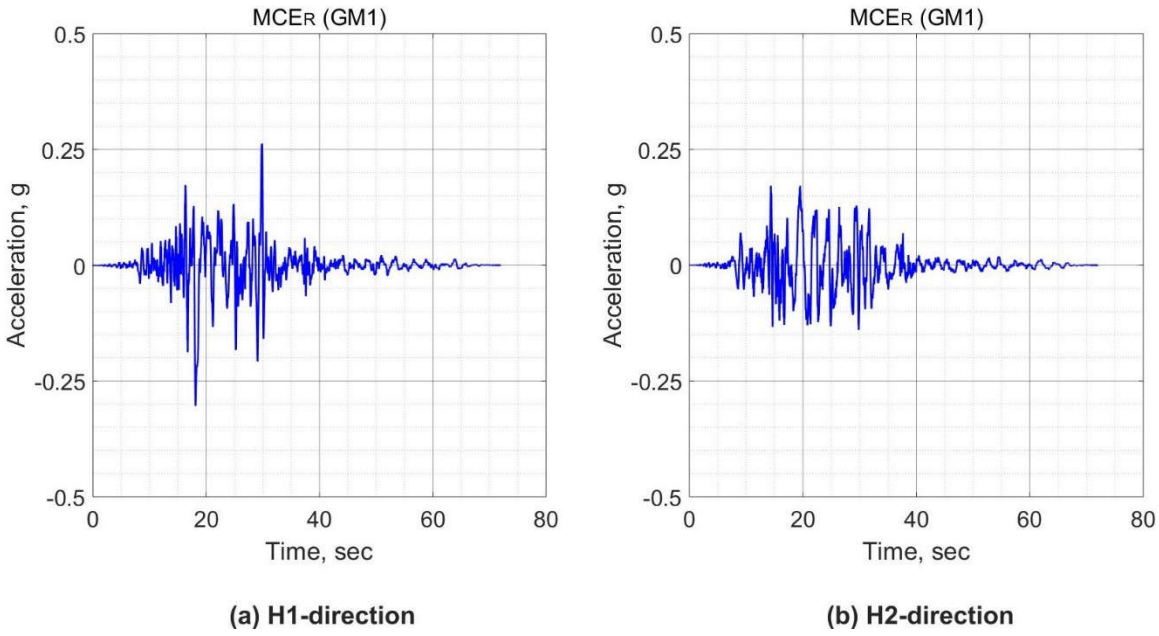

Figure A.8 Two Horizontal Components of the First Ground Motion for MCER.

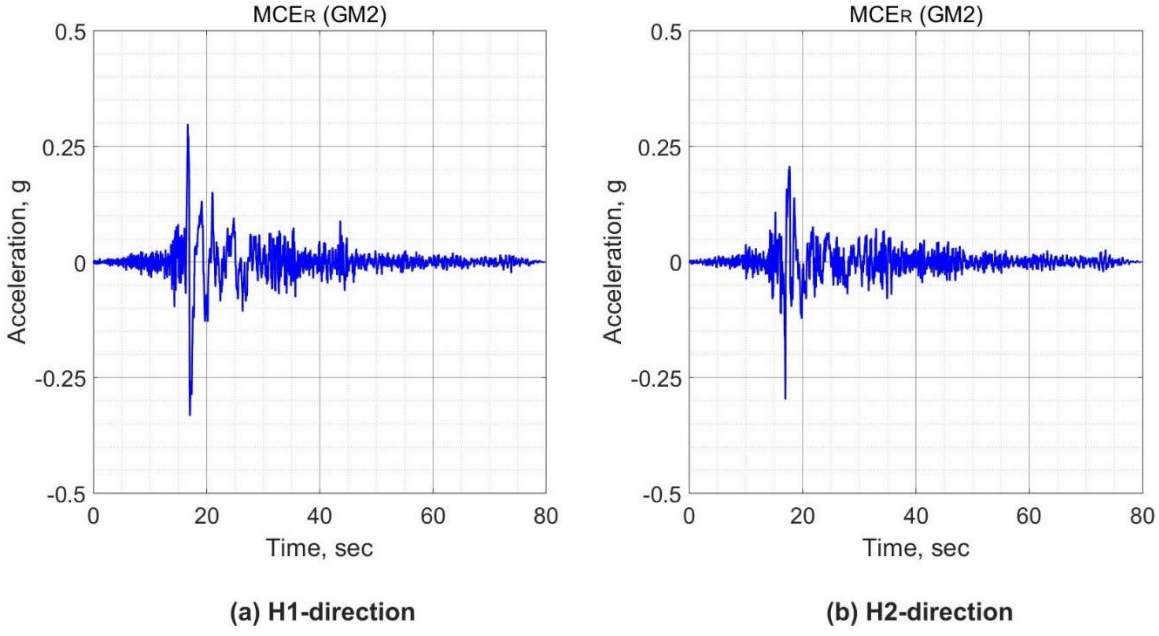

Figure A.9 Two Horizontal Components of the Second Ground Motion for MCER.

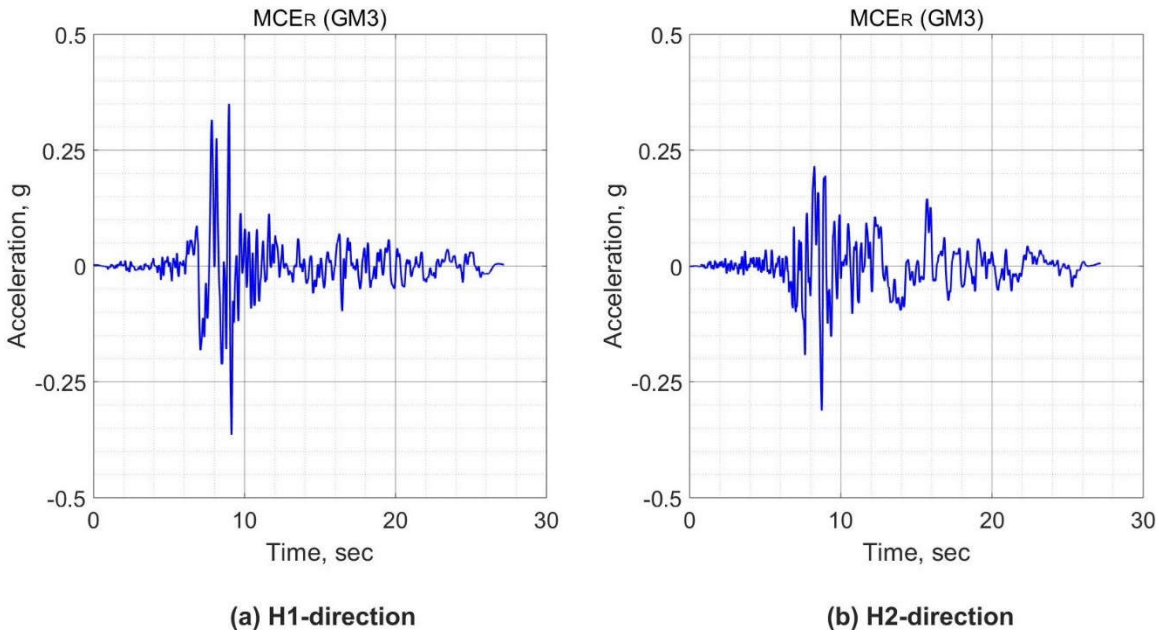

Figure A.10 Two Horizontal Components of the Third Ground Motion for MCER.

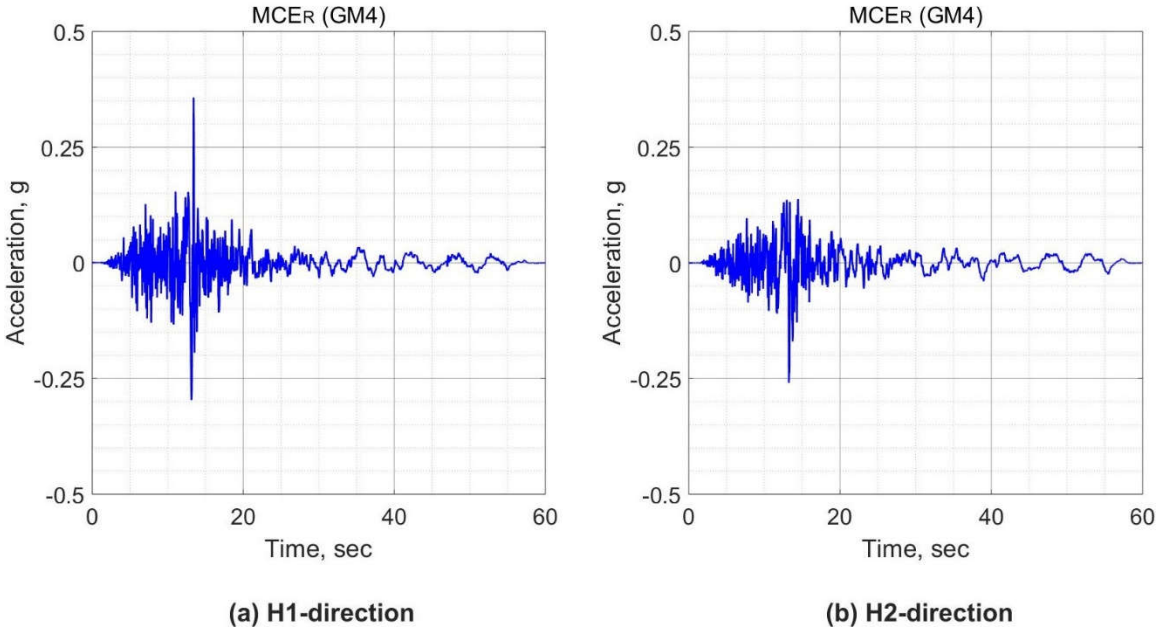

Figure A.11 Two Horizontal Components of the Fourth Ground Motion for MCER.

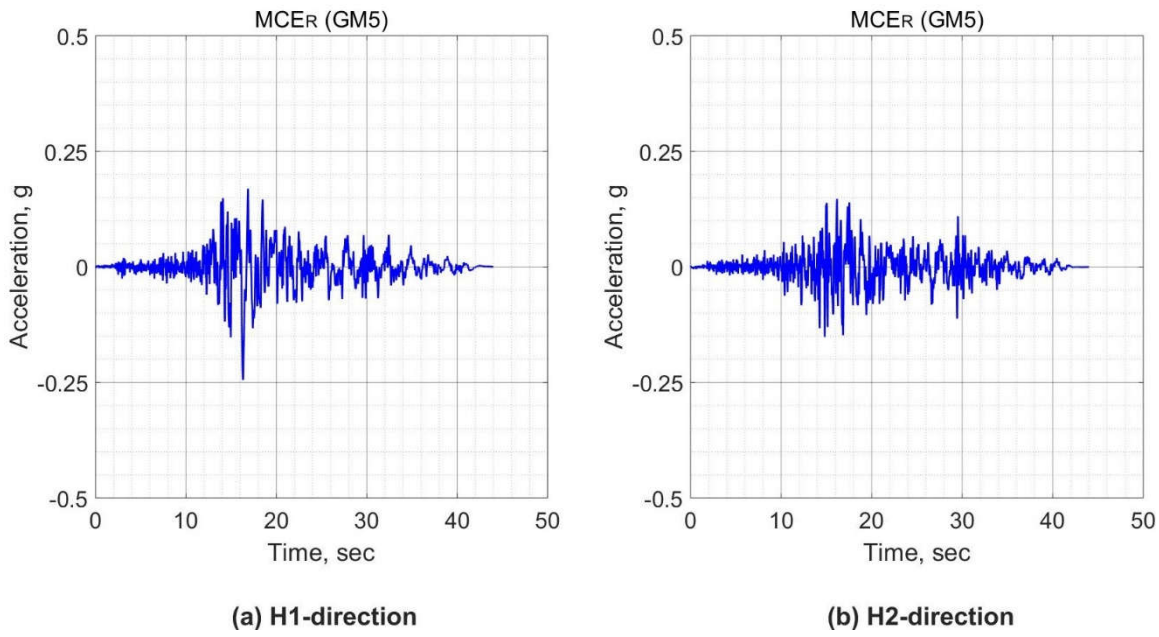

Figure A.12 Two Horizontal Components of the Fifth Ground Motion for MCER.

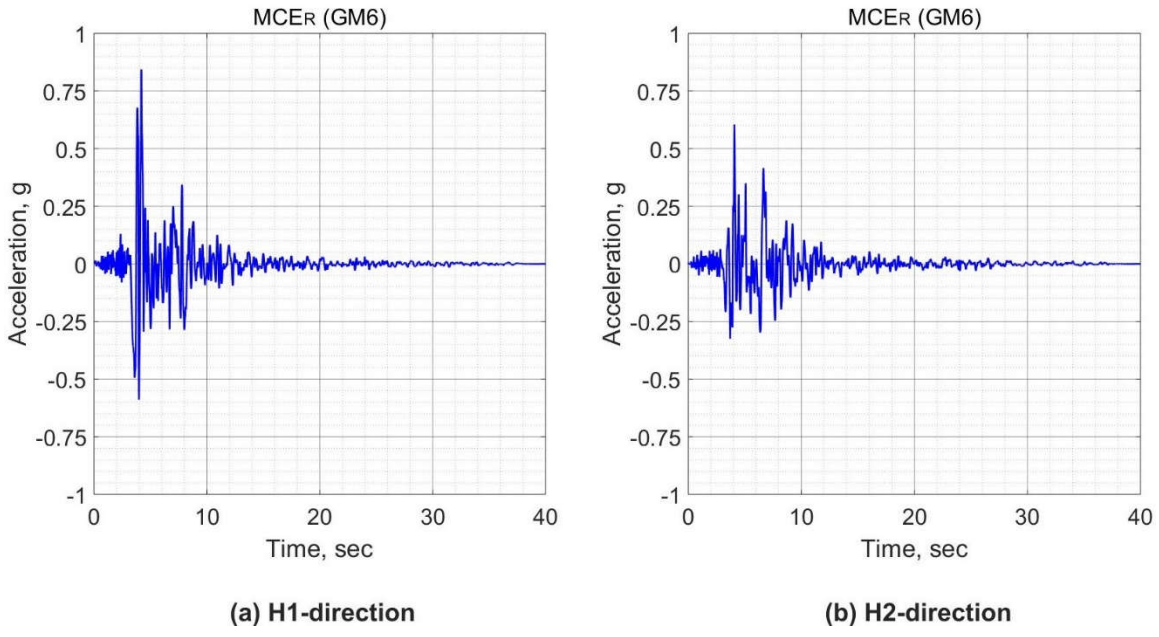

Figure A.13 Two Horizontal Components of the Sixth Ground Motion for MCER.

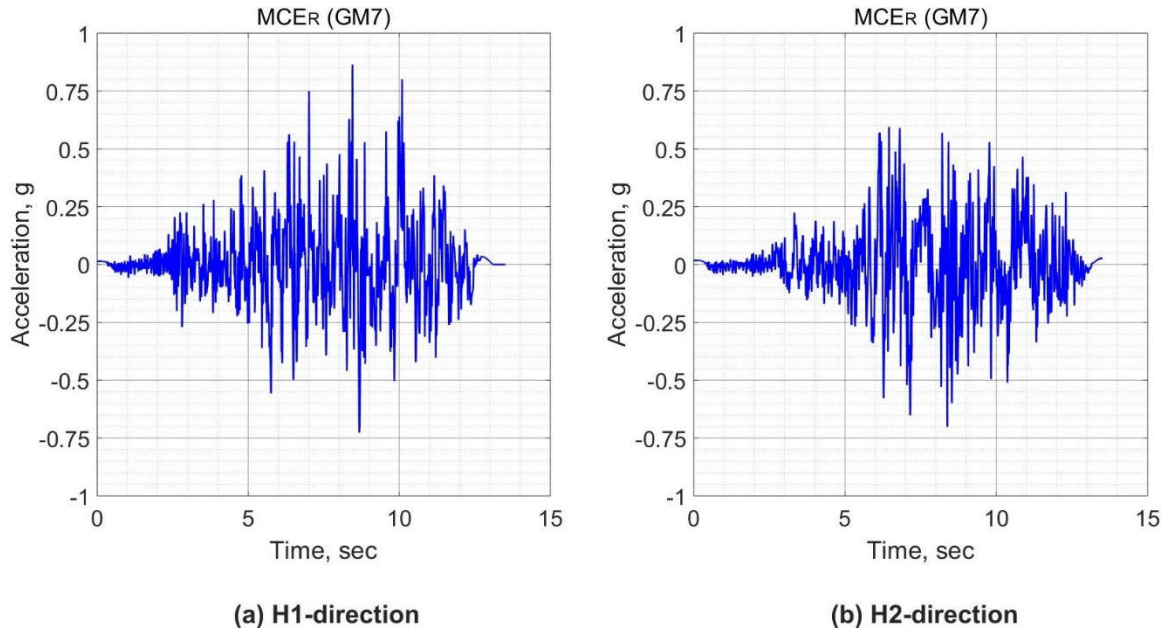

Figure A.14 Two Horizontal Components of the Seventh Ground Motion for MCER.

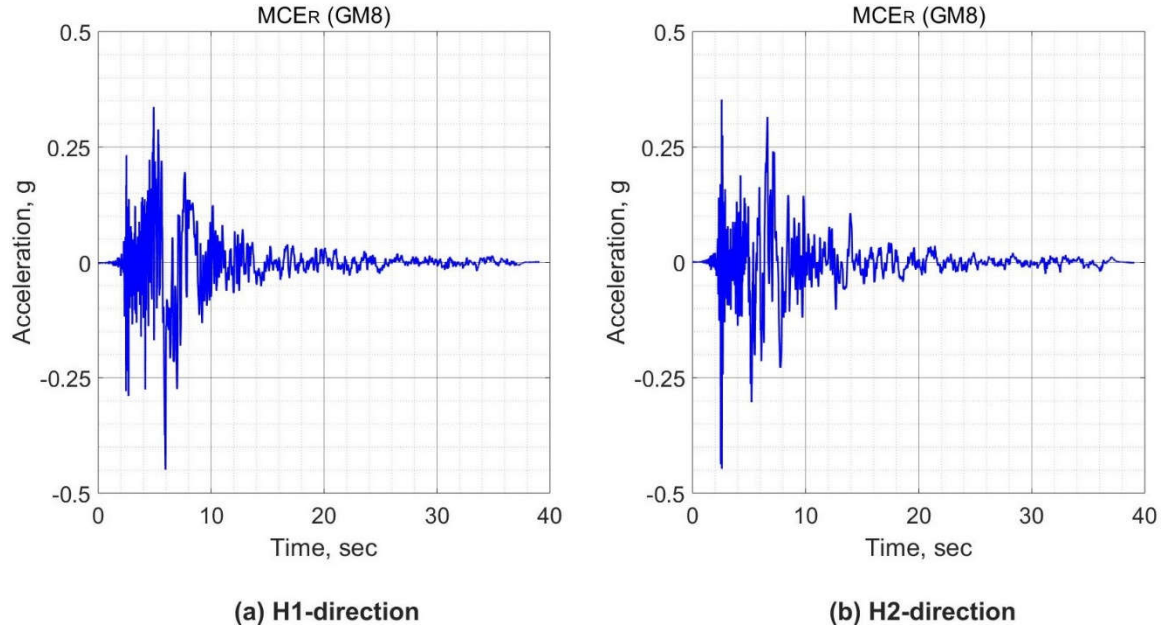

Figure A.15 Two Horizontal Components of the Eighth Ground Motion for MCER.

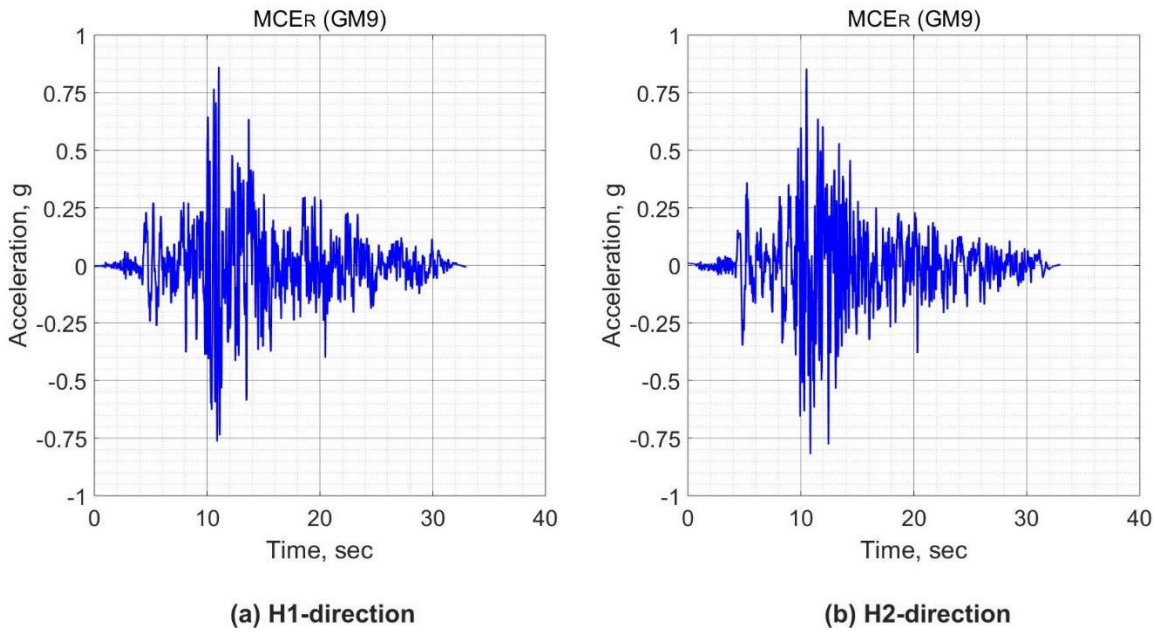

Figure A.16 Two Horizontal Components of the Ninth Ground Motion for MCER.

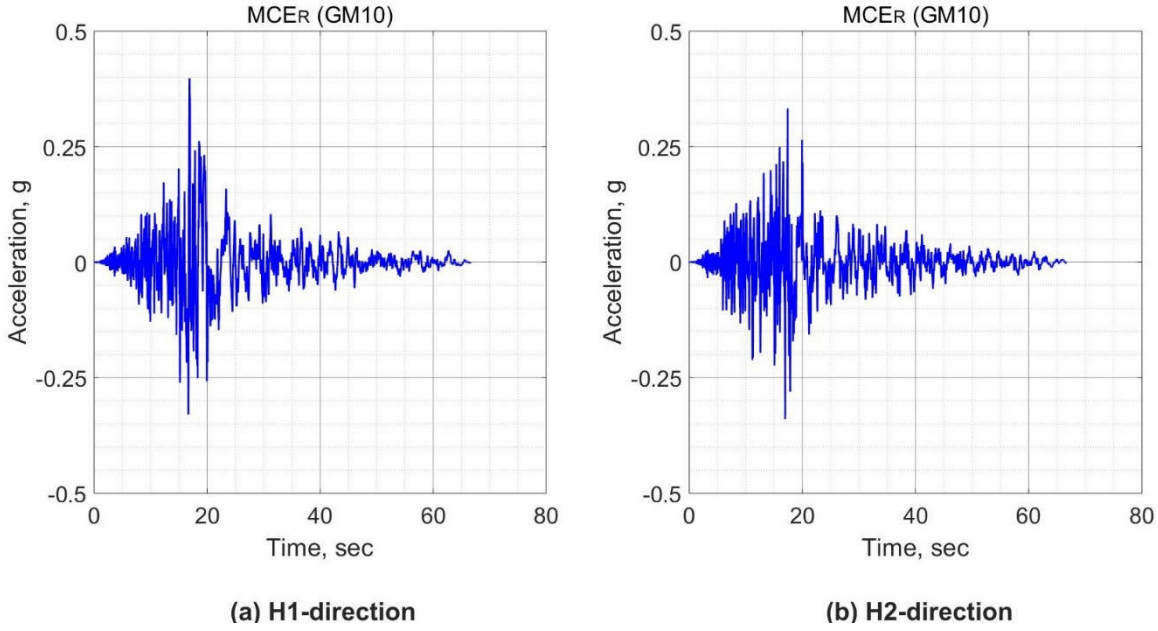

Figure A.17 Two Horizontal Components of the Tenth Ground Motion for MCER.

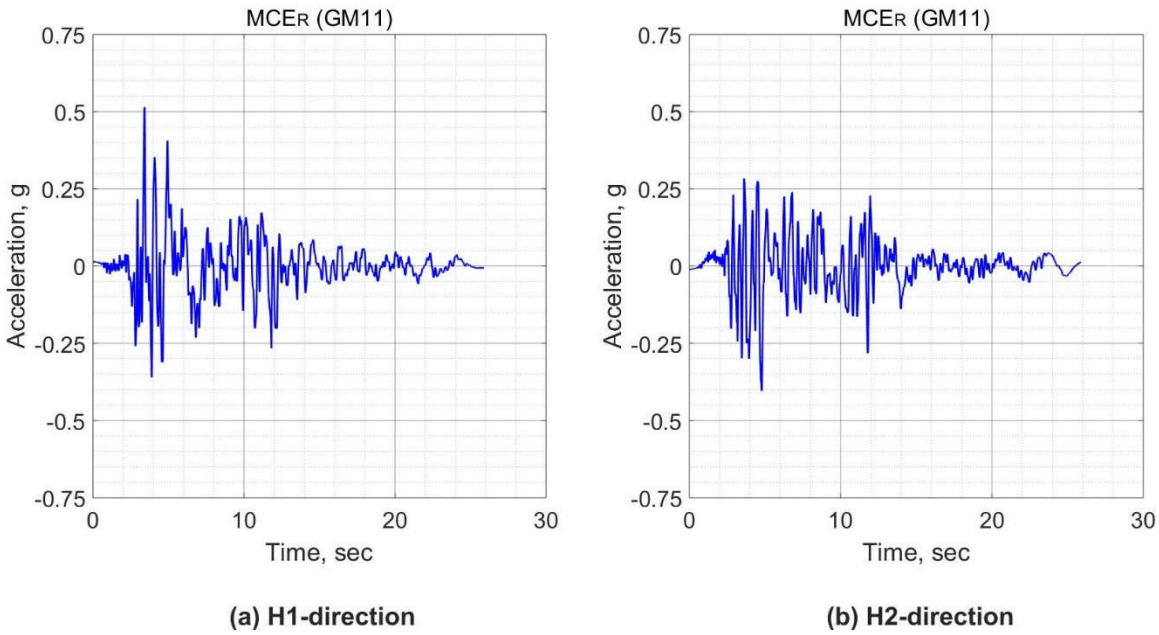

Figure A.18 Two Horizontal Components of the Eleventh Ground Motion for MCER.

APPENDIX B

Opensees Code for Simulation and Validation of Column Test.

This Opensees code uses the force-based beam column with fiber section for simulating the behavior of the column tested by Haber et al. (2014). in addition, the concrete02 and steel02 were used for simulation the concrete and the reinforcing steel bars, respectively.

```
# Create ModelBuilder (with two-dimensions and 3 DOF/node)
model basic -ndm 2 -ndf 3
# Units  kip   in  ksi

set height   108.0

# Create nodes
#    tag        X       Y
node   1       0.0     0.0
node   2       0.0     $height
node   3      -30.0    0.0
node   4       30.0   0.0

# Fix supports at base of columns
#    tag   DX   DY   RZ
fix   3     1    1   1
fix   4     1    1   1
# Define materials for nonlinear columns
# ------------------------------------------
# CONCRETE
# Core concrete (confined)
set   coreMatTag   11
###################   uniaxialMaterial Concrete01 $matTag $fpc $epsc0 $fpcu $epsU

uniaxialMaterial Concrete01  11  -5.77  -0.005  -1.16  -0.047 ;#-4.5  -0.017 ; #-1.16
-0.047
######-------------------------------------------------------------------------------
----------------
 ################  uniaxialMaterial Concrete02 $matTag $fpc $epsc0 $fpcu $epsU $lambda
$ft $Ets

 uniaxialMaterial Concrete02 12 -5.77   -0.005   -1.16   -0.047   0.01   0.0   0.0
#####-------------------------------------------------------------------------------
----------------------

# Cover concrete (unconfined)
set  coverMatTag   21 ;
uniaxialMaterial Concrete01  21  -4.35   -0.0019   -0.87   0.0075  ; #-1.7     -0.006
```

```
##-------------------------------------------------------------------------------
--------------
uniaxialMaterial Concrete02 22 -4.35   -0.0019   -0.87     -0.0075  0.01  0.0  0.0
##-------------------------------------------------------------------------------
----------------

# STEEL
# Reinforcing steel
set fy 75.0;     # Yield stress
set E 30000.0;   # Young's modulus
set  steelMatTag  3
#                        tag   fy E0    b
uniaxialMaterial Steel02  $steelMatTag  $fy $E 0.02 11  0.925  0.15
#-------------------------------------------------------------------------------

# Define cross-section for nonlinear columns

section Fiber 1 {

    # Create the concrete core fibers
  ### patch circ $matTag $numSubdivCirc $numSubdivRad $yCenter $zCenter $intRad $extRad
$startAng $endAng
  patch circ $coreMatTag   20   20   0.0   0.0   0.0   10.5    0   360   ;


    # Create the concrete cover fibers (top, bottom, left, right)

    patch circ $coverMatTag   14   14   0.0   0.0  10.5  12.0    0  360 ;


    # Create the reinforcing fibers (left, middle, right)
####    layer circ $matTag $numFiber $areaFiber $yCenter $zCenter $radius <$startAng
$endAng>


 layer circ $steelMatTag 11 0.79  0.0 0.0 10.5  0 360;

}


# Define column elements
# ----------------------

# Geometry of column elements
#                tag

geomTransf PDelta 1

# Create the coulumns using Beam-column elements
#               e            tag ndI ndJ nsecs secID transfTag
set eleType forceBeamColumn;

element   $eleType   1   1   2    1   HingeRadau  1   12.64   1  12.64     1;
```

```
###   element elasticBeamColumn $eleTag $iNode $jNode $A $E $Iz $transfTag
geomTransf Linear  2
element elasticBeamColumn 2   3   1    150.0    20000.0   10000.0   2
element elasticBeamColumn 3   1   4    150.0    20000.0   10000.0   2
# Define gravity loads
# --------------------

# Set a parameter for the axial load
set P 200.0;                # 10% of axial capacity of columns

# Create a Plain load pattern with a Linear TimeSeries
pattern Plain 1 "Linear" {
        # Create nodal loads at nodes 3 & 4
    #    nd    FX          FY  MZ
    load  2   0.0  [expr -$P] 0.0
}

# ------------------------------
# End of model generation
# ------------------------------
# ------------------------------
# Start of analysis generation
# ------------------------------

# Create the system of equation, a sparse solver with partial pivoting
system BandGeneral

# Create the constraint handler, the transformation method
constraints Transformation

# Create the DOF numberer, the reverse Cuthill-McKee algorithm
numberer RCM

# Create the convergence test, the norm of the residual with a tolerance of
# 1e-12 and a max number of iterations of 10
test NormDispIncr 1.0e-12  10 3

# Create the solution algorithm, a Newton-Raphson algorithm
algorithm Newton
# Create the integration scheme, the LoadControl scheme using steps of 0.1
integrator LoadControl 0.1

# Create the analysis object
analysis Static
# ------------------------------
# End of analysis generation
# ------------------------------
# ------------------------------
# Finally perform the analysis
# ------------------------------

# perform the gravity load analysis, requires 10 steps to reach the load level
```

```
analyze 10

recorder Node -file nodetwoDisp.out -time -node 2 1 -dof 1  disp

source dispconttest.tcl
```

APPENDIX C

Opensees code for simulation and validation the wall tested by Dazio et al. (2009)

This Opensees code uses the shell element with layered section for simulating the behavior of the tested concrete wall.

```
model basic -ndm 3 -ndf  6
# Create nodes
# ------------
# Units  N   mm  Mpa
# Set parameters for overall model geometry

set height   4520.0

# Create nodes
#    tag        X       Y    Z
# nodes
node 10001 0 0 0
node 10002 200 0 0
node 10003 0 565 0
node 10004 200 565 0
node 10005 0 1130 0
node 10006 200 1130 0
node 10007 0 1695 0
node 10008 200 1695 0
node 10009 0 2260 0
node 10010 200 2260 0
node 10011 0 2825 0
node 10012 200 2825 0
node 10013 0 3390 0
node 10014 200 3390 0
node 10015 0 3955 0
node 10016 200 3955 0
node 10017 0 4520 0
node 10018 200 4520 0
node 20002 400 0 0
node 20003 600 0 0
node 20004 800 0 0
node 20005 1000 0 0
node 20006 1200 0 0
node 20007 1400 0 0
node 20008 1600 0 0
node 20009 1800 0 0
node 20011 400 565 0
node 20012 600 565 0
```

```
node 20013 800 565 0
node 20014 1000 565 0
node 20015 1200 565 0
node 20016 1400 565 0
node 20017 1600 565 0
node 20018 1800 565 0
node 20020 400 1130 0
node 20021 600 1130 0
node 20022 800 1130 0
node 20023 1000 1130 0
node 20024 1200 1130 0
node 20025 1400 1130 0
node 20026 1600 1130 0
node 20027 1800 1130 0
node 20029 400 1695 0
node 20030 600 1695 0
node 20031 800 1695 0
node 20032 1000 1695 0
node 20033 1200 1695 0
node 20034 1400 1695 0
node 20035 1600 1695 0
node 20036 1800 1695 0
node 20038 400 2260 0
node 20039 600 2260 0
node 20040 800 2260 0
node 20041 1000 2260 0
node 20042 1200 2260 0
node 20043 1400 2260 0
node 20044 1600 2260 0
node 20045 1800 2260 0
node 20047 400 2825 0
node 20048 600 2825 0
node 20049 800 2825 0
node 20050 1000 2825 0
node 20051 1200 2825 0
node 20052 1400 2825 0
node 20053 1600 2825 0
node 20054 1800 2825 0
node 20056 400 3390 0
node 20057 600 3390 0
node 20058 800 3390 0
node 20059 1000 3390 0
node 20060 1200 3390 0
node 20061 1400 3390 0
node 20062 1600 3390 0
node 20063 1800 3390 0
node 20065 400 3955 0
node 20066 600 3955 0
node 20067 800 3955 0
node 20068 1000 3955 0
node 20069 1200 3955 0
node 20070 1400 3955 0
node 20071 1600 3955 0
```

```
node 20072 1800 3955 0
node 20074 400 4520 0
node 20075 600 4520 0
node 20076 800 4520 0
node 20077 1000 4520 0
node 20078 1200 4520 0
node 20079 1400 4520 0
node 20080 1600 4520 0
node 20081 1800 4520 0
node 30002 2000 0 0
node 30004 2000 565 0
node 30006 2000 1130 0
node 30008 2000 1695 0
node 30010 2000 2260 0
node 30012 2000 2825 0
node 30014 2000 3390 0
node 30016 2000 3955 0
node 30018 2000 4520 0
############################
# STEEL
# Reinforcing steel
set fy 580;     # Yield stress
set E 209000;   # Young's modulus
set  steelID  3

uniaxialMaterial Steel02  3 $fy $E 0.00  20  0.925  0.150
#-------------------------------------------------------------------------------------
------------------




    nDMaterial PlaneStressUserMaterial    1       40        7    46   0.7  -9.2  -
0.002    -0.021  0.0002  0.2
nDMaterial   PlateFromPlaneStress     4         1                1.25e10

nDMaterial   PlateRebar         10               3     90
nDMaterial   PlateRebar         11               3     0
section   LayeredShell      1000   10     4       25   11  0.2  10  0.345   4  24 4
24 4 24 4 24  10 0.345  11 0.2  4 25
section   LayeredShell     2000   10     4       25   11  0.4  10  1.47   4   24 4 24
4 24 4 24  10 1.47  11 0.4  4 25
############################
# createEles

element ShellMITC4 10001 10001 10002 10004 10003 2000
element ShellMITC4 10002 10003 10004 10006 10005 2000
element ShellMITC4 10003 10005 10006 10008 10007 2000
element ShellMITC4 10004 10007 10008 10010 10009 2000
element ShellMITC4 10005 10009 10010 10012 10011 2000
element ShellMITC4 10006 10011 10012 10014 10013 2000
element ShellMITC4 10007 10013 10014 10016 10015 2000
```

```
element ShellMITC4 10008 10015 10016 10018 10017 2000
element ShellMITC4 20001 10002 20002 20011 10004 1000
element ShellMITC4 20002 20002 20003 20012 20011 1000
element ShellMITC4 20003 20003 20004 20013 20012 1000
element ShellMITC4 20004 20004 20005 20014 20013 1000
element ShellMITC4 20005 20005 20006 20015 20014 1000
element ShellMITC4 20006 20006 20007 20016 20015 1000
element ShellMITC4 20007 20007 20008 20017 20016 1000
element ShellMITC4 20008 20008 20009 20018 20017 1000
element ShellMITC4 20009 10004 20011 20020 10006 1000
element ShellMITC4 20010 20011 20012 20021 20020 1000
element ShellMITC4 20011 20012 20013 20022 20021 1000
element ShellMITC4 20012 20013 20014 20023 20022 1000
element ShellMITC4 20013 20014 20015 20024 20023 1000
element ShellMITC4 20014 20015 20016 20025 20024 1000
element ShellMITC4 20015 20016 20017 20026 20025 1000
element ShellMITC4 20016 20017 20018 20027 20026 1000
element ShellMITC4 20017 10006 20020 20029 10008 1000
element ShellMITC4 20018 20020 20021 20030 20029 1000
element ShellMITC4 20019 20021 20022 20031 20030 1000
element ShellMITC4 20020 20022 20023 20032 20031 1000
element ShellMITC4 20021 20023 20024 20033 20032 1000
element ShellMITC4 20022 20024 20025 20034 20033 1000
element ShellMITC4 20023 20025 20026 20035 20034 1000
element ShellMITC4 20024 20026 20027 20036 20035 1000
element ShellMITC4 20025 10008 20029 20038 10010 1000
element ShellMITC4 20026 20029 20030 20039 20038 1000
element ShellMITC4 20027 20030 20031 20040 20039 1000
element ShellMITC4 20028 20031 20032 20041 20040 1000
element ShellMITC4 20029 20032 20033 20042 20041 1000
element ShellMITC4 20030 20033 20034 20043 20042 1000
element ShellMITC4 20031 20034 20035 20044 20043 1000
element ShellMITC4 20032 20035 20036 20045 20044 1000
element ShellMITC4 20033 10010 20038 20047 10012 1000
element ShellMITC4 20034 20038 20039 20048 20047 1000
element ShellMITC4 20035 20039 20040 20049 20048 1000
element ShellMITC4 20036 20040 20041 20050 20049 1000
element ShellMITC4 20037 20041 20042 20051 20050 1000
element ShellMITC4 20038 20042 20043 20052 20051 1000
element ShellMITC4 20039 20043 20044 20053 20052 1000
element ShellMITC4 20040 20044 20045 20054 20053 1000
element ShellMITC4 20041 10012 20047 20056 10014 1000
element ShellMITC4 20042 20047 20048 20057 20056 1000
element ShellMITC4 20043 20048 20049 20058 20057 1000
element ShellMITC4 20044 20049 20050 20059 20058 1000
element ShellMITC4 20045 20050 20051 20060 20059 1000
element ShellMITC4 20046 20051 20052 20061 20060 1000
element ShellMITC4 20047 20052 20053 20062 20061 1000
element ShellMITC4 20048 20053 20054 20063 20062 1000
element ShellMITC4 20049 10014 20056 20065 10016 1000
element ShellMITC4 20050 20056 20057 20066 20065 1000
element ShellMITC4 20051 20057 20058 20067 20066 1000
element ShellMITC4 20052 20058 20059 20068 20067 1000
```

```
element ShellMITC4 20053 20059 20060 20069 20068 1000
element ShellMITC4 20054 20060 20061 20070 20069 1000
element ShellMITC4 20055 20061 20062 20071 20070 1000
element ShellMITC4 20056 20062 20063 20072 20071 1000
element ShellMITC4 20057 10016 20065 20074 10018 1000
element ShellMITC4 20058 20065 20066 20075 20074 1000
element ShellMITC4 20059 20066 20067 20076 20075 1000
element ShellMITC4 20060 20067 20068 20077 20076 1000
element ShellMITC4 20061 20068 20069 20078 20077 1000
element ShellMITC4 20062 20069 20070 20079 20078 1000
element ShellMITC4 20063 20070 20071 20080 20079 1000
element ShellMITC4 20064 20071 20072 20081 20080 1000
element ShellMITC4 30001 20009 30002 30004 20018 2000
element ShellMITC4 30002 20018 30004 30006 20027 2000
element ShellMITC4 30003 20027 30006 30008 20036 2000
element ShellMITC4 30004 20036 30008 30010 20045 2000
element ShellMITC4 30005 20045 30010 30012 20054 2000
element ShellMITC4 30006 20054 30012 30014 20063 2000
element ShellMITC4 30007 20063 30014 30016 20072 2000
element ShellMITC4 30008 20072 30016 30018 20081 2000
#########################################################

fixY 0.0 1 1 1 1 1 1;

#equalDOF  20077  10017  10018  20074 20075 20076 20078 20079 20080 20081 30018    1
2



# Define gravity loads
# --------------------

# Set a parameter for the axial load

set P 695000.0;
# Create a Plain load pattern with a Linear TimeSeries
pattern Plain 1 Linear {

        # Create nodal loads at nodes 3 & 4
    #    nd    FX          FY  MZ
    load  20077   0.0  [expr -$P] 0.0  0  0  0

}



constraints Plain
numberer RCM
system BandGeneral
test NormDispIncr 1.0e-4 200 ;
algorithm BFGS -count 100
integrator LoadControl 0.1;
analysis Static
```

```
recorder Node -file SHN5static.out -time -node 20077  -dof 1 2 disp



analyze 10;

puts "gravity analyze ok..."
loadConst -time 0.0;

timeSeries Path 1 -dt 0.1 -filePath input.txt ;
pattern Plain 2 1 {
    sp 20077 1 1

 }
#pattern Plain 2 Linear {
#
#        # Create nodal loads at nodes 3 & 4
#    #    nd    FX          FY  MZ
#    load  20077   5134.0  0.0 0.0  0  0  0
#
#}
constraints Penalty 1e20 1e20;
numberer RCM;
system BandGeneral;
test NormDispIncr 1.0e-1 22000 2;
algorithm KrylovNewton;
integrator LoadControl 0.1;
analysis Static ;
recorder Element    -file  ele.out -time -ele  20060  forces;
recorder Node -file SHN5.out -time -node 20077  10017  -dof 1  disp
recorder Node -file reaction.out  -node 10001 10002 20002 20003 20004 20005 20006
20007 20008 20009 30002  -dof 1  reaction
analyze  6049
##
# ------------------------------
# End of model generation
# ------------------------------



# End of analysis generation
# ------------------------------



#source anady.tcl
#source analysiswall.tcl
#source dispAnalysisShell.tcl
```